Mucosal Associated Invariant T cells and CD161 expressing Natural Killer cells



Ayako Kurioka

Mansfield College, University of Oxford

Thesis submitted for the degree of

Doctor of Philosophy in Clinical Medicine

University of Oxford, Trinity Term 2015

Supervisor:

Professor Paul Klenerman, MRCP, FRCP, DPhil

Mucosal Associated Invariant T cells and CD161 expressing Natural Killer cells

Ayako Kurioka, Mansfield College

Submitted for DPhil in Clinical Medicine, Trinity Term 2015

Abstract

Mucosal-associated invariant T (MAIT) cells are a population of innate-like lymphocytes within the gut, liver and blood, expressing a semi-invariant T cell receptor (TCR) and high levels of the C-type lectin-like receptor, CD161. These cells recognise a metabolite of the microbial riboflavin synthesis pathway, presented by the highly conserved Major Histocompatibility Complex (MHC) class I-related protein, MR1, and are critical for the control of bacterial infections. The factors regulating the broad effector functions of MAIT cells have not been fully investigated. Utilising a novel flow cytometric killing assay, MAIT cells were shown here to require the induction of a cytotoxic phenotype through bacterial stimulation to efficiently kill target cells. Further in depth phenotypic analysis highlighted a distinct non-cytotoxic subset of CD4+ MAIT cells, with an altered cytokine-producing capacity, enriched within lymphoid tissues. Investigation into the potential role of these cells in psoriatic diseases revealed that MAIT cells within the synovial fluid of psoriatic arthritis patients are potently activated with increased IL-17 production, their frequency correlating with measures of clinical activity. MAIT cells also have an innate-like responsiveness to cytokines, a feature originally attributed to Natural Killer (NK) cells. Microarray analysis and mass cytometry experiments demonstrated that CD161 marks immature NK cells that have retained this ability to respond to innate cytokines during their differentiation, and is lost upon cytomegalovirus (CMV)-induced maturation in both healthy and human immunodeficiency virus (HIV)-infected patients. Thus, CD161 marks cells with innate-effector functions both in T cells and NK cells.

Acknowledgements

First and foremost, thank you to my supervisor, Paul, for all his support over the years that has made this journey possible. For letting me join the lab in the first place, and for always being so generous and open-minded. I cannot wish for a better supervisor.

I would also like to thank everyone from the Klenerman lab, for making it such a great place to work. Thank you particularly to the post-docs, Yu-hoi, Chris, Cormac and James for all your help with troubleshooting and technical advice, and to my office mates and fellow DPhil students, Jo, Alba, and Matt - for all the laughs and support through emergency coffee/tea breaks. Many thanks to everyone who has read my chapters and offered advice.

Thank you to the Nuffield Department of Medicine for my DPhil funding, which has made it possible for me to complete this work. Thank you also to Constantino and the Mexican Social Security Institute for the funding to visit and present my work in Mexico.

Thank you to all of my friends who have helped me survive my DPhil – Jo, Alba, Ruth, Jacqui, Leo, Matt, Rachel, Annette, Shoko, Alex, Jess, Nicole, Ingrid & Chris, thank you for all the good times we've shared, and for making my DPhil life in Oxford an unforgettable experience.

I'm eternally grateful to my parents for bringing me to the UK in the first place and letting me follow this path. I could never have dreamed of achieving something like this if it wasn't for your support. Thank you to Helen and Gary as well for taking me into their family as one of their own, and for always being ready to help with hugs and endless supplies of food!

Lastly, thank you to my fiancé, David, for your patience and understanding, particularly in the last few months during my time writing this thesis, and for always being my number one supporter even when I couldn't believe in myself. This thesis is dedicated to you.

TABLE OF CONTENTS

THESIS CONTRIBUTIONS 1

ABBREVIATIONS 3

1. INTRODUCTION 7

1.1. Innate and adaptive immunity 7

1.2. T cells 8
1.2.1. T cell memory 8
1.2.2. T cell subsets 10

1.3. Innate-like T cells 11
1.3.1. γδ T cells 13
1.3.2. Invariant Natural Killer T cells 15

1.4. Mucosal-associated invariant T (MAIT) cells 18
1.4.1. MR1 and its ligand 19
1.4.2. MAIT cell T cell receptor 21
1.4.3. MAIT cell development 22
1.4.4. MAIT cell tissue distribution 25
1.4.5. MAIT cell phenotype and effector functions 27
1.4.6. MAIT cell coreceptor usage 30
1.4.7. MAIT cells in bacterial infections 31
1.4.8. MAIT cells in viral infections 33
1.4.9. MAIT cells and autoimmunity 34

1.5. Innate-ness and CD161 expression 36

1.6. Natural Killer cells and the Innate lymphoid cell family 37
1.6.1. The ILC family 37
1.6.2. NK cell development 39
1.6.3. $CD56^{bright}$ and $CD56^{dim}$ NK cells 40
1.6.4. NK cell differentiation 44
1.6.5. NK cells in viral diseases 45
1.6.6. CD161 47
1.6.7. CD161 expression on NK cells in viral infections 49

1.7. Aims of Thesis 50

2. MATERIALS AND METHODS 51

2.1. Media and buffers 51

2.2. Cells 52
2.2.1. Peripheral blood samples 52
2.2.2. THP1 cells 52
2.2.3. B cell lines 52

2.3. Isolation of cells 52
2.3.1. PBMC separation 52

2.3.2. CD8+ T cell isolation 53
2.3.3. NK cell isolation 53

2.4. Irradiation of cells 53

2.5. Preparation of fixed bacteria 54

2.6. Cell culture 54
2.6.1. Bacterial activation of MAIT cells 54
2.6.2. Addition of blocking antibodies 55
2.6.3. T cell activation 55
2.6.4. PMA/ionomycin stimulation 55
2.6.5. IL-12+IL-18 stimulation 56
2.6.6. Proliferation assays 56

2.7. Flow cytometry 56
2.7.1. Surface staining 56
2.7.2. Intracellular cytokine staining 57
2.7.3. Transcription factor staining 57
2.7.4. Data acquisition and analysis 57

2.8. Cytometry by Time-of-Flight (CyTOF) 62
2.8.1. Antibody Conjugation 62
2.8.2. Staining of PMA/ionomycin stimulated cells 62
2.8.3. Staining of IL-12+IL-18 stimulated cells 63
2.8.4. Data acquisition and analysis 64

2.9. Statistical analysis 64

3. THE CYTOTOXICITY OF MAIT CELLS 65

3.1. Introduction 65

3.2. Aims 68

3.3. Materials and Methods 69
3.3.1. *In vitro* stimulation 69
3.3.2. Imagestream® analysis 69
3.3.3. Killing assays 70
3.3.4. Proliferation assays 71

3.4. Results 74
3.4.1. Resting blood-derived human MAIT cells have a unique cytotoxic profile 74
3.4.2. MR1-dependent activation of MAIT cells leads to degranulation and changes in their cytotoxic profile 76
3.4.3. Licensed MAIT cells can kill target cells in an MR1-dependent manner 79
3.4.4. Rapid GrB upregulation in MAIT cells is associated with Blimp1 and T-bet expression 84
3.4.5. MAIT cells readily proliferate in response to *E. coli* and maintain a highly cytotoxic profile… 86

3.5. Discussion 89

3.6. Summary 94

4. PHENOTYPE AND FUNCTION OF MAIT CELL SUBSETS 102

4.1. Introduction 102

4.2. Aims 105

4.3. Materials and Methods 105
4.3.1. Blood and tissue samples 106
4.3.2. *E. coli*-stimulation of MAIT cells 106
4.3.3. Apoptosis assays 107
4.3.4. Culture of MAIT cells in Th2-skewing conditions 107

4.4. Results 108
4.4.1. Frequencies of MAIT cell subsets in healthy adult blood 108
4.4.2. Cell surface phenotype heterogeneity of human MAIT cells 108
4.4.3. CD4+ MAIT cells have lower cytotoxic potential compared to CD4− MAIT cells 112
4.4.4. CD4+ MAIT cells have reduced Eomes expression 114
4.4.5. CD4+ MAIT cells have a lower capacity to secrete Th1 cytokines and degranulate… 118
4.4.6. CD4+ MAIT cells are skewed towards a Th2 cytokine profile 121
4.4.7. CD8 coreceptor blockade reduces CD8+ MAIT cell activation by *E. coli*-treated THP1 cells 121
4.4.8. CD4+ MAIT cells are enriched in tonsils and are highly active CD56+ cells in the liver…… 125

4.5. Discussion 128

4.6. Summary 135

5. MAIT CELLS IN PSORIASIS AND PSORIATIC ARTHRITIS 139

5.1. Introduction 139
5.1.1. Psoriasis 139
5.1.2. Psoriatic arthritis 142
5.1.3. Unconventional lymphocytes in psoriasis and PsA 143

5.2. Aims 145

5.3. Methods 145
5.3.1. Isolation of T cells from the skin 145
5.3.2. Psoriasis patients 146
5.3.3. Psoriatic arthritis (PsA) patients 146
5.3.4. Pre-activating MAIT cells for IL-17 production 146
5.3.5. RORγt inhibitor 147
5.3.6. Microarray analysis 147

5.4. Results 148
5.4.1. MAIT cells are present in healthy and psoriatic skin 148
5.4.2. The frequency and phenotype of MAIT cells of psoriasis and atopic dermatitis patients 150
5.4.3. A reduced frequency of MAIT cells from psoriasis and atopic dermatitis patients express IFNγ in response to PMA/ionomycin stimulation compared to healthy controls 153
5.4.4. MAIT cells are highly activated in the synovial fluid of psoriatic arthritis patients 155
5.4.5. CD161++ T cells in the synovial fluid of psoriatic arthritis patients are highly responsive to IL-12+IL-18 159
5.4.6. Increased frequency of IL-17-expressing T cells in the synovial fluid of PsA patients, including MAIT cells 162
5.4.7. Gene expression correlation analysis identifies genes highly associated with *ZBTB16* expression in CD8+ T cells 164
5.4.8. Effect of RORγt inhibitor on MAIT cells: optimization of IL-17 production from MAIT cells….. 169
5.4.9. RORγt inhibitor inhibits production of IL-17 from MAIT cells 172
5.4.10. RORγt inhibitor blocks MR1-induced IL-17 production from MAIT cells 176

5.4.11. RORγt inhibitor reduces the responsiveness of MAIT cells to IL-23+IL-18 stimulation 176

5.5. Discussion 178
5.5.1. MAIT cells are not enriched in psoriatic skin and PsA synovial fluid compared to blood 178
5.5.2. Regulation of IL-17 production from MAIT cells 181
5.5.3. Identifying correlates of innate-responsiveness and CD161 expression in T cells 183

5.6. Summary 185

6. CD161 EXPRESSION ON NK CELLS 211

6.1. Introduction 211

6.2. Aims 214

6.3. Methods 215
6.3.1. Patient information and cells 215
6.3.2. *In vitro* stimulation of NK cells 215
6.3.3. Screening for healthy CMV+ donors 216
6.3.4. Proliferation assays 216
6.3.5. Detection of apoptosis 217
6.3.6. Microarray analysis 217
6.3.7. Cytometry by time-of-flight (CyTOF) 218

6.4. Results 223
6.4.1. CD161 expression defines two distinct subsets of NK cells 223
6.4.2. Transcriptional analysis of CD161+ and CD161− NK cells 223
6.4.3. CD161+ NK cells are phenotypically immature compared to CD161− NK cells 228
6.4.4. CD161+ NK cells are high proliferative compared to CD161− NK cells 232
6.4.5. CD161+ $CD56^{dim}$ NK cells are highly responsive to cytokines IL-12+IL-18 235
6.4.6. Terminally differentiated NK cells expanded in CMV+ individuals are low in CD161 and PLZF expression 238
6.4.7. CD161+ NK cells are depleted in CMV-seropositive HIV donors and recovers with HAART 242
6.4.8. High dimensional analysis delineates NK cell populations in CMV+ and CMV− donors 245

6.5. Discussion 249
6.5.1. Phenotypic correlates of CD161 expression in NK cells 249
6.5.2. CD161 expression and innate responsiveness of NK cells 251
6.5.3. CD161 and proliferation of NK cells 251
6.5.4. CD161 and PLZF expression in NK cells 252
6.5.5. CD161 expression on NK cells in HIV infected patients 253

6.6. Summary 255

7. DISCUSSION 274

7.1. MAIT cells and their effector functions 274
7.1.1. License to kill: upregulation of GrB by MAIT cells 274
7.1.2. Can CD4+ MAIT cells kill? 276
7.1.3. Th2 cytokine production by CD4+ MAIT cells 277
7.1.4. Lineage decisions by MAIT cells 277

7.2. MAIT cells and their role in autoimmunity 279

7.2.1. MAIT cells in psoriatic disease 279
7.2.2. Activation of MAIT cells in autoimmune diseases 281

7.3. Innate-ness of cells and CD161 283
7.3.1. Innate-ness of T cells and CD161 283
7.3.2. Innate-ness of NK cells and CD161 283
7.3.3. PLZF: master transcription factor of innate-ness? 284

7.4. Parallels between NK cell and CD8+ T cell subsets 286
7.4.1. Cytokine responsiveness 286
7.4.2. Regulation of cytotoxicity 288
7.4.3. Enrichment in inflamed tissues 289
7.4.4. Implications of similarities between $CD56^{bright}$ NK cells and MAIT cells 290

7.5. Conclusions 293

REFERENCES 295

APPENDIX 351

List of publications 351

Thesis contributions

Chapter 3

Christian Clough
Optimization of granzyme and perforin stains. Performed Imagestream experiments for his thesis (MSc Integrated Immunology student)

Chapter 4

Aminu Jahun
Performed experiments contributing to phenotyping data and anti-CD8 blocking antibody experiments for his thesis (MSc Integrated Immunology student)

Christian Willberg
Performed staining of cells in tonsils and of 24 month old PBMCs

James Ussher
Performed experiments using intrahepatic lymphocytes and *E. coli*-treated THP1 cells

Lucy Walker
Performed the CBA experiments.

Verity Hill
Contributed to CLA1 staining experiments

Chapter 5

Sophie Zemendies
Collaboration on psoriasis project, helped with processing skin samples and PBMC experiments

Hussein Al-Mossawi
Collected PsA synovial fluid and blood samples, helped isolate SFMCs for some samples

Verity Hill
Helped perform *E. coli* and IL-23+IL-18 stimulation experiments using the RORγt inhibitor for her thesis (BA Biological Sciences student)

Yu-hoi Kang
Provided the CD161++, CD161+, and CD161- CD8+ T cell microarray data

Chapter 6

Joannah Fergusson
Collaboration on CyTOF experiments. Provided CyTOF data on polyfunctionality.

Yannick Simoni
Collaboration on CyTOF experiments and performed t-SNE analysis in R

Leo Swadling
Provided CyTOF data on polyfunctionality with Joannah Fergusson

Cormac Cosgrove
Performed staining of PBMCs from Swiss HIV Cohort study

Christian Willberg
Performed staining of 24 month old PBMCs

Alba Llibre
Performed experiments using NK cells and LLT1-expressing cell lines

Jacob Hurst
Performed comparison of PCA and t-SNE analysis shown in Methods section

Abbreviations

5-A-RU	5-amino-6-d-ribitylaminouracil
5-OP-RU	5-(2-oxopropylideneamino)-6-D-ribitylaminouracil
6-FP	6-formyl pterin
Ac-6-FP	acetyl-6-formylpterin
Act1	NF-κB Activator 1
AD	atopic dermatitis
AHR	aryl hydrocarbon receptor
AICD	activation induced cell death
APC	antigen presenting cell
ATCC	American Type Culture Collection
BCG	bacillus Calmette-Guérin
BCL	B cell line
BCL-xL	B-cell lymphoma-extra large
Blimp1	B lymphocyte-induced maturation protein 1
BMI	body mass index
BSA	bovine serum albumin
Btk	Bruton tyrosine kinase
BTN3A1	Butyrophilin 3A1
CBA	Cytometric bead assay
CCR	chemokine receptor
CD	Crohn's Disease
CDR	complementarity determining region
CFSE	carboxyfluorescein succinimidyl ester
ChIP	chromatin immunoprecipitation
ChIP-Seq	chromatin immunoprecipitation sequencing
CIA	collagen-induced arthritis
CIAI	collagen antibody-induced arthritis
CLA	cutaneous lymphocyte antigen
CLEC	C-type lectin-like receptor
CMV	Cytomegalovirus
CNS	central nervous system
CRP	C-reactive protein
CTL	cytotoxic T lymphocyte
CTV	CellTrace™ Violet
CUL3	Cullin-based E3 ubiquitin ligase
CXCL	C-X-C motif chemokine
CXCR	C-X-C chemokine receptor type
CyTOF	Cytometery by time-of-flight
DC	dendritic cell
DETC	dendritic epidermal T cells
DMARD	disease modifying anti-rheumatic drug
DN	double negative (CD4-CD8-)
DP	double-positive (CD4+CD8+)
E:T	effector-to-target cell ratio
E. coli	*Escherichia coli*
EAE	experimental autoimmune encephalomyelitis
EBV	Epstein-Barr virus
EDTA	Ethylenediaminetetraacetic acid
EGTA	ethylene glycol tetraacetic acid
ELISpot	Enzyme-Linked ImmunoSpot
Eomes	Eomesodermin

ER	endoplasmic reticulum
FACS	fluorescence activated cell sorting
FATAL	flurometric assessment of T lymphocyte antigen specific lysis
Fc	fragment crystallizable
FCS	foetal calf serum
FMO	fluorescence minus one
FTOC	fetal thymus organ cultures
GATA3	GATA binding protein 3
GEM	germline-encoded mycolyl lipid-reactive
GEM	germline-encoded, mycolyl lipid-reactive T cells
gMFI	geometric mean fluorescence intensity
Gr	granzyme
GSEA	gene set enrichment analysis
GVHD	graft-versus-host disease
GWAS	genome-wide association study
HAART	highly active antiretroviral therapy
HBV	hepatitis B virus
HCV	hepatitis C virus
HDAC1	Histone Deacetylase 1
HIV	human immunodeficiency virus
HLA	Human Leukocyte Antigen
HMBPP	(E)-4-Hydroxy-3-methyl-but-2-enyl pyrophosphate
HS	human serum
HSCT	hematopoietic stem cell transplantation
IBD	inflammatory bowel disease
ICS	intracellular cytokine staining
Id2	inhibitor of DNA binding 2
IEL	intraepithelial cells
IFN	interferon
Ig	Immunoglobulin
iGb3	isoglobotrihexosylceramide
IHL	intrahepatic lymphocytes
IL	interleukin
ILC	innate lymphoid cell
iNKT	invariant natural killer T cell
IPP	isopentenyl pyrophosphate
ITAM	Immunoreceptor tyrosine-based activating motif
ITIM	Immunoreceptor tyrosine-based inhibitory motif
KIR	killer-cell immunoglobulin-like receptor
LAMP	lysosomal-associated membrane protein
LCMV	lymphocytic choriomeningitis virus
MCMV	murine cytomegalovirus
LLT1	lectin-like transcript 1
LPS	lipopolysaccharide
LRC	leukocyte receptor complex
LTi	lymphoid tissue-inducer
LVS	live vaccine strain
MAIT	mucosal associated invariant T cell
MCMV	murine CMV
MHC	major histocompatibility complex
MIC	MHC class I polypeptide-related sequence
min	minutes
MR1	MHC class I-related gene protein
mRNA	messenger ribonucleic acid
MS	multiple sclerosis

NCR	natural cytotoxicity receptors
NES	Normalised Enrichment Score
NF-κB	nuclear factor kappa-B
NK	natural killer
NK-LDGL	NK-type lymphoproliferative disease of granular lymphocytes
NKRP	Natural Killer Receptor Protein
NKT	natural killer T
Ocil	osteoclast inhibitory lectin
PB	peripheral blood
PBMC	peripheral blood mononuclear cells
PBS	phosphate buffered saline
PD-1	programmed cell death protein 1
PD-1	programmed death 1
PFA	paraformaldehyde
PHA	phytohaemagglutinin
PLZF	promyelocytic leukaemia zinc finger
PMA	Phorbol 12-Myristate 13-Acetate
PS	phosphatidylserine
PsA	psoriatic arthritis
R	receptor
R10	RPMI1640 + 10% FCS+ L-Glutamine+ Penicillin-streptomicin solution
RA	rheumatoid arthritis
RAG	recombination-activating gene
RANKL	receptor activator of NF-κB ligand
RH10	RPMI1640 + 10% HS+ L-Glutamine+ Penicillin-streptomicin solution
ROR	RAR-related orphan receptor
rRL-6-CH_2OH	6-hydoxymethyl-8-D-ribityllumazine
RUNX3	runt-related transcription factor 3
S.E.M.	standard error of mean
SAP	SLAM-associated protein
SD	*Shigella dysenteriae*
SF	synovial fluid
SF	synovial fluid
SFMC	Synovial fluid mononuclear cells
SHCS	Swiss HIV cohort study
SHIP	haematopoietic cell-specific SH2 containing 5’ inositol phosphatase
SLAMF	signaling lymphocytic activation molecule
SLE	systemic lupus erythematosus
SLO	streptolysin O
SNP	single nucleotide polymorphisms
TAP	transporter associated with antigen processing
TB	tuberculosis
TCR	T cell receptor
TF	transcription factor
Th	T helper
ThPOK	Th-inducing POK-Kruppel factor
TLR	Toll-like receptor
TNF	tumour necrosis factor
TRAF3IP2	tumor necrosis factor receptor associated factor 3-interacting protein 2
UC	Ulcerative Colitis
UCB	umbilical cord blood
ULBP	UL-16-binding protein
Unstim	unstimulated
VbO1	*Vibrio cholera* O1
WGCNA	weighted gene co-expression network analysis

αGalACer	α-galacturonosylceramide
β2M	β-2-microglobulin
γc	common γ chain

Note: In this thesis, T cell subpopulations are referred to as CD161++ (bright), CD161+ (dim), or CD161− (negative) according to their expression levels of CD161, whereas NK cells are referred to as CD161+ (positive) and CD161− (negative), unless otherwise indicated. Within NK cells, the term CD56+ (positive) refers to the whole NK cell population as a whole, while $CD56^{bright}$ and $CD56^{dim}$ refers to subpopulations within NK cells distinguished by the level of CD56 expressed.

1. Introduction

1.1. Innate and adaptive immunity

The efficient detection and destruction of pathogens that threaten host viability requires the coordinated action of the two pillars of the immune system: the innate and adaptive immune responses. Innate immunity is mediated by defense mechanisms present from birth, which rapidly come into play following pathogen invasion. The cellular component of the innate immune system includes neutrophils, macrophages and Natural Killer (NK) cells. Initiation of the innate immune response involves the recognition of conserved structures on infectious agents, known as pathogen-associated molecular patterns (PAMPs), by pattern recognition receptors (PRRs) expressed by innate cells (Medzhitov, 1998). These cells can also recognize stress signals from infected or transformed cells, particularly important for the activation of NK cells. Importantly, the receptors that activate innate cells are germline-encoded, and are not specific to a particular pathogen. Activation of these cells leads the induction of inflammatory responses and innate host defenses, such as phagocytosis by neutrophils and macrophages, as well as direct cytotoxicity mediated by NK cells, thus providing the first line of defense. Many of these cells are present at the site of invasion or are immediately recruited, and quickly disappear after the removal of the pathogen.

The innate immune system is also critical for the subsequent development of the adaptive immune response, by processing antigen for presentation on Major Histocompatibility Complex (MHC) molecules, as well as releasing proinflammatory cytokines, chemokines, and interferons (IFN), which results in the recruitment and activation of the adaptive immune system. The adaptive immune system is

composed of T and B lymphocytes which express highly diverse, somatically-rearranged receptors. These receptors endow cells with the ability to specifically recognise the invading pathogen. Upon activation, T and B cells clonally expand and exert effector functions such as the production of antibodies, cytotoxicity, and secretion of immunomodulatory cytokines. The hallmark of the adaptive immune system is the presence of these antigen-specific effector cells and antibodies long after pathogen clearance, providing long-lasting immunity against previously encountered pathogens.

Recently, the dichotomy between cells of the innate and adaptive immune system has been blurred with the discovery of cells possessing both innate and adaptive characteristics, called innate-like T cells. This thesis will focus on cells that particularly behave in an innate-manner, innate-like T cells and NK cells.

1.2. T cells

1.2.1. T cell memory

T lymphocytes develop within the thymus and display an extremely diverse T cell receptor (TCR) repertoire when they mature and enter the circulation, due to somatic recombination of variable (V), diversity (D), joining (J) gene segments, mediated by the recombination activating gene (RAG) recombinase (Schatz et al., 1989). These T cells do not exhibit immediate effector functions, and remain naïve until they are activated by cognate antigen, presented by antigen-presenting cells (APCs) within secondary lymphoid organs. Following recognition of a specific antigen presented by MHC class I or class II molecules, naïve T cells differentiate into effector cells and undergo clonal expansion (Butz & Bevan, 1998). These cells then migrate to the site

of antigen presence to perform specialized functions, such as target cell lysis and secretion of immunomodulatory cytokines.

Following pathogen clearance, the majority of expanded antigen-specific effector T cells undergo contraction and cell death, while a fraction of these cells differentiate into long-lived memory T cells (Badovinac et al., 2002; Williams & Bevan, 2007). Immunological memory is thought to be an exclusive feature of T and B cells, and is defined as the presence of antigen-specific cells long after antigen clearance, which can mount enhanced recall responses following antigen re-challenge (Lau et al., 1994; Murali-Krishna, 1999).

T cells express the shortest isoform of the tyrosine phosphatase CD45, CD45RO, following antigen experience, while naïve T cells express CD45RA (Michie et al., 1992). CD45RA expression can therefore be used to divide T cells into memory subsets, in combination with the expression of lymph node homing receptors such as CCR7 (Romero et al., 2007; Sallusto et al., 1999). While CD45RA+CCR7+ naïve T cells and CD45RA−CCR7+ central memory T cells (T_{CM}) home to secondary lymphoid organs and can undergo rapid proliferation, CD45RA−CCR7− effector memory T cells (T_{EM}) are poised for rapid effector functions rather than proliferation, and lack lymph node homing receptors (Masopust et al., 2001; Sallusto et al., 1999). CD8+ T cells can also re-express CD45RA during terminal differentiation (CCR7−CD45RA+, T_{EMRA}) (Michie et al., 1992). This classification, however, underestimates the heterogeneity of memory T cell subsets within humans, which was demonstrated recently by the use of mass cytometry (Newell et al., 2012). Additionally, a subset of memory T cells which are retained in peripheral tissues such as the gut, lung and skin, called tissue-resident memory T cells, have been described recently. These cells provide immediate response against pathogen invasion through peripheral tissues (Jiang et al., 2012; Mackay et al., 2013).

1.2.2. T cell subsets

T cells are traditionally separated into two subsets according to CD4 and CD8 coreceptor expression. This CD4/CD8 lineage choice is determined during thymic selection by a network of transcription factors, including the master regulator of CD4-lineage choice, T helper (Th)-inducing POK-Kruppel factor (ThPOK), and runt-related transcription factor 3 (RUNX3), which silences *CD4* and promotes CD8+ T cell differentiation (He et al., 2005; Singer et al., 2008).

CD4+ T cells are activated by peptides presented by MHC class II molecules on professional APCs such as macrophages, dendritic cells (DCs) and B cells, and are called T helper (Th) cells due to their ability to secrete immunomodulatory cytokines. Naïve CD4+ T cells can differentiate into several lineages, including Th1, Th2, Th17, and regulatory T (T_{reg}) cells (Mosmann & Coffman, 1989; Park et al., 2005). These lineages are defined by the expression of prototypical cytokines and 'master' transcription factors, determined by the surrounding cytokine milieu during priming. Thus, TCR stimulation of naïve CD4+ T cells in the presence of interleukin (IL)-12 (Hsieh et al., 1993; Magram et al., 1996) and IFNγ (Scharton & Scott, 1993) leads to T-bet expression, which is required for the development of Th1 cells (Szabo et al., 2000). In contrast, IL-4 (Seder et al., 1992) and GATA binding protein 3 (GATA3) (Zheng & Flavell, 1997) induces Th2 cell differentiation. Th17 cells characteristically express the RAR-related Orphan receptor (ROR)γt (Ivanov et al., 2006), and their differentiation is induced by IL-23 and IL-1β in humans (Cosmi et al., 2008). In contrast, murine Th17 cells require TGFβ and IL-6 before they become responsive to IL-23 (Bettelli et al., 2006; Cua et al., 2003; Mangan et al., 2006). TGFβ in the absence of proinflammatory cytokines regulates Foxp3 expression to induce the differentiation of T_{reg} cells (Bettelli et al., 2006; Chen et al., 2003). All of these

differentiated CD4+ T cells that have attained specialized properties go onto play distinct roles within the immune system, as summarised in Figure 1-1.

CD8+ T cells recognise peptides presented by MHC class I molecules expressed on all nucleated cells, and differentiate into cytotoxic effector populations that can lyse infected or transformed cells. Cytotoxicity is mainly mediated through exocytosis of preformed granules containing granzyme and perforin (Heusel et al., 1994; Kägi et al., 1994a; Shresta et al., 1995), which induces apoptosis in target cells through caspase-dependent and independent mechanisms (Chowdhury & Lieberman, 2008). Fas ligand (FasL) expression on CD8+ T cells can also induce apoptosis in Fas-expressing target cells (Kägi et al., 1994b). CD8+ T cells also secrete abundant Th1-type cytokines such as IFNγ and TNFα upon activation (Barth et al., 1991). Memory CD8+ T cell differentiation requires IL-15, and the transcription factors T-bet and Eomesodermin (Eomes), which cooperate to induce the expression of cytolytic molecules (Intlekofer et al., 2005; Pearce et al., 2003). T-bet and Eomes are also required for the IL-15-dependent homeostasis of memory CD8+ T cells, as they maintain their expression of a subunit of the IL-15R, IL-2Rβ (Intlekofer et al., 2005).

1.3. Innate-like T cells

Recently, unconventional T cells with features of the innate immune system have been described. These cells respond rapidly to infection or tissue dysregulation in synchrony with the innate response, but express somatically-recombined TCRs - by definition, a characteristic of adaptive lymphocytes. However, unlike conventional T cells, innate-like T cells have a limited TCR repertoire and recognise a small number of conserved antigens. Functional maturation of these innate-like T cells is developmentally pre-programmed, and therefore, these cells display an effector

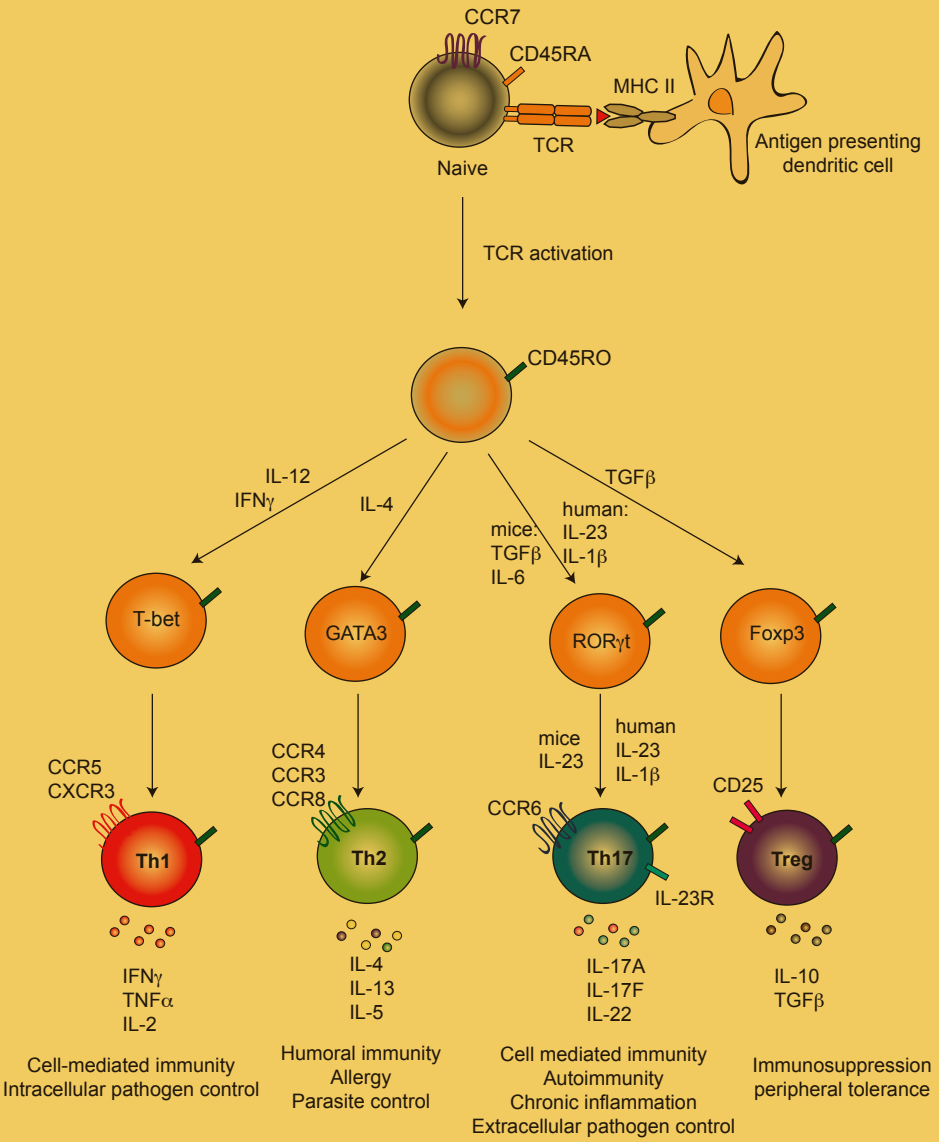


Figure 1-1. Differentiation of T helper cell (Th) subsets and regulatory T cells (Treg). T helper cells and regulatory T cells differentiate from naive CD4+ T cells following activation in the presence of indicated cytokines. Th1 cells differentiate in the presence of IL-12, enhanced by IFNγ, which induces the expression of T-bet. Th2 cells depend on IL-4 and GATA3 expression. Murine Th17 cells require TGFβ in combination with IL-6 (or IL-1β/IL-21) for intial expression of RORgt. This induces the expression of IL-23R, making the cells responsive to IL-23 and further enhancing Th17 differentiation. Human Th17 cells do not require TGFβ but instead require IL-23+IL-1β. Finally, activation in the presence of TGFβ induces Foxp3 expression, leading to the development of Tregs. Differentiated helper T cell subsets express the indicated cytokines upon TCR stimulation and home to inflamed tissues through the expression of different chemokine receptors. Adapted from Di Cesare *et al.*, 2009.

memory phenotype before exposure to foreign antigen, often within the thymus. These cells also preferentially home to tissues, and play a key role in bridging innate and adaptive immune responses by demonstrating rapid effector functions upon antigen encounter.

1.3.1. γδ T cells

One of the first innate-like T cells to be described was the γδ T cell population. While conventional T cells express a TCR composed of α and β chains, γδ T cells express a TCR encoded by the γ loci (Saito et al., 1984) and the δ loci (Chien et al., 1987). These γδ T cells appear before αβ T cells during fetal thymic development (Havran & Allison, 1988), and their frequency decreases as the αβ T cells expand, constituting 0.5-5% of the peripheral blood T cells in healthy human adults (Bonneville et al., 2010; Chien et al., 2014). Interestingly, the TCR expressed by γδ T cells can be highly related or invariant within tissues. For instance, cells in the peripheral blood preferentially express Vδ2 TCRs with biased γ chain pairing with Vγ9 (Triebel & Hercend, 1989). In contrast, Vδ1+ T cells, such as the Vγ5Vδ1+ murine skin dendritic epidermal T cells (DETCs), preferentially migrate to epithelial surfaces (Asarnow et al., 1988). The tissue-homing properties of γδ T cells are acquired during development, as successive waves of γδ thymocytes expressing different TCRs acquire different chemokine receptors (Bonneville et al., 2010). Thus, the first wave of Vγ5Vδ1 TCR-expressing thymocytes acquire CCR10 expression and home to the epidermis following the engagement of their TCR (Xiong et al., 2004). The second wave, in turn, express Vγ6Vδ1 TCR, and home to the mucosal epithelial surfaces (Itohara et al., 1990). Murine thymocytes expressing Vγ1Vδ6.3 TCR acquire the ability to home to the liver and spleen, due to the ligation of their TCR and subsequent induction of the transcription factor promyelocytic leukaemia zinc-finger (PLZF) (Kreslavsky et al., 2009), which also endows them with the ability to secrete

IFNγ and IL-4. In fact, the ability of γδ T cell subsets to express cytokines such as IFNγ and IL-17 is also predetermined by the strength of TCR signaling within the thymus (Jensen et al., 2008).

The TCR of γδ T cells enables them to recognize cellular dysregulation in infected or transformed cells, in a manner similar to PRRs. This dual reactivity is particularly exemplified by the Vγ9Vδ2+ T cells in peripheral blood, which recognize phosphoantigen metabolites of the isoprenoid biosynthesis pathway, such as (E)-4-Hydroxy-3-methyl-but-2-enyl pyrophosphate (HMBPP) produced by mycobacteria (Hintz et al., 2001). These cells can also recognize isopentenyl pyrophosphate (IPP), which accumulates during dysregulated metabolism in tumour cells (Tanaka et al., 1995). Butyrophilin 3A1 (BTN3A1) plays a crucial role in the phosphoantigen-mediated activation of Vγ9Vδ2+ T cells, even in cells which lack MHC surface expression (Harly et al., 2012). Current data suggests that BTN3A1 may not behave as an antigen-presenting molecule as initially suggested, but instead acts as a sensor of intracellular phosphoantigen (Sandstrom et al., 2014; Wang et al., 2013), and conveys this to circulating Vγ9Vδ2+ T cells through an unknown mechanism (Gu et al., 2015). γδ T cells can also recognize self-lipids presented by the non-polymorphic MHC-related molecules, CD1c (Spada et al., 2000) and CD1d (Uldrich et al., 2013). Furthermore, the Vδ1+ subset can be activated by the stress-induced non-classical MHC molecules, MHC class I polypeptide-related sequence A (MICA) and MICB (Groh et al., 1998), which are recognized by γδ T cells directly through their TCR, as well as through their NKG2D receptor (Strid et al., 2008; Wu et al., 2002). Additionally, γδ T cells can be regulated by both inhibitory and activating NK receptors which bind MHC class Ia and Ib (Trichet et al., 2006).

γδ T cell populations show a broad functional phenotype, secreting a range of Th1 and Th2 cytokines (Ferrick et al., 1995), as well as exhibiting direct cytotoxicity of

infected target cells (Bukowski et al., 1994) and tumour cells (Bas et al., 2006; Fisch et al., 1990). This polyfunctionality enables their immunosurveillance function, particularly in neonates (Gibbons et al., 2009; Ramsburg et al., 2003). A protective role for γδ T cells in infections is supported by the observation that subsets of γδ T cells dramatically expand during infection in patients e.g. expansion of Vγ9Vδ2 T cells during infection by HMBPP-producing mycobacteria (Havlir et al., 1991; Modlin et al., 1989). These expanded γδ T cells can provide protection against fatal mycobacterial infections (Shen et al., 2002), by directly lysing infected cells through the secretion of granulysin (Dieli et al., 2001). Recently, IL-17 production from subsets of γδ T cells has also been demonstrated, which is not only critical in protection against *Listeria monocytogenes* infection in a murine model (Hamada et al., 2008), but has also been implicated in autoimmune conditions such as psoriasis (Cai et al., 2011).

1.3.2. Invariant Natural Killer T cells

In 1987, three groups described a population of murine CD4−CD8− (double negative; DN) thymocytes expressing low levels of TCR, with biased expression of Vβ8 (Budd et al., 1987; Ceredig et al., 1987; Fowlkes et al., 1987). Subsequently, this population was found to express the NK cell marker, NK1.1 in mice (Sykes, 1990), or CD161 in humans (Exley et al., 1997), which has led to these cells being referred to as invariant NKT (iNKT) cells (Godfrey et al., 2004; Makino et al., 1995). In addition to the biased usage of the Vβ8 and Vβ2 chain (Sykes, 1990), these DN T cells were found to use an invariant TCRα chain rearrangement of Vα14-Jα18 in mice (Lantz & Bendelac, 1994), or Vα24-Jα18 in humans (Porcelli et al., 1993).

This unique TCR enables iNKT cells to recognise ligands presented by the non-polymorphic MHC class I-like molecule, CD1d (Bendelac et al., 1995). CD1d

presents conserved lipid antigens (Beckman et al., 1994), such as the prototypic glycosphingolipid, α-galactosylceramide (αGalCer) (Kawano et al., 1997). Several other glycolipid antigens have been described for iNKT cells, such as the closely related α-galacturonosylceramide (αGalACer) (Kinjo et al., 2005; Mattner et al., 2005), as well as mammalian glycolipids such as isoglobotrihexosylceramide (iGb3) (Zhou et al., 2004). All of these iNKT cells that can be detected with α-GalCer-loaded CD1d tetramers are collectively called Type I NKT cells. For the remainder of this thesis, the term 'iNKT cell' will be used to describe Type I NKT cells.

Type II NKT cells, in contrast, are CD1d-restricted NKT cells that recognize a range of hydrophobic antigens, such as sulfatide (Patel et al., 2012) and lysophosphatidylcholine (Maricic et al., 2014). Type II NKT cells express a more diverse TCR repertoire compared to Type I NKT cells (Gadola et al., 2002), with TCRs composed of Vα3.2-Jα9 or Vα8 paired with Vβ8 (Park et al., 2001).

In humans, the NKT cell family is even more diverse, consisting of both αβ and γδ T cells restricted by four additional CD1 family members, CD1a, CD1b, CD1c, and CD1e (Godfrey et al., 2010). These include the dermal CD1a-restricted T cells that are activated by skin oils (de Jong et al., 2014) or lipid neoantigens generated by bee venom-derived phospholipase A2 (Bourgeois et al., 2015), as well as germline-encoded mycolyl lipid-reactive (GEM) TCR expressing T cells reactive to CD1b (Van Rhijn et al., 2013), and CD1c-restricted T cells that recognize the mycobacterial lipid phosphomycoketide (Ly et al., 2013). Interestingly, TCR-independent activation of NKT cells has also been described; for instance, microbial activation of iNKT cells has been shown to be dominated by IL-12 signaling, rather than CD1d-mediated TCR signaling (Brigl et al., 2011).

Upon activation, iNKT cells can rapidly produce a broad range of cytokines, partly due to their constitutively high expression of cytokine mRNAs (Stetson et al., 2003). iNKT cells can be further divided into CD4+ and CD4− subsets that produce a different range of cytokines and differ in their cytotoxic capacity. Thus, CD4+ iNKT cells secrete large amounts of IL-4, IL-13, and IL-10, while the CD4− subset are the dominant IFNγ-producers and the cytotoxic subset (Gumperz et al., 2002; Lee et al., 2002). CD8+ iNKT cells have also been found in humans (Takahashi et al., 2002). Recently, IL-17-producing CD4− iNKT cells that express RORγt have also been described (Coquet et al., 2008). Thus according to their coreceptor expression, iNKT cells are functionally compartmentalized and are thought to play different roles in health and disease; for example, liver CD4− iNKT cells are much more effective at mediating tumour rejection compared to their CD4+ counterparts (Crowe et al., 2005).

The innate-like properties of iNKT cells are imprinted during their development. iNKT cell precursors are selected by CD4+CD8+ double-positive (DP) cortical thymocytes expressing CD1d, rather than by cortical epithelial cells that select conventional MHC-restricted T cells (Bendelac, 1995). Interaction of the signaling lymphocytic activation molecule 1 (SLAMF1) and SLAMF6 receptors between cortical DP thymocytes and iNKT cell precursors leads to signaling through the adaptor SLAM-associated protein (SAP) (Griewank et al., 2007). As this signal is required for the positive selection of iNKT cells, SAP-deficient mice and patients with SAP-deficient X-linked lymphoproliferative disorder both lack iNKT cells, but not conventional T cells (Nichols et al., 2005; Pasquier et al., 2005). Intriguingly, forced positive selection of MHC-class II restricted T cells by cortical thymocytes, rather than thymic epithelial cells, induces iNKT cell-like properties in these conventional T cells, including SAP-dependent development, lower expression of their TCR, and rapid secretion of IL-4 (Li et al., 2007a, 2007b). Thus, the unique selecting cell type of NKT cells in the thymus is key in determining their differentiation programme.

Another factor that is crucial to their constitutively activated, memory phenotype is the expression of PLZF. This key transcription factor is induced in iNKT cells immediately after positive selection, even in SAP-deficient iNKT thymocytes (Kovalovsky et al., 2008; Savage et al., 2008). PLZF-deficient mice have severely reduced frequencies of iNKT cells, and the residual iNKT cells in these mice remain functionally immature (Gleimer et al., 2012; Kovalovsky et al., 2008; Savage et al., 2008). Specifically, these cells lack the characteristic memory phenotype of iNKT cells, home to lymph nodes rather than peripheral tissues, and are unable to secrete IL-4 and IFNγ upon stimulation. Ectopic PLZF expression in CD4+ thymocytes induced these cells to acquire an innate-like phenotype, secreting IL-4, and preferentially migrating to non-lymphoid tissues (Kovalovsky et al., 2010; Savage et al., 2008, 2011), suggesting that PLZF regulates the acquisition of innate-like effector functions by iNKT cells.

Interestingly, the CD4-lineage inducer ThPOK has also been shown to be important for the functional maturation and development of CD4+ iNKT cells, as ThPOK-deficient mice preferentially develop into an unusual CD8+ or DN (Engel et al., 2010), IL-17-producing population (Enders et al., 2012). This has been shown to be due to the repression of RORγt expression by ThPOK (Engel et al., 2012). Thus, iNKT cells that produce IL-17 (NKT-17) have low expression of ThPOK, which is permissive for their RORγt expression (Engel et al., 2012). This CD8+ RORγt+ phenotype of NKT-17 cells is similar to another population of innate-like T cells: mucosal-associated invariant T cells.

1.4. Mucosal-associated invariant T (MAIT) cells

During an extensive analysis of the TCR repertoire of human CD4−CD8− DN T cells, Porcelli *et al*. (1993) identified two invariant TCR rearrangements prevalent in these

cells. One of these was the invariant TCRα chain of human iNKT cells. The second Vα7.2-Jα33 rearrangement identified in this study was subsequently shown to be characteristic of a novel population restricted by a novel MHC-class Ib molecule, distinct from CD1 (Tilloy et al., 1999). This molecule was identified to be the non-polymorphic and highly evolutionarily conserved, MHC class I-related protein 1 (MR1) (Treiner et al., 2003). The relative abundance of Vα7.2-Jα33 transcripts in human gut biopsies, as well as the enrichment of homologous Vα19-Jα33 transcripts in murine lamina propria lymphocytes, compared to intraepithelial lymphocytes or mesenteric lymph nodes of mice (Treiner et al., 2003), has led to this population being called, 'mucosal-associated' invariant T cells (MAIT) cells.

1.4.1. MR1 and its ligand

MR1 is an antigen-presenting molecule first sequenced in 1995 (Hashimoto et al., 1995), and in contrast to the highly polymorphic MHC class I molecules that have undergone extensive duplication, MR1 is encoded by a single gene outside the MHC locus on chromosome 1 and is highly conserved among mammals (Riegert et al., 1998; Tsukamoto et al., 2013). Thus the α1-α2 domains of human and mouse MR1 are 89-90% identical, compared to that of CD1 which is 60-62% identical (Riegert et al., 1998; Yamaguchi et al., 1998). MR1 expression is essential for the development of MAIT cells, as MAIT cells are absent in $MR1^{-/-}$ mice (Treiner et al., 2003). The MR1 transcript is ubiquitously expressed (Hashimoto et al., 1995; Riegert et al., 1998) in a similar manner to MHC class I expression. However, endogenous surface expression of MR1 is difficult to detect (Huang et al., 2005), except at low levels on certain B cell lines detected by a capture assay (Chua et al., 2011). In transduced cells overexpressing MR1, MR1 is co-localised with lysosomal-associated membrane protein (LAMP) and calreticulin, suggesting that MR1 resides in late endosomes (Huang et al., 2008). Studies showing that MR1 is β-2-microglobulin (β2M)-

associated (Treiner et al., 2003), requires folding for surface expression (Miley et al., 2003), and that mutations at residues critical for MHC class I molecules to bind peptides also abrogated MAIT hybridoma activation (Huang et al., 2005), together suggested that MR1 has an antigen presentation function. However, MR1 surface expression was shown to be independent of the endoplasmic reticulum (ER) peptide-loading complex components, such as the transporter associated with antigen processing (TAP) (Tilloy et al., 1999; Treiner et al., 2003), and was not affected by protease inhibitors (Huang et al., 2008), suggesting that MR1 is loaded either with a peptide outside the ER, or a non-peptide ligand.

Two seminal papers in 2010 showed that MR1-restricted MAIT cells could be activated by various species of bacteria and yeast, and were critical for early protection against bacterial infections (Gold et al., 2010; Le Bourhis et al., 2010). Together with the absence of these cells in germ free mice (Le Bourhis et al., 2010; Treiner et al., 2003), these reports suggested that MR1 presents a conserved microbial ligand. The nature of the ligand presented by MR1 was discovered by Kjer-Nielsen *et al.* (2012) when they found that 6-formyl pterin (6-FP), a natural photodegradation product of folic acid (vitamin B9) in the RPMI culture media, induced refolding of MR1 (Ussher et al., 2014b). Although 6-FP could not activate MAIT cells, mass spectrometry analysis of MR1 refolded in the supernatant of *Salmonella enterica* serovar *Typhimurium* cultures identified a potent ligand, reduced 6-hydoxymethyl-8-D-ribityllumazine (rRL-6-CH_2OH) – a metabolic byproduct of riboflavin (vitamin B2) biosynthesis. Thus MAIT cells can be activated by organisms possessing the riboflavin synthesis pathway, including *Mycobacteria*, *Enterobacter*, *Pseudomonas*, *Salmonella*, and *Candida* species, but not by those lacking this pathway (e.g. *Streptococcus pyrogenes* and *E. faecalis*) (Gold et al., 2010; Le Bourhis et al., 2010). Subsequently, MR1 tetramers loaded with rRL-6-CH_2OH have

allowed the specific detection of human and murine MAIT cells (Reantragoon et al., 2013).

A subsequent study demonstrated that an early intermediate of bacterial riboflavin synthesis, 5-amino-6-d-ribitylaminouracil (5-A-RU), is critical in activating MAIT cells (Corbett et al., 2014). Non-enzymic condensation of 5-A-RU with glyoxal or methylglyoxal byproducts (bacterial or host-derived metabolites) generated unstable intermediates, such as 5-(2-oxopropylideneamino)-6-D-ribitylaminouracil (5-OP-RU), which could activate MAIT cells (Corbett et al., 2014). MR1 refolded with 5-A-RU and methylgyoxal produced a mass spectrometry peak consistent with that initially found when MR1 was refolded in *S. enterica* supernatant by Kjer-Nielson *et al.* (2012), which demonstrated that 5-OP-RU is the true MR1 ligand. Subsequent studies have also identified non-stimulatory ligands such as acetyl-6-formylpterin (Ac-6-FP) that can act to inhibit MAIT cell activity (Eckle et al., 2014; Soudais et al., 2015).

1.4.2. MAIT cell T cell receptor

The majority of MAIT cells express the canonical TCR α chain, Vα7.2-Jα33 in humans and Vα19-Jα33 in mice, which is preferentially paired with Vβ2, Vβ13.2 and Vβ22 in humans, or Vβ6 or Vβ8 in mice (Lepore et al., 2014; Reantragoon et al., 2013; Tilloy et al., 1999). A minor population of human MAIT cells also express Vα7.2-Jα12 and Vα7.2-Jα20 (Lepore et al., 2014; Reantragoon et al., 2013). Vβ usage can also be variable (Kawachi et al., 2006; Reantragoon et al., 2013; Tilloy et al., 1999), with only half of the MR1-tetramer-positive cells expressing Vβ6 or Vβ8 in mice infected with mycobacteria (Sakala et al., 2015).

The MAIT cell TCR is highly evolutionarily conserved within mammals (López-Sagaseta et al., 2013; Tilloy et al., 1999). Mutagenesis studies of the TCR has

demonstrated that the TCR α chain makes the majority of contacts with MR1 (Reantragoon et al., 2012). In particular, the conserved Tyr95α residue within the CDR3α loop is critical for MAIT cell activation, as it is positioned directly over the ligand-binding cavity and forms a hydrogen bond with the vitamin B metabolite bound by MR1 (Patel et al., 2013; Reantragoon et al., 2012; Young et al., 2013).

In contrast to the invariant CDR3α loop, which is highly conserved in length and amino acid sequence, the CDR3β loop, encoded by the Vβ-Dβ-Jβ rearrangement, is highly variable (López-Sagaseta et al., 2013; Reantragoon et al., 2012; Tilloy et al., 1999). CDR3β loop is also important for the MAIT cell activation, as recognition of MR1 is lost when the CDR3β loop is swapped with one from a non-MAIT TCR (Reantragoon et al., 2012). Structural studies have shown that the CDR3β loop provides ancillary contacts that can vary due to loop hypervariability and alternative Vβ gene usage, which may contribute to ligand discrimination (Gold et al., 2014; López-Sagaseta et al., 2013; Patel et al., 2013). In line with this, the MAIT cell TCR engages MR1 through the Vα CDR loops in a conserved manner, regardless of whether the ligand is stimulatory or not, and regardless of the CDR3β loop sequence (López-Sagaseta et al., 2013; Patel et al., 2013), and the inhibitory MR1 ligand Ac-6-FP was shown to act by preventing the CDR3β chain from binding MR1 (Eckle et al., 2014).

1.4.3. MAIT cell development

MAIT cells are absent in nude mice (Tilloy et al., 1999) and are present in the human thymus as well as in murine fetal thymus organ cultures (FTOCs) (Martin et al., 2009), suggesting that MAIT cells are selected in the thymus. Experiments using murine FTOCs showed that MAIT cell progenitors are selected by MR1 expressed by

hematopoietic cells, and not epithelial cells (Martin et al., 2009), specifically the CD4+CD8+ DP thymocytes (Gold et al., 2012; Seach et al., 2013).

The exact signals leading to the development of MAIT cells remain to be determined. During iNKT cell development, sustained TCR signaling leads to the expression of PLZF, which is essential to their intrathymic acquisition of an effector memory phenotype within the thymus (Savage et al., 2008). MAIT cells also require PLZF for their development, as PLZF-deficient wild-type mice lacked MAIT cells (Rahimpour et al., 2015). Unlike iNKT cells however, murine and human MAIT cells exit the thymus as naïve cells (Martin et al., 2009). Second trimester fetal MAIT thymocytes indeed show no PLZF expression, but MAIT cells in fetal peripheral tissues (small intestine, liver and lung) expressed higher levels of PLZF compared to those in the lymphoid tissues (Leeansyah et al., 2014), which was associated with the downregulation of lymph node homing markers, acquisition of CD45RO, as well as increased responsiveness to bacterial stimulation. Therefore, developing MAIT cells increase their expression of PLZF post-thymically, but prior to microbial colonization, which is required for the acquisition of their memory phenotype and innate reactivity to bacteria. Indeed, MAIT cells in invariant Vα19-Jα33 TCR transgenic (Vα19i-transgenic) mice have a naïve phenotype and express no or little PLZF, in contrast to MAIT cells from wild-type mice (Martin et al., 2009; Rahimpour et al., 2015). Thus, although MAIT cells lack intrathymic PLZF expression in contrast to iNKT cells, both of these populations require PLZF expression for their development and acquisition of innate effector functions (Leeansyah et al., 2014; Rahimpour et al., 2015; Savage et al., 2008) (summarised in Figure 1-2).

Other similarities between MAIT cell and iNKT cell development and maintenance includes their dependency on RORγt, as patients with loss-of-function mutations in

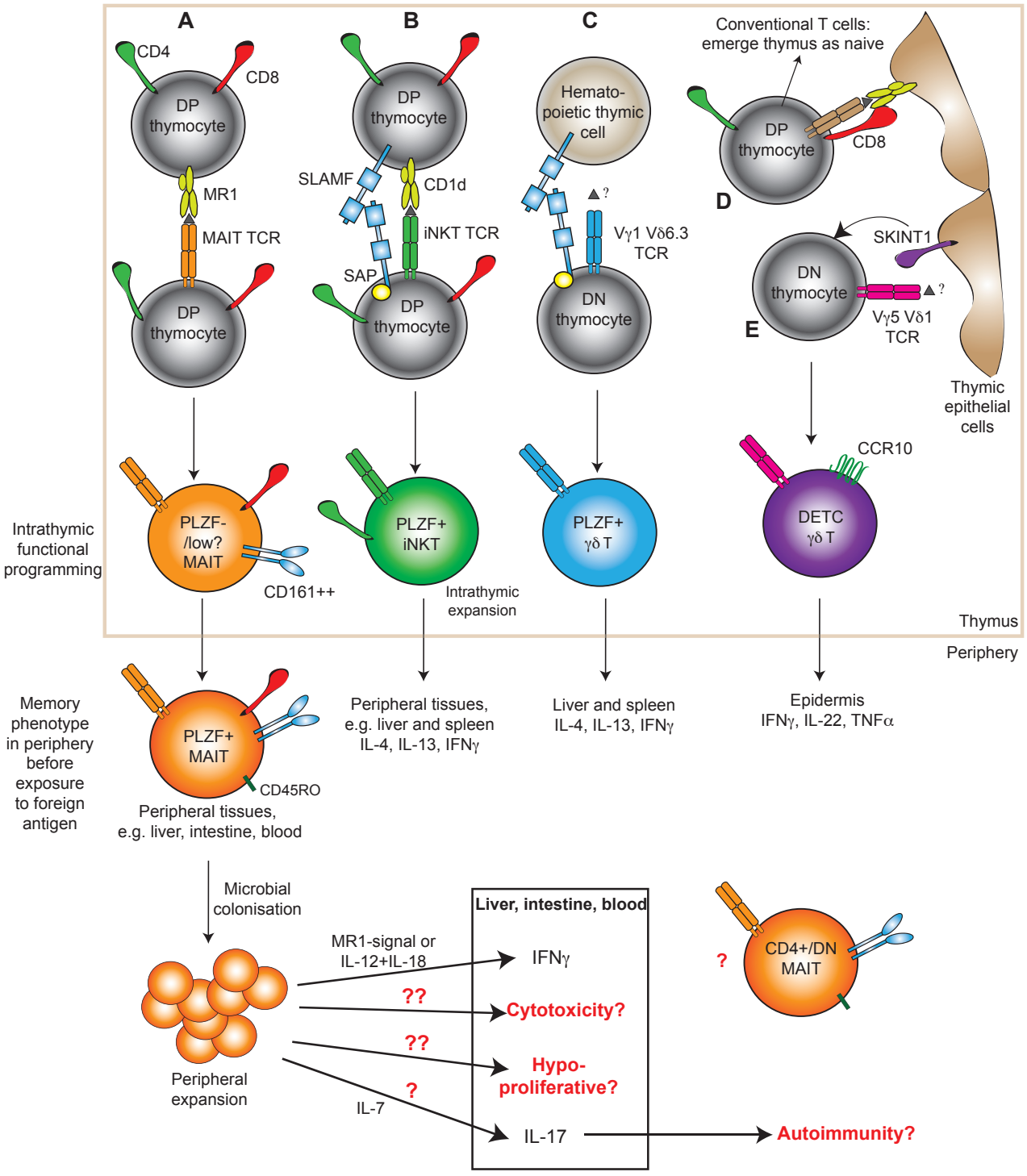


Figure 1-2. Model showing differences in lineage commitment of innate-like T cells, and the questions on MAIT cells addressed in this thesis. Development of A) MAIT, B) iNKT, C) iNKT-like γδ T, D) conventional T cells, E) and dendritic epidermal γδ T cells (DETCs). Precursors of MAIT and iNKT cells are selected by antigen presented by CD8+CD4+ double-positive (DP) thymocytes. iNKT-like γδ T cells are also selected on thymic cells of hematopoietic origin. iNKT-like γδ T and iNKT cells require SLAMF interactions mediated by SAP. Conventional T cells are selected by antigen presented by cortical epithelial cells, while DETCs also interact with epithelial cells expressing SKINT1. Conventional T cells emerge as naive cells from the thymus, while innate-like T cells undergo functional programming which endows them with tissue-homing and memory properties. MAIT cells express increasing levels of PLZF extrathymically, but before exposure to foreign antigen. Remaining questions about MAIT cells highlighted in red concerning the cytotoxicity and proliferative capacity of MAIT cells, the regulation of IL-17 production and whether they may be involved in autoimmune diseases is probed in this thesis. Furthermore, functional differences in MAIT cell subsets are probed. Modified from Bonneville *et. al.*, 2010.

RORC completely lacked both MAIT cells and iNKT cells (Okada et al., 2015). This is due to the regulation of DP thymocyte survival by RORγt (Sun et al., 2000); the short half-life of DP thymocytes in the absence of RORγt limits the accessibility of the most distal 5' segments of the TCR Vα array, including those encoding the Vα chain of MAIT cells (*TRAV1.2* encoding Vα7.2) and iNKT cells (*TRAV10* encoding Vα24) (Guo et al., 2002; Okada et al., 2015). Additionally, *STAT3*-deficient patients show a reduction in iNKT and MAIT cell frequency (Wilson et al., 2015). As STAT3 is activated by cytokines such as IL-21 and IL-23, this study suggests that IL-21 and IL-23 responsiveness is required for the survival/maintenance of iNKT cells and MAIT cells, respectively.

In contrast to the intrathymic expansion of iNKT cells, which occurs unaffected in germ free mice, expansion of MAIT cells is dependent on microbial colonization and occurs in the periphery, as MAIT cells are undetectable in germ free mice (Le Bourhis et al., 2010; Treiner et al., 2003). Reconstitution of germ-free mice with a single strain of bacteria that possesses the riboflavin synthesis pathway leads to the expansion of MAIT cells (Le Bourhis et al., 2010). MAIT cell frequency consequently increases early in life (Dusseaux et al., 2011). Early studies have suggested that B cells are important for this peripheral expansion (Martin et al., 2009; Treiner et al., 2003). Another feature that contrasts to iNKT cells is the independence of MAIT cell development on the expression of SAP, as MAIT cells are present in SAP-deficient patients, who lack iNKT cells (Martin et al., 2009).

1.4.4. MAIT cell tissue distribution

MAIT cells are called "mucosal-associated" because the Vα7.2-Jα33 transcript was enriched in the human gut compared to skin tissues when they were initially characterised (Treiner et al., 2003). MR1-tetramer studies have also confirmed their

enrichment in the gut, although different anatomical locations within the gastrointestinal tract are reported to have different frequencies of MAIT cells. A higher frequency of MAIT cells are present in the jejunum (~60% of CD4− T cells) (Reantragoon et al., 2013), compared to reported frequencies in healthy ileum (1.5% of T cells) (Serriari et al., 2014), colon (10% of T cells) (Cosgrove et al., 2013; Fergusson et al., 2015), and rectum (2% of T cells) (Leeansyah et al., 2013). MAIT cells are further enriched within the liver (20-50% of T cells) compared to the intestine (Dusseaux et al., 2011; Tang et al., 2013). In contrast, MAIT cells are rare in lymphoid tissues (Dusseaux et al., 2011; Leeansyah et al., 2014), suggesting that they preferentially home to peripheral tissues. This is most likely due to their expression of gut-homing integrin α4β7 (Gold et al., 2010; Treiner et al., 2003), as well as chemokine receptors CCR9, CCR6, and CXCR6, which are involved in trafficking to peripheral tissues such as the intestine and the liver (Dusseaux et al., 2011). In contrast, they lack the expression of CCR7 and CD62L, which controls trafficking to the lymph nodes (Billerbeck et al., 2010; Dusseaux et al., 2011). MAIT cells are also abundant in human peripheral blood (1-10% of T cells) (Dusseaux et al., 2011). A recent study has also demonstrated the presence of MAIT cell TCR transcripts in previously unreported tissues, such as kidneys, prostate and ovaries (Lepore et al., 2014).

In contrast to the abundance of MAIT cells in human tissues, MAIT cells are rare in commonly used laboratory strains of mice. Early studies of MAIT cells in wild-type mice showed they comprised ~2% of DN T cells in murine mesenteric lymph nodes and ~10% of DN T cells in gut lamina propria (Kawachi et al., 2006; Tilloy et al., 1999), and thus the majority of murine studies have used Vα19i-transgenic mice (Kawachi et al., 2006). MR1-tetramers have also allowed the characterization of wild-type murine MAIT cells, showing an enrichment of MAIT cells in the lung (mean 3.3%

of T cells in C57BL/6 mice), liver (0.6% of T cells), and lamina propria (0.7% of T cells).

1.4.5. MAIT cell phenotype and effector functions

In addition to the unique chemokine receptor expression of MAIT cells, which endows them with tissue-homing properties, MAIT cells have a unique phenotype that has been characterized in detail. Although cord blood MAIT cells are naïve, they already share a pre-programmed transcriptional signature associated with adult MAIT cells (Walker et al., 2012), in line with the acquisition of their innate reactivity and activated phenotype during development (Leeansyah et al., 2014). In adults, MAIT cells express a uniform effector memory phenotype (Billerbeck et al., 2010; Dusseaux et al., 2011).

One of the key characteristics of human MAIT cells is the high expression of the C-type lectin-like receptor, CD161. This receptor was shown to be expressed at a high surface density by CD8+ T cells when it was cloned as a homologue of the NKRP1 family of glycoproteins expressed on rodent NK cells (please see Section 1.6.6) (Lanier et al., 1994). Subsequent characterization of this population (Billerbeck et al., 2010; Takahashi et al., 2005; Turtle et al., 2009) and the identification that the majority of CD161++ T cells are MAIT cells (Dusseaux et al., 2011; Martin et al., 2009), has led to the high expression of CD161, along with the expression of a Vα7.2+ TCR, to become the primary flow cytometric method of identifying human MAIT cells in the absence of the MR1-tetramer. Indeed, CD161++Vα7.2+ T cells have been shown to overlap with the cells stained by the MR1-tetramer (Reantragoon et al., 2013). CD161 expression on MAIT cells is high in the thymus, fetal organs (Leeansyah et al., 2014), as well as cord blood (Dusseaux et al., 2011; Martin et al., 2009; Walker et al., 2012). However, the significance of the high

expression of CD161 on MAIT cells, and the factors that may regulate its expression, is still unclear. Ligation of CD161 has been shown to have a costimulatory effect on other T cells, increasing cytokine production, proliferation, and transendothelial migration (Aldemir et al., 2005; Exley et al., 1998; Poggi et al., 1997). Of note, some murine T cells, including iNKT cells, express the related NKRP1 molecule, NK1.1 (encoded by NKRP1B/C). However, NK1.1 cannot be used as a surrogate marker for murine MAIT cells as only a minority of MAIT cells from Vα19i-transgenic and wild-type mice express NK1.1 (Kawachi et al., 2006; Martin et al., 2009).

MAIT cells also express high levels of IL-18R, which enables this population to rapidly release IFNγ in response to innate cytokines such as IL-12 and IL-18 (Ussher et al., 2014a). This was further confirmed by the activation of MAIT cells by *E. faecalis*, which lacks the riboflavin synthesis pathway, or toll-like receptor (TLR) agonists, in an IL-12- and IL-18-dependent manner (Jo et al., 2014; Ussher et al., 2014a). As conventional T cells require TCR signaling before the expression of cytokine receptors such as IL-18R (Tomura et al., 1998), this feature of MAIT cells is reminiscent of other innate T cells, which can be rapidly activated by cytokines alone. For instance, iNKT cells constitutively express IL-12R and their response to bacteria such as *S. pneumoniae*, predominantly depends on IL-12 rather than their TCR (Brigl et al., 2011). Similarly, in a murine model of bacterial lung infection, the control of intracellular *M. bovis* bacillus Calmette-Guérin (BCG) and *F. tularensis* live vaccine strain (LVS) growth by murine MAIT cells required IL-12 (Chua et al., 2012; Meierovics et al., 2013), but not MR1 signaling (Chua et al., 2012). MAIT cells may therefore be important in displaying immediate function upon infection, even with bacteria which may impede MR1 loading, such as *Salmonella* (Buchmeier & Heffron, 1991; Martin et al., 2013) or in viral infections.

In addition to IFNγ, which can be induced both in a TCR-dependent and TCR-independent manner (Ussher et al., 2013), MAIT cells can express a broad range of cytokines. Other Th1 cytokines such as TNFα have also been consistently reported to be secreted by MAIT cells (Dusseaux et al., 2011; Gold et al., 2010). Rapid IL-4, IL-5 and IL-10 expression has been described in MAIT cells from Vα19i-transgenic mice (Kawachi et al., 2006), although the expression of these cytokines from human MAIT cells ranges from none (Dusseaux et al., 2011; Miyazaki et al., 2011; Tang et al., 2013) to low (Cho et al., 2014; Lepore et al., 2014). Interestingly, MAIT cells have a constitutively high expression of RORγt and the associated ability to express IL-17A (Billerbeck et al., 2010; Dusseaux et al., 2011; Walker et al., 2012). Furthermore, MAIT cells are the dominant IL-17-producing T cell population within the liver (Tang et al., 2013). IL-23 has also been reported to induce TCR-independent production of IL-17 in mice (Chiba et al., 2012).

Other innate T cells such as iNKT cells and γδ T cells have been shown to have high cytotoxic function (Bukowski et al., 1994; Crowe et al., 2005). However, the cytotoxic capacity of MAIT cells and whether they may play a role in infection has been less extensively investigated until recently. Memory CD8+ T cells, or cytotoxic T lymphocytes (CTLs), classically mediate the killing of target cells through the secretion of cytotoxic granule effector molecules such as granzymes and perforin. In humans, there are five isoforms of granzymes that differ in substrate specificities: Granzyme A (GrA), GrB, GrK, GrH, and GrM (Chowdhury et al., 2008). Due to the toxicity of these effector molecules, killing is a highly regulated function and requires the recognition of the target cell by the TCR (Jenkins et al., 2009; Stinchcombe et al., 2006). The delivery of granzymes to the target cell also requires the polymerization of perforin (Baran et al., 2009). GrB and GrA have been shown to be secreted by MAIT cells stimulated with bacterially-pulsed APCs (Dusseaux et al., 2011), but in a previous analysis of the phenotype of CD161++CD8+ T cells, these cells lacked the

expression of GrB and perforin (Billerbeck et al., 2010), and the signals regulating the expression of these cytotoxic effector molecules by MAIT cells are unknown (Figure 1-2).

Finally, despite evidence of peripheral expansion of MAIT cells after birth (Dusseaux et al., 2011; Martin et al., 2009), adult MAIT cells uniquely lack the expression of Ki67 in the periphery (Dusseaux et al., 2011) and have been shown to proliferate poorly in mice (Kawachi et al., 2006). MAIT cells were also non-proliferative when stimulated by a combination of PHA, IL-2, IL-7 and IL-15 for 10 days (Dusseaux et al., 2011), or exposed to bacterially-infected APCs (Le Bourhis et al., 2010). In contrast to adult MAIT cells, cord blood MAIT cells are highly responsive and proliferative to TCR stimulation (Turtle et al., 2011). However, proliferative responses of MAIT cells to cytokines have not been probed in detail, and the ability of MAIT cells to respond to homeostatic cytokines such as IL-15 will be important to investigate, as conventional CD8+ T cells and iNKT cells require IL-15 for homeostasis (Kennedy et al., 2000; Ranson et al., 2003). Furthermore, although MAIT cells are rare in wild-type mice, the frequency of MAIT cells increased to ~25% of αβ T cells in the lung following *F. tularensis* LVS infection (Meierovics et al., 2013), suggesting that MAIT cells are able to expand in response to bacterial infections.

1.4.6. MAIT cell coreceptor usage

Although MAIT cells were initially identified within the DN population (Porcelli et al., 1993), in humans the majority of MAIT cells are CD8+, with a small fraction of DN cells, as well as a very minor population that express the CD4 coreceptor (Reantragoon et al., 2013). Interestingly, more than half of CD8+ MAIT cells express the homodimer CD8αα, with a smaller frequency of cells expressing the CD8αβ heterodimer. This is unique to MAIT cells, as conventional CD8+ T cells express the

CD8αβ coreceptor (Reantragoon et al., 2013; Walker et al., 2012). The significance of CD8αα expression on MAIT cells is unknown; transcriptional profiling of CD8αα and CD8αβ MAIT cells showed no differences at the mRNA level (Walker et al., 2012). CD8αα expression is acquired early in MAIT cell development, as MAIT cells which were predominantly CD8αβ in the thymus and fetal lymphoid tissues transitioned to a CD8αα phenotype in peripheral tissues in second trimester fetuses (Leeansyah et al., 2014). In Vα19i-transgenic mice, the majority of MAIT cells are DN rather than CD8+, and the remaining ~40% of MAIT cells express CD4 (Reantragoon et al., 2013).

As the majority of previous functional and phenotypic studies on MAIT cells have been performed on CD8+ MAIT cells in humans and DN MAIT cells in mice, functional descriptions of CD4+ MAIT cells are lacking. A recent study using MR1-tetramers demonstrated that murine CD4+ MAIT cells are particularly enriched within lymphoid tissues (Rahimpour et al., 2015). Whether this is true in humans has not been demonstrated. Furthermore, the transcription factors that may be responsible for determining coreceptor usage, and functional differences between subsets of MAIT cells, if any, remain unknown.

1.4.7. MAIT cells in bacterial infections

The high degree of evolutionary conservation of MR1 and its recognition of intermediates of the riboflavin pathway, conserved in various species of bacteria and yeast, suggests that MAIT cells play a critical and non-redundant role in microbial protection. Indeed, a number of papers have suggested that MAIT cells play a protective role in bacterial infections. For instance, $MR1^{-/-}$ mice lacking MAIT cells have a higher bacterial burden in the first few days following intraperitoneal injection of *E. coli* or intravenous injection of *M. abscessus* (Le Bourhis et al., 2010), and were

overwhelmed by a fatal burden of intraperitonially injected *Klebsiella pneumonia* (Georgel et al., 2011). Additionally, aerosol infection models have demonstrated that MAIT cells are essential for the early control of bacterial burden in the lung (Chua et al., 2012; Meierovics et al., 2013). Interestingly, mice were protected from *F. tularensis* LVS even in the absence of conventional αβ T cells, but were overcome in $MR1^{-/-}$ mice (Meierovics et al., 2013), suggesting that MAIT cells may be important for microbial control in immunocompromised patients.

Various studies of MAIT cell frequencies in patients also point towards their involvement in bacterial infections. For example, there is a higher frequency of MAIT cells in the lung of patients with *M. tuberculosis* infection, with lower frequencies of MAIT cells in the blood (Gold et al., 2010; Le Bourhis et al., 2010). Reduced MAIT cell frequencies were only observed in patients with active *M. tuberculosis* infection but not in latent infection (Gold et al., 2010), suggesting that MAIT cells are recruited to the lung in active disease. Peripheral MAIT cells in these patients also have increased expression of the exhaustion marker, programmed cell death protein 1 (PD-1) (Jiang et al., 2014; Saeidi et al., 2015), and their responsiveness to *M. bovis* BCG is increased upon PD-1 blockade (Jiang et al., 2014).

In addition to pulmonary infections, MAIT cells have been suggested to be involved in enteric infections as well, as MAIT cells are reduced early in the blood of patients that received an attenuated strain of *Shigella dysenteriae 1* (SD1) (Martin et al., 2013), as well as in *Vibrio cholera* O1 (VbO1)-infected children (Leung et al., 2014a). Interestingly, activation of MAIT cells was specific to vaccine responders that developed a SD1-lipopolysaccharide (LPS)-specific immunoglobulin (Ig) A response (Martin et al., 2013) and correlated with protective VbO1-LPS-specific IgA and IgG antibody responses (Leung et al., 2014a). These two studies suggest that MAIT cells

may potentially play a role in the development of protective antibody responses against polysaccharide antigens.

Lastly, low frequencies of MAIT cells have been associated with increased susceptibility to other microbial infections. For example, reduced MAIT cell frequencies have been associated with increased severity of cystic fibrosis and increased susceptibility to *P. aeruginosa* infection (Smith et al., 2014). Furthermore, a significant depletion of MAIT cells in critically ill patients with sepsis was a risk factor for subsequent nosocomial infections (Grimaldi et al., 2014).

1.4.8. MAIT cells in viral infections

Interestingly, although MR1$^{-/-}$ mice were not susceptible to influenza compared to control mice (Le Bourhis et al., 2010), MAIT cell frequencies are affected during human viral infections. Thus, in a cohort of critically ill patients, patients with severe viral infections also had a reduced frequency of MAIT cells (Grimaldi et al., 2014), in addition to bacterially-infected patients. Furthermore, peripheral blood CD161++CD8+ T cells, the majority of which are MAIT cells, are depleted in chronic hepatitis C virus (HCV)-infected patients (Billerbeck et al., 2010).

MAIT cells have also been found to be severely depleted from the periphery of patients infected with human immunodeficiency virus (HIV) (Cosgrove et al., 2013; Fernandez et al., 2015; Leeansyah et al., 2013; Saeidi et al., 2015), as well as HIV/*M. tuberculosis*-co-infected patients (Wong et al., 2013). The loss of MAIT cells occurs as early as 2-3 weeks after HIV infection (Wong et al., 2013), and does not recover with successful highly active antiretroviral therapy (HAART) (Cosgrove et al., 2013; Leeansyah et al., 2013). CD8+ MAIT cells in the rectal mucosa (Leeansyah et al., 2013) and colon (Cosgrove et al., 2013) were better preserved, although CD4+ MAIT

cells were specifically lost from the rectal mucosa, in line with the significant loss of all CD4+ T cells in the rectal mucosa in HIV-infected patients (Leeansyah et al., 2013). As peripheral CD8+ MAIT cells were not specifically infected by HIV (Cosgrove et al., 2013), the depletion of MAIT cells from the blood of HIV-infected patients has been suggested to be due to either the activation-induced cell death (AICD) of MAIT cells from HIV-induced microbial translocation into the periphery (Cosgrove et al., 2013), or exhaustion and downregulation of the MAIT cell marker CD161 (Leeansyah et al., 2013). Although a recent tetramer study confirmed the loss of MAIT cells from the peripheral blood of HIV-infected patients, with no detectable loss of CD161 expression on MAIT cells (Fernandez et al., 2015), the increased expression of PLZF in CD161−Vα7.2+ T cells in infected patients and the loss of the Vβ2/Vβ13 expression bias in the residual CD161+Vα7.2+ T cells observed in previous reports remains to be explained (Leeansyah et al., 2013). Nevertheless, the loss of MAIT cells may potentially have a profound effect on microbial protection in HIV-infected patients, as exemplified by the loss of mucosal Th17 cells SIV-infected rhesus macaques (Raffatellu et al., 2008).

The ability of MAIT cells to be activated by viruses through TLR stimulation and inflammatory cytokines also suggests that they may play a larger role in the immune system that is not limited to protection against bacterial infection.

1.4.9. MAIT cells and autoimmunity

There is an increasing interest in the possible involvement of MAIT cells in autoimmune diseases. Various reports have associated MAIT cells with multiple sclerosis (MS), although both regulatory and pathogenic roles have been implicated. In a murine model of experimental autoimmune encephalomyelitis (EAE), MAIT cells suppressed autoimmune inflammation in Vα19i-transgenic mice (Croxford et al.,

2006), as the adoptive transfer of Vα19-Jα33 TCR+ cells into wild-type mice with EAE protected the mice from pathology. The suppressive action of MAIT cells was associated with a reduction in pathological Th1 cytokines, and an increase in IL-10 in peripheral lymphoid tissue, which was further supported by a study showing that human MAIT cells suppressed IFNγ production from conventional T cells in a contact-dependent manner (Miyazaki et al., 2011). The canonical Vα7.2-Jα33 sequence was also found to be enriched in the central nervous system (CNS) lesions from MS autopsy samples (Illés et al., 2004). The presence of MAIT cells in the CNS of MS patients has also been confirmed by immunohistochemistry (Annibali et al., 2011; Willing et al., 2014). In contrast, the reports concerning the frequency of MAIT cells in the blood of MS patients are variable, either showing no difference (Illés et al., 2004), a reduction (Miyazaki et al., 2011; Willing et al., 2014), or increase (Annibali et al., 2011), compared to healthy controls. As peripheral blood MAIT cell frequency decreases with age (Novak et al., 2014), it has been suggested that the increased frequency of MAIT cells in MS patients observed in an early report (Annibali et al., 2011) may be due to the higher average age of the healthy control group, compared to the MS cohort in this study (Willing et al., 2014).

A number of studies have also linked MAIT cells with intestinal inflammatory disorders. For example, reduced frequencies of MAIT cells have been demonstrated in the blood of patients with inflammatory bowel disease (IBD) (Serriari et al., 2014) (both Crohn's Disease (CD) and ulcerative colitis (UC)). Together with an increase in the frequency of MAIT cells in the inflamed ileum of patients with CD, this study suggests that MAIT cells are recruited to the inflamed tissues in IBD patients. MAIT cells are also depleted from the blood and gut in patients with coeliac disease (Dunne et al., 2013). Recent studies have also highlighted an interesting role that MAIT cells may play in the pathology of type 2 diabetes and obesity, as MAIT cells are lost from the blood in these patients (Magalhaes et al., 2015). MAIT cells were

enriched within the adipose tissue of these obese patients, and the frequency of blood MAIT cells recovered 3 months after bariatric surgery. Strikingly, almost all of the MAIT cells in the adipose tissue of obese patients expressed IL-17 after stimulation, in contrast to the low frequency of blood MAIT cells that express IL-17 (~10%) (Magalhaes et al., 2015). Increased IL-17 from peripheral blood MAIT cells has also been observed in obese children (Carolan et al., 2015). Interestingly, overexpression of MAIT cells delayed the onset of diabetes in non-obese diabetic mice, suggesting that they may also have a suppressive role that is altered in disease (Shimamura et al., 2011). Altered MAIT cell frequencies have been observed in juvenile type 1 diabetes (Harms et al., 2015), as well as inflammation of the gallbladder (cholecystitis) (Kim et al., 2015).

Finally, MAIT cells may also play role in arthritic diseases. MAIT cells exacerbate collagen-induced arthritis (CIA), as $MR1^{-/-}$ wild-type mice had milder joint inflammation and bone destruction compared to $MR1^{+/+}$ mice (Chiba et al., 2012). Furthermore, $MR1^{-/-}$ mice were protected from severe collagen antibody-induced arthritis (CAIA), and while adoptive transfer of MAIT cells into $MR1^{-/-}$ mice enhanced pathology (Chiba et al., 2012), suggesting that MAIT cells may be active drivers of inflammatory arthritis. Indeed, depletion of blood MAIT cells has also been reported in patients with systemic lupus erythromatosis (SLE) and rheumatoid arthritis (RA) (Cho et al., 2014), with a corresponding increase in the frequency of MAIT cells in the joints of patients with arthritic disease (Billerbeck et al., 2010; Cho et al., 2014).

1.5. Innate-ness and CD161 expression

Recently, the expression of CD161 on T cells was shown to identify T cells that share a common transcriptional phenotype, regardless of TCR usage (Fergusson et al., 2014). These cells had a MAIT-cell like phenotype, including the increased

expression of RORγt, IL-18R and PLZF compared to their CD161– counterparts. CD161-expressing T cells thus displayed an innate-like phenotype previously only associated with unconventional T cells, and showed the ability to respond to IL-12 and IL-18 by secreting IFNγ, which was restricted to cells with high CD161 expression. CD161 is also expressed by a large fraction of NK cells, and the ability of cells to respond to IL-12 and IL-18 is a function originally described in NK cells (Fehniger et al., 1999). Whether this transcriptional phenotype and functional correlation with CD161 holds true in NK cells, however, has not been investigated.

1.6. Natural Killer cells and the Innate lymphoid cell family

Natural killer (NK) cells are the original members of a population of cells that have been recently collectively referred to as innate lymphoid cells (ILCs). The proposed definition of ILCs are cells that 1) lack RAG-dependent rearranged antigen receptors, 2) lack myeloid cell and DC markers, and 3) have a lymphoid morphology (Spits et al., 2013; Spits & Cupedo, 2012).

1.6.1. The ILC family

NK cells were first discovered in 1975 as cells able to lyse tumour cells without prior sensitization, mediating cytotoxicity in a non-specific fashion (Herberman et al., 1975; Kiessling et al., 1975). Together with the lymphoid tissue-inducer (LTi) cells (Mebius et al., 1997), NK cells have been extensively characterized in health and disease. However, an array of recent papers describing unusual NK-cell like populations such as IL-22-producing NK-22 (Cella et al., 2009), Th2-cytokine producing natural helper cells (Moro et al., 2010) or nuocytes (Neill et al., 2010) led to the rediscovery of the ILC family as a population of developmentally related cells that depend on the

common cytokine receptor γ chain (γc) and the transcriptional repressor, inhibitor of DNA binding 2 (Id2) for their development (Hoyler et al., 2012; Yokota et al., 1999).

Importantly, three groups of ILCs have been defined with distinct patterns of cytokine production that mirrors that of T helper cell subsets. These are called group 1 ILCs (ILC1), group 2 ILC (ILC2), and group 3 ILC (ILC3) (Spits et al., 2013). ILC2s produce IL-5 and IL-13 in response to epithelial cell-derived IL33 and/or IL-25 (Moro et al., 2010; Neill et al., 2010; Price et al., 2010). Their production of IL-13 is critical for helminth expulsion (Fallon et al., 2006; Neill et al., 2010; Price et al., 2010), while they can also drive atopic dermatitis and allergic inflammations (Halim et al., 2012; Kim et al., 2013). ILC3s in turn are characterized by their innate ability to secrete IL-17A, IL-17F, IL-22, and GM-CSF (Artis & Spits, 2015; Takatori et al., 2009). IL-22 production by ILC3s is critical in containing commensal bacteria (Sonnenberg et al., 2012), and IL-23-responsive ILC3s also mediate colitis (Buonocore et al., 2010) and accumulate in the inflamed intestine of CD patients (Geremia et al., 2011). ILC3s also include the LTi cells involved in organizing tertiary lymphoid structures and tissue repair (Boos et al., 2007; Scandella et al., 2008).

Lastly, group 1 ILCs were initially proposed to include NK cells and non-NK cells, which secrete IFNγ, and express T-bet (Bernink et al., 2013; Fuchs et al., 2013). ILC1 cells are important anti-bacterial cells, involved in the protection against *S. enteria* (Klose et al., 2013). Furthermore, ILC1s accumulate in the inflamed intestine of CD patients (Bernink et al., 2013). There also seems to be some plasticity between ILC1 and ILC3 cells (Bernink et al., 2015; Klose et al., 2013). Thus, ILCs secreting both IFNγ and IL-17 in response to IL-23, or IFNγ and IL-22 in response to IL-12+IL-18 have been reported (Buonocore et al., 2010; Satoh-Takayama et al., 2009). It is thought that both NK cells and ILC1s depend on IL-15 for their development (Cooper et al., 2002; Kennedy et al., 2000; Klose et al., 2014; Mrózek

et al., 1996), although a population of ILC1s expressing CD56 and CD94, called intraepithelial ILC1s, develop independently of IL-15 (Fuchs et al., 2013). The dependency of ILC1s and NK cells on IL-15 is in contrast to ILC2s and ILC3s, which rely on IL-7 and are depleted in IL-7Rα$^{-/-}$ mice (Moro et al., 2010; Vonarbourg et al., 2010).

More recently, NK cells have been shown to be a distinct lineage from the helper ILC subsets, as an Id2+ common progenitor was identified that gave rise to all helper-like ILC subsets, including ILC1 cells, but not conventional NK cells (Klose et al., 2014). Thus, NK cells constitute the cytotoxic arm of ILCs, equivalent to CTLs within T cells (Artis et al., 2015). Of note, liver ILC1s express GrA and GrC at a higher level than liver NK cells (Robinette et al., 2015) and show cytotoxic capacity (Sojka et al., 2014), but transcriptional profiling of the murine ILC family has demonstrated that ILC1s and NK cells are distinguished by Eomes expression (Klose et al., 2014; Robinette et al., 2015). This is consistent with the dependence of NK cell maturation on Eomes (Gordon et al., 2012). Further separating ILCs from conventional NK cells is the fact that helper ILC1 cells require T-bet for their development, and ILC3s require T-bet to differentiate into NKp46+ ILC3s, (Klose et al., 2014) whereas NK cells can develop in the absence of T-bet, due to the redundancy between T-bet and Eomes (Gordon et al., 2012; Klose et al., 2014; Townsend et al., 2004).

1.6.2. NK cell development

All lymphocytes arise from a common lymphoid progenitor (CLP), which is a precursor for B cells, T cells, ILCs, and DCs. ILC precursors are thought to be a subset of these cells that express the integrin α4β7 (α-lymphoid precursor) with heterogenous CXCR6 expression, which are unable to develop into T and B cells (Cherrier et al., 2012; Klose et al., 2014; Possot et al., 2011). These cells are also

similar to previously described stage I NK cell precursors in human secondary lymphoid organs (Figure 1-3). As described above, lineage tracing has shown that helper ILCs, including LTi cells, originate from a Id2+ common progenitor that is distinct from that of NK cells (Klose et al., 2014). The next step seems to be the transient high expression of PLZF in precursors that gives rise to helper ILCs but not LTi or NK cells, as NK cells developed independently of PLZF (Constantinides et al., 2014).

Committed NK cell precursors that have diverged from other ILC precursors are thought to develop into Stage II NK cells (CD34+α4β7+CD45RA+c-kit+CD94−), where they start to acquire CD161, followed by CD56 (Bennett et al., 1996), as well as IL-15Rα expression, and differentiate into stage III NK cells (CD34−α4β7−CD45RA+c-kit+CD94−) (Freud et al., 2006). Finally, with the acquisition of high CD94, CD56, and NKp46 expression, stage IV NK cells (CD34−α4β7−CD45RA+c-kit+/−CD94+) acquire the $CD56^{bright}$ NK cell phenotype (Freud et al., 2006).

1.6.3. $CD56^{bright}$ and $CD56^{dim}$ NK cells

NK cells have been well characterized in human peripheral blood, where two NK cell subsets can be described, based on the expression level of CD56: $CD56^{bright}$ and $CD56^{dim}$ NK cells. The majority of peripheral blood NK cells are $CD56^{dim}$ NK cells, while the ratio is inversed in secondary lymphoid organs, where the $CD56^{bright}$ NK cells dominate (Lanier et al., 1986). $CD56^{bright}$ NK cells are described as the immunoregulatory population, based on their ability to secrete cytokines including IFNγ and IL-10, while they express low amounts of granzymes and perforin, and are poorly cytotoxic *ex vivo* (Cooper et al., 2001; Fehniger et al., 1999). $CD56^{dim}$ NK cells, on the other hand, have a highly cytotoxic phenotype, expressing high levels of GrB,

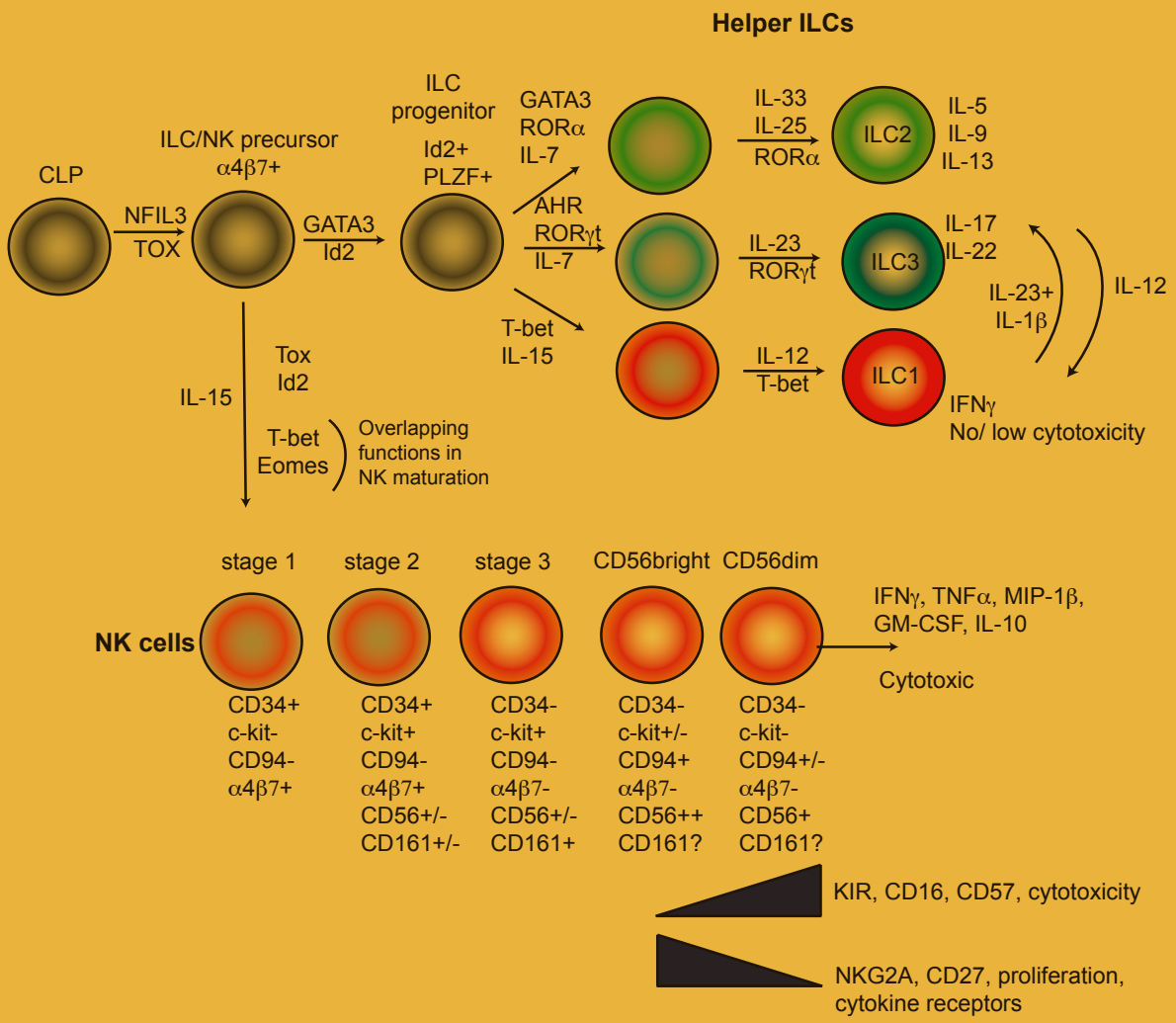


Figure 1-3. Development of ILCs and NK cells. ILCs and NK cells develop from haematopoetic stem cells via a common lymphoid progenitor (CLP) that expresses α4β7 integrin. Helper type ILCs share a common progenitor that expresses Id2 and PLZF at a high level, and indicated transcription factors can influence the differentiation of ILC1, ILC2, and ILC3s. There is some plasticity between mature ILC1 and ILC3s depending on the cytokine milieu. Immature NK cells do not express PLZF at this early stage and instead depend on transcription factors such as thymocyte selection-associated high mobility group box protein (TOX), eomesodermin (Eomes), and T-bet to fully mature. The different stages of NK cell development can be identified by their expression of CD34, c-kit, and CD94. Maturation continues in the periphery and is associated with increased cytotoxicity and loss of proliferative capacity. CD161 is expressed early during the differentiation of NK cells, before CD56. However how the expression changes during peripheral maturation has not been characterised in detail. Model modified from Rankin *et. a*l, 2013 and Yu *et. al.*, 2013.

GrA, and perforin at the resting condition (Jacobs et al., 2001; Wendt et al., 2006). This enables this population to efficiently lyse virus-infected and tumour cell lines without prior activation (Jacobs et al., 1992; Nagler et al., 1989).

However, this dichotomy based on cytokine production and cytotoxicity may be too simplistic, as $CD56^{bright}$ NK cells can also be cytotoxic. For example, $CD56^{bright}$ NK cell population can kill activated autologous CD4+ T cells in MS (Bielekova et al., 2006; Jiang et al., 2011). Furthermore, immature DCs are killed by $CD56^{bright}$ NK cells in lymph nodes in a TRAIL-dependent manner (Hayakawa et al., 2003; Piccioli, 2002), and IL-2-activated peripheral blood $CD56^{bright}$ NK cells can become efficient killers (Ferlazzo et al., 2004b; Jacobs et al., 1992; Nagler et al., 1989).

Instead, the signals that $CD56^{bright}$ and $CD56^{dim}$ NK cells are highly responsive to, and their kinetics, seem to differ between the two subsets. $CD56^{bright}$ NK cells express high levels of cytokine receptors which enables these cells to produce abundant IFNγ and proliferate in response to cytokines such as IL-2, IL-15, IL-12, IL-18, and IFNα (Baume et al., 1992; Cooper et al., 2001). As $CD56^{bright}$ NK cells are the dominant NK cell population in lymph nodes and inflammatory sites, this allows them to interact with DCs and T cells at these sites (Dalbeth et al., 2004; Fehniger et al., 2003; Ferlazzo et al., 2004a). However, in addition to cytokines, NK cell activity is regulated by an array of activating and inhibitory receptors (Figure 1-4). Interestingly, $CD56^{bright}$ NK cells secrete little IFNγ in response to target cell recognition mediated by receptors such as NKG2D, even though the receptor is equally expressed by $CD56^{bright}$ and $CD56^{dim}$ cells (Fauriat et al., 2010b). In turn, $CD56^{dim}$ NK cells are the earliest and dominant IFNγ-secreting population in response to activating receptor ligation (De Maria et al., 2011; Fauriat et al., 2010b). Furthermore, $CD56^{dim}$ NK cells are able to form more conjugates with infected or transformed cells (Jacobs et al., 2001; Wendt et al., 2006), and the expression of low-affinity FcγRIII (CD16) is largely

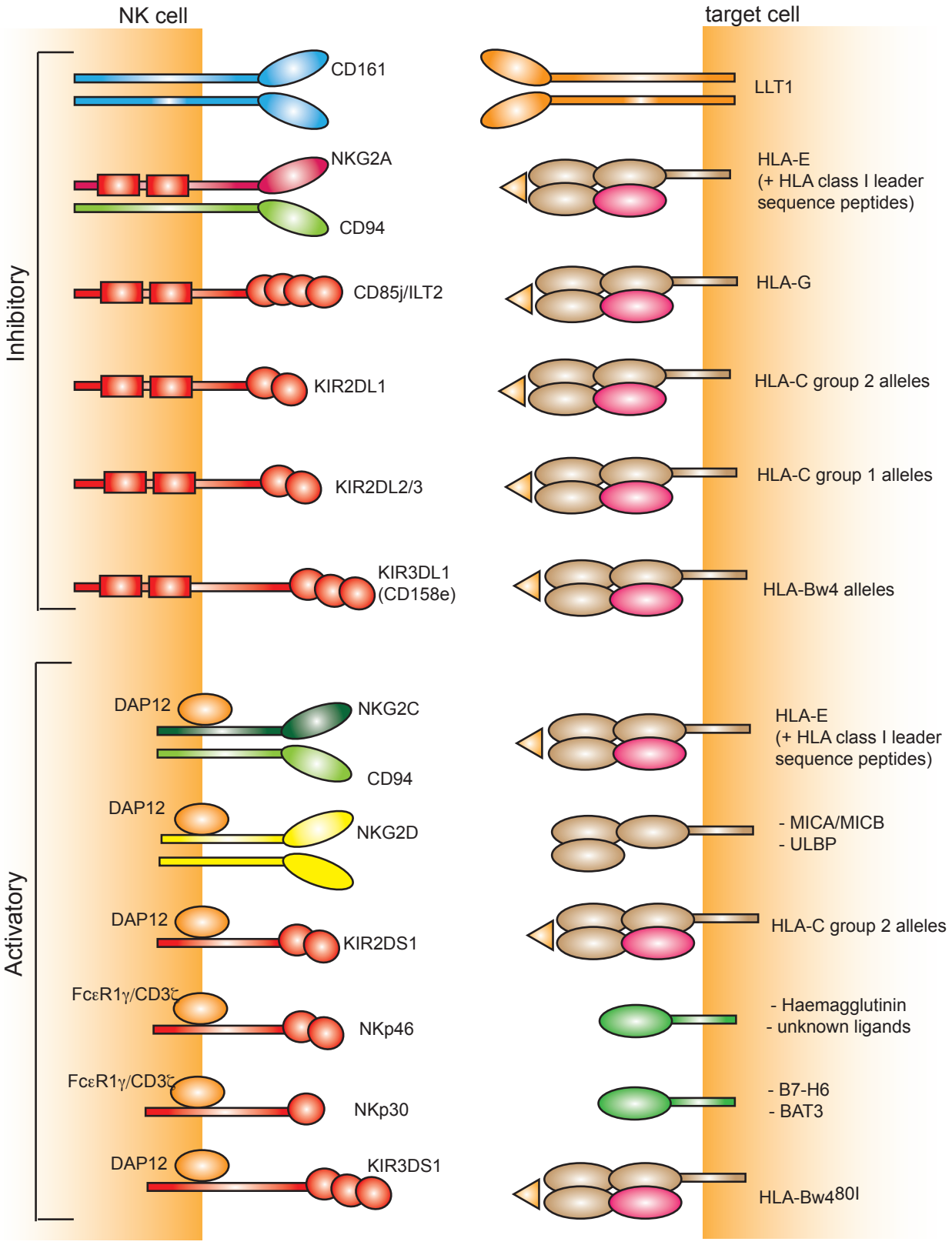


Figure 1-4. NK cell receptors and their ligands. NK cells express an array of inhibitory and activatory receptors that consist of C-type lectin-like receptors (NKG receptors, CD161) and receptors encoded by the leukocyte receptor complex (LRC) of immunoglobulin-related genes on chromosome 19 (killer-cell immunoglobulin-like receptor KIRs, and immunoglobulin-like transcript ILTs, and NKp46). NKp30 is encoded in the class III region of the MHC locus. Inhibitory receptors have immunoreceptor tyrosine-based inhibitory motifs (ITIM; red boxes), while activating receptors bind adaptor proteins that contain immunoreceptor tyrosine-based activating motif (ITAM; orange circles) (DAP12, FcεR1γ/CD3ζ). CD161 has been shown to be inhibitory for NK cell cytotoxicity and cytokine secretion. Model modified from Moffet-King *et. al*., 2002

restricted to $CD56^{dim}$ NK cells. These features, together with high expression of cytolytic molecules, allow $CD56^{dim}$ NK cells to efficiently lyse target cells either directly or indirectly through CD16-mediated antibody-dependent cellular cytotoxicity (ADCC). The expression of a family of receptors called killer immunoglobulin-like receptors (KIRs), which modulates the responsiveness of NK cells to activating receptor ligation, is also restricted to $CD56^{dim}$ NK cells (discussed below).

1.6.4. NK cell differentiation

During the differentiation of human NK cells, $CD56^{bright}$ NK cells are thought to give rise to $CD56^{dim}$ NK cells. This is supported by studies showing that $CD56^{bright}$ NK cells have longer telomeres (Romagnani et al., 2007), and in $RAG2^{-/-}$ $\gamma c^{-/-}$ mice transplanted with human hematopoietic stem cells, $CD56^{bright}$ NK cells differentiated linearly into $CD56^{dim}$ NK cells, acquiring CD16 and KIR expression, which was dependent on IL-15 (Huntington et al., 2009; Juelke et al., 2010). This has also been shown *in vitro* by culturing $CD56^{bright}$ NK cells in the presence of synovial or skin fibroblasts, or cytokines (Chan et al., 2007; Ferlazzo et al., 2004b).

The differentiation of $CD56^{bright}$ NK cells into $CD56^{dim}$ NK cells is accompanied by a loss of the expression of markers such as CD94 (Yu et al., 2010), NKG2A (Béziat et al., 2010), and CD27 (Vossen et al., 2008), which are highly expressed in $CD56^{bright}$ NK cells. In turn, the expression of CD16 and the terminal differentiation marker CD57 (Lopez-Vergès et al., 2010) correlates with increased granzyme and perforin expression (Björkström et al., 2010; Lopez-Vergès et al., 2010).

The maturation of NK cells is also accompanied with the increased expression of a family of receptors called KIRs. KIRs are a diverse and polymorphic family of receptors, encoded by the leukocyte receptor complex (LRC) (Wende et al., 1999).

These receptors either have two or three Ig-like extracellular domains (2D or 3D), and the length of their cytoplasmic tail (L for long, S for short) determines the name of the protein (e.g. KIR2DL3). The long cytoplasmic tail of KIR molecules contains immunoreceptor tyrosine-based inhibitory motifs (ITIMs), and confers an inhibitory signal upon engagement, while short-tailed receptors associate with adaptor proteins that contain immunoreceptor tyrosine-based activating motifs (ITAM), and thus are activating (Jamil & Khakoo, 2011) (Figure 1-4). Both inhibitory and activatory KIRs bind polymorphic Human Leukocyte Antigen (HLA) class I ligands, and the extent of NK cell inhibition/activation varies depending on the allelic forms expressed (Jamil et al., 2011). For example, the inhibitory receptors KIR2DL2 and KIR2DL3 are specific for HLA-C alleles with asparagine at position 80 (HLA-C1 alleles) (Colonna et al., 1993). In contrast, KIR2DL1 binds HLA-C alleles with lysine at position 80 (HLA-C2 alleles) (Figure 1-4) (Mandelboim et al., 1996).

The ligation of KIRs by their self-MHC class I ligands is required for conferring intrinsic responsiveness of NK cells to activating receptors, a process called NK cell education (Anfossi et al., 2006; Kim et al., 2005). The cytotoxicity and responsiveness of $CD56^{dim}$ NK cells to activating receptor ligation therefore correlates with an increased number of self-MHC ligand/KIR interactions. Hypo-responsiveness due to lack of licensing, however, can be overcome by the presence of cytokines such as IL-2 (Juelke et al., 2009; Kim et al., 2005).

1.6.5. NK cells in viral diseases

NK cells are key effectors in the host defense against viral diseases, and patients with defective NK cell function have increased susceptibility to viral infections, in particular to recurrent and disseminating herpesgroup virus infections (Biron et al., 1989; Jawahar et al., 1996; Joncas et al., 1989; Quinnan et al., 1982). In mice,

depletion of NK cells leads to increased mortality following influenza infection (Stein-Streilein & Guffee, 1986), Ebola (Warfield et al., 2004), and murine cytomegalovirus (MCMV) (Bukowski, 1985), amongst others.

NK cells express a range of activating and inhibitory receptors (Figure 1-4) which are critical in mediating NK cell cytotoxicity against virus-infected cells. In addition to KIRs, NK cells express natural cytotoxicity receptors (NCR), NKp30, NKp44 and NKp46, which are activating receptors that recognise virally derived products, as well as tumour ligands (Arnon et al., 2004; Pende et al., 1999). NKp46 and NKp44, for instance, bind haemagglutinin of influenza virus (Arnon et al., 2001; Mandelboim et al., 2001), and mice lacking the murine homolog of NKp46 succumb to lethal influenza infection (Gazit et al., 2006).

NK cells can also recognise stress-induced ligands such as MICA, MICB, and UL-16-binding protein (ULBP) through the NKG2D receptor, which induces lysis of target cells even in the presence of MHC class I (Bauer et al., 1999). Viral evasion mechanisms targeting NKG2D highlight the importance of this receptor, as human CMV secretes UL16, which binds ULBP and blocks the interaction between NKG2D and its activating ligand (Kubin et al., 2001). Synergy between all of these activating receptors is required for efficient activation of NK cells (Bryceson et al., 2006), and down-modulation of these receptors in infected patients may contribute to increased pathology.

NK cell dysfunction has been reported in HIV infection, with the impairment of NK cell cytotoxicity, including the ability to induce antibody-dependent cellular cytotoxicity (ADCC), correlating with disease progression (Ahmad & Menezes, 1996; Brenner et al., 1991; Sirianni et al., 1994). In turn, strong NK cell functionality correlates with improved clinical states (Szelc et al., 1992). Genome-wide association studies

(GWAS) have shown a strong association between slower HIV disease progression and the co-expression of the activating receptor KIR3DS1 and its ligand, HLA-Bw4 molecules that express isoleucine at position 80 (Bw4*80I) (Long et al., 2008; Martin et al., 2002), which may confer enhanced cytotoxicity against infected HLA-Bw4-80I-expressing cells (Alter et al., 2007). NK cells in HCV infected patients also seem to be altered, with increased cytotoxicity and impaired ability to produce IFNγ (Ahlenstiel et al., 2010). The activity of NK cells is thought to affect the outcome of HCV infection, as patients with homozygous carriage of *KIR2DL3:HLA-C-1* had a higher probability to clear the HCV virus compared to individuals without this background (Khakoo et al., 2004).

Reduced NK cell activity in HCV and HIV patients has also been correlated with reduced expression of NKp46 and NKp30 (De Maria et al., 2003; Nattermann et al., 2006). This phenotype could be induced *in vitro*, as culturing NK cells with HCV-infected cells induced the downregulation of NKp30 (Holder et al., 2013), as well as NKG2D (Yoon et al., 2011), with reduced cytotoxicity against target cells. Reduced NCR expression has also been described in Hantavirus (Björkström et al., 2011), Chikunguya virus (Petitdemange et al., 2011), and hepatitis B virus (HBV) infections (Béziat et al., 2012). Modulation of some of these receptors may be protective in some cases, however, as in acute HCV infected patients, individuals who subsequently cleared the virus had reduced frequencies of cells expressing NKp30, NKp46, and NKG2D, compared to those who progressed to chronic infection (Alter et al., 2011).

1.6.6. CD161

As described above, CD161 is one of the earliest markers expressed during NK cell maturation from CD34+ hematopoietic stem cell precursors (Azzoni et al., 1998;

Bennett et al., 1996; Montaldo et al., 2012). CD161, or NKRP1A, is the only member of the NKRP1 family of genes expressed in humans, while in rodents there are seven genes of the Nkrp1 family, *Nkrp1a-g* (Fergusson et al., 2011; Lanier et al., 1994). In mice, these proteins are preferentially expressed on murine NK cells; the first member to be discovered was *Nkrp1c*, which encodes the canonical NK cell marker NK1.1 in C57BL/6 mice (Ryan et al., 1992). NKRP1A, C, and F contain a positively charged amino acid in their transmembrane domain, and thus are thought to be activating receptors (Aust et al., 2009). However, only the cross-linking of NKRP1C has been demonstrated to enhance cytotoxicity and cytokine secretion (Aust et al., 2009; Ryan et al., 1992), while NKRP1A has been shown to be inhibitory in one study (Poggi et al., 1998). In contrast, NKRP1B and NKRP1D lack charged transmembrane residues and have a cytoplasmic ITIM domain, which delivers inhibitory signals when ligated (Carlyle et al., 1999; Iizuka et al., 2003).

In 2005, two groups identified the ligand for CD161 as lectin-like transcript 1 (LLT1) (Aldemir et al., 2005; Rosen et al., 2005). LLT1 is the human ortholog of C-type lectin related-b protein, osteoclast inhibitory lectin (Ocil), which binds the inhibitory NKRP1B and NKRP1D receptors in mice (Carlyle et al., 2004). LLT1 expression has been described on activated or infected APCs such as B cells, plasmacytoid dendritic cells, and monocyte-derived dendritic cells (Aldemir et al., 2005; Germain et al., 2011; Rosen et al., 2008), as well as on NK cells and T cells (Boles et al., 1999; Germain et al., 2011). CD161+NK cells have reduced cytotoxicity and cytokine secretion towards LLT1-expressing target cells (Aldemir et al., 2005; Rosen et al., 2005), and LLT1 expression on B cell tumours has been shown to inhibit NK cells (Germain et al., 2015). Crosslinking of CD161 also blocks NK cell degranulation (Rosen et al., 2008), suggesting that CD161 acts as an inhibitory receptor on NK cells.

1.6.7. CD161 expression on NK cells in viral infections

Changes in the frequency of CD161-expressing NK cells have been frequently reported in viral infections. Lower expression of CD161 in acute HCV-infected patients predicted viral clearance (Alter et al., 2011), while higher CD161 expression has been reported in patients with chronic HCV compared to acute infections (Lunemann et al., 2014). Patients chronically infected with HIV have a depletion of CD161+ NK cells compared to healthy controls (Alter et al., 2004; Luteijn et al., 2011), which is replenished by successful HAART treatment, along with a recovery of NK cell cytotoxicity (Azzoni et al., 2002). However, the contrary has also been reported, where HAART treated patients showed reduced expression of CD161 compared to untreated and uninfected donors (Jacobs et al., 2004). Furthermore, the emergence of a dysfunctional CD56−CD16+ NK cell population with impaired lytic capacities has been described in HIV (Mavilio et al., 2005), which was characterized by a significantly downregulated expression of CD161 in one study of HIV-1 subtype C infected patients (Kulkarni et al., 2012).

Thus, CD161 expression is heterogeneous and reduced in the context of some viral infections, but in the absence of a comprehensive phenotypic and functional analysis of NK cells based on CD161 expression, the significance of these changes are unknown. Furthermore, CD161-expressing T cells were shown to share a core transcriptional programme regardless of TCR expression (Fergusson et al., 2014), which was associated with an increased responsiveness to innate cytokines IL-12 and IL-18. Whether this transcriptional signature and functional correlation with CD161 holds true within NK cells is unknown.

1.7. Aims of Thesis

This thesis will address the functional properties of MAIT cells and their subsets in health and autoimmune disease, particularly in psoriasis and psoriatic arthritis. Furthermore, whether CD161-expressing NK cells share functional features with CD161-expressing T cells, including MAIT cells, will be investigated. These aims are summarised below:

1. Investigate the regulation of the cytotoxic potential of MAIT cells, and demonstrate specific lysis of target cells
2. Determine the overlapping and distinct features of MAIT cell subsets, according to coreceptor expression
3. Investigate the phenotype and function of MAIT cells in psoriasis and psoriatic arthritis, and use a novel RORγt inhibitor to inhibit IL-17 production from MAIT cells
4. Perform a comprehensive phenotypic and functional comparison of CD161+ and CD161− NK cells. Do they share features with CD161+ T cells, and how does CD161 expression change in the context of viral infections?

2. Materials and Methods

2.1. Media and buffers

R10

RPMI 1640 (Sigma Aldrich) + 10% heat-inactivated fetal calf serum (FCS; Gibco) + 2mM L-Glutamine (Gibco) + 1X Penicillin-Streptomicin solution (Gibco)

RH10

RPMI 1640 (Sigma Aldrich) + 10% heat-inactivated and filtered human serum (Sigma Aldrich) + 2mM L-Glutamine (Gibco) + 1X Penicillin-Streptomicin solution (Gibco)

Freezing mix

90% heat inactivated FCS (Gibco) + 10% dimethyl sulfoxide (DMSO; Sigma Aldrich)

MACS buffer

Phosphate buffered saline (PBS) + 2mM ethylenediaminetetraacetic acid (EDTA; Sigma Aldrich) + 0.5% heat inactivated FCS (Gibco)

THP1 media

R10 + 50μM β-mercaptoethanol (Sigma Aldrich)

CyTOF buffer

PBS + 0.05% sodium azide + 2mM EDTA + 2% FCS (Gibco)

2.2. Cells

2.2.1. Peripheral blood samples

Adult peripheral blood mononuclear cells (PBMCs) were obtained from healthy donor whole blood leukocyte cones (NHS Blood and Transplant, UK), or from healthy volunteers. PBMCs from 24 month old donors were obtained from a cohort of Swedish infants (Saghafian-Hedengren et al., 2010). Umbilical cord blood (UCB) samples were obtained from Stem Cell Services (NHS Blood and Transplant, UK). Further details of blood and tissue samples specific for each chapter are detailed in the Materials and Methods section in the relevant chapter.

2.2.2. THP1 cells

THP1 cells (ECACC, UK) were maintained at 2 x 10^5 cells/ml in THP1 culture media.

2.2.3. B cell lines

Primary B cells from a healthy donor were Epstein-Barr virus (EBV)-transformed to generate B cell lines (BCL). They were maintained at 5 x 10^5 cells/ml in R10 media.

2.3. Isolation of cells

2.3.1. PBMC separation

Whole blood was diluted with PBS and layered over Lymphoprep^{TM} separation medium (Axis Shield Diagnostics), then centrifuged for 22min at 2200 rpm (22°C with no brake). The PBMC layer was collected with a Pasteur pipette and washed twice

with R10, first at 1800 rpm for 10min, followed by another wash at 1600 rpm for 5min. Cells were counted by Trypan Blue exclusion for further use or freezing.

For freezing, freshly isolated PBMCs were resuspended in freezing mix and aliquoted into cryovials. Cells were initially frozen at −80°C, and transferred into liquid nitrogen for long-term storage.

For thawing, frozen cells were partially thawed using a 37°C water bath, transferred into a 15ml Falcon tube and slowly resuspended in warm R10. Cells were washed and resuspended in R10 for further use.

2.3.2. CD8+ T cell isolation

CD8+ T cells were isolated from PBMCs by positive selection with CD8 Microbeads (Miltenyi Biotec) using MS MACS columns (Miltenyi Biotec), following the manufacturer's protocol. Purity was consistently >90%.

2.3.3. NK cell isolation

NK cells were isolated from PBMCs by negative selection with EasySep^{TM} Human NK cell enrichment kit (STEMCELL Technologies) following the manufacturer's protocol. Purity was consistently >85%.

2.4. Irradiation of cells

Cell lines or autologous feeder cells were irradiated with 30 gry of radiation prior to co-culture with T cells.

2.5. Preparation of fixed bacteria

Using a pipette tip, a single colony of *E. coli* (DH5α; Invitrogen) was picked from a Luria-Bertani (LB) agar plate and the tip was dropped into 5ml of LB media, and cultured overnight in a shaker incubator. An empty pipette tip (without picking any colonies) was dropped into 5ml of LB media and cultured overnight as a negative control. The *E. coli* was then fixed in 1% paraformaldehyde (PFA) for 20 minutes, and washed extensively in sterile, filtered PBS. The negative control was prepared in identical fashion and used as a sterility control, in order to control for any microorganisms that may have contaminated the *E. coli* culture either during the incubation period, fixation process, or during the washes.

2.6. Cell culture

2.6.1. Bacterial activation of MAIT cells

THP1 cells or BCLs were incubated with PFA-fixed *E. coli* overnight at a ratio of 25 bacteria per cell (2 x 10^6 *E. coli* : 8 x 10^4 THP1/BCL), or the sterility control. THP1 cells or BCLs were subsequently washed twice in R10 and PBMCs or enriched CD8+ T cells were added for 5 hours or overnight, as indicated. PBMCs were added at a ratio of 5 x 10^5 PBMCs : 8 x 10^4 THP1. Enriched CD8+ T cells were added at ratio of 2 x 10^5 CD8+ T cells : 8 x 10^4 THP1, unless otherwise indicated. For intracellular cytokine staining, Brefeldin A (eBioscience) was added at 3μg/ml for the final 4 hours of the stimulation. For degranulation assays, anti-CD107a PE-Cy7 antibody (Biolegend) was added at the beginning of the stimulation of T cells.

2.6.2. Addition of blocking antibodies

An anti-MR1 antibody (Clone 26.5, kindly provided by T.H. Hansen), or IgG2a isotype control (BD Biosciences) were used at 5µg/ml for blocking experiments. Anti-IL-12p40/70 antibody (eBioscience) and anti-IL-18 antibody (MBL International) or IgG1 isotype control (BD Biosciences) was used at 5µg/ml for blocking experiments.

2.6.3. T cell activation

For the TCR-mediated activation of T cells, anti-CD3/CD28/CD2 beads were prepared using the T cell Activation/Expansion kit (Miltenyi Biotec), by coating anti-biotin MACSiBead Particles with CD3-biotin, CD28-biotin, and CD28-biotin at 10µg/ml following the manufacturer's protocol. Anti-CD3/CD28/CD2 beads were incubated with PBMCs or enriched CD8+ T cells at a bead-to-cell ratio of 1:2. Alternatively, anti-biotin MACSiBead were coated with CD3-biotin alone at 10µg/ml for anti-CD3 stimulations. Dynabeads® Human T-Activator CD3/CD28 beads (Thermo Fisher Scientific) were used at a bead-to-cell ratio of 1:1.

2.6.4. PMA/ionomycin stimulation

PBMCs were incubated with 250ng/ml Phorbol 12-Myristate 13-Acetate (PMA) and 250ng/ml ionomycin (both Sigma Aldrich) for 5 hours. For the negative control, an equivalent dilution of DMSO (Sigma Aldrich) was added for 5 hours. Brefeldin A (Sigma Aldrich) was added at 10µg/ml for the final 4 hours of the stimulation.

2.6.5. IL-12+IL-18 stimulation

PBMCs were incubated with IL-12 and IL-18 (both Miltenyi Biotec) at 50ng/ml overnight. Brefeldin A (eBioscience) was added at 3µg/ml for the final 4 hours of the incubation.

2.6.6. Proliferation assays

PBMCs were labeled with 5µM CellTrace^{TM} Violet (CTV; Invitrogen) according to the manufacturer's protocol. Briefly, PBMCs were washed twice in PBS before resuspending in PBS, and 5mM stock concentration of CTV was added at 1:1000 in 15ml Falcon tubes. After mixing, cells were kept at room temperature in the dark for 10min, before the addition of ice cold R10 for 5min. Cells were subsequently washed in R10 three times, changing the Falcon tube each time. After the final wash, CTV-labeled cells were cultured in RH10 for 5-6 days at 37°C, either left unstimulated or stimulated with the indicated cytokines or antigens, detailed in each chapter. Following proliferation, cells were harvested and stained with the live-dead dye, then fixed and permeablised for the staining of extracellular as well as intracellular markers to account for any downregulation of surface receptors.

2.7. Flow cytometry

2.7.1. Surface staining

Cells were washed and resuspended in PBS, and flurochrome-conjugated antibodies and live-dead dye was added at optimised dilutions (Table 2-1). Cells were incubated at 4°C for 25min before washing with PBS, and fixed in 1% formaldehyde (Sigma Aldrich) for 20 min at 4°C. Cells were then washed and resuspended in PBS for flow cytometer acquisition or further intracellular staining.

2.7.2. Intracellular cytokine staining

Following surface staining and fixation with 1% formaldehyde, cells were washed with PBS and resuspended in 1X Permeabilisation buffer (eBioscience) for 25min at room temperature. Cells were then washed in 1X Permeabilisation buffer and resuspended with antibodies diluted in 1X Permeabilisation buffer for 25min at room temperature. Following incubation with antibodies, cells were washed and resuspended in PBS. Cytotoxic effector molecules were stained following the same protocol.

2.7.3. Transcription factor staining

Transcription factors and nuclear proteins were stained using the Foxp3/Transcription Factor Staining Buffer Set (eBioscience), according to the manufacturer's protocol. Briefly, cells were surface stained and after washing, cells were resuspended in 1X Fixation/Permeabilisation buffer for 60min at room temperature. After washing with 1X Permeabilisation buffer, the cells were incubated with the relevant antibodies in 1X Permeabilisation buffer at room temperature for 45min. The cells were subsequently washed and resuspended in PBS.

2.7.4. Data acquisition and analysis

Data were acquired on a MacsQuant Analyser (Miltenyi Biotec) or LSRII (BD Biosciences) and analysed using FlowJo software (Tree Star, Inc.). Gating strategies used in this thesis were as shown in Figure 2-1, unless otherwise indicated. The expression of markers was determined according to the appropriate isotype control or fluorescence minus one (FMO) sample.

Table 2-1. Antibodies used in flow cytometry experiments.

Marker	Flurochrome	Clone	Company	Dilution
Annexin V	FITC	n/a	Miltenyi Biotec	1:20
Bcl6	APC	BCL-UP	eBioscience	1:25
Blimp1	Alexa Fluor 488	IC36081G	R&D Systems	1:25
Caspase 3	PE	CCP32	BD Biosciences	1:5
CCL4 (MIP1β)	PE	24006	R&D Systems	1:50
CCR2	PerCP-Cy5.5	K036C2	BioLegend	1:25
CCR3	PE	5E8	BD Biosciences	1:25
CCR4	PerCP-Cy5.5	L291H4	BioLegend	1:25
CCR5	PerCP-Cy5.5	HEK/1/85a	BioLegend	1:25
CCR6	PerCP-Cy5.5	11A9	BD Biosciences	1:25
CCR7	PerCP-Cy5.5	G043H7	BioLegend	1:100
CCR9	PE	112509	R&D Systems	1:25
CD107a	PE-Cy7	H4A3	BD Biosciences	1:20
	PE-Cy7	H4A3	BioLegend	1:1000
CD127	FITC	MB15-18C9	Miltenyi Biotec	1:50
CD14	APC-Cy7	HCD14	BioLegend	1:100
	Pacific blue	TuK4	Invitrogen	1:100
CD158e1/e2	PE	Z27.3.7	Beckman Coulter	1:50
CD16	eFluor450	eBioCB16	eBioscience	1:50
	FITC	eBioCB16	eBioscience	1:50
CD160	Alexa Fluor 647	BY55	BioLegend	1:50
CD161	PE	191B8	Miltenyi Biotec	1:100
	APC	191B8	Miltenyi Biotec	1:100
CD19	APC-Cy7	HIB19	BioLegend	1:50
	Pacific blue	SJ25-C1	Invitrogen	1:50
CD244	PE-Cy5.5	C1.7	BioLegend	1:5
CD25	PE	BC96	BioLegend	1:50
CD27	Alexa Fluor 700	O323	eBioscience	1:50
CD3	PE-Cy7	UCHT1	BioLegend	1:100
	eFluor450	UCHT1	eBioscience	1:100
	FITC	UCHT1	BioLegend	1:50
	APC	OKT13	eBioscience	1:50
	Pacific Orange	UCHT1	Invitrogen	1:50
	FITC	UCHT1	BioLegend	1:50
	APC-Cy7	HIT3a	BioLegend	1:100
CD38	FITC	HIT2	BD Biosciences	1:50
CD4	PerCP-Cy5.5	OKT4	eBioscience	1:100
	Alexa Fluor 700	RPA-T4	BD Biosciences	1:100
	Qdot 605	S3.5	Invitrogen	1:200
	PE-Cy7	SK3	BD Biosciences	1:100
	VioGreen	VIT4	Miltenyi Biotec	1:50
CD45	FITC	5B1	Miltenyi Biotec	1:50
CD45RA	PE-Cy7	HI100	BioLegend	1:50
	PerCP-Cy5.5	HI100	BioLegend	1:50
CD45RO	PE-Cy7	UCHL1	BioLegend	1:50

CD56	APC	AF12-7H3	Miltenyi Biotec	1:50
	PE-Cy7	CMSSB	eBioscience	1:50
	Brilliant Violet 421	HCD56	BioLegend	1:100
	FITC	NCAM16.2	BD Biosciences	1:50
	PE-Cy7	MEM-188	BioLegend	1:50
CD57	Pacific blue	HCD57	BioLegend	1:1000
	APC	HCD57	BioLegend	1:50
	FITC	HCD57	BioLegend	1:50
CD62L	PE	DREG-56	Abcam	1:100
	PE-Cy7	DREG-56	BioLegend	1:50
CD69	FITC	FN50	eBioscience	1:40
CD8α	PerCP-Cy5.5	RPA-T8	BioLegend	1:100
	PerCP-Cy5.5	SK1	BioLegend	1:100
	PerCP-Cy5.5	RPA-T8	eBioscience	1:100
	Alexa Fluor 700	RPA-T8	BD Biosciences	1:100
	VioGreen	BW135/80	Miltenyi Biotec	1:50
	eFluor450	OKT8	eBioscience	1:100
CD85j	FITC	555942	BD Biosciences	1:50
CD8β	PE	2ST8.5H7	Beckman Coulter	1:50
CD94	FITC	DX22	eBioscience	1:50
CLA1	Pacific blue	HECA-452	BioLegend	1:100
CX3CR1	FITC	2A9-1	BioLegend	1:25
CXCR3	PE	1C6/CXCR3	BD Biosciences	1:25
CXCR4	PE	12G5	eBioscience	1:25
CXCR6	Alexa Fluor 647	TG3/CXCR6	BioLegend	1:10
Eomes	eFluor660	WD1928	eBioscience	1:25
FasL	PE	NOK-1	eBioscience	1:25
Foxp3	Alexa Fluor 700	PCH101	eBioscience	1:25
GATA3	PE	TWAJ	eBioscience	1:25
GM-CSF	PerCP-Cy5.5	BVD2-21C11	BioLegend	1:25
Granulysin	PE	DH2	BioLegend	1:50
Granzyme A	PerCP-Cy5.5	CB9	BioLegend	1:100
	FITC	356412	R&D Systems	1:50
Granzyme B	APC	GB11	Invitrogen	1:100
	Alexa Fluor 700	GB11	BD Biosciences	1:50
Granzyme K	FITC	24C3	Immunotools	1:25
	PE	24C3	Immunotools	1:25
IFNγ	Alexa Fluor 700	B27	BD Biosciences	1:50
	FITC	45-15	Miltenyi Biotec	1:50
	PE	45-15	Miltenyi Biotec	1:50
	PerCP-Cy5.5	4S.B3	eBioscience	1:50
IL-13	PerCP-Cy5.5	JES10-5A2	BioLegend	1:25
IL-17A	PE	eBio64CAP17	eBioscience	1:10
	PE	eBio64DEC17	eBioscience	1:10
	Alexa Fluor 488	BL168	BioLegend	1:10
	FITC	BL168	BioLegend	1:10
IL-18Rα	PE	H44	eBioscience	1:25

IL-1β	PE	CRM56	eBioscience	1:25
IL-2	PerCP-Cy5.5	MQ1-17H12	BD Biosciences	1:100
IL-22	PerCP-eFluor710	22URTI	eBioscience	1:25
	APC	142928	R&D Systems	1:25
IL-4	APC	MP4-25D2	BioLegend	1:25
IL-6	Alexa Fluor 700	MQ2-13A5	eBioscience	1:25
Ki67	FITC	B56	BD Biosciences	1:50
KLRG1	FITC	13F12F2	Kindly provided by H. Pircher	1:100
Live/dead	near IR	n/a	Invitrogen	1:1250
	Pacific blue	n/a	Invitrogen	1:1250
MDR1	PE	UIC2	BioLegend	1:50
NKG2A	PE	Z199	Beckman Coulter	1:50
NKG2C	Alexa Fluor 488	134591	R&D Systems	1:25
	PE	134591	R&D Systems	1:25
	PerCP	134591	R&D Systems	1:10
NKG2D	PE	149810	R&D Systems	1:50
NKp30	APC	AF29-4D12	Miltenyi Biotec	1:50
NKp44	PE	Z231	Beckman Coulter	1:50
NKp46	APC	9E2	Miltenyi Biotec	1:50
NKp80	APC	4A4.D10	Miltenyi Biotec	1:50
PD-1	BV421	EH12.2H7	BioLegend	1:50
Perforin	FITC	δG9	BD Biosciences	1:50
	Pacific blue	B-D48	BioLegend	1:100
Phosphatidylserine	Alexa Fluor 488	1H6	Merck Milipore	1:100
PLZF	APC	6318100	R&D Systems	1:25
RORγt	PE	Q21-559	BD Biosciences	1:25
STAT3 (pY705)	PE	4/P-STAT3	BD Phosflow	1:25
T-bet	PE	4B10	Santa Cruz Biotechnology	1:25
	PE	eBio4B10	eBioscience	1:25
TCR γδ	PE-Cy5	IMMU510	Beckman Coulter	1:50
TGFβ	PE	TW4-2F8	BioLegend	1:25
ThPOK	PE	11H11A14	BioLegend	1:25
TIM-3	PE	344823	R&D Systems	1:50
TNFα	PerCP-Cy5.5	MAb11	BioLegend	1:50
	PE-Cy7	MAb11	BD Biosciences	1:25
	PE-Cy7	MAb11	BioLegend	1:100
Vα7.2	PE	3C10	BioLegend	1:100
	APC	3C10	BioLegend	1:50
	PE-Cy7	3C10	BioLegend	1:100
	FITC	3C10	BioLegend	1:50

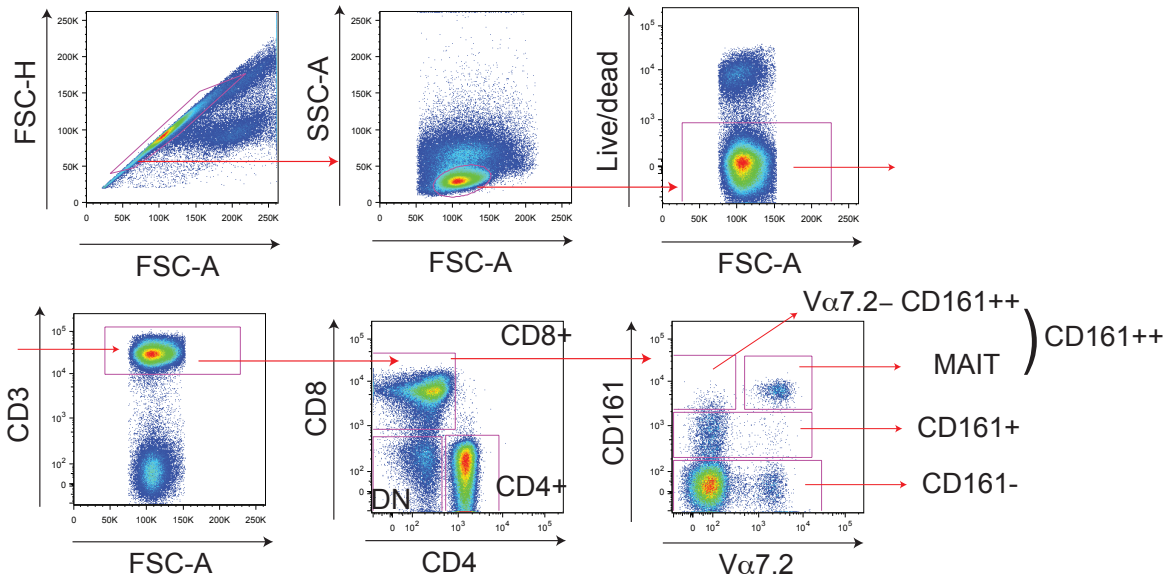


Figure 2-1. Gating strategy used to identify T cell subsets according to CD161 and Vα7.2 expression. Cells were gated as singlets, lymphocytes, live cells, CD3+ cells to identify T cells. CD8+ T cells were further gated as shown, to identify CD161++, CD161+, and CD161– populations. The CD161++ subset can be divided into Vα7.2+ MAIT cells and Vα7.2– non-MAIT cells. Gates based on CD8+ T cells were then used to define corresponding populations in double-negative (DN) or CD4+ T cells, where indicated.

2.8. Cytometry by Time-of-Flight (CyTOF)

2.8.1. Antibody Conjugation

Purified antibodies lacking carrier proteins were labeled with heavy-metal maleimide-coupled MAXPAR chelating polymers according to the protocol provided by DVS Sciences.

2.8.2. Staining of PMA/ionomycin stimulated cells

For data shown in Chapter 6, Appendix Figure VI-1, PBMCs were thawed and rested overnight at 37°C, then cultured at 3-4x10^6/ml in complete RPMI, with 1X Brefeldin A, 1X monensin (both eBioscience), 2.5µg/ml anti-CD107a, 1.25µg/ml anti-CD107b, and 10µM TAPI-2 (metalloproteinase inhibitor to prevent stimulation-induced cleavage of surface markers) (VWR International). Cells were stimulated for 3 hours with 150ng/ml PMA and 1µM ionomycin (Sigma Aldrich).

Following stimulation, cells were stained as previously described (Newell et al., 2012) in CyTOF buffer with fluorescently-tagged antibodies for 30min on ice and washed (see Chapter 6, Appendix Table VI-2). After washing, cells were incubated with metal-conjugated surface antibodies for 30min on ice, including secondary antibodies against the fluorescent tags. Cells were then stained with a live-dead marker (20uM maleimido-mono-amine-DOTA in PBS) for 30min, then fixed overnight at 4°C with 2% PFA in PBS. After two washes in 1X Permeabilisation buffer (eBioscience), cells were stained with intracellular antibodies on ice for 45min, washed then labeled for 20 minutes with 250nM iridium interchelator (DVS Sciences) in 2% PFA. Cells were washed twice before dilution to 5x10^5 cells/ml in distilled water for acquisition. Further details are provided in Chapter 6.

2.8.3. Staining of IL-12+IL-18 stimulated cells

For experiments shown in Chapter 6, Figure 6-9, frozen PBMCs were thawed and washed in R10+DNAse (Sigma Aldrich). PBMCs were depleted of CD4+ T cells, monocytes, and B cells, using anti-Mouse IgG Microbeads (Miltenyi) following staining with anti-CD4, or anti-CD33+anti-CD13, or anti-CD20 antibodies, respectively. Cells were cultured in RPMI 10% FCS for 20 hours with IL-12 and IL-18 (both 50ng/ml, Miltenyi Biotec), and 1X Brefeldin A (eBioscience) was added at 3µg/ml) for the last 4 hours.

Cells were first stained with the viability marker Cisplatin (Sigma Aldrich) at 5µM in PBS for 5min on ice, then with metal-conjugated surface antibodies and fluorochrome-conjugated antibodies, in RPMI+10% FCS at 37°C for 15min (See Chapter 6, Table 6-2). After washing, cells were stained in 1% bovine serum albumin (BSA)/PBS buffer with the remaining surface antibodies, including secondary antibodies against the fluorescent tags, at 4°C for 15min. Cells were then fixed in Fixation/Permeabilisation buffer (eBioscience) for 30min at 4°C. Following washing in Permeabilisation buffer (eBioscience), cells were incubated with intracellular antibodies for 30min at 4°C in Permeabilisation buffer. A unique dual combination of metal barcodes was added to each sample for barcoding as previously described (Becher et al., 2014; Wong et al., 2015), and cells were DNA labeled with 250nM iridium interchelator in 2% PFA (DVS Sciences). Cells were fixed in 2% PFA overnight at 4°C. Cells were washed twice before dilution to $5x10^5$ cells/ml in distilled water for acquisition. Further details are provided in Chapter 6.

2.8.4. Data acquisition and analysis

Cells were acquired on CyTOF using dual-count mode and analysed with noise-reduction turned off. Any zero values were randomized using a uniform distribution of values between zero and minus-one using an R script. The signal of each parameter was then normalized based on the EQ Four Element Calibration beads (Fluidigm) (Finck et al., 2013). The cells were gated and de-barcoded to identify each sample using Boolean gating in FlowJo Version 10 (Tree Star).

2.9. Statistical analysis

All graphs were generated and statistical analyses performed using Prism software version 6 (GraphPad). Data in figures and text are presented as means with standard error of the mean (S.E.M.). ****P<0.0001, ***P<0.001, **P<0.01, *P<0.05, ns = non-significant, by the indicated statistical test in each figure legend. Flow cytometric coexpression analysis was performed using SPICE software Version 5.3 (Roederer et al., 2011).

3. The Cytotoxicity of MAIT cells

3.1. Introduction

The cytotoxic cells of the innate and adaptive immune system, NK cells and CD8+ T cells, respectively, are characterized by their ability to induce the apoptosis of infected or transformed cells. The primary mechanism by which cytotoxic cells kill target cells is through the granule exocytosis pathway, mediated by serine proteases called granzymes being released from the granules of the effector cell and gaining entry to the cytoplasm of the target cell (Shi et al., 1992). The pore-forming protein perforin is critical for the release of granzymes into the target cell cytosol (Pardo et al., 2004), as internalized granzymes are retained in endosome-like-vesicles in the absence of perforin, and are unable to induce apoptosis (Froelich et al., 1996; Pinkoski et al., 1998). Although target cells can also take up granzymes by receptor-mediated endocytosis (Motyka et al., 2000), perforin-deficient mice are unable to lyse tumour cells or clear lymphocytic choriomeningitis virus (LCMV) and *L. monocytogenes* infections (Kägi et al., 1994a; van den Broek, 1996; Walsh et al., 1994), suggesting that perforin-mediated entry of granzymes is critical for the efficient lysis of target cells.

Perforin on its own cannot induce apoptosis, as this requires granzymes gaining access to their substrates in the target cell. In humans there are five granzymes with diverse substrate specificities: granzyme (Gr) A, GrB, GrH, GrK, and GrM (Chowdhury et al., 2008). GrB is the prototypical granzyme and is critical for efficient lysis of target cells, as cells from GrB-deficient mice induce apoptosis at a much slower rate compared to those from wild-type mice (Heusel et al., 1994; Pardo et al., 2004). The proteolytic cleavage of GrB substrates, caspase 3 and 7, activates these enzymes to induce a caspase cascade, which results in rapid DNA fragmentation

and degradation of cytoskeletal and nuclear proteins (Chowdhury et al., 2008). GrB also cleaves the proapoptotic Bcl-2 family member, Bid, which leads to permeabilisation of the mitochondrial outer membrane and release of cytochrome c into the cytosol (Sutton et al., 2000). Cytochrome c in turn induces the assembly of a complex composed of Apoptotic protease activating factor 1 (Apaf1) and caspase 9, called the apoptosome, which initiates an apoptotic protease cascade (Li et al., 1997). In conventional CD8+ T cells, GrB can be induced upon activation, either through their TCR or by cytokines such as IL-15 (Liu et al., 2002; Nowacki et al., 2007), and its expression is associated with high expression of T-bet (Cruz-Guilloty et al., 2009; Intlekofer et al., 2005). Furthermore, mice deficient for the transcriptional repressor, B lymphocyte-induced maturation protein 1 (Blimp1), failed to induce GrB which was required for the control of influenza virus (Kallies et al., 2009). Thus, GrB expression is tightly regulated in CD8+ T cells and the ability to upregulate GrB is a critical determinant of cytotoxicity.

CD8+ T cells also express the granzymes GrA and GrK, which are closely related trypsin-like serine proteases (Bratke et al., 2005). GrA and GrK induce cell death mainly through proteolysis of components of the ER-associated SET complex, which leads to single-stranded DNA nicks and consequent DNA degradation, as well as through the generation of reactive oxygen species (Bovenschen et al., 2009; Pardo et al., 2004). GrK also has unique substrates not shared with GrA, including Bid (Zhao et al., 2007). However, recent studies have suggested that GrA and GrK are inefficient inducers of cell death (Cooper et al., 2011; Joeckel et al., 2011; Metkar et al., 2008). Although murine models have shown that GrA is important for the cytotoxic function of T cells (Pardo et al., 2004; Shi et al., 1992), human GrA is significantly less cytotoxic compared to murine GrA when delivered to target cells at the same concentration (Kaiserman et al., 2014; Susanto et al., 2013). Furthermore, GrA delivered to target cells *in vitro* using perforin was less cytotoxic when compared

to GrB at equivalent concentrations (Metkar et al., 2008). Similarly, although GrK has been shown to be important for the clearance of influenza in mice (Jenkins et al., 2008), GrK+ cells from LCMV-infected mice lacking GrA and GrB could not induce cell death (Joeckel et al., 2011). In humans, GrK expression is particularly enriched within the $CD56^{bright}$ NK cell subset, which has been described to have low cytotoxic potential (Bratke et al., 2005; Jacobs et al., 2001). Interestingly, in an analysis of the cytotoxic phenotype of virus-specific CD8+ T cells, lytic activity inversely correlated with GrK expression, while GrA expression did not correlate with cytotoxicity (Harari et al., 2009). This contrasted with the strong correlation between perforin and GrB expression and the ability of these CD8+ T cells to lyse target cells. Thus, a hierarchy among these granzyme and perforin molecules determines cytotoxic efficiency, with expression of perforin and GrB, but not GrA or GrK, correlating with cytotoxic function.

Up to 20% of peripheral blood CD8+ T cells in humans express the TCRα chain Vα7.2 recombined with Jα33, Jα12, or Jα20, which is preferentially paired with a limited number of Vβ chains, and are a developmentally distinct subset of innate-like T cells called MAIT cells (Lepore et al., 2014; Reantragoon et al., 2013). These cells can also be identified by their high expression of the C-type lectin-like receptor, CD161. MAIT cells are restricted by the non-polymorphic antigen-presenting molecule, MR1, which presents ligands derived from riboflavin precursors (Corbett et al., 2014; Kjer-Nielsen et al., 2012). As this metabolite is produced by a wide range of bacteria, MAIT cells are critical in the control of bacterial infections, including BCG, *K. pneumonia*, and *E. coli* (Chua et al., 2012; Georgel et al., 2011; Le Bourhis et al., 2010). Murine models have demonstrated that this is primarily mediated through the secretion of cytokines such as IFNγ and TNFα, and the induction of nitric oxide in infected macrophages (Chua et al., 2012; Meierovics et al., 2013). Thus, *in vitro* control of *F. tularensis* LVS by MAIT cells was not associated with the lysis of

infected cells, and early *in vivo* control of BCG was independent of MR1, suggesting that cytotoxic activity may not play a large role in the control of bacterial infections in mice.

However, in contrast to Vα19-Jα33 TCR transgenic mice models, the majority of human MAIT cells are CD8+, a phenotype associated with high cytotoxic function in conventional T cells. Indeed, GrB and GrA secretion from human MAIT cells has been previously demonstrated (Dusseaux et al., 2011). However, the expression of other granzymes and perforin, and the factors regulating the cytotoxicity of human MAIT cells, require further investigation. This is a critical point, given their high frequencies in tissues, effector-memory phenotype and cytotoxic potential; such activity must be tightly regulated in order to limit immunopathology.

3.2. Aims

1. Investigate the cytotoxic profile of *ex vivo* human MAIT cells
2. Determine the signals regulating the cytotoxicity of MAIT cells
3. Demonstrate direct cytotoxicity of MAIT cells using a novel flow cytometric killing assay

3.3. Materials and Methods

Chapter specific materials and methods are listed below. Please see Chapter 2 for all other methods.

3.3.1. *In vitro* stimulation

PFA-fixed *E. coli* (DH5α, Invitrogen) or a sterility control was added to THP1 cells at 25 Bacteria-per-Cell (BpC) overnight. Subsequently, THP1s were washed and CD8+ T cells isolated using CD8 Microbeads (Miltenyi Biotec; purities were ≥90%) and anti-CD107a PE-Cy7 antibody (Biolegend) were added to the wells overnight.

For profiling of granule contents after cytokine stimulation of CD8+ T cells, enriched CD8+ T cells were stimulated for 16 hours with the following cytokines/mitogens: recombinant human IL-2 (Roche), IL-12, IL-18, IL-15, IL-23, TGFβ, IL-1β (all Miltenyi Biotec), IL-21, IL-7 (both PeproTech Inc) all at 50ng/ml; PMA (50ng/ml) and ionomycin (250ng/ml) (Sigma-Aldrich); or anti-CD3/CD28/CD2-coated beads (Miltenyi Biotec). For time-course PBMC stimulations, *E. coli* was added at 10BpC or anti-CD3/CD28/CD2-coated beads at a 1:1 ratio.

3.3.2. Imagestream® analysis

CD8+ T cells were negatively enriched from PBMCs using EasySep^{TM} CD8+ T cell separation kit (StemCell Technologies) and stained with anti-CD161 APC (Miltenyi Biotec), together with anti-CD107a FITC (BD Biosciences), anti-Granzyme A PerCP-Cy5.5 (Biolegend) or anti-Granzyme K FITC (Immunotools). Cells were fixed before analysis by flow cytometry and image capture with Imagestream® imaging cytometer (Amnis Corporation). 15,000 events were collected on the Imagestream® for co-

localisation analysis. Post-acquisition spectral compensation and statistical co-localisation analysis was performed using IDEAS® image analysis software package (Amnis Corporation).

Co-localisation was quantified using a 'Bright Detail Similarity Score', defined as a log-transformed Pearson's correlation coefficient of the intensities of the spatially correlated pixels within the whole cell, as a measure of the degree to which two images were linearly correlated. A score of >2.0 was considered co-localised.

3.3.3. Killing assays

The assay was based on the fluorometric assessment of T lymphocyte antigen specific lysis (FATAL) assay (Sheehy et al., 2001). BCLs were either coincubated with PFA-fixed *E. coli* at 25BpC or the sterility control overnight. Cells were harvested and the *E. coli*-treated BCLs were stained with CellTrace^{TM} carboxyfluorescein succinimidyl ester (CFSE; Invitrogen), while the negative control BCLs were stained with CTV (Invitrogen) as detailed in Chapter 2 (2.6.6.). After extensive washing, the CFSE- and CTV-labeled cells were mixed at a 1:1 ratio before plating.

To prepare effector cells, PBMCs were either used *ex vivo*, or cultured with PFA-fixed *E. coli* at 10Bpc for 6 days. CD8+ T cells were isolated from these PBMCs using CD8 Microbeads (Miltenyi Biotec), and added to the wells at the indicated effector cell: target cell (E:T) ratios overnight, with an anti-CD107a antibody. E:T indicates the ratio of CD8+ T cells to CFSE+ target cells, unless otherwise indicated. CD8+ T cell purities were ≥90%. Experiments were done in duplicate. An MR1-blocking antibody (Clone 26.5), a FasL-blocking antibody (Biolegend) or an appropriate isotype control was added at 5μg/ml for blocking experiments. To block

degranulation, 5mM ethylene glycol tetraacetic acid (EGTA; Sigma-Aldrich) with 1mM $MgCl_2$ (Affymetrix) was used.

Following incubation, cells were stained with a live-dead maker (Invitrogen) before fixation/permeabilisation for the staining of relevant markers. Gating is shown in Figure 3-1. Only live BCLs were analysed. Based on the frequencies of live CFSE+ and live CTV+ BCLs in wells containing no effectors (E:T=0:1), the expected frequency of target cells can be found:

$$\text{Expected ratio (ER)} = \frac{\%\text{CFSE+ cells}}{\%\text{ CTV+ cells}}$$

Using this ratio, the % specific killing can be calculated:

$$\%\text{ specific killing} = 100 \times \left[\frac{(\text{ER} \times \%\text{CTV+}) - \%\text{CFSE+ cells}}{(\text{ER} \times \%\text{CTV+})} \right]$$

For the post-hoc estimation of the actual E:T ratio in each well, the frequency of CD161++ CD8+ T cells within live cells was divided by the expected frequency of CFSE+ cells in each well (ER × %CTV+ cells).

3.3.4. Proliferation assays

PBMCs were labeled with CTV (Invitrogen) as detailed in Chapter 2 (2.6.6), and cultured for 6 days with either PFA-fixed *E. coli* at the indicated BpC, or the sterility

control. Alternatively, THP1 cells were cultured with *E. coli* at 25BpC overnight before irradiation and were co-cultured with CTV-labeled CD8+ T cells enriched with CD8 Microbeads (Miltenyi Biotec) for 6 days at a ratio of $2.5x10^5$ CD8+ T cells: $8x10^4$ THP1 cells. Autologous irradiated feeder cells were added at a ratio of $2.5x10^5$ CD8+ T cells: $5x10^4$ feeder cells.

For cytokine-induced proliferation, CTV-labeled PBMCs were cultured for 6 days with the following stimuli: recombinant human IL-2 (100IU/ml), IL-15 (25ng/ml), IL-18 (50ng/ml), IL-12 (50ng/ml), PHA (2µg/ml), anti-CD3- or anti-CD3/CD28/CD2-coated beads (Miltenyi Biotec) at a 1:1 ratio, or the indicated combinations.

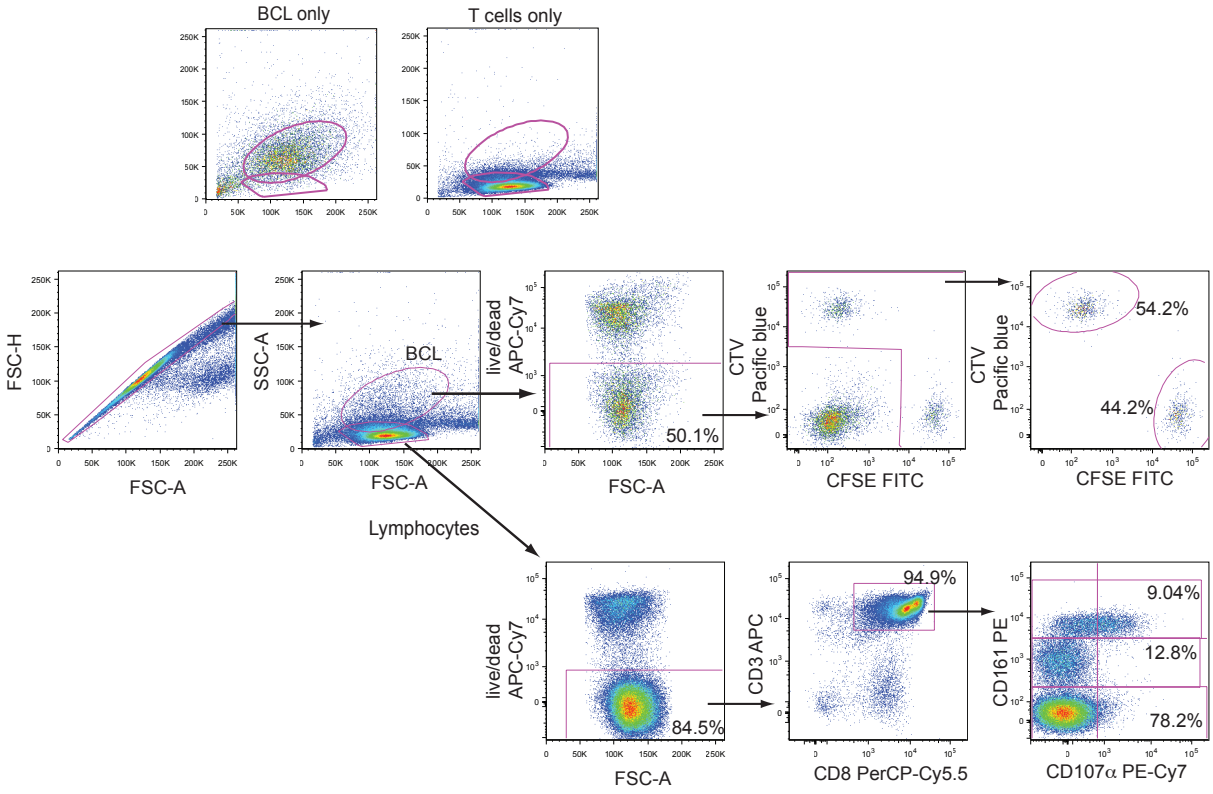


Figure 3-1.Flow cytometry gating strategy used to analyse specific killing of target cells mediated by MAIT cells. Enriched CD8+ T cells were cocultured with a 1:1 ratio of CFSE+ B cell lines (BCLs) that were pre-treated with *E. coli*, and negative control CTV+ BCLs that were treated with the sterility control. Cells were cocultured overnight at indicated ratios and CD107a and specific killing was assessed. For this, single cells were gated, and BCLs and T cell populations were gated based on control wells with only BCLs or T cells. T cells were further identified as live, CD3+CD8+ T cells, and CD107a expression was analysed according to CD161 expression. For the analysis of BCLs, live BCLs were gated and CTV–CFSE– cells were excluded to exclude non-BCLs from the analysis. Target cell killing was determined from the frequency of CTV+ negative control BCLs compared to CFSE+ *E. coli*-treated BCLs.

3.4. Results

3.4.1. Resting blood-derived human MAIT cells have a unique cytotoxic profile

To investigate whether MAIT cells express cytotoxic effector molecules at rest, the expression of GrA, GrK, GrB and perforin in CD161++CD8+ T cells from adult peripheral blood was analysed. *Ex vivo* peripheral blood CD161++CD8+ T cells expressed almost no GrB (3.1±0.9%) compared to either CD161+ (47.6%, $P<0.0001$) or CD161− subpopulations (18.5%, $P<0.01$; Figure 3-2A), in line with a previous report (Billerbeck et al., 2010). The amount of perforin expressed by these cells, as measured by geometric mean fluorescence intensity (gMFI), was also significantly lower than other CD8+ T cell subpopulations (both $P<0.0001$). In contrast, a higher frequency of CD161++CD8+ T cells expressed GrA (96.6±1.2%), compared to CD161+ (87.2%, $P<0.05$) and CD161− CD8+ T cells (31.3%, $P<0.0001$). A greater fraction of CD161++CD8+ T cells also expressed GrK (91.1±1.2%), compared to CD161+CD8+ T cells (32.9%, $P<0.0001$) and CD161− CD8+ T cells (16.3%, $P<0.0001$). Cord blood CD161++CD8+ T cells were also GrA+GrK+ (Appendix Figure III-1A), suggesting this is an inherent feature of this subset.

To investigate whether this cytotoxic profile was characteristic of MAIT cells, or of the CD161++CD8+ T cell population as a whole, granzyme and perforin expression was assessed in CD161++CD8+ T cells according to Vα7.2 TCR expression (Figure 3-2B). Within CD161++CD8+ T cells, there was no difference in expression of GrA and perforin between Vα7.2+ and Vα7.2− cells. However, the frequency of cells expressing GrB was significantly lower in the Vα7.2+ MAIT cells ($P<0.05$), while the proportion of cells expressing GrK was significantly higher ($P<0.001$) compared to Vα7.2− CD161++CD8+ T cells (Figure 3-2C).

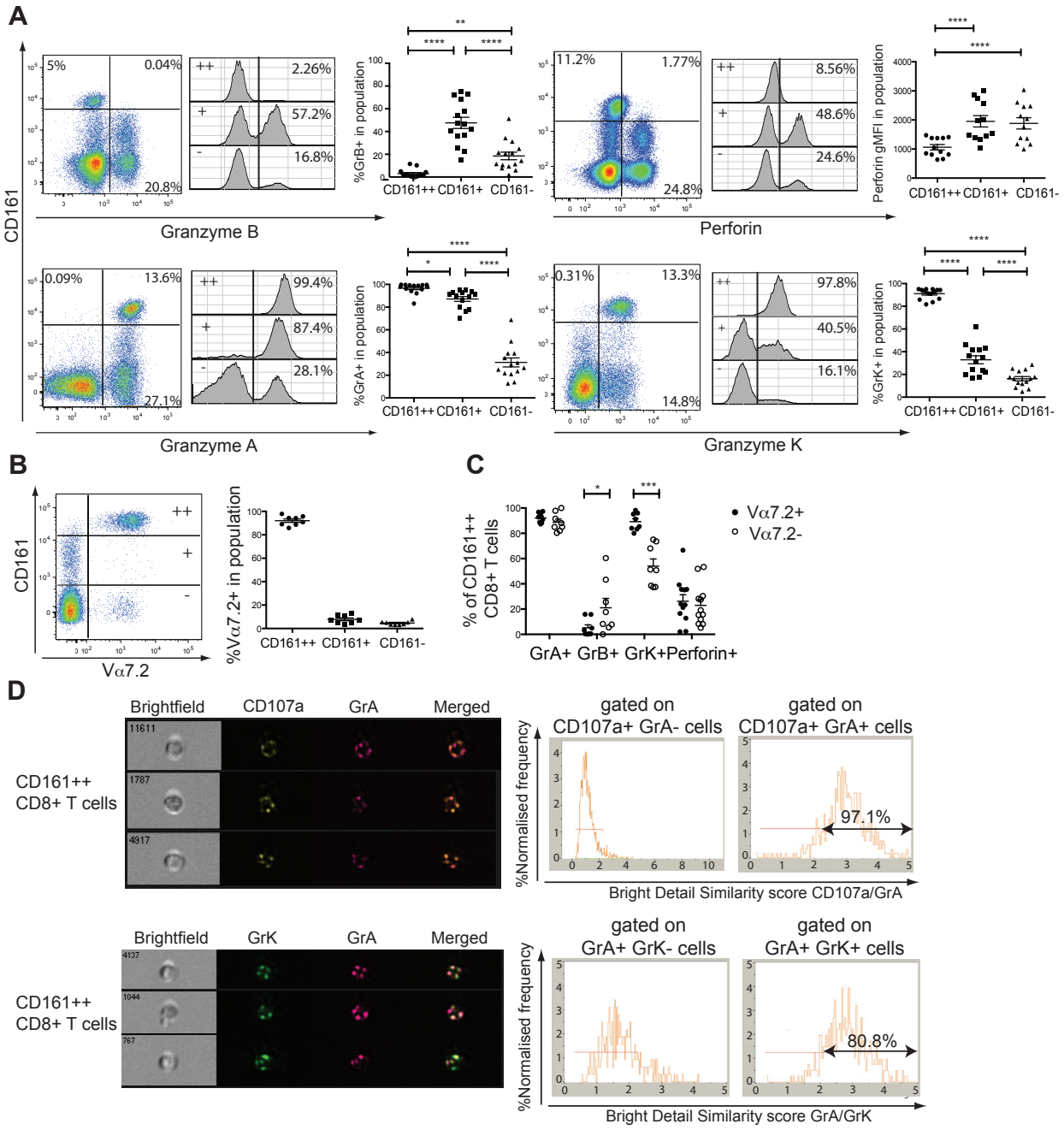


Figure 3-2. Resting blood-derived human MAIT cells have a unique cytotoxic profile. A) Expression of GrB, perforin, GrA, and GrK in peripheral blood CD8+ T cells from healthy donors according to CD161 expression levels. For each marker, representative staining gated on CD8+ T cells (left), representative staining gated on CD161++, CD161+, and CD161- CD8+ T cells (middle), and cumulative data for 12-15 healthy individuals (right) are shown. Results shown as mean ± S.E.M, *P<0.05, **P<0.01, ****P<0.0001 by repeated measures one way ANOVA, with Bonferroni's multiple comparisons test. B) CD161++CD8+ T cells are predominantly Vα7.2+, compared with CD161+ and CD161- CD8+ T cells. Representative staining of Vα7.2 TCR on CD8+ T cells according to CD161 expression levels and cumulative data are shown (n=8). C) Expression of GrB, perforin, GrA, and GrK in Vα7.2+ and Vα7.2- cells, gated within the CD161++CD8+ T cell population. Cumulative data is shown, analyzed by paired t-test (n=8-12). D) Representative images showing Imagestream® analysis of colocalization of GrA, GrK, and CD107α expression within CD161++CD8+ T cells. Histograms of normalized cell frequency against co-localization as measured by Bright Detail Similarity scores; >2.0 is defined as colocalized. Imagestream experiments performed by Christian Clough.

Analysis of the simultaneous expression of perforin and granzymes in MAIT cells confirmed that the majority of the population coexpressed GrA and GrK, while a mean of 30% of MAIT cells coexpressed GrA, GrK, and perforin (Appendix Figure III-1B, C).

Using ImageStream technology, GrA was seen to colocalise with CD107a, a marker of cytotoxic granules, as well as with GrK in CD161++CD8+ Tcells (Figure3-2D), suggesting that GrA and GrK are preformed within lytic granules. Thus, CD161++CD8+ T cells, including the MAIT cells, have the potential to release GrA, GrK and perforin immediately upon target cell interaction.

3.4.2. MR1-dependent activation of MAIT cells leads to degranulation and changes in their cytotoxic profile

Next, the regulation of the cytotoxic potential of MAIT cells was investigated *in vitro*. MAIT cells can be activated both through the cognate interaction between MR1 and the TCR, as well as through IL-12 and IL-18 stimulation in a TCR-independent manner (Ussher et al., 2014a). Therefore, we tested if either pathway, or a combination of these signals, could induce a cytotoxic phenotype within MAIT cells.

THP1 cell lines were pre-exposed to PFA-fixed *E. coli*, and then cultured with enriched CD8+ T cells overnight, after which the cytotoxic profile of MAIT cells was evaluated. MAIT cells degranulated extensively in response to *E. coli* as measured by CD107a expression (Figure 3-3A; 66.3%, $P<0.0001$). This was almost completely blocked by an anti-MR1-blocking antibody (20.9%; $P<0.0001$), while blocking IL-12 or IL-18 had minimal effect on the degranulation of the cells.

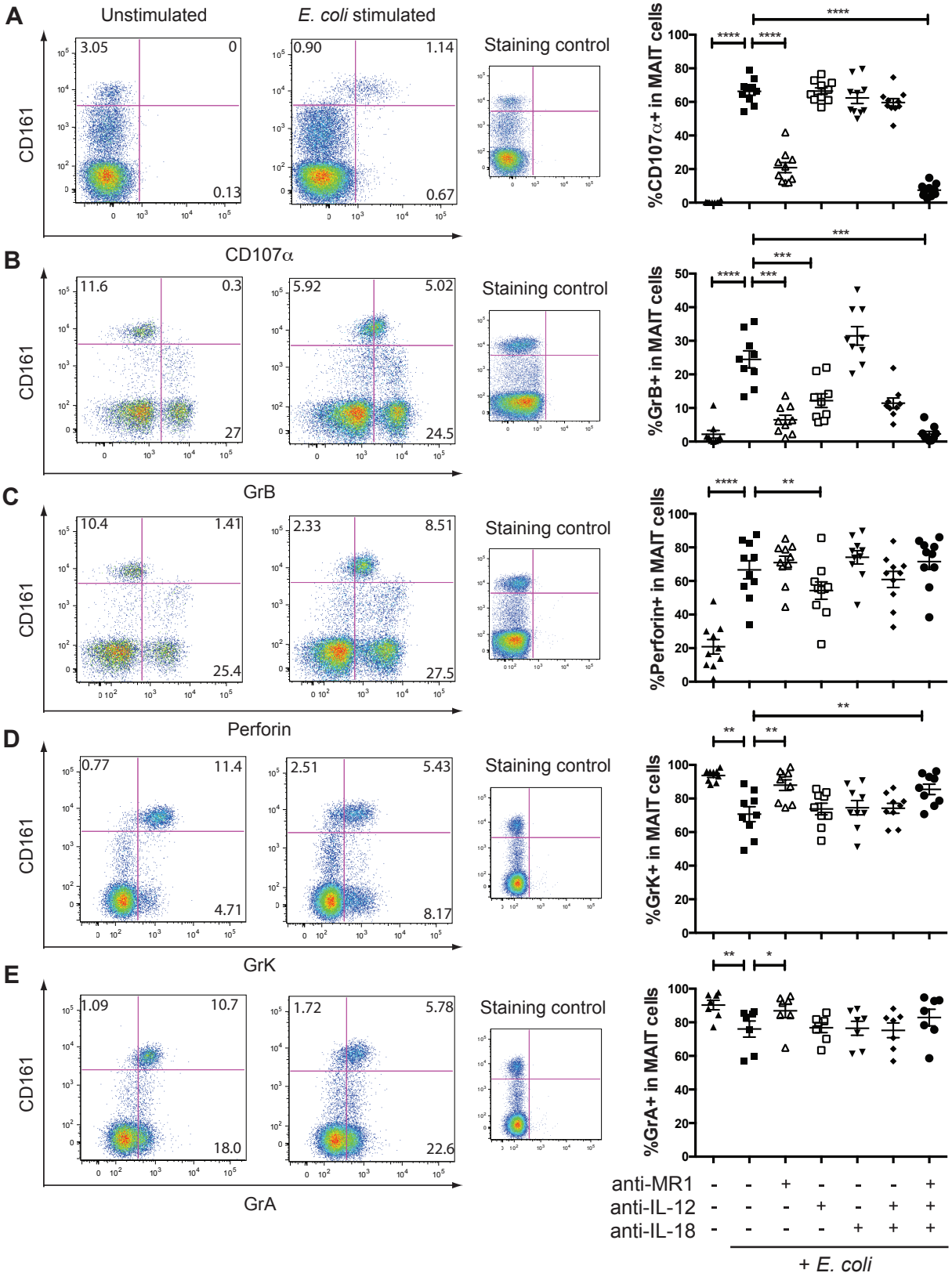


Figure 3-3. Bacterial stimulation leads to degranulation and changes in cytotoxic profile of MAIT cells. Enriched CD8+ T cells were cocultured with THP1 cells exposed to *E. coli*, in the presence or absence of blocking antibodies against MR1, IL-12, IL-18 or isotype controls, and assayed for the expression of A) CD107α, B) GrB, C) Perforin, D) GrK, and E) GrA. Representative plots gated on CD8+ T cells are shown on the left panel and cumulative data on the right panel for each marker, with bars indicating mean ± S.E.M (n=7-10). Staining control shows isotype control (conjugated with matched fluorochromes) used for gating for each marker. (Staining control for D and E are the same). *P<0.05, **P<0.01, ***P<0.001, ****P<0.0001, ns=non-significant by repeated measures one way ANOVA, with Bonferroni's multiple comparisons test.

Resting MAIT cells had characteristically low expression of GrB and perforin. However, the frequency of MAIT cells expressing GrB increased to ~35% in response to *E. coli* (P<0.0001; Figure 3-3B). Importantly, the addition of either anti-MR1-blocking antibody, or IL-12-blocking antibody, significantly reduced the induction of GrB (6.5%, P<0.001; 12.2%, P<0.001, respectively), and the combination of anti-MR1, anti-IL-12, and anti-IL-18-blocking antibodies inhibited GrB upregulation completely (2.28%, P<0.001). Confirming the need for a TCR signal, direct stimulation of MAIT cells with anti-CD3/CD28/CD2 beads, but not with anti-CD3 beads or cytokines alone, also led to significant upregulation of GrB (Appendix Figure III-2A). This suggests that TCR signals are necessary for rapid GrB upregulation in response to *E. coli*, and that costimulation either with IL-12 or CD2/CD28 is also required.

Of note, there was a dose-dependent increase of GrB expression with increasing concentrations of *E. coli* (Appendix Figure III-3A, B). At the highest BpC, however, there was no further increase in GrB expression, even though these cells were maximally activated as measured by CD69 expression (Appendix Figure III-3A). This may be due to the downregulation of the TCR upon exposure to high doses of bacteria, as shown by Vα7.2 downregulation, in turn limiting further TCR-mediated upregulation of GrB. There was a loss of the CD161++ population with increasing doses of *E. coli* as previously described (Leeansyah et al., 2013), but there was no loss of CD161 expression from the maximally activated CD69+ MAIT cells (Appendix Figure III-3A). There was no difference in the frequency of MAIT cells or other CD8+ T cell populations when the cells were stained extracellularly or intracellularly for CD161 after activation (data not shown). Therefore, in this activation model, downregulation of CD161 expression on MAIT cells was not observed.

In response to *E. coli*-treated THP1 cells, MAIT cells also upregulated perforin (20.8% versus 66.7%, $P<0.0001$; Figure 3-3C). However, unlike GrB, perforin upregulation could not be blocked by the addition of the MR1-blocking antibody. IL-12-blocking antibody also had only a small effect on the upregulation of perforin (66.7% versus 54.3%; $P<0.01$). Therefore, multiple factors may be contributing to perforin upregulation; indeed, direct stimulation of MAIT cells with IL-7, IL-15, or IL-2 upregulated perforin (Appendix Figure III-2B). This contrasts with the TCR- and costimulation-dependent GrB upregulation described above, and suggests that GrB expression in MAIT cells may be more tightly regulated than perforin.

In contrast to GrB and perforin, the frequency of GrK- and GrA-expressing MAIT cells were both significantly reduced in response to *E. coli* (Figure 3-3D, E), and this loss was blocked by the anti-MR1-antibody. Stimulation of MAIT cells directly with anti-CD3/CD28/CD2 beads or PMA/ionomycin, but not cytokines, also reduced the percentage of MAIT cells expressing GrK, and to a limited extent, GrA, although this did not reach significance (Appendix Figure III-2C, D). There was also no significant increase in GrA or GrK expression as measured by gMFI when cells were directly stimulated with cytokines, such as IL-12+IL-18 (Appendix Figure III-2C, D). Furthermore, there was no significant upregulation of granulysin or FasL when MAIT cells were stimulated with anti-CD3/CD28/CD2 beads or *E. coli* (Appendix Figure III-2E, F). Thus, MAIT cells modify their granule contents upon physiological activation.

3.4.3. Licensed MAIT cells can kill target cells in an MR1-dependent manner

MAIT cells are activated by a broad range of bacteria through recognition of their ligand, a metabolic precursor of riboflavin, presented by MR1 (Kjer-Nielsen et al., 2012). Whether this recognition leads to cytotoxicity, and what mechanisms are

involved, have not been probed in detail. Furthermore, when administered to target cells, GrA and GrK, expressed by resting MAIT cells, have been suggested not to induce apoptosis, while GrB, not expressed by resting MAIT cells, induces apoptosis at equivalent concentrations (Joeckel et al., 2011; Metkar et al., 2008).

To test the capacity of *ex vivo* MAIT cells to kill target cells, a flow cytometry-based killing assay was developed, based on the published FATAL assay (Sheehy et al., 2001). Briefly, EBV-transformed B cell lines (BCLs) were either incubated with PFA-fixed *E. coli* or sterility control overnight and stained with CFSE and CTV dyes, respectively. These were mixed at a 1:1 ratio and cocultured with enriched CD8+ T cells at various E:T ratios. Specific killing of CFSE+ target cells, but not CTV+ control cells, was then calculated based on the ratio of CFSE+ and CTV+ cells in wells without effector cells (see Materials and Methods). Additionally, CD107a externalization by the CD161++CD8+ T cells was measured. Therefore, by combining the FATAL assay with the LAMP-1 assay (Betts et al., 2003) and phenotyping the effector cells, this assay allows the identification of the cell population responsible for cytolysis; thus, removing the necessity to sort enrich specific or rare effector populations. Using this modified FATAL assay, resting MAIT cells were found to only kill up to 30% of *E. coli*-treated BCLs even the highest E:T ratios, in an MR1-dependent manner (Figure 3-4A, B).

Next, whether pre-activation of MAIT cells would enhance their killing capacity was investigated. PBMCs isolated from the same donors were either pre-stimulated with PFA-fixed *E. coli* for 6 days (licensed) or freshly thawed (*ex vivo*); both were enriched for CD8+ T cells in parallel. Licensed MAIT cells were significantly more cytotoxic compared to *ex vivo* MAIT cells, killing up to 70% of *E. coli*-treated BCLs ($P<0.0001$; Figure 3-4C, D). The frequency of CD161++CD8+ T cells did not significantly differ between *ex vivo* and licensed cells (Appendix Figure III-4A), and indeed post-hoc

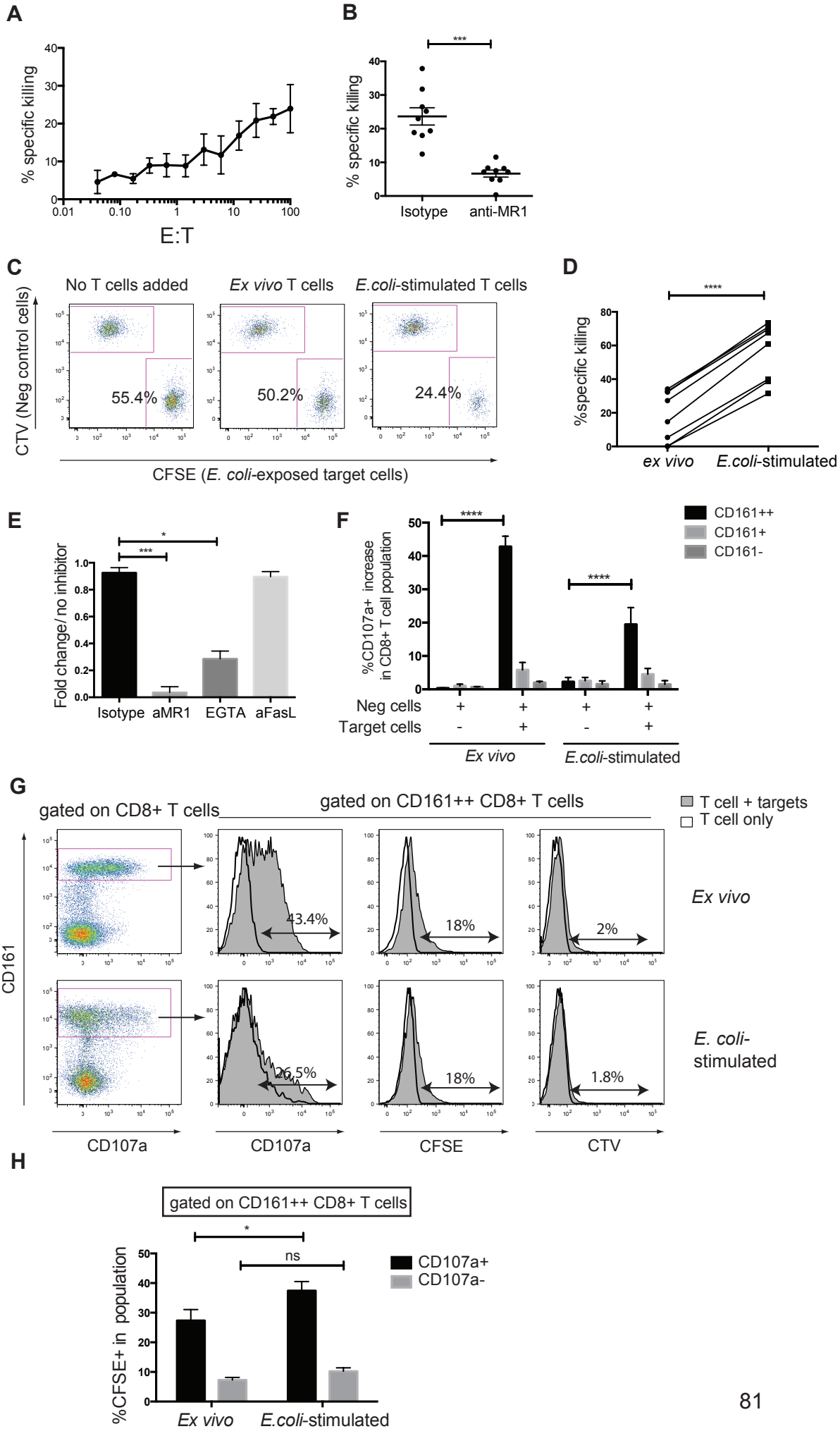

A
% specific killing
E:T
B
% specific killing
Isotype
anti-MR1
C
No T cells added
Ex vivo T cells
E.coli-stimulated T cells
CTV (Neg control cells)
55.4%
50.2%
24.4%
CFSE (E. coli-exposed target cells)
D
%specific killing
ex vivo
E.coli-stimulated
E
Fold change/ no inhibitor
Isotype
aMR1
EGTA
aFasL
F
CD161++
CD161+
CD161-
%CD107a+ increase in CD8+ T cell population
Neg cells
Target cells
Ex vivo
E.coli-stimulated
G
gated on CD8+ T cells
gated on CD161++ CD8+ T cells
T cell + targets
T cell only
CD161
43.4%
18%
2%
26.5%
18%
1.8%
Ex vivo
E. coli-stimulated
CD107a
CD107a
CFSE
CTV
H
gated on CD161++ CD8+ T cells
ns
CD107a+
CD107a-
%CFSE+ in population
Ex vivo
E.coli-stimulated

Figure 3-4. *E. coli*-stimulated MAIT cells can efficiently kill target cells in an MR1- and degranulation-dependent manner. BCLs were either incubated with PFA-fixed *E. coli* or sterility control and stained with CFSE and CTV dyes, respectively, and co-cultured with enriched CD8+ T cells. A) Percentage of specific killing of target BCLs by *ex vivo* MAIT cells at various E:T ratios. Mean ± S.E.M of duplicate results of three independent experiments shown (n=10). B) %specific killing of target cells by *ex vivo* MAIT cells with and without an anti-MR1 blocking antibody at E:T=50:1. (n=9) C) Example plots showing the frequency of live *E. coli*-exposed BCLs and negative control BCLs without effector cells (left), with *ex vivo* MAIT cells (middle), or with MAIT cells stimulated with *E. coli* for 6 days (right), added at E:T=10:1. D) %specific killing of target cells by *ex vivo* and *E. coli*-stimulated MAIT cells from the same donors at E:T=10:1. Mean ± S.E.M of duplicate results of three independent experiments are shown (n=8). E) Inhibition of killing at E:T=10:1 by *E. coli*-stimulated MAIT cells in presence of anti-MR1 antibody, EGTA, or anti-FasL antibody, compared to killing with no inhibitor. Repeated measures one-way ANOVA, with Bonferroni's multiple comparisons test. (n=5) F) Cumulative data showing increase in %CD107α+ cells in indicated CD8+ T cell populations, compared to wells with T cells only. Analyzed by two-way ANOVA, comparing increase in CD107α + expressing cells when target cells are added, within each CD8+ T cell population, with Bonferroni's multiple comparisons test. CFSE+ *E. coli*-exposed BCL = Target cells, CTV+ negative control BCL = Neg cells. (n=8) G) Representative plots of *ex vivo* and *E. coli*-stimulated CD8+ T cells from the killing assays. Histograms showing expression of CD107α, and CFSE and CTV acquired through trogocytosis in CD161++CD8+ T cells. H) Trogocytosis of CFSE from *E. coli*-exposed BCL membranes onto degranulating CD161++CD8+ T cells (n=8). Analyzed by two-way ANOVA, comparing wells with *ex vivo* and *E. coli*-stimulated cells, with Bonferroni's multiple comparisons test. For all tests, ***P<0.0001, ***P<0.001, **P<0.01, *P<0.05, ns=non-significant.

adjustment of the E:T to the actual ratio of CD161++CD8+ T cells to target cells showed licensed MAIT cells were more cytotoxic on a per cell basis (Appendix Figure III-4B). Target cell killing by the *E. coli*-stimulated CD8+ T cells was abolished with the addition of the anti-MR1 blocking antibody, confirming MAIT cells were mediating the killing (Figure 3-4E). Inhibition of degranulation and perforin polymerization with EGTA also prevented killing, suggesting this process was degranulation-mediated (Figure 3-4E). Blocking FasL did not affect this killing, consistent with the low FasL expression on activated MAIT cells (Appendix Figure III-2F).

Only the CD161++CD8+ T cell population degranulated in response to *E. coli*-treated BCL, confirming that this population was responsible for target cell killing (Figure 3-

4F, G). Interestingly, following immunological synapse formation between effector cells and their target cells, effector cells can take membrane patches from their target cells, a phenomenon known as trogocytosis, and this can be used to quantify cell-cell interactions (Poupot et al., 2008). As the cytotoxicity assay here uses two amine-reactive dyes that bind to both cytosolic and membrane proteins, which are less prone to dye transfer than the lipophilic dye used in the original FATAL assay (Sheehy et al., 2001), trogocytosis of the target cell membrane by the T cells could be quantified from the frequency of CFSE+ and CTV+ cells, indicating prior synapse formation. This showed that CD161++CD8+ T cells made immunological synapses with the CFSE+ target cells, and not with the CTV+ control cells (Figure 3-4G; Appendix III-4C). *Ex vivo* CD161++CD8+ T cells degranulated more readily than *E. coli*-stimulated CD161++CD8+ T cells in response to the same target cells (Figure 3-4F), yet were less cytotoxic than the latter, consistent with the hypothesis that MAIT cells needed licensing by granzyme exchange to become highly cytotoxic. When CD107a+ cells within CD161++CD8+ T cells were compared, the frequency of cells that had acquired CFSE was significantly higher in the *E. coli*-stimulated, licensed cells than in *ex vivo* cells (Figure 3-4H), suggesting there is also increased synapse formation between the target cells and *E. coli*-stimulated CD161++CD8+ T cells compared to *ex vivo* CD161++CD8+ T cells.

Overall these data suggest that *E. coli*-stimulated, licensed MAIT cells maintain the capacity to degranulate and possess enhanced killing capacity compared to *ex vivo* MAIT cells.

3.4.4. Rapid GrB upregulation in MAIT cells is associated with Blimp1 and T-bet expression

Next, the kinetics of MAIT cell licensing was probed by examining GrB and perforin upregulation in response to *E. coli*. MAIT cells showed no change in the expression of GrB and perforin within the first 6 hours of stimulation (Figure 3-5A, B), but dramatically upregulated these effector molecules by 18 hours, with most cells expressing GrB and perforin by 30 hours. This upregulation was specific to the MAIT cell population, the kinetics of which was similar to anti-CD3/CD28/CD2 stimulation (Figure 3-5C, D). Of note, although GrB could not be upregulated by cytokines alone in a 16 hour culture, and required TCR stimulation (Appendix III-2A), long-term MAIT cell stimulation with cytokines such as IL-12, IL-15, and IL-21 for 6 days induced significant upregulation of GrB, comparable to TCR stimulation (Appendix III-5A, B).

The transcription factors T-bet and Blimp1 are both important for GrB expression in CD8+ T cells (Cruz-Guilloty et al., 2009; Kallies et al., 2011). To investigate whether these transcription factors are associated with GrB upregulation in MAIT cells, PBMCs were stimulated with *E. coli* for 24 hours, with or without the addition of MR1- and IL-12-blocking antibodies. As expected from the THP1 coculture model, MAIT cells stimulated with *E. coli* upregulated GrB (Figure 3-5E, F), but also coexpressed T-bet and Blimp1 in an MR1- and IL-12-dependent manner (Figure 3-5G). Cells expressing T-bet or Blimp1 were more likely to express GrB (Figure 3-5H, I), supporting a role for these transcription factors in the upregulation of GrB in MAIT cells.

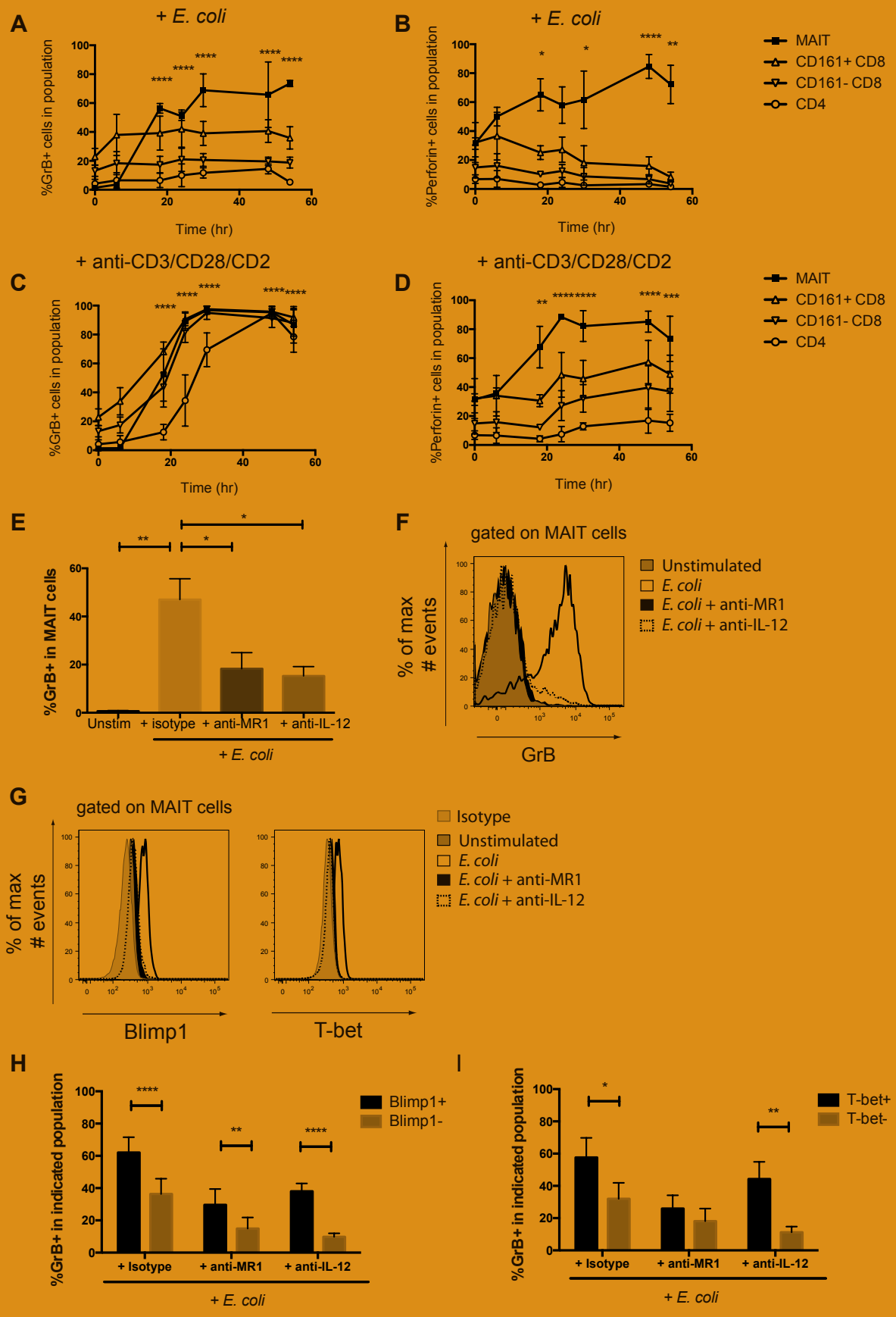

A
+ E. coli
%GrB+ cells in population
Time (hr)
B
+ E. coli
%Perforin+ cells in population
Time (hr)
MAIT
CD161+ CD8
CD161- CD8
CD4
C
+ anti-CD3/CD28/CD2
%GrB+ cells in population
Time (hr)
D
+ anti-CD3/CD28/CD2
%Perforin+ cells in population
Time (hr)
MAIT
CD161+ CD8
CD161- CD8
CD4
E
%GrB+ in MAIT cells
Unstim
+ isotype
+ anti-MR1
+ anti-IL-12
+ E. coli
F
gated on MAIT cells
% of max
# events
GrB
Unstimulated
E. coli
E. coli + anti-MR1
E. coli + anti-IL-12
G
gated on MAIT cells
% of max
# events
Blimp1
T-bet
Isotype
Unstimulated
E. coli
E. coli + anti-MR1
E. coli + anti-IL-12
H
%GrB+ in indicated population
Blimp1+
Blimp1-
+ Isotype
+ anti-MR1
+ anti-IL-12
+ E. coli
I
%GrB+ in indicated population
T-bet+
T-bet-
+ Isotype
+ anti-MR1
+ anti-IL-12
+ E. coli

Figure 3-5. GrB and perforin upregulation in *E. coli*-stimulated MAIT cells is rapid and associated with Blimp1 and T-bet expression. A-D) PBMCs were stimulated with A, B) PFA-fixed *E. coli*, or C, D) anti-CD3/CD28/CD2 coated beads, and stained for GrB and perforin at the indicated time points (n=3). Asterisks (*) indicate significant increases in effector molecules in MAIT cells compared to the unstimulated controls, by a two-way ANOVA, with Bonferroni's multiple comparisons test. E-I) PBMCs were stimulated with PFA-fixed *E. coli* for 24 hours with and without blocking antibodies to MR1 and IL-12, and stained for GrB, T-bet, and Blimp1 (n=7). E) Cumulative data for frequency of GrB expressing MAIT cells and F) representative example of GrB expression in MAIT cells after *E. coli* stimulation, ± blocking antibodies to MR1 or IL-12. One-way ANOVA, Bonferroni's multiple comparisons test. G) Representative T-bet and Blimp1 expression in MAIT cells unstimulated or stimulated with PFA-fixed *E. coli* ± blocking antibodies to MR1 or IL-12. H) Frequency of GrB expressing cells in T-bet+ or T-bet- MAIT cells. I) Frequency of GrB expressing cells in Blimp1+ or Blimp1- MAIT cells. Results analyzed by two-way ANOVA with Bonferroni's multiple comparisons test. Bars indicate mean ± S.E.M. *P<0.05, **P<0.01, ***P<0.001, ****P<0.0001, ns=non-significant.

3.4.5. MAIT cells readily proliferate in response to *E. coli* and maintain a highly cytotoxic profile

Finally, we asked how the granule content of MAIT cells changed during proliferation. MAIT cells have been previously described to be hypoproliferative (Dusseaux et al., 2011; Le Bourhis et al., 2010). However, when CTV-labeled PBMCs were cultured with PFA-fixed *E. coli* for 6 days, MAIT cells proliferated in a dose-dependent manner to *E. coli* (Figure 3-6A, B). The proliferation of MAIT cells was confirmed by Ki67 staining (Figure 3-6C), and was inducible when enriched CD8+ T cells were directly stimulated with *E. coli*-treated THP1s (Appendix Figure III-6A), confirming this is a specific effect and not bystander proliferation. Interestingly, although most cells remained CD161++ (Figure 3-6A), CD161 was downregulated on MAIT cells with increasing rounds of cell divisions (Appendix Figure III-6B). To investigate the relative contributions of the TCR signal and innate cytokines for MAIT cell proliferation, blocking antibodies to MR1 or IL-12 and IL-18 were added. Addition of the MR1-blocking antibody, but not IL-12- or IL-18-blocking antibodies, significantly

inhibited MAIT cell proliferation (Figure 3-6D), demonstrating that *E. coli*-induced MAIT cell expansion is largely TCR-dependent. Of note, proliferation of MAIT cells at 10BpC could not be completely inhibited by the anti-MR1 blocking antibody, suggesting that other cytokines may be contributing to their proliferation. Indeed, CD161++CD8+ T cells readily proliferated in response to IL-2, IL-15, or IL-12 in the absence of exogenous TCR stimulation (Appendix Figure III-7).

To investigate how the cytotoxic profile of MAIT cells changed with proliferation, PFA-fixed *E. coli* were added to CTV-stained PBMCs, and after 6 days, GrB, perforin, GrK, and GrA expression assessed. MAIT cells cultured with *E. coli* acquired a highly cytotoxic profile; ~100% of cells expressed GrB and ~90% of cells expressed perforin (Figure 3-6E). GrB and perforin expression did not require proliferation, as CTV^{high}, non-proliferating cells also expressed high levels of both cytotoxic mediators. Additionally, although resting MAIT cells all express GrA, stimulated MAIT cells upregulated GrA as measured by gMFI (Figure 3-6F). In turn, there was a significant loss of GrK expression by activated MAIT cells (Figure 3-6F).

Therefore, MAIT cells are highly proliferative to antigenic and cytokine stimuli *in vitro*, and their activation, irrespective of proliferation, is associated with increased expression of perforin, GrB, and GrA, and decreased expression of GrK.

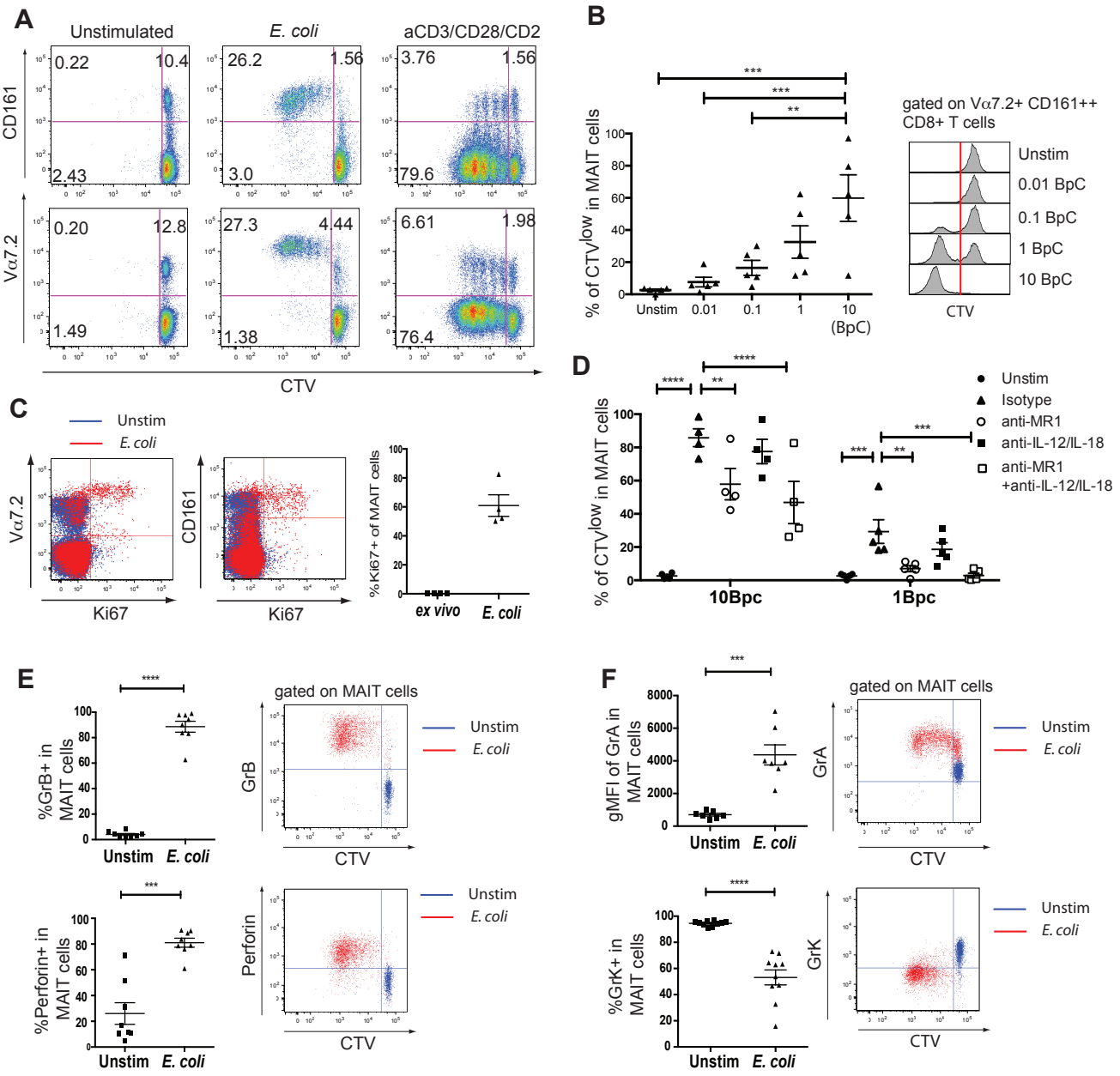


Figure 3-6. MAIT cells are readily proliferative in response to *E. coli* and maintain a highly cytotoxic profile. PBMCs from healthy donors were CTV-labeled and cultured with PFA-fixed *E. coli* for 6 days. BpC = bacteria per cell ratio. A) Representative plot showing dilution of CTV against CD161 expression (upper panel) and Vα7.2 expression (lower panel) at 10 BpC or with anti-CD3/CD28/CD2 beads, gated on CD8+ T cells. B) Cumulative data (left) and representative flow cytometry histograms are shown for each BpC. One-way ANOVA, with Bonferroni's multiple comparisons test. C) Representative plot (left) and cumulative data (right) showing Ki67 staining in CD8+ T cells after *E. coli*-stimulation at 10 BpC (n=4). D) Proliferation of MAIT cells in response to *E. coli* with anti-MR1, IL-12, and IL-18 blocking antibodies at the indicated BpCs. Results pooled from two independent experiments and analyzed by two way ANOVA, with Bonferroni's multiple comparisons test. E) GrB and perforin, and F) GrA and GrK expression in CTV labeled-MAIT cells following *E. coli* stimulation for 6 days. Cumulative data (left) and representative staining is shown (right). Gating for granzymes and perforin based on isotype controls. Results analyzed by paired t-test (n=8). Bars indicate mean ± S.E.M. *P<0.05, **P<0.01, ***P<0.001, ****P<0.0001, ns=non-significant.

3.5. Discussion

In this study, the regulation of MAIT cell cytotoxicity and their ability to specifically kill target cells was investigated. This revealed that the unique cytotoxic granule content of resting MAIT cells changes dramatically upon activation, licensing these cells to kill target cells with greater efficiency.

At rest, almost all CD161++CD8+T cells, including MAIT cells and non-MAIT Vα7.2− T cells, expressed GrA and GrK within cytotoxic granules and, therefore, are poised to release these immediately upon degranulation. In contrast, they express low levels of perforin, no GrB, and little granulysin or FasL. This is consistent with the effector memory phenotype of MAIT cells; while effector cells can exhibit immediate lytic function following LCMV infection, memory T cells required exposure to antigen to acquire cytotoxicity (Bachmann et al., 1999; Wherry et al., 2003). *Ex vivo* MAIT cells were able to specifically kill a small fraction of the *E. coli*-treated target cells in an overnight killing assay. Whether this is mediated by GrA and GrK initially released during the degranulation of MAIT cells, or by GrB induced following activation, has not been fully investigated here. As TCR-mediated upregulation of GrB only occurred between 6 and 18 hours of stimulation, preliminary experiments based on a 4 hour killing assay was also performed (Appendix III-4D, E). This suggested that there is a lack of killing by *ex vivo* CD8+ T cells, and the addition of an anti-MR1 antibody did not affect this killing, while *E. coli*-stimulated CD8+ T cells could mediate MR1-dependent killing. Therefore, *ex vivo* MAIT cells are inefficient killers, despite preformed GrK and GrA in their granules, and require the upregulation of GrB to mediate efficient killing.

Of note, the killing assay performed in this study uses mixed effector populations that may have impacted the linearity of the assay. For example, at high E:T ratios, the

greater number of non-MAIT CD8+ T cells may have stochastically inhibited the interaction between MAIT cells and their target cells, as there was a higher probability of MAIT cells encountering non-MAIT CD8+ T cells than target cells, compared to MAIT cells at low E:T ratios. Furthermore, not all the killing observed in the 4 hour killing assay using the licensed MAIT cells was abolished in the presence of an anti-MR1 blocking antibody (Appendix III-4D, E), and 10% specific killing was observed in the presence of *ex vivo* CD8+ T cells which was could not be blocked by an anti-MR1 antibody. Whether this residual killing is background killing mediated by other CD8+ T cells, or whether MAIT cells may be killing the target cells in a TCR-independent manner, needs to be further clarified by repeating the assays using FACS-sorted MAIT cells.

GrA and GrK have been suggested to have non-cytotoxic functions mediating inflammation (Cooper et al., 2011; Joeckel et al., 2011; Metkar et al., 2008), directly activating monocytes to produce proinflammatory cytokines such as IL-1β and TNFα (Metkar et al., 2008). GrK also binds to Gram-negative bacteria and LPS, synergistically increasing LPS-induced release of proinflammatory cytokines (Wensink et al., 2014). Interestingly, GrA release by γδ T cells is critical in the control of BCG growth by inducing TNFα production in infected macrophages (Spencer et al., 2013), and similarly, degranulation of resting MAIT cells may assist in the control of bacterial infection through phagocyte activation, rather than through lysis. Once GrA and GrK are released from the cell, the signals that may aid the replenishment of the granules are unknown. Of note, direct stimulation of MAIT cells with various cytokines such as IL-12+IL-18 did not significantly increase the amount of GrA or GrK expressed by *ex vivo* MAIT cells as measured by gMFI, but long-term culture with *E. coli* induced a significant upregulation of GrA in MAIT cells, suggesting that GrA can be replenished through continued antigenic stimulation.

Following antigen exposure, MAIT cells rapidly transition to a more classical cytotoxic effector cell, displaying high levels of GrB and perforin. This is consistent with previous work showing that activated MAIT cells can secrete GrB (Dusseaux et al., 2011), and that GrB expression in CD8+ T cells positively correlates with recent antigenic stimulation (Harari et al., 2009; Migueles et al., 2008; Nowacki et al., 2007). Early upregulation of GrB by activated MAIT cells was dependent upon engagement of the TCR with MR1 and IL-12 or costimulation through CD2/CD28. This is in contrast to perforin, which could be induced by multiple cytokines. Of note, long-term stimulation of MAIT cells with cytokines such as IL-12 and IL-15 could also induce GrB, but not in shorter cultures, in line with studies using IL-7 or IL-15 to induce GrB expression in MAIT cells (Leeansyah et al., 2015; Sattler et al., 2015). Indeed, *in vivo* administration of exogenous IL-15 induces GrB in murine effector memory CD8+ T cells (Liu et al., 2002; Yajima et al., 2005). This suggests that GrB upregulation either requires antigenic stimulation or persistent stimulation with cytokines, which may be indicative of ongoing inflammation. Release of GrB by MAIT cells, however, is ultimately dependent on MR1. Interestingly, a recent study has demonstrated that GrB upregulation of MAIT cells in response to *E. coli* is defective in HIV patients (Leeansyah et al., 2015). Furthermore, GrB has been shown to be upregulated in MAIT cells from obese patients, and only returned to normal levels 6 months after bariatric surgery (Magalhaes et al., 2015). Therefore, GrB may be a useful marker for MAIT cell activation.

Amongst the granzymes, GrB is the most potent, especially in humans (Kaiserman et al., 2006). The tight regulation of MAIT cell cytotoxicity may therefore be important in limiting immune-mediated pathology. The data here also suggest that the transcription factors Blimp1 and T-bet may be involved in this regulation of GrB expression in MAIT cells. In conventional CD8+ T cells, T-bet and Blimp1 are independently regulated, with Blimp1-deficiency resulting in a failure to produce GrB

(Cruz-Guilloty et al., 2009; Kallies et al., 2009). Interestingly, a murine homologue of Blimp1 called Hobit has also been shown induce GrB expression in iNKT cells (van Gisbergen et al., 2012), which also do not express GrB and perforin at rest (Farr et al., 2014). Whether Blimp1 and T-bet plays a similarly critical role in GrB expression in MAIT cells remains to be determined.

Following GrB and perforin upregulation, the highly cytotoxic, licensed MAIT cells were able to kill up to 70% of *E. coli*-treated BCLs. While both *ex vivo* and licensed MAIT cells degranulated upon exposure to target cells, *ex vivo* MAIT cells showed significantly less cytotoxicity compared to licensed MAIT cells, consistent with changes in granule content with activation. Blocking experiments showed killing by these licensed MAIT cells was dependent on TCR-mediated degranulation, and not Fas-mediated killing, which is important in iNKT cell cytotoxicity (Wingender et al., 2010). The ability of activated MAIT cells to kill target cells may play an important role in bacterial control *in vivo*. Indeed, MAIT cells have been demonstrated to kill epithelial cells infected with *S. flexneri* (Martin et al., 2013), which may be important for preventing cytosolic bacteria from crossing the mucosal barrier. Other intracellular bacteria such as *M. tuberculosis* can replicate in macrophages and B cells, surviving inside a segregated endosomal compartment (Pieters, 2008; Souwer et al., 2012). Thus, efficient killing of mycobacteria-infected THP1 cells, as demonstrated recently (Lepore et al., 2014), may lead to enhanced clearance of such bacteria. Interestingly, *in vitro* control of bacterial growth by murine MAIT cells was mediated by cytokine production, and not by infected-cell lysis (Chua et al., 2012; Meierovics et al., 2013). Murine GrB is less cytotoxic than human GrB (Kaiserman et al., 2006), and cytokine-induced nitric oxide has been shown to be critical for mycobacterial control in mice, but its role is controversial in humans (Yang et al., 2009). Furthermore, the majority of MAIT cells are CD8+ in humans, and their cytotoxicity is regulated in a manner to conventional cytotoxic CD8+ T cells, while

murine MAIT cells are DN and CD4+ (Reantragoon et al., 2013). Therefore, it is possible that direct killing of cells by MAIT cells plays a lesser role in the murine models of infections than in humans. *In vitro* bacterial growth control assays inhibiting GrB activity, as well as assessing the expression of GrB in MAIT cells from sites of infection, such as in the lungs of *M. tuberculosis*-infected patients, may be able to demonstrate a role for GrB in bacterial control in humans. Successful killing of infected cells will ultimately depend upon various factors including ligand availability for MR1-loading, inhibitors of cytolysis expressed by the infected cell, and inhibitory/costimulatory signals (Toossi et al., 2011; Willberg et al., 2007).

Lastly, although MAIT cells have been suggested to be hypoproliferative (Dusseaux et al., 2011), in this study, adult MAIT cells were demonstrated to proliferate in response to cytokines as well as TCR stimulation. Furthermore, MAIT cell expansion could be induced through *E. coli*-stimulation in an MR1-dependent manner, in line with recent studies showing *in vitro* MAIT cell proliferation in response to bacteria or the MAIT cell ligand, 5-OP-RU (Leeansyah et al., 2014; Rahimpour et al., 2015). Interestingly, MAIT cells downregulated CD161 with increasing rounds of cell division (Appendix III-6B), in agreement with previous observations that MAIT cell clones can be CD161− (Gold et al., 2010). As CD161 costimulates T cell proliferation (Germain et al., 2011), downregulation of CD161 with proliferation may be beneficial for the continued survival of the cells by limiting activation-induced cell death (AICD). Additionally, a greater proportion of CD161++CD8+ T cells, including the Vα7.2+ MAIT cells, proliferated when stimulated with IL-2 or IL-15 compared to CD161+CD8+ T cells (Appendix III-7). However, PHA induced limited proliferation of MAIT cells, despite high activation. Given the sensitivity of MAIT cells to AICD (Cosgrove et al., 2013; Gérart et al., 2013), MAIT cell proliferation most likely depends on a balance between expansion and AICD, and may explain the variation between MAIT cell proliferation studies. *In vivo*, once MAIT cells are recruited to sites

of infection/inflammation, their functional impact, including cytotoxic activity, may be further perpetuated by their proliferation.

3.6. Summary

1. *Ex vivo* peripheral blood MAIT cells have a unique cytotoxic profile within CD8+ T cells: GrA+, GrK+, perforin^{low}, GrB−
2. MAIT cells readily degranulate and rapidly upregulate GrB and perforin expression in response to bacterial stimulation. The early expression of GrB in this model was dependent on MR1 and required costimulation by IL-12. Degranulation was completely MR1 dependent
3. MAIT cells expressing high levels of GrB and perforin were cytotoxic and induced efficient killing of target cells, compared to *ex vivo* MAIT cells
4. MAIT cells can proliferate readily in response to cytokines and in response to *E. coli* in an MR1-dependent manner

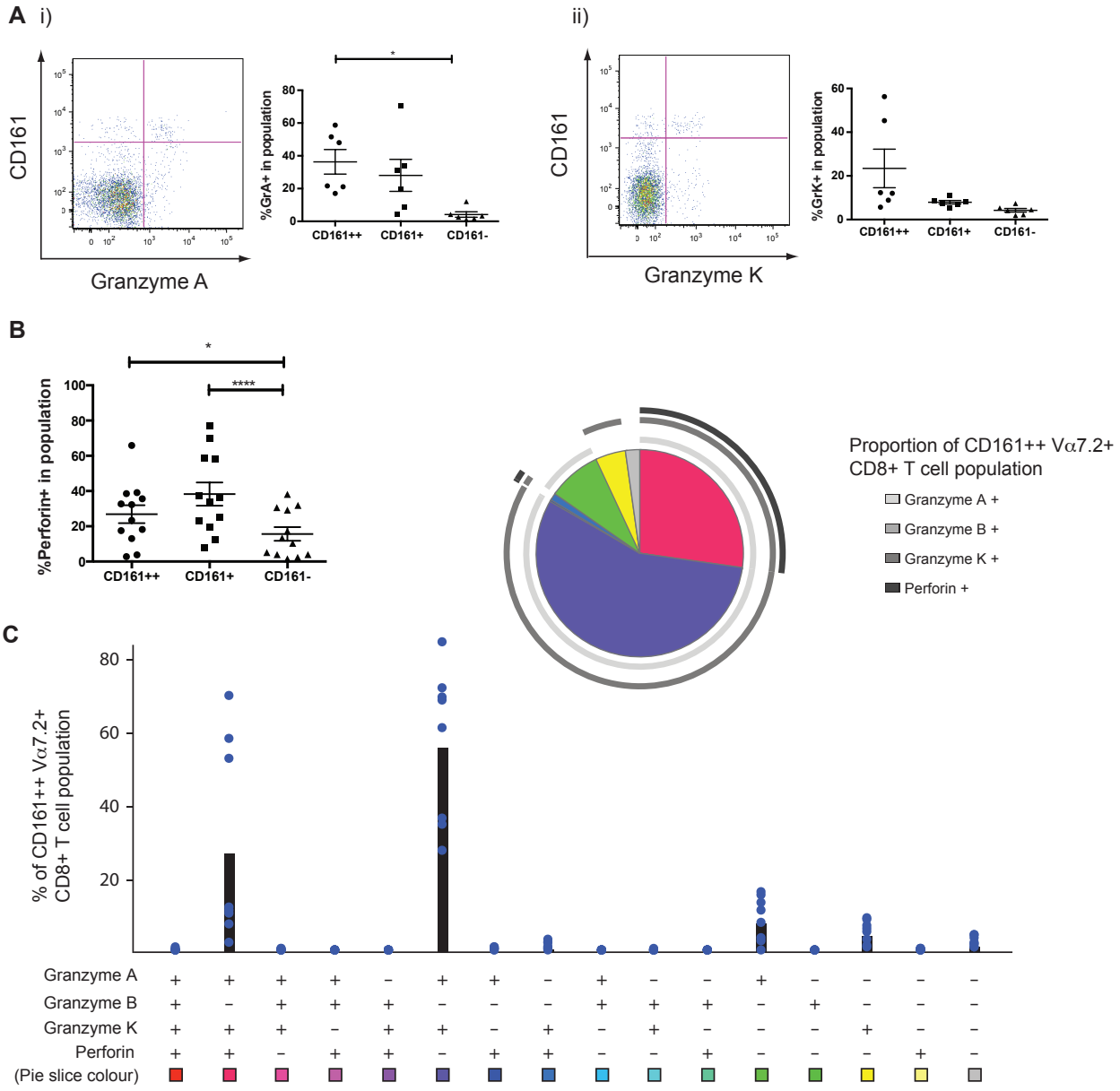
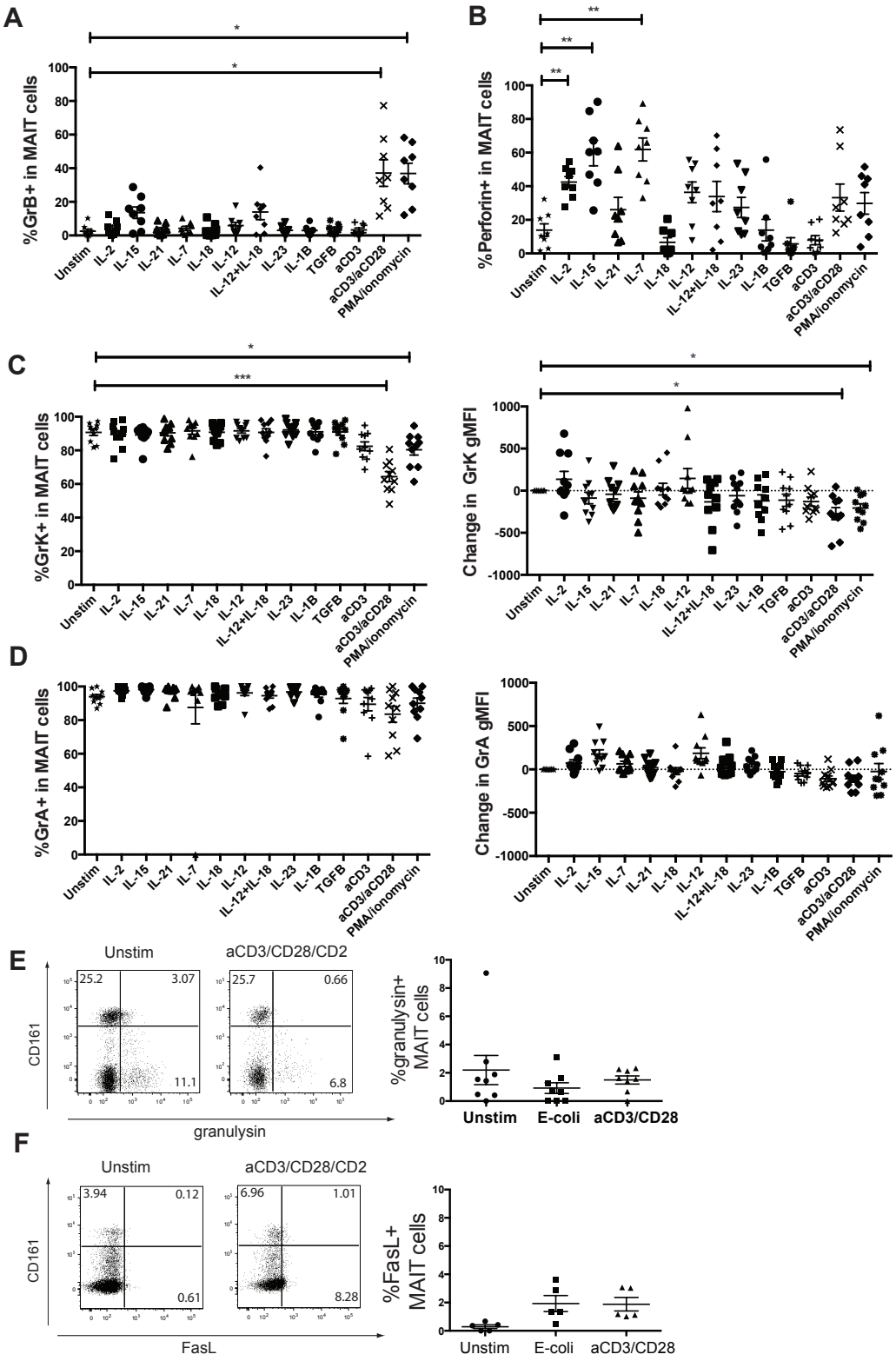


Figure Appendix III-1. GrA and GrK expression in cord blood CD8+ T cells, and simultaneous analysis of cytotoxic-granule composition of adult peripheral blood MAIT cells. A) Frequency of GrA and GrK expressing cells in cord blood CD8+ T cells according to CD161 expression levels. Representative plot and cumulative data for 6 donors is shown. Results shown as mean ± S.E.M, analyzed by repeated measures one way ANOVA, with Bonferroni's multiple comparisons test. B) Frequency of perforin expressing cells in adult peripheral blood CD8+ T cells from healthy donors according to CD161 expression levels. Cumulative data for 12 healthy individuals is shown. Results shown as mean ± S.E.M, analyzed by repeated measures one way ANOVA, with Bonferroni's multiple comparisons test. *P<0.05, ****P<0.0001. C) Simultaneous analysis of cytotoxic-granule composition of MAIT cells in *ex vivo* adult peripheral blood, on the basis of GrA, GrB, GrK, and perforin expression. All the possible combinations of the different markers are shown on the x-axis of the graph, and the percentage of MAIT cells expressing each of these combinations are shown on the y-axis. Each dot represents a healthy donor (n=8). Data is summarized in the pie chart, with each slice corresponding to the average proportion of MAIT cells positive for the combinations of markers shown on the graph.



Appendix Figure III-2. Changes in cytotoxic granule content of MAIT cells with cytokine and TCR-stimulation. Enriched CD8+ T cells were stimulated for 16 hours with the indicated cytokines, anti-CD3- or anti-CD3/CD28/CD2 coated beads, or PMA/ionomycin, and analysed for expression of A) GrB (n=8), B) Perforin (n=8), C) GrK (n=10), or D) GrA (n=10) in MAIT cells. Fold change is calculated from the ratio of the gMFI of GrA or GrK in MAIT cells after stimulation, compared to that of unstimulated MAIT cells. Results analyzed by repeated measures one-way ANOVA with Bonferroni's multiple comparisons test. E, F) Expression of E) granulysin (n=8) and F) intracellular FasL (n=5) in CD8+ T cells after stimulation of PBMCs with *E. coli* or anti-CD3/CD28/CD2 beads for 16 hours. NK cells were used as a positive control for staining. Representative staining (left) and cumulative data (right) is shown. Bars indicate mean ± S.E.M. *P<0.05, **P<0.01, ***P<0.001.

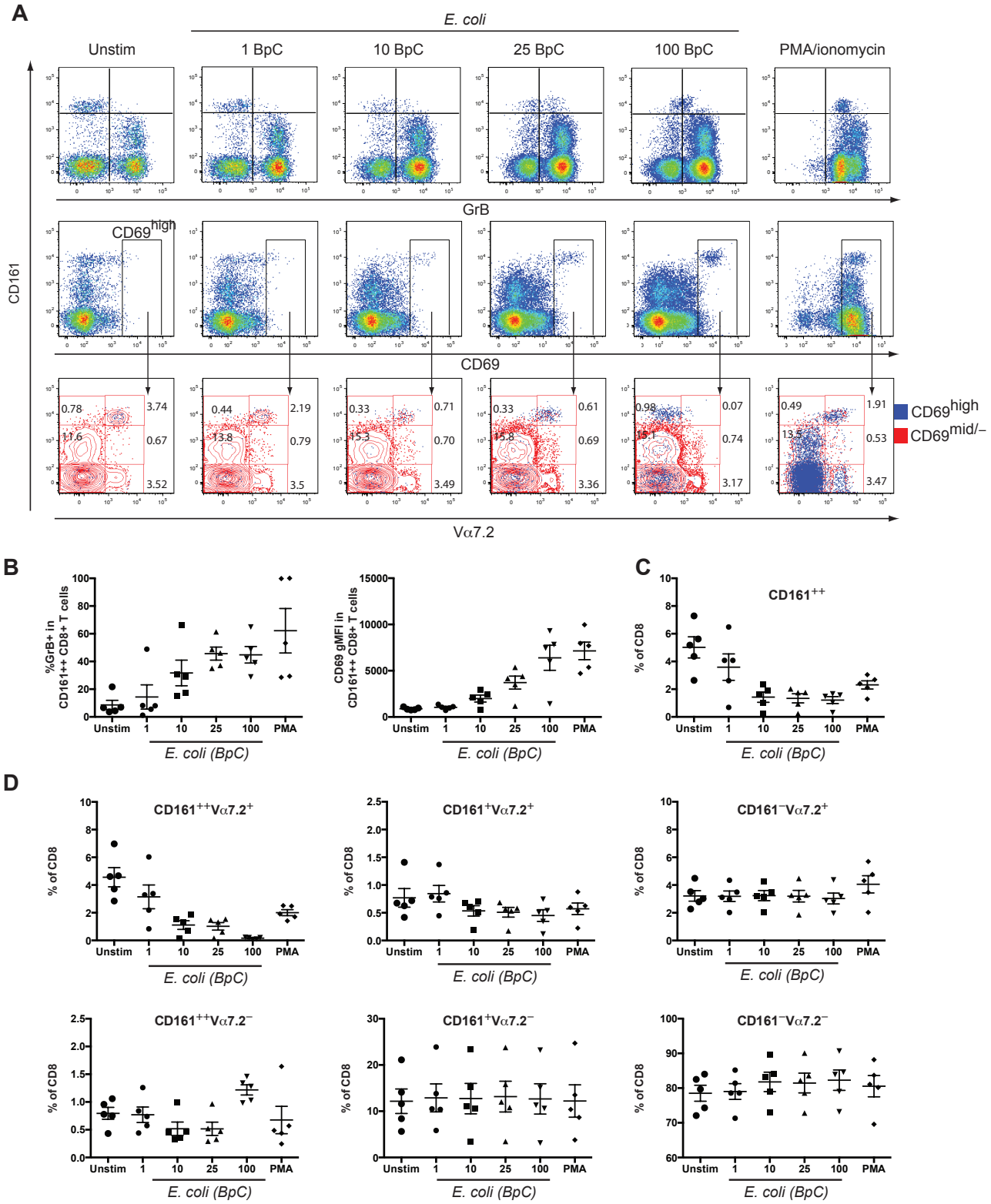
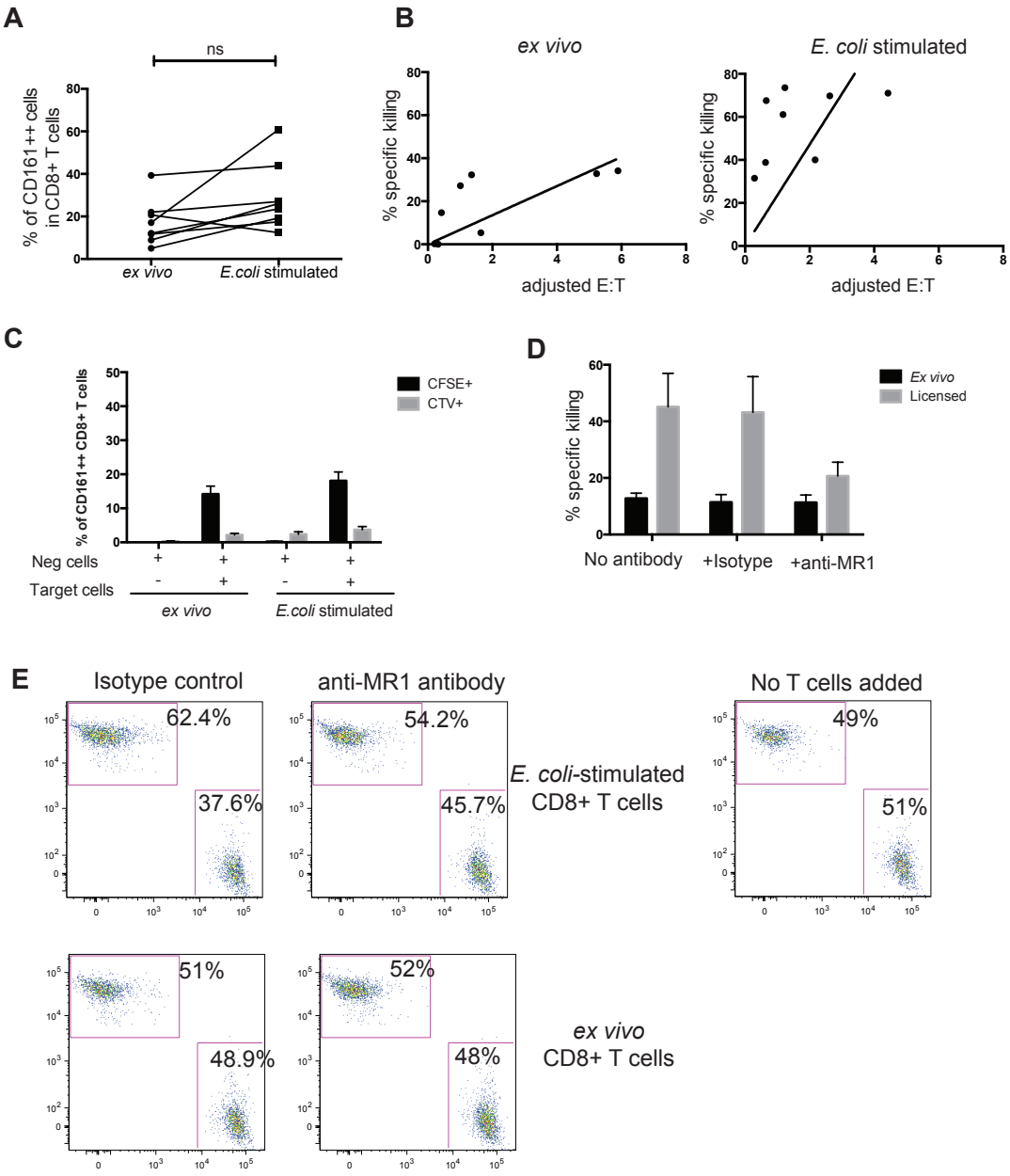
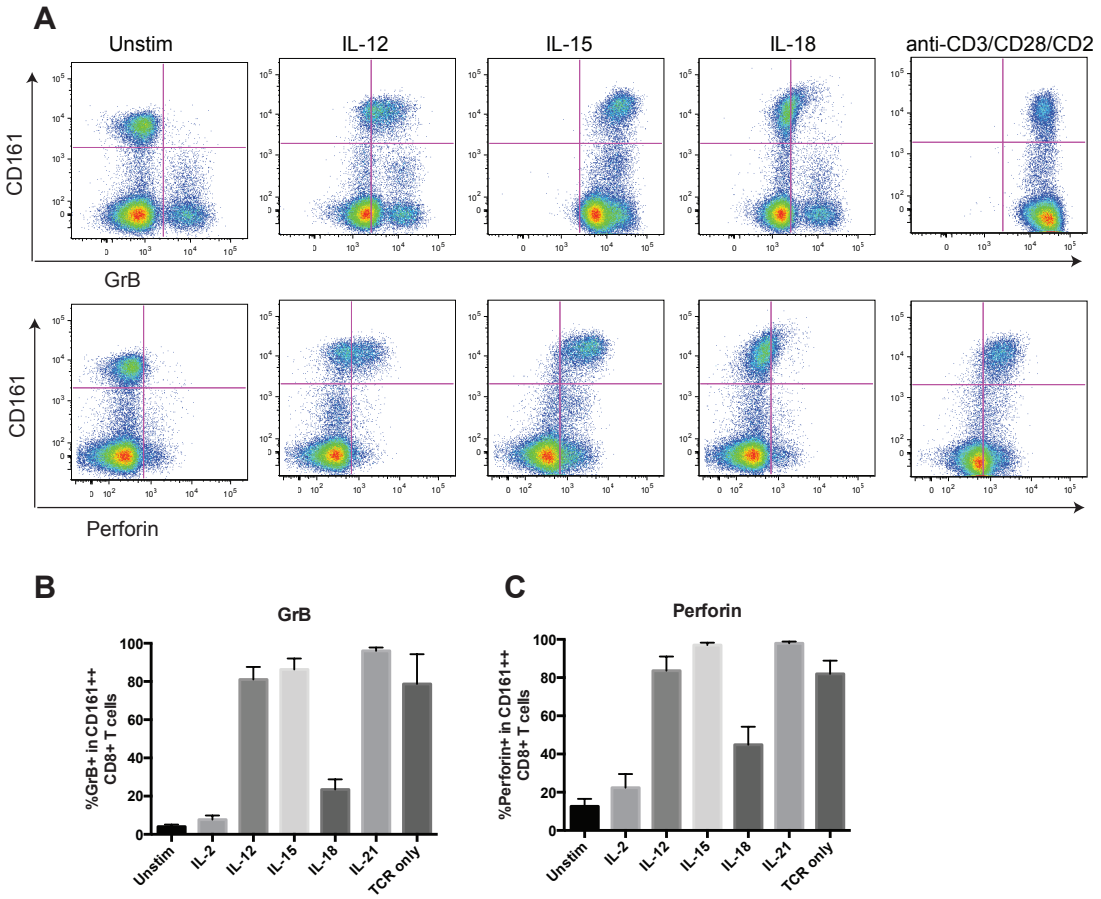


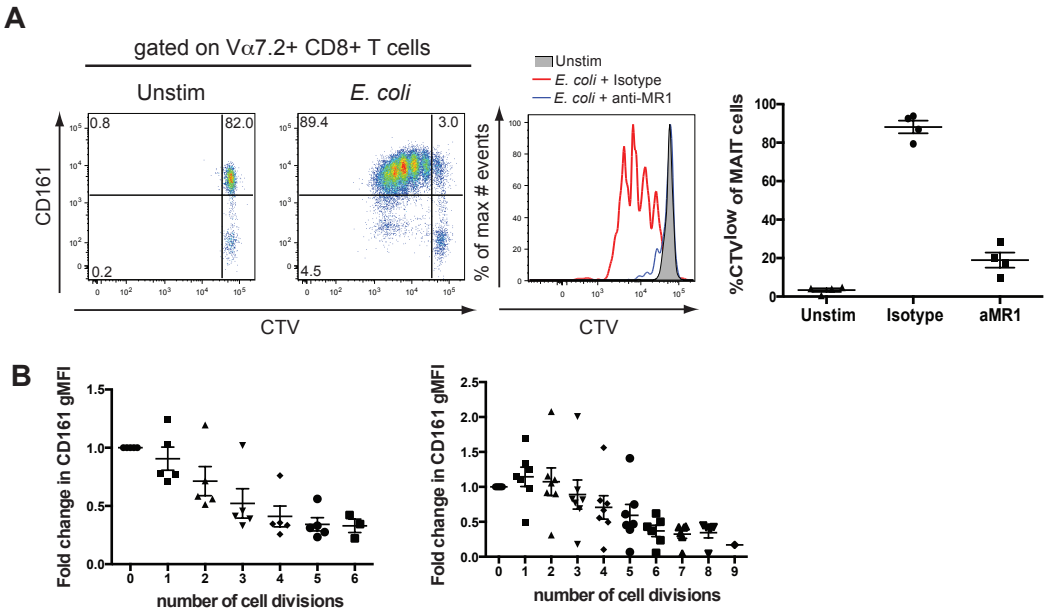
Figure Appendix III-3. Changes in the expression of GrB, CD69, CD161 and Vα7.2 in MAIT cells with increasing concentration of *E. coli*. Enriched CD8+ T cells were stimulated overnight with *E. coli*-treated THP1 cells at the indicated BpCs or PMA/ionomycin. A) Representative plots showing GrB (top), CD69 (middle), and Vα7.2 (bottom) expression against CD161 from the same donor. In the bottom panel, the highly activated CD69^{high} cells are overlaid in blue, and the numbers represent the percentages of the indicated populations within the CD8+ T cells. B) Cumulative data showing percentage of GrB+ cells (left) and gMFI of CD69 (right) within CD161++CD8+ T cells. C) Frequency of CD161++CD8+ T cells within CD8+ T cells. D) Frequency of the indicated populations within CD8+ T cells. For all data, mean ± S.E.M are shown (n=5).



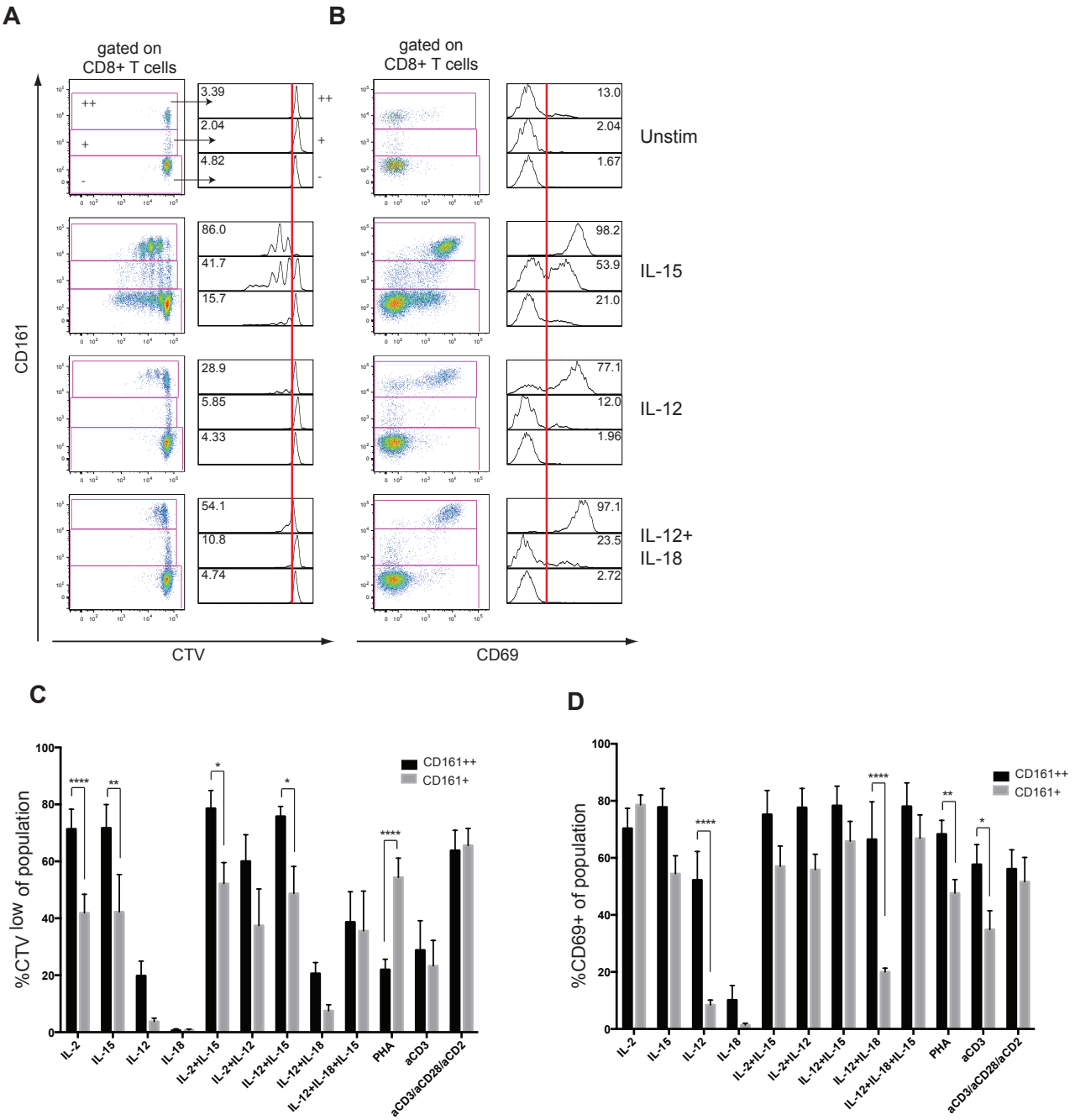
Appendix III-4. *E. coli*-stimulated MAIT cells have a higher cytotoxic capacity compared to *ex vivo* MAIT cells. Killing of target cells by CD8+ T cells as measured by the FATAL assay. CD8+ T cells either pre-activated/licensed by stimulation with *E. coli* or *ex vivo* cells from the same donor were cultured with target BCL cells that had been either pre-treated with *E. coli* (CFSE+) or treated with the sterility control (CTV+). Specific killing of the CFSE+ cells was calculated from the ratio of the frequency of live, CFSE+ and CTV+ cells (detailed in Materials and Methods). A-C) Killing of target cells by CD8+ T cells in an overnight killing assay. A) Frequency of CD161++CD8+ T cells within the CD8+ T cells, in the same donors either *ex vivo* or stimulated with *E. coli* for 6 days. B) Percentage specific killing plotted against E:T adjusted for actual ratio of CD161++CD8+ T cells to CFSE+ target cells in each well calculated from the expected ratio (See Materials and Methods). C) Trogocytosis of CFSE and CTV from the CFSE+ *E. coli*-treated BCL or CTV+ negative control BCL membranes onto CD161++CD8+ T cells. CFSE+ *E. coli*-exposed BCL = Target cells, CTV+ negative control BCL = Neg cells. D-E) Killing of target cells by CD8+ T cells in a 4 hour killing assay. D) % specific killing of target cells by CD8+ T cells either pre-activated with *E. coli* (licensed) or *ex vivo* cells, either in the presence or absence of an anti-MR1 blocking antibody. E) Representative plots showing the ratio between CFSE+ and CTV+ target cells following a 4 hour incubation with *ex vivo* or *E. coli*-stimulated CD8+ T cells, compared to wells without any T cells added (right) (n=3).



Appendix Figure III-5. Cytokine-induced upregulation of GrB and perforin in CD161++CD8+ T cells. PBMCs were stimulated with the indicated cytokines or anti-CD3/CD28/CD2 beads (TCR only) and cultured for 6 days, after which the expression of B) GrB and C) perforin within MAIT cells was assessed. (n=5).



Appendix Figure III-6. MR1-specific proliferation of MAIT cells. THP1 cells pre-exposed to *E. coli* and irradiated were used to stimulate enriched CTV-labeled CD8+ T cells for 6 days, with or without anti-MR1 blocking antibody. A) Representative staining gated on Vα7.2+ CD8+ T cells showing dilution of CTV. Histogram gated on CD161++ Vα7.2+ MAIT cells. B) Downregulation of CD161 in MAIT cells with increasing rounds of cell division, both in enriched CD8+ T cells (left) and PBMCs (right) in response to *E. coli*. Graph shows fold change in gMFI of CD161 in proliferating CD161+Vα7.2+ CD8+ T cells compared to non-dividing CD161++ Vα7.2+CD8+ T cells in the same well.



Appendix Figure III-7. CD161++CD8+ T cells, including the MAIT cells, proliferate in response to cytokines and TCR-stimulation. PBMCs from healthy donors were CTV-labeled and cultured for 6 days with the indicated stimuli. A) Representative staining of CD8+ T cells showing dilution of CTV and B) CD69 expression in response to cytokines, according to CD161 expression levels. C) Frequency of CD161++ and CD161+CD8+ T cells diluting CTV after stimulation with the indicated stimuli (n=5-11). CD161−CD8+ T cells were not included in the analysis as they include naïve T cells. Frequency of CTV^{low} cells in unstimulated cells was subtracted for each donor. D) Frequency of CD161++ and CD161+ CD8+ T cells expressing CD69 after 6 days of culture with the indicated stimuli (n=5-11). Frequency of CD69 expression in unstimulated cells was subtracted for each donor. Significance is indicated for differences between CD161++ and CD161+CD8+ T cells analyzed by a two-way ANOVA with Bonferroni's multiple comparisons test.

4. Phenotype and Function of MAIT cell subsets

4.1. Introduction

The invariant TCR α chain expressed by MAIT cells was originally identified within the CD4−CD8− double-negative (DN) T cell population (Porcelli et al., 1993). However, the development of MR1-tetramers has shown unequivocally that MAIT cells can be divided into CD8+, CD4+, and DN subsets (Reantragoon et al., 2013). Interestingly, the frequency of each subset and their distribution varies between mammalian species, age, and tissue. In ruminants and Vα19-Jα33 TCR transgenic (Vα19i-transgenic) mice, the majority of the MAIT cells are DN cells (Kawachi et al., 2006; Tilloy et al., 1999), whereas within humans they are predominantly CD8+ (Dusseaux et al., 2011; Reantragoon et al., 2013; Walker et al., 2012). Furthermore, while more than half of these CD8+ MAIT cells express the CD8αα homodimer in adults, MAIT cells in second trimester fetal thymi express the CD8αβ heterodimer, with CD8αα expression associated with the acquisition of a memory phenotype (Leeansyah et al., 2014; Walker et al., 2012). The frequency of these CD8+ MAIT cells in the periphery falls with age, with less than 50% of peripheral blood MAIT cells expressing CD8 in individuals of 100 years of age (Lee et al., 2014; Novak et al., 2014; Walker et al., 2014). Furthermore, a recent study using MR1-tetramers in wild-type mice has demonstrated that, similar to humans, certain laboratory strains of mice have a larger fraction of MAIT cells that are CD8+ (Rahimpour et al., 2015). In this study, the distribution of murine MAIT cell subsets differed between tissues, with an enrichment of CD4+ MAIT cells in lymph nodes. Altogether, these reports highlight the heterogeneity of the frequency and distribution of MAIT cell subsets. However, the functional relationship between the different subsets, especially in humans, is poorly understood.

MAIT cells share many developmental and functional features with iNKT cells (see Chapter 1). Similar to MAIT cells, CD1d-restricted iNKT cells consist of CD4+ and CD4− subsets (Godfrey et al., 2004), where the CD4− subset is composed of DN cells in mice, and DN and CD8αα+ cells in humans (Gumperz et al., 2002; Lee et al., 2002). The functional differences between these iNKT cell subsets are well documented. CD4− iNKT cells secrete more Th1-type cytokines such as IFNγ, as well as IL-17, while CD4+ iNKT cells are the dominant producers of Th2 and immunoregulatory cytokines such as IL-4, IL-10, and IL-13 (Coquet et al., 2008; Gumperz et al., 2002; Liu et al., 2008). The balance between these subsets is thought to be key in determining the protective or pathological role of iNKT cells in disease; for example, while CD4+ iNKT cells protected non-obese diabetic mice from developing type 1 diabetes, CD4− iNKT cells secreting IL-17 exacerbated the disease (Simoni et al., 2011). In contrast, the adoptive transfer of CD4+, but not DN, iNKT cells enhanced the development of atherosclerotic lesions in mice (To et al., 2009), and indeed there is an enrichment of CD4+, but not DN, iNKT cells in human atherosclerotic plaques (Chan et al., 2005; Kyriakakis et al., 2010). The cytolytic and Th1 cytokine-producing CD4− iNKT cells are also the main effector population in tumour rejection (Crowe et al., 2005) and control of microbial infections (Emoto et al., 1995, 2006). In contrast, IL-13 secreted by CD4+ iNKT cells inhibits the activity of tumour antigen-specific CD8+ T cells (Osada et al., 2005; Terabe et al., 2008). Diverse roles for MAIT cells have also been described, where they may secrete Th1/17 (Chua et al., 2012; Meierovics et al., 2013), Th2 (Kawachi et al., 2006), or regulatory cytokines (Croxford et al., 2006; Miyazaki et al., 2011). However, most of the previous studies have focused on the dominant population of MAIT cells in mice (DN) and humans (CD8+). Therefore, whether the different subsets have the potential to play a different function in disease remain unknown.

CD4 and CD8 coreceptor molecules are transmembrane glycoproteins that enhance conventional T cell signaling by binding MHC class II (CD4) or class I (CD8) molecules on APCs. This recruits the Src tyrosine kinase $p56^{lck}$ to the TCR-complex, thus reducing the number of MHC-peptide molecules required for T cell activation (Janeway, 1992). The purpose of CD4 or CD8 expression on cells not restricted by MHC class I or II molecules, such as MAIT cells, is unclear. Although there has been one report of CD8 blockade completely abrogating MAIT cell activation (Gold et al., 2012), DN MAIT cells are highly functional without expressing coreceptors (Kawachi et al., 2006; Meierovics et al., 2013). In fact, although the CD8β chain is required for efficient CD8 coreceptor function (Arcaro et al., 2000), a large fraction of adult human MAIT cells express the CD8αα homodimer. CD8αα sequesters $p56^{lck}$ away from the TCR due to its exclusion from lipid rafts, and therefore is thought to be inhibitory (Cheroutre & Lambolez, 2008; Madakamutil et al., 2004). Thus, MAIT cells most likely do not require coreceptors for their activation, but their coreceptors may modulate their activation.

The developmental basis for coreceptor expression, or the lack of it, by MAIT cells is unknown. However, it is unlikely to reflect thymic modulation of coreceptor expression in response to MHC class I or II ligation by CD8 or CD4, respectively. MAIT cell development contrasts with conventional T cells and is more similar to iNKT cells, as MAIT cell selection is dependent on MR1 expressed by DP thymocytes, rather than by the cortical thymic epithelium (Gold et al., 2012; Seach et al., 2013; Treiner et al., 2003). Human MAIT cells are mostly CD4−CD8+ in the second trimester fetal thymus (Leeansyah et al., 2014). The factors involved in determining this phenotype are unknown, but in conventional T cells and iNKT cells, this process is thought to be controlled by a network of transcriptional repression involving ThPOK and Runx3 (Chakravarti & Godfrey, 2010). ThPOK, the master regulator of the CD4 lineage, directly inhibits the activity of Runx3, while Runx3 binds

to the CD4 silencer, thus repressing the CD4 phenotype (He et al., 2010). Indeed, the lack of CD8+ iNKT cells in mice is not due to deletion of CD8+ iNKT cells during thymic development, but because of their high expression of ThPOK (Engel et al., 2010). ThPOK-deficient iNKT cells fail to express CD4, and mainly express CD8, although the overall frequency of thymic or peripheral iNKT cells is not affected (Engel et al., 2010; Wang et al., 2010). Furthermore, a recent study using a humanized mouse model of iNKT cells showed that the development of CD8αβ+ iNKT cells involved the suppression of ThPOK and increased expression of Eomes (Wen et al., 2015). Whether differential expression of ThPOK and Eomes may account for the differences in MAIT cell subsets has not been investigated.

4.2. Aims

1. Examine the frequency of CD4+, CD8+ and DN MAIT cells in human peripheral blood, tonsils, liver, and bone marrow
2. Perform a detailed analysis of phenotypic differences between CD4+, CD8+ and DN MAIT cells
3. Investigate the functional differences between CD4+, CD8+ and DN MAIT cells
4. Examine the effect of CD8 coreceptor blockade on CD8+ MAIT cells using an anti-CD8 blocking antibody

4.3. Materials and Methods

Chapter specific materials and methods are detailed below. For all other methods, please refer to Chapter 2.

4.3.1. Blood and tissue samples

PBMCs were isolated from healthy adult donors, 24-month old donors, and UCB as detailed in Chapter 2.

Intrahepatic lymphocytes were collected from donors after portal flush using cold preservation solution following removal of the right lobe of the donor's livers (non-pathological liver grafts preceding liver transplantation), and were provided by A. Bertoletti.

Tonsils were obtained following routine tonsillectomy from the Ear, Nose and Throat Department at the John Radcliffe Hospital, Oxford. Single cells were collected by mechanical disruption of tonsil samples.

The bone marrow samples were obtained from hip joints. The sample was filtered (40µm), washed with PBS and homogenized, before layering on Lymphoprep^{TM} (Axis Shield Diagnostics) for density gradient separation.

4.3.2. *E. coli*-stimulation of MAIT cells

THP1 cells (ECACC, UK) were incubated overnight with PFA-fixed *E. coli* (DHα, Invitrogen) at a ratio of 25 bacteria per cell (BpC), or a sterility control. THP1 cells were washed extensively, and PBMCs, intrahepatic lymphocytes, or enriched CD8+ T cells were added to the THP1 cells for a 5 hour stimulation. Brefeldin A (eBioscience) was added for the final 4 hours of the stimulation. Alternatively, for the assessment of degranulation, anti-CD107a-PE-Cy7 (BioLegend) was added from the start of the stimulation. For the assessment of GrB and perforin upregulation, PBMCs were added to *E. coli*-treated THP1 cells for 24 hours. PBMCs were added

at a ratio of $5x10^5$ cells : $8x10^4$ THP1 cells. Liver mononuclear cells were added at a ratio of 6-7.$2x10^5$ cells : $8x10^4$ THP1 cells. Enriched CD8+ T cells were added at a ratio of $2x10^5$ cells : $8x10^4$ THP1 cells.

For anti-CD8 blocking experiments, anti-human CD8α (clone LT8, Novus Biologicals) blocking antibodies or IgG2a isotype control (R&D Systems) antibody was added at the indicated concentrations at the beginning of the co-culture of PBMCs or enriched CD8+ T cells with THP1 cells.

4.3.3. Apoptosis assays

Following stimulation with *E. coli*-treated THP1 cells, MAIT cell apoptosis was detected by Annexin V surface staining (Miltenyi Biotec), in Annexin V binding buffer (Miltenyi Biotec) for 15min. Staurosporine (Sigma Aldrich) was added as a positive control.

4.3.4. Culture of MAIT cells in Th2-skewing conditions

PBMCs were cultured in RH10 with 100ng/ml IL-4 (PreproTech Inc) and 50U/ml IL-2 (Miltenyi Biotec) for 6 days, as previously described (Xue et al., 2015), before washing and stimulation with PMA and ionomycin (both 250ng/ml; Sigma Aldrich) for 5 hours. Brefeldin A (Sigma Aldrich) was added at 10µg/ml for the final 4 hours of the stimulation.

4.4. Results

4.4.1. Frequencies of MAIT cell subsets in healthy adult blood

MAIT cells detected by the MR1-tetramer directly correspond to cells that can be identified as CD3+CD161++Vα7.2+ T cells (Magalhaes et al., 2015; Reantragoon et al., 2013). Therefore, this definition of MAIT cells has been used in this study.

Following the gating strategy shown in Figure 4-1A, MAIT cells accounted for a mean of 2.39 ± 0.37% of circulating T cells in healthy adult peripheral blood (Figure 4-1B), comparable to previous reports (Cosgrove et al., 2013; Magalhaes et al., 2015). Within different T cell subsets, MAIT cells were found at an average frequency of 7.16 ± 0.92% within CD8+, 12.25 ± 1.64% within DN, and 0.13 ± 0.03% of CD4+ T cells. Conversely, gating on all CD3+MAIT cells, the majority were found to be either CD8+ (71.77 ± 2.28%) or DN (20.96 ± 1.92%), while CD4 MAIT cells only accounted for 4.79 ± 0.67% of total MAIT cells in adult peripheral blood (Figure 4-1C), in line with previous studies (Miyazaki et al., 2011; Reantragoon et al., 2012).

4.4.2. Cell surface phenotype heterogeneity of human MAIT cells

To assess whether different MAIT cell subsets may traffic to different tissues, the expression of chemokine receptors was compared. Of the chemokine receptors tested, MAIT cell subsets were uniformly high for CCR2, CCR5, CCR6, and had low or little expression of CCR3, CXCR3, CXCR4 (Figure 4-2A, B), as previously reported in CD8+ MAIT cells (Dusseaux et al., 2011). Although some differences in expression were seen for CCR2, CCR5 and CCR6, the most striking difference between the subsets was the expression of CCR4 and CCR7. 16.20 ± 4.60% of CD4+ MAIT cells expressed CCR4, which was significantly higher than the CD8+

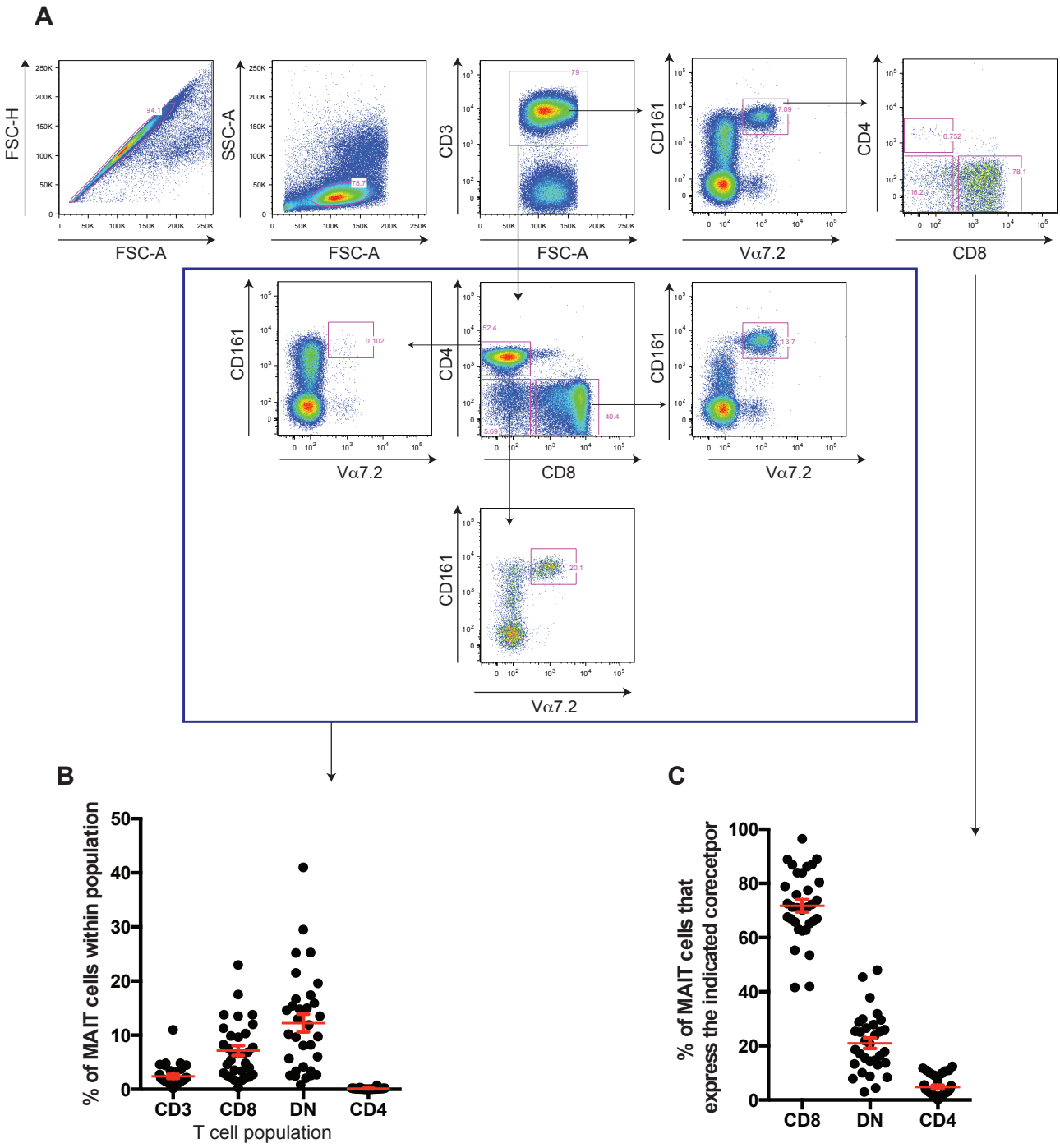


Figure 4-1. Frequency of MAIT cell subsets in healthy adult peripheral blood. A) Gating strategy used to identify MAIT cells and their subsets in this study. B) Cumulative frequencies (mean ± S.E.M.) of MAIT cells within total CD3+, CD8+, CD4+ and CD4−CD8− double-negative (DN) T cells (n=32). C) Analysis of CD4 and CD8 coreceptor expression on CD3+CD161++Vα7.2+ MAIT cells (mean ± S.E.M) (n=32).

(0.97 ± 0.23%) and DN (1.74 ± 0.56%) MAIT cells. CCR7 expression was similarly only found on CD4+ MAIT cells (25.13 ± 3.30%), while absent on CD8+ and DN subsets. In our hands, we could not detect CCR9 or CXCR6 on MAIT cells, although previous reports have shown that MAIT cells can express these chemokine receptors (Billerbeck et al., 2010; Dusseaux et al., 2011). Therefore, differences between the subsets with regard to these receptors needs further investigation.

Next, we investigated whether other cell surface markers previously described to be expressed by CD8+ MAIT cells differed in expression levels in CD4+ and DN MAIT cells (Figure 4-2C). Firstly, CD8+ and DN MAIT cells expressed a low level of the early activation marker CD69 (23.10 ± 4.5% and 25.24 ± 5.55%, respectively), suggesting a level of constitutive activation during circulation. However, the expression of CD69 on CD4+ MAIT cells was virtually absent. In contrast, CD25 (IL-2Rα) was exclusively found on CD4+ MAIT cells (42.97 ± 2.63%). Of note, this CD25+CD4+ MAIT cell population lacked expression of Foxp3 and was unable to produce TGF-β (data not shown), so are not regulatory T cells. Additionally, the cytokine receptors IL-18R and CD127 were highly expressed in all subsets of MAIT cells, albeit at a slightly lower frequency in CD4+ MAIT cells. Lastly, NK cell receptors CD56, NKG2A and CD94 were consistently expressed in CD8+ and DN MAIT cells, but CD4+ MAIT cells lacked their expression, suggesting a lack of cytotoxic potential.

Additionally, 40.65 ± 6.44% of CD4+ MAIT cells expressed CD62L (L-selectin), an adhesion molecule associated with homing to lymphoid tissues (Figure 4-2C). Based on the expression of CCR7 and CD45RA to define memory subsets of T cells (Sallusto et al., 1999), most MAIT cells exhibited an effector memory phenotype (CCR7−CD45RA−), but 20% of the CD4+ MAIT cells had a central memory phenotype (CCR7+CD45RA−CD45RO+; Figure 4-2D, E). Together with their CD62L

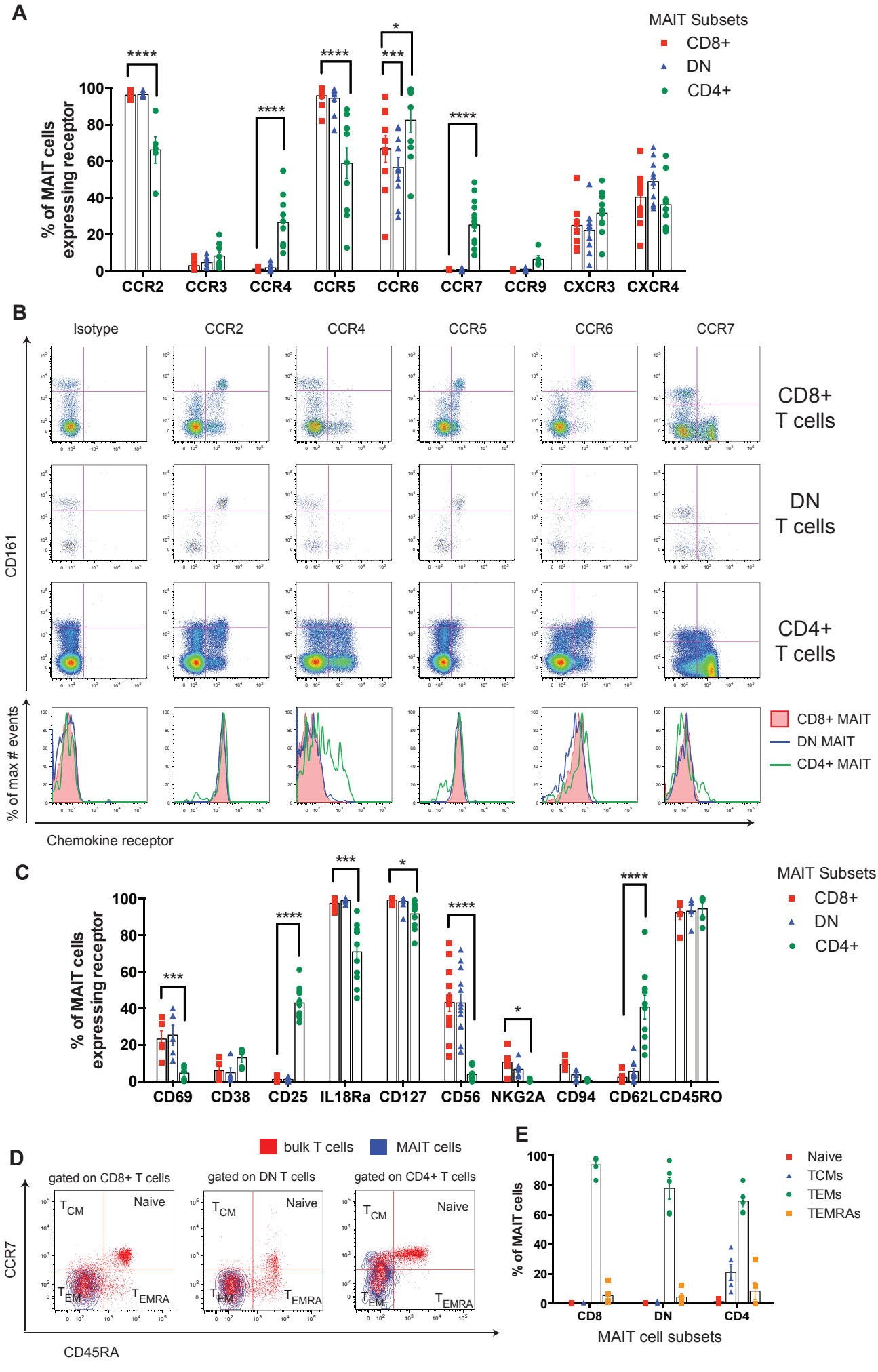

A
MAIT Subsets
CD8+
DN
CD4+
% of MAIT cells expressing receptor
CCR2
CCR3
CCR4
CCR5
CCR6
CCR7
CCR9
CXCR3
CXCR4
B
Isotype
CCR2
CCR4
CCR5
CCR6
CCR7
CD8+ T cells
DN T cells
CD4+ T cells
CD161
% of max # events
Chemokine receptor
CD8+ MAIT
DN MAIT
CD4+ MAIT
C
MAIT Subsets
CD8+
DN
CD4+
% of MAIT cells expressing receptor
CD69
CD38
CD25
IL18Ra
CD127
CD56
NKG2A
CD94
CD62L
CD45RO
D
bulk T cells
MAIT cells
gated on CD8+ T cells
gated on DN T cells
gated on CD4+ T cells
CCR7
CD45RA
Naive
E
Naive
TCMs
TEMs
TEMRAs
% of MAIT cells
CD8
DN
CD4
MAIT cell subsets

Figure 4-2. CD4+ MAIT cells have a unique chemokine receptor expression profile. A) Cumulative data for percentage of CD8+, DN, and CD4+ MAIT cells expressing the indicated chemokine receptors. Bars indicate mean ± S.E.M. ****P<0.0001, ***P<0.001, *P<0.05 by two-way repeated measures ANOVA with Dunnett's multiple comparisons test, compared to CD8+ MAIT cells. All other comparisons were not significant (n=5-15). B) Representative flow cytometry plots gated on total CD8+ (top row), DN (second row), CD4+ (third row) T cells showing expression of indicated chemokine receptors. Bottom row shows histograms for cells gated on CD8+, CD4+ or DN MAIT cells. C) Cumulative data for percentage of CD8+, DN, CD4+ MAIT cells expressing the indicated surface receptors. Bars indicate mean ± S.E.M. ****P<0.0001, ***P<0.001, *P<0.01 by two-way repeated measures ANOVA with Dunnett's multiple comparisons test, compared to CD8+ MAIT cells. All other comparisons were not significant (n=5-13). D) Analysis of the frequency of memory subsets within MAIT cells based on CCR7 and CD45RA expression. Red shows the bulk T cell subset and red shows MAIT cells within each T cell subset. E) Cumulative data showing the frequency of indicated memory subsets within CD8+, DN, or CD4+ MAIT cells. Bars indicate mean ± S.E.M. (n=5). In all graphs CD8+ cells are shown in red, DN cells in blue, and CD4+ cells in green. Data includes experiments performed by Aminu Jahun.

expression, this suggests that a subset of CD4+ MAIT cells may preferentially home to lymphoid tissues.

4.4.3. CD4+ MAIT cells have lower cytotoxic potential compared to CD4− MAIT cells

The lack of NK cell receptor expression on CD4+ MAIT cells suggests that these cells may have low cytotoxic potential. In Chapter 3, CD8+ MAIT cells were demonstrated to have a unique cytotoxic profile, expressing GrA, GrK and low levels of perforin at resting conditions. To investigate whether this phenotype was shared with DN and CD4+ MAIT cells, the frequency of cells expressing GrA, GrK, GrB and perforin was analysed (Figure 4-3A-D). This showed that DN MAIT cells expressed GrA, GrK and perforin at comparable frequencies to CD8+ MAIT cells, but CD4+ MAIT cells expressed significantly less GrA (33.67 ± 7.22% vs. 97.63 ± 0.56%; p<0.0001), GrK (35.55 ± 4.87% vs. 95.36 ± 1.22%; p<0.0001), and perforin (7.07% ±

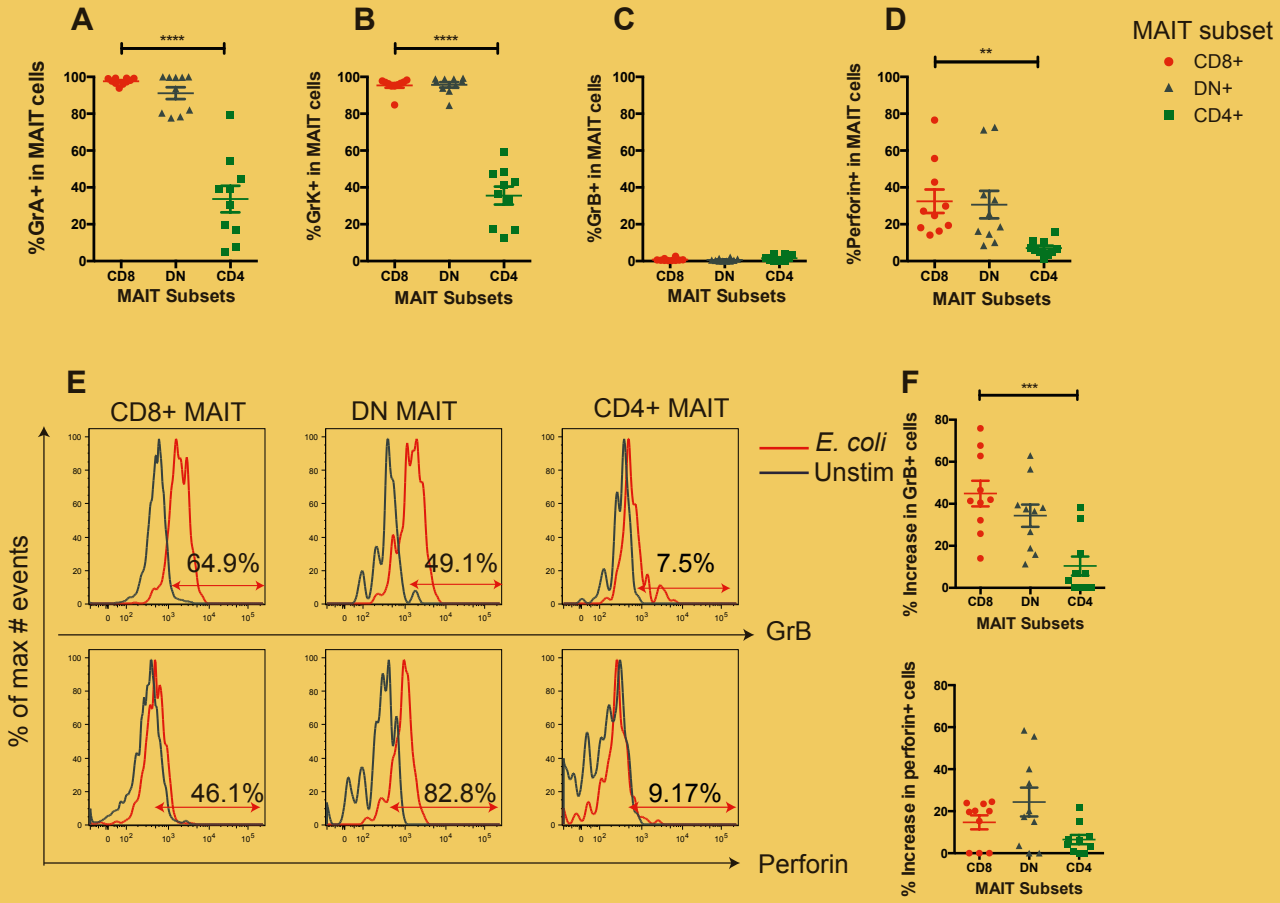


Figure 4-3. CD4+ MAIT cells have lower cytotoxic potential than CD4– MAIT cells. A-D) Frequency of CD8+, DN, CD4+ MAIT cells expressing (A) Granzyme (Gr) A, (B) GrK, (C) GrB, or (D) perforin, showing mean ± S.E.M. ****P<0.0001, **P<0.01 by repeated measures one-way ANOVA with Bonferroni's multiple comparisons test, compared to CD8+ MAIT cells (n=10). E-F) Upregulation of GrB and perforin in MAIT cell subsets following stimulation with *E. coli*-treated THP1 cells for 24 hours. E) Representative staining showing GrB and perforin upregulation in MAIT cells. Percentages indicate frequency of cells expressing indicated effector molecule, based on staining control. F) The fraction of cells expressing GrB or perforin at resting conditions was subtracted to show increases in GrB or perforin expression after *E. coli*-stimulation. ***P<0.001 by by repeated measures one-way ANOVA with Bonferroni's multiple comparisons test, compared to CD8+ MAIT cells (n=10). All other comparisons were non-significant.

1.32% vs. 32.47 ± 6.38%; $p<0.01$) compared to CD8+ MAIT cells. All subsets expressed little GrB at resting conditions.

CD8+ MAIT cells can rapidly upregulate GrB and perforin following bacterial stimulation, which arms these cells with the ability to efficiently kill target cells (Chapter 3). To investigate whether CD4+ MAIT cells, with even lower cytotoxic potential than resting CD8+ MAIT cells, can become efficient killers, MAIT cells were stimulated with *E. coli*-treated THP1 cells for 24 hours and GrB and perforin expression was analysed. As shown in Figure 4-3E, the increase in the fraction of CD4+ MAIT cells expressing GrB was significantly lower compared to CD8+ MAIT cells (15.38 ± 3.83% vs. 44.87 ± 6.08%). There was no significant difference in the ability of DN MAIT cells to upregulate GrB when compared to CD8+ MAIT cells (Figure 4-3F). In contrast, there was no significant difference between all subsets in their ability to upregulate perforin in response to bacterial stimulation.

4.4.4. CD4+ MAIT cells have reduced Eomes expression

Next we looked at the differences in transcription factor expression in MAIT cell subsets, as expression of these master regulators closely correlates with the effector functions of cells, and may also highlight developmental differences between the subsets. Within peripheral CD8+ T cells, MAIT cells uniquely express the transcription factor RORγt (Billerbeck et al., 2010; Dusseaux et al., 2011). Furthermore, MAIT cells secrete IFNγ upon stimulation (Ussher et al., 2013), and therefore are expected to express the Th1 lineage transcription factor, T-bet (Szabo et al., 2000), which is crucial for IFNγ production by iNKT cells (Matsuda et al., 2006; Townsend et al., 2004). Eomes is highly homologous to T-bet and together with T-bet, controls IFNγ production and the cytotoxic potential of T cells (Intlekofer et al., 2005; Pearce et al., 2003).

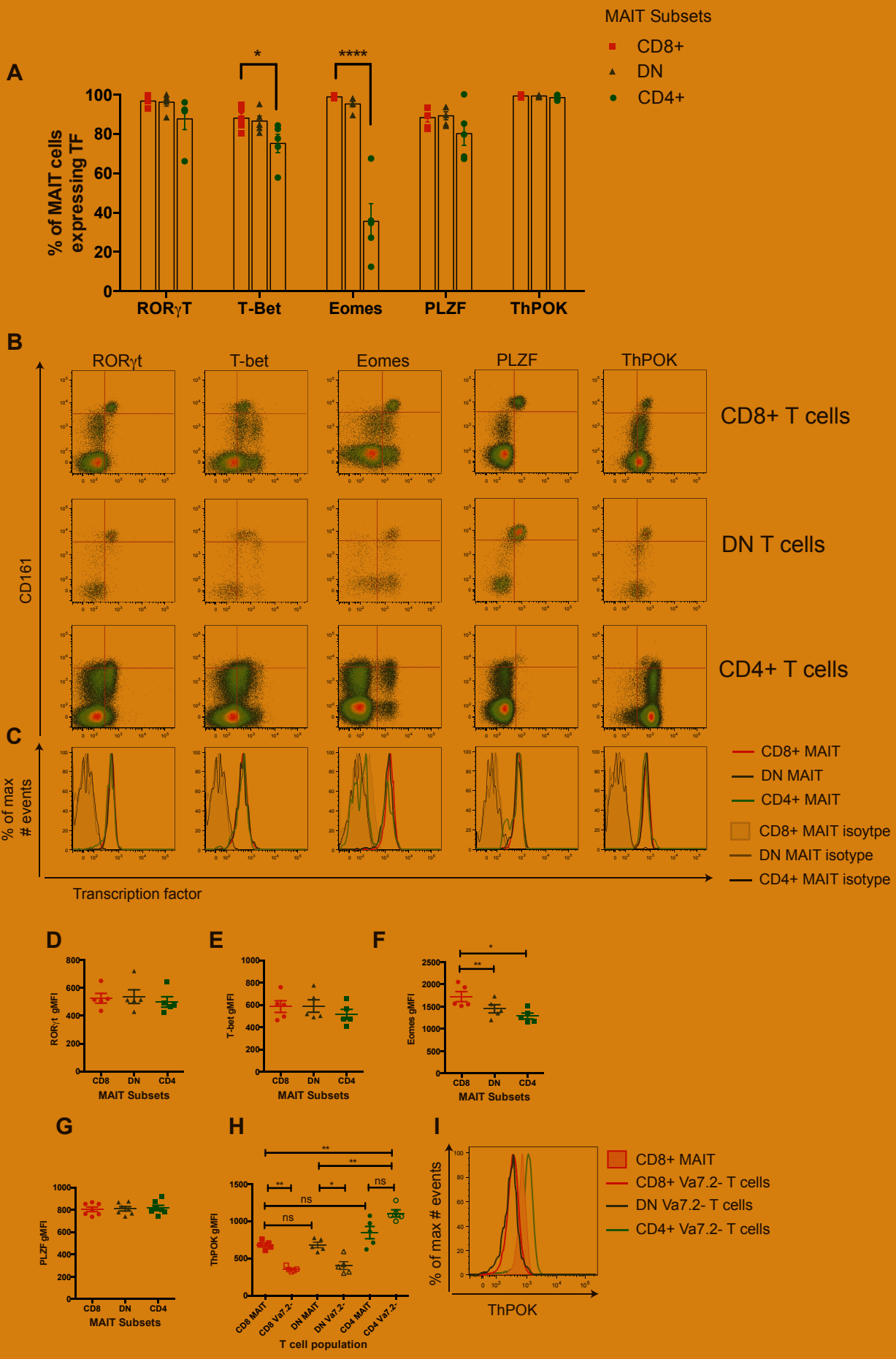

A
MAIT Subsets
CD8+
DN
CD4+
% of MAIT cells expressing TF
RORγT
T-Bet
Eomes
PLZF
ThPOK
B
RORγt
T-bet
Eomes
PLZF
ThPOK
CD8+ T cells
DN T cells
CD4+ T cells
CD161
C
% of max # events
Transcription factor
CD8+ MAIT
DN MAIT
CD4+ MAIT
CD8+ MAIT isoytpe
DN MAIT isotype
CD4+ MAIT isotype
D
RORγt gMFI
MAIT Subsets
E
T-bet gMFI
MAIT Subsets
F
Eomes gMFI
MAIT Subsets
G
PLZF gMFI
MAIT Subsets
H
ThPOK gMFI
T cell population
I
% of max # events
ThPOK
CD8+ MAIT
CD8+ Va7.2- T cells
DN Va7.2- T cells
CD4+ Va7.2- T cells

Figure 4-4. CD4+ MAIT cells have reduced Eomes expression. Expression of the indicated transcription factors was assessed in CD8+, DN, and CD4+ MAIT cells. A) Cumulative data showing the frequency of CD8+, DN, and CD4+ MAIT cells expressing the indicated transcription factors. Bars indicate mean ± S.E.M., ****P<0.0001, ***P<0.001, *P<0.05 by two-way repeated measures ANOVA with Dunnett's multiple comparisons test, compared to CD8+ MAIT cells. All other comparisons were not significant (n=5-10). B) Representative flow cytometry plots gated on total CD8+ (top row), DN (second row), CD4+ (third row) T cells showing expression of indicated transcription factors. C) Overlaid histograms of cells gated on CD8+, CD4+ or DN MAIT cells showing the expression of the indicated transcription factor, overlaid with their respective isotype control stains in grey as per legend. D-F) Geometric mean fluorescence intensity (gMFI) of (D) RORγt (E) T-bet or (F) Eomes (G) PLZF expressed in CD8+, DN, or CD4+ MAIT cells, showing the mean ± S.E.M. **P<0.01, *P<0.05 by repeated measures one-way ANOVA with Bonferroni's multiple comparisons test, compared to CD8+ MAIT cells. All other comparisons were not significant (PLZF n=7, n=5 for others). H) gMFI of ThPOK expressed in MAIT cells (closed symbols) or conventional Vα7.2- T cells (open symbols), within the CD8+, DN, or CD4+ T cells. **P<0.01, *P<0.05, ns=non-significant by repeated measures one-way ANOVA with Bonferroni's multiple comparisons test (n=5). I) Overlaid histogram showing the expression of ThPOK in CD8+ MAIT cells (red tinted) compared to conventional Vα7.2- CD8+, DN, or CD4+ T cells. In all graphs CD8+ cells are shown in red, DN cells in blue, and CD4+ cells in green. Data includes staining performed by Aminu Jahun.

To see if the DN and CD4+ MAIT cells share expression of these transcription factors with CD8+ MAIT cells, MAIT cells were stained for RORγt, T-bet, and Eomes using an optimised protocol. All three subsets of MAIT cells expressed high levels of RORγt and were found to be T-bet^{low}, although CD4+ MAIT cells had a slightly lower frequency of cells expressing T-bet compared to CD8+ and DN MAIT cells (Figure 4-4A, B). However, there was no significant difference between the three subsets in terms of the level of RORγt and T-bet expressed on a per cell basis, shown as overlaying histograms (Figure 4-4C) and as measured by gMFI (Figure 4-4D, E). In contrast, only 35.58 ± 9.0% of CD4+ MAIT cells expressed Eomes compared to CD8+ and DN MAIT cells, in which the majority of cells expressed Eomes (Figure 4-4A, C). Moreover, the level of Eomes expressed was significantly lower on a per cell basis in the CD4+ MAIT cells, as measured by gMFI (Figure 4-4F), consistent with their low cytotoxic potential compared to their CD8+ counterparts. Interestingly, the frequency of CD4+ MAIT cells expressing GrA and GrK (~35%) is similar to the

frequency of CD4+ MAIT cells expressing Eomes. The Eomes+T-bet^{low} memory phenotype has been previously shown to be associated with high expression of GrA and GrK in CD8+ T cells (Smith et al., 2012), and thus the cytotoxic potential of MAIT cells may be similarly regulated by these two transcription factors.

The transcription factor PLZF is a master regulator of innate-like T cells (Kovalovsky et al., 2008; Savage et al., 2008), and human CD8+ MAIT cells have also been shown to express PLZF at high levels (Dusseaux et al., 2011; Fergusson et al., 2014). MAIT cell development in wild-type mice is almost entirely dependent on PLZF, although a small proportion of CD4+ MAIT cells developed in the absence of PLZF (Rahimpour et al., 2015), which may suggest that a fraction of CD4+ MAIT cells may not express PLZF. However, all three subsets uniformly expressed PLZF (Figure 4-4A), and at high levels on a per cell basis (Figure 4-4G) with no significant difference seen between any of the populations.

Finally, the expression of ThPOK was examined, a transcription factor associated with CD4 lineage commitment during thymic development (Xi He, Park, & Kappes, 2010; Xiao He et al., 2005). ThPOK is also expressed by iNKT cells throughout their differentiation (Engel et al., 2010), and is required for the normal development of γδ T cells (Alonzo et al., 2010). We found that a high proportion of all three subsets of MAIT cells expressed ThPOK (Figure 4-4A). Levels of expression were found to be similar regardless of coreceptor expression, as measured by gMFI (Figure 4-4H), although there were a few donors that expressed higher levels of ThPOK in CD4+ MAIT cells. Interestingly, when comparing the gMFI of ThPOK expressed by MAIT cells to conventional CD4+, CD8+ or DN T cells (Vα7.2−), MAIT cells were found to consistently express higher levels of ThPOK compared to conventional CD8+ and DN T cells, while expressing lower levels compared to conventional CD4+ T cells (Figure 4-4H, I), showing that MAIT cells are ThPOK^{low}.

In summary, all MAIT cells have a RORγt+T-bet^{low}PLZF+ThPOK^{low} phenotype, and while CD8+ and DN MAIT cells are enriched for Eomes expression, a large fraction of CD4+ MAIT cells lack this transcription factor.

4.4.5. CD4+ MAIT cells have a lower capacity to secrete Th1 cytokines and degranulate

Next, to determine the functional differences between the three MAIT cell subsets, *E. coli*-treated THP1 cells were used to probe the MR1-dependent activation of MAIT cells. THP1 cells were cultured with PFA-fixed *E. coli* overnight before washing and co-culturing with PBMCs for 5 hours. There was a clear production of IFNγ from all three subsets of MAIT cells after stimulation with *E. coli*-treated THP1 cells, which was completely blocked by the addition of an anti-MR1 blocking antibody (Figure 4-5A, B). There was no further reduction in IFNγ by the addition of an anti-IL-12 and anti-IL-18 blocking antibody in this model (Figure 4-5B), consistent with previous work (Ussher et al., 2013). IL-17 was expressed by all MAIT cell subsets and its expression was completely MR1-depenent (Figure 4-5C).

Using this model, the frequency of cytokine producing cells within each subset was further compared. There was no difference in the frequency of CD8 and DN MAIT cells producing IFNγ (58.09 ± 5.34% and 52.06 ± 5.51%, respectively), but the frequency of CD4+ MAIT cells producing IFNγ was significantly lower (18.82 ± 3.45%, $p<0.0001$; Figure 4-5D). A significantly reduced fraction of CD4+ MAIT cells also produced TNFα (Figure 4-5E) and MIP1β (Figure 4-5F) in response to MR1-presented antigen when compared to the CD8+ and DN MAIT cells. The difference in IL-2 production was difficult to determine due to the small frequency of MAIT cells

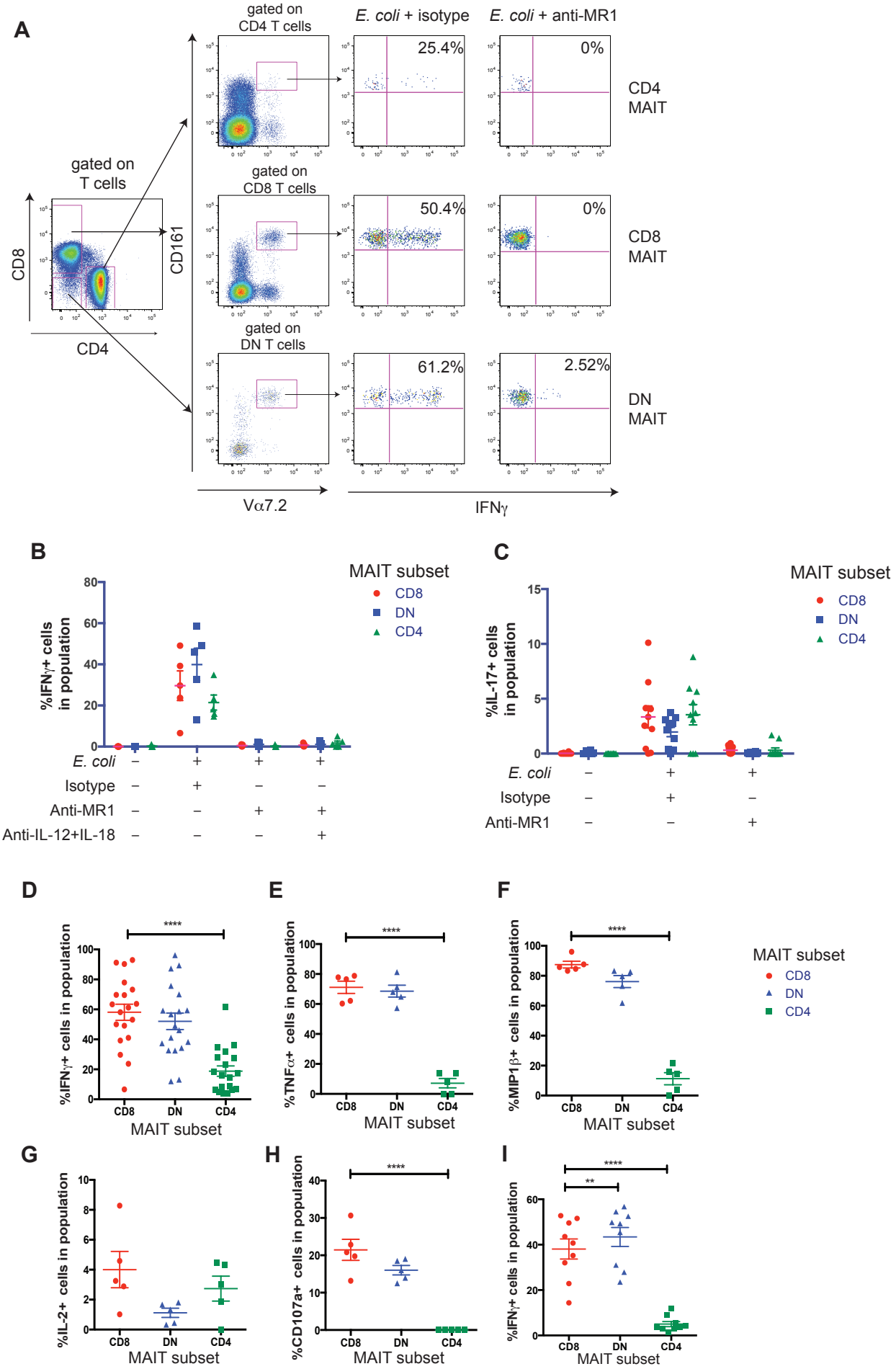

A
gated on T cells
CD8
CD4
CD161
gated on CD4 T cells
gated on CD8 T cells
gated on DN T cells
E. coli + isotype
E. coli + anti-MR1
25.4%
0%
50.4%
0%
61.2%
2.52%
CD4 MAIT
CD8 MAIT
DN MAIT
Vα7.2
IFNγ
B
%IFNγ+ cells in population
MAIT subset
CD8
DN
CD4
E. coli
Isotype
Anti-MR1
Anti-IL-12+IL-18
C
%IL-17+ cells in population
MAIT subset
CD8
DN
CD4
E. coli
Isotype
Anti-MR1
D
%IFNγ+ cells in population
MAIT subset
E
%TNFα+ cells in population
MAIT subset
F
%MIP1β+ cells in population
MAIT subset
MAIT subset
CD8
DN
CD4
G
%IL-2+ cells in population
MAIT subset
H
%CD107a+ cells in population
MAIT subset
I
%IFNγ+ cells in population
MAIT subset

Figure 4-5. CD4+ MAIT cells have reduced production of Th1 cytokines and do not degranulate. THP1 cells were used as antigen-presenting cells and cultured with *E. coli* overnight before co-culturing with PBMCs for 5 hours, to induce MR1-dependent activation of CD4+, CD8+ and DN MAIT cells. A) PBMCs were cultured for 5 hours with *E. coli*-treated THP1 cells in the presence or absence of anti-MR1 blocking antibody. Representative staining is shown. B) Cumulative data for the frequency of MAIT cells expressing IFNγ in response to *E. coli*-treated THP1s in the presence or absence of blocking antibodies against MR1, IL-12, IL-18, or isotype controls for 5 hours (n=5). C) Cumulative data from two independent experiments showing the frequency of MAIT cells expressing IL-17 in response to *E. coli*-treated THP1s in the presence or absence of anti-MR1 blocking antibody, (n=10). D-H) Frequency of CD8+, DN, or CD4+ MAIT cells expressing (D) IFNγ (E) TNFα (F) MIP1β (G) IL-2 (H) CD107a in response to *E. coli*-treated THP1s. ****P<0.0001 by repeated measures one-way ANOVA with Dunnett's multiple comparisons test, compared to CD8+ MAIT cells. All other comparisons were non-significant. (n=19 for IFNγ, from three independent experiments; n=5 for all others). I) Cumulative data for percentage of MAIT cells producing IFNγ in response to overnight IL-12+IL-18 stimulation. ****P<0.0001, **P<0.01 by repeated measures one-way ANOVA with Dunnett's multiple comparisons test, compared to CD8+ MAIT cells (n=9).

producing IL-2 (Figure 4-5G). Importantly, while similar frequencies of CD8 and DN MAIT cells were able to degranulate (Figure 4-5H), there was a complete lack of degranulation from the CD4+ MAIT cells.

Lastly, as MAIT cells can also be activated in an MR1-independent manner through cytokines (Ussher et al., 2014a), PBMCs were stimulated overnight with IL-12+IL-18, with Brefeldin A added for the last four hours of stimulation, and the expression of IFNγ by MAIT cell subsets was compared. Only a mean of 5.01% of CD4+ MAIT cells produced IFNγ (Figure 4-5I), compared to the high proportion of IFNγ+ CD8+ and DN MAIT cells following IL-12+IL-18 stimulation. This was also confirmed using a cytometric bead array (CBA)-assay using FACS-sorted subsets of MAIT cells (Appendix Figure IV-1).

Together, these results suggest that CD4+ MAIT cells have a low capacity to secrete Th1 cytokines in response to MR1- and MR1-independent signals, compared to other subsets of MAIT cells, and do not degranulate after short-term activation.

4.4.6. CD4+ MAIT cells are skewed towards a Th2 cytokine profile

Next, the potential of MAIT cells to produce Th2 cytokines was investigated. PBMCs were cultured in Th2 skewing conditions (IL-4+IL-2) as described in Materials and Methods, and restimulated with PMA/ionomycin for 5 hours (Figure 4-6A). CD4+ MAIT cells contained a significantly higher fraction of cells expressing IL-4 (7.73% ± 1.85) and to a lesser extent, IL-13 (3.66% ± 1.32), compared to the CD8+ MAIT cells (0.69% ± 0.38 and 0.37% ± 0.18, respectively) and DN MAIT cells (0.17% ± 0.15 and 0.65 ± 0.48, respectively)(Figure 4-6B, C). In turn, CD4+ MAIT cells produced significantly less IFNγ compared to their CD8+ and DN counterparts in response to PMA/ionomycin (Figure 4-6D), in line with their reduced capacity to produce IFNγ in previous assays. Interestingly, low production of IL-4 and IL-13 was unique to MAIT cells within the CD8+ T cell population, as other populations within CD8+ T cells were able to produce IL-4 and IL-13 to similar or greater levels compared to CD4+ T cells (Figure 4-6E, F). A similar trend was visible within the DN T cell population, whereas within the CD4+ T cell population, there was no difference in the ability of MAIT cells to produce IL-4 and IL-13 compared to conventional CD4+ T cell populations. This suggests that IL-4 and IL-13 production may be uniquely suppressed within CD8+ and DN MAIT cells compared to CD4+ MAIT cells.

4.4.7. CD8 coreceptor blockade reduces CD8+ MAIT cell activation by *E. coli*-treated THP1 cells

Thus far, no clear differences could be observed between the CD8+ and DN MAIT cells in phenotype and function. Given that the ratio of DN MAIT cells to CD8+ MAIT cells has been reported to increase with age (Novak et al., 2014; Walker et al., 2014), we asked whether there may be difference in survival after antigen-dependent

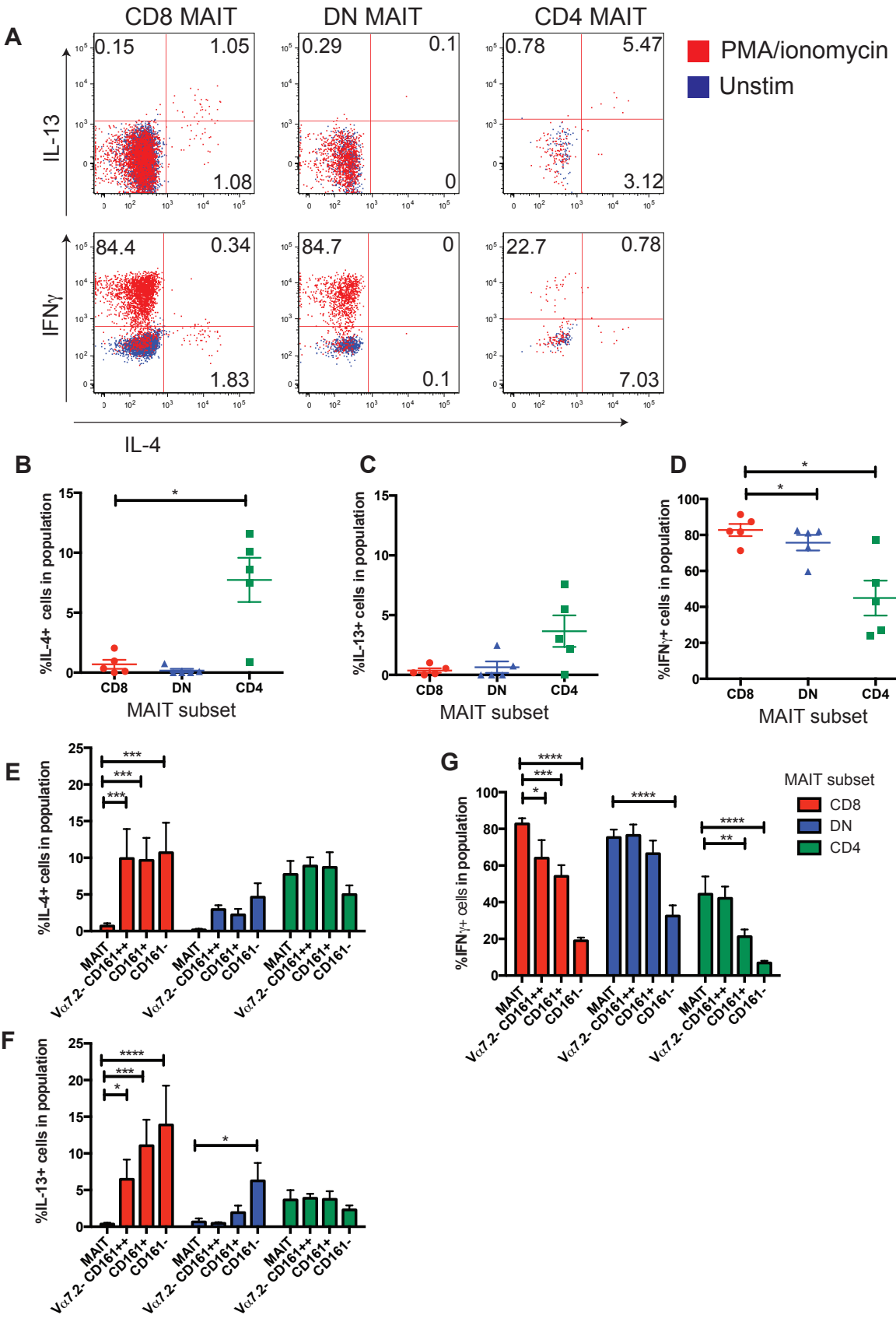


Figure 4-6. CD4+ MAIT cells are skewed towards a Th2 response. PBMCs were cultured in Th2 skewing conditions (IL-4+IL-2, see Materials and Methods) and restimulated with PMA/ionomycin for 5 hours. A) Representative plots showing IL-4, IL-13, and IFNγ production in response to PMA/ionomycin from MAIT cells. B-D) Cumulative data for percentage of MAIT cells expressing (B) IL-4 (C) IL-13 (D) IFNγ. *P<0.05 by repeated measures one-way ANOVA with Dunnett's multiple comparisons test, compared to CD8+ MAIT cells (n=5). All other comparisons were not significant. E-G) Cumulative data for percentage of MAIT cells, Vα7.2-CD161++, CD161+ (dim), CD161- cells within CD4+, CD8+, or DN T cells producing (E) IL-4, (F) IL-13, or (G) IFNγ. ****P<0.0001, ***P<0.001, **P<0.01, *P<0.05 by two-way repeated measures ANOVA with Dunnett's multiple comparisons test, compared to MAIT cells in each T cell population, (n=5).

activation. Therefore, PBMCs were added to *E. coli*-treated THP1 cells and expression of the apoptosis marker Annexin V on MAIT cells was assessed (Figure 4-7A). This in fact showed that the increase in Annexin V-expressing cells following stimulation was significantly greater in DN MAIT cells, compared to CD8+ T cells (Figure 4-7B). Thus, although both CD8+ and DN MAIT cells are similarly activated in an MR1-dependent manner, the CD8+ MAIT cell population may be protected from AICD.

We wanted to further investigate the role of the CD8 coreceptor in the function of MAIT cells. If CD8 acted as a coreceptor, it would be predicted to increase the avidity and to decrease the TCR off rate for cognate antigen (Garcia et al., 1996). The enhanced antigen sensitivity mediated by CD8 can be visualized as a shift in an antigen dose response curve (Engel et al., 2010). Therefore, the number of PFA-fixed *E. coli* cultured with each THP1 cell was titrated, and MAIT cell activation was measured by IFNγ production (Figure 4-7C). However, there was no difference between the CD8+ and DN MAIT cell in their ability to make IFNγ at low doses of *E. coli*, suggesting that the CD8 coreceptor does not modify the antigen sensitivity of MAIT cells.

To investigate whether the activation of MAIT cells is affected when the CD8 coreceptor is blocked, PBMCs were incubated with *E. coli*-treated THP1 cells over 5 hours, in the presence or absence of an anti-CD8α blocking antibody (clone LT8). Due to the residual loss of CD8 staining from the presence of the anti-CD8 antibody, CD4− MAIT cells were gated in the following experiments. Adding a serially titrated concentration of the anti-CD8 blocking antibody showed that there is a dose-dependent reduction in the frequency of IFNγ+ MAIT cells with CD8 coreceptor blockade, compared to the isotype control (Figure 4-7D). This effect was also seen when measuring different outputs of TCR signaling, namely TNFα, CD107a, and

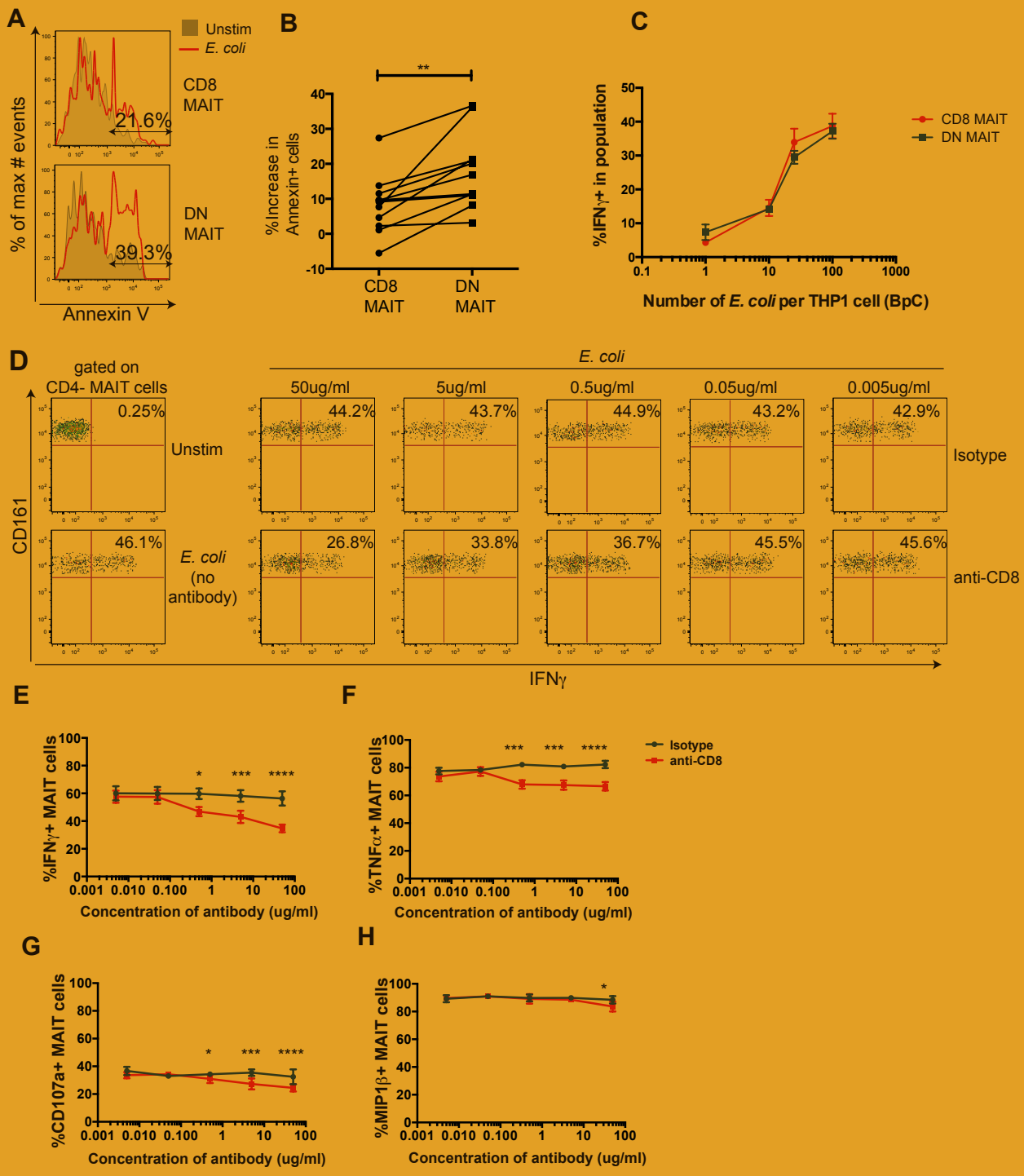


Figure 4-7. CD8 coreceptor blockade reduces CD8+ MAIT cell activation by *E. coli*-treated THP1 cells. A) Representative flow cytometry plot of Annexin V staining of CD8+ (top) or DN (bottom) MAIT cells following incubation with *E. coli*-treated THP1 cells for 5 hours, B) Cumulative data showing the increase in the frequency of Annexin V+ MAIT cells compared to unstimulated cells. **P<0.01 by paired t-test (n=11). C) MAIT cell sensitivity to antigen titration was evaluated by culturing an increasing number of *E. coli* per THP1 cell (Bacteria per cell - BpC) overnight, before washing and incubation with PBMCs at the fixed ratio $5x10^5$ PBMC: $8x10^4$ THP1. Cumulative frequencies of CD8+ or DN MAIT cells producing IFNγ are shown (n=5). D) Representative plots of IFNγ expression in CD4− MAIT cells cultured in the presence of increasing concentrations of blocking antibody against CD8, or isotype control, or in the absence of antibodies (far left column). E-H) Cumulative data for the frequency of CD4− MAIT cells expressing (E) IFNγ, (F) TNFα, (G) CD107a, or (H) MIP1β in the presence (red) or absence (blue) of a blocking antibody against CD8. Each symbol and bar represents the mean ± S.E.M. (n=5). ****P<0.0001, ***P<0.001, *P<0.05 by two-way repeated measures ANOVA with Dunnett's multiple comparisons test, compared to MAIT cells cultured at the corresponding concentration of isotype control antibody. All other comparisons were non-significant. The anti-CD8 antibody titration experiments were performed by Aminu Jahun.

MIP1β (Figure 4-7E-H). Interestingly, the degree to which CD8-coreceptor blockade affected the response of MAIT cells differed depending on the response measured, with the inhibitory effect of CD8 coreceptor blockade increasing as follows: MIP1β < CD107a < TNFα, IFNγ.

To confirm the specificity of this effect, anti-CD8 blocking antibody was added to magnetically enriched CD8+ T cells and the CD8-depleted population. The purity of CD8+ T cells was >95%, while in the CD8-depleted population the frequency of CD8+ T cells was <0.5%. When either population was cultured with *E. coli*-treated THP1s in the presence of the anti-CD8 blocking antibody, there was a significant reduction in the frequency of IFNγ+ and TNFα+ MAIT cells in the CD8+ MAIT cells but not in the DN MAIT cell population (Appendix Figure IV-2).

4.4.8. CD4+ MAIT cells are enriched in tonsils and are highly active CD56+ cells in the liver

Having studied the differences in the phenotype and function of MAIT cell subsets in healthy adult peripheral blood, whether their coreceptor usage differed by age, or within tissues, was assessed. Coreceptor usage of MAIT cells in tonsils, bone marrow, and the liver was compared to that of blood from cord blood, 24 month old, and adult donors. This revealed that CD4+ MAIT cells were uniquely enriched within tonsilar MAIT cells, accounting for a mean of 43.9 ± 7.78% of total MAIT cells (Figure 5-8A). CD8+ and DN MAIT cells both made up an average of 26.28 ± 6.16% and 23.5 ± 3.08% respectively of the remaining MAIT cells in the tonsil. This was in contrast to the distribution of MAIT cell subsets in the memory T cell fraction of a bone marrow sample (Figure 5-8B), and within intrahepatic lymphocytes (IHL), where the CD8+ MAIT cell population constituted the majority of MAIT cells, similar to

peripheral blood (Figure 5-8C). Furthermore, there was no significant difference in the coreceptor expression of blood MAIT cells with age, when comparing cord, 24 month old, or adult peripheral blood (Figure 5-8D).

Next, as the highest frequency of total MAIT cells can be found in the liver (Dusseaux et al., 2011; Tang et al., 2013), we looked to see if there were phenotypic and functional differences in subsets of MAIT cells specific to the liver. Although the coreceptor expression of liver MAIT cells did not significantly differ compared to blood MAIT cells (Figure 5-8C), all subsets of MAIT cells expressed high levels of the NK cell marker CD56, compared to peripheral blood MAIT cells in adults and paediatric samples (Figure 5-8E, F). Thus, while blood CD4+ MAIT cells expressed very little CD56 regardless of age (3.6 ± 1.03% in adults), an average of 51.87 ± 6.9% of intrahepatic CD4+ MAIT cells expressed CD56. Activation of all subsets of liver-derived MAIT cells was entirely MR1-dependent, as shown by culturing hepatic MAIT cells with *E. coli*-treated THP1 cells for 5 hours (Figure 5-8G, H). Interestingly, within the liver, the CD8+ MAIT cell population had the highest frequency of IFNγ+ cells compared to the DN and CD4+ MAIT cells. CD56 expression was also associated with a higher frequency of IFNγ+ MAIT cells (Figure 5-8I). This was especially true within the liver CD4+ subset, with 42.80 ± 6.19% of CD56+ CD4+ MAIT cells secreting IFNγ, while only 13.97 ± 2.46% of CD56- CD4+ MAIT cells responded by making IFNγ, suggesting that CD56 expression is associated with a greater Th1 response from CD4+ MAIT cells within the liver.

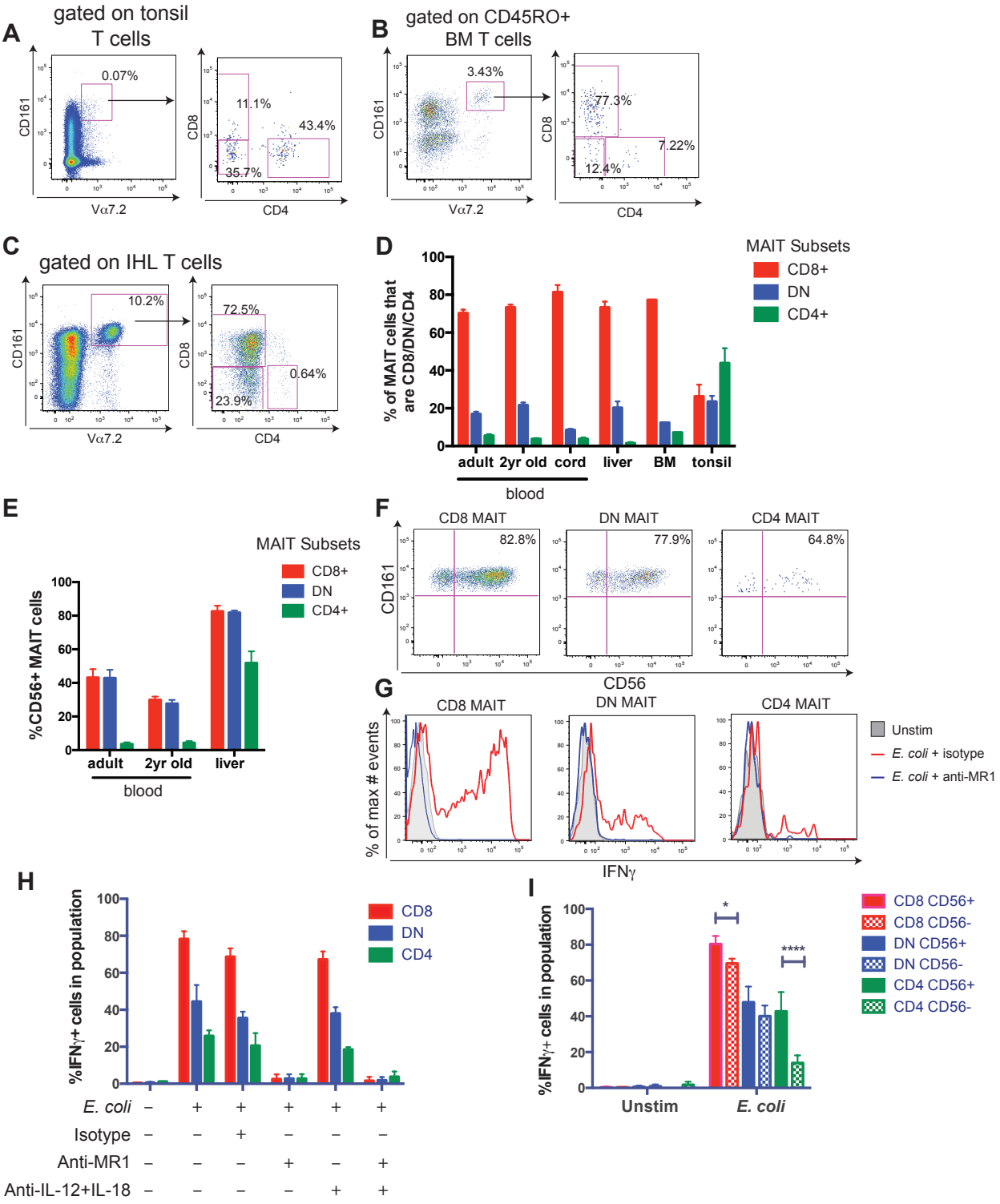


Figure 4-8. CD4+ MAIT cells are enriched within tonsils and are highly activated in the liver. A-C) Representative staining showing the expression of coreceptors on MAIT cells from A) tonsils, B) a bone marrow sample, or C) intrahepatic lymphocyte samples (IHL). D) Cumulative frequencies of CD8+ (red), DN (blue) or CD4+ (green) cells within total MAIT cells in the indicated tissues. n=32 (adult blood), 28 (2yr old blood), 3 (cord blood), 3 (liver), 1 (BM), 6 (tonsil). E) Cumulative frequencies of CD56-expressing MAIT cells within blood and liver, according to coreceptor expression. F) Representative staining showing CD56 expression on intrahepatic MAIT cells. G-H) IHL cells were cultured with *E. coli*-treated THP1 cells for 5 hours. Representative staining (G) and cumulative frequencies (H) of IFN γ-expressing intrahepatic MAIT cells, in the presence or absence of an anti-MR1 blocking antibody: (blue line) or isotype control (red line). I) Expression of IFNγ by the indicated intrahepatic MAIT cell subsets according to CD56 expression. ****P<0.0001, *P<0.05 by two-way repeated measures ANOVA with Tukey's multiple comparisons test, comparing CD56+ and CD56− cells within each MAIT cell subset (n=3). Staining of 2yr old paediatric samples and tonsil cells performed by Chris Willberg, and staining of intrahepatic lymphocytes and *E. coli*-stimulation experiments were performed by James Ussher.

4.5. Discussion

In this study, we have performed a detailed comparison of the CD4+, CD8+ and DN MAIT cell subsets in parallel, in terms of their phenotype, cytokine secretion, cytotoxicity, and transcription factor expression. This has highlighted many of their distinct and overlapping characteristics.

Very little has been previously reported on CD4+ MAIT cells. In contrast to Vα19i-transgenic mice, where >40% of MAIT cells express CD4, only a small proportion of human and wild-type mice MAIT cells express CD4 (Rahimpour et al., 2015; Reantragoon et al., 2013), rendering the study of this population difficult. The development of the MR1-tetramer confirmed that the CD4+ MAIT cells can be identified as the CD4+CD161++Vα7.2+ T cells in humans (Reantragoon et al., 2013), and, thus, we have defined MAIT cells as CD161++Vα7.2+ T cells in this study. Based on this definition, several key features were found to be unique to CD4+ MAIT cells.

Firstly, a fraction of the CD4+ MAIT cells were found to differ in their expression of tissue homing receptors compared to their CD4− counterparts. CD4+ MAIT cells uniquely expressed the lymph node homing receptors, CCR7 and CD62L. Consistent with this phenotype, there was a significant enrichment of CD4+ MAIT cells within tonsil T cells, constituting the largest population of MAIT cells compared to the CD8+ and DN subsets. The enrichment of CD4+ MAIT cells in lymphoid tissues is similar to the recently reported enrichment of CD4+ MAIT cells within lymph nodes in wild-type mice (Rahimpour et al., 2015). Furthermore, this finding also mirrors the phenotype of the CD4+ subset of iNKT cells, where a small proportion of CD4+ iNKT cells have also been shown to be CCR7+CD62L+ (Kim et al., 2002; Sandberg et al.,

2002). However, another study looking at fetal MAIT cells only observed an enrichment of CD4+ MAIT cells within the intestine, but not in the spleen or mesenteric lymph node (Leeansyah et al., 2014), suggesting that the lymph node homing properties of CD4+ MAIT cells may be acquired later in their development. PLZF is thought to be important to confer tissue-homing properties to iNKT cells, as ectopic expression of PLZF in conventional thymocytes can convert naïve lymph node homing ($CD44^{low}$ $CD62L^{high}$) cells into effector cells with tissue-homing properties ($CD44^{high}CD62L^{low}$) (Kovalovsky et al., 2010; Raberger et al., 2008). Although both CD4+ iNKT cells (Savage et al., 2008) and CD4+ MAIT cells express high levels of PLZF, it will be interesting to compare the level of PLZF expressed in these minor lymphoid tissue homing CD4+ MAIT cells with peripheral-tissue homing MAIT cells.

In addition to lymph node homing receptors, CD4+ MAIT cells also uniquely expressed CCR4. CCR4 expression has been similarly reported in a small proportion of CD4+ iNKT cells (Kim et al., 2002). CCR4 is mainly involved in the trafficking to the skin, where endothelial cells and dermal dendritic cells express the CCR4 ligands CCL17 and CCL22 (Campbell et al., 1999). We also found a higher frequency of cutaneous lymphocyte antigen (CLA1)-expressing MAIT cells in the CD4+ subset compared to its CD4− counterparts (Appendix IV-3A), suggesting that CD4+ MAIT cells may preferentially home to the skin. Although a previous study has reported that MAIT cells are present in psoriatic lesions (Teunissen et al., 2014), only the CD8+ subset was studied, and, thus, the contribution to disease from CD4+ MAIT cells remains unknown.

Another unique feature of CD4+ MAIT cells was their ability to secrete more IL-4 and IL-13 compared to their CD4− counterparts. This supports the recent findings in Vα19i-transgenic mice showing that CD4+ MAIT cells were the dominant producers

of IL-4 (Sakala et al., 2015), and a previous study in humans (Lee et al., 2014). The lower capacity of CD4+ MAIT cells to produce Th1 cytokines IFNγ and TNFα suggests that within peripheral blood, the CD4+ MAIT cells are skewed towards a Th2 rather than a Th1 response. As they express comparable levels of T-bet to CD4− MAIT cells, other factors such as their low Eomes expression may be associated with their lower IFNγ production and cytotoxic function. Indeed, overexpression of Runx3, the silencer of CD4 expression during T cell development, induces Eomes and suppresses IL-4 secretion (Yagi et al., 2010). The hypothesis that Eomes accounts for many of the differences between CD4+ and CD4− MAIT cells is supported by studies of iNKT cells, where human DN and CD8αβ+ iNKT cells were reported to have a higher expression of Eomes compared to CD4+ iNKT cells, which correlated with their cytotoxic capacities (Knox et al., 2014; O'Reilly et al., 2011; Wen et al., 2015). Low Eomes expression in the CD4+ MAIT cell population has also been recently reported by Leeansyah *et al*., (2015), along with a reduced expression of PLZF and the transcription factor Helios. Other transcription factors may therefore also differ between the MAIT cell subsets, and requires further investigation. Additional experiments using FACS-sorted MAIT cells and quantifying cytokine production using techniques such as CBA and ELISAs will be important to directly compare the cytokine profile of each subset of MAIT cells, in particular for differences between the CD8αα and CD8αβ subsets as CD8β can be downregulated in even in unstimulated MAIT cells during culture (Walker et al., 2012).

It is also important to note that the CD4+CD161++Vα7.2+ T cell population, although defined as MAIT cells in this study, may include conventional CD4+ T cells expressing CD161 and Vα7.2, as the Vα7.2 antibody does not recognise the joining region of the TCRα chain. Therefore, the proportion of CD4+CD161++Vα7.2+ T cells that are MAIT cells will need to be determined using an MR1-tetramer, or by single-cell TCR sequencing analysis.

In this study, CD8+ and DN MAIT cells were functionally and phenotypically similar. However, there was a consistently greater upregulation of Annexin V on DN MAIT cells compared to CD8+ MAIT cells following MR1-dependent activation. A possible explanation may be provided by the expression of the CD8αα homodimer by most CD8+ MAIT cells. CD8αα expression is thought to be induced on high-affinity CD8αβ T cells, and can protect cells from AICD (Huang et al., 2011). In line with this, CD8αα expression on T cells is associated with cells that are constitutively activated and display a memory phenotype, such as CD8αα+ skin resident T cells (Zhu et al., 2013) and murine CD8αα+ intraepithelial cells (IEL) (Cheroutre et al., 2008). CD8αα is also transiently expressed on CD8+ T cells during LCMV and influenza infection in mice, promoting their survival and differentiation into memory cells (Madakamutil et al., 2004; Zhong & Reinherz, 2005). Additionally, CD8αα is expressed on various cells other than T cells, such as NK cells, where it has been shown to rescue degranulation-induced apoptosis (Addison et al., 2005). Further research into the possibility that the CD8 coreceptor, specifically the CD8αα homodimer, promotes the survival of MAIT cells through the expression of anti-apoptotic molecules such as B-cell lymphoma 2 (BCL-2), and whether it directly interacts with MR1 or other MHC class I-like molecules, will be of future interest.

Whether the CD8 coreceptor, regardless of CD8α and CD8β chain expression, may affect the activation of MAIT cells was also investigated. Although CD8 was not necessary for the activation of MAIT cells, CD8+ MAIT cell responses were reduced in a dose-dependent manner by the addition of an anti-CD8α blocking antibody. As the structure and residues of the CD8-binding domain of MHC class I is conserved between MR1 and MHC class I molecules, it has been suggested that MR1 may bind CD8αα (Reantragoon et al., 2012, 2013). It is well attested that the binding of CD8 to MHC class I stabilizes the TCR/peptide-MHC class I interaction (Laugel et al., 2007), and the results here support the idea that the CD8 coreceptor also plays a similar

role to stabilize the MAIT TCR/riboflavin-MR1 interaction. We found that there was a hierarchy in cellular responses of MAIT cells that are affected by CD8 coreceptor blockade – the order was as follows, from least affected to most affected: MIP1β < CD107a < TNFα ≤ IFNγ. This is consistent with previous work on conventional CD8+ T cells showing that the TCR signaling threshold differs between cellular responses (Laugel et al., 2007; Valitutti et al., 1996). This series is also similar to the hierarchy in cellular responses elicited by peptide-MHC class I stimulation demonstrated by Van den berg *et al.* (2013), where the activation threshold, as measured by the minimum peptide concentration required for activation, increased as follows: MIP1β < CD107a < TNFα < IL-2 < IFNγ. Importantly, however, we cannot rule out that, in our assays, CD8 is acting as a simple adhesion molecule, or is hindering the interaction between MR1 and the MAIT cell TCR, particularly because there was no difference in the sensitivity of CD8+ and DN MAIT cells to serially titrated concentrations of *E. coli*. In order to confirm the function of the CD8 coreceptor on MAIT cell activation, further studies disrupting the potential CD8-binding site of MR1 will be necessary (Purbhoo et al., 2001). Furthermore, no work was done here investigating the role of the CD4 coreceptor on MAIT cells, and similarly, a direct interaction between MR1 and CD4 remains to be demonstrated.

There was a significant increase in the expression of CD56 on all subsets of intrahepatic MAIT cells compared to peripheral blood MAIT cells, which was associated with a higher effector function, especially in the CD4+ subset, secreting abundant IFNγ in response to MR1-presented antigen. Due to limited tissue samples, we were unable to look at the expression of CD56 or cytotoxic molecules in tonsils and bone marrow. However, as CD56 expression has been previously associated with increased cytotoxic effector function of T cells (Kelly-Rogers et al., 2006; Pittet et al., 2000), CD4+ MAIT cells may have heterogenous cytotoxic capacities depending on the tissue they reside in, and their activation status. Increased CD56

expression in T cells and NK cells have been reported in *in vitro* cultures of cells with common γ-chain cytokines such as IL-2, IL-15 and IL-21, as well as IL-23 (Bonanno et al., 2009; Cookson & Reen, 2003; Kelly-Rogers et al., 2006; van de Wetering et al., 2009). Indeed, when we compared the expression of CD56 on CD8+ T cells during *in vitro* cultures in the presence of various cytokines, a significant increase in the expression of CD56 on CD161++CD8+T cells could be readily induced by IL-12, IL-2, IL-15, and IL-2, either in combination with each other or alone (Appendix IV-3B, C). It is therefore possible that the intrahepatic cytokine milieu upregulates CD56 expression on all MAIT cell subsets, and lowers their activation threshold and/or skews them towards a Th1 response. Indeed, intrahepatic lymphocytes are dominated by rapidly-acting innate cells, including MAIT cells, γδ T cells, NK cells, and T cells expressing NK cell receptors e.g. CD56, and constitutive expression of cytokines such as IL-15 (Golden-Mason et al., 2004) and IL-7 (Tang et al., 2013) may activate and induce CD56 upregulation in MAIT cells.

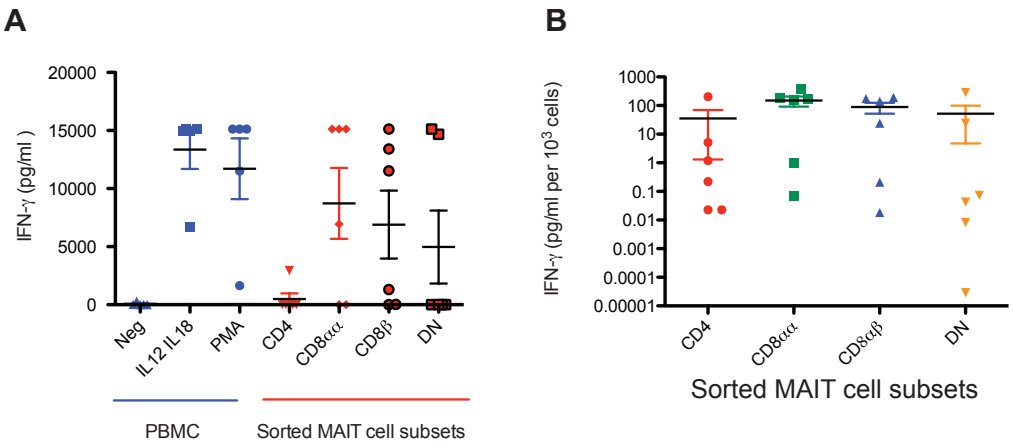
We have shown here that all human MAIT cells are PLZF+, T-bet^{low}, RORγt+, and ThPOK^{low}. ThPOK expression is vital for the differentiation of CD4+ conventional T cells as well as iNKT cells (Engel et al., 2010; He et al., 2008). To date, this is the first report of the expression of ThPOK in MAIT cells. Here, we show that all three subsets of MAIT cells express less ThPOK than conventional CD4+ T cells, but at a greater level than conventional CD8+ and DN T cells. Interestingly, a similar pattern of ThPOK downregulation has been reported specifically in the type-17 iNKT cells (iNKT17) (Engel et al., 2012). ThPOK negatively regulates Th17 differentiation (Engel et al., 2012), and thus only cells that express low levels of ThPOK are permissive for the differentiation of iNKT17 cells, which express RORγt and are able to produce IL-17 (Coquet et al., 2008; Enders et al., 2012). Furthermore, ThPOK-deficient mice lack CD4+ iNKT cells and instead harbor a population of CD8+ iNKT cells, with the majority of the cells, regardless of CD8 expression, exhibiting an

iNKT17 phenotype with low production of IFNγ and IL-4 (Enders et al., 2012; Engel et al., 2010). However, the complete lack of ThPOK expression renders the cells hyporesponsive and with low levels of the activation marker CD69, as well as lower expression of PLZF (Engel et al., 2012; Vahl et al., 2013). Based on the role of ThPOK in iNKT cell function and development, it is tempting to hypothesize that MAIT cells express a reduced amount of ThPOK permissive for the expression of RORγt and secretion of IL-17, while retaining some expression that is essential for their functional maturation and development. For this, ThPOK could be overexpressed or knocked out to in order to investigate whether the level of ThPOK expression affects RORγt expression levels in MAIT cells.

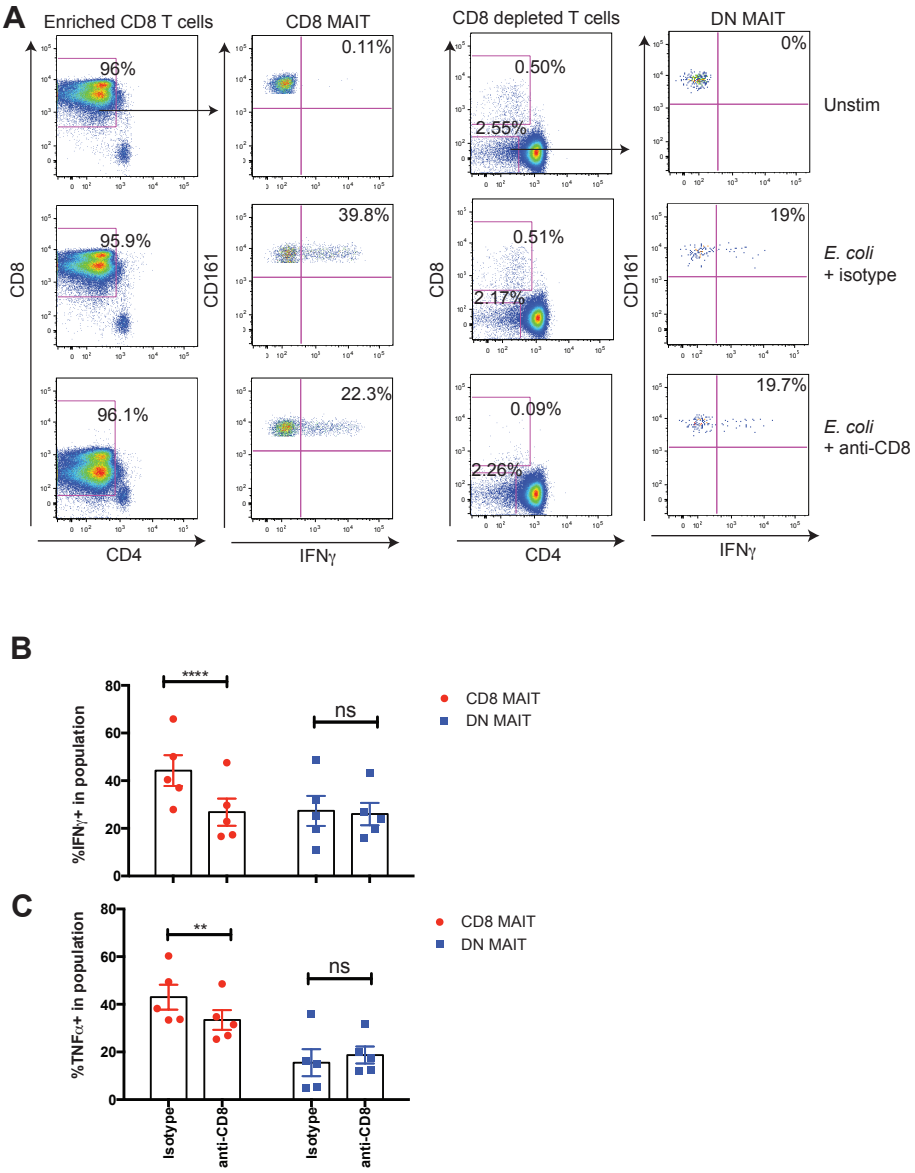
In conclusion, we have explored the heterogeneous as well as homogeneous phenotypes and functions of the three defined subsets of MAIT cells. The overrepresentation of CD4+ MAIT cells in lymphoid organs reported here in humans and recently in mice (Rahimpour et al., 2015) and their Th2 cytokine profile supports the notion that they may play a distinct role in health and disease, and future studies will be warranted to further investigate the development and function of these cells compared to their CD4− counterparts. Furthermore, the CD8 coreceptor ligation was not required for the activation of CD8+ MAIT cells, but may play a fine-tuning role enhancing the MR1-dependent activation of MAIT cells. Understanding the functional differences between subsets will help us understand the distinct role each subset may play in health and disease.

4.6. Summary

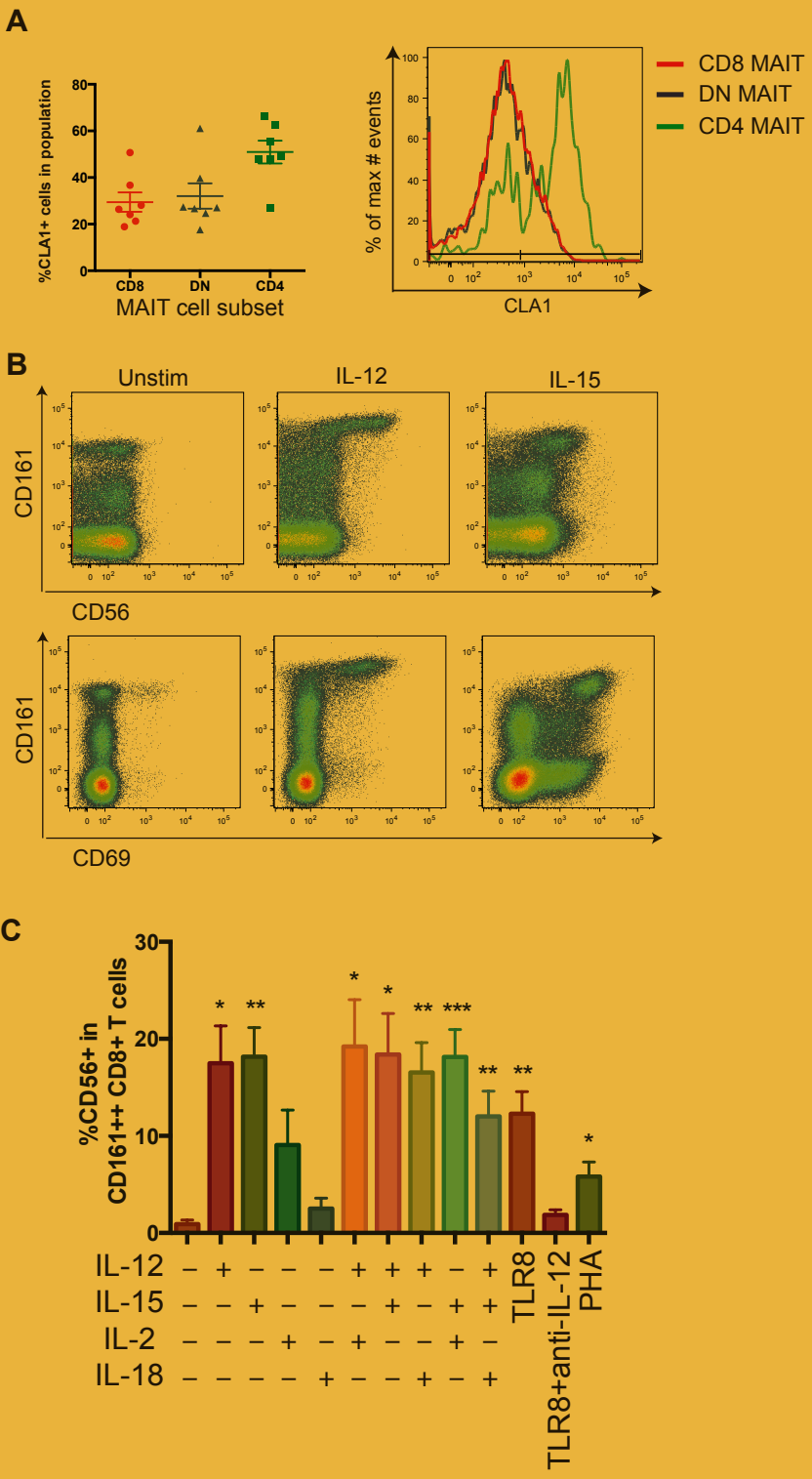
1. CD4+ MAIT cells are uniquely enriched within the human tonsil compared to CD4− MAIT cells, in line with their distinct lymphoid homing trafficking machinery
2. CD4+ MAIT cells are skewed towards a Th2 cytokine profile, and express significantly less Th1 cytokines than CD4− MAIT cells. CD4+ MAIT cells also lacked the capacity to degranulate and express cytotoxic molecules. All three subsets are proficient producers of IL-17
3. MAIT cells are uniformly T-bet^{low}, PLZF+, RORγt+, ThPOK^{low}. CD4+ MAIT cells express significantly less Eomes compared to CD8+ and DN MAIT cells
4. CD8+ MAIT cells do not require CD8 coreceptor ligation for their activity



Appendix Figure IV-1. Cytometric bead array (CBA) assay to detect cytokine production from indicated FACS-sorted MAIT cell subsets, following IL-12+IL-18 stimulation for 48 hours. A) IFNγ production measured by a CBA assay following stimulation of unsorted PBMCs (blue) (10^6 cells per well) or FACS-sorted MAIT cell subsets (red) with IL-12+IL-18 stimulation for 48 hours. No other cytokines were detected. B) IFNγ production measured by a CBA assay, adjusted per 10^3 cells of indicated MAIT cell subset. Graphs depict the mean concentration of cytokines ± S.E.M. Experiments performed by Lucy Walker.



Appendix Figure IV-2. Anti-CD8 blocking antibody does not affect the activation of the DN population of MAIT cells. A) Representative plots showing the effect of the anti-CD8 blocking antibody on IFNγ expression from either CD8+ MAIT cells within enriched CD8+ T cells (left) or DN MAIT cells within CD8-depleted T cells (right), both cultured with *E. coli*-treated THP1s for 5 hours. B-C) Cumulative data showing the (B) IFNγ or (C) TNFα expression from either CD8+ MAIT cells within enriched CD8+ T cells or DN MAIT cells within CD8-depleted T cells, in the presence or absence of blocking antibody against CD8. ****P<0.0001, **P<0.01, ns=non-significant by two-way repeated measures ANOVA, with Bonferroni's multiple comparisons test, comparing the cells cultured with isotype controls versus cells cultured with anti-CD8 blocking antibody (n=5).



Appendix Figure IV-3. Expression of cutaneous lymphocyte antigen 1 (CLA1) and induction of CD56 on MAIT cells. A) Expression of CLA1 on MAIT cell subsets. Cumulative frequencies (left) and representative plot showing the expression of CLA1 on indicated MAIT cell subsets. ***P<0.001 by repeated measures one-way ANOVA with Dunnett's multiple comparisons test, compared to CD8+ MAIT cells. n=6, from two independent experiments. B-C) CD56 expression on CD161++CD8+ T cells after culture with indicated cytokines or stimuli for 6 days. Representative staining (B) and cumulative frequencies (C) are shown. ***P<0.001 by repeated measures one-way ANOVA with Dunnett's multiple comparisons test, compared to unstimulated cells. n=10, from two independent experiments. All graphs show mean ± S.E.M. CLA1 staining includes data generated by Verity Hill.

5. MAIT cells in psoriasis and psoriatic arthritis

5.1. Introduction

5.1.1. Psoriasis

Psoriasis is a chronic inflammatory skin disease characterized by inflamed scaly lesions and epidermal hyperplasia (acanthosis; thickening of the epidermis), due to the hyperproliferation of keratinocytes (Perera et al., 2012; van Beelen et al., 2007). Furthermore, it is also characterized by the infiltration of CD8+ T cells in the epidermis, and DC and CD4+ T cell infiltration into the dermis (Austin et al., 1998; Gudjonsson et al., 2004; Paukkonen et al., 1992; Perera et al., 2012). This inflammatory disease affects 125 million people globally, but its etiology is still unclear (Langley et al., 2005).

T cells have been shown to critical drivers of psoriasis pathology, as T cells in non-lesional skin from psoriatic patients induced spontaneous psoriatic lesions when grafted onto immunocompromised mice lacking T, B and NK cells (Boyman et al., 2004). Psoriasis was initially thought to be a Th1-mediated disease, due to an increase in the frequency of IFNγ-producing T cells in the periphery and skin lesions of psoriatic patients (Austin et al., 1999; Szabo et al., 1998). Recent research however supports the involvement of the IL-23/IL-17 pathway in the pathogenesis of psoriasis. Genome-wide association studies (GWAS) have highlighted single nucleotide polymorphisms (SNPs) in *IL23A* encoding the cytokine IL-23, as well as *IL12RB* and *IL23R*, encoding the common IL-12/23p40 subunit and IL-23R, respectively, which are associated with the development of psoriasis (Capon et al., 2007; Cargill et al., 2007; Hébert et al., 2012; Nair et al., 2009). Increased IL-23

mRNA (Chan et al., 2006; Lee et al., 2004) and protein expression (Piskin et al., 2006) in the lesional skin of psoriatic patients has been reported, and indeed, overexpression or injection of IL-23, but not IL-12, induces severe inflammation of murine skin, similar to epidermal hyperplasia seen in psoriatic skin (Chan et al., 2006; Wiekowski et al., 2001; Zheng et al., 2007). Thus, treatment with a neutralizing IL-12/23p40 antibody has shown high efficacy in clinical trials for psoriatic patients (Kauffman et al., 2004; Krueger et al., 2007; Toichi et al., 2006).

Murine models of psoriasis are commonly based on IL-23 injection in mice, or the application of the TLR7/8 agonist imiquimod, which induces psoriasiform skin inflammation and hyperplasia (Van Belle et al., 2012; Zheng et al., 2007). Skin inflammation in such murine models was initially shown to be dependent on IL-22, through IL-23 injection in IL-22R-deficient mice (Zheng et al., 2007) and through the use of IL-22-neutralizing antibodies (Ma et al., 2008; Van Belle et al., 2012). IL-22 exerts its effect by modulating defensins (Wolk et al., 2006) and by inducing keratinocyte activation and hyperproliferation (Boniface et al., 2005; Sa et al., 2007; Zheng et al., 2007). Although IL-22 mRNA expression is upregulated in psoriatic skin compared to normal skin (Boniface et al., 2007), two clinical trials of IL-22-blockade (ILV-095 and IL-094) in psoriasis patients have so far been unsuccessful and have been terminated (Antoniu, 2012)[1].

Instead, another key role for IL-23 in psoriasis is its ability to drive Th17 cell proliferation and differentiation (Wilson et al., 2007). IL-23-induced epidermal hyperplasia has been subsequently shown to require both IL-22 and IL-17, as skin inflammation was reduced in IL-17$^{-/-}$ mice, despite high levels of IL-22 (Rizzo et al., 2010). Psoriasis-like inflammation in imiquimod-induced models is also completely

[1] Source: https://clinicaltrials.gov/ct2/show/NCT01010542

abrogated in mice deficient for IL-23 or IL-17R (Cai et al., 2011; van der Fits et al., 2009), highlighting a critical role for IL-17 in psoriatic disease.

Clinical evidence for the involvement of IL-17 in psoriasis is extensive. IL-17 is found at increased levels in psoriatic lesions, but not in non-lesional skin (Harper et al., 2009; Lowes et al., 2008; Teunissen et al., 1998). Both Th17 cells and Tc17 cells are increased in these lesions, with a particular increase of Th17 cells in the dermis (Kryczek et al., 2008), and Tc17 cells within the epidermis (Kryczek et al., 2008; Ortega et al., 2009; Res et al., 2010). In the periphery of psoriasis patients, Th17 cells have also been reported to be increased (Benham et al., 2013; Kagami et al., 2010). Reduced clinical severity has been correlated with a reduction in IL-17 in psoriatic lesions (Zaba et al., 2007) as well as reduced Th17 and Tc17 cells in the periphery (Eysteinsdóttir et al., 2013), although one study did not find a correlation between the frequency of Th17 cells in blood and skin disease severity (Kagami et al., 2010). Interestingly, there is a strong genetic association of psoriasis with HLA-C (Gudjonsson et al., 2003; Mallon et al., 1997). Two-thirds of psoriasis patients carry the *HLA-Cw*0602* allele (Gudjonsson et al., 2004; Mallon et al., 1997), and genetic association studies have shown that *HLA-Cw6* is a risk factor for psoriasis (Nair et al., 2009), implicating conventional CD8+ T cells in the pathogenesis of psoriasis.

IL-17 induces keratinocyte activation together with IFNγ and IL-22, leading to the production of antibacterial peptides such as defensins and S100 proteins (Morizane & Gallo, 2012), as well as chemokines CCL20 and IL-8 (Liang et al., 2006). Together, this leads to the recruitment of CCR6-expressing T cells and neutrophils to the site of inflammation (Homey et al., 2000; Yao et al., 1995). Furthermore, IL-17 downregulates filaggrin and adhesion molecules required for barrier formation (Gutowska-Owsiak et al., 2012). Thus IL-17-blockade (Hueber et al., 2010; Leonardi et al., 2012; Papp et al., 2012) has shown promising results in treating psoriasis.

Furthermore, as RORγt is required for the induction of IL-17 transcription and for the development of Th17-dependent autoimmune diseases in mice (Ivanov et al., 2006; Lee et al., 2012), RORγt inhibitors have been developed which have been shown to successfully inhibit IL-17 production (Huh et al., 2011; Huh & Littman, 2012), and the expression of Th17 signature genes in PBMCs of psoriatic patients (Skepner et al., 2014).

5.1.2. Psoriatic arthritis

10~30% of patients with psoriasis also suffer from an erosive, poly-articular disease with joint destruction, loss of functionality, and hyperplasia of the synovial lining cells, a condition known as psoriatic arthritis (PsA) (Langley et al., 2005; Perera et al., 2012). Development of PsA has been associated with the same loci in GWAS studies as psoriasis (Hébert et al., 2012), and IL-17 is thought to play a key role in its pathology. IL-17 overexpression in the knee joint of naïve mice induces joint inflammation and cartilage proteoglycan loss (Lubberts et al., 2001), as well as inducing increased cartilage erosion in the joints of mice with collagen-induced arthritis (CIA) and streptococcal cell wall-induced arthritis (Koenders et al., 2005; Lubberts et al., 2001). Murine arthritis models have also shown that IL-17 enhances joint inflammation by inducing proinflammatory cytokines and chemokines, such as IL-1β, TNFα, and IL-8 (Chabaud et al., 1999; Jovanovic et al., 1998). Furthermore, IL-17 induces osteoclastogenesis and bone resorption through the induction of receptor activator of nuclear factor kappa-B (NF-κB) ligand (RANKL) (Kotake et al., 1999). IL-17 can also cause the destruction of cartilage matrix (Chabaud et al., 2000; Koshy et al., 2002) and inhibit matrix synthesis by activating chondrocytes (LeGrand et al., 2001). In murine models of CIA and adjuvant-induced arthritis, antibody blockade of IL-17 or deficiency of IL-17 leads to reduced joint damage (Bush et al., 2002; Lubberts et al., 2004; Nakae et al., 2003).

There are also human studies supporting a role for IL-17 in PsA. High concentrations of IL-17 have been detected in the synovial fluid of PsA patients (Celis et al., 2012; Raychaudhuri et al., 2012), with an increased frequency of Th17 cells in the periphery (Jandus et al., 2008; Yoo et al., 2012) as well as the joint (Leipe et al., 2010; Raychaudhuri et al., 2012). A correlation between the frequency of IL-17-producing CD4+ cells and the extent of disease activity has also been reported (Leipe et al., 2010). Interestingly, a GWAS study has shown a strong association between the development of PsA and the tumor necrosis factor receptor associated factor 3-interacting protein 2 (*TRAF3IP2*) gene encoding the IL-17-receptor adaptor protein, NF-κB Activator 1 (*Act1*), which showed a less significant association in patients with psoriasis alone (Hüffmeier et al., 2010). CD8+ T cells have also been implicated in PsA pathogenesis, as CD8+ T cells outnumber CD4+ T cells in the synovial fluid of PsA patients (Costello et al., 1999), and the susceptibility to PsA is most strongly associated with HLA genes of the MHC class I locus (Eder et al., 2012; Winchester et al., 2012), and transcription factor genes involved in the differentiation of memory CD8+ T cells (Bowes et al., 2015).

5.1.3. Unconventional lymphocytes in psoriasis and PsA

Recently, there is increasing interest in the role of unconventional, innate lymphocytes producing IL-17, such as γδ T cells and innate lymphoid cells (ILCs), in the development of psoriasis and PsA. In an imiquimod-induced model of psoriasis-like skin inflammation, RORγt+ ILCs and γd T cells were found to be the main IL-17- and IL-22-producers in plaques (Cai et al., 2011; Pantelyushin et al., 2012). Depletion of γδ T cells and ILCs protected these mice from plaque formation (Pantelyushin et al., 2012) and IL-23-induced epidermal hyperplasia and inflammation (Cai et al., 2011). The role for γδ T cells in human psoriasis is also

supported by the increased frequencies of IL-17-producing γδ T cells in psoriatic lesions (Cai et al., 2011). In a CIA model, γδ T cells have also been shown to be a major source of IL-17, and antibody-mediated depletion of these cells led to a significant reduction in disease severity and incidence (Roark et al., 2007). A recent study has also shown an increase in IL-17-producing ILC3s in the synovial fluid of PsA patients compared to the periphery (Leijten et al., 2015).

The role of MAIT cells in these psoriatic diseases has not been examined in detail. Like γδ T cells and ILC3s, MAIT cells constitutively express RORγt, CCR6, and IL-23R (Walker et al., 2012), and are able to produce high levels of IL-17 (Billerbeck et al., 2010; Dusseaux et al., 2011), particularly in inflamed tissues such as the adipose tissue of obese patients (Magalhaes et al., 2015). The loss of MAIT cells from the periphery has been reported in various autoimmune conditions including IBD (Serriari et al., 2014), diabetes and obesity (Carolan et al., 2015; Magalhaes et al., 2015), and MS (Miyazaki et al., 2011; Willing et al., 2014). Furthermore, there is a corresponding accumulation of MAIT cells in inflamed tissues of patients (Annibali et al., 2011; Magalhaes et al., 2015; Serriari et al., 2014), suggesting that MAIT cells are being recruited from the periphery into inflamed loci. Importantly, $MR1^{-/-}$ mice were less susceptible to CIA, and adoptive transfer of MAIT cells induced arthritis in $MR1^{-/-}$ mice in a model of collagen antibody-induced arthritis (CIAI) (Chiba et al., 2012), suggesting MAIT cells may act as effector cells in joint inflammation. This is supported by a recent study showing that the loss of MAIT cells in the periphery of systemic lupus erythematosus (SLE) and rheumatoid arthritis (RA) patients positively correlated with disease severity, and an increase in MAIT cells was found in the synovial fluid of RA patients compared to paired blood samples (Cho et al., 2014).

We therefore wanted to examine the functionality of MAIT cells in the blood and inflamed tissue of psoriasis and PsA patients, and correlate their frequency with

disease activity. Furthermore, in collaboration with ORCA Pharmaceuticals Ltd., we tested the effect of a novel RORγt inhibitor on MAIT cells to delineate the RORγt-dependent and -independent functions of these cells, as well as testing this novel inhibitor in human cells for its therapeutic potential.

5.2. Aims

1. Detect and quantify MAIT cells in healthy and psoriatic skin
2. Analyse the frequency and function of peripheral blood MAIT cells in psoriasis patients
3. Analyse the frequency and function of MAIT cells and MAIT-cell like CD161++ T cells in the peripheral blood and synovial fluid of PsA patients
4. Demonstrate the effect of RORγt blockade on MAIT cell function using a novel RORγt inhibitor

5.3. Methods

5.3.1. Isolation of T cells from the skin

Human skin samples were obtained from healthy donors during plastic surgery or from biopsies of lesional skin of psoriatic patients, and processed as previously described (Salimi et al., 2013). Subcutaneous fat was removed before the samples were dissected and incubated in collagenase P (Roche). Following overnight digestion at 37°C, the tissue was collected and filtered through a 70μm strainer (VWR International). After a wash in cold 10mM EDTA solution, the cells were resuspended in cold RPMI, and filtered through a 40μm strainer. Cells were then layered onto Lymphoprep^{TM} for density gradient separation, and rested overnight in R10 before FACS analysis.

5.3.2. Psoriasis patients

PBMCs from 10 psoriasis patients and 10 atopic dermatitis patients were isolated and frozen until use. Patient information is provided in Appendix Table V-9. Samples were treated identically to 10 frozen healthy control samples (leukocyte cone donors), in two separate experiments.

5.3.3. Psoriatic arthritis (PsA) patients

7 synovial fluid samples and paired peripheral blood samples were obtained from 5 PsA patients. Patient information is summarized in Table 5-1. Synovial fluid samples were washed in PBS before being layered onto Lymphoprep^{TM} (Axis Shield Diagnostics) for the isolation of cells by density gradient separation. Synovial fluid mononuclear cells (SFMC) were used immediately, and remaining cells were frozen in liquid nitrogen until further use for transcription factor staining. For *E. coli*-stimulations, SFMC was added to *E. coli*-treated THP1 cells at a ratio of $5x10^5$ SFMC:$8x10^4$ THP1 cells, as with PBMCs.

5.3.4. Pre-activating MAIT cells for IL-17 production

$2x10^6$ PBMCs from healthy donors were thawed and cultured with either anti-CD3/CD28/CD2 beads (Miltenyi Biotec) at a 2:1 ratio or PFA-fixed *E. coli* at 10BpC in 48 well plates in R10 for 7 days, with the following cytokines: IL-23, IL-18, IL-2, IL-6 (50ng/ml; all Miltenyi Biotec), IL-1β (50ng/ml PreproTech), and IL-7 (20ng/ml; Miltenyi Biotec) for initial optimization experiments. Cells were washed and restimulated with 250ng/ml PMA and 500ng/ml ionomycin (both Sigma Aldrich) for 5 hours, with Brefeldin A (10µg/ml; Sigma Aldrich) added for the final 4 hours. Subsequently, PBMCs were cultured with anti-CD3/CD28/CD2 beads and IL-23, IL-7 and IL-1β as

above and restimulated with PMA/ionomycin or *E. coli*-treated THP1 cells, as indicated.

5.3.5. RORγt inhibitor

The ORX1091 compound was added to PBMCs at indicated concentrations during 7 day pre-activation cultures of MAIT cells as described above. DMSO was added to negative control wells. Alternatively, the ORX1091 compound was added to PBMCs for 24 hours, before IL-12+IL-18 or IL-23+IL-18 (all 50ng/ml; Miltenyi Biotec) was added for a further 16 hours. Brefeldin A was added for the last 4 hours. Designed by ORCA Pharmaceuticals Ltd., and molecular weight=436.54. In murine T cells, half maximal inhibitor concentration (IC_{50})= 105±69nM.

5.3.6. Microarray analysis

Microarrays of CD161 subsets within CD8+ T cells were obtained from the publication by Billerbeck *et al.,* (2010). Genes significantly upregulated in CD161++ or CD161+ subsets (>2 fold, P<0.05) compared to the CD161− subset of CD8+ T cells are listed in Appendix Table V-1. Pavlidis Template Matching (PTM) of whole microarray data was performed using MeV Version 4.9 (TM4; Saeed et al., 2003). The threshold for matching was set as the size of the correlation coefficient (R>0.9). Venn diagrams were generated using GenePattern[2].

[2] http://www.broadinstitute.org/cancer/software/genepattern/

5.4. Results

5.4.1. MAIT cells are present in healthy and psoriatic skin

The presence of MAIT cells within the skin, and whether there is a change in their frequency in psoriatic skin compared to healthy skin, was investigated. Within dermal T cells in one healthy donor, 0.16% of cells expressed CD161 and Vα7.2 (Figure 5-1A). The presence of MAIT cells was confirmed in a second healthy donor, as these cells could be expanded with anti-CD3/CD28/CD2 stimulation (Figure 5-1B). Other stimuli that induce the proliferation of peripheral blood MAIT cells (IL-2, IL-12, or *E. coli*; see Chapter 3) did not expand these cells. Examination of psoriatic lesional skin showed that MAIT cells were also present in psoriatic skin at a low frequency (range 0-4.17%), and expressed IL-18R as seen in blood (Ussher et al., 2013) (Figure 5-1C). Although there seemed to be a slight increase in the frequency of MAIT cells within all T cells as well as within CD8+ T cells in psoriatic skin compared to healthy skin, these were not significant differences (Figure 5-1D). There was also no difference the frequency of MAIT cells within DN T cells. CD4+ T cells could only be detected in one psoriatic skin sample, but no other healthy or psoriatic skin samples. Thus, although CD4+ MAIT cells express the skin-homing markers CCR4 and CLA1 (Chapter 4), no CD4+ MAIT cells could be identified in healthy or psoriatic skin. The assessment of coreceptor usage of MAIT cells also did not show any differences in the ratio of CD8 and DN MAIT cells within psoriatic skin (Figure 5-1E).

A potential reason for the lack of isolated CD4+ T cells may be due to the enrichment of epidermal cells during sample processing (CD4+ T cells are enriched in the dermis, while CD8+ T cells are localised in the epidermis (Mueller et al., 2014)), or due to the effect of neutral protease activity in the collagenase preparations, which can degrade

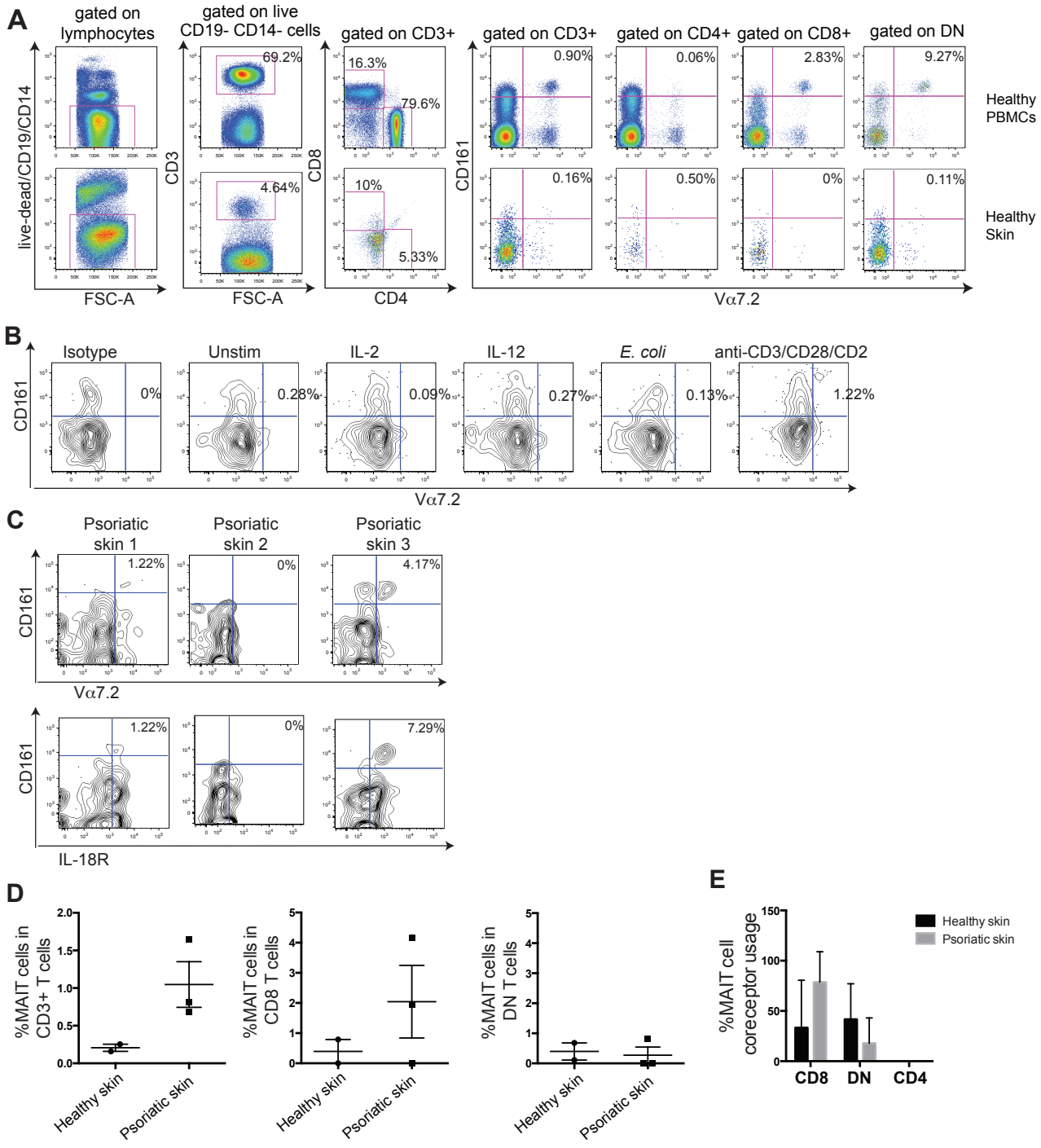


Figure 5-1. IL-18R+ MAIT cells are present in healthy and psoriatic skin. A) Gating strategy for identifying MAIT cells, comparing flow cytometry staining of healthy MAIT cells from the periphery to cells from the skin. B) Culture of dermal MAIT cells with indicated cytokines or anti-CD3/CD28/CD2 beads for 5 days. The frequency of MAIT cells within CD8+ T cells is indicated. C) IL-18R expression and Vα7.2 expression on CD8+ MAIT cells from psoriatic skin samples. D) Comparative frequencies (mean ± S.E.M.) of MAIT cells within CD3+ (left), CD8+ (centre), and double-negative (DN) (right) T cells from healthy (n=2) and psoriatic skin (n=3). All comparisons between healthy skin and psoriatic skin non-significant by an unpaired t-test. Data for CD4+ T cells not shown (no CD4+ T cells detected in four out of five skin samples). E) The frequency of MAIT cells that are CD8+, DN, or CD4+ in healthy and psoriatic skin.

certain epitopes and may have affected the detectable expression of CD4 (Clark et al., 2006). Given the very small number of MAIT cells that could be detected within healthy or psoriatic skin samples, these results would need to be confirmed using other methods such as immunohistochemistry.

5.4.2. The frequency and phenotype of MAIT cells of psoriasis and atopic dermatitis patients

Due to the insufficient number of MAIT cells that could be isolated from psoriatic skin to perform functional studies, a comprehensive analysis of the function and phenotype of MAIT cells in the blood of psoriasis patients was performed. These were compared to PBMCs from healthy controls and atopic dermatitis (AD) patients. AD is a common relapsing skin condition, and similarly to psoriasis, is characterized by epithelial hyperplasia and T cell and DC infiltrates (Di Cesare et al., 2008). AD is, however, a Th2-mediated disease, characterized by abnormal IgE production, eosinophilia and production of Th2 cytokines (Di Cesare et al., 2008; Wierenga et al., 1991). Increased IL-17 has been observed in acute and chronic atopic lesions compared to non-lesional skin (Gittler et al., 2012; Koga et al., 2008; Toda et al., 2003), but in contrast to the strong association between IL-17/Th17 cells and the clinical score in psoriasis, IL-17 does not increase in chronic lesions compared to acute atopic dermatitis lesions (Gittler et al., 2012; Koga et al., 2008; Nograles et al., 2009). In turn, increased production of IL-22 and Th2 cytokines are associated with progression to chronic disease (Gittler et al., 2012; Nograles et al., 2009). Given the different cytokine profiles involved in psoriasis and AD, we hypothesized that MAIT cell frequency and function may be affected differently.

Firstly, the frequency of MAIT cells in peripheral blood samples from 10 psoriasis patients, 10 AD patients, and 10 healthy controls were determined by flow cytometry. Although there was a trend towards a lower frequency of MAIT cells in the blood of psoriasis patients (2.89 ± 0.47%) compared to healthy controls (6.36 ± 1.04%) and AD patients (5.66 ± 2.39%), there was no statistically significant difference between the three groups of donors (Figure 5-2A). There was also no significant difference in the frequencies of MAIT cells within DN or CD4+ T cells in the periphery of psoriasis patients (Appendix Figure V-1A).

MAIT cells also express IL-18R at a uniquely high level compared to conventional T cells (Ussher et al., 2013). A significant increase in the expression of IL-18R mRNA in lesional skin has also been reported (Pietrzak et al., 2008), suggesting that IL-18R+ cells may infiltrate into the psoriatic lesion. Examination of the phenotype of MAIT cells in psoriasis patients, however, showed there was no significant difference in the expression of IL-18R on CD8+ MAIT cells (Figure 5-2B), as well as CD4+ and DN MAIT cells (Appendix Figure V-1B).

T cells in psoriatic lesions have been shown to have an increased expression of GrB and perforin (Yawalkar et al., 2001), and increased perforin expression in the periphery of psoriasis patients have also been demonstrated (Behrendt et al., 2000; Prpić Massari et al., 2007). Therefore, changes in the cytotoxic profile of MAIT cells in psoriasis patients were investigated by staining for GrA, GrB, GrK and perforin in *ex vivo* cells (Figure 5-2C-F). Again, there was no significant difference in the expression of cytolytic molecules by MAIT cells between patient groups, with a clear GrA+GrK+GrB−perforin^{low} phenotype in all CD8+ MAIT cells. There was also no difference in the expression of granzymes and perforin by CD4+ or DN MAIT cells between patient groups (data not shown).

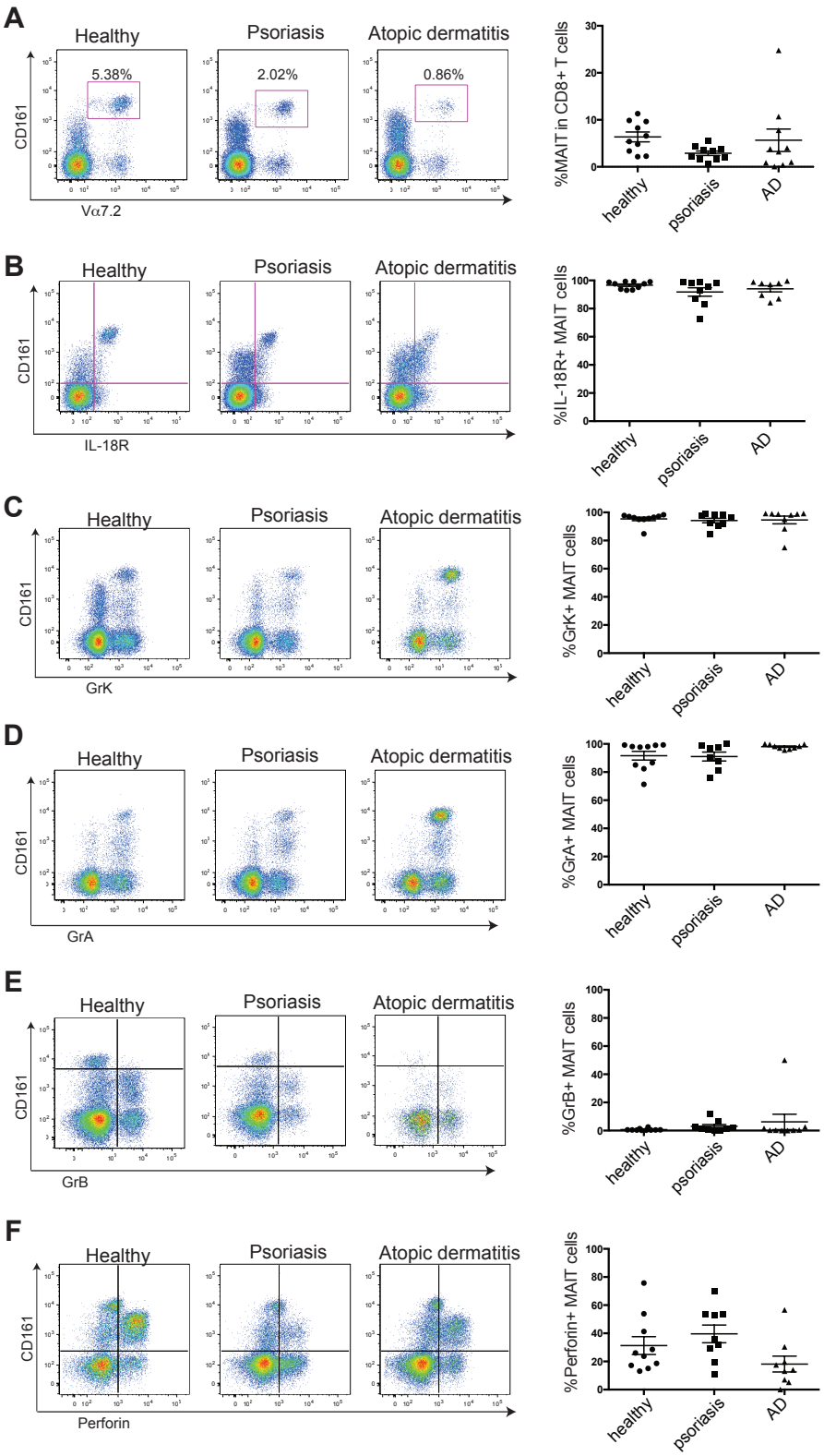


Figure 5-2. The frequency and phenotype of MAIT cells in the periphery of psoriasis and atopic dermatitis (AD) patients are not significantly different compared to MAIT cells from healthy controls. A) Representative staining (left) and cumulative frequencies (right) of MAIT cells within CD8+T cells are shown for healthy (n=10), psoriasis (n=10), and AD (n=10) patients. B) Representative staining of IL-18R expression and cumulative frequencies of IL-18R+ MAIT cells from healthy (n=10), psoriasis (n=9), and AD (n=8) patients are shown. C-F) Granzyme K (GrK) (C), GrA (D), GrB (E), and perforin (F) expression by CD8+ MAIT cells. Representative staining and cumulative frequencies of cells expressing the indicated granzyme/perforin are shown for each. Healthy (n=10), psoriasis (n=9), AD (n=9). All comparisons were non-significant. All representative stains are gated on peripheral blood CD8+ T cells of a healthy (left), psoriasis (centre) or AD (right) patient.

5.4.3. A reduced frequency of MAIT cells from psoriasis and atopic dermatitis patients express IFNγ in response to PMA/ionomycin stimulation compared to healthy controls

To look for differences in the ability of MAIT cells to respond in an MR1-dependent manner and -independent manner (Ussher et al., 2013), PBMCs were either cultured with THP1 cells that had been pre-treated with PFA-fixed *E. coli* for 5 hours (Figure 5-3A), or stimulated with IL-12+IL-18 cytokines overnight (Figure 5-3B). A high proportion of MAIT cells in all groups of patients responded by secreting IFNγ to both stimuli, and there was no significant difference between healthy controls and psoriasis or AD patients, in CD8+ MAIT cells, or CD4+ and DN MAIT cells (Appendix Figure V-1C, D).

Finally, the ability of MAIT cells to secrete proinflammatory cytokines that have been associated with increased pathology in psoriasis patients was assessed. PBMCs were stimulated with PMA/ionomycin for 5 hours in the presence of Brefeldin A, and stained intracellulary for IFNγ, IL-17, and IL-22 expression (Figure 5-3C-E). Due to the extensive downregulation of the CD4 coreceptor upon PMA/ionomycin stimulation in this assay, analysis was performed on CD8+ and CD8− T cells. Interestingly, there was a significantly lower frequency of both CD8+ and CD8− MAIT cells secreting IFNγ in psoriasis and AD patients in response to PMA/ionomycin, which was a specific effect on MAIT cells (Figure 5-3C). Although previous studies had demonstrated an increase in IL-17-expressing peripheral CD8+ and CD8− T cells in psoriasis (Benham et al., 2013; Jandus et al., 2008; Leipe et al., 2010), no significant increase in the frequency of CD8+ or CD8− T cells expressing IL-17 could be observed in this study. IL-22 has also been shown to be increased in human psoriatic lesions (Boniface et al., 2007), as well as in plasma (Wolk et al., 2006).

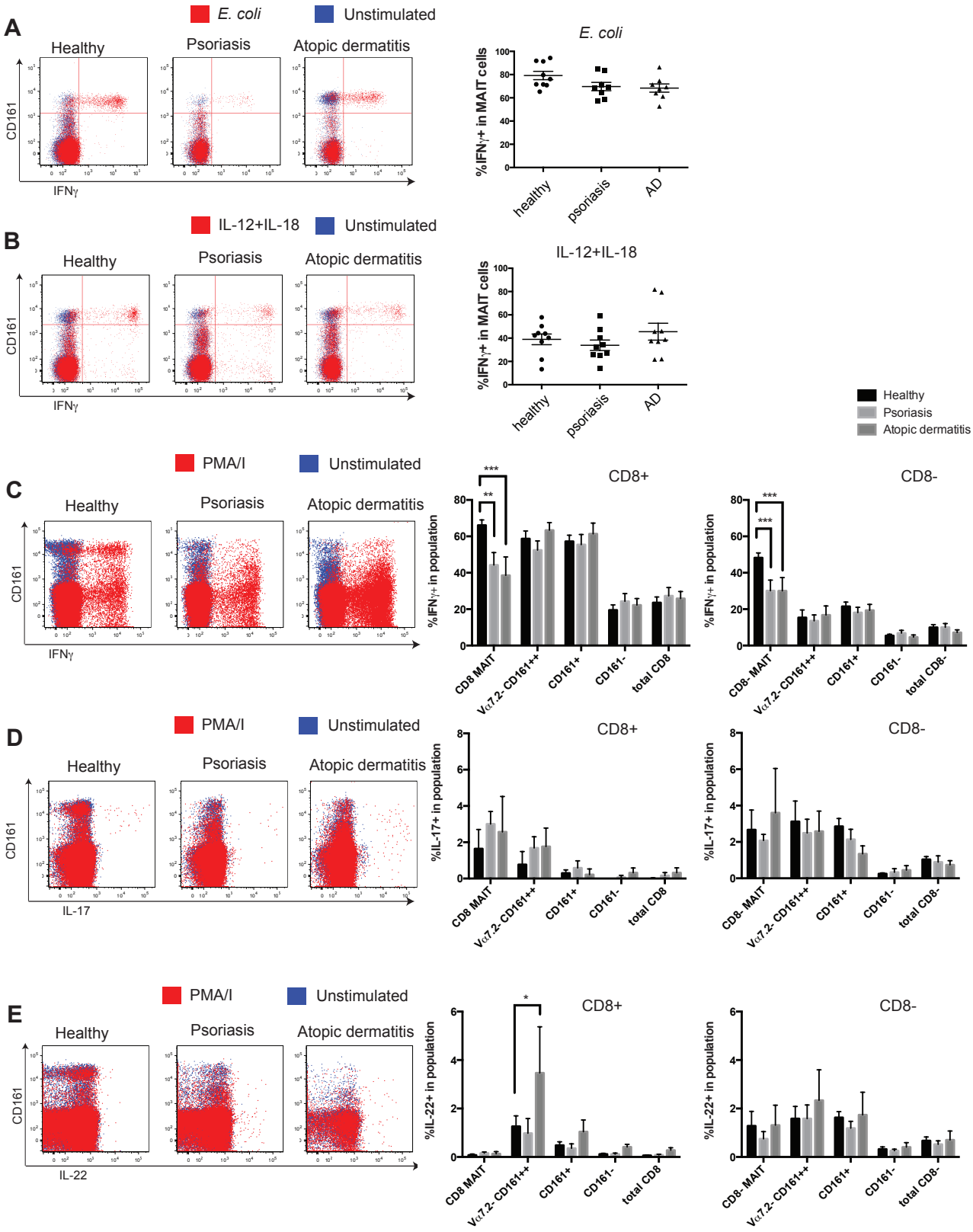


Figure 5-3. A reduced frequency of MAIT cells from psoriasis and atopic dermatitis (AD) patients express IFNγ in response to PMA/ionomycin stimulation. Representative stains (left) and cumulative frequencies (right) are shown for the following experiments: A-B) IFNγ-expression from CD8+ MAIT cells after A) culture with *E. coli*-treated THP1 cells for 5 hours, or B) overnight stimulation with IL-12+IL-18. Healthy (n=9), psoriasis (n=8), and AD (n=9) patients. C-E) Expression of IFNγ (C), IL-17 (D) and IL-22 (E) from T cells after stimulation with PMA/ionomycin (PMA/I) for 5 hours. For each cytokine, frequencies of cytokine-producing cells from indicated populations of CD8+ and CD8− T cells are shown. Healthy controls n=10, psoriasis n=10, AD n=10. ***P<0.001, **P<0.01, *P<0.05 by two-way repeated measures ANOVA with Dunnett's multiple comparisons test, compared to healthy controls within each indicated population. All other comparisons were non-significant. All representative stains are gated on peripheral blood CD8+ T cells of a healthy (left), psoriasis (centre) or AD (right) patient. PMA/I = PMA/ionomycin.

However there was no significant increase in the frequency of MAIT cells expressing IL-22 in psoriasis patients. Interestingly, there was a significant increase in the frequency of Vα7.2−CD161++CD8+ T cells expressing IL-22 in AD patients compared to healthy controls (Figure 5-3E). As increased IL-22 production has been strongly correlated with progression to chronic AD (Gittler et al., 2012; Nograles et al., 2009), it will be interesting to investigate whether this population may be increased in the lesional skin of AD patients.

5.4.4. MAIT cells are highly activated in the synovial fluid of psoriatic arthritis patients

Approximately 30% of patients with psoriasis suffer from the inflammatory joint disease, PsA (Christophers, 2001). As murine MAIT cells can exacerbate joint inflammation in a CIA model (Chiba et al., 2012), and they have the potential to secrete the osteoclastogenic and proinflammatory cytokine IL-17, the frequency, function and phenotype of MAIT cells from paired peripheral blood (PB) and synovial fluid (SF) samples from PsA patients were analysed (Table 5-1).

Firstly, the frequency of MAIT cells in SF samples from PsA patients was compared to paired PBMC samples. Although one donor showed a strikingly high frequency of MAIT cells within SF CD8+ T cells (Figure 5-4A), there was no significant increase in the frequency of MAIT cells within SF CD8+ T cells compared to paired PB samples (13.83 ± 9.45% vs. 5.506 ± 1.32%; Figure 5-4B). In fact, some donors had a higher frequency of MAIT cells within CD8+ T cells in the periphery compared to the inflamed joint, suggesting that there is no particular enrichment of MAIT cells within the joint due to their recruitment from the periphery. CD4+ and DN MAIT cells showed similar findings (Figure 5-4A, B). Strikingly, however, a higher frequency of

all subsets of SF MAIT cells expressed CD69 (70.35 ± 13.23%) compared to MAIT cells in paired PB samples (14.68 ± 5.57%) (Figure 5-4C).

Interestingly, when the frequency of MAIT cells in the SFMC was correlated with clinical disease activity parameters, a positive correlation was observed between the frequencies of SF CD8+ MAIT cells and the C-reactive protein (CRP) level in the blood (R=0.6794, P=0.0436) of patients with PsA (Figure 5-4D).

Next, whether the ability of MAIT cells to respond to MR1-dependent stimuli is preserved in the SF of PsA patients was tested, by culturing PBMCs or SFMCs for 5 hours with *E. coli*-treated THP1 cells. MAIT cells isolated from the SF of PsA patients responded readily to *E. coli*-treated THP1 cells by producing IFNγ (Figure 5-4E). Although there was no difference in the frequency of IFNγ-producing CD8+ MAIT cells between paired SF and PB samples, there was a significantly higher frequency of IFNγ+ CD8+ MAIT cells in the SF samples compared to healthy control PB samples (Figure 5-4F). A similar result was found for CD4+ and DN MAIT cells (Appendix Figure V-2A).

Changes in the cytotoxic granule content of MAIT cells were also investigated in CD8+ T cells of PsA patients. Staining for GrA, GrB, GrK, and perforin showed that there is no significant change in the cytolytic content of CD8+ MAIT cells in the SF in PsA patients (Appendix V-2B). Interestingly, however, there was a dramatic increase in the expression of GrA and GrK in non-MAIT CD8+ T cells, as the majority of all CD8+ T cells expressed GrA and GrK (Appendix V-2C, D). There was no overall change in expression of GrB or perforin in CD8+ T cells *ex vivo* (Appendix V-2E, F).

Sampling information:	
Number of SF samples	7
Number of patients	5
Number of patients where SF from both knees were sampled	1
Number of patients where SF before and after treatment were taken	1
Number of SF samples that had paired PB samples	6
Patient information (n=5)	
Male, no. (%)	4 (80%)
Age, mean ± SEM years	42.8 ± 3.499
Smoking, no. (%)	1 (20%)
B27 positive	0 (0%)
Cormorbidities (NASH) (%)	1 (20%)
Cormorbidities (Psoriasis) (%)	1 (20%)
Treatment information (n=7)	
Number of SF samples taken during treatment, no. (%)	4 (57%)
Biologics (%)	0 (0%)
DMARDs (LFN, MTX) (%)	4 (57%)
No treatment (%)	3 (43%)
CRP, mean ± SEM gm/dl (in all SF samples n=7)	5.786 ± 1.470

Table 5-1. Clinical data for PsA patients. DMARDs = disease modifying anti-rheumatic drugs, LFN = leflunomide, MTX = methotrexate, CRP = C-reactive protein level, NASH = non-alcoholic steatohepatitis. SF = synovial fluid, PB = peripheral blood. SEM = standard error of the mean. B27 = HLA-B27.

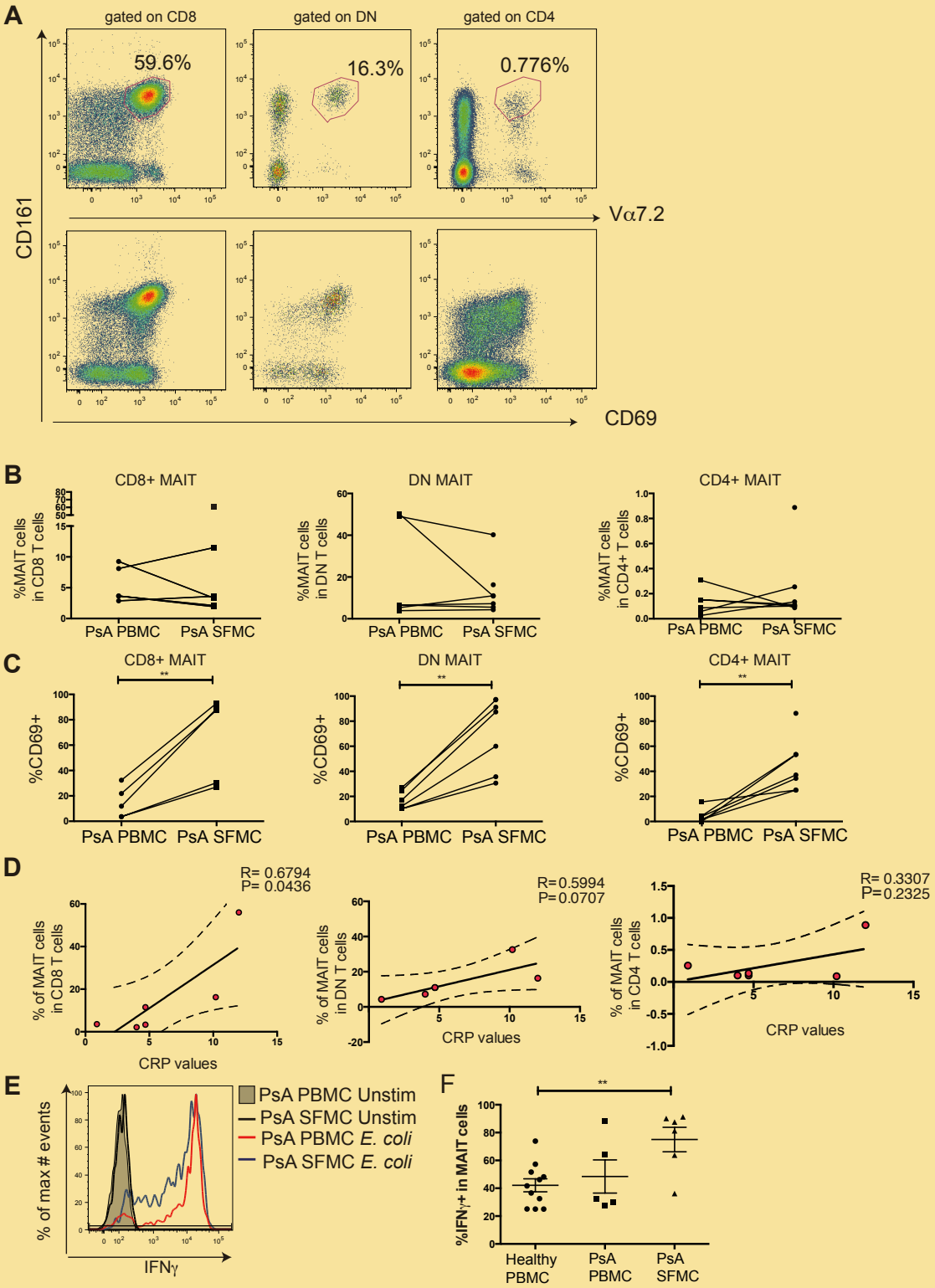


Figure 5-4. MAIT cells are highly activated in the synovial fluid of PsA patients and their frequency correlates with clinical activity. A) Staining of CD8+, DN and CD4+ T cells in the synovial fluid of a PsA patient with a high frequency of MAIT cells. B) Frequencies of MAIT cells within CD8+, DN, and CD4+ T cells in the blood (PBMC) and synovial fluid (SFMC) of PsA patients. Connecting lines indicate paired samples from the same patient. N=7 for SFMC, n=5 for PBMC samples.C) Expression of CD69 on MAIT cells in paired PBMC and SFMC samples. **P<0.01 by paired t-test. (n=5) D) Correlation between the frequency of MAIT cells within indicated T cell subset of SFMC and C-reactive protein (CRP) levels (n=6). Regression coefficient (solid line) with 95% confidence intervals (broken lines) are shown. E-F) IFNγ expression from CD8+ MAIT cells from PsA PBMC and SFMC samples, stimulated with *E. coli*-treated THP1 cells for 5 hours. Representative staining from one PsA patient (E) and cumulative frequencies (F) of IFNγ+ CD8+ MAIT cells compared to peripheral blood MAIT cells from healthy controls (healthy PBMC n=11) is shown. PsA SFMC n= 6, PsA PBMC n=5. **P<0.01 by one-way ANOVA with Dunnett's multiple comparisons test.

5.4.5. CD161++ T cells in the synovial fluid of psoriatic arthritis patients are highly responsive to IL-12+IL-18

As MAIT cells can also produce IFNγ in response to IL-12+IL-18, we next investigated whether SF MAIT cells may show heightened responsiveness to cytokines. PBMCs or SFMCs were stimulated overnight with IL-12+IL-18 and the frequency of T cells expressing IFNγ was assessed (Figure 5-5A). This showed that a higher frequency of SF CD8+ MAIT cells produced IFNγ compared to paired PB samples (57.0 ± 9.09% vs. 26.41 ± 10.46%). Interestingly, there was also a significantly higher frequency of IFNγ+ cells within Vα7.2− CD161++ CD8+ T cells, as well as within the CD161++ CD4+ T cells from SF samples (Figure 5-5B). This increase in IFNγ-expressing cell frequency was particularly striking in the Vα7.2−CD161++ CD4+ T cells. Furthermore, when the frequency of IFNγ-producing cells within SF samples was correlated with clinical disease activity, there was a correlation between the frequency of CD161++CD4+T cells secreting IFNγ in response to IL-12+IL-18 and CRP levels (R=0.8931, P=0.0153), while there was no significant correlation between CRP levels and the frequency of IFNγ+CD8+MAIT cells from SF samples (Figure 5-5C), suggesting that the MAIT-like responsiveness of CD161++CD4+ T cells to innate cytokines is correlated with levels of joint inflammation.

T cells expressing CD161 share a transcriptional signature associated with an increased ability to respond to the innate cytokines IL-12 and IL-18, which includes the genes encoding PLZF, RORγt, and IL-18R (Fergusson et al., 2014). In order to investigate the reason for the heightened, MAIT-cell like responsiveness to IL-12+IL-18 by CD161++CD4+ T cells, and to a lesser extent, CD8+MAIT cells in SF samples,

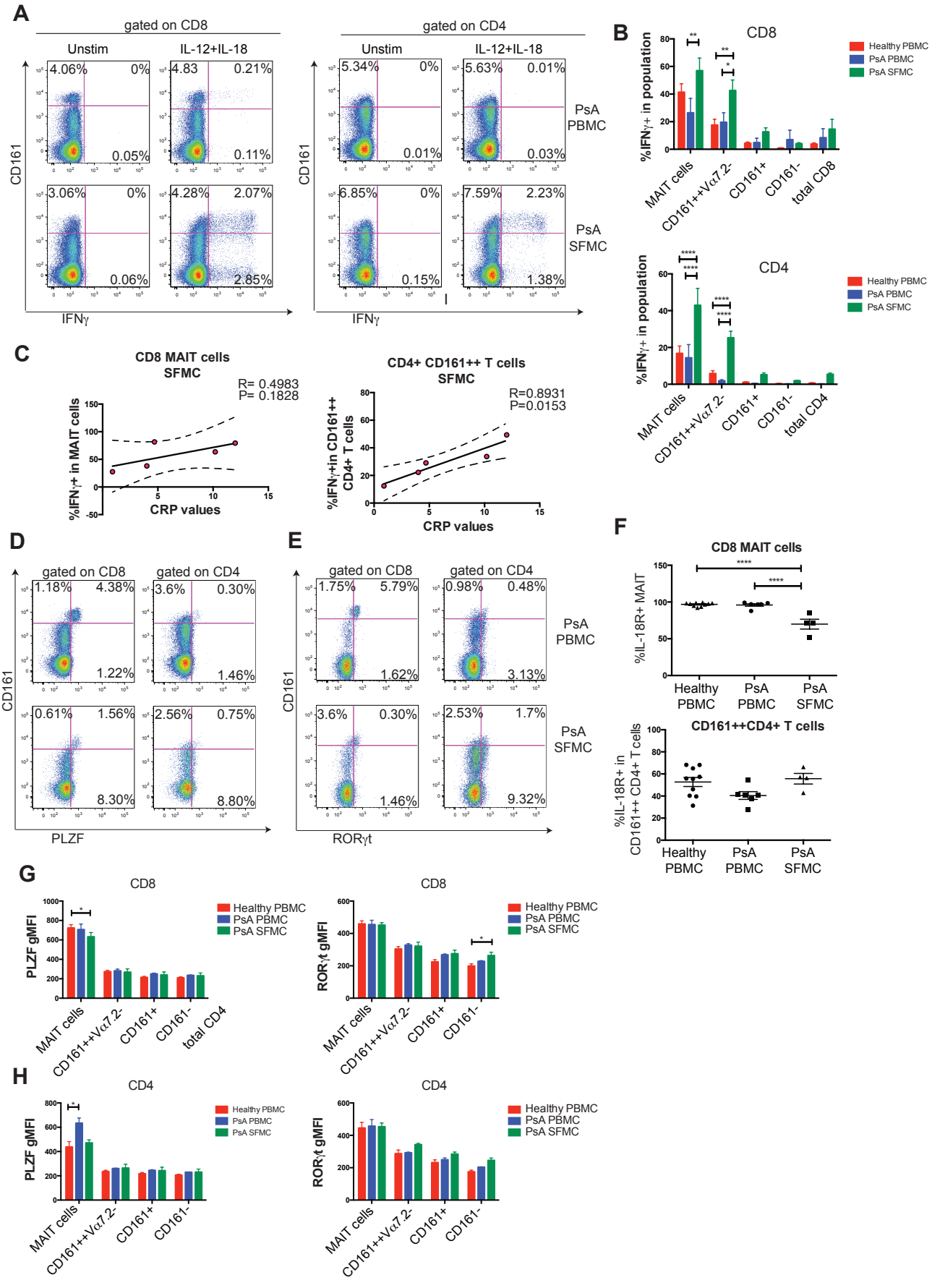

A
gated on CD8
gated on CD4
Unstim
IL-12+IL-18
CD161
IFNγ
PsA PBMC
PsA SFMC
B
CD8
CD4
%IFNγ+ in population
Healthy PBMC
PsA PBMC
PsA SFMC
MAIT cells
CD161++Vα7.2-
CD161+
CD161-
total CD8
total CD4
C
CD8 MAIT cells SFMC
R= 0.4983
P= 0.1828
%IFNγ+ in MAIT cells
CRP values
CD4+ CD161++ T cells SFMC
R=0.8931
P=0.0153
%IFNγ+in CD161++ CD4+ T cells
D
PLZF
E
RORγt
F
CD8 MAIT cells
%IL-18R+ MAIT
CD161++CD4+ T cells
%IL-18R+ in CD161++ CD4+ T cells
Healthy PBMC
PsA PBMC
PsA SFMC
G
CD8
PLZF gMFI
RORγt gMFI
H
CD4

Figure 5-5. CD161++ T cells in the synovial fluid of PsA patients are highly responsive to IL-12+IL-18. A-B) IFNγ production from T cells in response to overnight IL-12+IL-18 stimulation in paired PsA PBMC and SFMC samples or healthy control PBMC samples. A) Representative staining of paired PBMC (top) and SFMC (bottom) CD8+ and CD4+ T cells, and B) cumulative frequencies of IFNγ+ cells in the indicated subsets of CD8+ and CD4+ T cells. PsA PBMC n=5, PsA SFMC n=6, healthy PBMC n=16. ****P<0.0001, **P<0.01, *P<0.05 by two-way ANOVA with Bonferroni's multiple comparisons test. All other comparisons were non-significant. C) The frequency of IFNγ+ cells in CD8+ MAIT cells or CD161++CD4+ T cells following IL-12+IL-18 stimulation was correlated with C-reactive protein (CRP) levels. Regression coefficient (solid line) with 95% confidence intervals (broken lines) are shown (n= 5). D-E) Representative staining of PLZF (D) and RORγt (E) in CD8+ and CD4+ T cells in paired PBMC and SFMC samples from PsA patients. F) IL-18R expression in CD8+ MAIT cells and CD161++CD4+ T cells in SFMC (n=4) and PBMC samples (n=6) from PsA patients, or healthy control PBMCs (n=10). ****P<0.0001 by one-way ANOVA with Bonferroni's multiple comparisons test. All other comparisons were non-significant. G-H) Expression level of PLZF (G) and RORγt (H) as measured by gMFI in the indicated subsets of CD8+ and CD4+ T cells from PsA PBMC (n=3), PsA SFMC (n=3), and healthy PBMCs (n=5). ****P<0.0001, **P<0.01, *P<0.05 by two-way ANOVA with Bonferroni's multiple comparisons test, compared to healthy PBMCs. All other comparisons were non-significant.

changes in the expression of PLZF (Figure 5-5D), RORγt (Figure 5-5E), and IL-18R (Figure 5-5F) in these cells was assessed. Contrary to expectations, there was a significant reduction in the expression of IL-18R in CD8+ MAIT cells in SFMC samples (Figure 5-5F), compared to paired PBMC samples or healthy controls, which was mirrored by a slightly lower PLZF expression (Figure 5-5G). There was also no significant difference between the expression of IL-18R in CD161++CD4+ T cells between paired SF and PB samples. The amount of PLZF expressed by these cells, as measured by gMFI, again trended towards a lower expression in CD4+MAIT cells in SFMC compared to paired PBMC samples (Figure 5-5H). There was no difference in the amount of RORγt expressed by CD8+ MAIT cells or CD161++CD4+ T cells (Figure 5-5G, H). These results suggest that the increased frequency of IFNγ-expressing CD161++CD4+ T cells in response to IL-12 and IL-18 in SF samples from PsA patients is not associated with an increase in IL-18R, RORγt, or PLZF expression.

5.4.6. Increased frequency of IL-17-expressing T cells in the synovial fluid of PsA patients, including MAIT cells

Finally, the expression of cytokines previously associated with inflammatory joint diseases was assessed. Amongst these, IL-17 has been repeatedly associated with PsA pathology and is increased in the joint of PsA patients (Celis et al., 2012; Raychaudhuri et al., 2012). TNFα has also been shown to promote bone resorption and proliferation of synovial fibroblasts (Ritchlin et al., 2003; Yokota et al., 2006), while GM-CSF is produced by the synovium of arthritic patients (Alvaro-Gracia et al., 1991) and can exacerbate arthritis in CIA models (Campbell et al., 1997). Additionally, IFNγ can also enhance osteoclastogenesis (Kotake et al., 2005) and is present in the synovial tissue of patients with arthritis (Ritchlin et al., 1998).

Therefore, paired PBMCs and SFMCs from patients with PsA, or PBMC samples from healthy controls were stimulated *ex vivo* for 5 hours with PMA/ionomycin and the percentages of cells expressing IL-17, IFNγ, GM-CSF, and TNFα were determined within CD8+ and CD8− T cells (due to the extensive downregulation of CD4 upon PMA/ionomycin stimulation). In SF samples from PsA patients, there was a significant increase in the percentage of MAIT cells staining for IL-17 compared to paired PB samples (Figure 5-6A; 8.89 ± 5.17% vs. 2.31 ± 1.37%; $P<0.01$), as well as compared to PB samples from healthy donors (0.48 ± 0.08%; $P<0.01$). This increase in the frequency of IL-17-expressing cells was, in fact, seen in all CD8+ T cell subsets, in particular the CD161-positive subsets (Figure 5-6B). Furthermore, although there was no significant difference in the proportion of MAIT cells expressing IFNγ, GM-CSF, or TNFα (Figure 5-6A, B), there was a significant increase in the frequency of IFNγ+ (63.51 ± 8.38% vs. 13.90 ± 3.67%; $P<0.01$) and

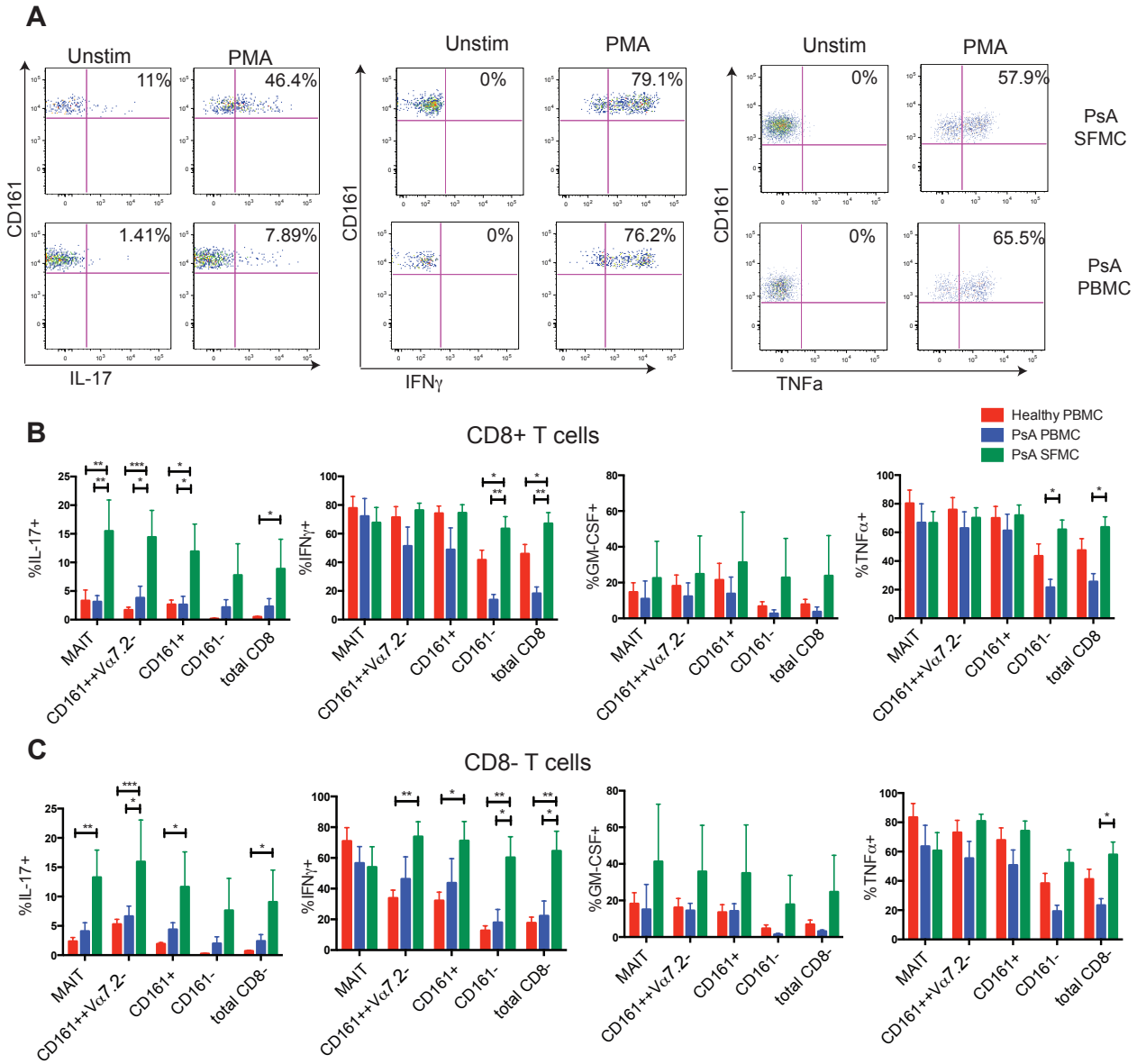


Figure 5-6. Increased frequency of IL-17-expressing T cells in the synovial fluid of PsA patients, including MAIT cells. Cells from the peripheral blood (PBMC) and the synovial fluid (SFMC) of psoriatic arthritis (PsA) patients, and PBMCs from healthy controls were stimulated with PMA/ionomycin for 5 hours in the presence of brefeldin A, and the expression of IFNγ, IL-17, GM-CSF, and TNFα was assessed. A) Representative staining of IL-17, IFNγ, and TNFα expression from CD8+ MAIT cells from paired SFMC and PBMC samples from a PsA patient. B-C) Expression of IL-17, IFNγ, GM-CSF, and TNFα from indicated subsets of CD8+ (B) and CD8− (C) T cells from SFMC and PBMC samples from PsA patients, or healthy control PBMCs. For IL-17, IFNγ and TNFα, healthy PBMC n=10, PsA PBMC n=6, PsA SFMC n=5. For GM-CSF, healthy PBMC n=4, PsA PBMC n=2, PsA SFMC n=2. ****P<0.0001, ***P<0.001, **P<0.01, and *P<0.05 by two-way repeated measures ANOVA with Tukey's multiple comparisons test. All other comparisons were not significant.

TNFα+ cells (62.07 ± 6.58% vs. 21.6 ± 5.59%; P<0.05) within the CD161− CD8+ T population in the SF compared to PB in paired donors. This led to a significant increase in IFNγ- and TNFα-expressing cells within the whole CD8+ T cell population in the SF compared to PB samples. A similar increase in the frequency of cells expressing IL-17, IFNγ and TNFα was seen in the CD8− T cell subsets compared to healthy PB samples as well (Figure 5-6C). In particular, the proportion of CD8− T cells expressing IFNγ was significantly greater in SF samples compared to healthy PB samples in PsA patients in all subsets except MAIT cells (i.e. in CD161++Vα7.2−, CD161+, CD161− T cells), leading to a significant increase in IFNγ-expressing cells in the CD8− T cell population as a whole (Figure 5-6C). Together, these results show that compared to healthy PB samples, there is a significant increase in the frequency of cells producing IL-17 in all CD161-expressing T cell subsets including MAIT cells, while significantly increased frequencies of IFNγ+ cells was also observed in all non-MAIT CD8− T cells, as well as the CD161− T cell subset in CD8+ T cells. This also suggests that the increased frequency of SF CD161++CD4+ T cells expressing IFNγ in response to IL-12+IL-18 may be due to their increased capacity to secrete IFNγ.

5.4.7. Gene expression correlation analysis identifies genes highly associated with *ZBTB16* expression in CD8+ T cells

The high frequency of IFNγ-expressing SF CD161++CD4+ T cells following IL-12 and IL-18 stimulation further confirms a recent report on peripheral blood cells showing that CD161 expression strongly correlates with the ability of T cells to respond to innate cytokines, regardless of TCR usage (Fergusson et al., 2014). However the master transcription factor regulating CD161 expression and its associated phenotype, including the MAIT-cell like high responsiveness to innate cytokines, has not yet been determined. Both RORγt and PLZF have been

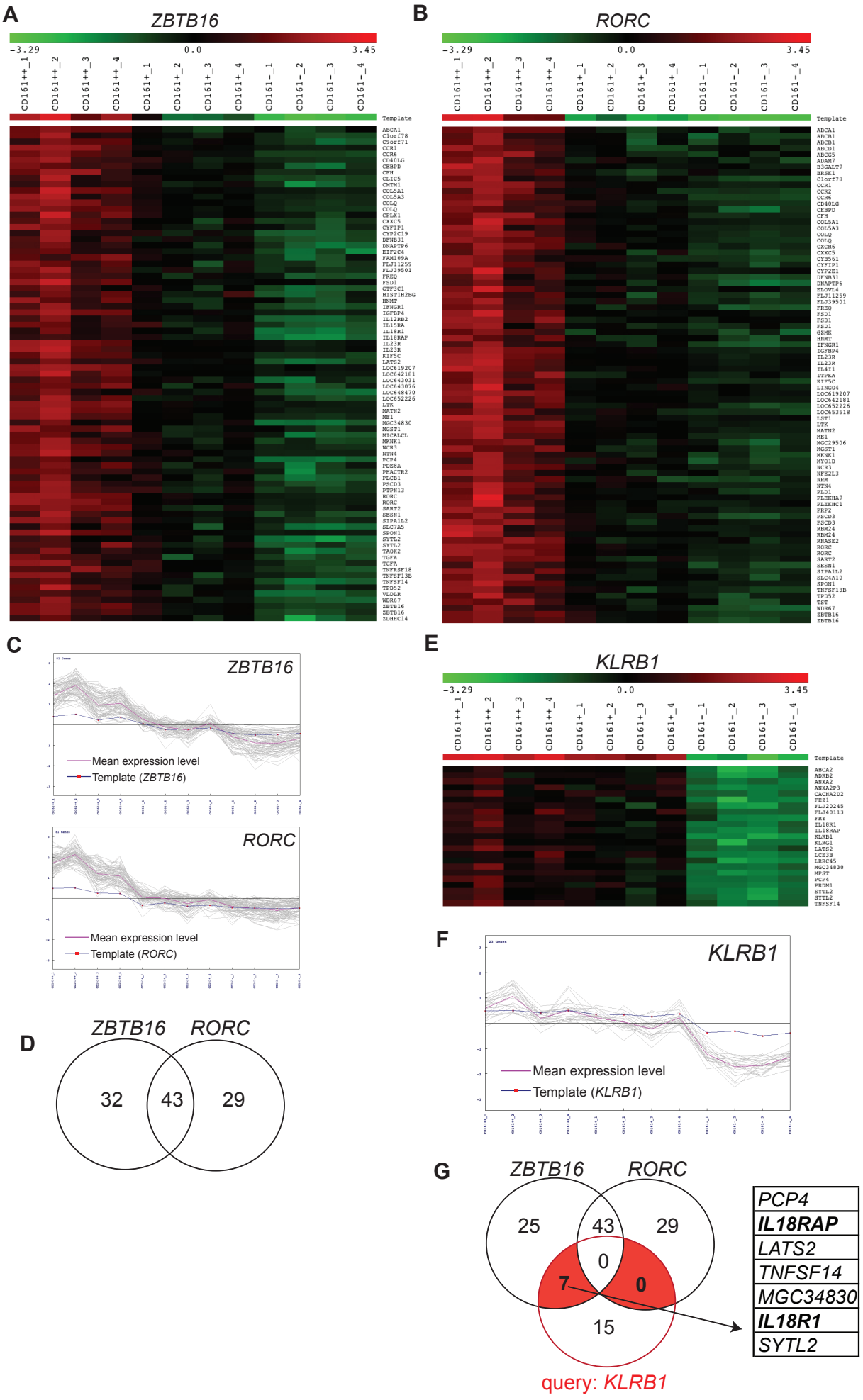
suggested to regulate CD161 expression. CD161 marks cells capable of producing of IL-17 across all T cell subtypes (Cosmi et al., 2008; Maggi et al., 2010), and the overexpression of RORγt in CD161−CD4+ T cells induces the expression of CD161 (Maggi et al., 2010). Conversely, a significantly reduced expression of CD161 in iNKT, γδ T, CD8 and NK cells has been observed in a PLZF-deficient patient (Eidson et al., 2011). In order to probe the role of these two transcription factors within MAIT cells, microarray data comparing the transcriptional phenotype of CD161++, CD161+, and CD161− CD8+ T cells was analysed (Billerbeck et al., 2010). Given the dominance of MAIT cells within CD161++CD8+ T cells, and the shared phenotype between Vα7.2− and Vα7.2+CD161++ cells (Fergusson et al., 2014), genes highly expressed in the CD161++ CD8+ T cells were considered to be shared with MAIT cells.

First, it was hypothesized that a transcriptional signature associated with expression levels of genes encoding the transcription factors PLZF (encoded by *ZBTB16*) and RORγt (encoded by *RORC*) will be present in this dataset, and that highly coexpressed genes are more likely to be co-regulated. Pavlidis template matching (PTM) is an algorithm that can be tailored to use a specific gene expression pattern as a template, to search for gene expressions that match to the template within the entire dataset (Pavlidis & Noble, 2001). The match is based on the Pearson correlation between the template and the genes in the dataset, and the threshold criterion for matching can be set as either the size of the correlation coefficient (R) or the significance (P-value) of the correlation coefficient (Shin et al., 2014). Using *ZBTB16* (Figure 5-7A) or *RORC* (Figure 5-7B) as the template gene, PTM analysis was used to define a set of genes with highly correlated gene expression trajectories matching that of either *ZBTB16* or *RORC* (correlation coefficient R>0.9). Genes highly correlated with *ZBTB16* and *RORC* differed slightly in their expression profiles (Figure 5-7C). Amongst the 81 genes identified as either highly correlated with

RORC or *ZBTB16* expression, 43 were shared between the two genes, while 32 genes were uniquely correlated with *ZBTB16*, and 29 were uniquely correlated to *RORC* (Figure 5-7D), which are listed in Appendix Table V-2.

KLRB1, the gene encoding CD161, was not found amongst either list of genes matching the expression profile of *ZBTB16* or *RORC*. The cluster of 23 genes identified to have an expression pattern matched with *KLRB1* also did not include *ZBTB16* or *RORC*, or other transcription factors that have been associated with CD161 expression (Figure 5-7E). This appeared to be because the gene expression level of *KLRB1* is not significantly different between CD161++ cells and CD161+ cells (Figure 5-7F; Appendix Table V-1), whereas both *ZBTB16* and *RORC* are expressed at a significantly higher level in CD161++ cells compared to CD161+ and CD161− cells (Appendix Table V-1), suggesting that the high protein level expression in CD161++ cells may be regulated at the post-transcriptional level. However, when the genes identified to have matched expression profiles with *ZBTB16*, *RORC*, or *KLRB1* were compared, genes with a matched expression profile to *KLRB1* did not overlap with genes matched with *RORC*, and instead shared 7 genes solely with genes matched with *ZBTB16*, including *IL18R1* and *IL18RAP*. These 7 genes are listed in Figure 5-7G (full list of genes provided in Appendix Table V-3). Furthermore, when the correlation coefficient threshold was lowered to R>0.85, *ZBTB16* but not *RORC* appeared on the list of genes with matched expression profiles to *KLRB1* (data not shown). Therefore, at the gene expression level, this analysis suggests that *KLRB1* shares an expression pattern of a set of genes highly correlated with *ZBTB16* expression, but not with *RORC* expression.

Genes with matched expression profiles to *IL18RAP* (Figure 5-7H) and *IL18R1* (Figure 5-7I) also shared a greater number of genes matched with *ZBTB16*


A
ZBTB16
-3.29
0.0
3.45
CD161++_1
CD161++_2
CD161++_3
CD161++_4
CD161+_1
CD161+_2
CD161+_3
CD161+_4
CD161-_1
CD161-_2
CD161-_3
CD161-_4
Template
B
RORC
-3.29
0.0
3.45
CD161++_1
CD161++_2
CD161++_3
CD161++_4
CD161+_1
CD161+_2
CD161+_3
CD161+_4
CD161-_1
CD161-_2
CD161-_3
CD161-_4
Template
C
ZBTB16
Mean expression level
Template (ZBTB16)
RORC
Mean expression level
Template (RORC)
D
ZBTB16
RORC
32
43
29
E
KLRB1
-3.29
0.0
3.45
CD161++_1
CD161++_2
CD161++_3
CD161++_4
CD161+_1
CD161+_2
CD161+_3
CD161+_4
CD161-_1
CD161-_2
CD161-_3
CD161-_4
Template
F
KLRB1
Mean expression level
Template (KLRB1)
G
ZBTB16
RORC
25
43
29
0
7
0
15
query: KLRB1
PCP4
IL18RAP
LATS2
TNFSF14
MGC34830
IL18R1
SYTL2

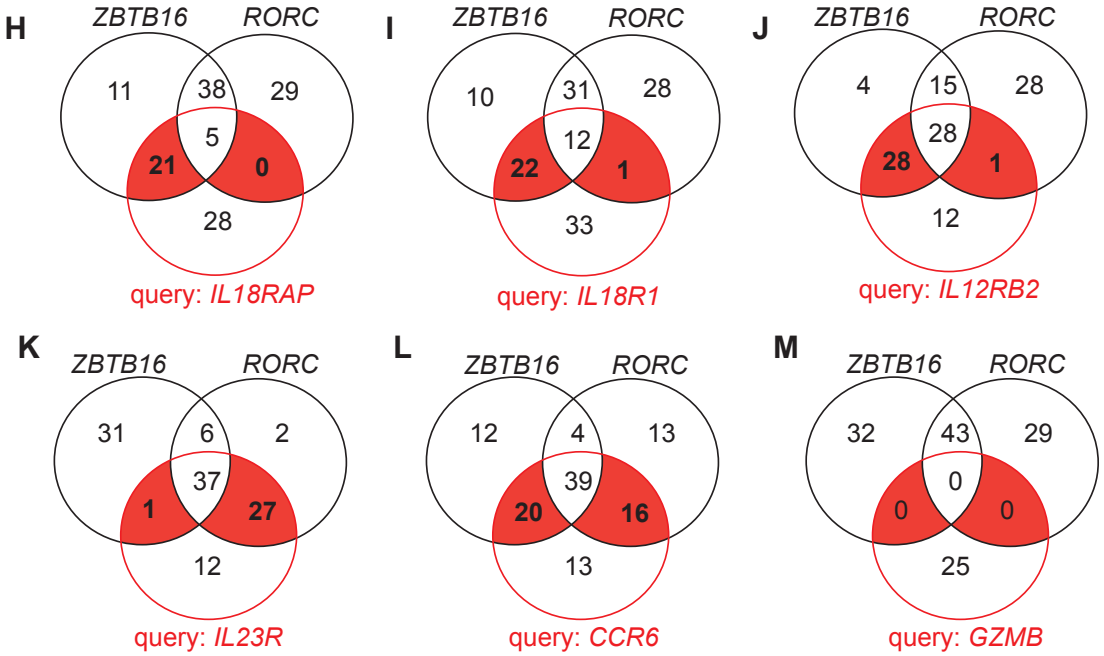


Figure 5-7. Gene correlation analysis based on Pavlidis Template Matching (PTM) identifies genes highly associated with *ZBTB16* expression in CD8+ T cells. Microarray data of CD161++, CD161+, and CD161- CD8+ T cells was analysed for genes that match the expression profile of *ZBTB16* and *RORC* by PTM. A, B) Heatmap showing normalized gene expression of genes that match the gene expression profile of the template gene, *ZBTB16* (A) or *RORC* (B) by PTM analysis (correlation coefficient R>0.9). C) Expression graphs showing the degree of congruence between the template genes *ZBTB16* (top) or *RORC* (bottom) and respective genes identified with matched expression profiles by PTM analysis. D) Number of genes that overlap between genes identified as highly correlated to *ZBTB16* and *RORC* by PTM analysis. E) Heatmap showing normalized gene expression of genes that match the gene expression profile of template gene *KLRB1* (correlation coefficient R>0.9). F) Expression graphs showing the degree of congruence between the template genes *KLRB1* and genes identified with matched expression profiles by PTM analysis. G) Venn diagram showing the number of genes with expression profiles that are uniquely matched to or shared by *ZBTB16, RORC*, and *KLRB1* by PTM analysis (correlation coefficient R>0.9). Red areas highlight the number of genes matched to *KLRB1* that are shared with *ZBTB16* or *RORC* only. H-M) Venn diagram showing the number of genes with expression profiles that are uniquely matched to or shared by *ZBTB16*, *RORC*, and the indicated query gene highlighted in red. Results are shown for H) *IL18RAP*, I) *IL18R1* J) *IL12RB2* K) *IL23R* L) *CCR6* M) *GZMB*. Correlation coefficient R>0.9. Red areas highlight the number of genes matched to the query gene that are shared with *ZBTB16* or *RORC* only.

expression than *RORC*, suggesting that these two genes may also be regulated by or together with *ZBTB16* (Appendix Table V-4, V-5). *IL12RB2* expression also showed a similar result, sharing a greater number of genes highly correlated with *ZBTB16* than *RORC* (Figure 5-7J; Appendix Table V-6). These results support previous studies showing reduced *il18r1* and *il12r* expression in PLZF-deficient mice (Gleimer et al., 2012). In turn, genes with an expression pattern matched with *IL23R* shared a greater number of genes matched with the expression profile of *RORC* (Figure 5-7K; Appendix Table V-7), in line with the fact that the regulation of IL-23R expression is well established to be mediated by RORγt (Huh et al., 2011; Ivanov et al., 2006). Finally, genes highly correlated with *CCR6* expression, which encodes the chemokine receptor CCR6, shared similar numbers of genes matched with *ZBTB16* as it did with *RORC* (Figure 5-7L; Appendix Table V-8). Although CCR6 has been traditionally associated with RORγt expression and Th17 cells (Annunziato et al., 2007; Hirota et al., 2007), this result supports a recent paper showing that CCR6 expression is independently regulated by both PLZF and RORγt in human Th17 cells (Singh et al., 2015). The PTM analysis ensures that only genes that have similar expression profiles are highlighted; for example, performing this analysis for genes associated with *GZMB* (encoding GrB) expression showed that there is no overlap between the genes matched with *ZBTB16* nor *RORC,* as expected (Figure 5-7M).

These results therefore support a greater correlation of *KLRB1*, *IL12RB2*, *IL18R1*, and *IL18RAP* expression with *ZBTB16*, while the *IL23R* expression profile overlaps with *RORC* expression profiles in CD8+ T cells.

5.4.8. Effect of RORγt inhibitor on MAIT cells: optimization of IL-17 production from MAIT cells

The role of the transcription factor RORγt in the function of MAIT cells was further investigated *in vitro*. The critical role of RORγt in the generation of IL-17-producing T cells has led to the identification of small molecules targeting RORγt. These compounds have been shown to reduce the clinical severity of imiquimod-induced psoriasis in mice (Skepner et al., 2014) and adjuvant-induced arthritis in rats (Cascão et al., 2012). These inhibitors also abrogate IL-17 production from *ex vivo* human PBMCs (Solt et al., 2011), memory CD161+CD4+ T cells (Huh et al., 2011), as well as γδ T cells (Skepner et al., 2014). However, the effect of RORγt inhibitors on MAIT cells has not yet been tested, and was investigated using a novel RORγt inhibitor developed by ORCA Pharmaceuticals Ltd., which has not yet been used on human cells.

As the detection of *ex vivo* IL-17 production from peripheral blood MAIT cells using flow cytometry has been very low in previous assays (Figures 5-3D, 5-6B), IL-17 production from MAIT cells was optimised in order to accurately evaluate the effect of the RORγt inhibitor. IL-7 has been shown to license MAIT cells for IL-17 production in the liver (Tang et al., 2013), and extremely high production of IL-17 has been reported in MAIT cells from the adipose tissue of severely obese patients (Magalhaes et al., 2015), suggesting that local cytokines and/or TCR activation may prime the MAIT cells to produce higher levels of IL-17. Furthermore, combination of IL-23 with cytokines such as IL-1β, IL-18, IL-2, and IL-6 has been shown to increase the production of IL-17 from CD4+, CD8+, γδ T, and ILCs (Buonocore et al., 2010; Lalor et al., 2011; Lee et al., 2012; Leung et al., 2014b; Sutton et al., 2009). Therefore, MAIT cells were primed with combinations of these cytokines, with or without TCR stimulation, either provided by PFA-fixed *E. coli* or anti-CD3/CD28/CD2 beads (TCR beads), to investigate whether these conditions would increase the frequency of MAIT cells producing IL-17. PBMCs were cultured for 7 days under

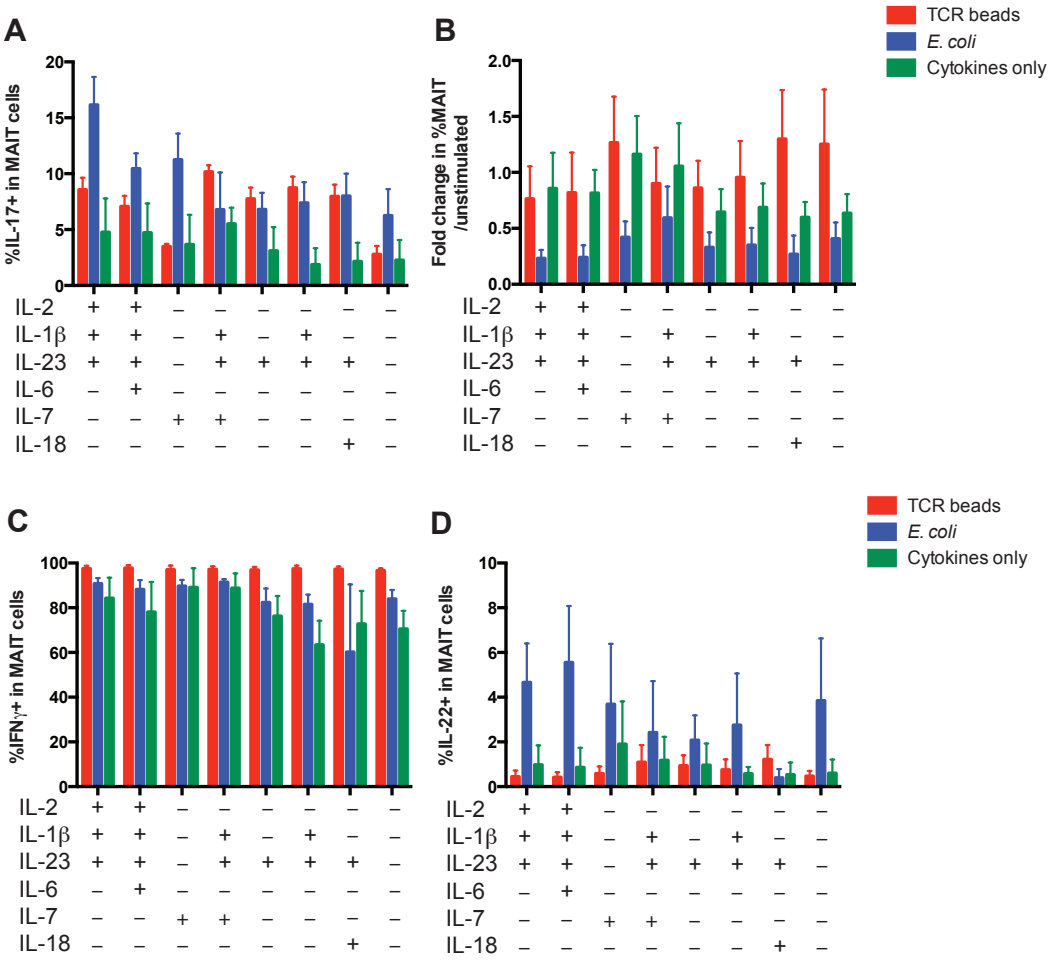


Figure 5-8. Optimisation of IL-17 production from MAIT cells. MAIT cells were cultured in the presence of anti-CD3/CD28/CD2 beads (red bars), *E. coli* (blue bars), or nothing (green bars) with the addition of the indicated combinations of cytokines for 7 days, and restimulated with PMA and ionomycin for 5 hours (n=3). A) Cumulative frequencies of IL-17+ cells within MAIT cells shown for the indicated conditions. B) Fold change in the frequency of MAIT cells within CD8+ T cells after culture with the indicated conditions, compared to the frequency of MAIT cells without any stimulation. C) Cumulative frequencies of IFNγ+ cells within MAIT cells shown for the indicated conditions. D) Cumulative frequencies of IL-22+ cells within MAIT cells shown for the indicated conditions.

these conditions, and restimulated with PMA/ionomycin for 5 hours. Brefeldin A was added for the last 4 hours of the stimulation.

Only an average of 2.27 ± 1.8% of MAIT cells cultured in the absence of cytokines produced IL-17 upon stimulation, while 16.17 ± 2.49% of MAIT cells cultured with *E. coli* in the presence of IL-2+IL-23+IL-1β produced IL-17; the highest frequency amongst all conditions tested (Figure 5-8A). However, the relative fold change in the frequency of MAIT cells within CD8+ T cells compared to unstimulated controls was mostly below 0.5 in all the *E. coli*-treated conditions, possibly due to AICD following the long-term culture (Figure 5-8B). In contrast, the frequency of MAIT cells remained constant or even increased in cultures with TCR beads, and clear production of IL-17 was induced from MAIT cells, with the TCR+IL-1β+IL-23+IL-7 condition inducing IL-17 expression in 10.17 ± 0.58% of CD8+ MAIT cells. All the tested conditions induced a high frequency of IFNγ+ cells (Figure 5-8C). As the TCR+IL-1β+IL-23+IL-7 condition also induced the highest frequency of IL-22+ cells within TCR bead-stimulated conditions (Figure 5-8D), with good survival of MAIT cells, this condition was used in subsequent experiments to test the effect of the RORγt inhibitor on IL-17 production from MAIT cells. IL-17 production from CD4+ or DN MAIT cells did not differ compared to CD8+ MAIT cells (data not shown), so analysis was focused on CD8+ MAIT cells for the following experiments.

5.4.9. RORγt inhibitor inhibits production of IL-17 from MAIT cells

To investigate the effect of the novel RORγt inhibitor on MAIT cells, PBMCs were cultured with TCR beads+IL-7+IL-23+IL-1β, either in the presence or absence of increasing concentrations of the RORγt inhibitor. Cells were washed, restimulated with PMA/ionomycin, and stained for IL-17, IFNγ, and IL-22 production. Addition of the RORγt inhibitor blocked the production of IL-17 from CD8+ MAIT cells in a dose-

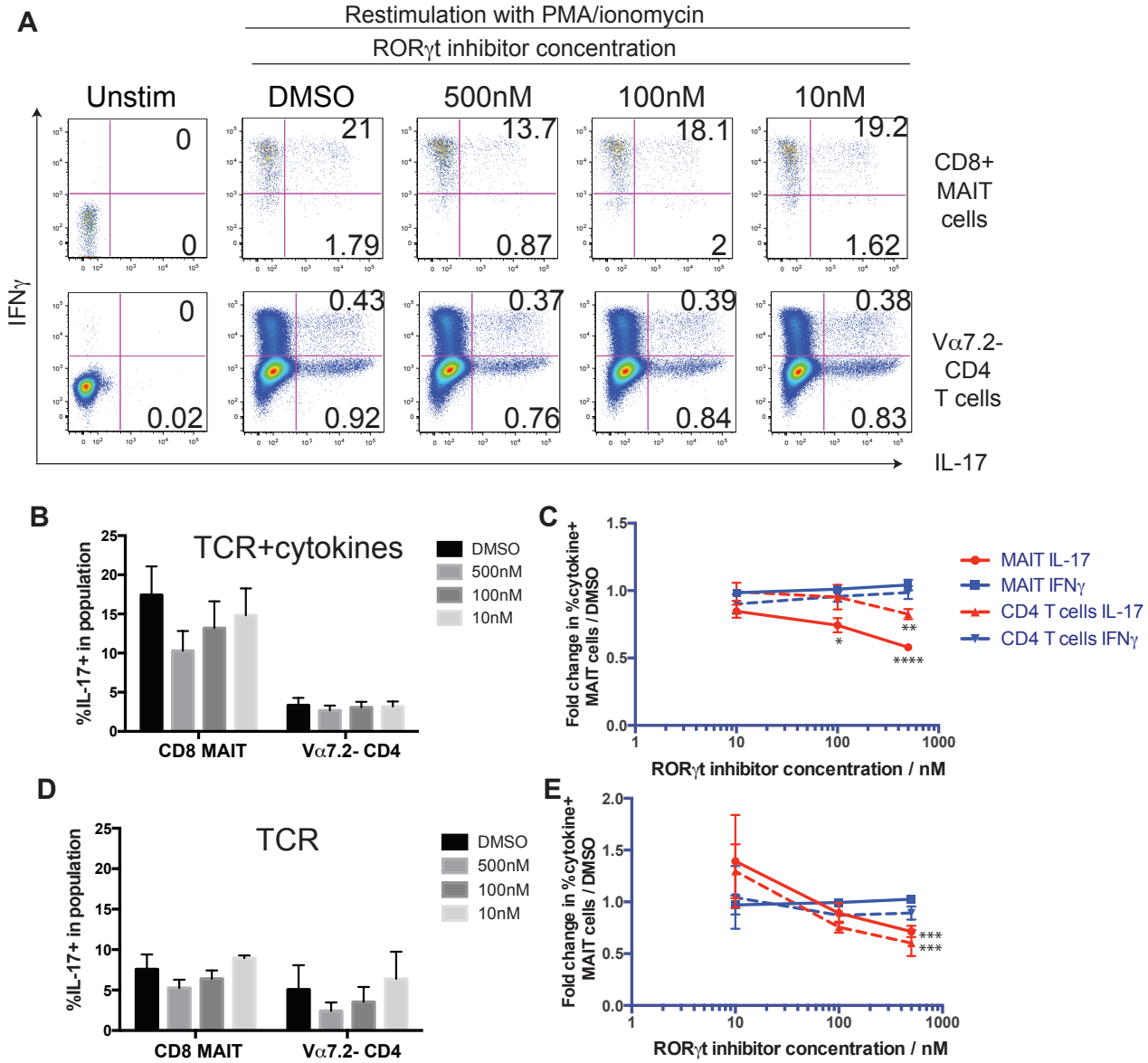


Figure 5-9. RORγt inhibitor reduces IL-17 production from CD8+ MAIT cells in a dose-dependent manner. A) Representative plots showing IL-17 expression from MAIT cells (top) and Vα7.2− CD4+ T cells (bottom) following preactivation with TCR beads+IL-23+IL-1β+IL-7 and restimulation with PMA/ionomycin, with increasing concentrations of the RORγt inhibitor. B) Cumulative frequencies of IL-17+ cells in CD8+ MAIT cells or Vα7.2− CD4+ T cells after preactivation with TCR beads+IL-23+IL-1β+IL-7 (TCR + cytokines) with increasing concentrations of the RORγt inhibitor, and restimulation with PMA/ionomycin (n=3). (C) Fold change in the frequency of IFNγ+ (blue) and IL-17+ (red) MAIT cells or Vα7.2− CD4+ T cells cultured with TCR beads+IL-23+IL-1β+IL-7 (TCR + cytokines) with increasing concentrations of the RORγt inhibitor, compared to cells with no inhibitor (DMSO only), (n=3). ****P<0.0001, **P<0.01, *P<0.05 by two-way repeated measures ANOVA with Dunnett's multiple comparisons test, compared to fold change at 10nM. All other comparisons were non-significant. (D) Cumulative frequencies of IL-17+ from CD8+ MAIT or Vα7.2− CD4+ T cells after culture with TCR beads and increasing concentrations of the RORγt inhibitor, and restimulation with PMA/ionomycin (n=3). (I) Fold change in the frequency of IFNγ+ (blue) and IL-17+ (red) MAIT cells or Vα7.2− CD4+ T cells cultured with TCR beads with increasing concentrations of the RORγt inhibitor, compared to cells with no inhibitor (DMSO only), (n=3). ***P<0.001 by two-way repeated measures ANOVA with Dunnett's multiple comparisons test, compared to fold change at 10nM. All other comparisons were non-significant

dependent manner in these preliminary experiments (Figure 5-9A, B). At the highest concentration of the RORγt inhibitor, 10.30 ± 2.52% of MAIT cells expressed IL-17, compared to 17.43 ± 3.65% of MAIT cells cultured with DMSO alone (0.58 fold reduction; Figure 5-9C). The RORγt inhibitor also had an effect on the production of IL-17 from conventional Vα7.2− CD4+ T cells, albeit to a smaller extent; at 500nM, the RORγt inhibitor reduced the frequency of IL-17+Vα7.2−CD4+T cells by 0.826 fold compared to DMSO controls. This is in contrast to IFNγ production, which was unaffected by RORγt inhibition in both MAIT and the Vα7.2−CD4+ T cells (Figure 5-9C). This inhibitory effect of the RORγt inhibitor on IL-17 expression was observed even in cells cultured with TCR beads only, without IL-23+IL-1β+IL-7 (Figure 5-9D, E).

Interestingly, while the frequency of IL-17+ MAIT cells greatly increased in the presence of IL-23+IL-1β+IL-7 compared to cells cultured with TCR beads only (17.43 ± 3.65% vs. 7.57 ± 1.83%, respectively), the frequency of IL-17+ Vα7.2−CD4+ T cells did not increase with the addition of the cytokines IL-23+IL-1β+IL-7 (3.34 ± 0.94% vs. 5.08 ± 3.00%). Accordingly, the RORγt inhibitor had a greater effect on IL-17 production from MAIT cells cultured with TCR beads+IL-23+IL-1β+IL-7 compared to those cultured with TCR beads only (0.579 vs. 0.715 fold reduction at 500nM, respectively), while there was a smaller effect of RORγt inhibition on IL-17 production from CD4+ T cells cultured with TCR beads+IL-23+IL-1β+IL-7 compared to TCR beads only (0.826 vs. 0.603 fold reduction at 500nM). As RORγt inhibitors have been shown to inhibit the expression of IL-23R as well as IL-17 (Huh et al., 2011), these observations suggest that: 1) MAIT cells are more sensitive to IL-23, IL-1β and IL-7 than conventional CD4+ T cells, and 2) RORγt inhibition may reduce IL-23R expression on MAIT cells, thus rendering the cells less responsive to skewing by IL-23.

5.4.10. RORγt inhibitor blocks MR1-induced IL-17 production from MAIT cells

Next, the effect of the RORγt inhibitor on MR1-dependent activation of MAIT cells was investigated. MAIT cells were pre-activated with TCR beads+IL-23+IL-1β+IL-7 in the presence or absence of the RORγt inhibitor, and were cultured with *E. coli*-treated THP1 cells for 5 hours. There was a clear production of IL-17 from MAIT cells (7.52 ± 1.60%) in response to *E. coli*-treated THP1 cells, but not in response to sterility control-treated THP1s (Figure 5-10A). In these experiments, IL-17 production from MAIT cells was almost completely blocked by the RORγt inhibitor at the highest concentration. The inhibition was dose-dependent (Figure 5-10B); at 1μM, IL-17 production was reduced by 0.24 fold when compared to the DMSO control, while at 10nM, the RORγt inhibitor only reduced the IL-17 production from MAIT cells by 0.96 fold. IFNγ production from the MAIT cells was completely unaffected by the RORγt inhibitor (Figure 5-10C). Furthermore, there was no difference in the relative expression of CD161 comparing MAIT cells treated with DMSO and the RORγt inhibitors (Figure 5-10D). Both IFNγ- and IL-17-production from these pre-activated MAIT cells remained MR1-dependent (Figure 5-10E).

5.4.11. RORγt inhibitor reduces the responsiveness of MAIT cells to IL-23+IL-18 stimulation

In addition to MR1-dependent activation, MAIT cells may be activated in an MR1-independent manner by IL-12+IL-18 (Ussher et al., 2014a). As the transcriptional signature associated with such innate responsiveness in T cells included the gene encoding the transcription factor RORγt (Fergusson et al., 2014), the effect of RORγt inhibition on the innate responsiveness of MAIT cells to IL-12+IL-18 or IL-23+IL-18

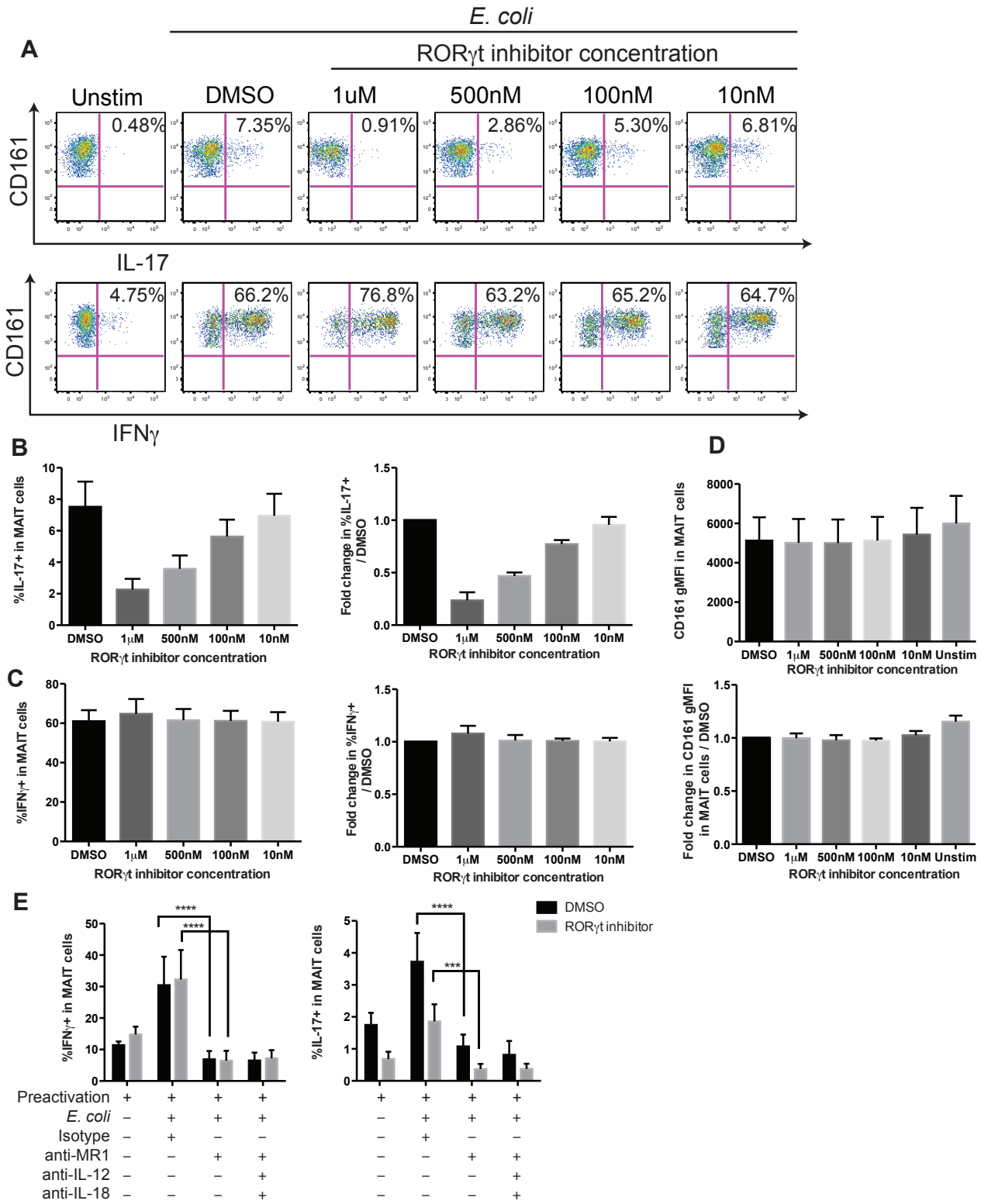


Figure 5-10. RORγt inhibitor inhibits MR1-induced IL-17 production from MAIT cells. A-D) MAIT cells were cultured with TCR beads+IL-23+IL-1β+IL-7 and increasing concentrations of the RORγt inhibitor, and were restimulated with *E. coli*-treated THP1s for 5 hours. A) Representative staining showing IL-17 and IFNγ production from MAIT cells B-C) Cumulative frequencies (left) or fold change (right) compared to DMSO controls of IL-17+ MAIT cells (B), and IFNγ producing MAIT cells (C), are shown (n=3 for 1μM, n=6 for other concentrations). D) Expression of CD161 on MAIT cells as measured by gMFI (top) or fold change compared to DMSO controls (bottom) with increasing concentrations of RORγt inhibitor. (n=3 for 1μM, n=6 for other concentrations). E) IFNγ and IL-17 production from preactivated (cultured with TCR beads+IL-23+IL-1β+IL-7) MAIT cells stimulated with *E. coli*-treated THP1 cells in the presence or absence of blocking antibodies against MR1, IL-12, IL-18, or isotype controls, and in the presence or absence of the RORγt inhibitor (500nM) as indicated. ****P<0.0001, ***P<0.001 by two-way repeated measures ANOVA with Bonferroni's multiple comparisons test, compared to the isotype control (n=6). Data includes experiments performed by Verity Hill.

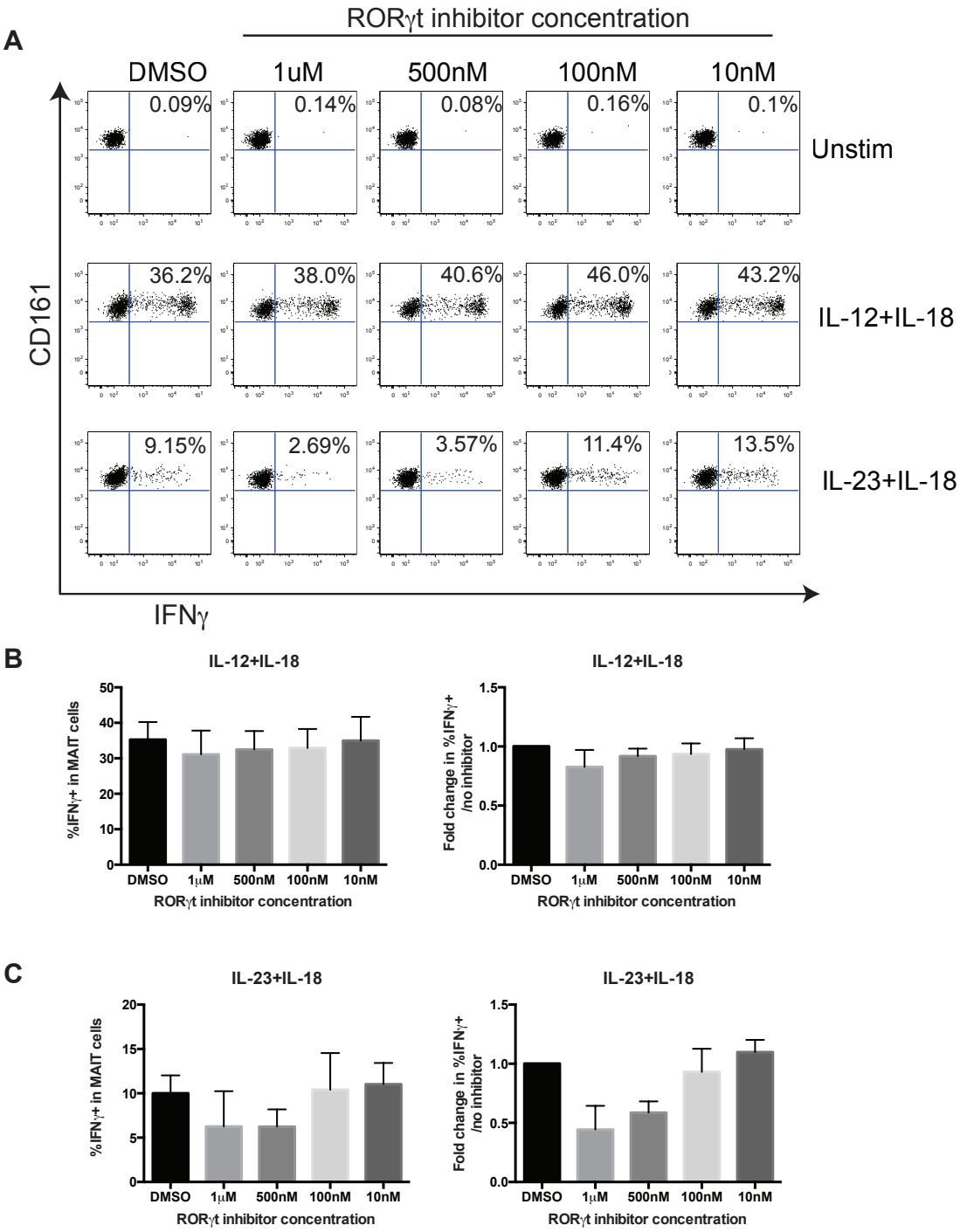


Figure 5-11. RORγt inhibitor reduces the responsiveness of MAIT cells to IL-23+IL-18 stimulation. MAIT cells were cultured with increasing concentrations of the RORγt inhibitor for 24 hours, followed by overnight stimulation with IL-12+IL-18 or IL-23+IL-18, with Brefeldin A added for the last 4 hours. IFNγ expression was then assessed from MAIT cells. A) Representative staining showing IFNγ expression from MAIT cells from the same donor cultured with increasing concentrations of the RORγt inhibitor and stimulated with IL-12+IL-18 or IL-23+IL-18. Staining is representative of two independent experiments. B) Cumulative frequencies (left) and fold change (right) in IFNγ+ MAIT cells stimulated with IL-12+IL-18, following culture with increasing concentrations of the RORγt inhibitor (n=3 for 1μM, n=5 for other concentrations). C) Cumulative frequencies (left) and fold change (right) in IFNγ+ MAIT cells stimulated with IL-23+IL-18, following culture with increasing concentrations of the RORγ t inhibitor (n=5). Experiments performed by Verity Hill.

was assayed. *Ex vivo* MAIT cells were cultured in the presence of the RORγt inhibitor for 24 hours, before the addition of either IL-12+IL-18 or IL-23+IL-18 for the following 20 hours, with Brefeldin A added for the last 4 hours of the assay. These preliminary experiments showed that IFNγ expression in MAIT cells following IL-12+IL-18 stimulation was completely unaffected by the addition of the RORγt inhibitor (Figure 5-11A, B). In contrast, IFNγ expression induced by IL-23+IL-18 was reduced by the addition of the RORγt inhibitor in a dose-dependent manner (Figure 5-11C), suggesting that the RORγt inhibitor is reducing the responsiveness of MAIT cells to IL-23, but not to IL-12 or IL-18.

5.5. Discussion

5.5.1. MAIT cells are not enriched in psoriatic skin and PsA synovial fluid compared to blood

Psoriasis is characterized by an enrichment of IL-17+ CD8+ T cells in the lesional skin (Ortega et al., 2009; Res et al., 2010). Given the high expression of RORγt and IL-17 by peripheral blood MAIT cells (Billerbeck et al., 2010; Dusseaux et al., 2011), the frequency of MAIT cells within psoriatic skin compared to healthy skin *in situ* was quantified. There was no difference between the frequency of MAIT cells in healthy skin compared to psoriatic skin, which is supported by a recent study where the frequency of MAIT cells that had spontaneously migrated out from healthy skin were compared with that from psoriatic skin (Teunissen et al., 2014). However, the number of MAIT cells detectable by flow cytometry was so low that this data needs to be interpreted with caution. Furthermore, isolation of lymphocytes from skin involved collagenase exposure, which has been suggested to potentially affect the expression of CD molecules (Clark et al., 2006; Mulder et al., 1994). Resting the isolated dermal

lymphocytes overnight allowed some re-expression of MAIT cell markers. Thus, the enumeration of MAIT cells from these skin samples needs to be corroborated with immunohistochemistry stains of psoriatic skin biopsies.

Although there was a trend towards a lower frequency of MAIT cells in the blood of psoriasis patients compared to healthy donors, there was no significant difference between the frequency of MAIT cells in healthy donors and psoriasis patients. As MAIT cell frequency decreases with age (Novak et al., 2014; Walker et al., 2014), this study should be repeated with age-matched healthy donors and psoriasis patients. In terms of functional differences, there was a specific reduction in IFNγ-producing MAIT cells in response to PMA/ionomycin stimulation. Reduced frequencies of IFNγ-expressing peripheral MAIT cells has also been noted in other inflammatory diseases such as Crohn's disease (Serriari et al., 2014) and SLE (Cho et al., 2014), and may indicate skewing of cytokine secreting profiles. However, there was no significant increase in the frequency of IL-17+ CD4+ or CD8+ T cells from the peripheral blood of psoriasis patients. This contrasts with previous reports of increased frequencies of IL-17-producing CD4+ (Benham et al., 2013; Kagami et al., 2010) and CD8+ T cells (Teunissen et al., 2014) in the periphery of psoriasis patients. These findings therefore need to be repeated with a larger cohort of patients and corroborated through other methods to quantify IL-17 production, such as an ELISA assay, combined with further studies of MAIT cells within the skin.

In a small cohort of PsA patients, an increased frequency of synovial fluid MAIT cells expressing IL-17 was observed. Interestingly, this increased ability to express IL-17 was not unique to MAIT cells, as all CD161+ CD8+ as well as CD8− T cells within the joint showed significantly increased frequencies of IL-17+ cells. This supports a recent publication demonstrating that MAIT cells comprise only a minority of CD8+ T cells capable of secreting IL-17 in the synovial fluid of PsA patients (Menon et al.,

2014). The mechanism for this is unknown, as increased RORγt was only detected in the SF CD161− CD8+ T cell fraction of PsA patients. Furthermore, MAIT cells were not significantly enriched in joint samples compared to their paired blood samples, as some donors had higher frequencies of MAIT cells in their blood compared to the synovial fluid, in contrast to MAIT cells in the synovial fluid of RA patients (Cho et al., 2014).

However, preliminary experiments suggested that CD8+ MAIT cell frequency within the joint correlated with disease activity, as measured by CRP levels. This may be due to the recruitment of MAIT cells to the site of inflammation by chemokines, or may suggest that MAIT cells are directly involved in joint inflammation. Infiltration of MAIT cells into inflamed or infected tissues have also been observed in many conditions, including MS (Willing et al., 2014) and obesity (Magalhaes et al., 2015). The high variability of MAIT cell frequency, even in the blood of healthy donors, suggests that these findings need to be confirmed in a much larger cohort of PsA patients. Importantly, several of the SF samples were collected from patients on disease modifying anti-rheumatic drugs (DMARDs), or taken from the same patient at different time points, or from differentially affected knees, which this preliminary study has not taken into account. Another limitation of this study is that patients here only showed mild or moderate inflammation with relatively low CRP levels (<12mg/ml). Although PsA is characterized by lower levels of CRP compared to RA (Lindqvist et al., 2008), other arthritis studies that have looked at MAIT cell frequencies included patients with CRP levels up to 150mg/ml (Cho et al., 2014; Menon et al., 2014). These studies also incorporate other measures of disease activity and active synovitis such as the Disease Activity Score in 28 joints (DAS 28), which would be important to further support the relationship between MAIT cell frequency and arthritic disease severity.

5.5.2. Regulation of IL-17 production from MAIT cells

Interestingly, the fraction of IL-17+ cells in stimulated healthy blood MAIT cells was significantly increased by the addition of Th17 skewing cytokines, IL-23+IL-1β+IL-7, compared to cells that had been cultured with TCR beads only. This was in contrast to conventional CD4+ T cells, which did not show an increase in the proportion of cells expressing IL-17 after culture with Th17 skewing cytokines. Due to the high expression of cytokine receptors such as IL-23R and IL-7R at basal conditions (Billerbeck et al., 2010; Leeansyah et al., 2015; Tang et al., 2013), MAIT cells may be more responsive to such cytokines than conventional CD4+ T cells.

The current study of PsA patients, as well as two recent studies, have shown that in psoriasis and PsA patients, the dominant CD8+ T cell population producing IL-17 in response to PMA/ionomycin stimulation in the inflamed tissues do not appear to be MAIT cells (Menon et al., 2014; Teunissen et al., 2014). This is in contrast to the periphery (Billerbeck et al., 2010) and liver (Tang et al., 2013) where IL-17 is exclusively produced by MAIT cells within the CD8+ T cell population. However, the sensitivity of MAIT cells to IL-23 and the inflammatory milieu may be particularly important in the early phase of such autoimmune diseases. For instance, in a model of IL-23-induced skin inflammation, dermal γδ T cells were the major IL-17-producers in response to IL-23 stimulation, and acanthosis was attenuated in mice lacking γδ T cells (Cai et al., 2011). Thus, the involvement of innate lymphocytes, with constitutive IL-23R expression and preferential localization within tissues, may precede the involvement of conventional IL-17-producing T cells in the development of psoriasis. Indeed, IL-23 and IL-1β-induced IL-17-production from γδ T cells can enhance IL-17 production by Th17 cells, thus modulating the adaptive immune response during the development of EAE (Sutton et al., 2009). Although MR1-independent IL-17 production in response to IL-23 has been demonstrated *in vitro* from murine MAIT

cells (Chiba et al., 2012), such innate IL-17 production has yet to be demonstrated from human MAIT cells. The innate response of MAIT cells is an area that warrants further investigation, in particular for autoimmune conditions such as arthritis, where bacterially-derived MR1 ligands are not present in the sterile conditions of the synovial fluid.

Several RORγt small-molecule inhibitors block Th17 differentiation and IL-17 production from rodent and human T cells (Huh et al., 2011; Skepner et al., 2014; Solt et al., 2011). In a series of preliminary experiments, a novel RORγt inhibitor was shown to block IL-17 production from human MAIT cells in a dose-dependent manner, both in response to polyclonal stimulation and TCR stimulation. Furthermore, the inhibitor is able to specifically inhibit the expression of functional IL-23R by MAIT cells, as the inhibitor abrogated their response to IL-23 and IL-18, but not IL-12+IL-18. Importantly, IFNγ production from MAIT cells and conventional CD4+ T cells was completely unaffected by the inhibitor. No difference in IL-22 production from MAIT cells was seen with RORγt inhibition, most likely due to the dominant role of the aryl hydrocarbon receptor (AHR) transcription factor in the production of this cytokine (Veldhoen et al., 2008). Thus, this novel RORγt inhibitor may be therapeutically effective in treating IL-17-driven autoimmune diseases.

Inhibiting the upstream RORγt, rather than individual cytokines and their receptors downstream, for the treatment of Th17-related diseases may have a broader biological effect. Indeed, patients with defects in genes encoding RORγt or components of the IL-23/IL-17 pathway have increased susceptibility to fungal and bacterial diseases (Blauvelt et al., 2015; Okada et al., 2015). On the other hand, RORγt deficiency in mice does not completely abolish IL-17A production, as the related nuclear receptor RORα is also involved in Th17 cell differentiation (Yang et al., 2008). Furthermore, the number of adverse events in psoriasis patients during

most clinical trials of anti-IL-23 (Papp et al., 2008) and anti-IL-17 (Leonardi et al., 2012; Rich et al., 2013) blocking antibodies are not significantly different from placebo controls, although some studies have reported increased adverse effects (Papp et al., 2012). Ultimately, RORγt inhibitors are a promising therapeutic strategy for the treatment of IL-17-driven diseases, but careful clinical trials will be required to identify the long-term risks involved in RORγt inhibition.

5.5.3. Identifying correlates of innate-responsiveness and CD161 expression in T cells

The frequency of SF CD161++CD4+ T cells expressing IFNγ in response to IL-12+IL-18 stimulation correlated significantly with CRP levels in PsA patients, and was strikingly increased in SF compared to paired blood samples. However, there was no significant increase in the expression of key factors associated with the innate-responsiveness of T cells, namely IL-18R, PLZF, and RORγt (Fergusson et al., 2014), in PsA SF samples compared to paired PB samples. Instead, there was an increased frequency of CD8− T cells expressing IFNγ in response to PMA/ionomycin, particularly in the CD161++Vα7.2− T cell subset, suggesting that the increased frequency of cells expressing IFNγ in synovial fluid CD161++CD4+ T cells may, in part, be due to the increased capacity of these cells to make Th1 cytokines. Therefore, this further confirms that innate responsiveness of T cells is not acquired in chronic inflammation and is restricted to cells expressing CD161 at a high level.

An increased frequency of cells expressing IFNγ in response to IL-12 and IL-18 has also been observed in synovial fluid NK cells from arthritic patients, compared to their peripheral blood counterparts (de Matos et al., 2007), suggesting there is a general increase in IFNγ production from lymphocytes in the synovial fluid. IFNγ is not

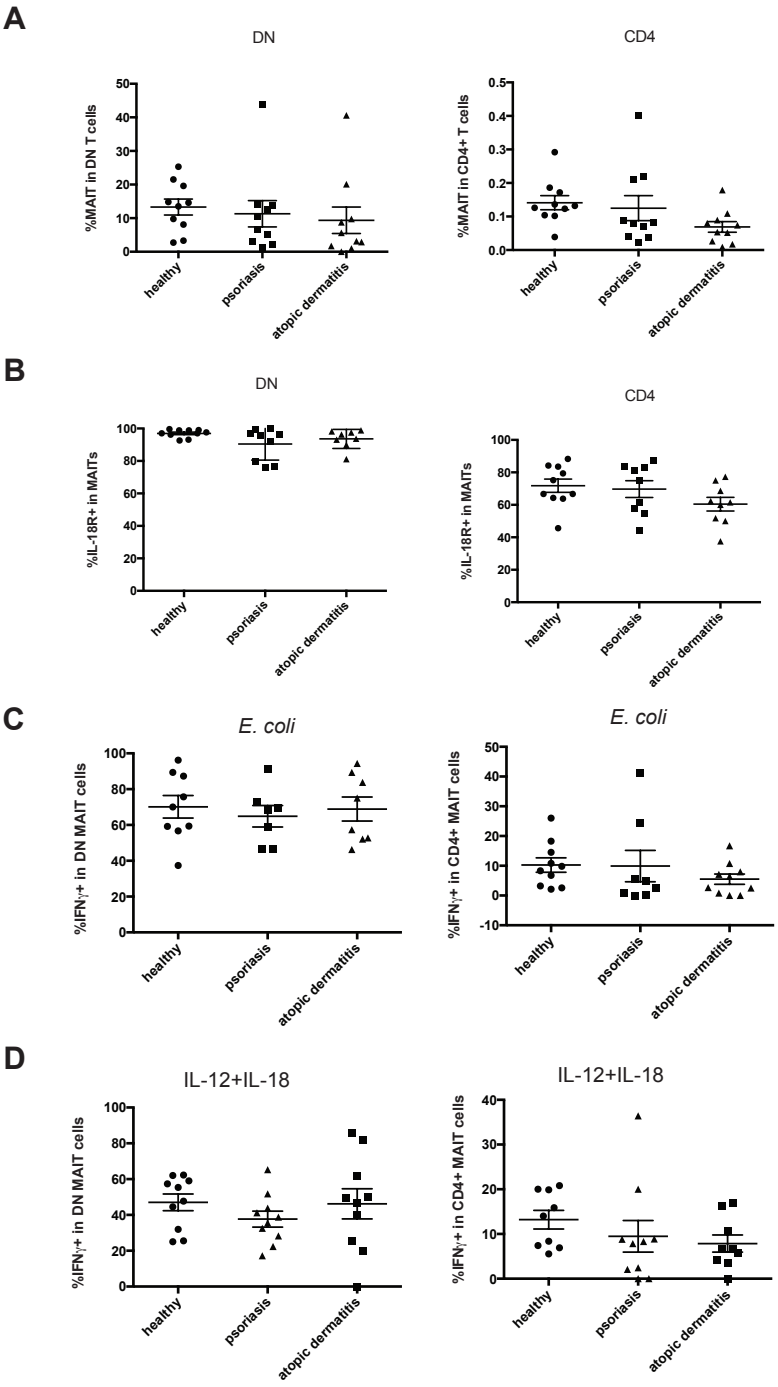
necessary for the development of arthritis in murine models (Sarkar et al., 2009). However, serum levels of IFNγ, IL-12, and IL-18, in addition to IL-17, have been shown to correlate with disease severity in psoriasis patients (Arican et al., 2005). Furthermore, high levels of IFNγ and IL-18 are present in the synovial tissue of arthritis patients (Ritchlin et al., 1998; Rooney et al., 2004). IFNγ can enhance IL-23 and IL-1β production by DCs (Kryczek et al., 2008), as well as osteoclastogenesis (Kotake et al., 2005). Additionally, a single intradermal injection of IFNγ into non-lesional skin of psoriasis patients induced the infiltration of T cells and DCs with similar inflammatory characteristics of psoriasis (Johnson-Huang et al., 2012). Therefore, IFNγ production from CD161++ T cells in the synovial fluid of PsA patients could play a role in the maintenance of the inflammatory state of the joint.

A gene expression correlation analysis of the transcriptome of CD161++, CD161+, and CD161− CD8+ T cells was performed to further understand the biology underlying CD161 expression. This showed that there was a greater overlap between modules of genes highly correlated with *KLRB1*, *IL18R1*, *IL18RAP*, and *IL12RB2* and expression profiles of genes highly correlated with *ZBTB16* expression, compared to *RORC* expression. Various studies also show that the lack of/reduced PLZF expression is associated with reduced *il12rb1* and *il18r1* expression in mice (Gleimer et al., 2012) and humans (Schlums et al., 2015), as well as affecting the expression of CD161 in humans (Eidson et al., 2011; Schlums et al., 2015). However, in a study examining MAIT cells in the fetal thymus, MAIT cells were already shown to express CD161 at a high level, and showed little PLZF protein expression (Leeansyah et al., 2014), suggesting that PLZF may not be the only regulator of CD161 expression. A recent study has also demonstrated that PLZF and RORγt co-regulate each other (Singh et al., 2015). Thus, although inhibition of RORγt did not affect the expression of CD161 on MAIT cells, further analysis will be required to define the key genes regulating the “CD161 phenotype”.

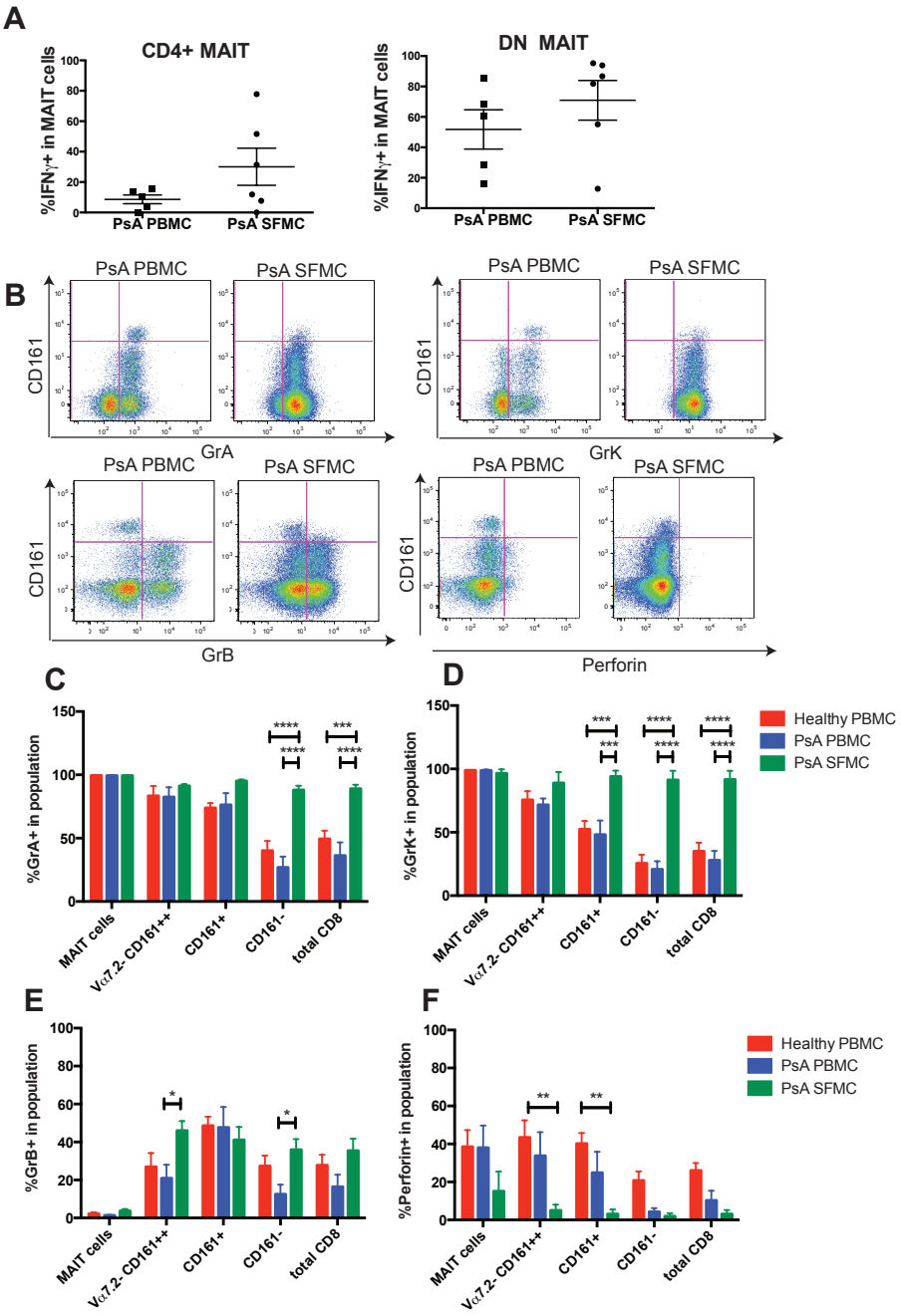
The PTM analysis performed in this study has several disadvantages, mainly due to the lack of an unbiased way to quantitatively evaluate the functional significance of correlated gene expression patterns, and greatly underestimates the complexity of genes that are regulated by a whole network of genes. Network-based analyses such as weighted gene co-expression network analysis (WGCNA) allows the identification of biological networks of highly co-regulated genes (Langfelder & Horvath, 2008). Thus WGCNA analysis of the combined transcriptome of all CD161-expressing T cells may be able to identify key regulators of the module of genes associated with CD161 expression. Furthermore, future work using Chip-Seq analysis will be able to confirm the interaction between PLZF and/or RORγt on the *KLRB1* promoter in MAIT cells.

5.6. Summary

1. MAIT cells are present in healthy and psoriatic skin
2. MAIT cells are highly activated in the synovial fluid of PsA patients, and their frequency correlates with clinical disease
3. A increased proportion of the non-MAIT, CD161++CD4+ population expresses IFNγ in response to IL-12+IL-18 in the synovial fluid of PsA patients
4. A novel RORγt inhibitor is able to inhibit IL-17 production and the responsiveness of MAIT cells to IL-23 in a dose-dependent manner
5. CD161 expression and responsiveness to IL-12+IL-18 by MAIT cells is not affected by RORγt inhibition. Gene expression correlation analysis suggests that PLZF is a more likely candidate transcription factor associated with CD161 expression and innate responsiveness to IL-12 and IL-18 in CD8+ T cells



Appendix Figure V-1. Phenotype and function of peripheral blood CD4+ and DN MAIT cells from psoriasis and atopic dermatitis patients. A) Frequencies of MAIT cells within CD4+ T cells and DN T cells. n=10 for all three groups of patients. B) Cumulative frequencies of IL-18R+ DN (left) and CD4+ (right) MAIT cells from healthy (n=10), psoriasis (n=9), and atopic dermatitis (n=8) patients. C) IFNγ-expression from peripheral blood DN (left) and CD4+ (right) MAIT cells from healthy (n=9), psoriasis (n=8), or atopic dermatitis (n=8) patients following culture with *E. coli*-treated THP1 cells for 5 hours. D) IFNγ expression from peripheral DN (left) or CD4+ (right) MAIT cells of healthy (n=9), psoriasis (n=9), or atopic dermatitis (n=9) patients following overnight stimulation with IL-12 and IL-18.



Appendix Figure V-2. PsA synovial fluid T cells express GrA and GrK. A) IFNγ expression from CD4+ (left) and DN MAIT cells (right) from PsA samples, stimulated with *E. coli*-treated THP1 cells for 5 hours. PBMC n=5, SFMC n=6. B) Representative staining showing the expression of Granzyme A (GrA), GrK, GrB, or perforin in CD8+ T cells from PBMC (left) and SFMC (right) samples. C) Cumulative frequencies of cells expressing GrA (C), GrK (D), GrB (E), and perforin (F) in the indicated CD8+ T cell population. ****P<0.0001, ***P<0.001, **P<0.01, *P<0.05 by two way repeated measures ANOVA with Tukey's multiple comparisons test. All other comparisons were non-significant.

Appendix Table V-1. Genes significantly upregulated in CD161++ cells compared to CD161- CD8+ T cells (left) or CD161+ CD8+ T cells (right). (P<0.05, >2 fold change). From Billerbeck *et. al.* 2010.

Upregulated in CD161++ vs CD161-		
Symbol	logFC	P.Value
LTK	6.41815433	2.91E-13
RORC	5.88212323	3.59E-13
ME1	5.73909545	2.16E-12
KLRB1	5.10128809	1.00E-12
ZBTB16	4.96964065	7.91E-12
LOC642181	4.91842052	7.05E-12
IL23R	4.80116015	9.52E-11
ZBTB16	4.78802096	5.72E-10
IL23R	4.75408883	3.57E-10
MATN2	4.68648581	7.77E-12
COLQ	4.64757185	1.27E-12
NTN4	4.63287471	1.51E-11
IL18RAP	4.62410673	1.70E-10
COL5A3	4.60364269	7.66E-10
COLQ	4.46717201	2.76E-10
RORC	4.38751364	1.31E-11
CCR6	4.28784824	6.07E-12
PCP4	4.23112406	1.65E-10
IL4I1	4.04723998	2.97E-09
CXCR6	3.96559806	1.89E-10
LOC619207	3.88332089	6.07E-11
CD40LG	3.73625751	2.22E-09
CEBPD	3.70527371	3.07E-09
COL5A1	3.68485203	1.55E-09
CYP2E1	3.62834021	5.54E-08
SIPA1L2	3.54450097	8.41E-11
CCR2	3.4845828	6.31E-10
SPON1	3.47826449	1.80E-10
BLK	3.4561377	1.75E-08
LATS2	3.36165616	2.21E-08
RBM24	3.34179765	4.23E-08
RBM24	3.30811374	1.76E-06
CA2	3.26420415	4.89E-07
KIF5C	3.24243512	6.06E-10
IL18R1	3.21954786	4.52E-09
ITPKA	3.21477887	5.74E-08
PRP2	3.20400507	1.62E-09
RNF165	3.14538912	7.21E-05
TLE1	3.12467913	7.25E-07
LOC653518	3.09922081	1.08E-09
PHLDA1	3.08930402	6.40E-08
PLEKHA7	3.08006666	1.56E-08
NCR3	3.06715672	2.02E-09
CCL20	2.96410288	7.31E-06
PRSS35	2.94598929	8.27E-09
CA2	2.91951933	3.92E-07
FEZ1	2.91343848	1.40E-07
MGC34830	2.8587093	1.04E-08
CDKN1A	2.8285429	7.99E-05
CFH	2.82506288	1.20E-07
IL8	2.8231864	0.00142985
DNAPTP6	2.80383429	4.75E-08
FSD1	2.79824678	3.12E-09
P2RY14	2.7717714	7.40E-06
TNF	2.72973772	1.82E-07
IGFBP4	2.70348176	5.01E-09
CFH	2.69903269	1.14E-07
MAF	2.67684265	1.58E-05
PLEKHC1	2.64293183	6.39E-06
TNFSF14	2.63778811	3.33E-08
THBS1	2.58224484	3.02E-07
B3GALT2	2.57670458	9.69E-07
CAMTA1	2.57542888	1.95E-08
ELOVL4	2.56066433	1.06E-07
MAP3K8	2.5462322	1.12E-06
PLCB1	2.53557204	1.01E-06
CENTG2	2.53357244	2.27E-07
PHACTR2	2.532127	7.50E-07
TGFA	2.52963103	7.21E-07
PRDM1	2.48533289	4.41E-07

Upregulated in CD161++ vs CD161+		
Symbol	logFC	P.Value
LTK	4.49873737	5.98E-11
IL23R	3.930369	5.42E-09
RORC	3.91055364	1.59E-10
LOC642181	3.88269198	2.32E-10
IL23R	3.75711123	3.28E-09
IL4I1	3.65074325	1.26E-08
LOC619207	3.55061435	2.26E-10
LOC650761	3.51663379	1.25E-07
ME1	3.49587823	3.11E-09
CA2	3.48776177	2.07E-07
BLK	3.43640438	1.89E-08
MATN2	3.41137848	8.26E-10
RBM24	3.22998115	6.70E-08
CYP2E1	3.22296297	2.67E-07
ITPKA	3.18617455	6.47E-08
RORC	3.17520888	1.49E-09
COL5A1	3.02634242	2.45E-08
NTN4	3.00214978	8.06E-09
FSD1	2.96766528	1.35E-09
COL5A3	2.86344231	5.12E-07
CSF3R	2.86324954	4.26E-07
CA2	2.78558858	7.16E-07
COLQ	2.7835688	2.40E-09
PLEKHA7	2.7624561	6.87E-08
LILRA5	2.76221228	2.89E-06
RBM24	2.75453855	1.54E-05
NRGN	2.73647454	0.00019723
CCL20	2.71514197	1.99E-05
PRP2	2.67934489	2.00E-08
SPI1	2.66895804	1.29E-05
PLEKHC1	2.66343985	5.83E-06
SCRN1	2.63022068	8.88E-09
GALNAC4S-6S	2.62895382	3.13E-05
PTPNS1	2.61287028	4.77E-05
SPON1	2.60787794	1.10E-08
COLQ	2.60764205	4.68E-07
RBP7	2.57414434	1.96E-06
NAPSB	2.55678664	2.79E-05
MS4A6A	2.50942941	0.00010104
CXCR6	2.48099985	1.35E-07
MS4A6A	2.48069554	3.71E-06
SPI1	2.47661225	2.64E-05
HK3	2.46383403	2.92E-07
RAB31	2.45487021	9.75E-06
STAB1	2.45308276	4.50E-07
FOLR3	2.44817622	4.90E-08
AIF1	2.44807742	4.83E-06
SERPINA1	2.42014283	1.20E-05
CHST13	2.41833756	3.05E-07
CD300LF	2.41808504	1.43E-07
CSF1R	2.40595305	6.07E-06
CD14	2.39177876	2.23E-06
SCGB3A1	2.38610174	0.00015029
CD83	2.38336871	0.00076849
GP9	2.36658013	0.00054424
S100A12	2.36273328	8.04E-06
ZBTB16	2.35292653	3.13E-07
MS4A7	2.35065	4.89E-05
SIPA1L2	2.34448218	3.03E-08
CACNA2D3	2.34349896	4.78E-06
LILRA2	2.32732664	2.72E-06
HCK	2.32590342	1.20E-06
IL13RA1	2.3213418	3.79E-05
CYBB	2.31337965	2.49E-05
MS4A6A	2.31311012	0.00010043
CDKN1A	2.31111333	0.00055712
CD1D	2.30209812	0.00012675
RGS18	2.29805058	0.00040199
S100A9	2.29573223	1.70E-05
SLC11A1	2.29171723	1.98E-06

CTSH	2.45347362	1.39E-05	LMO2	2.28999649	3.79E-05
SLC4A10	2.45009931	2.42E-05	BASP1	2.28701527	4.84E-05
SYTL2	2.44599144	1.18E-07	FCN1	2.28174109	6.89E-06
NAPSB	2.42422742	4.96E-05	GNA15	2.27741866	9.66E-06
ROR2	2.38609669	1.12E-05	FPR1	2.25486805	4.65E-06
CCR1	2.36881222	7.58E-08	**CCR6**	2.2545114	6.17E-08
LOC91461	2.36465176	2.24E-05	P2RY14	2.25371861	7.29E-05
MICALCL	2.35791888	6.14E-07	NALP12	2.25188549	1.16E-06
PRDM1	2.3572165	2.17E-07	ASGR2	2.24895293	1.84E-06
CFH	2.35246618	3.44E-07	LST1	2.24685738	1.96E-07
SYTL2	2.30474862	1.27E-07	BTK	2.24548178	0.00012441
GNA15	2.30335342	8.47E-06	LST1	2.24502285	1.13E-06
PLD1	2.28543345	1.16E-05	IGSF6	2.24374525	9.54E-06
CTSH	2.28255309	1.75E-07	S100A8	2.24147325	9.21E-06
FLJ39501	2.26444766	1.34E-07	PRSS35	2.24115134	3.32E-07
GALNAC4S-6S	2.26362828	0.00014885	KLF4	2.24040166	0.00047522
SLC11A1	2.25944628	2.36E-06	CD14	2.23806945	3.41E-06
CXXC5	2.25727195	2.00E-06	IRAK3	2.23481916	4.41E-07
GPBAR1	2.25687095	1.95E-06	TMIGD2	2.23401209	9.77E-06
IL8	2.25599277	0.0017313	RTN1	2.22137145	3.64E-06
LOC653518	2.25237568	1.79E-06	SLC4A10	2.22127513	6.94E-05
ADM	2.24918702	1.21E-06	GP1BB	2.21911441	0.00056227
ZBTB16	2.24379415	3.89E-06	SLC7A7	2.21902107	1.42E-05
SLAMF1	2.24376145	2.36E-07	LTBR	2.21012837	2.30E-05
CD33	2.24046067	5.01E-05	BRSK1	2.20522287	1.43E-07
CCL3L3	2.23584848	4.83E-07	NCR3	2.19637458	1.98E-07
PTPN13	2.22266922	7.87E-05	CLEC12A	2.19481009	3.17E-06
KIT	2.21588059	2.67E-07	**ZBTB16**	2.19303538	1.62E-05
STAB1	2.21344094	1.65E-06	CD36	2.19202163	6.55E-05
BHLHB2	2.20394522	7.53E-07	ASGR1	2.19048711	6.72E-06
CSF3R	2.19836504	1.08E-05	CSPG2	2.1904574	5.82E-05
PSCD3	2.19619364	1.50E-06	NFE2	2.18935441	7.57E-05
SLCO3A1	2.16850865	1.06E-05	B3GALT2	2.18696506	7.12E-06
FLJ20245	2.16749734	9.45E-07	SERPINA1	2.18101816	3.12E-05
IL17RE	2.1618486	8.04E-06	LILRB3	2.17461517	7.33E-06
NALP12	2.15841118	1.96E-06	ELOVL4	2.16457752	9.41E-07
KLF4	2.15526065	0.00067006	IFI30	2.16330288	6.54E-06
CCL3L3	2.15512174	4.10E-07	CCR2	2.16283013	4.43E-07
MAF	2.14738961	3.66E-06	LST1	2.15982971	3.33E-06
TNFSF13B	2.13231207	1.42E-07	CD40LG	2.15863024	3.25E-06
CCL3L1	2.12868501	1.52E-07	LYZ	2.14884699	0.0001751
TSPAN15	2.11230927	2.24E-06	JUP	2.1375059	6.49E-06
ADAM19	2.11174511	1.94E-05	LILRA3	2.12679899	7.40E-06
CD14	2.10158027	1.04E-05	CD68	2.12327646	5.31E-06
VLDLR	2.09901075	7.02E-07	ALDH3B1	2.10474758	3.50E-07
PODXL	2.09723982	1.33E-05	CAMTA1	2.10253824	2.96E-07
IGSF6	2.09033569	2.13E-05	EMR2	2.0948387	2.78E-05
LILRA3	2.08514148	9.32E-06	LOC649635	2.09104229	2.22E-07
P2RY14	2.08287122	0.00011779	PYGL	2.07683711	5.46E-05
LOC644365	2.07435694	1.69E-06	CPVL	2.07221725	6.41E-05
LOC648470	2.06520642	9.26E-07	MARCKS	2.07207569	2.15E-05
AIF1	2.06339956	3.39E-05	LY86	2.06132369	2.16E-06
IFI30	2.0581206	1.17E-05	LGALS2	2.054363	0.00012674
RBP7	2.05233194	2.75E-05	FCER1A	2.05109022	6.10E-06
PTPRM	2.04154424	1.62E-05	KIAA1598	2.05074053	1.93E-05
ASGR1	2.03954762	1.53E-05	IL17RE	2.04830619	1.49E-05
B3GALT7	2.03557873	7.82E-07	CYP1B1	2.04521407	0.00012357
TNFRSF4	2.03046235	1.48E-06	C4orf18	2.04346527	1.24E-05
CLEC1B	2.02101363	0.00206367	CD163	2.04293983	0.00014186
SERPINA1	2.00756692	9.10E-05	LOC644365	2.04242194	2.05E-06
CDH2	2.00691643	0.00076662	MAFB	2.03915147	4.48E-05
TYROBP	2.00665656	0.00016474	CPVL	2.03875153	4.33E-05
CATSPER1	2.00063634	1.36E-05	KIF5C	2.02624628	3.92E-07
CD83	1.99647059	0.00025103	PLD1	2.02006001	4.57E-05
CYBRD1	1.98969957	3.61E-05	TBXAS1	2.01874387	9.64E-06
LRRC25	1.9892117	5.53E-07	TNFAIP2	2.01435834	0.00013274
LRRC6	1.9888514	1.36E-05	FN5	2.0116632	0.00030795
PLXDC2	1.98720429	6.99E-06	ROR2	2.00907891	7.35E-05
SYTL2	1.98688361	2.31E-05	RAB32	2.00331186	4.38E-05
FEZ1	1.98294806	4.79E-07	IGFBP4	2.00122576	2.97E-07
SPRY1	1.98127317	4.18E-05	CD33	1.99796559	0.00016197
LOC652226	1.97818872	4.03E-06	RNASE2	1.99437272	6.54E-06

RNASE2	1.97290737	7.43E-06	TNFRSF21	1.99386207	1.19E-05
LGALS3	1.97238964	2.29E-05	ALOX5	1.99150691	4.20E-05
TSPAN18	1.9710867	2.81E-05	**ZBTB16**	1.99072175	1.57E-05
HCK	1.96827888	9.00E-06	SYK	1.98566234	0.00013986
SCGB3A1	1.96728051	0.00088622	MNDA	1.98466578	6.45E-05
IRAK3	1.96483648	2.22E-06	CD86	1.98404335	2.51E-06
CAP2	1.96381698	8.91E-05	PRAM1	1.97489522	7.73E-07
PPAP2C	1.95721942	1.06E-05	MCEMP1	1.97200656	1.48E-06
C4orf18	1.95429697	2.06E-05	CST3	1.96571233	9.47E-06
FES	1.94922478	4.50E-06	TNS3	1.9611746	3.93E-05
HNMT	1.94481705	4.15E-07	LOC653518	1.95875499	9.52E-06
CD300LF	1.94231163	2.33E-06	LRRC25	1.95774612	6.78E-07
PLA2G7	1.94034175	3.03E-06	GPBAR1	1.94834952	1.12E-05
LST1	1.93946001	6.67E-06	FES	1.92886512	5.10E-06
KYNU	1.93934957	0.00154075	B3GALT7	1.92868436	1.54E-06
ALOX5	1.9342713	5.73E-05	HLA-DRA	1.9276711	0.00029933
LAMA2	1.93416533	1.59E-05	LOC653518	1.92707651	7.00E-07
TBXAS1	1.93071434	1.60E-05	CLEC12A	1.91362559	1.41E-06
TST	1.92921336	1.60E-05	HLA-DRA	1.90954737	0.00043655
ADRB2	1.92865798	9.57E-07	PLXNB2	1.90618905	1.64E-05
IL12RB2	1.92450709	6.86E-07	FLJ22662	1.89882119	2.78E-05
MS4A7	1.92390591	0.0003588	CEBPD	1.898293	1.72E-05
RTN1	1.92010653	1.98E-05	SLC24A4	1.89246362	0.00035353
C1orf78	1.91577495	1.61E-06	HDC	1.88720214	5.22E-06
SYK	1.915091	0.00019949	CD86	1.8765445	7.23E-05
NFE2	1.91317991	0.00028727	CD83	1.86383828	0.00047457
HES4	1.91011593	0.00019004	TSPAN15	1.86365826	9.95E-06
SCRN1	1.90978548	6.45E-07	CFD	1.8615485	1.09E-05
HK3	1.90593678	7.04E-06	SLC15A3	1.86127548	2.13E-06
CD36	1.90283212	4.18E-05	EPB41L3	1.84466765	0.00011852
CLEC12A	1.89914345	5.73E-06	ZNF385	1.83654863	4.80E-06
CHST13	1.89807154	6.17E-06	AQP9	1.83537188	1.25E-05
PDE5A	1.89797468	0.00146747	OSCAR	1.82945615	1.96E-06
RGS18	1.89718403	0.00202543	NCF1C	1.82655487	4.95E-05
CD36	1.89665604	0.00027644	MTMR11	1.82348758	1.68E-05
CSF1R	1.89506307	8.51E-05	TGFBI	1.82093648	2.98E-05
LOC646786	1.89150541	4.80E-05	CCR1	1.81515976	2.32E-06
CPVL	1.88919651	9.60E-05	NTN4	1.81086481	4.09E-05
WDR67	1.88856311	8.33E-07	CUEDC1	1.80721329	3.03E-06
AFF3	1.88131468	0.00016101	SPRY1	1.80169588	0.00011256
BASP1	1.87805532	0.00034479	RIN2	1.80143998	3.70E-05
LYN	1.87194889	3.09E-05	TLR8	1.79855145	0.00022932
ASGR2	1.87060418	1.62E-05	ABCA1	1.7970662	1.87E-05
ABCA1	1.85990438	1.27E-05	GPBAR1	1.79394816	2.25E-05
MS4A6A	1.85936177	9.25E-05	ECGF1	1.79355429	2.74E-06
CLEC7A	1.8582141	4.57E-07	CLEC12A	1.78788532	1.16E-05
FOLR3	1.85817598	1.76E-06	THBS1	1.78299189	2.64E-05
CYP1B1	1.85392429	0.00031973	RNASE6	1.77849658	9.62E-06
TGFA	1.85346911	8.81E-06	KIF5C	1.77666295	1.25E-06
FN5	1.85190767	0.00065139	SULF2	1.77642318	1.91E-05
DFNB31	1.84751589	1.07E-06	UNQ5783	1.77376387	1.29E-05
LST1	1.84671834	2.37E-06	CCR2	1.77353262	1.26E-05
S100A12	1.84646594	0.00011757	P2RX1	1.77114246	2.44E-05
MARCKS	1.84620963	7.45E-05	FGD2	1.76186619	0.00048523
CAPN12	1.84365857	6.13E-06	LILRA5	1.75470862	1.53E-05
LST1	1.84356496	2.10E-05	CD36	1.74488823	0.0001034
FCN1	1.84245027	7.35E-05	C5AR1	1.74364074	0.00045887
GPBAR1	1.8397963	1.70E-05	ANPEP	1.73786668	3.32E-06
C3AR1	1.83636811	2.27E-05	LOC91461	1.73162586	0.00051344
CPVL	1.83414725	0.00021843	BCL11A	1.72799242	0.00024702
S100A8	1.82963265	8.51E-05	PRICKLE1	1.72395161	0.00011108
CLEC7A	1.82582589	1.97E-06	VENTX	1.7109934	0.00036207
CYP2C19	1.82328011	1.84E-05	HNMT	1.70997963	2.87E-05
PIK3AP1	1.82060171	2.33E-05	PLXDC2	1.70492401	3.92E-05
RNASE6	1.81869957	7.42E-06	FLJ33641	1.70114751	0.00023347
CAPN12	1.81728434	2.45E-06	KIT	1.69751545	7.28E-06
GP9	1.81675472	0.00441334	ALDH1A1	1.69321125	4.49E-05
CLEC12A	1.81137048	2.91E-05	PLA2G7	1.69014659	1.53E-05
KLRG1	1.80998571	1.08E-05	CTSH	1.68875905	0.00060906
TNFSF14	1.8066124	3.07E-06	SIGLEC10	1.68175307	0.00043464
C6orf59	1.8056149	0.00019876	GPX1	1.67548076	0.00016531
DUSP6	1.80168518	0.0002327	CENTA2	1.67280674	3.48E-05

SERPINA1	1.80157897	0.00022206	HNMT	1.66892249	2.83E-06
CCL3	1.79972011	1.42E-05	GPR162	1.66692352	1.25E-05
CD1D	1.79516097	0.00122274	CAP2	1.66539111	0.0004385
ITGAX	1.78998447	4.83E-05	C1QR1	1.66435543	6.27E-05
NTN4	1.78996826	4.63E-05	IRF8	1.65712188	0.00054531
FOSB	1.78903876	0.00043579	MGST1	1.65333659	3.49E-06
IFNGR1	1.78753491	3.57E-06	TSPAN18	1.65285795	0.00017523
OACT1	1.78700826	1.94E-06	CTSH	1.65256485	9.63E-06
LOC653158	1.77830666	0.00048855	ATP6V0A1	1.65246422	8.31E-06
MGST1	1.77729455	1.44E-06	TLR7	1.63936367	0.00034359
KCNT1	1.77727389	0.00191906	DAB2IP	1.63920555	0.00030221
MEF2C	1.76252876	0.00355296	CD68	1.63787957	0.00024702
LEPREL2	1.76032136	6.88E-05	P2RY13	1.63700813	6.55E-05
BTK	1.76007915	0.00115413	FLJ20273	1.63563557	9.21E-06
MAFB	1.75952971	0.00020164	NCF2	1.6339949	0.000418
MGC5457	1.75738915	0.00086995	ALDH2	1.63006448	7.89E-06
SPRY1	1.75513249	3.17E-05	MS4A7	1.6295748	1.07E-05
LILRB3	1.75368974	7.88E-05	SPRY1	1.62809367	7.07E-05
TNS3	1.75046513	0.00012796	OSCAR	1.62711306	1.93E-05
TRIB1	1.74832527	0.00029043	PTPNS1	1.62341516	3.60E-05
KLRC1	1.74534509	5.85E-05	NRIP1	1.62313542	5.74E-06
KIAA0427	1.74514555	2.35E-06	ASGR2	1.62235223	2.61E-05
SPI1	1.73553758	0.00085884	TRIB1	1.62155824	0.00057731
ALDH3B1	1.73468212	3.92E-06	PTGS2	1.61602972	0.0004959
CACNA2D2	1.73237526	3.75E-06	TLR8	1.60831125	7.10E-05
GNB4	1.72615762	9.40E-05	TAL1	1.60629777	0.00043672
HIST2H3C	1.72421017	7.44E-05	TBC1D9	1.60335676	0.00029298
FPR1	1.72268798	9.24E-05	CLEC4A	1.5997924	0.00011188
ANXA2P3	1.72246584	2.23E-06	FLJ20701	1.59592385	7.67E-05
LIM2	1.72019696	6.23E-06	AFF3	1.59521338	0.00074
CDKN1A	1.71699684	5.73E-05	GNB4	1.59520544	0.00020588
CD14	1.71657505	6.78E-05	CXCL16	1.59443291	8.18E-06
CEBPA	1.71477398	8.30E-05	TNFSF13B	1.58522534	1.03E-05
KIAA1598	1.71342784	0.00012949	SGK	1.58520688	0.00019199
TSPAN18	1.71080112	9.42E-05	IL1RN	1.57647511	2.35E-05
LGALS2	1.70597559	0.00071951	HLA-DMB	1.57588285	0.00021629
FCGR1A	1.70138487	0.00080158	SPRY1	1.57437783	4.54E-05
IL15	1.70007589	4.02E-05	ABCD1	1.57355358	1.16E-05
CYFIP1	1.69601105	9.05E-06	FCER1G	1.57252195	0.00071688
GP1BB	1.69510592	0.00468454	ECGF1	1.57124091	1.36E-05
SULF2	1.692142	3.27E-05	CFH	1.57118984	7.44E-05
IL15RA	1.69123362	6.07E-06	CSF2RA	1.56486871	1.28E-05
FLJ22662	1.69102371	9.50E-05	FER1L3	1.56472277	0.00054754
RAVER2	1.68766214	3.30E-05	PFC	1.56194198	3.12E-05
HPGD	1.68717776	7.71E-05	ADM	1.56191634	7.92E-05
HNMT	1.68714778	3.33E-05	CLEC4A	1.56018757	9.07E-05
SLAMF7	1.68574738	0.00010139	NCF1B	1.55715038	7.36E-05
NCAM1	1.68351345	0.00010079	LST1	1.55668965	4.20E-05
CST3	1.68278145	5.31E-05	CLEC7A	1.55563087	4.16E-06
CLIC4	1.68221047	0.00014247	GPR177	1.55271765	4.85E-05
PLEKHG3	1.67939536	4.69E-05	HMOX1	1.55018837	0.00017577
C1orf61	1.67745961	5.81E-05	CSF3R	1.54958868	2.44E-05
MS4A6A	1.67741998	0.00337051	CFH	1.54583419	5.02E-05
SLC7A7	1.67701145	0.00026449	IGF2BP2	1.54162323	0.00017111
LINGO4	1.67652656	1.77E-05	LYZ	1.53887932	0.00021414
PDZD4	1.67645406	4.11E-05	TNFSF13B	1.53816571	8.40E-06
BRSK1	1.67535884	4.58E-06	LEPREL2	1.53796574	0.00026395
SYTL2	1.67375718	0.00010193	PPGB	1.53328297	9.93E-06
ECGF1	1.67347956	6.28E-06	PRDM1	1.52907633	0.00077506
CLEC12A	1.67099473	7.23E-06	LILRA5	1.52618441	0.00010382
SIGLEC10	1.67044984	0.00046202	FSD1	1.52528409	1.02E-05
C10orf128	1.66666247	2.79E-05	APOBEC3A	1.52303112	3.21E-05
POLR2L	1.66626156	2.82E-05	RETN	1.52115598	0.00051167
LRFN4	1.66580046	9.87E-06	CIAS1	1.51923116	8.39E-06
CLIC5	1.66308223	7.88E-06	KCTD12	1.51694909	0.00014718
RAB31	1.6602667	0.00054279	EMR3	1.51267375	0.00036792
ASGR2	1.66002901	2.02E-05	DPP4	1.51216627	7.09E-05
ZNF385	1.65790844	1.57E-05	RUNX2	1.51163616	2.26E-05
TNFRSF18	1.65584733	0.00027733	CFH	1.50810061	0.00018492
PRICKLE1	1.65564627	0.00016617	CD300C	1.50124766	5.26E-05
PRDM1	1.65507466	6.64E-05	IL1B	1.50087754	0.00024252
SPI1	1.6548692	0.00139849	CXorf20	1.49758701	0.00013402

RGS2	1.65155791	0.00031034	P2RY14	1.49639841	0.00046533
FAM20C	1.64953247	1.90E-05	LINGO4	1.49598054	6.09E-05
IL6	1.64642952	0.00429963	FLJ39501	1.49590344	2.17E-05
FAM13A1	1.64452889	0.00010066	DKFZP564O08	1.49392046	0.00011607
DUSP5	1.64421653	0.00066984	ADAM12	1.48637041	0.00020684
C20orf103	1.6426751	6.73E-05	LOC653518	1.48209752	4.80E-05
MNDA	1.64212309	0.00041315	SLC37A2	1.48066987	3.51E-05
MYO1D	1.6402818	3.87E-06	TMEM176B	1.4796439	0.0002997
BCL3	1.63910466	1.04E-05	VMD2	1.47614886	3.53E-05
TNFRSF18	1.63679715	1.51E-05	C20orf103	1.47523587	0.00019874
ALDH2	1.63597308	7.57E-06	INTS6	1.47253031	0.00016674
SKAP2	1.63523307	0.00010385	CREB5	1.46232531	4.14E-05
SART2	1.63507418	1.03E-05	OLFM1	1.4607545	6.44E-05
LTBR	1.63371118	0.00048275	HMFN0839	1.46046162	3.14E-05
RBM9	1.63289353	1.65E-05	CSF2RA	1.45957193	0.00021664
LOC649635	1.63055127	5.00E-06	MOSC1	1.45741242	4.60E-05
LOC650761	1.62753579	0.00070717	AMICA1	1.45112404	1.33E-05
SLC24A4	1.62673459	0.00131665	PNKD	1.44618426	0.00012203
ABCA2	1.6230217	2.19E-05	PILRA	1.44605714	6.51E-05
HIST2H2AA3	1.62244929	6.62E-06	SULF2	1.43896046	0.0001214
FER1L3	1.62186189	0.00039611	MATN2	1.43795252	3.97E-05
PLAUR	1.62149202	6.59E-05	G0S2	1.43512765	5.91E-05
TPM2	1.62124559	0.00011679	SART2	1.4345964	4.41E-05
FAM13A1	1.62088976	1.67E-05	DAPK1	1.43398947	0.0002041
CUEDC1	1.6194172	1.11E-05	CRISPLD2	1.4326196	5.56E-05
MGC29506	1.61704658	9.26E-05	CXXC5	1.41918523	0.00031455
SPRY1	1.61257041	3.51E-05	SEMA4A	1.41799052	3.05E-05
TBC1D9	1.6120103	0.0002785	CD300LB	1.41740195	0.00056214
S100A9	1.61196849	0.00060013	ERGIC1	1.4058871	0.00035513
PYGL	1.60978774	0.00064326	OLIG1	1.40208083	2.08E-05
AUTS2	1.60700803	1.81E-05	SLC1A2	1.40040613	0.00038817
CENTD3	1.60657063	4.42E-05	NLRP3	1.39994396	6.18E-05
SESN1	1.60097342	4.98E-06	PDLIM7	1.3933948	0.00011227
EMR2	1.60087965	0.00041714	LOC196264	1.38708332	0.00079915
GPR65	1.60018459	1.40E-05	TST	1.38550082	0.00046673
CMTM1	1.59845434	5.95E-05	HSPC159	1.38446701	0.00099443
PTAFR	1.59845192	0.00017162	CLEC7A	1.38194485	4.87E-05
ZDHHC14	1.59799847	6.10E-05	CD163	1.36889079	0.00037382
FCER1A	1.59791781	9.56E-05	RBM9	1.35846107	0.00011776
P2RX1	1.59698003	7.39E-05	DHRS9	1.34890336	5.77E-05
NETO2	1.59668237	0.00042248	KCTD12	1.33803187	0.00011106
PRAM1	1.59526513	1.03E-05	PTAFR	1.33295701	0.00090225
NAPSB	1.59479896	0.00140199	LOC389816	1.33103996	5.39E-05
PTPNS1	1.58871527	0.00396299	LRP3	1.31546648	0.00015677
HDC	1.5854221	3.77E-05	LILRA3	1.3141136	0.00030135
KLRG1	1.58398295	0.00034535	PSCD3	1.30915216	0.00028117
CYB561	1.58026451	5.29E-05	MARCO	1.30854395	0.00020091
OSCAR	1.57934941	1.12E-05	ALDH1A1	1.30351621	0.00011271
PLAUR	1.57757047	9.92E-05	UNQ3033	1.3024588	0.00019716
LILRA2	1.5728551	0.00020096	ARHGAP10	1.30244516	5.92E-05
CD163	1.57126119	0.00149822	C10orf47	1.30226516	0.00040065
RAB32	1.56937653	0.00048697	NCAPG2	1.28977216	0.00010056
CACNA2D3	1.56557743	0.00034957	PGM5	1.2887873	0.00015271
RORA	1.56392802	0.00011115	FCGR2A	1.28354157	0.00022497
AIM2	1.56353529	0.0001595	PPAP2C	1.28303709	0.00076067
CYBRD1	1.56274085	0.00039464	CYFIP1	1.27991538	0.00018392
LOC653610	1.55734996	2.05E-05	CSTA	1.27525062	4.55E-05
ERN1	1.55649101	7.26E-06	PLAUR	1.27286036	0.00074803
TRIM7	1.55620592	0.00028678	LOC652226	1.26369898	0.00046164
LMO2	1.55339565	0.00147901	IFNGR2	1.26150109	0.0003812
ADAM8	1.55148901	3.57E-05	PDIA5	1.26008787	0.00036836
LST1	1.55043035	4.38E-05	HLX1	1.2535134	0.00023886
ABCC3	1.54775556	0.00294276	CD302	1.25201189	0.00035445
FCAR	1.54732788	6.28E-05	PLAUR	1.25164242	0.00077857
MS4A6A	1.54305709	0.00340563	PLAUR	1.25000102	0.00016221
C1QR1	1.543035	0.00013598	SULF2	1.24801576	0.00093387
MTMR11	1.53981986	0.00010293	ARHGAP22	1.24783403	0.0001125
GADD45G	1.53980795	0.00023069	LAPTM4B	1.24328302	0.00041984
ALDH1A1	1.53889594	0.00012109	PFKFB3	1.24007482	0.00035904
P2RY13	1.53779611	0.00012428	OACT1	1.23939497	0.0001187
IRF8	1.53669665	0.00104477	QPCT	1.23852664	0.0003183
P2RY14	1.53626641	0.00036607	FVT1	1.23597766	0.00011934

IER3	1.53514103	0.00067397
CSPG2	1.53457563	0.00157636
CLEC7A	1.53428838	1.54E-05
RPPH1	1.5336999	2.36E-05
FCHO2	1.52635076	0.00173597
CCR2	1.52557769	6.57E-05
FGD2	1.52079864	0.0016818
LAG3	1.52073693	3.74E-05
PTGS2	1.5203377	0.00084599
LILRA3	1.51691133	7.29E-05
CYFIP1	1.51587254	0.00057522
CD86	1.51547552	5.43E-05
KIT	1.51538197	0.00035453
SIGLEC5	1.5141448	0.00039436
KIF5C	1.51360143	8.62E-06
MAFF	1.51267489	0.00010265
PRDM1	1.51139563	0.00085616
TLR8	1.51028577	0.00109371
CCL3L1	1.50901311	9.50E-05
G0S2	1.50419616	3.58E-05
LTB4R	1.50250509	5.66E-05
SLC4A4	1.49967421	0.00034969
MCEMP1	1.49919295	3.60E-05
FLJ20701	1.49700702	0.00014663
FAM43A	1.49694676	0.00014748
C3orf57	1.49492527	0.00257933
OSCAR	1.49393899	4.91E-05
FLJ12331	1.49392276	0.00019718
DENND3	1.49246798	8.78E-05
GBP5	1.48861003	5.19E-05
TNFSF13B	1.48589883	2.14E-05
PDZK1IP1	1.4812453	0.00226844
EOMES	1.4795733	0.00020681
IL1B	1.47917899	0.00027845
SLC16A3	1.47907161	8.73E-05
CPLX1	1.47862085	3.29E-05
LOC285513	1.47544194	5.72E-05
TNFRSF21	1.47412195	0.00028162
TNFRSF1B	1.47198361	0.0001323
IL1RN	1.47045668	5.01E-05
DKFZp686O24	1.46774029	0.00012383
RIN2	1.46732386	0.0002944
LOC650919	1.46592787	0.0001367
FSD1	1.46532734	1.61E-05
CIAS1	1.46420498	1.28E-05
KLRF1	1.46325099	0.00447397
CD163	1.45878265	0.00020513
LAT2	1.45787643	0.00238053
LONRF3	1.45635635	0.00029027
ELOVL6	1.45445452	0.00020173
HMOX1	1.45355458	0.00032497
SLC4A4	1.45175888	0.00018705
IL13RA1	1.45137789	0.00277417
HOP	1.45118123	0.00011919
SCAP2	1.44943142	4.12E-05
HIST1H2BG	1.44139586	2.07E-05
MGC52282	1.43905249	1.51E-05
CREB5	1.43728074	4.98E-05
HTRA1	1.434225	0.0004356
FZD2	1.43371525	0.00043803
SULF2	1.43270215	0.00012682
AQP9	1.43249449	0.00017442
TCF4	1.43136616	0.00259744
MKNK1	1.42911835	3.77E-05
LILRB2	1.42780901	0.00024153
SLC7A5	1.42508556	3.33E-05
GPR171	1.42401118	6.17E-05
IL15	1.42245663	9.55E-05
ARHGAP24	1.42194681	0.00103206
FLJ12078	1.41964308	0.00308719
TREML1	1.41756396	0.00117974
CENTA2	1.41677444	0.0001922
CYP2S1	1.23167694	0.00010471
DKK3	1.22667402	0.00041397
CXCL2	1.22624043	0.00059991
LTB	1.22289628	4.95E-05
CDA	1.22135278	0.00049397
TLR5	1.22092831	0.00045628
LAPTM4B	1.21602121	0.00026082
ASB9	1.2124826	0.00035122
USP13	1.21198385	0.00041831
HOMER3	1.21028248	0.00068357
SLC16A3	1.20722858	0.00060675
IFITM3	1.20707761	0.00070085
FVT1	1.20610035	0.00018918
ATBF1	1.19770639	0.00091499
CPLX1	1.19538601	0.00028561
RTN3	1.1925133	0.00049656
MERTK	1.19122663	0.00036703
CCR6	1.18357104	0.00030884
DNAPTP6	1.18228725	0.00084669
CAPG	1.17864596	0.00036134
ACPP	1.17684255	0.00071636
LOC652616	1.17070555	0.00067002
FAM20C	1.16469092	0.00062392
CD302	1.15995823	0.00085444
GPX1	1.14793774	0.00096669
SAMD4A	1.14226512	0.00089047
ESPN	1.13159721	0.0001939
EDG2	1.13068353	0.00064329
KCNMB1	1.12964128	0.00017651
IL18R1	1.12559741	0.0009802
NRG1	1.12297315	0.00070367
PSG6	1.11944352	0.00036426
CYP27A1	1.11436524	0.00040762
SDSL	1.10989173	0.00075467
EYA2	1.10692562	0.00035912
FCGR1B	1.10662257	0.00046339
LRTM1	1.10228728	0.00075313
LTC4S	1.10198735	0.00093888
GRN	1.09997744	0.00059222
FLT4	1.09576208	0.00071154
DUSP16	1.08107645	0.00055606
C1orf78	1.07322834	0.00075754
ANG	1.06725061	0.0003634
CLEC7A	1.06498723	0.00061319
PRR5	1.0485448	0.00050691
SCMH1	1.04703709	0.00060226
BCL3	1.03807361	0.00100581
S100Z	1.03540232	0.00085996
UNC93B1	1.02659687	0.00095195
CPNE2	1.02307516	0.00034628
TTYH3	1.02295844	0.00062616
IL23A	1.02114539	0.00077886
FLJ22386	1.01838378	0.00054391
BTBD11	1.01669304	0.0008657
LOC389816	1.00990057	0.00039726
ABCB1	1.00984039	0.00098756
CAMK1	1.00592626	0.00076748
ELK3	1.00168713	0.00102117
ZNF503	1.00048832	0.00075888
PILRA	0.99664275	0.0007274
TBC1D8	0.94433536	0.00093933
TNFRSF25	0.94101627	0.00095014
LYPLA2P1	0.93343636	0.00074725

FLJ20273	1.41396933	4.66E-05
PERP	1.41351076	0.00078467
CD86	1.40806725	0.00106626
CAMK1	1.40781721	2.83E-05
ECGF1	1.40536756	4.65E-05
GTF3C1	1.40492492	5.14E-05
MAP3K5	1.40473575	9.51E-05
HIST1H2AE	1.4044246	0.00023201
LOC653264	1.40000279	0.00018486
KCNK7	1.39918833	0.00272992
FCGR2A	1.39853119	9.62E-05
IL29	1.39703917	3.63E-05
ADAM15	1.39505315	0.00014578
HLA-DRA	1.39383986	0.00424603
KLRC1	1.39244692	0.00056191
TLR8	1.39159995	0.00029765
SLC17A3	1.3910124	8.79E-05
MGC14376	1.39058765	0.0035174
RPS24	1.38966003	0.00027914
ELK3	1.38628795	4.60E-05
HIST2H2AC	1.38609766	3.31E-05
OLFM1	1.38595751	0.00011067
NCF4	1.38567747	0.00035608
KCNMB1	1.38530201	2.08E-05
CENTG2	1.38327636	0.00185469
HIST1H2BD	1.38259786	0.00027298
IGF2BP2	1.38250317	0.00047673
CD68	1.38232722	0.0004792
USP13	1.38084497	0.00011979
ATP2B4	1.37957987	0.0007327
HIST1H2BC	1.37640778	0.0024056
IRF5	1.3753823	0.00039843
GZMK	1.37481257	4.54E-05
MOSC1	1.37390226	8.54E-05
LILRA5	1.37347222	0.00029105
ANKRD13D	1.36974902	0.00143051
CTNNA1	1.36877232	0.00015043
FCGR1B	1.36857436	5.78E-05
CCR6	1.3674044	7.43E-05
CFD	1.36715965	0.00027829
IGSF4	1.36471632	3.41E-05
KIAA1754L	1.36417541	5.67E-05
CXCL2	1.36349716	0.00022584
RNASE4	1.36309168	0.00013191
ODF2L	1.35937108	0.00030964
PRSS22	1.35812056	0.00050384
SERPINB2	1.35798479	0.00451946
ABCB1	1.35586102	5.35E-05
CD300LB	1.35583484	0.00082754
EPB41L3	1.35465823	0.00187307
PILRA	1.35426481	0.00012729
LOC653518	1.35389965	0.00012231
GFPT2	1.35152345	6.44E-05
ATF3	1.35081883	0.00032108
MCTP1	1.35074938	0.00268722
VENTX	1.35008311	0.00261903
RASSF4	1.34955177	9.61E-05
LYZ	1.34919866	0.000714
HSH2D	1.34908603	0.00050404
MYO1F	1.34795187	0.00012928
FAM46C	1.34542523	0.00174169
ACPP	1.34524303	0.00021043
LOC221136	1.34366853	0.00041858
S100P	1.34326796	0.00136927
MPST	1.34281666	2.95E-05
STX11	1.34267347	4.02E-05
ADAM7	1.34218463	0.00010143
GPR162	1.34206879	0.00012799
PTGDS	1.34167929	0.00119537
LOC389816	1.34109058	4.98E-05
LOC646064	1.33989041	0.00026883
KLF12	1.33795345	0.00330768

RHOC	1.33745307	0.00071881
METRNL	1.3369798	0.00103942
LIPC	1.33639319	0.00020903
RAB11FIP1	1.33542311	0.00021308
BCL6	1.33483961	7.63E-05
EDG8	1.33247577	0.00020414
PLAUR	1.33117826	8.61E-05
DDAH2	1.33013057	0.00469267
FHOD1	1.32989743	0.00011281
GPR68	1.32743798	0.00016884
ABCD1	1.32726052	7.46E-05
TPM2	1.32683809	0.00053969
CYBB	1.32642769	0.00392415
LRP3	1.32507031	0.00014589
LILRB4	1.32058315	0.00097955
CENPM	1.31736367	0.0001062
CMTM1	1.31565638	0.00011067
CXCL16	1.31533312	6.86E-05
CLEC4A	1.31487426	0.00047172
C1orf96	1.31449879	0.00115308
CLC	1.31248088	0.00205908
CRISPLD2	1.31158943	0.00013747
RHOC	1.3093424	0.00019427
FLJ21986	1.30767138	0.00075499
S100Z	1.30651229	9.75E-05
NEO1	1.30554846	5.57E-05
CLEC4A	1.30414387	0.00075846
GPR177	1.30315346	0.00028209
C10orf87	1.30166698	0.00021325
FAM38A	1.3001284	0.00024018
TANC1	1.29794149	7.93E-05
MERTK	1.29789335	0.00016209
CTSZ	1.29752853	0.00037373
RUNX2	1.29677983	0.00011488
MAPK10	1.29657394	0.00017057
ABCB1	1.29537136	9.74E-05
MS4A7	1.29535317	0.0001269
RAB11FIP1	1.29497988	0.00331715
PCOLCE	1.29486425	9.36E-05
CERK	1.29418213	0.00015037
DMN	1.29395837	0.00050464
CREB5	1.29285126	0.00392914
LOC644677	1.28826308	0.0004222
USP54	1.28772813	0.0003268
RORA	1.28689279	0.00138191
BCL11A	1.28530827	0.00299861
CREB3L2	1.28524174	9.49E-05
SMAD3	1.28379077	0.00030836
HIST1H2BB	1.28326788	3.48E-05
NBPF9	1.2830271	0.00118356
SEMA4A	1.2830236	8.80E-05
HOMER3	1.28200632	0.00040901
DDX39	1.28026576	6.55E-05
NAG8	1.27945549	0.00274088
FHL1	1.2793391	0.00091285
CASP5	1.27904545	8.97E-05
ADAM12	1.27775789	0.00082012
SERPINB2	1.27769451	0.00282461
CD4	1.2751586	0.00247177
FLJ33641	1.27491595	0.00271512
DHRS9	1.27415727	0.00010406
SRC	1.27298636	0.00150035
FOSL2	1.2724923	0.00063957
CD302	1.27234743	0.00037663
FREQ	1.26743239	7.84E-05
CD1C	1.26696304	0.0031851
SLC37A2	1.26647576	0.00017613
DPP4	1.26468288	0.00040714
REPS2	1.26247903	0.00039763
LRIG1	1.26170403	0.00051544
GDPD5	1.26041166	0.00017591
UNQ3033	1.25999474	0.00027081

GPR65	1.2596121	0.00037402
ZFYVE28	1.25901346	0.00216299
NCF4	1.25859857	0.00011159
CSF3R	1.25855207	0.00021074
MPPED2	1.25753293	0.00291332
MATN2	1.25575613	0.00016049
TAOK2	1.25467834	0.00012287
ATBF1	1.25429198	0.00061442
LOC196264	1.25325114	0.00183541
SLC22A15	1.25256449	0.00265766
HSPA2	1.24970013	0.00014053
NLRP3	1.24839337	0.00019645
OLIG1	1.24832884	7.27E-05
APOBEC3A	1.24653202	0.00024883
NLF2	1.24600623	0.00074116
ODF2L	1.24360648	0.00010964
CACNA2D4	1.2414317	0.0007156
HLA-DMB	1.24022657	0.00175775
C15orf48	1.24003239	0.00015657
DUSP2	1.23982711	0.00278318
LOC196549	1.2383971	0.00016549
FAM7A1	1.23801843	0.00042908
CSF2RA	1.23703639	0.00015705
ATG16L2	1.23636079	0.00013479
HMFN0839	1.23544638	0.00017739
HOXA5	1.23461042	0.00151291
RDX	1.23268597	0.00017711
CAMK2N1	1.23095002	0.00021488
PTMS	1.22964605	0.00014829
RIMS3	1.2288802	0.00022105
OSM	1.22850876	0.00275793
AGPAT4	1.22835207	0.0007052
HIST2H2AA3	1.22811713	0.00030186
CLCF1	1.22793255	0.00016517
C1orf24	1.22534438	0.00168228
RASD1	1.22240656	0.00456383
LOC654053	1.21913078	0.00020648
CARD15	1.21854646	0.00192884
FAM91A2	1.21850396	0.00071069
B4GALT5	1.21761398	0.00030859
KLRC1	1.21650654	0.00393116
FGL2	1.21545809	0.00379835
ESM1	1.21366179	9.49E-05
LOC651158	1.21122553	0.00124271
FOLR2	1.20944898	0.00313406
DRD1IP	1.20919968	0.00211708
ELF2	1.20890152	9.98E-05
GUCY1A3	1.20884069	0.00164979
CBLN4	1.20744143	0.00229465
LIMS1	1.20597566	0.00114614
KYNU	1.204002	0.00101121
CDKN1C	1.20398667	0.00137954
FLJ11155	1.20368972	0.00455055
MATK	1.20137252	0.0003508
CERK	1.19883601	0.00030431
MARCO	1.19810263	0.00045867
MGC61571	1.19806072	0.00052458
DAPK1	1.19755932	0.00103515
COL4A3	1.19645895	0.00189254
UNC93B1	1.19604338	0.00024126
PRR5	1.19571687	0.00014677
DPY19L1	1.19533198	0.0006218
TMEM51	1.19527634	0.00058202
HIST1H2BE	1.19284474	0.00261602
CSF2RA	1.1926332	0.00130365
ANPEP	1.19252543	0.00020316
HSPA6	1.19058209	0.00185908
EMR3	1.19035625	0.00270747
PSCD3	1.18988027	0.00066923
HSPC159	1.18974002	0.00325166
ADAM15	1.18899618	0.00021285
JUP	1.18895573	0.00205941

CACNB1	1.18889916	0.00081962
ANXA2P1	1.1879628	0.00016953
HLA-DRB6	1.18492298	0.00054078
PLEKHA5	1.18432017	0.00214185
ADCY9	1.18375301	0.00188473
ATP8B4	1.18339099	0.0012598
S100A11	1.18224391	0.00029521
PDE8A	1.1817765	0.00028735
IL1A	1.18094509	0.00103785
TICAM1	1.17930449	0.00018785
PNKD	1.17855308	0.00081897
KISS1	1.17828533	0.00102841
PFKFB3	1.17724116	0.00057467
ANXA2P1	1.17673288	0.000441
ERN1	1.17667056	0.00039171
SYNE2	1.17602204	0.00021375
NCF1C	1.17571771	0.00268769
FLT4	1.17230215	0.00038953
RHBDF2	1.17126229	0.00034142
SLC22A4	1.17118532	0.00011767
FAS	1.17019043	0.00129544
GALC	1.16982019	0.00023531
LOC646537	1.16893731	0.00460498
CYB561	1.16831439	0.00014097
CES1	1.16664487	0.00204205
NBEAL2	1.1644276	0.00141219
FLJ11151	1.16435283	0.00045051
ZC3H12A	1.16268352	0.00052203
LOC389634	1.16263639	0.00385015
SPIRE1	1.16239339	0.00086092
DPRXP4	1.16134093	0.00022948
RHBDF2	1.1608709	0.00115812
PTPNS1	1.16047706	0.00092255
CLIP2	1.15822628	0.00097823
ACTN4	1.15804678	0.0002083
SNAI3	1.15617805	0.00016533
FLJ43093	1.15587523	0.00186274
UST	1.15250202	0.00031808
ABCG1	1.15188947	0.00468872
CFH	1.15177014	0.00049009
CSTA	1.15159207	0.0001307
GAS7	1.15015235	0.0006728
ALOX5AP	1.14990645	0.0002971
TNNI2	1.14983602	0.00103152
RASGRP4	1.14898113	0.00160164
TGFBI	1.14881265	0.00219153
SLCO3A1	1.14851584	0.00032446
USP45	1.14756651	0.00400953
ATN1	1.14749814	0.00065184
VCL	1.14631262	0.00096102
ARHGAP18	1.14350987	0.00214205
NEK3	1.14322866	0.00157871
DKFZP586D09	1.14209241	0.00027858
GANC	1.14197631	0.00136887
PHTF1	1.13889751	0.00471632
RHEBL1	1.13786723	0.00176648
ALCAM	1.1373687	0.00070839
LAMA2	1.13566654	0.0002525
FLJ45337	1.13511096	0.00095125
KCTD15	1.134985	0.00034114
CCL4	1.13437194	0.00032778
HLX1	1.13421145	0.00059868
FSIP1	1.13161875	0.00127335
PLXNC1	1.13048554	0.00061782
CD58	1.12987977	0.00055876
UNQ5783	1.12871422	0.00112578
UCK2	1.12686166	0.00064169
DKFZP564O08	1.12500586	0.00151078
CTNND1	1.12265631	0.00190726
GOLPH4	1.1222266	0.000736
C14orf161	1.12140518	0.00032463
FUT7	1.1211894	0.00060115

GPR114	1.11896848	0.00188475
FBN2	1.11850805	0.00036467
C4orf18	1.11847261	0.00088856
PPP2R3A	1.11763118	0.00393021
TNFAIP6	1.11615301	0.00497875
GYG1	1.11463624	0.00047956
LOC647466	1.11349234	0.00360649
PMAIP1	1.10973376	0.00426036
DOC2B	1.10893817	0.00262741
GALNT10	1.10827446	0.00125119
PTGDR	1.10809826	0.00079968
CTNNA1	1.10647308	0.00078729
LOC348645	1.1064301	0.00351769
HTRA4	1.10642949	0.00107545
ANXA2	1.10291252	0.00032684
GAA	1.10197772	0.00037012
MGC31967	1.09990385	0.00034432
CLIP2	1.09946066	0.00065294
C20orf134	1.09776316	0.00028175
PRG2	1.09727505	0.00112352
DGCR5	1.09661661	0.00386272
IER5	1.09567249	0.00372027
LRRN6C	1.09481743	0.00112234
LY86	1.09465646	0.0014434
PRDM8	1.09462909	0.00102487
HIST1H2AD	1.09114547	0.00411102
PRO0628	1.09053051	0.00303057
HIP1	1.08901	0.00112949
FRY	1.08869337	0.00026268
QPCT	1.08822461	0.00100089
LIMK1	1.08685865	0.00098356
LOC645769	1.08618259	0.00289337
ELOVL6	1.08545359	0.00368864
TCF7L2	1.08494309	0.00070767
ST3GAL4	1.08432285	0.00071859
LPAL2	1.08370134	0.0006408
LOC652037	1.08327711	0.00119508
IFI44L	1.08270842	0.00111143
LAT1-3TM	1.08244023	0.0037022
PTPN13	1.08232149	0.0022412
TNFRSF12A	1.0815253	0.0005453
SLC43A2	1.08124814	0.00154666
PACSIN1	1.08075821	0.00241915
LOC643169	1.07842412	0.00253734
FURIN	1.07782678	0.00140146
NPDC1	1.07631362	0.00257401
SERPINA9	1.07534734	0.00340204
TRIM7	1.07463361	0.00158563
ATP1B1	1.07439513	0.00230474
LOC653127	1.07419411	0.00271082
GZMA	1.07415872	0.00107293
RHBDF2	1.07387675	0.00166672
CYP27B1	1.07372803	0.00158567
HM13	1.07356774	0.00067969
METRNL	1.07174037	0.0019388
BTBD14A	1.06873109	0.00051989
PARP8	1.06824765	0.00107341
CCL4L1	1.06596292	0.00082758
FAM7A3	1.06539446	0.00214346
PDE4B	1.0653747	0.00041374
NCF1B	1.06373004	0.00228248
LRRC33	1.06319138	0.00115954
GAS1	1.06206816	0.00079387
RTKN	1.06179524	0.00125757
DUSP1	1.06115759	0.00378755
HLA-DQB1	1.06006714	0.00089819
LOC648604	1.05641898	0.00495925
FYN	1.05342886	0.00443764
DOK3	1.05323007	0.00398507
ASTN	1.0521493	0.00082095
NMUR1	1.05153174	0.00084628
SCD5	1.05056919	0.0004148

NAIP	1.04857189	0.00218203
PRKCD	1.04812925	0.00042994
C20orf195	1.04752669	0.00125214
RRBP1	1.04680649	0.00301568
GALM	1.04637197	0.00080272
LOC653785	1.04559419	0.0003036
ZDHHC1	1.04525332	0.00248332
CILP	1.0442479	0.00079448
POU2F2	1.04423942	0.00415703
PLOD3	1.0435445	0.00054461
LOC646309	1.04347073	0.00294918
GAS1	1.04346967	0.00083819
C10orf47	1.04326827	0.00253903
LOC643700	1.04299767	0.00205087
NRIP1	1.03997639	0.00058631
KIF13A	1.03867343	0.00484026
PRF1	1.03808843	0.00092213
SAMD4A	1.03770823	0.00194171
PTGDR	1.03708072	0.00313736
HIST1H4A	1.03407445	0.00468122
FLJ11259	1.03397749	0.00059834
LOC648998	1.03356583	0.00212501
ST3GAL6	1.03334629	0.00200377
SLCO3A1	1.031266	0.00047864
METRNL	1.03078815	0.00205895
CD72	1.02846897	0.00498844
LOC645040	1.02833481	0.00097256
CR1	1.02807043	0.00302135
CLK2	1.02688234	0.00239987
SYNE2	1.02687028	0.00110381
ELSPBP1	1.02612205	0.00370947
EIF2C4	1.02438563	0.0004728
AHNAK	1.02258986	0.0011638
HIST1H2AH	1.02222521	0.00074163
C1orf24	1.02201421	0.00083624
FLJ11292	1.02167484	0.00312434
FAM63B	1.02145854	0.00378107
YPEL1	1.02120464	0.00072767
ETV6	1.020523	0.00079243
HYAL2	1.01929048	0.00036533
FLJ46831	1.0188289	0.00140619
WNT1	1.01728532	0.00113279
FEZ1	1.01719079	0.00375726
STOM	1.016788	0.00120692
C15orf48	1.01643155	0.00183361
KIAA1539	1.01546014	0.00128026
TYRO3	1.01213272	0.00384028
PDLIM7	1.01001087	0.00198788
CECR6	1.00922795	0.00171291
IFI44	1.00862679	0.0017009
CHD9	1.00849	0.00118555
INTS6	1.00788595	0.00406904
DIP2A	1.00678099	0.0025914
MGST2	1.00449026	0.00136175
C15orf5	1.00083739	0.00401624
RHOQ	1.00047397	0.00153912
TTK	0.99928422	0.00268815
SLC15A3	0.99814064	0.00131838
LOC644846	0.99800566	0.003018
ATXN2L	0.99793758	0.00196037
ANG	0.99739507	0.00066732
SBF2	0.9972492	0.00471601
SLC44A3	0.99684741	0.00115807
DKK2	0.99655889	0.00314991
CARD14	0.99570189	0.00212491
MARLIN1	0.99496677	0.0017903
RNU43	0.99461476	0.00130789
ESM1	0.99053937	0.00192622
C3orf60	0.98993183	0.00102716
JSRP1	0.98971326	0.00109343
MXD1	0.9879889	0.00277206
LOC651291	0.98712364	0.00198225

PPAPDC1B	0.98427454	0.00467264
CXorf20	0.98344609	0.00465485
LOC440132	0.9824175	0.00119883
MMP25	0.98136677	0.00402525
LRIG1	0.97882971	0.00314053
MAN2A2	0.977237	0.00224633
CST7	0.97695922	0.00115044
ADAMDEC1	0.97643107	0.00380719
HSPA2	0.9755047	0.00331742
NADK	0.97265002	0.00051205
PILRA	0.97237547	0.00089835
TPD52	0.97042877	0.00136598
GALIG	0.96931656	0.00128736
ARNTL	0.96870989	0.00098903
LOC388578	0.96734012	0.00174557
CD74	0.96536429	0.00356326
LYAR	0.96397151	0.00228195
NFKBIA	0.9602873	0.00222187
LOC652616	0.96009302	0.0032655
ALDH1A1	0.95965138	0.00176642
RXRA	0.95890031	0.00106072
C1orf188	0.95801676	0.00391372
CD58	0.9574376	0.00319442
HES1	0.95690538	0.00362797
ANXA2	0.95614468	0.00470043
LILRA5	0.9560568	0.00414013
NCAPG2	0.95584653	0.00153318
CRHR1	0.95267473	0.00255267
C8G	0.95131438	0.00299586
HM13	0.94907808	0.00266106
SDSL	0.94819193	0.00267473
PPP2R2B	0.94797451	0.0028012
LOC401233	0.94314566	0.00245071
DYRK1B	0.9418872	0.00226622
ATP2B4	0.94166408	0.00121151
NRM	0.9384433	0.00160479
IRAK2	0.93837723	0.00135005
LOC653257	0.93825814	0.00276846
CYP27A1	0.9381531	0.00175991
RAPGEF1	0.9378152	0.00492492
CD300C	0.93473293	0.0035724
HYPE	0.93453939	0.00381657
C1R	0.9325158	0.0012279
SLC45A3	0.93012428	0.00415537
LRRC45	0.9297971	0.00329768
LOC650557	0.92804152	0.00431042
PPAP2B	0.92591652	0.00245002
SLC1A5	0.92541466	0.00328457
SLC43A3	0.92536402	0.00226913
CACNB3	0.9247505	0.00215178
CDC42EP4	0.92230404	0.00400695
EMILIN2	0.91948762	0.00367157
SCO2	0.91930449	0.00184531
AMICA1	0.91666238	0.00122384
CYP2S1	0.91649818	0.00153231
ATF7IP2	0.9162595	0.00220011
PAQR6	0.91575002	0.00243689
FLJ43855	0.91351301	0.00213524
ARHGAP22	0.91285357	0.00185369
REC8L1	0.91225151	0.00203089
LOC648041	0.9118637	0.00357671
PBX4	0.91130743	0.0023698
CD302	0.91068169	0.0046212
ATP2B4	0.91017078	0.00145079
SMAD7	0.90902199	0.00275225
HIST2H2BF	0.90818374	0.0022081
ABCC13	0.90773487	0.00162564
GATA1	0.90769422	0.00388342
LOC646550	0.90766156	0.00420687
LOC136288	0.90679897	0.00311417
GABRP	0.90648436	0.00192747
SNRP70	0.90591713	0.00268953

ID2	0.90423351	0.00194749
GRIPAP1	0.90415229	0.00394791
STX3A	0.90376611	0.00146742
DCBLD1	0.90344406	0.00246374
PRKAG3	0.90253404	0.00437104
C22orf5	0.90191	0.00231744
LOC90835	0.90014488	0.0032739
KLHL17	0.8986744	0.00390877
PLEKHF1	0.89802006	0.00193957
SLC2A8	0.8978429	0.00177789
EDG2	0.89713879	0.00399947
SP140	0.89585739	0.0037469
CCDC46	0.89566362	0.00393541
LOC653337	0.89413683	0.0016369
LOC652651	0.89294588	0.00172019
CSF2RB	0.89290446	0.00126056
C20orf75	0.89014732	0.0035297
TFEB	0.88931118	0.00173339
IRF5	0.887794	0.0034333
PTCH	0.88756777	0.00375962
B4GALT1	0.88754606	0.00295544
PTPRE	0.88618059	0.00400009
LOC647384	0.88555494	0.00136175
SOD2	0.88200451	0.00487567
EBI2	0.88076944	0.00207756
RAB6B	0.88035492	0.00273936
MAPK8IP3	0.87740807	0.0041798
HYPK	0.87590785	0.00326273
NPC1	0.87326477	0.00426671
LOC646354	0.87186245	0.00434085
LOC643550	0.87144786	0.00293769
INCA	0.86890524	0.00235872
MGC13005	0.86848427	0.00419688
POGZ	0.86628703	0.00179648
LEPREL1	0.86626997	0.00420548
LOC389816	0.86545857	0.00149464
PRNP	0.86537866	0.00211619
DSC2	0.864576	0.00297568
LOC650968	0.8627841	0.00442251
CD151	0.86166803	0.00412357
LRRTM2	0.85933253	0.00323786
ARSJ	0.85842138	0.00233826
PTPRE	0.85800373	0.00303935
YWHAH	0.85695658	0.00485883
NFE2L3	0.85691537	0.00304447
SSH3	0.85517077	0.00426554
ZSWIM4	0.84899226	0.00253053
BMPR1A	0.84758585	0.00233628
MYO1C	0.84743486	0.00371123
LOC650546	0.84144372	0.00250414
FAM26B	0.84112945	0.00399921
PTPRN	0.83960632	0.00450252
C17orf58	0.83828323	0.00420774
ERVWE1	0.83764312	0.00423354
SLC31A2	0.83555471	0.00308984
ESPN	0.83492374	0.00264231
LOC649679	0.8321905	0.00392699
WDFY2	0.83183545	0.00408222
FLJ40113	0.8303592	0.00215579
RBMY1A1	0.82880572	0.0042374
FLJ33387	0.82861051	0.00398155
SRGN	0.82763849	0.0021578
GBF1	0.82621493	0.00285129
S100A4	0.82595005	0.00266767
CAV2	0.8243491	0.00196872
LOC643031	0.82305	0.00201368
GDPD3	0.81919686	0.00421212
SNTB2	0.81767209	0.0032401
LRRC45	0.81669283	0.00358552
NOD1	0.81568731	0.00255952
CASP1	0.81490074	0.00493207
IL1F7	0.81372365	0.00334903

LOC644548	0.81291047	0.00460239
LOC643176	0.81147032	0.0046451
PHCA	0.80931868	0.00236157
PFKFB3	0.80439898	0.00294218
DPP8	0.80321973	0.00379428
SLC22A4	0.80209584	0.00323065
SOLH	0.80132715	0.00493536
APLP2	0.79374056	0.00499535
PPGB	0.7832318	0.0049767
HSPA1A	0.78191904	0.00416975
LOC643009	0.77962234	0.00482229
PLS3	0.77932989	0.00399098
ANXA5	0.77794028	0.00452938
RASGRP4	0.75761057	0.00449714
LRRC49	0.74945858	0.00447877
C15orf38	0.72984369	0.00499026

Appendix Table V-2. Comparison of genes with matched expression profiles to *ZBTB16* and *RORC*, identified by PTM analsyis (R>0.9) of expression dataset of CD161++, CD161+, and CD161- CD8+ T cells. Columns list genes uniquely matched to *ZBTB16* or *RORC*, or genes matched to both *ZBTB16* and *RORC*. Numbers indicate the number of genes in column.

ZBTB16 only 32	RORC only 29	ZBTB16 and RORC 43
GTF3C1	BRSK1	CYFIP1
CLIC5	PRP2	PSCD3
EIF2C4	ABCB1	SPON1
TGFA	LST1	LTK
FAM109A	NRM	CEBPD
VLDLR	CXCR6	CFH
CYP2C19	PLD1	IL23R
CPLX1	MGC29506	C1orf78
IL18RAP	IL4I1	RORC
PHACTR2	ABCD1	MGST1
MGC34830	CCR2	NTN4
MICALCL	LOC653518	HNMT
PDE8A	ABCG5	SIPA1L2
LOC648470	LINGO4	CXXC5
IL12RB2	ELOVL4	WDR67
IL15RA	PLEKHC1	FLJ11259
TNFSF14	SLC4A10	TNFSF13B
TNFRSF18	RNASE2	SART2
PTPN13	B3GALT7	LOC652226
ZDHHC14	PLEKHA7	KIF5C
SYTL2	GZMK	SESN1
C9orf71	MYO1D	MKNK1
LOC643031	TST	FLJ39501
SLC7A5	ITPKA	ME1
PCP4	NFE2L3	FREQ
LATS2	ADAM7	DNAPTP6
LOC643076	CYP2E1	CCR6
TAOK2	RBM24	FSD1
CMTM1	CYB561	DFNB31
HIST1H2BG		TPD52
PLCB1		ABCA1
IL18R1		CCR1
		IFNGR1
		IGFBP4
		ZBTB16
		COLQ
		NCR3
		CD40LG
		COL5A1
		COL5A3
		LOC619207
		MATN2
		LOC642181

Appendix Table V-3. Comparison of genes with matched expression profiles to *ZBTB16*, *RORC*, or *KLRB1*, identified by PTM analsyis (R>0.9) of expression dataset of CD161++, CD161+, and CD161- CD8+ T cells. Columns list genes uniquely matched to or shared by *ZBTB16*, *RORC,* or *KLRB1*. Numbers indicate the number of genes in column.

ZBTB16 only 25	KLRB1 only 15	RORC only 29	ZBTB16 and KLRB1 7	ZBTB16 and RORC 43	RORC and KLRB1 0	all three 0
GTF3C1	MPST	BRSK1	PCP4	CYFIP1		
CLIC5	ABCA2	PRP2	IL18RAP	PSCD3		
EIF2C4	LRRC45	ABCB1	LATS2	SPON1		
TGFA	ANXA2	LST1	TNFSF14	LTK		
FAM109A	KLRB1	NRM	MGC34830	CEBPD		
VLDLR	CACNA2D2	CXCR6	IL18R1	CFH		
CYP2C19	ADRB2	PLD1	SYTL2	IL23R		
CPLX1	PRDM1	MGC29506		C1orf78		
PHACTR2	FRY	IL4I1		RORC		
MICALCL	LCE3B	ABCD1		MGST1		
PDE8A	FEZ1	CCR2		NTN4		
LOC648470	FLJ40113	LOC653518		HNMT		
IL12RB2	FLJ20245	ABCG5		SIPA1L2		
IL15RA	ANXA2P3	LINGO4		CXXC5		
TNFRSF18	KLRG1	ELOVL4		WDR67		
PTPN13		PLEKHC1		FLJ11259		
ZDHHC14		SLC4A10		TNFSF13B		
C9orf71		RNASE2		SART2		
LOC643031		B3GALT7		LOC652226		
SLC7A5		PLEKHA7		KIF5C		
LOC643076		GZMK		SESN1		
TAOK2		MYO1D		MKNK1		
CMTM1		TST		FLJ39501		
HIST1H2BG		ITPKA		ME1		
PLCB1		NFE2L3		FREQ		
		ADAM7		DNAPTP6		
		CYP2E1		CCR6		
		RBM24		FSD1		
		CYB561		DFNB31		
				TPD52		
				ABCA1		
				CCR1		
				IFNGR1		
				IGFBP4		
				ZBTB16		
				COLQ		
				NCR3		
				CD40LG		
				COL5A1		
				COL5A3		
				LOC619207		
				MATN2		
				LOC642181		

Appendix Table V-4. Comparison of genes with matched expression profiles to *ZBTB16*, *RORC*, or *IL18RAP*, identified by PTM analsyis (R>0.9) of expression dataset of CD161++, CD161+, and CD161- CD8+ T cells. Columns list genes uniquely matched to or shared by *ZBTB16, RORC,* or *IL18RAP*. Numbers indicate the number of genes in column.

ZBTB16 only	RORC only	IL18RAP only	ZBTB16 and IL18RAP	ZBTB16 and RORC	RORC and IL18RAP	all three
11	29	28	21	38	0	5
C9orf71	BRSK1	KLRB1	GTF3C1	CYFIP1		CEBPD
LOC643031	PRP2	LAMA2	IL15RA	PSCD3		IFNGR1
CLIC5	ABCB1	BHLHB2	EIF2C4	SPON1		ZBTB16
SLC7A5	LST1	LRRC6	TNFSF14	LTK		DNAPTP6
LOC643076	NRM	PRDM1	VLDLR	CFH		WDR67
TNFRSF18	CXCR6	ADRB2	CYP2C19	IL23R		
TGFA	PLD1	FRY	ZDHHC14	C1orf78		
FAM109A	MGC29506	PRSS22	SYTL2	RORC		
PTPN13	IL4I1	LCE3B	PCP4	MGST1		
PDE8A	ABCD1	CREB3L2	IL18RAP	NTN4		
CPLX1	CCR2	KLRG1	LATS2	HNMT		
	LOC653518	SRGN	TAOK2	SIPA1L2		
	ABCG5	MPST	PHACTR2	CXXC5		
	LINGO4	ABCA2	CMTM1	FLJ11259		
	ELOVL4	ANXA2	MGC34830	TNFSF13B		
	PLEKHC1	CACNA2D2	HIST1H2BG	SART2		
	SLC4A10	ERN1	MICALCL	LOC652226		
	RNASE2	DOPEY2	PLCB1	KIF5C		
	B3GALT7	UCK2	IL18R1	SESN1		
	PLEKHA7	SLCO3A1	LOC648470	MKNK1		
	GZMK	CILP	IL12RB2	FLJ39501		
	MYO1D	CENTG2		ME1		
	TST	FEZ1		FREQ		
	ITPKA	FLJ40113		CCR6		
	NFE2L3	UST		FSD1		
	ADAM7	ANXA2P1		DFNB31		
	CYP2E1	FLJ20245		TPD52		
	RBM24	ADAM8		ABCA1		
	CYB561			CCR1		
				IGFBP4		
				COLQ		
				NCR3		
				CD40LG		
				COL5A1		
				COL5A3		
				LOC619207		
				MATN2		
				LOC642181		

Appendix Table V-5. Comparison of genes with matched expression profiles to *ZBTB16*, *RORC*, or *IL18R1*, identified by PTM analsyis (R>0.9) of expression dataset of CD161++, CD161+, and CD161- CD8+ T cells. Columns list genes uniquely matched to or shared by *ZBTB16, RORC,* or *IL18R1*. Numbers indicate the number of genes in column.

ZBTB16 only 10	IL18R1 only 33	RORC only 28	ZBTB16 and IL18R1 22	ZBTB16 and RORC 31	RORC and IL18R1 1	all three 12
C9orf71	KLRB1	BRSK1	GTF3C1	CYFIP1	MYO1D	PSCD3
IL15RA	CHD9	PRP2	CLIC5	SPON1		IFNGR1
LOC643076	FHOD1	ABCB1	EIF2C4	LTK		SESN1
TNFRSF18	ATN1	LST1	TNFSF14	CEBPD		C1orf78
PHACTR2	LRRC6	NRM	VLDLR	CFH		MKNK1
TGFA	PRDM1	CXCR6	CYP2C19	IL23R		ZBTB16
FAM109A	ADRB2	PLD1	PTPN13	RORC		FLJ39501
MICALCL	RAB11FIP1	MGC29506	ZDHHC14	MGST1		DNAPTP6
PDE8A	CREB3L2	IL4I1	SYTL2	NTN4		CCR6
CPLX1	ST3GAL4	ABCD1	LOC643031	HNMT		DFNB31
	NADK	CCR2	SLC7A5	SIPA1L2		CXXC5
	KLRG1	LOC653518	PCP4	FLJ11259		WDR67
	POLR2L	ABCG5	IL18RAP	TNFSF13B		
	SLAMF1	LINGO4	LATS2	SART2		
	MPST	ELOVL4	TAOK2	LOC652226		
	GBP5	PLEKHC1	CMTM1	KIF5C		
	ABCA2	SLC4A10	MGC34830	ME1		
	PRNP	RNASE2	HIST1H2BG	FREQ		
	SMAD3	B3GALT7	PLCB1	FSD1		
	ANXA2	PLEKHA7	IL18R1	TPD52		
	RDX	GZMK	LOC648470	ABCA1		
	CACNA2D2	TST	IL12RB2	CCR1		
	PCOLCE	ITPKA		IGFBP4		
	ADAM19	NFE2L3		COLQ		
	UCK2	ADAM7		NCR3		
	MAF	CYP2E1		CD40LG		
	CAPN12	RBM24		COL5A1		
	LRFN4	CYB561		COL5A3		
	PHCA			LOC619207		
	CENTG2			MATN2		
	FLJ40113			LOC642181		
	ANXA2P1					
	FLJ20245					

Appendix Table V-6. Comparison of genes with matched expression profiles to *ZBTB16*, *RORC*, or *IL12RB2*, identified by PTM analsyis (R>0.9) of expression dataset of CD161++, CD161+, and CD161- CD8+ T cells. Columns list genes uniquely matched to or shared by *ZBTB16, RORC,* or *IL12RB2*. Numbers indicate the number of genes in column.

ZBTB16 only 4	**IL12RB2 only** 12	**RORC only** 28	**ZBTB16 and RORC** 15	**ZBTB16 and IL12RB2** 28	**IL12RB2 and RORC** 1	**all three** 28
LOC643076	LOC654053	BRSK1	ABCA1	GTF3C1	MYO1D	PSCD3
TNFRSF18	PRNP	PRP2	CCR1	CLIC5		SPON1
TGFA	C1orf188	ABCB1	CYFIP1	EIF2C4		CEBPD
FAM109A	PHCA	LST1	LTK	VLDLR		C1orf78
	LAMA2	NRM	CFH	CYP2C19		SIPA1L2
	CHD9	CXCR6	IL23R	CPLX1		CXXC5
	FLJ40113	PLD1	RORC	IL18RAP		WDR67
	ANXA2P1	MGC29506	MGST1	PHACTR2		LOC652226
	LRRC6	IL4I1	NTN4	MGC34830		KIF5C
	CLEC4E	ABCD1	HNMT	MICALCL		SESN1
	SLC17A3	CCR2	FLJ11259	PDE8A		MKNK1
	KLRG1	LOC653518	TNFSF13B	LOC648470		FLJ39501
		ABCG5	SART2	IL12RB2		ME1
		LINGO4	LOC619207	IL15RA		FREQ
		ELOVL4	FSD1	TNFSF14		DNAPTP6
		PLEKHC1		PTPN13		CCR6
		SLC4A10		ZDHHC14		DFNB31
		RNASE2		SYTL2		TPD52
		B3GALT7		C9orf71		IFNGR1
		PLEKHA7		LOC643031		IGFBP4
		GZMK		SLC7A5		ZBTB16
		TST		PCP4		COLQ
		ITPKA		LATS2		NCR3
		NFE2L3		TAOK2		CD40LG
		ADAM7		CMTM1		COL5A1
		CYP2E1		HIST1H2BG		COL5A3
		RBM24		PLCB1		MATN2
		CYB561		IL18R1		LOC642181

Appendix Table V-7. Comparison of genes with matched expression profiles to *ZBTB16*, *RORC*, or *IL23R*, identified by PTM analsyis (R>0.9) of expression dataset of CD161++, CD161+, and CD161- CD8+ T cells. Columns list genes uniquely matched to or shared by *ZBTB16, RORC,* or *IL23R*. Numbers indicate the number of genes in column.

ZBTB16 only	IL23R only	RORC only	ZBTB16 and RORC	RORC and IL23R	ZBTB16 and IL23R	all three
31	12	2	6	27	1	37
GTF3C1	BLK	ABCG5	CEBPD	BRSK1	TGFA	CYFIP1
CLIC5	CA2	ABCD1	DNAPTP6	PRP2		PSCD3
EIF2C4	LEPREL2		HNMT	ABCB1		SPON1
FAM109A	P2RY14		DFNB31	LST1		LTK
VLDLR	LOC644365		WDR67	NRM		CFH
CYP2C19	TSPAN18		FLJ11259	CXCR6		IL23R
CPLX1	GNB4			PLD1		C1orf78
IL18RAP	PRSS35			MGC29506		RORC
PHACTR2	AFF3			IL4I1		MGST1
MGC34830	DKFZp686O24166			CCR2		NTN4
MICALCL	ELK3			LOC653518		SIPA1L2
PDE8A	CAP2			LINGO4		CXXC5
LOC648470				ELOVL4		TNFSF13B
IL12RB2				PLEKHC1		SART2
IL15RA				SLC4A10		LOC652226
TNFSF14				RNASE2		KIF5C
TNFRSF18				B3GALT7		SESN1
PTPN13				PLEKHA7		MKNK1
ZDHHC14				GZMK		FLJ39501
SYTL2				MYO1D		ME1
C9orf71				TST		FREQ
LOC643031				ITPKA		CCR6
SLC7A5				NFE2L3		FSD1
PCP4				ADAM7		TPD52
LATS2				CYP2E1		ABCA1
LOC643076				RBM24		CCR1
TAOK2				CYB561		IFNGR1
CMTM1						IGFBP4
HIST1H2BG						ZBTB16
PLCB1						COLQ
IL18R1						NCR3
						CD40LG
						COL5A1
						COL5A3
						LOC619207
						MATN2
						LOC642181

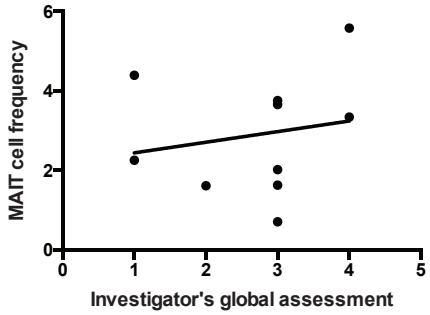
Appendix Table V-8. Comparison of genes with matched expression profiles to *ZBTB16*, *RORC*, or *CCR6*, identified by PTM analsyis (R>0.9) of expression dataset of CD161++, CD161+, and CD161- CD8+ T cells. Columns list genes uniquely matched to or shared by *ZBTB16, RORC,* or *CCR6*. Numbers indicate the number of genes in column.

ZBTB16 only	CCR6 only	RORC only	ZBTB16 and CCR6	RORC and CCR6	ZBTB16 and RORC	all three
12	13	13	20	16	4	39
IL15RA	PRNP	BRSK1	GTF3C1	PRP2	ABCA1	CYFIP1
SLC7A5	CERK	ABCG5	CLIC5	ABCB1	MGST1	PSCD3
IL18RAP	SNAI3	LINGO4	EIF2C4	ELOVL4	HNMT	SPON1
LOC643076	PRSS35	PLEKHC1	TNFSF14	NRM	FLJ11259	LTK
FAM109A	ELK3	LST1	TNFRSF18	SLC4A10		CEBPD
CMTM1	LOC650227	RNASE2	TGFA	CXCR6		CFH
HIST1H2BG	ALCAM	B3GALT7	VLDLR	PLD1		IL23R
MICALCL	PHCA	PLEKHA7	PTPN13	MGC29506		C1orf78
CYP2C19	HYAL2	TST	ZDHHC14	GZMK		RORC
PDE8A	TSPAN18	ITPKA	C9orf71	MYO1D		NTN4
CPLX1	CTSH	NFE2L3	LOC643031	IL4I1		SIPA1L2
SYTL2	C10orf128	ABCD1	PCP4	ADAM7		CXXC5
	SLAMF1	RBM24	LATS2	CYP2E1		WDR67
			TAOK2	CYB561		TNFSF13B
			PHACTR2	CCR2		SART2
			MGC34830	LOC653518		LOC652226
			PLCB1			KIF5C
			IL18R1			SESN1
			LOC648470			MKNK1
			IL12RB2			FLJ39501
						ME1
						FREQ
						DNAPTP6
						CCR6
						FSD1
						DFNB31
						TPD52
						CCR1
						IFNGR1
						IGFBP4
						ZBTB16
						COLQ
						NCR3
						CD40LG
						COL5A1
						COL5A3
						LOC619207
						MATN2
						LOC642181

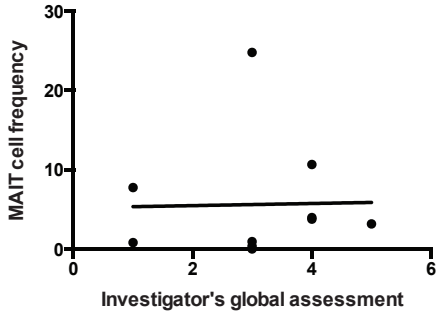
A

	Sample type	Patient number	Date frozen	Date biopsy taken	Investigator's global assessment
Psoriasis	PBMCs	Ps200	07/06/2011		2
		Ps201	09/06/2011		1
		Ps150	07/06/2011		3
		Ps125	04/07/2011		4
		Ps202	07/06/2011		3
		Ps54			3
		Ps55			4
		Ps56			3
		Ps51			3
		Ps213	03/08/2011		1
	Psoriatic skin biopsy	Ps1219		12/07/2013	1
		Ps1300		28/11/2013	2
		Ps1298		28/11/2013	2
Atopic dermatitis	PBMCs	AD203	28/07/2011		1
		AD120	04/07/2011		4
		AD33	04/07/2011		5
		AD13	09/05/2011		3
		AD11	07/06/2011		4
		AD201	06/07/2011		1
		AD22	15/02/2005		4
		AD205	08/08/2011		4
		AD200	06/07/2011		1
		AD204			2

B



C



Appendix Table V-9. Patient information for the psoriasis and atopic dermatitis PBMCs and skin biopsies. A) Table showing patient information and the Investigator's global assessment (IGA) score for each patient. B-C) CD8+ MAIT cell frequency in the PBMCs of psoriasis (B) and atopic dermatitis (C) patients are plotted against the IGA score.

6. CD161 expression on NK cells

6.1. Introduction

NK cells are the most classical population of ILCs, expressing a heterogeneous repertoire of germline-encoded receptors that allows them to distinguish infected or stressed cells from healthy cells. In particular, NK cells express inhibitory MHC class I-specific receptors such that they recognise “missing self” and can be activated by the loss of MHC class I molecules on transformed or infected cells (Bix et al., 1991; Kärre et al., 1986). These receptors include the killer cell immunoglobulin-like receptors (KIRs) and C-type lectin-like CD94/NKG2A heterodimers (Anfossi et al., 2006; Karlhofer et al., 1992; Lazetic et al., 1996). In turn, activating receptors such as NKG2D homodimers (Bauer, 1999) and natural cytotoxicity receptors (NCRs) of the immunoglobulin superfamily (Arnon et al., 2004; Mandelboim et al., 2001) allows the recognition of “self” cells that express viral antigens or stress-induced molecules (see Chapter 1, Figure 1-4). The combined engagement of these activating and inhibitory receptors determines whether NK cells are activated to lyse target cells.

NK cells are traditionally divided into two main subsets according to the level of CD56 expression: $CD56^{bright}$ and $CD56^{dim}$ NK cells (Lanier et al., 1986). $CD56^{dim}$ NK cells are thought to differentiate from $CD56^{bright}$ NK cells, as $CD56^{dim}$ NK cells have shorter telomeres than $CD56^{bright}$ NK cells (Romagnani et al., 2007). Furthermore, in an experiment using humanized mice engrafted with human haematopoietic stem cells, $CD56^{bright}$ NK cells were shown to differentiate into $CD56^{dim}$ NK cells (Huntington et al., 2009). A clear pathway for NK cell differentiation following the $CD56^{bright}$ to $CD56^{dim}$ transition is less well defined. The consensus is that

proliferative capacity and responsiveness to cytokines such as IL-12+IL-18 is associated with $CD56^{bright}$ NK cells (Baume et al., 1992; Cooper et al., 2001), and thus are "immature" functions. In contrast, $CD56^{dim}$ NK cells are more responsive to activating receptor ligation and are highly cytotoxic effector cells (De Maria et al., 2011; Nagler et al., 1989). Therefore increased cytotoxicity is endowed to "mature" NK cells. Upon maturation, $CD56^{dim}$ NK cells acquire the terminal differentiation marker CD57 (Lopez-Vergès et al., 2010) as well as the Fc receptor III for IgG, CD16, and inhibitory KIR receptors specific for self-MHC class I molecules (Anfossi et al., 2006; Björkström et al., 2010).

Recently, a terminally differentiated population of NK cells with memory-like properties has been described in the context of CMV (Paust et al., 2010; Sun et al., 2009, 2012). NK cells are critical for the control of murine CMV (MCMV), as expression of the Ly49H receptor, which directly interacts with the m157 protein of MCMV, was necessary to clear the infection (Brown et al., 2001). Interestingly, primary MCMV infection has been shown to induce the clonal expansion of Ly49H+ NK cells, which persist in tissues for months after infection, and upon re-challenge, undergo secondary expansion with enhanced effector functions (Sun et al., 2009). These NK cells thus exhibit memory-like properties that were previously only attributed to cells of the adaptive immune system.

In humans, CMV infections are asymptomatic in healthy individuals, but immunosuppressed individuals, such as HIV patients, are at high risk of developing disease. CMV also skews the NK cell receptor repertoire in humans, with cells expressing the activating heterodimer NKG2C/CD94 expanding in recipients of solid organ (Lopez-Vergès et al., 2011) or umbilical cord blood (UCB) transplantation (Foley et al., 2012b) during primary CMV infection or reactivation. After haematopoietic cell transplantation, NKG2C+ NK cells from CMV-seropositive donors

expanded in CMV-seropositive recipients, whereas NKG2C+ NK cells from CMV-seronegative donors did not, suggesting that there is a secondary response against CMV antigen (Foley et al., 2012a). These cells have an enhanced ability to secrete IFNγ in response to target cells, or even more so, upon CMV reactivation (Foley et al., 2012a, 2012b; Lopez-Vergès et al., 2011). Therefore, it has been suggested that these cells represent the human counterparts of Ly49H+ NK cells with memory-like properties. These NKG2C+ cells can be identified by their high expression of CD57, and they express inhibitory KIRs specific for self-MHC class I molecules (Béziat et al., 2012; Gumá et al., 2004; Lopez-Vergès et al., 2011). Furthermore, in a patient who completely lacked T cells, all NK cells expressed the activating NKG2C/CD94 heterodimer, suggesting that NKG2C+ NK cells are important effector cells in the control of CMV infection (Kuijpers et al., 2008).

CD161 is one of the earliest markers expressed during NK cell maturation from CD34+ haematopoietic stem cell precursors, in addition to markers such as CD56 and NKp44 (Bennett et al., 1996; Montaldo et al., 2012). On mature NK cells, expression of CD161 has been suggested to correlate with the cytotoxic function of CD16+ NK cells (Konjević et al., 2009), and ligation of CD161 with its ligand LLT1 inhibits NK cell cytotoxicity and cytokine secretion (Aldemir et al., 2005; Rosen et al., 2005, 2008). There have been various reports of modulated expression of CD161 on NK cells during viral infections. For instance, reduced CD161 expression in acute HCV infection predicated viral clearance (Alter et al., 2011), while it has also been correlated with increased liver inflammation in chronic HCV infection (Cosgrove et al., 2014). Patients with chronic HIV infection have also been reported to have depleted CD161+ NK cells compared to healthy donors (Alter et al., 2004; Luteijn et al., 2011). In patients where viral replication is suppressed by Highly Active Antiretroviral Therapy (HAART), this CD161+ NK cell population is replenished and shows a recovery in cytotoxicity against target cells (Azzoni et al., 2002), although another

report suggested the opposite occurs, with a reduced CD161+ NK cell population in HAART treated patients compared to untreated and uninfected donors (Jacobs et al., 2004). CD161 was also found to be significantly downregulated in an exhausted CD56−CD16+ NK cell subset in HIV patients compared to slow progressors and healthy controls (Kulkarni et al., 2012). In the context of CMV seropositive donors, reports on CD161 expression have been variable, with some reporting no change (Achour et al., 2014; Gumá et al., 2004; Noyola et al., 2012) and others reporting a downregulation on NKG2C+ NK cells in HCV/HBV patients (Béziat et al., 2012).

Despite reports on the expression of CD161 in different viral infections, comprehensive phenotypic and functional analyses of NK cells based on CD161 expression have not been performed. Furthermore, CD161-expressing T cells share a transcriptional signature, regardless of TCR expression (Fergusson et al., 2014), which was associated with an increased responsiveness to innate cytokines IL-12 and IL-18. Whether this transcriptional signature and functional correlation with CD161 holds true within NK cells is unknown.

6.2. Aims

1. Describe the phenotype of CD161+ NK cells in relation to the CD161− NK cell population
2. Investigate differences in the functional capacity of CD161+ and CD161− NK cells
3. Investigate the expression of CD161 on NK cells from chronic HIV patients from the Swiss HIV cohort, and the effect of HAART on CD161 expression
4. Investigate whether CD161+ NK cells share transcriptional or functional features with CD161-expressing T cells, as described by Fergusson *et al.* (2014)

6.3. Methods

Chapter-specific materials and methods are detailed below. Please see Chapter 2 for further details of other methods.

6.3.1. Patient information and cells

PBMCs were isolated from healthy adult donors, 24-month old donors, and UCB as detailed in Chapter 2. PBMCs were obtained from a cohort of treatment-naïve patients from the Swiss HIV Cohort study (n=27), sampled prior to, and 1 year and 2 years into HAART. Cells were isolated as detailed in section 2.3.1, frozen and stored in liquid nitrogen until use. After thawing, cells were rested overnight before staining. Clinical data for the patients are shown in Table 6-1.

	Treatment time point		
	Pre treatment	1 year post treatment	2 years post treatment
n	27	27	27
Gender Male Female	 24 3		
Age Median (IQR)	 40 (34.0, 45.0)		
CD4 count (cells/ml)	202 (185,299)	414 (333, 569)	515 (405, 620)
Viral load (log10 cpm) Median (IQR)	 4.64 (4.13, 4.98)	 0 (0,0)	 0 (0,0)
Time since diagnosis (months) Median (IQR)	 10 (2,86)		
CMV seropositive	25	not tested	not tested

Table 6-1. Clinical characteristics of treatment cohort from Swiss HIV Cohort Study. Modified from Cosgrove *et. al.*, 2013.

K562 cells were obtained from the American Type Culture Collection (ATCC).

6.3.2. *In vitro* stimulation of NK cells

PBMCs were cultured with K562 cells at a ratio of PBMCs : K562 cells = 10:1 for 6 hours. Anti-CD107a PE-Cy7 (BD Biosciences) was added at the beginning of the stimulation, and after 1 hour, Brefeldin A (eBioscience) was added for the remaining

time. For IL-12+IL-18 stimulations, PBMCs were cultured for 20 hours with 50ng/ml IL-12 and IL-18 (Miltenyi Biotec), with Brefeldin A (eBioscience) added for the last 4 hours.

6.3.3. Screening for healthy CMV+ donors

For the screening of T cell responses to CMV, PBMCs were cultured with CMV lysate (Virusys Corporation) at 5µg/ml overnight and Brefeldin A (eBioscience) was added after 1 hour of stimulation. Donors were considered CMV+ if the frequency of IFNγ+ CD4+ T cells was higher than the frequency of IFNγ+ cells from unstimulated CD4+ T cells. The donors who tested positive for CMV had a mean of %2.757 ± 1.830 of CD4+ T cells making an IFNγ response. Alternatively, lab volunteers that had been previously tested for CMV responses by tetramer staining or Enzyme-Linked ImmunoSpot (ELISpot) assays were also included in the healthy CMV+ cohort for comparison with HIV-infected individuals.

6.3.4. Proliferation assays

PBMCs were labeled with CTV as described in Chapter 2 (2.6.6). Cells were resuspended and cultured with the indicated concentrations of cytokines: IL-2 (100IU/ml; Roche Diagnostics), IL-15 (25ng/ml; Miltenyi Biotec), PHA (2µg/ml; Sigma Aldrich), IL-18 (50ng/ml; Miltenyi Biotec), IL-12 (50ng/ml; Miltenyi Biotec) or the indicated combinations of stimuli for 5 days.

For crosslinking of receptors, purified anti-CD16 (BD Biosciences), anti-NKG2C (R&D Systems), or an isotype control (BD Biosciences) was diluted in PBS to 5µg/ml, and added to a flat bottom ELISA plate (Greiner Bio-One Limited). After an overnight incubation at 4°C, the plate was washed three times with PBS, before adding R10 for

2 hours at 37°C. $5x10^5$ CTV-labeled PBMCs were cultured in 200µl for 5 days, with or without the addition of IL-15 at 50ng/ml.

For the proliferation of sorted NK cells, PBMCs were labeled with CTV as detailed in Chapter 2 (2.6.6.), and NK cells were enriched from CTV-labeled PBMCs using the EasySep Human NK cell enrichment kit (StemCell Technologies). Enriched NK cells were stained for surface markers, and sorted on the MoFlo XDP (Beckman Coulter). NK cells were defined as singlet, alive, CD14−CD19−CD3−CD56+ cells, sorted as CD161+ or CD161− NK cells, and cultured for 5 days in the presence of IL-15 (50ng/ml; Miltenyi Biotec).

6.3.5. Detection of apoptosis

For apoptosis assays, PBMCs were cultured for 5 days as described in Section 6.3.4. or staurosporine (Sigma-Aldrich) as a positive control. Cells were harvested and stained with phosphatidylserine AlexaFluor488 (Millipore) on ice for one hour with the live-dead marker, before staining with other markers.

6.3.6. Microarray analysis

Fresh PBMCs from four healthy volunteers were sorted by surface antibody staining using a MoFlo MLS cell sorter (Beckman Coulter), defined as singlet, alive, CD14−CD19− CD3− CD56+ cells that are CD161+ or CD161−. Purified cell populations were snap frozen and stored at −80°C before shipping to Miltenyi Biotec, Germany for RNA extraction and gene expression analysis performed with the 8x60K Agilent Whole Human Genome Oligo Microarray, which is provided as a commercial service (Miltenyi Biotec). Raw microarray image files were processed using Agilent feature extraction, and differential gene expression was analysed using the Rosetta

Resolver gene expression data analysis system (Rosetta Biosoftware). After filtering out probes not detected in more than 4 samples in R, 776 genes were differentially regulated between CD161+ and CD161− NK cells to a significant level (P<0.01, >2 fold change). Hierarchical clustering of differentially regulated genes was completed using the heatmap function in GENE-E[3] (Broad Institute).

Whole microarray data of CD161 subsets within CD8+ T cells were obtained from the publication by Billerbeck *et. al*. (2010). Gene lists for comparison with NK cell data were obtained from genes significantly up/downregulated in CD161++ or CD161+ subsets (>2 fold, P<0.05) compared to the CD161− subset of CD8+ T cells. Gene set enrichment analysis (GSEA) was performed using GSEA version 2.1.0 (Mootha et al., 2003; Subramanian et al., 2005).

6.3.7. Cytometry by time-of-flight (CyTOF)

For experiments shown in Appendix Figure VI-1, PBMCs were stimulated with PMA/ionomycin for 3 hours and were stained and acquired by CyTOF as described in Chapter 2 (2.8). The panel of antibodies and heavy metal isotopes are listed in Appendix Table VI-2, and the gating strategy is shown in Figure 6-1A.

For experiments shown in Figure 6-9 and Appendix Figure VI-4, PBMCs depleted of CD4+ T cells, monocytes and B cells were stimulated with IL-12+IL-18 (both 50ng/ml, Miltenyi Biotec) overnight, with Brefeldin A (eBioscience) added for the last 4 hours. The panel of markers and heavy metal isotopes are listed in Table 6-2. Monocytes, myeloid and plasmacytoid DC, mast/basophils, and B cells were excluded from the analysis based on the markers CD14, CD11c, CD123, FcεR1 and CD19. Gating strategy is shown in Figure 6-1B.

[3] http://www.broadinstitute.org/cancer/software/GENE-E/.

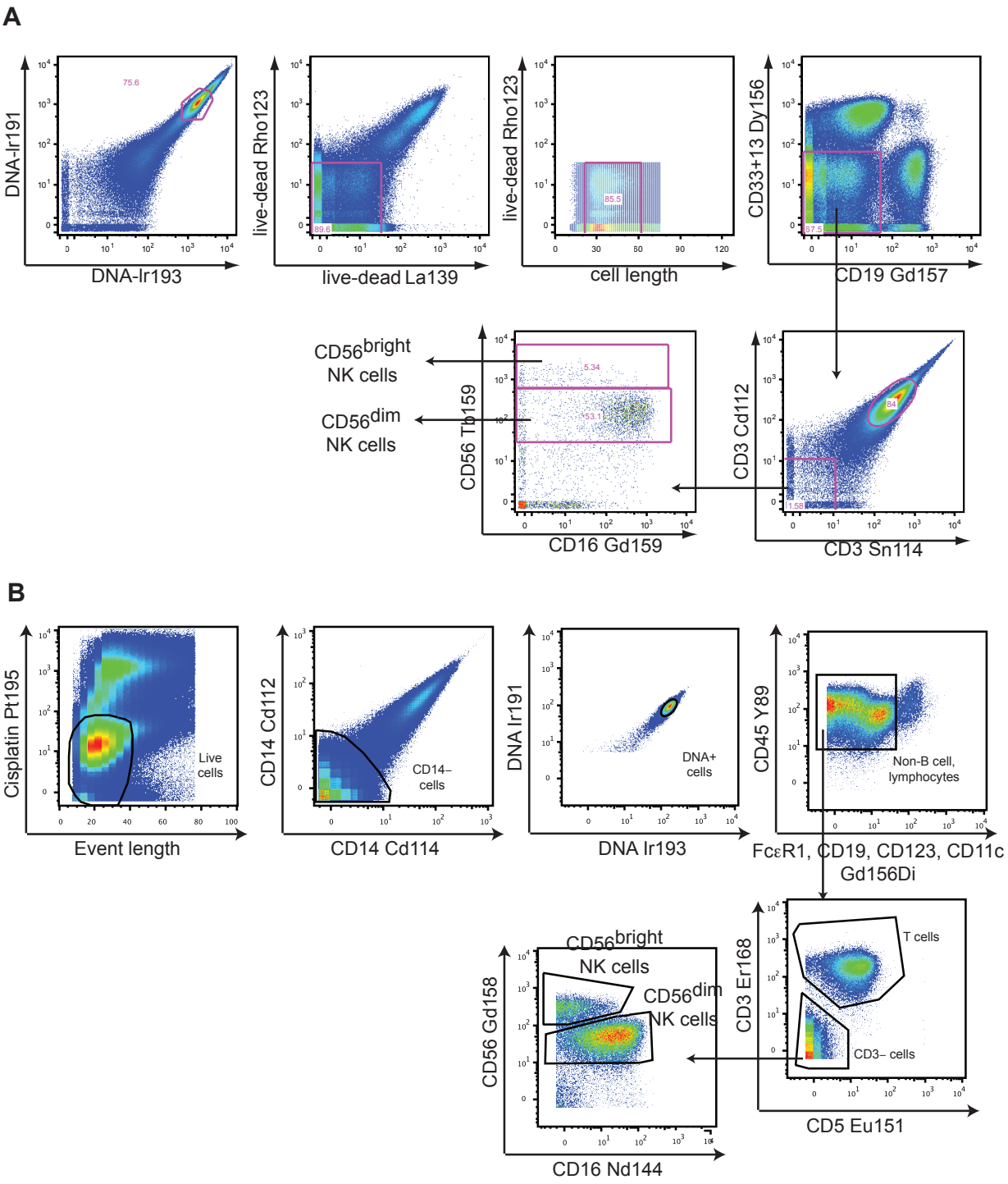


Figure 6-1. Gating strategy for identifying NK cells by mass cytometry. A) For experiments using Panel 1 (Table 6-1, Appendix Figure VI-1), single cells were identified by DNA content and cell length, live cells by exclusion of dead cells, and lymphocytes by the exclusion of CD33+CD13+ monocytes. CD19+ B cells were further excluded from the analysis. NK cells were gated as CD3-CD56+ cells. B) For experiments using Panel 2 (Table 6-2, Figure 6-9), monocyte, B cell, and CD4+ T cell-depleted peripheral blood and cord blood samples were stimulated with IL-12+IL-18 overnight and acquired by CyTOF. Live cells were identified as Cisplatin- and DNA+ cells. Lymphocytes were further identified by the expression of CD45, and monocytes (CD14+), mast/basophils (FcεR1+), plasmacytoid DCs (CD123+), myeloid DCs (CD11c+) were excluded. B cells (CD19+) were also excluded from the analysis. NK cells were gated as CD3-CD5-CD56+ cells.

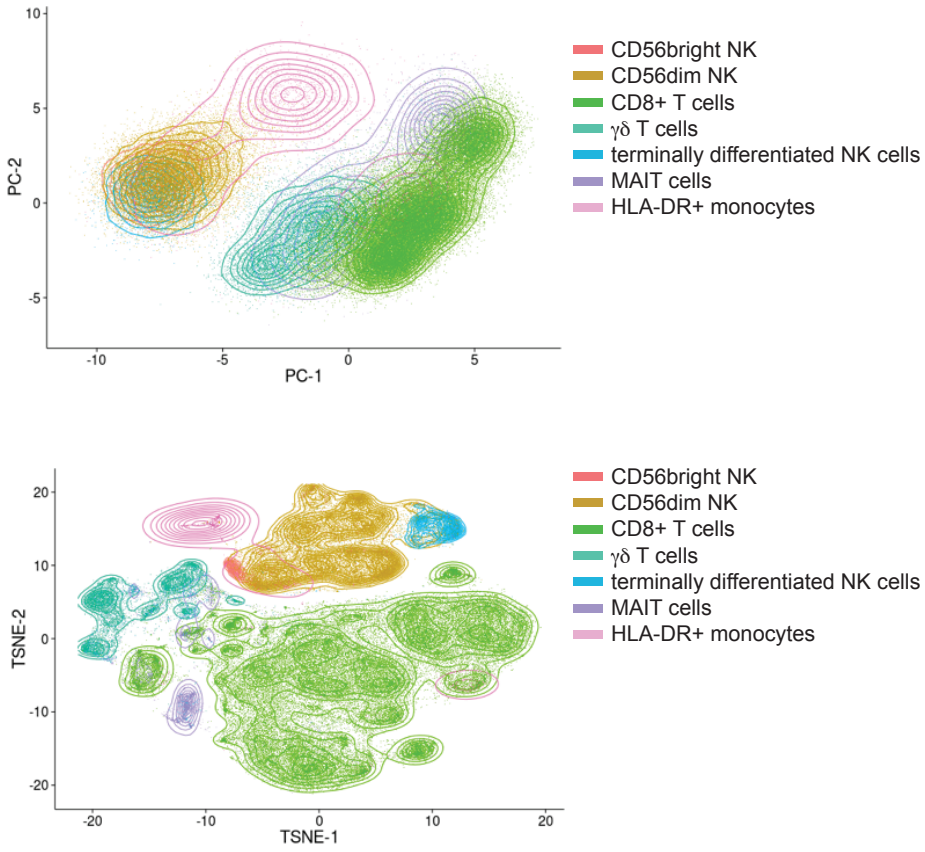
Table 6-2. CyTOF panel for experiments in Figure 6-9.

Atomic mass	Markers
103	Barcode (BC)
104	BC
105	BC
106	BC
108	BC
110	BC
113	BC
89	CD45
112/114	CD14
115	CD57
141	HLA-DR
142	NKG2D
143	IFNγ
144	CD16
145	CD69
146	CD8
147	TNFα
148	CCR4
149	CCR6
150	KLRG1
151	CD5
152	CD122
154	CXCR6
155	T-bet
156	FCεER1a, CD11c, CD19, CD123
158	CD56
159	CD161
160	NKp44
161	NKp30
162	Vα7.2
163	CD127
164	Granzyme B
165	IL-18R
166	NKp46
167	c-Kit-APC
168	CD3
169	CD25
170	NKG2C
171	CRTH2-FITC
172	CD94
173	IL-23R-biotin
174	CD160
175	Perforin
176	γδ TCR-PE
191/193	DNA
195	Cisplatin (Live/dead)

Biaxial gating was performed on FlowJo Version 10 software (Treestar). t-distributed stochastic neighbor embedding (t-SNE) analysis was either performed in Cytobank (www.cytobank.org; Cytobank Inc) or in R.

t-SNE analysis is a method that enables the visualization of high-dimensional data in low-dimensional space, while preserving the overall structure of high-dimensional data (Amir et al., 2013; Becher et al., 2014). t-SNE depicts each cell as a point in high-dimensional space, where each dimension is a parameter (e.g. expression level of one marker), and the pairwise distance between each point for each parameter is calculated. The points are then mapped into a two-dimensional map, where each cell's location in the plot is based on information from all of the original dimensions. Cells with similar phenotypes are depicted as nearby points or clusters, while dissimilar cells are depicted as distant points.

Compared to linear methods of dimensionality reduction, such as Principal Component Analysis, which mostly focuses on keeping dissimilar data points far apart, the non-linear dimensionality reduction by t-SNE is particularly important for keeping cells sharing similar phenotypes in high-dimensional space together in the resulting map. This is demonstrated by the figure below, where annotated populations are overlapping and not separated by PCA but t-SNE analysis shows good separation of annotated cells from the same sample (analysis by Jacob Hurst):



For Cytobank analysis, live, CD45+CD14−CD19−FcεR1−CD123−CD11c− cells were gated, and t-SNE analysis was performed based on the remaining parameters with proportional sampling, so that the algorithm samples from gated populations preserving their relative abundance. For further NK cell analysis, CD3−CD5−CD56+ cells were gated within these cells using Cytobank, exported and reanalyzed in Cytobank. For further analysis in R, FCS files were imported into R via the read.FCS function in the flowCore package, as described previously (Wong et al., 2015). t-SNE analysis was performed using custom R scripts using R packages that perform the Barnes-Hut implementation of t-SNE. Cells from each cluster identified by t-SNE were grouped and the median intensity values for each cluster for every marker was calculated for the generation of heatmaps.

6.4. Results

6.4.1. CD161 expression defines two distinct subsets of NK cells

NK cells were defined as CD19−CD14−CD3−CD56+ cells in this study. CD161 is expressed by the majority of peripheral blood NK cells in healthy adult donors, with a mean of 80.05 ± 2.65% of all NK cells expressing CD161 (Figure 6-2A). Analysis of CD161 expression within cord blood samples, in contrast, showed that CD161 is expressed by almost all CD56-positive NK cells, with a distinctive lack of the CD161− NK cell subset (Figure 6-2B, C). This is in line with previous reports of CD161 expression on cord blood NK cells (Bennett et al., 1996; Wang et al., 2007). In a paediatric cohort of 24 month old donors, however, the percentage of NK cells expressing CD161 was significantly reduced compared to NK cells within cord blood (Figure 6-2C). The frequency of CD161-expressing NK cells did not differ between 24 month year old donors and adult donors, suggesting that the CD161− NK cells arises from the CD161+ NK cell subset within the first two years of life. Dissection of NK cells into the $CD56^{bright}$ and $CD56^{dim}$ NK cell populations (Figure 6-2D, E) showed that there is a significant enrichment of CD161+ cells within the $CD56^{dim}$ subset, compared to the $CD56^{bright}$ NK cell subset.

6.4.2. Transcriptional analysis of CD161+ and CD161− NK cells

To further explore the CD161+ NK cell phenotype, mRNA microarray analysis was performed on FACS-sorted CD161+ and CD161− NK cell populations following the gating strategy shown in Figure 6-2A. Comparison of CD161+ to CD161− NK cells revealed a number of differentially expressed transcripts. Based on a cutoff of a 2-fold difference in transcript abundance and a p-value of less than 0.01, 776 genes were identified as differentially regulated between the two subsets, as illustrated by

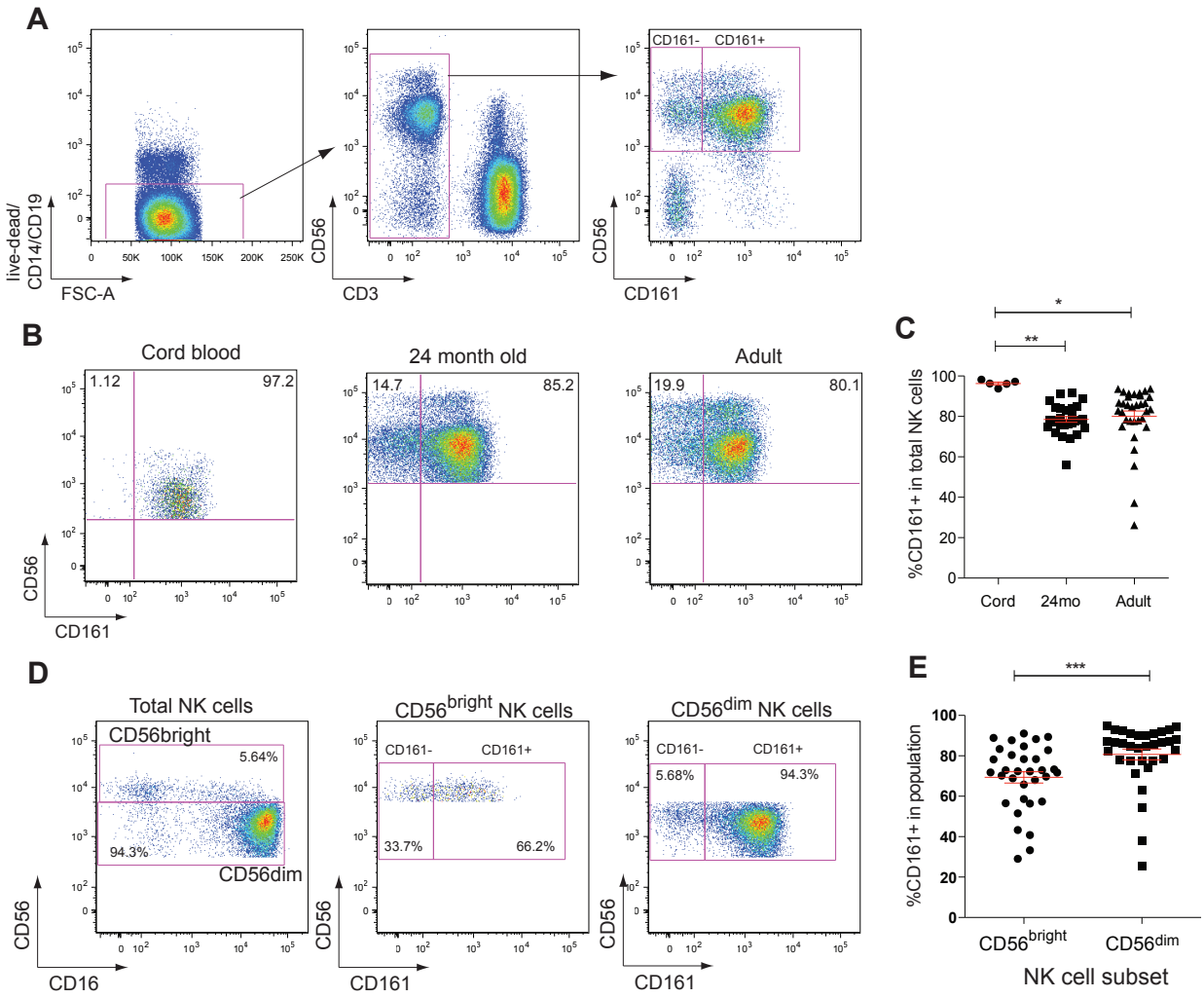


Figure 6-2. CD161 expression defines two distinct subsets of NK cells. A) Gating strategy used to identify CD161+ and CD161− NK cells. NK cells were defined as CD3−CD56+ throughout this study. B) Representative staining showing the expression of CD161 in umbilical cord blood, 24 month olds (24mo), and adult individuals on total NK cells (CD3−CD56+ cells). C) Cumulative frequencies of CD161+ NK cells in cord blood (n=5), 24 month olds (n=28), and adult individuals (n=33). **P<0.01, *P<0.05 by one-way ANOVA with Tukey's multiple comparisons test. All other comparisons were non-significant. D) Representative staining showing the expression of CD161 on $CD56^{bright}$ and $CD56^{dim}$ NK cells in adult peripheral blood. E) Cumulative frequencies of CD161+ cells within $CD56^{bright}$ and $CD56^{dim}$ NK cells. ***P<0.001 by a paired t-test (n=33).

the heatmap in Figure 6-3A (genes listed in Appendix Table VI-1). Many of the significantly expressed genes were detected at low signal intensities (Figure 6-3B). Therefore, genes that were not significantly detected in at least four samples were filtered out prior to analysis.

Within the differentially expressed genes, we identified genes associated with NK cell function. For example, the gene encoding the activating receptor CD160 was upregulated within the CD161+ subset (Figure 6-3C). CD160 elicits both cytolytic activity and cytokine secretion when triggered by engaging MHC class I molecules, such as HLA-C (Barakonyi et al., 2004; Le Bouteiller et al., 2011). Expression of this receptor was confirmed at the protein level by flow cytometry, and found to be particularly upregulated in CD161+ cells within the $CD56^{dim}$ NK cell subset. Additionally, *MKI67*, encoding Ki67, which is expressed during all active phases of the cell cycle, was also significantly upregulated within the CD161+ NK cell subset compared to the CD161− cells, and confirmed at the protein level (Figure 6-3D), suggesting that CD161 expression identifies NK cells that have recently proliferated.

Within the CD161− NK cell subset, *KLRC1*, encoding the inhibitory C-type lectin-like receptor NKG2A was upregulated and could be confirmed at the protein level (Figure 6-3E). However this association was lost upon comparison of CD161+ and CD161− NK cells within $CD56^{bright}$ and $CD56^{dim}$ NK cell populations separately, with NKG2A expressed in all $CD56^{bright}$ NK cells (Béziat et al., 2010). Although there was no significant difference between the expression of *NCAM1* (encoding CD56) by CD161+ and CD161− NK cells, as there is a slight enrichment of the $CD56^{bright}$ NK cell subset within the CD161− cells (Figure 6-2E), it cannot be ruled out that some genes found to be differentially regulated between CD161+ and CD161− NK cells may in fact reflect an enrichment of $CD56^{dim}$ cells within the CD161+ subset and the $CD56^{bright}$ cells within the CD161− subset.

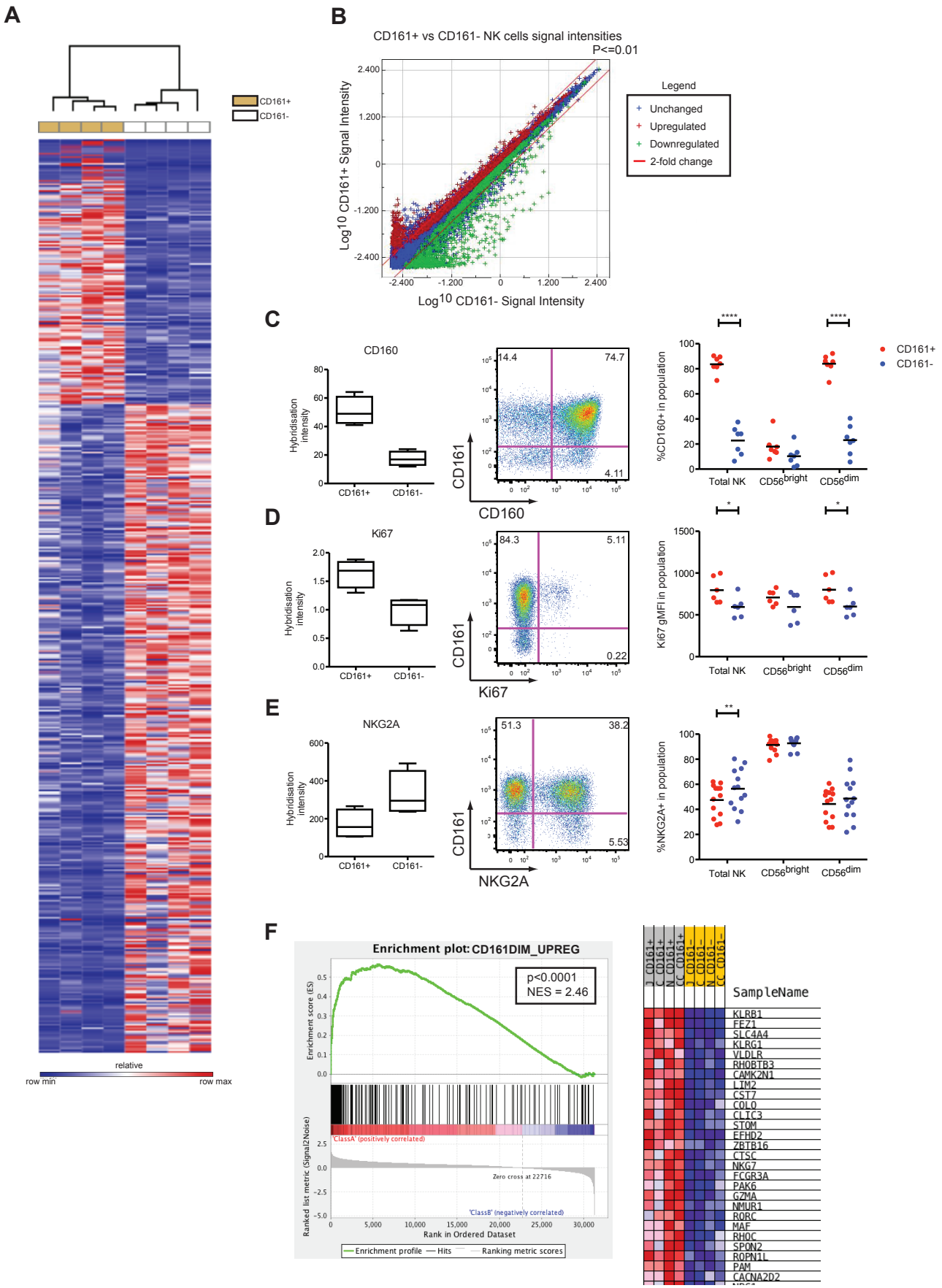

A
CD161+
CD161-
relative
row min
row max
B
CD161+ vs CD161- NK cells signal intensities
P<=0.01
Log10 CD161+ Signal Intensity
Log10 CD161- Signal Intensity
Legend
Unchanged
Upregulated
Downregulated
2-fold change
C
CD160
Hybridisation intensity
CD161+
CD161-
14.4
74.7
4.11
CD161
CD160
%CD160+ in population
Total NK
CD56bright
CD56dim
D
Ki67
84.3
5.11
0.22
Ki67
Ki67 gMFI in population
E
NKG2A
51.3
38.2
5.53
NKG2A
%NKG2A+ in population
F
Enrichment plot: CD161DIM_UPREG
p<0.0001
NES = 2.46
Enrichment score (ES)
Ranked list metric (Signal2Noise)
'ClassA' (positively correlated)
Zero cross at 22716
'ClassB' (negatively correlated)
Rank in Ordered Dataset
Enrichment profile
Hits
Ranking metric scores
SampleName
KLRB1
FEZ1
SLC4A4
KLRG1
VLDLR
RHOBTB3
CAMK2N1
LIM2
CST7
COL0
CLIC3
STOM
EFHD2
ZBTB16
CTSC
NKG7
FCGR3A
PAK6
GZMA
NMUR1
RORC
MAF
RHOC
SPON2
ROPN1L
PAM
CACNA2D2

Figure 6-3. Microarray analysis of CD161+ vs. CD161− NK cells. A) Heatmap illustrating the significantly differentially expressed transcripts between CD161+ and CD161− NK cells in 4 donors. Subsets clustered by one minus Pearson correlation by GENE-E. B) Scatter plots of signal intensities of all mRNA probes in CD161+ (y-axis) vs. CD161− (x-axis) NK cells. The signal intensities of each probe are represented by a dot and are shown in a double logarithmic scale. Red diagonal lines define the areas of 2-fold differential signal intensities. Blue cross: unchanged genes, red cross: significantly upregulated genes ($p<0.01$), green cross: significantly downregulated genes ($p<0.01$). C) Expression of CD160 by gene array (left), representative plot by flow cytometry (centre) and cumulative frequencies of CD161+ and CD161− cells expressing CD160 (right) within total NK (CD3−CD56+ cells), $CD56^{bright}$ and $CD56^{dim}$ NK cells. D) Expression of Ki67 by gene array (left), representative plot by flow cytometry (centre) and gMFI of Ki67 expressed in CD161+ and CD161− cells (right) within total, $CD56^{bright}$, and $CD56^{dim}$NK cells. E) Expression of NKG2A by microarray (left), representative plot by flow cytometry (centre) and cumulative frequencies of CD161+ and CD161− cells expressing NKG2A (right) within total, $CD56^{bright}$, and $CD56^{dim}$ NK cells. For C-E) ****$P<0.0001$, **$P<0.01$, *$P<0.05$ by repeated measures two-way ANOVA with Bonferroni's multiple comparisons test, comparing CD161+ cells to CD161− cells within each population of NK cells. n=7 for CD160, n=6 for Ki67, and n=13 for NKG2A for the analysis of each marker by flow cytometry. F) Gene set enrichment analysis (GSEA) summary plots for CD161+ vs. CD161− NK cell ranked genes, and CD161+(dim) CD8+ T cell upregulated gene set. Normalised enrichment score (NES) = 2.46, $p<0.0001$, and heatmap showing the expression level of genes enriched in CD161+ NK cells (red = positively correlated, blue =negatively correlated).

Finally, as CD161 expression on T cells identifies cells that share a core transcriptional signature, regardless of TCR usage (Fergusson et al., 2014), it was investigated whether genes upregulated within CD161+ NK cells were also shared with CD161-expressing T cells. For this, the whole microarray data was analysed using GSEA (Subramanian et al., 2005), which orders the genes into a ranked list according to their differential expression between CD161+ and CD161− NK cells, and can identify whether sets of genes upregulated in CD161-expressing T cells are enriched within a particular location of the NK cell ranked list. In contrast to CD161-expressing T cells (Fergusson et al., 2014), there was no significant enrichment of genes upregulated in CD161++CD8+ T cells within CD161+ NK cells (data not shown). However, a significant enrichment of genes upregulated in CD161+ (dim) CD8+ T cells in comparison to CD161− CD8+ T cells was found within CD161+ NK cells (Normalised Enrichment Score (NES) = 2.46, $P<0.0001$) (Figure 6-3F). These

genes included *ZBTB16,* which encodes the transcription factor PLZF, and suggests that CD161+ NK cells and CD161+ CD8+ T cells share a transcriptional signature, but not CD161+ NK cells and CD161++CD8+ T cells.

6.4.3. CD161+ NK cells are phenotypically immature compared to CD161− NK cells

Given that CD161− NK cells appear postnatally, we tested the hypothesis that CD161+ NK cells represent a more immature subset compared to CD161− NK cells, which would therefore display a more differentiated phenotype. In order to account for an enrichment of $CD56^{bright}$ or $CD56^{dim}$ NK cells in either population, the CD161+ and CD161− NK cells within all populations - total NK cells, $CD56^{bright}$ NK cells, and $CD56^{dim}$ NK cells - were analysed.

The expression of the terminal differentiation marker CD57 on CD161+ and CD161− NK cells varied between donors and there was no significant difference between the two CD161 subsets (Figure 6-4A). CD16 is another marker exclusively expressed in the mature $CD56^{dim}$ NK cell population and upon binding of the fragment crystallisable (Fc) region of IgG antibodies coating an infected cell, NK cells can release granzymes and perforin to induce apoptosis. CD16 expression was significantly enriched within the CD161− $CD56^{bright}$ NK cells ($P<0.0001$), suggesting that the CD161− $CD56^{bright}$ NK cells may be more mature than CD161+ $CD56^{bright}$ NK cells. The contrary was found in the $CD56^{dim}$ NK cell population, although both subsets expressed high levels of CD16 (Figure 6-4B).

Next, the expression of NKp30 and NKp46 was compared between CD161+ and CD161− NK cells. These activating receptors can bind viral and tumour proteins

(Mandelboim et al., 2001; Poggi et al., 2005) and are downregulated in mature NK cells (Björkström et al., 2010), with NKp46 particularly enriched within immature $CD56^{bright}$ NK cells (Krämer et al., 2012). Expression of both NKp30 and NKp46 was found to be significantly enriched within CD161+ NK cells, particularly in the $CD56^{dim}$ NK cells for NKp30 (Figure 6-4C) and in both $CD56^{bright}$ and $CD56^{dim}$ NK cells for NKp46 (Figure 6-4D), supporting the notion that CD161+ NK cells are less mature than their CD161− counterparts. CD161+ NK cells were also enriched for the expression of the activating receptor NKp80 (Vitale et al., 2001) within the $CD56^{dim}$ NK cell population (Figure 6-4E).

The inhibitory C-type lectin-like receptor KLRG1 decreases with age (Hayhoe et al., 2010) and maturation of human NK cells (Bigley et al., 2012; Lopez-Vergès et al., 2010). KLRG1 expression was slightly enriched within the CD161+ NK cell subset (Figure 6-4F), consistent with a less mature phenotype. Additionally, the expression of the activation marker CD69 was significantly higher in the CD161+ $CD56^{dim}$ NK cell subset (Figure 6-4G), indicating that a fraction of this subset is constitutively activated in the periphery.

The expression of inhibitory receptors which recognize MHC class I molecules on the surface of their target cells, such as CD94/NKG2 heterodimeric receptors and KIR receptors, was also examined (Moesta & Parham, 2012). There was no difference in the expression of CD94 between CD161+ and CD161− NK cells (Figure 6-4H), in a similar manner to NKG2A (Figure 6-3E), even though both have been associated with immature NK cells (Béziat et al., 2010; Yu et al., 2010). Interestingly, however, KIR3DL1/S1 (CD158e), the inhibitory isoform of which recognizes the HLA-Bw4 motif on target cells (Song et al., 2014), was slightly enriched within the CD161− NK cell population (Figure 6-4I). CD85j is another inhibitory receptor of the immunoglobulin-like receptor superfamily, which recognises both classical and non-classical MHC

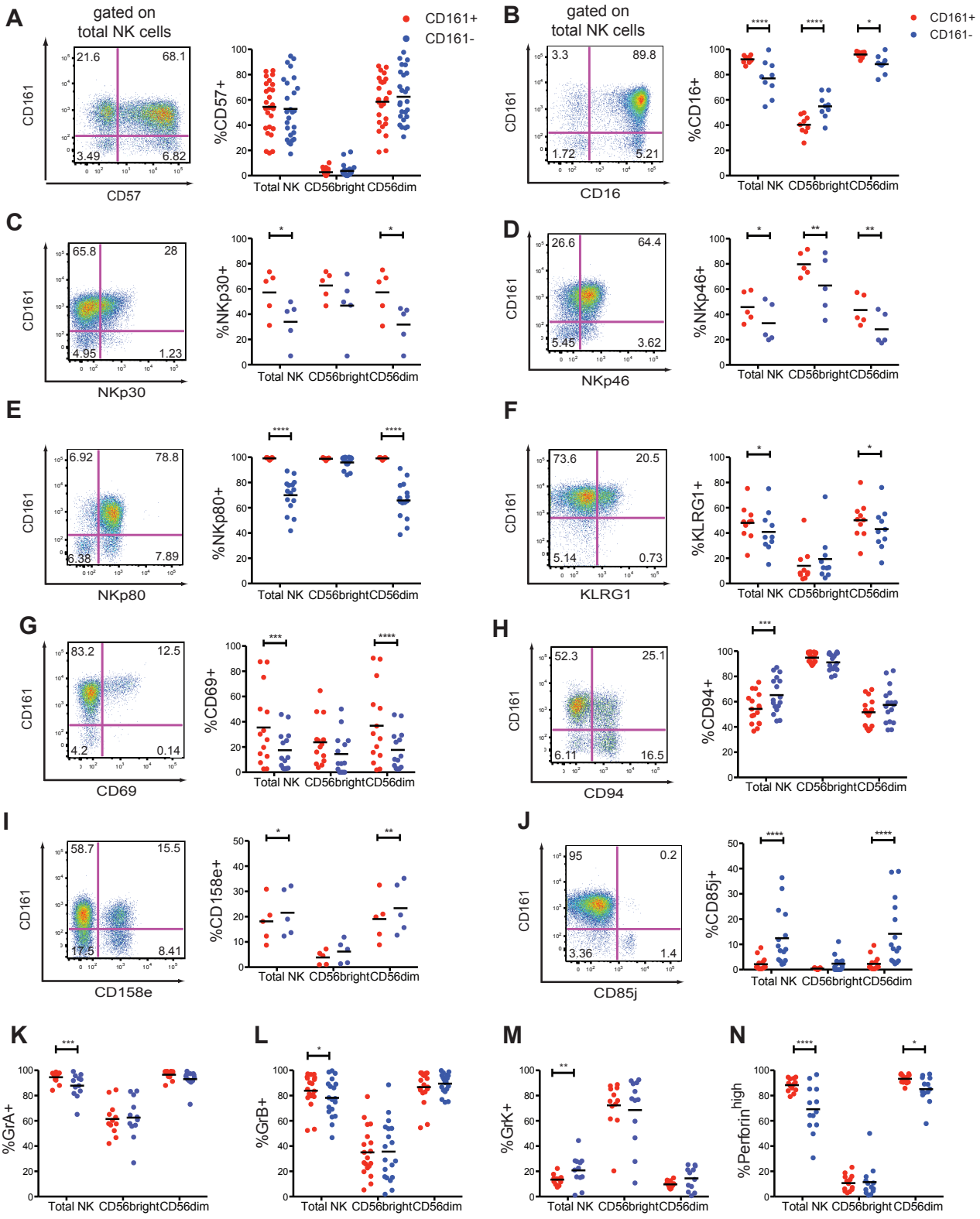

A
gated on
total NK cells
CD161
CD57
21.6
68.1
3.49
6.82
%CD57+
Total NK
CD56bright
CD56dim
CD161+
CD161-
B
gated on
total NK cells
CD16
3.3
89.8
1.72
5.21
%CD16+
C
NKp30
65.8
28
4.95
1.23
%NKp30+
D
NKp46
26.6
64.4
5.45
3.62
%NKp46+
E
NKp80
6.92
78.8
6.38
7.89
%NKp80+
F
KLRG1
73.6
20.5
5.14
0.73
%KLRG1+
G
CD69
83.2
12.5
4.2
0.14
%CD69+
H
CD94
52.3
25.1
6.11
16.5
%CD94+
I
CD158e
58.7
15.5
17.5
8.41
%CD158e+
J
CD85j
95
0.2
3.36
1.4
%CD85j+
K
%GrA+
L
%GrB+
M
%GrK+
N
%Perforin^high

Figure 6-4. CD161+ NK cells are phenotypically immature compared to CD161- NK cells. CD161+ and CD161− NK cells from adult peripheral blood were assessed for the expression of different markers. Representative plots, gated on total NK cells (CD3−CD56+) (left), and frequencies of receptor-positive cells within the CD161+ and CD161− fractions of indicated NK cell populations (right) are shown for 5-26 healthy donors. Expression of A) CD57 (n=26), B) CD16 (n=9), C) NKp30 (n=5), D) NKp46 (n=5), E) NKp80 (n=15), F) KLRG1 (n=10), G) CD69 (n=14), H) CD94 (n=17), I) CD158e (n=5), J) CD85j (n=15) is shown. ****P<0.0001, ***P<0.001, **P<0.01, *P<0.05 by repeated measures two-way ANOVA with Bonferroni's multiple comparisons test, comparing CD161+ cells to CD161− cells within each population of NK cells. All other comparisons were non-significant. K-N) Expression of cytotoxic effector molecules in CD161+ and CD161− NK cells. Cumulative frequencies of indicated population of NK cells expressing K) Granzyme A (GrA) (n=12), L) GrB (n=19), M) GrK (n=12), and N) Perforin at a high level (perforin^{high}) (n=13) are shown. In all graphs, CD161+ cells are shown in red, CD161− cells are shown in blue. ****P<0.0001, ***P<0.001, **P<0.01, *P<0.05 by repeated measures two-way ANOVA with Bonferroni's multiple comparisons test, comparing CD161+ cells to CD161− cells within each population of NK cells.

class I molecules (Navarro et al., 1999). Expression of CD85j was almost exclusive to CD161− NK cells within the CD56^{dim} NK population (Figure 6-4J). As KIR and CD85j expression is associated with NK cell maturation (Björkström et al., 2010; Lopez-Vergès et al., 2010), these results support the hypothesis that CD161− NK cells are more mature compared to CD161+ NK cells.

Lastly, although cytotoxic capacity is thought to increase with NK cell maturation (Lopez-Vergès et al., 2010), there was no significant difference in the expression of GrA, GrB, or GrK (Figure 6-4K-N) between CD161+ and CD161− within either NK cell subsets, CD56^{bright} or CD56^{dim}. All NK cells expressed the cytotoxic effector molecule perforin, but CD56^{dim} NK cells were particularly enriched for perforin^{high} cells. These perforin^{high} cells were slightly enriched in the CD161+ CD56^{dim} NK cells compared to their CD161− counterparts, although perforin was expressed at high levels by both subsets regardless of CD161 expression (Figure 6-4N).

All together, these results suggest that CD161− NK cells are enriched for a more differentiated phenotype compared to CD161+ NK cells, particularly within $CD56^{dim}$ NK cells.

6.4.4. CD161+ NK cells are high proliferative compared to CD161− NK cells

The proliferative capacity of NK cells is thought to decrease during maturation, as $CD56^{bright}$ NK cells exhibit a higher capacity to proliferate after cytokine stimulation compared to $CD56^{dim}$ NK cells (Caligiuri et al., 1990; Vitale et al., 2004). CD161+ NK cells had a significantly higher expression of Ki67 (Figure 6-3D), and the more mature CD161− NK cells may be expected to be hypoproliferative. To assess the proliferative capacity of CD161-expressing NK cells, PBMCs were stained with CTV and stimulated with different combinations of cytokines or PHA for 5 days. Strikingly, CD161+ NK cells divided more extensively than CD161− NK cells, evidenced by the significantly greater dilution of CTV when stimulated with IL-2 or IL-15, either alone, together, or combined with IL-12, as well as PHA (Figure 6-5A, B). However there was no significant difference in the expression of CD69 in response to IL-2, IL-15, or PHA, suggesting that the reduced proliferation in CD161− NK cells is not due to their inability to respond to the cytokines. In all other conditions, expression of the activation marker CD69 was consistently higher in the CD161+ NK cell subset, reaching significance for all conditions with IL-12 or IL-15 (Figure 6-5C). Furthermore, there was no significant difference in phosphatidylserine staining, a marker of apoptosis, between CD161+ and CD161− NK cells after culture with IL-2 or IL-15 (Figure 6-5D), suggesting that the lower proliferative response of the CD161− NK cells in response to IL-2 and IL-15 was not due to higher rates of AICD in the CD161− NK cell subset. The higher proliferation observed from CD161+ NK cells

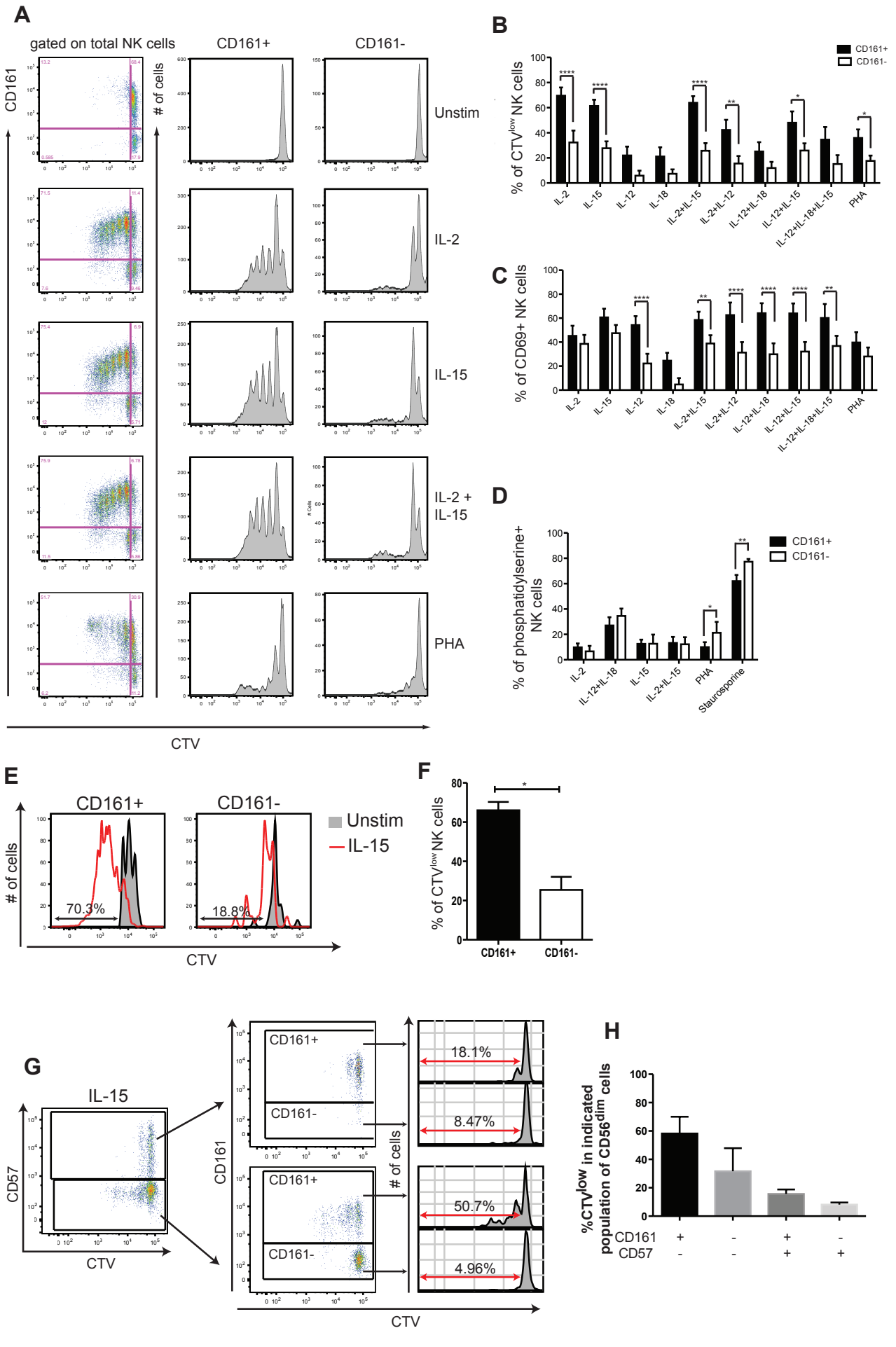

A
gated on total NK cells
CD161+
CD161-
CD161
# of cells
Unstim
IL-2
IL-15
IL-2 +
IL-15
PHA
CTV
B
CD161+
CD161-
% of CTV^low NK cells
IL-2
IL-15
IL-12
IL-18
IL-2+IL-15
IL-2+IL-12
IL-12+IL-18
IL-12+IL-15
IL-12+IL-18+IL-15
PHA
C
% of CD69+ NK cells
D
% of phosphatidylserine+ NK cells
IL-12+IL-18
Staurosporine
E
Unstim
IL-15
70.3%
18.8%
F
G
CD57
CD161+
CD161-
18.1%
8.47%
50.7%
4.96%
H
%CTV^low in indicated population of CD56^dim cells

Figure 6-5. CD161+ NK cells have a greater proliferative capacity than CD161− NK cells. PBMCs from healthy donors were CTV-labeled and cultured for 5 days with the indicated stimuli. A) Representative staining of CTV for CD161+ and CD161− NK cells from one healthy donor. B-C) Frequency of CD161+ and CD161− NK cells either (B) diluting CTV, or (C) expressing CD69, after simulation with the indicated combinations of cytokines and PHA (n=14). Graphs show frequencies of CTV^{low} and CD69+ cells following background subtraction. ****P<0.0001, **P<0.01, *P<0.05 by repeated measures two-way ANOVA, with Bonferroni's multiple comparisons test, comparing CD161+ and CD161− NK cells. D) Frequency of CD161+ and CD161− NK cells expressing phosphatidylserine after 5 days culture with the indicated stimuli (n=4). **P<0.01, *P<0.05 by repeated measures two-way ANOVA with Bonferroni's multiple comparisons test. All other comparisons were non-significant. E-F) CTV-labeled FACS-sorted CD161+ and CD161− NK cells were stimulated with IL-15 for 5 days or left unstimulated, and the frequency of cells diluting CTV (CTV^{low}) was analysed (n=3). *P<0.05 by paired t-test. E) Representative staining and F) cumulative data is shown. G) Representative staining for CTV on CD57+ and CD57− NK cells, according to CD161 expression. H) Frequency of cells diluting CTV on indicated $CD56^{dim}$ NK cell subsets stimulated with IL-15, according to CD161 and CD57 expression. (n=3). $CD56^{bright}$ NK cells were excluded as they do not express CD57.

was also confirmed using FACS-sorted CD161+ and CD161− NK cells (Figure 6-5E, F). Together, these results suggest that CD161+ NK cells have a greater proliferative capacity compared to CD161− NK cells.

CD57 expression on NK cells (Björkström et al., 2010; Lopez-Vergès et al., 2010) and CD8+ T cells (Brenchley et al., 2003) has been demonstrated to identify cells with low proliferative capacity. Analysis of CD161 and CD57 expression on NK cells proliferating following IL-15 stimulation for 5 days, however, showed that within both CD57− and CD57+ populations, the CD161+ NK cells showed greater dilution of the CTV dye (Figure 6-5G). Although these results did not reach significance due to low numbers of samples and need to be repeated (Figure 6-5H), as the frequency of CD57 expressing cells does not differ between CD161+ and CD161− NK cells (Figure 6-4A), this shows that CD161 expression correlates with the proliferative capacity of NK cells.

6.4.5. CD161+ CD56^{dim} NK cells are highly responsive to cytokines IL-12+IL-18

A key functional characteristic of NK cells is their ability to recognize and kill target cells that have lost their expression of MHC class I molecules. Therefore, differences in target cell recognition between CD161+ and CD161− NK cells were investigated. NK cells were cultured with MHC-class I deficient K562 target cell lines, and IFNγ secretion, as well as degranulation based on CD107a expression, was compared based on CD161 expression (Figure 6-6A, B). Although the frequency of NK cells expressing IFNγ and CD107a in response to K562 cells were comparable to previous publications (Anfossi et al., 2006; Björkström et al., 2010), there was no difference in the frequency of CD161+ and CD161− cells degranulating in either CD56^{bright} or CD56^{dim} NK cell populations. Furthermore, assaying the simultaneous production of IFNγ, TNFα, GM-CSF, MIP-1β, and CD107α expression across PMA/ionomycin-stimulated NK cells by mass cytometry (cytometry by time-of-flight (CyTOF)) did not reveal any significant difference in the ability of CD161+ and CD161− NK cells to degranulate or produce cytokines (Appendix Figure VI-1).

CD56^{bright} NK cells are characterized by their greater ability to secrete cytokines after stimulation in response to innate cytokines such as IL-12 and IL-18, which is lost from CD56^{dim} NK cells as they differentiate (Björkström et al., 2010; Lopez-Vergès et al., 2010). Interestingly, CD161 expression on T cells was recently shown to identify cells with the ability to respond to IL-12 and IL-18 in a TCR-independent, “NK-like” manner (Fergusson et al., 2014). Therefore, to ask whether this functional correlate with CD161 existed in NK cells, IFNγ production in response to overnight stimulation with IL-12+IL-18 was assayed in CD161+ and CD161− NK cells. This showed that although the majority of CD56^{bright} NK cells secreted IFNγ regardless of CD161

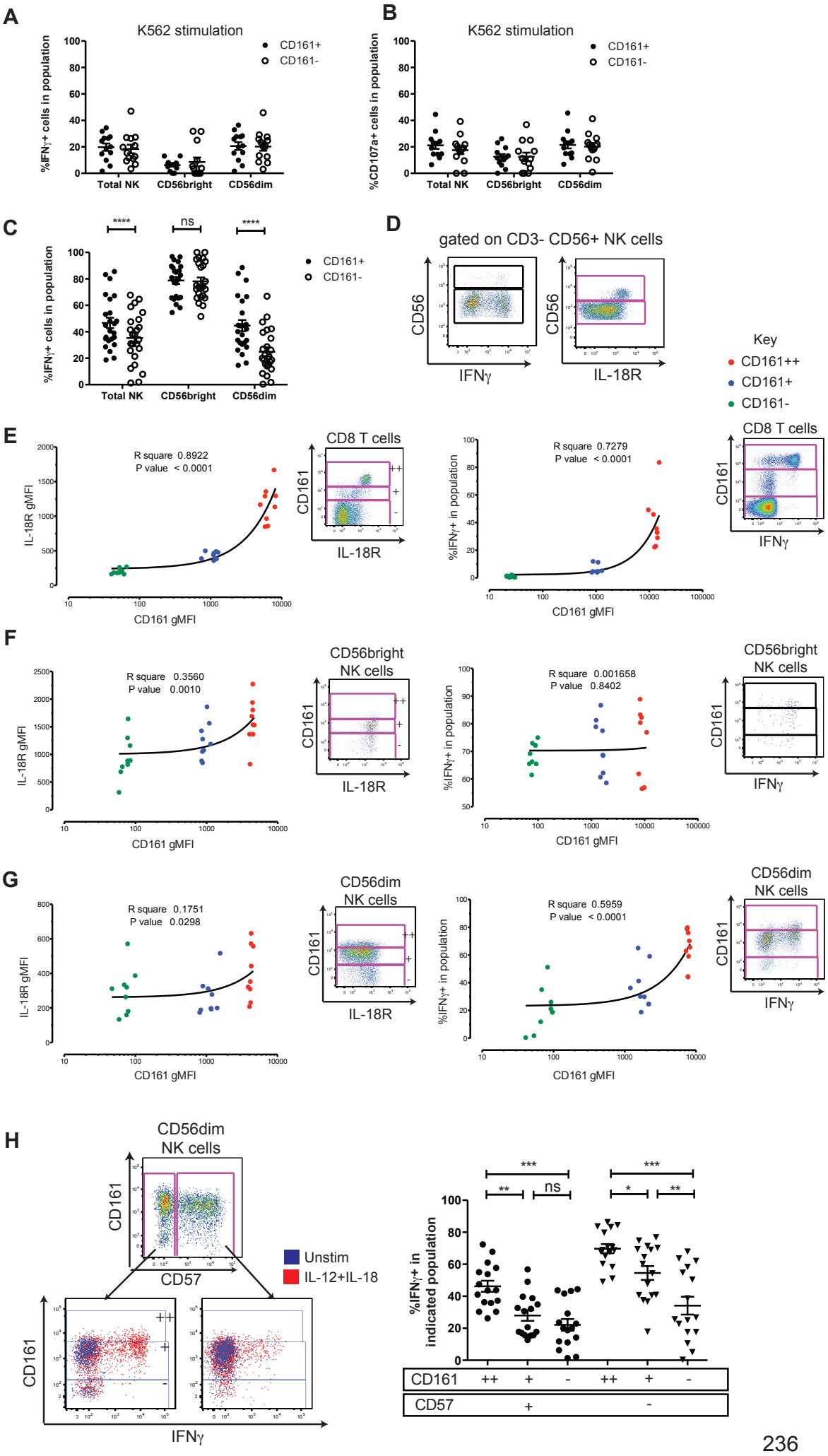

A
K562 stimulation
%IFNγ+ cells in population
CD161+
CD161-
Total NK
CD56bright
CD56dim
B
K562 stimulation
%CD107a+ cells in population
C
%IFNγ+ cells in population
****
ns
****
D
gated on CD3- CD56+ NK cells
CD56
IFNγ
IL-18R
Key
CD161++
CD161+
CD161-
E
R square 0.8922
P value < 0.0001
IL-18R gMFI
CD161 gMFI
CD8 T cells
CD161
IL-18R
R square 0.7279
P value < 0.0001
%IFNγ+ in population
IFNγ
F
R square 0.3560
P value 0.0010
CD56bright NK cells
R square 0.001658
P value 0.8402
G
R square 0.1751
P value 0.0298
CD56dim NK cells
R square 0.5959
P value < 0.0001
H
CD56dim NK cells
CD57
Unstim
IL-12+IL-18
%IFNγ+ in indicated population
***
**
ns
*
CD161 ++ + - ++ + -
CD57 + -

Figure 6-6. CD161 expression correlates with increased responsiveness to IL-12+IL-18 stimulation within CD56^{dim} NK cells. A-B) IFNγ production A) and CD107a mobilization B) by CD161+ and CD161− NK cells in response to K562 stimulation for 6 hours is shown. The comparisons between CD161+ and CD161− NK cells were non-significant by repeated measures two-way ANOVA with a Bonferroni's multiple comparisons test. N=13. C) IFNγ production by CD161+ and CD161− NK cells in response to overnight IL-12+IL-18 stimulation is shown. ****P<0.0001 by repeated measures two-way ANOVA with a Bonferroni's multiple comparisons test. N=24. D) Representative staining for IFNγ production in response to IL-12+IL-18 (left), and IL-18R expression (right) gated on all CD3-CD56+ NK cells. E-G) gMFI of CD161 for CD161++ (red), CD161+ (blue), and CD161− (green) subsets in CD8+ T cells (E), CD56^{bright} NK cells (F), or CD56^{dim} NK cells (G), correlated with gMFI of IL-18R within corresponding subsets (left) or IFNγ expression in response to overnight stimulation with IL-12+IL-18. (n=9). For all populations, representative staining showing IL-18R and IFNγ expression on indicated cells from the same donor, and gating of CD161++, CD161+ and CD161− subsets based on CD8+ T cells, are shown. H) Representative staining showing IFNγ production in response to IL-12+IL-18 from CD57+ and CD57− cells within the CD56^{dim} NK cell population (left). CD161++, CD161+, and CD161− subsets were gated within CD57+ and CD57− NK cells as indicated, and the frequency of IFNγ+ cells in each population was graphed (right). ***P<0.001, **P<0.01, *P<0.05, or non-significant (ns) by repeated measures one-way ANOVA with Bonferroni's multiple comparisons test. Results are shown for comparisons between CD161++, CD161+ and CD161− subsets within CD57+ and CD57− NK cells.

expression, a consistently higher frequency of CD161-expressing CD56^{dim} NK cells produced IFNγ compared to their CD161− NK cell counterparts (P<0.0001) (Figure 6-6C, D). The ability of all CD56^{bright} NK cells to respond to IL-12+IL-18 was associated with their uniformly high expression of IL-18R (Figure 6-6D).

Within T cells, CD161 expression correlates with their expression of IL-18R at the protein level, which confers their responsiveness to IL-12 and IL-18 stimulation (Fergusson et al., 2014). Thus gating on CD161++, CD161+, and CD161− cell subsets in CD8+ T cells and plotting the expression levels of IL-18R at the population level (taken as gMFI) in relation to that of CD161 expression shows a highly significant correlation (P<0.0001) between the levels of CD161 expressed and the expression of IL-18R (R=0.892) in CD8+ T cells (Figure 6-6E), confirming previous reports (Fergusson et al., 2014). Furthermore, overnight stimulation of CD8+ T cells with IL-12+IL-18 leads to IFNγ production from these cells, the frequency of which

correlates with the level of CD161 expressed (Figure 6-6E). Gating on corresponding CD161++, CD161+, and CD161− cells in NK cells also showed a weak but significant correlation between CD161 and IL-18R expression in $CD56^{bright}$ (Figure 6-6F) and $CD56^{dim}$ NK cells (Figure 6-6G), although the correlation coefficient (R=0.356 for $CD56^{bright}$, R=0.175 for $CD56^{dim}$) was very low in contrast to that seen in CD8+ T cells (R=0.892). The IFNγ response to IL-12 and IL-18 within the $CD56^{dim}$ cells, however, strongly correlated with CD161 expression (R=0.5959, P<0.0001), in a similar manner to CD8+ T cells (Figure 6-6G). There was no correlation between IFNγ production and CD161 expression levels in $CD56^{bright}$ NK cells (Figure 6-6F). These results suggest that CD161 expression marks $CD56^{dim}$ cells, but not $CD56^{bright}$ NK cells, with an increased ability to respond to IL-12 and IL-18, which is shared with CD161-expressing T cells.

CD57 expression has been shown to be a major determinant in the responsiveness of $CD56^{dim}$ NK cells to IL-12 and IL-18 (Lopez-Vergès et al., 2010), independent of other markers of differentiation or KIR expression (Björkström et al., 2010). However, gating on CD161++, CD161+, and CD161− subsets within $CD56^{dim}$ NK cells showed that the frequency of IFNγ+ cells clearly increased with increasing CD161 expression within both CD57+ and CD57− $CD56^{dim}$ NK cells, confirming that CD161 expression correlates with IL-12 and IL-18 responsiveness, independently of CD57 (Figure 6-6H).

6.4.6. Terminally differentiated NK cells expanded in CMV+ individuals are low in CD161 and PLZF expression

Previous analysis has shown that CD161− NK cells exhibit a more functionally mature phenotype compared to their CD161+ counterparts. CMV infection has been demonstrated to accelerate the differentiation of NK cells, leading to the persistence

of terminally differentiated NK cells expressing the activating heterodimer NKG2C/CD94 and CD57 (Foley et al., 2012a; Lopez-Vergès et al., 2011). Previous studies examining CD161 expression on these NKG2C+CD57++ NK cells have reported varied results, with some reporting no significant difference (Achour et al., 2014; Gumá et al., 2004; Noyola et al., 2012), while a significant downregulation of CD161 has been shown in CMV-seropositive HCV/HBV patients and Chikungunya virus infected patients (Béziat et al., 2012; Petitdemange et al., 2011).

In order to investigate whether terminal differentiation induced by CMV infection may affect the expression of CD161 on NK cells, PBMCs were incubated with CMV lysate overnight to identify individuals with CMV-specific memory T cells, and the frequency and phenotype of NK cells within these patients was examined (Figure 6-7A). Individuals with memory CD4+ T cells that responded to the CMV-lysate had a significantly greater frequency of CD161− cells within their $CD56^{dim}$ NK cell population (Figure 6-7B), but not $CD56^{bright}$ NK cells (data not shown). Furthermore, CD57 (Figure 6-7C) and NKG2C (Figure 6-7D, E) expression on these CD161− NK cells was significantly higher in CMV+ donors but not in CMV− donors, suggesting that there is an enrichment of cells expressing NKG2C and CD57 within the CD161- population. Indeed, NKG2C+CD57++ cells were found exclusively in CMV+ donors (although not reaching statistical significance due to high donor variability) (Figure 6-7F, G), and there was a significantly lower expression of CD161 on these terminally differentiated NKG2C+CD57++ NK cells ($P<0.0001$) in CMV+ donors (Figure 6-7H).

We next wanted to probe the mechanism involved in CD161 downregulation in CMV+ donors. CD161 expression has been previously associated with the transcription factor PLZF. For instance, a PLZF-deficient patient had reduced CD161 expression on NK cells (Eidson et al., 2011). Furthermore, *ZBTB16* expression, encoding PLZF, is upregulated within most CD161+ T cells, including MAIT cells

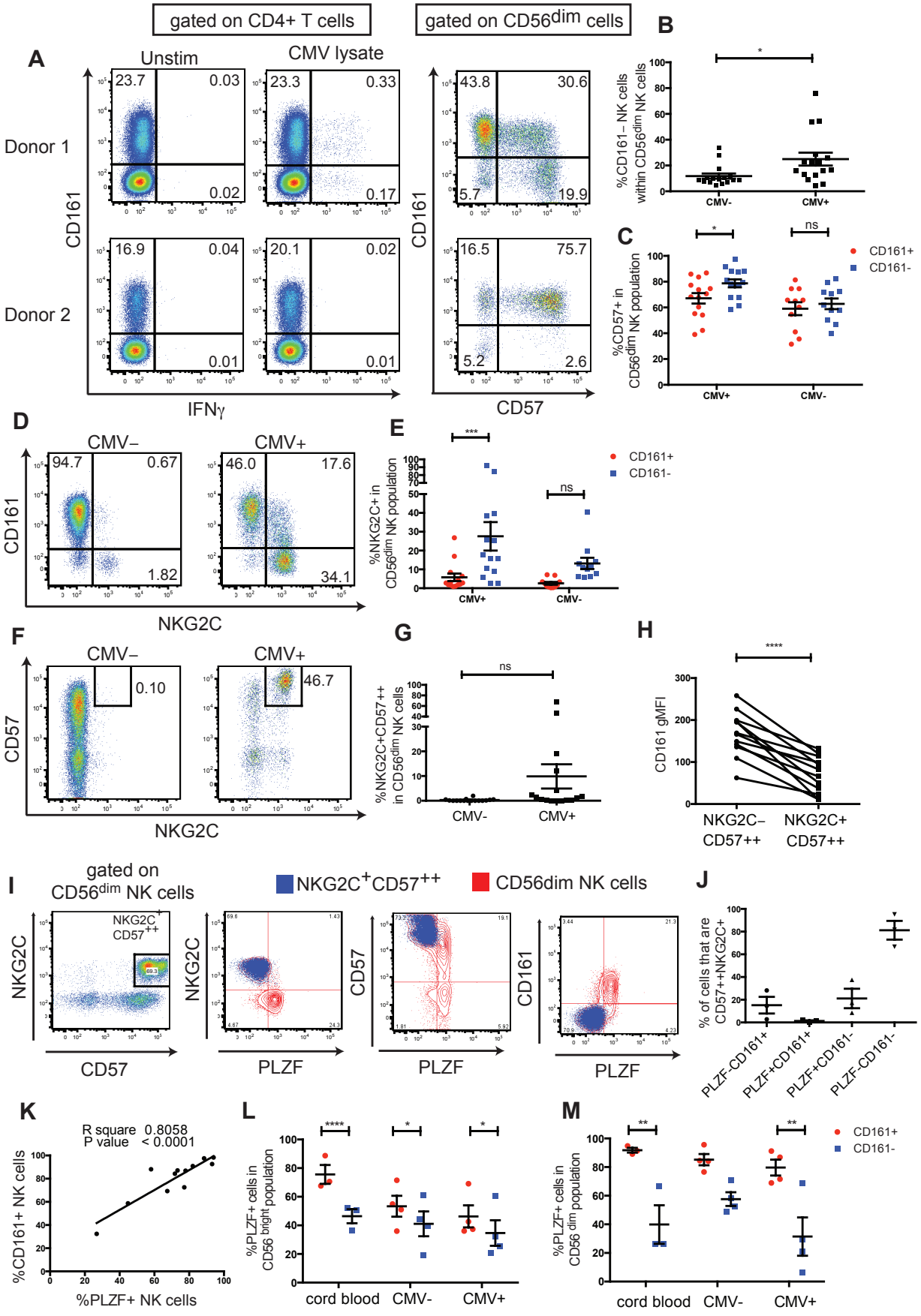

gated on CD4+ T cells
gated on CD56dim cells
A
Unstim
CMV lysate
Donor 1
Donor 2
CD161
IFNγ
CD57
23.7
0.03
0.02
23.3
0.33
0.17
43.8
30.6
5.7
19.9
16.9
0.04
0.01
20.1
0.02
0.01
16.5
75.7
5.2
2.6
B
%CD161− NK cells within CD56dim NK cells
CMV-
CMV+
C
%CD57+ in CD56dim NK population
CD161+
CD161-
ns
D
CMV−
CMV+
NKG2C
94.7
0.67
1.82
46.0
17.6
34.1
E
%NKG2C+ in CD56dim NK population
***
F
0.10
46.7
G
%NKG2C+CD57++ in CD56dim NK cells
H
CD161 gMFI
****
NKG2C− CD57++
NKG2C+ CD57++
I
gated on CD56dim NK cells
NKG2C+CD57++
CD56dim NK cells
NKG2C+ CD57++
PLZF
J
% of cells that are CD57++NKG2C+
PLZF-CD161+
PLZF+CD161+
PLZF+CD161-
PLZF-CD161-
K
R square 0.8058
P value < 0.0001
%CD161+ NK cells
%PLZF+ NK cells
L
%PLZF+ cells in CD56 bright population
cord blood
CMV-
CMV+
M
%PLZF+ cells in CD56 dim population

Figure 6-7. Terminally differentiated NK cells expanded in CMV+ individuals are low in CD161 and PLZF expression. A) Representative staining showing IFNγ production from CD4+ T cells in response to stimulation with CMV lysate, and the expression of CD161 and CD57 on $CD56^{dim}$ NK cells from the same donors. B) Cumulative frequencies of CD161− NK cells within the $CD56^{dim}$ NK cell population within CMV+ (n=16) and CMV− (n=16) individuals. *P<0.05 by an unpaired t-test. Data combined from four independent experiments. C-E) Expression of NKG2C and CD57 on CD161+ and CD161- NK cells, according to CMV status. Cumulative frequencies of C) CD57+ cells or D, E) NKG2C+ cells in indicated population of $CD56^{dim}$ NK cells is shown. N= 14 for CMV+, n=11 for CMV− individuals. ***P<0.0001, *P<0.05 by repeated measures two-way ANOVA with Bonferroni's multiple comparisons test. F-G) Representative staining (F) showing NKG2C and CD57 expression on $CD56^{dim}$ NK cells in CMV− and CMV+ individuals, and the cumulative frequencies (G) of NKG2C+CD57++ cells within $CD56^{dim}$ NK cells in CMV+ and CMV− individuals.(n=16). H) gMFI of CD161 on CD57++NKG2C+ and CD57++NKG2C− cells in CMV+ individuals (n=12). ****P<0.0001 by paired t-test. I) Representative staining showing PLZF, CD161, NKG2C and CD57 expression on $CD56^{dim}$ NK cells from a CMV+ individual. NKG2C+CD57++ NK cells are shown in blue, while bulk $CD56^{dim}$ NK cells are shown in red. J) Enrichment of NKG2C+CD57++ cells in $CD56^{dim}$ NK cells from CMV+ donors within the PLZF−CD161− double-negative population (n=3). K-M) PLZF and CD161 expression on NK cells from cord blood (n=3), CMV+ (n=4) and CMV− (n=4) adults. K) Frequency of total NK cells expressing CD161, correlated with the frequency of cells expressing PLZF. L-M) Cumulative frequency of CD161+ and CD161− $CD56^{bright}$ (L) or $CD56^{dim}$ (M) NK cells expressing PLZF. ****P<0.0001, **P<0.01, *P<0.05 by repeated measures two-way ANOVA with Bonferroni's multiple comparisons test.

(Fergusson et al., 2014). Therefore it was investigated whether lower CD161 expression on NKG2C+CD57++ $CD56^{dim}$ NK cells may be associated with reduced PLZF expression. Comparison of PLZF expression in relation to the expression of NKG2C, CD161, and CD57 in $CD56^{dim}$ NK cells revealed that NKG2C+CD57++ cells extensively downregulated PLZF (Figure 6-7I). Within three CMV+ donors with a large NKG2C+CD57++ population (<50% of $CD56^{dim}$ NK cells), cells lacking the expression of both CD161 and PLZF were highly enriched for these NKG2C+CD57++ NK cells (Figure 6-7J). To investigate whether the lower expression of PLZF in CD161− NK cells was specific to CMV+ donors, PLZF and CD161 expression in NK cells from cord blood, as well as adult CMV− and CMV+ donors was assessed. This showed that the frequency of NK cells expressing PLZF strongly correlated with the frequency of NK cells expressing CD161 (R=0.8058, P<0.0001; Figure 6-7K). PLZF expression was higher in CD161+ NK cells from both

cord and adult blood, regardless of CMV status, although the difference did not reach statistical significance in the $CD56^{dim}$ population of CMV− adult donors (Figure 6-7L, M). Therefore, CD161+ NK cells are enriched for PLZF expression, while CD161− NK cells, although not completely lacking in PLZF expression, have a significantly lower expression of PLZF, which is further downregulated in CMV+ donors.

6.4.7. CD161+ NK cells are depleted in CMV-seropositive HIV donors and recovers with HAART

We next wanted to investigate whether CD161 expression changes in other viral diseases. It has been previously reported that CD161 expression on NK cells is reduced in the periphery of chronic HIV patients (Alter et al., 2004; Jacobs et al., 2004; Tarazona et al., 2002). To investigate whether this subset recovers in patients receiving HAART, the frequency of CD161+ NK cells in 27 patients with chronic HIV infection from the Swiss HIV cohort study (SHCS) were followed for two years of HAART. Samples were taken prior to the start of treatment (T-0), at one year (T-1), and two years (T-2) into treatment and analysed by flow cytometry in a blinded manner.

Previous findings that the frequency of CD161+ NK cells were dramatically lower in HIV patients was initially confirmed by comparing the frequency of CD161+ NK cells in these HIV patients to that in healthy controls (Appendix Figure VI-2). However, our initial comparison did not take into account the CMV seropositivity of the “healthy” controls. CMV infection and reactivation is common in immunosuppressed HIV patients (Cheung & Teich, 1999; Sabin et al., 1995), and indeed 24 out of 27 patients were CMV seropositive in the SHCS cohort. In order to control for CD161 downregulation that occurs in CMV+ donors, the frequency of CD161+ NK cells in

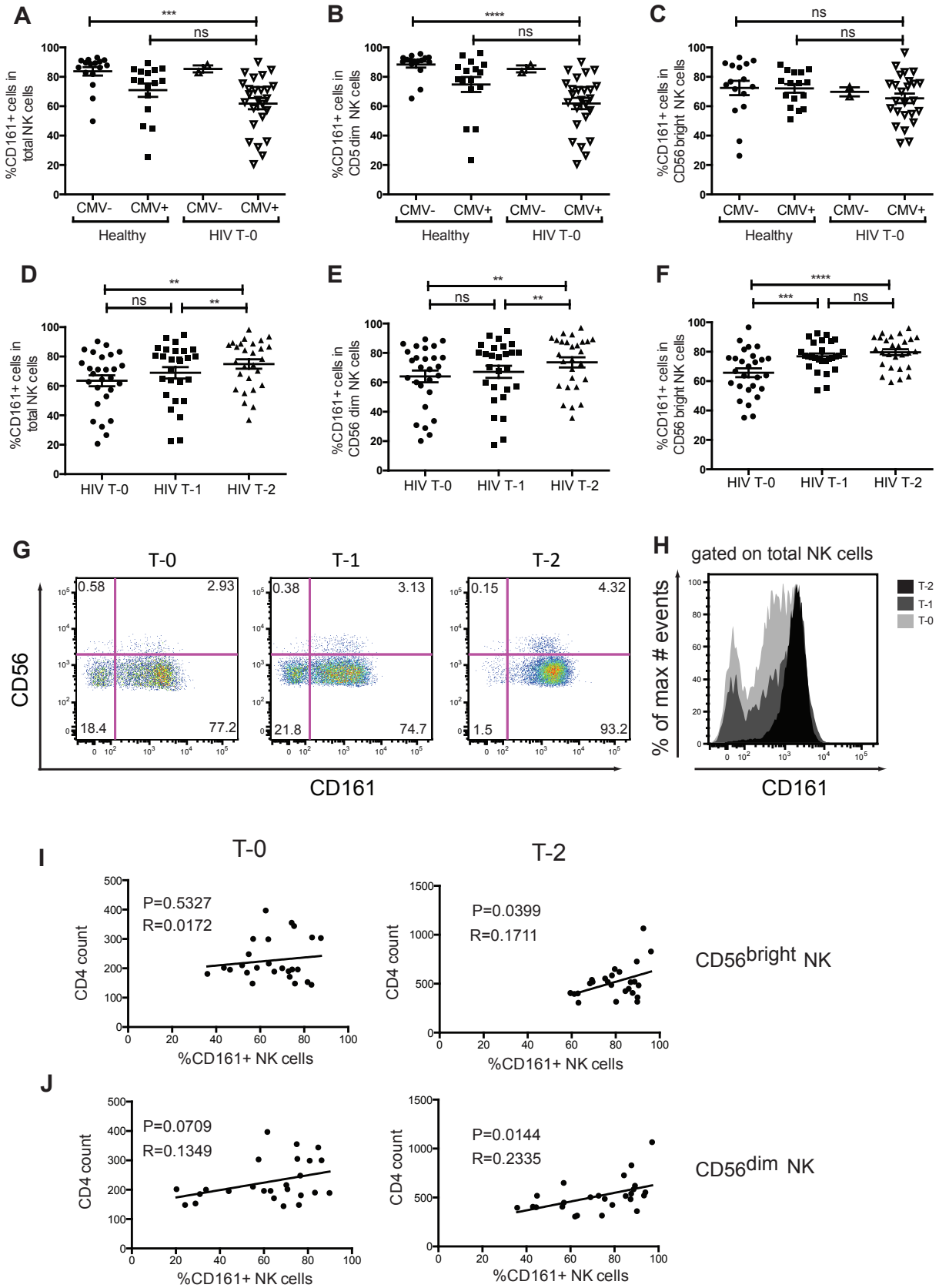

A
B
C
D
E
F
G
H
I
J
%CD161+ cells in total NK cells
%CD161+ cells in CD5 dim NK cells
%CD161+ cells in CD56 bright NK cells
%CD161+ cells in CD56 dim NK cells
CMV-
CMV+
Healthy
HIV T-0
HIV T-1
HIV T-2
ns
T-0
T-1
T-2
CD56
CD161
gated on total NK cells
% of max # events
P=0.5327
R=0.0172
P=0.0399
R=0.1711
P=0.0709
R=0.1349
P=0.0144
R=0.2335
CD4 count
%CD161+ NK cells
CD56bright NK
CD56dim NK

Figure 6-8. CD161+ NK cells are depleted in CMV-seropositive HIV donors and recover with HAART. The frequency of CD161-expressing NK cells in patients with chronic-stage HIV infection from the Swiss HIV cohort study, who were followed for two years of HAART, with samples taken prior to the start of the treatment (T-0), at one year (T-1), and two years (T-2) into treatment. Patients were tested for CMV-seropositivity prior to the start of treatment (Table 6-1). The frequency of CD161+ NK cells within A) total NK cells (CD3−CD56+), B) $CD56^{dim}$ NK cells, and C) $CD56^{bright}$ NK cells is shown for HIV patients at T-0 (n=25 for CMV+, n=2 for CMV−), compared to CMV+ (n=16) and CMV− (n=16) healthy donors. ****P<0.0001, ***P<0.001, or non-significant (ns) by two-way ANOVA with Bonferroni's multiple comparisons test. Other comparisons were non-significant. D) Frequency of CD161+ NK cells within HIV patients followed for two years of HAART. CD161+ cells within A) total NK cells, B) $CD56^{dim}$ NK cells, and C) $CD56^{bright}$ NK cells are shown for HIV patients at T-0, T-1, and T-2. ****P<0.0001, ***P<0.001, **P<0.01, *P<0.05, or non-significant (ns) by repeated measures one-way ANOVA, with Bonferroni's multiple comparisons test. G) Representative staining showing CD161 expression on total NK cells from one patient at T-0 (left), T-1 (centre), and T-2 (right). H) Histogram overlaying CD161 expression on total NK cells from one patient. I-J) Correlation between CD4 counts and CD161 expression on I) $CD56^{bright}$ NK cells or J) $CD56^{dim}$ NK cells at T-0 and T-2. (N=27). Staining performed by Cormac Cosgrove.

HIV patients tested for CMV seropositivity, and healthy donors that had been tested for a CMV-specific memory T cell response (Figure 6-7B), were compared. We found that within total NK cells (Figure 6-8A) and $CD56^{dim}$ NK cells (Figure 6-8B), there was a significantly lower frequency of cells expressing CD161 in CMV+HIV patients, compared to healthy CMV− donors, but not compared to healthy CMV+ donors. There was no significant difference in CD161 expression in $CD56^{bright}$ NK cells between healthy donors and HIV patients, regardless of CMV status (Figure 6-8C). This suggests that CD161 downregulation on NK cells in HIV patients may be associated with their CMV seropositive status, due to the lower expression of CD161 on $CD56^{dim}$ NK cells in CMV+ individuals. Indeed, the two CMV seronegative HIV patients had a high expression of CD161, with 83% and 87.8% of $CD56^{dim}$ NK cells expressing CD161, respectively, compared to a mean of 61.90 ± 3.84% of $CD56^{dim}$ NK cells from CMV+ HIV patients expressing CD161.

Next, we wanted to investigate whether CD161 expression recovers with successful HAART treatment. Surprisingly, a comparison of CD161 expression in total NK cells

(Figure 6-8D), CD56^{dim} NK cells (Figure 6-8E), and CD56^{bright} NK cells (Figure 6-8F) showed that in all populations, there was a significant increase in the frequency of cells expressing CD161 with treatment (T-0 vs. T-2). This is also illustrated in Figure 6-7G and H, and suggests that HIV itself has an impact on the downregulation CD161 and expansion of terminally differentiated NK cells in CMV-seropositive individuals. Interestingly, there was a small but significant correlation between CD4 counts and frequency of cells expressing CD161 in both CD56^{bright} (Figure 6-8I) and CD56^{dim} NK cells (Figure 6-8J) in these patients after, but not before, two years of HAART treatment.

6.4.8. High dimensional analysis delineates NK cell populations in CMV+ and CMV− donors

Previous analysis has shown that CD161 expression marks CD56^{dim} NK cells that have a greater ability to respond to innate cytokines, a feature that is shared with CD161-expressing T cells (Fergusson et al., 2014). Whether this functional correlate is preserved during differentiation induced by CMV, and if there are other correlates of innate responsiveness, however, has not been investigated. In order to comprehensively analyse the innate responsiveness of NK cells in the context of CMV, PBMCs from CMV+ (n=5) and CMV− (n=4) adults, as well as cord blood samples (n=2), were stimulated with IL-12 and IL-18 and the expression of 39 markers was simultaneously assessed by CyTOF (Table 6-2).

In the acquired samples, most CMV+ donors had an expanded population of NKG2C+CD57+ cells within their CD56^{dim} NK cell population (Figure 6-9A, B), and CD161 expression was confirmed to correlate with responsiveness to IL-12+IL-18 as measured by IFNγ, NKp30, CD69, and CD25 within CD56^{dim} NK cells, as well as

within T cells (Appendix Figure VI-3). Next, to reduce the dimensionality of the data, t-Distributed Stochastic Neighbour Embedding (t-SNE) analysis was performed. t-SNE depicts each cell as a point in high-dimensional space, where each dimension is a parameter (Amir et al., 2013; Becher et al., 2014). The points from the high-dimensional space are mapped into low-dimensional space in a way that best conserves the pairwise comparisons between the points in high-dimensional space (see Section 6.3.7.). The resulting map therefore maps each cell's location in the resulting plot based on information from all of the original dimensions.

t-SNE analysis of the expression of 36 parameters on live lymphocytes generated a two-dimensional composite map based on all donors that clearly delineates cell subsets as distinct niches, or clusters (Figure 6-9C). The clusters were coloured by their expression of lineage defining markers so that MAIT cells, γδ T cells, NK cells, and conventional CD8+ T cells could be identified (Figure 6-9C). Three NK cell clusters could be identified according to CD3 and CD56 expression, where one cluster (NK1) clearly contained the $CD56^{bright}$ NK cell subset, which overlapped with the NK2 subset containing a large fraction of $CD56^{dim}$ NK cells. A separate $CD56^{dim}$ NK cell cluster (NK3) formed a distinct cluster separated from the other NK cells. When the t-SNE plots of CMV+ and CMV− donors were compared, the clearest difference was the presence of this NK3 cluster in CMV+ donors but not in CMV− donors, characterized by high staining for NKG2C (Figure 6-9D) and CD57 expression (Figure 6-9E), and low expression of CD161 (Figure 6-9F) and IFNγ in response to IL-12 and IL-18 stimulation (Figure 6-9G) compared to the NK1 cluster. t-SNE analysis of the expression of these parameters on NK cells alone also identified 5 distinct clusters (Appendix VI-4). Interestingly, two of these NK cell clusters were high in NKG2C expression (cluster 1 and 2), and while one of these NKG2C+CD161−IFNγ− clusters (cluster 1) was only present in CMV+ individuals, cluster 2 was present in CMV− adults but not cord blood, suggesting that CMV may

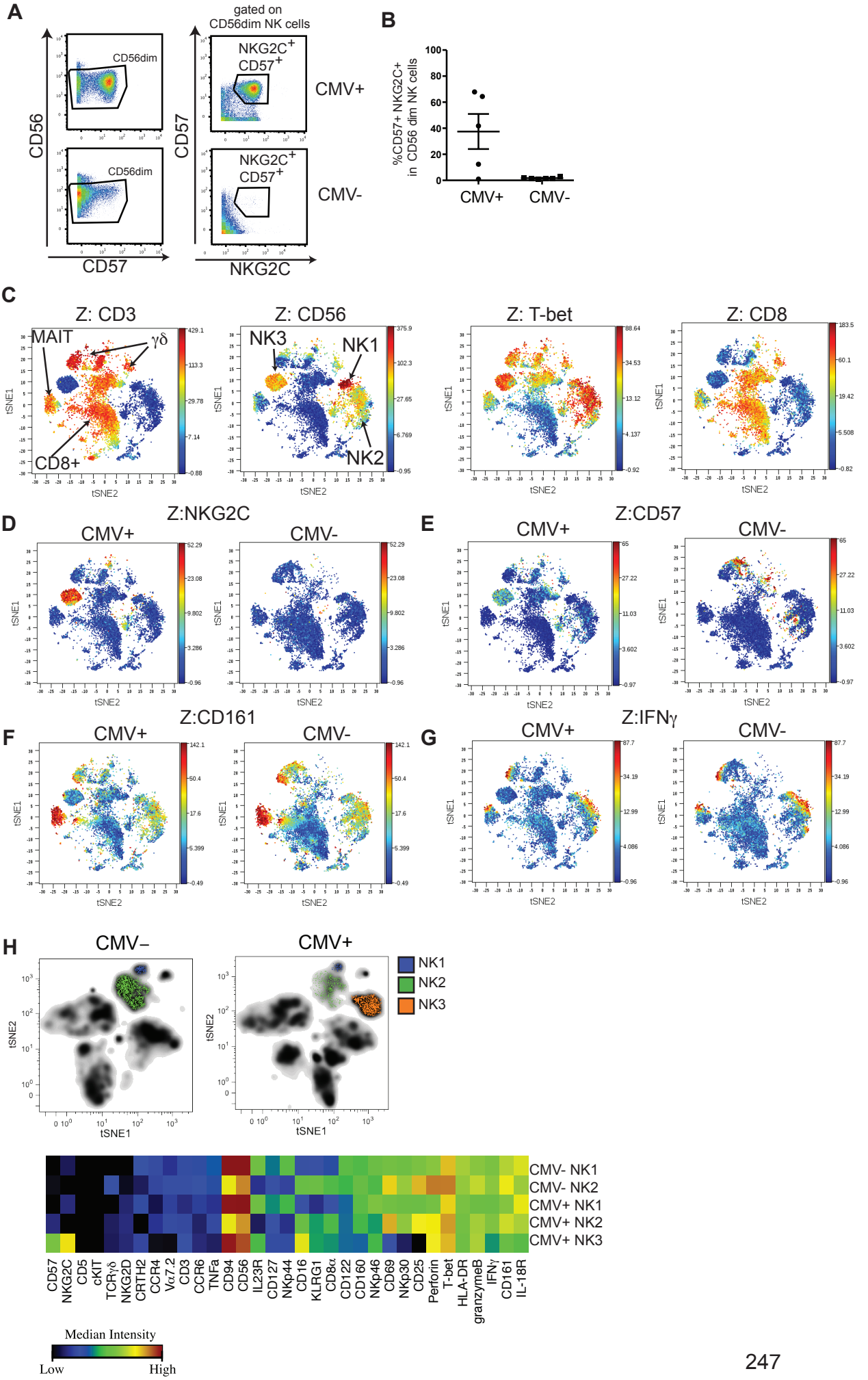

A
gated on
CD56dim NK cells
CD56dim
NKG2C+
CD57+
CMV+
CMV-
CD56
CD57
NKG2C
B
%CD57+ NKG2C+
in CD56 dim NK cells
100
80
60
40
20
0
CMV+
CMV-
C
Z: CD3
Z: CD56
Z: T-bet
Z: CD8
MAIT
γδ
CD8+
NK3
NK1
NK2
tSNE1
tSNE2
D
Z:NKG2C
CMV+
CMV-
E
Z:CD57
CMV+
CMV-
F
Z:CD161
CMV+
CMV-
G
Z:IFNγ
CMV+
CMV-
H
CMV–
CMV+
NK1
NK2
NK3
tSNE1
tSNE2
CMV- NK1
CMV- NK2
CMV+ NK1
CMV+ NK2
CMV+ NK3
CD57
NKG2C
CD5
cKIT
TCRγδ
NKG2D
CRTH2
CCR4
Vα7.2
CD3
CCR6
TNFa
CD94
CD56
IL23R
CD127
NKp44
CD16
KLRG1
CD8α
CD122
CD160
NKp46
CD69
NKp30
CD25
Perforin
T-bet
HLA-DR
granzymeB
IFNγ
CD161
IL-18R
Median Intensity
Low
High

Figure 6-9. t-SNE analysis delineates NK cell populations in CMV+ and CMV- donors. Peripheral blood and cord blood samples depleted of B cells, monocytes, and CD4+ T cells were stimulated with IL-12+IL-18 overnight and acquired by CyTOF, as detailed in Materials and Methods. t-SNE analysis was used to broadly assess phenotypic profiles of NK cells across 11 donors. A) Representative staining for NKG2C and CD57 on $CD56^{dim}$ NK cells from CMV+ and CMV− individuals identifying expanded NKG2C+CD57+ cells in CMV+ donors. B) Cumulative frequencies of NKG2C+CD57+ cells between CMV+ and CMV− donors acquired in the CyTOF experiment. C-G) Data from all samples were aggregated and t-SNE analysis was used to delineate clusters using Cytobank. The resulting plot was coloured according to the median intensity of the indicated markers (Z) to annotate indicated clusters (C). D-G) t-SNE plots for CMV+ and CMV− individuals are shown, coloured according to the expression of the markers indicated as Z. Plots are coloured according to levels of D) NKG2C, E) CD57, F) CD161, and G) IFNγ. H) t-SNE analysis was performed on CMV+ and CMV− donors, using R. Populations of NK cells were identified by manual gating and used to colour code clusters within the t-SNE plot. The median intensities of each marker was calculated for the NK cell populations identified (top) and plotted as a heatmap (bottom). t-SNE analysis in R was performed by Yannick Simoni.

induce the expansion of these NKG2C+CD161− IFNγ− cells (cluster 2), which further differentiates into cluster 1.

NK cell clusters were further analaysed in R to generate a comprehensive overview of marker expression in each cluster. For the three NK cell clusters identified in Figure6-8H, the median intensities of each marker was quantified and summarised using a heatmap illustration. This shows a clearly lower expression of NKp30, CD25, CD69, IFNγ, CD160, and to a lesser extent, CD161 and IL-18R in the CMV+ donor-specific NK3 cluster, while they expressed higher levels of NKG2C, CD57, and CD16. Of note, as there was a high background for CD161 (shift of negative cells), the reduction in CD161 expression on these terminally differentiated NK cells was not as clear as observed in previous flow cytometry experiments, but the median intensity of CD161 was lower in NK3 compared to other NK2 ($CD56^{dim}$ NK cell) populations. Thus, together with NKp30 and CD160, CD161 expression marks $CD56^{dim}$ NK cells that have retained their responsiveness to innate cytokines; an ability that is lost upon CMV-induced terminal differentiation.

6.5. Discussion

In this study, the transcriptional signature, phenotypic properties and functional capacity of human CD161+ and CD161− NK cells was investigated. CD161 expression was found to mark functionally immature NK cells with a higher proliferative capacity, higher responsiveness to cytokines within $CD56^{dim}$ NK cells, and was dramatically downregulated in terminally differentiated NK cells expanded in CMV+ donors.

6.5.1. Phenotypic correlates of CD161 expression in NK cells

All NK cells expressed CD161 at a high level in cord blood, but a distinct CD161− NK population was present in 24 month old samples, suggesting that CD161− NK cells emerge from CD161+ NK cells early in life. Detailed phenotypic analysis using flow and mass cytometry indeed showed that CD161− NK cells are enriched for CD57+NKG2C+ NK cells expanded in CMV+ donors, which are also characterized by reduced expression of CD160, NKp30, CD69, IL-18R and CD25. Thus, CD161 may be an immature NK cell marker, which is downregulated during CMV-induced differentiation. Interestingly, not all the properties of CD161+ NK cells are consistent with these cells being more immature than the CD161− NK cells. For instance, CD161− cells are present in the $CD56^{bright}$ NK cell population, and there was no difference in CD57 expression between CD161+ and CD161− cells in CMV-negative donors. CD16 and granzyme expression was also not significantly different between the two populations, in contrast to populations defined by other NK cell maturation markers such as CD57 and CD62L. Instead, CD161 expression may be associated with an independent maturation pathway, or may be closely associated with education; indeed, a dissociation between differentiation as measured by CD57

expression and education as measured by KIR expression has been previously described (Björkström et al., 2010).

What is the significance of downregulating CD161 during NK cell differentiation? CD161 ligation has been shown to inhibit NK cell cytotoxicity (Aldemir et al., 2005; Rosen et al., 2005, 2008), and this could be confirmed using MHC-class I deficient target cells expressing the ligand for CD161, LLT1 (Appendix Figure VI-5). However, there was largely no difference in the cytotoxic profile of CD161+ and CD161− NK cells, nor the ability of CD161+ and CD161− NK cells to degranulate in response to MHC-class I-deficient cells. The downmodulation of the inhibitory molecule CD161 during differentiation may enhance the ability of NK cells to kill infected or transformed cells, but would also result in unchecked cytotoxicity that could be harmful to "self". Interestingly, expression of CD85j and CD158e (KIR3DL1/KIR3SL1), which recognise classical MHC class I molecules, was enriched within the CD161− NK cell population. As NK cells are licensed through ligation of KIRs by self-specific HLA ligands (Anfossi et al., 2006; Fauriat et al., 2010a), it is tempting to speculate that downregulation of CD161 may be associated with increased education and expression of other inhibitory receptors that recognise classical MHC class I molecules. Indeed, NKG2C+CD57+ cells have clonal expression pattern of inhibitory KIRs specific for self-HLA class I molecules (Béziat et al., 2012, 2013). A population of NKG2C-negative NK cells expressing inhibitory self-KIRs can also expand in CMV+ individuals (Béziat et al., 2013; Della Chiesa et al., 2014; Lee et al., 2015; Zhang et al., 2013). As CMV induces the downregulation of MHC class I molecules, except for HLA-E, cells expressing inhibitory self-KIRs and NKG2C (which binds HLA-E) may selectively expand (Della Chiesa et al., 2014). Whether educated cells are already enriched cells within CD161− NK cells, or whether CD161 is downregulated during the expansion of these self-KIR expressing cells, remains to be investigated.

6.5.2. CD161 expression and innate responsiveness of NK cells

As CD161 expression in T cells identifies cells with high expression of IL-18R and an innate ability to respond to the cytokines IL-12 and IL-18, regardless of TCR usage, (Fergusson et al., 2014), whether this association holds true beyond T cells was tested in NK cells. All $CD56^{bright}$ NK cells secreted IFNγ, regardless of their CD161 expression, and IL-18R expression in $CD56^{dim}$ NK cells only weakly correlated with CD161 expression. However, within $CD56^{dim}$ NK cells, IFNγ production in response to IL-12 and IL-18 was strongly correlated with CD161 expression. This suggests that CD161 marks $CD56^{dim}$ NK cells that have retained the ability to respond to IL-12+IL-18 during differentiation, as multidimensional analysis showed that this functional association was preserved in CMV+ donors. It is likely that within NK cells, innate responsiveness is controlled by additional factors, especially within $CD56^{bright}$ NK cells. For example, NK cells have constitutive IFNγ promoter activity and upregulate IFNγ transcription during maturation in the bone marrow, in contrast to T cells, where such constitutive IFNγ expression is restricted to memory cells (Stetson et al., 2003). Additionally, the haematopoietic cell-specific SH2 containing 5' inositol phosphatase (SHIP1) has been suggested to negatively regulate the cytokine responsiveness of NK cells (Trotta et al., 2005), as SHIP1 expression is lower in $CD56^{bright}$ cells compared to $CD56^{dim}$ NK cells, and overexpression of SHIP1 reduced the responsiveness of $CD56^{bright}$ NK cells to cytokines.

6.5.3. CD161 and proliferation of NK cells

The most striking functional difference between CD161+ and CD161− NK cells was their proliferative capacity in response to cytokines. The hyperproliferative capacity of CD161+ NK cells most likely reflects their heightened ability to respond to cytokines, as preliminary experiments have shown that CD161− NK cells can proliferate in

response to activating receptor ligation, but not in the presence of cytokines alone (Appendix Figure VI-6A). This is line with reports that the *in vitro* expansion of NKG2C+CD57++ NK cells, which are enriched for CD161− cells, requires NKG2C ligation in addition to IL-15 or IL-12 (Gumá et al., 2006; Rölle et al., 2014). Interestingly, CD161 was downregulated during IL-15-induced proliferation (Appendix Figure VI-6B, C), similar to a previous study showing CD161 downregulation with IL-2 stimulation (Azzoni et al., 1998). The absence of CD161− NK cells in cord blood and their presence in 24 month old samples strongly suggests that CD161− NK cells emerge from CD161+ NK cells. Furthermore, the stable presence of a small frequency of CD161− NK cells in CMV− donors suggests that the emergence of CD161− NK cells is not dependent on CMV infection. One possibility may be that proliferation of CD161+ NK cells is accompanied by the downregulation of CD161 during NK cell differentiation. Indeed, the significant and almost complete loss of CD161 expression on the expanded NK cells of patients with NK-type lymphoproliferative disease of granular lymphocytes (NK-LDGL) suggests that expansion of NK cells is associated with CD161 downregulation (Pascal et al., 2004). Further investigation into the relationship between proliferation and the expression of CD161 will be required to fully understand how the CD161− NK cell population emerges early in life and expands during terminal differentiation of NK cells.

6.5.4. CD161 and PLZF expression in NK cells

PLZF expression was found to strongly correlate with the frequency of NK cells expressing CD161, and CD161+ NK cells were enriched for PLZF expression, regardless of age or CMV status. However, not all CD161− NK cells lacked PLZF expression, in line with residual expression of CD161 in a PLZF-deficient patient (Eidson et al., 2011), which suggests that there are additional factors regulating CD161 expression. PLZF has recently been shown to be the most downregulated

transcription factor in NKG2C+CD57+ NK cells expanded in CMV+ donors, due to hypermethylation of a *ZBTB16* intronic sequence (Schlums et al., 2015), which was also associated with extensive downregulation of the genes encoding CD161, IL-18R and IL-12R. It is interesting to note that PLZF and CD161 expression in T cells mark "innate" T cells with the ability to respond to cytokines alone (Fergusson et al., 2014), while in these terminally differentiated, so-called "adaptive" NK cells, the downmodulation of PLZF and CD161 expression is associated with a reduced ability to respond to innate cytokines (Schlums et al., 2015). Of note, this study also found that another member of the BTB-zinc finger (BTB-ZF) family, *ZBTB32*, was hypomethylated in these cells - a gene that was upregulated by 35-fold in CD161− NK cells compared to CD161+ NK cells (Appendix Table VI-1). Thus, several members of the BTB-ZF family, including ZBTB32 and PLZF, may regulate CD161 expression and innate-responsiveness to cytokines.

6.5.5. CD161 expression on NK cells in HIV infected patients

In the present study of HIV-infected patients, CD161 expression in $CD56^{dim}$ NK cells was significantly reduced compared to healthy CMV− donors, but not compared to healthy CMV+ donors. Although only two HIV patients were CMV seronegative, both donors had high expression of CD161, which did not change with HAART (data not shown). Therefore, CD161 downregulation may be associated with CMV reactivation or re-infection due to progressive immunodeficiency during HIV infection (Mela et al., 2005). Prior infection with CMV is a risk factor for a low CD4 count, progression to AIDS and mortality in HIV patients (Sabin et al., 1995), and whether CMV-driven differentiation, and possibly exhaustion, of NK cells may reduce the ability of NK cells to mediate HIV control requires further investigation.

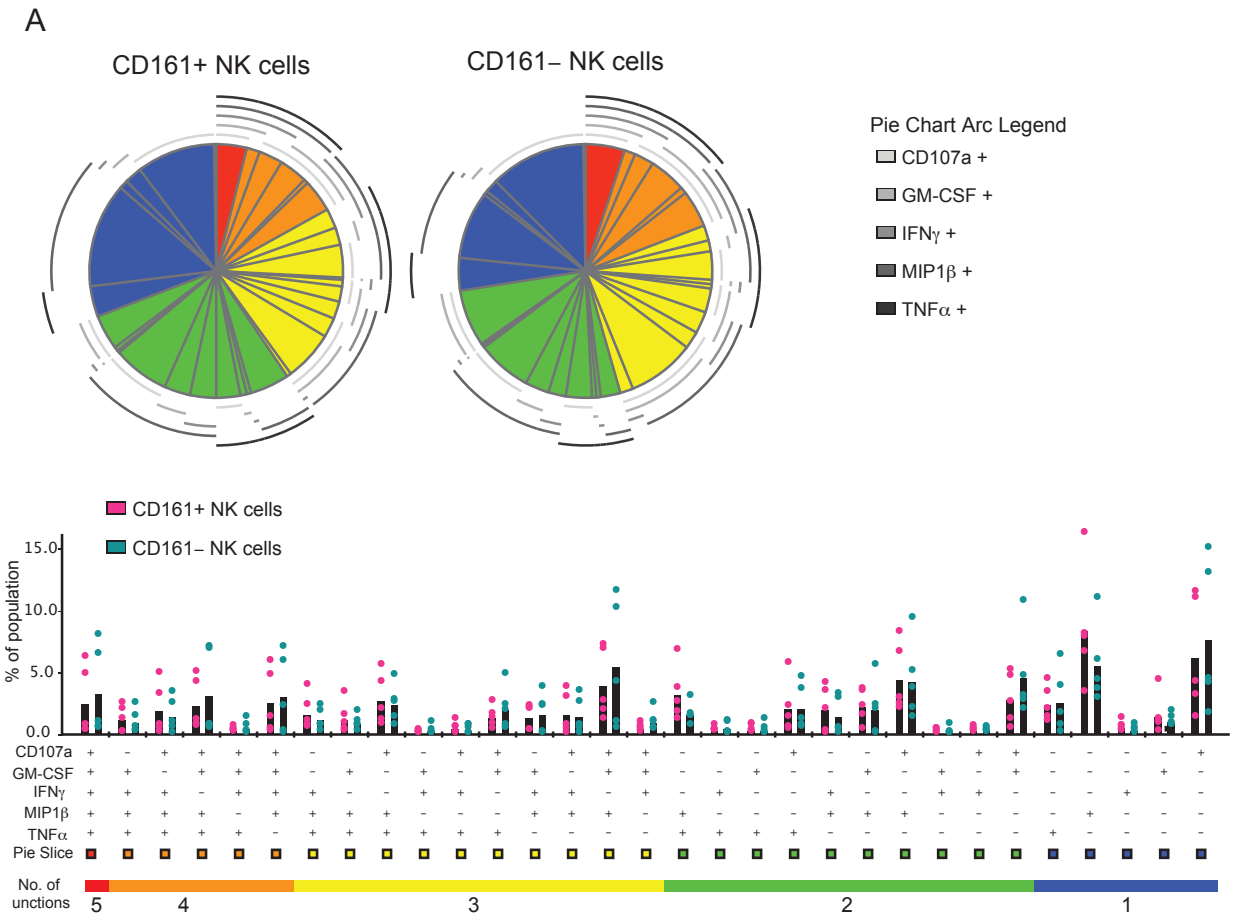
Interestingly, longitudinal analysis of CD161 expression in NK cells before and during HAART treatment in these patients showed that there was a significant recovery in CD161 expression in both $CD56^{bright}$ and $CD56^{dim}$ NK cell subsets over time. This may be due to HIV patients re-establishing better control of CMV following HAART treatment. In $CD56^{dim}$ NK cells, a significant increase in CD161 expression was only observed after two years of HAART treatment, which may correspond with reduced CMV viraemia (Lopez-Vergès et al., 2011). However, the recovery of CD161 expression on $CD56^{bright}$ NK cells, which do not contain CMV-induced expansions, suggests that HIV may also have direct effects on CD161 expression. CD161 downregulation in HIV patients has also been reported in a population of dysfunctional CD56− NK cells (Kulkarni et al., 2012) that are defective at target cell lysis and cytokine secretion (Mavilio et al., 2005), the emergence of which is not CMV-associated (Milush et al., 2013). Whether these changes are directly induced by HIV, or are due to differentiation/proliferation of NK cells is unknown. *In vitro* experiments culturing NK cells with HIV-infected cells may be able to address whether HIV can directly affect CD161 expression, as has been shown for HCV-induced downregulation of NKp30 (Holder et al., 2013).

Regardless of whether it is induced by CMV or directly by HIV, the loss of the CD161+ NK cell subset in HIV infected patients may potentially lead to cells having a reduced proliferative capacity in response to homeostatic cytokines, reduced activating NCR expression, as well as a reduced capacity to secrete IFNγ in response to innate cytokines. Indeed, a reduced ability of NK cells from HIV infected patients to respond to IL-12+IL-18 has been reported, although whether this may be linked to CD161 is unknown (Meier et al., 2005). As CMV-associated expansion of terminally differentiated NK cells has been reported in many viral infections, including EBV (Saghafian-Hedengren et al., 2013) and HCV/HBV (Béziat et al., 2012), phenotypic and functional analyses of NK cells during viral infections should control

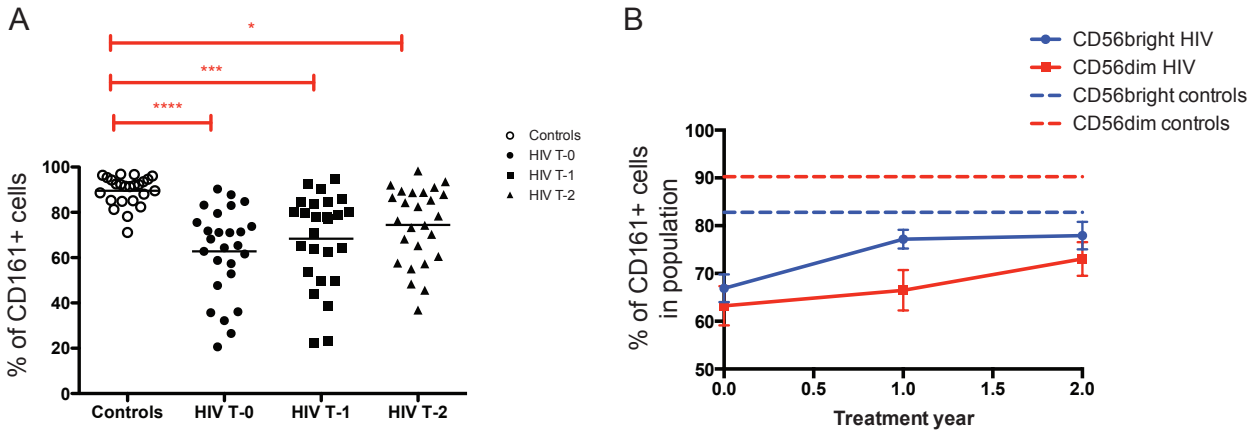
for changes in the NK cell repertoire that is driven by CMV, in order to identify the specific changes that affect NK cell function in the viral infection in question.

6.6. Summary

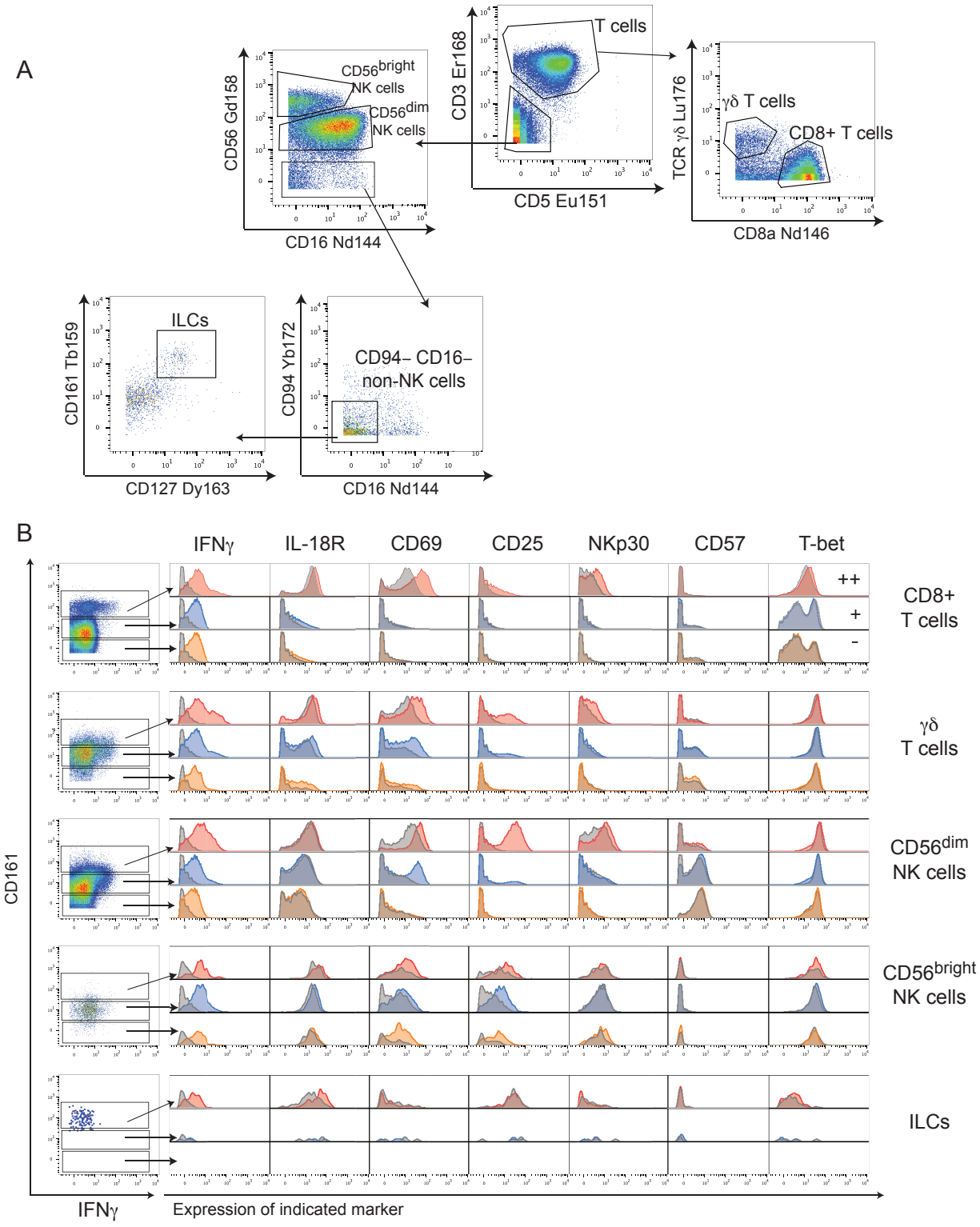
1. CD161 is a marker of immature NK cells, expressed on all NK cells in cord blood
2. CD161+ NK cells are highly proliferative in response to cytokines and are enriched for the expression of activating receptors NKp30, NKp46, and CD160
3. CD161 expression correlates with responsiveness to innate cytokines IL-12+IL-18 within $CD56^{dim}$ NK cells
4. CD161 is downregulated on $CD56^{dim}$ NK cells during CMV-induced terminal differentiation of NK cells in healthy donors as well as HIV-infected patients. CD161 expression on NK cells recovers with HAART
5. CD161+ NK cells are highly enriched for the expression of PLZF, which is further downregulated in CD161− NK cells during CMV-induced terminal differentiation



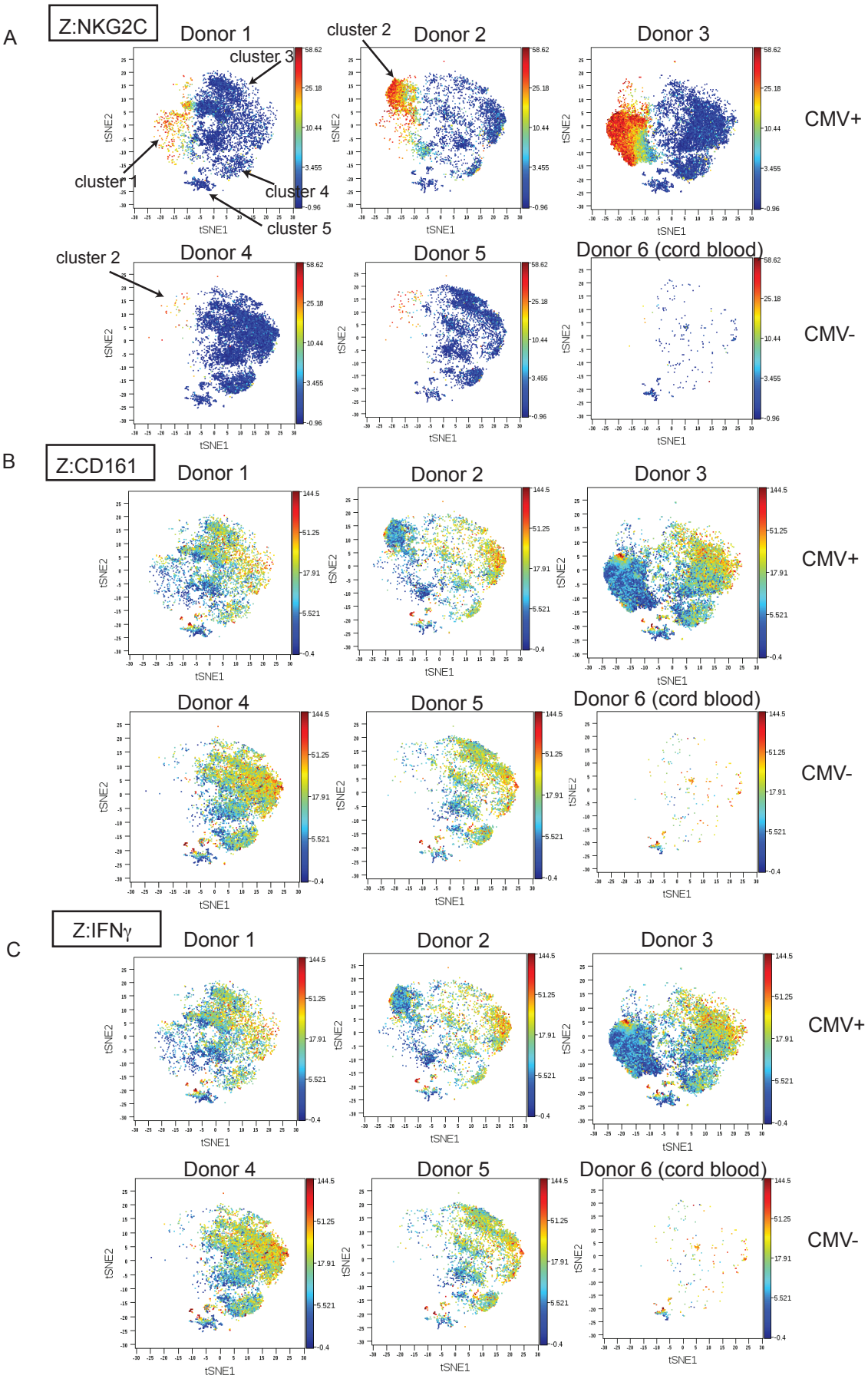
Appendix Figure VI-1. CyTOF data showing the polyfunctionality of CD161+ and CD161− NK cells in response to PMA/ionomycin stimulation. PBMCs were stimulated with PMA/ionomycin for 3 hours as detailed in Chapter 2, and gated as shown in Figure 6-1A. NK cells gated as CD3-CD56+ cells were analysed for the simulatenous expression of CD107a, GM-CSF, IFNγ, MIP1β, and TNFa, and analysed by SPICE. Cells which did not secrete anything were excluded from the analysis. Colours in the pie charts represent 5-function (red), 4-function (orange), 3-function (yellow), 2-function (green), or 1-function (blue) cells, within the responding cells of the CD161+ NK cell subset (left) or the CD161− NK cell subset (right). The pie chart arcs indicate the cytokine/CD107a expression for individual fractions of the pie charts. The scatter charts below show the responses in CD161+ or CD161− NK cells broken down into different functional categories. The pie chart between CD161+ and CD161− NK cells did not differ when broken down into $CD56^{bright}$ and $CD56^{dim}$ NK cells (data not shown).



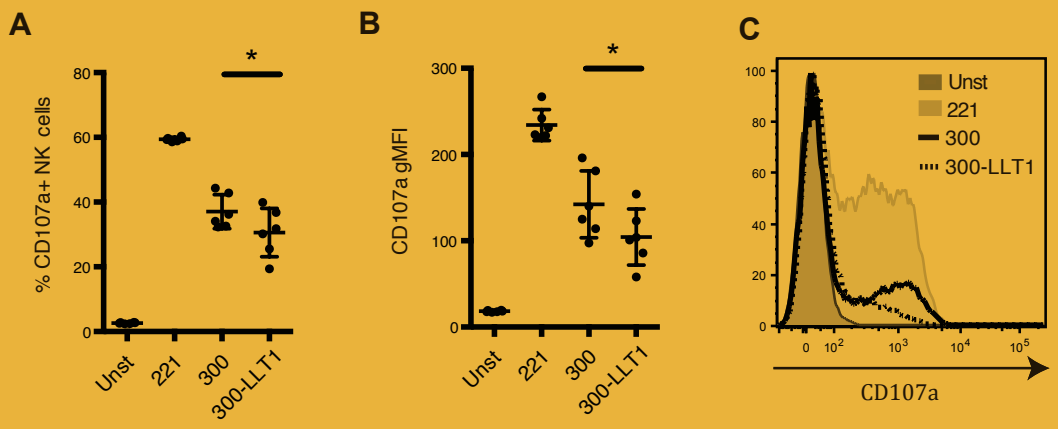
Appendix Figure VI-2. CD161 expression on NK cells in HIV patients, compared to healthy controls with unknown CMV serostatus. A) Expression of CD161 on total NK cells from healthy controls (n=24) or HIV patients (n=27) from the Swiss HIV cohort study, who were followed for two years of HAART, with samples taken prior to the start of the treatment (T-0), at one year (T-1), and two years (T-2) into treatment. ****P<0.0001, ***P<0.001, *P<0.05 by two-way ANOVA with Bonferroni's multiple comparisons test, compared to controls. B) The change in mean frequency of CD161+ NK cells within $CD56^{dim}$ NK cells (solid blue) and $CD56^{bright}$ NK cells (solid red) during two years of HAART, compared to mean frequencies of CD161+ cells within $CD56^{bright}$ NK cells (dotted blue) and $CD56^{dim}$ NK cells (dotted red) in healthy controls (n=24).



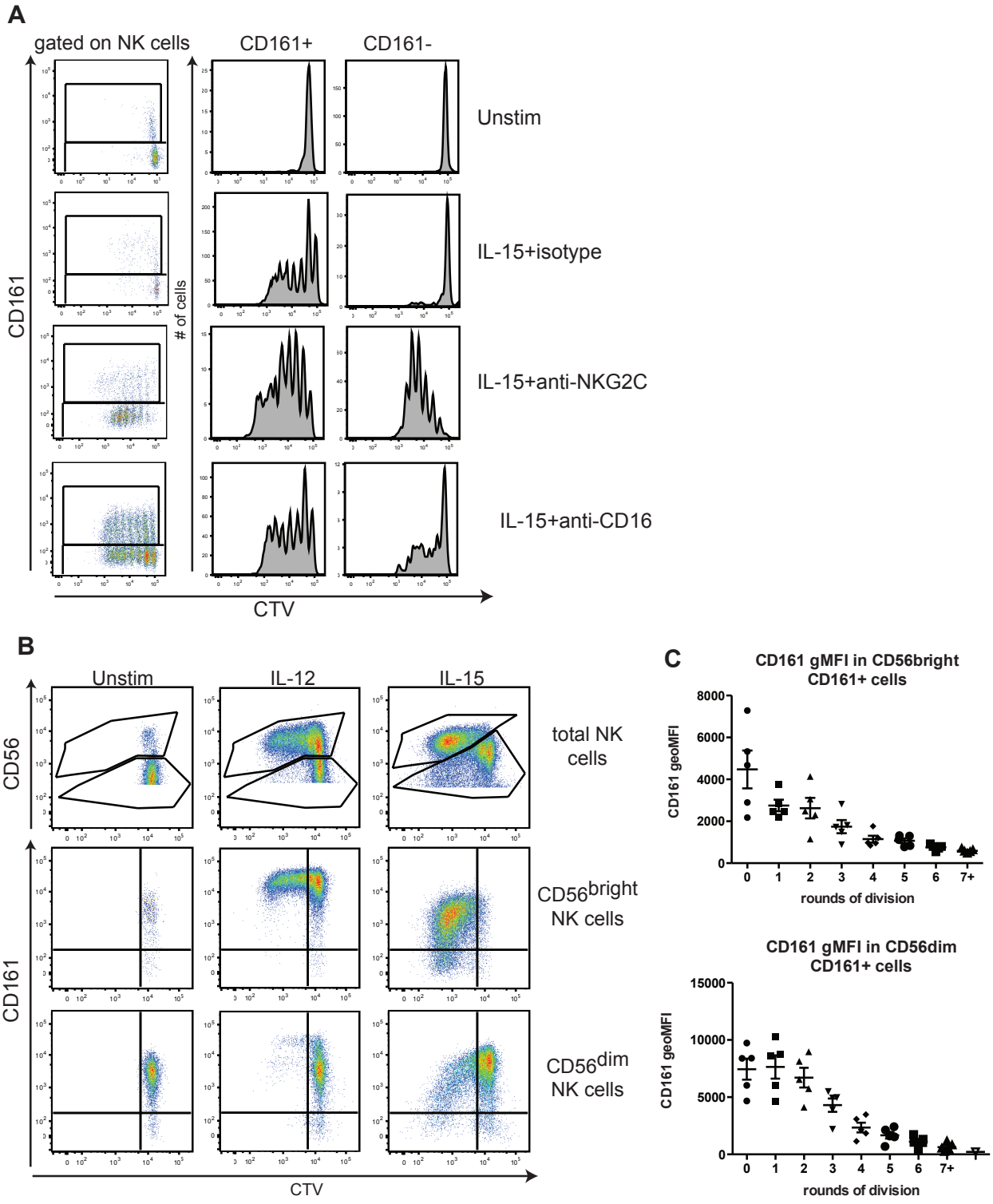
Appendix Figure VI-3. Profiling of innate-like T cells and ILCs by mass cytometry. B cell, monocyte, and CD4+ T cell-depleted peripheral blood and cord blood samples were stimulated with IL-12+IL-18 overnight and acquired by CyTOF. A) Gating strategy to analyse innate-like T cells and ILCs by mass cytometry. After following the gating strategy identified in Figure 6-1B, T cells were gated as CD3+CD5+ cells, and γδ T cells and CD8+ T cells were identified by gating on γδ TCR+ cells and CD8+ cells, respectively. NK cells were gated as CD3−CD5−CD56+ cells. Helper-type ILCs were defined as CD3−CD5−CD56−CD94−CD16−CD161+ and CD127+. B) For the indicated populations, histograms are used to compare the expression of surface and intracellular markers within CD161++ (red), CD161+ (blue), and CD161− (yellow) subsets from one donor. For each population, the unstimulated cells are shown in grey. Gates to identify CD161++, CD161+, and CD161− cells in all populations were based on CD8+ T cells.



Appendix Figure VI-4. t-SNE analysis gating on NK cells (CD3-CD5-CD56+ cells) only. Analysis continued from Figure 6-9. The analysis delineates 5 distinct clusters of NK cells, highlighted by the arrows. Plots are coloured by the expression level of the marker indicated by Z. A) Colouring of t-SNE plots according to NKG2C expression levels. B) Colouring of t-SNE plots according to CD161 expression levels. C) Colouring of t-SNE plots according to IFNγ expression levels.



Appendix Figure VI-5. LLT1 inhibits NK cell degranulation. NK cells were co-cultured with HLA-A, B, C-null .221 cells (221), or the murine pre-B cell line 300-19 either transfected with LLT1 (300-LLT1) or untransfected cells (300), and the expression of CD107a on NK cells was assessed. The percentage of CD107a-expressing NK cells (A) as well as CD107a gMFI values (B) were lower when 300-LLT1 cells were used as targets compared to the untransfected 300 cells. Representative FACS plot showing NK cell degranulation (C) (n=6). Data from Alba Llibre.



Appendix Figure VI-6. Downregulation of CD161 on proliferating NK cells. A) CTV-labeled NK cells were stimulated with IL-15 and plate-bound anti-NKG2C or anti-CD16 antibody, or isotype control for 5 days. B) Expression of CD161 on NK cells proliferating in response to IL-12 and IL-15 following stimulation for 5 days. C) Expression of CD161 as measured by gMFI with increasing rounds of divisions in response to IL-15 stimulation in $CD56^{bright}$ CD161+ NK cells (top) and $CD56^{dim}$ CD161+ NK cells (bottom) (n=5).

Appendix Table VI-1. Genes significantly up/downregulated in CD161+ NK cells compared to CD161- NK cells (P<0.01, >2 fold change), after filtering out probes not detected in more than 4 samples.

GeneName	Fold.Change	P.value
LRIT1	11.58883	0.00219
EPHB1	11.46734	0.00225
lincRNA:chr7:96292589-96310764_F	10.6393	0.00452
lincRNA:chr18:53497402-53506427_R	10.51485	0.00888
A_33_P3305973	8.72807	0.00383
PCDHGA3	8.06123	0.00109
lincRNA:chr19:35305854-35305927_R	7.88077	0.00185
THC2681728	7.77927	0.00374
LOC440600	7.66841	0.00191
KRT19P2	7.60378	0.00051
FAM19A5	7.34541	0.00509
ARNTL2	7.11732	3.00E-05
POM121L1P	7.03228	0.00794
LOC402382	6.63936	0.00032
KRT4	6.35655	0.00574
lincRNA:chr10:50217119-50223094_R	6.34384	4.53E-10
lincRNA:chr1:79897287-79954287_R	6.33358	0.00408
lincRNA:chr12:132832202-132857482_R	6.0783	0.00469
DLGAP5	6.04587	0.0019
lincRNA:chr8:123989344-123994919_R	5.96057	0.00059
PABPN1L	5.88941	0.0034
A_33_P3228603	5.55843	0.00759
lincRNA:chr11:110066015-110071440_F	5.49261	0.0051
NHSL1	5.39421	0.00979
KIF19	5.0835	0.00337
lincRNA:chr7:25978475-25989975_F	4.9988	0.00328
BCAS1	4.95295	2.00E-05
TWIST2	4.70419	0.0066
LOC100507084	4.70272	1.37E-17
SPC25	4.31379	0.00412
RBFOX3	4.28036	0.00063
ADRB1	4.18074	1.22E-06
BCAS1	3.97205	6.00E-05
UOX	3.96827	0.00365
FAM22D	3.95211	0.00968
ENST00000358739	3.90872	7.35E-06
LRP12	3.86966	1.27E-22
RORC	3.82559	0.00025
TDRD1	3.77387	0.00208
GP5	3.73929	0.00012
AFAP1L1	3.69192	0.00152
KLRB1	3.67139	4.23E-15
lincRNA:chr15:25245397-25265969_R	3.61207	0.00208
KIAA0226	3.49556	0.00748
NHEDC1	3.4723	0.00012
GLI3	3.44416	4.00E-05
CCL23	3.42177	0.00177
PRICKLE2	3.2503	0.00356
SLC6A4	3.24996	1.00E-05
lincRNA:chr13:31404935-31457531_F	3.17322	3.42E-07
LGR6	3.1523	0.00398
BRSK1	3.13476	0.00013
C13orf33	3.12717	0.00355
FEZ1	3.06226	9.86E-12
lincRNA:chr4:15669186-15683175_R	3.03911	0.00793
ORC1	3.03102	2.20E-06
MED20	3.01214	0.00107
KRT72	2.9994	2.85E-06
MLF1	2.98473	0.00539
DKFZp779M0652	2.92281	0.00024
SOX30	2.91728	0.00201
UNC45B	2.91327	9.59E-09
FAM132B	2.87727	0.00055
HES6	2.87382	2.00E-05
THC2721084	2.87257	0.00013
OCA2	2.82985	5.64E-07
SLC4A10	2.82845	0.00728
KRT2	2.82586	4.00E-05
GREB1	2.82196	0.00767
RNF157	2.82014	0.0024
SLC4A4	2.81913	2.66E-21

HIST1H4L	2.78855	4.29E-07
MELK	2.78221	2.42E-06
MYRIP	2.77679	0.0056
GALNT9	2.7697	0.00252
GPR124	2.75326	1.84E-07
VIT	2.74784	0.00186
HES6	2.70835	2.00E-05
RLBP1	2.70237	1.37E-06
CELA1	2.67637	2.00E-04
CT45A5	2.67543	0.00092
LGR6	2.65052	2.00E-05
lincRNA:chr2:120459730-120511405_R	2.6238	9.11E-07
SPR	2.57179	0.00865
BIRC5	2.56514	0.00048
lincRNA:chr11:69216919-69339519_F	2.55935	0.00424
LAYN	2.55713	6.80E-10
AK125574	2.55156	0.00019
DEPDC1B	2.55128	0.00093
lincRNA:chr7:139487141-139489421_F	2.54075	1.62E-07
HES6	2.47098	8.26E-07
TKTL1	2.4585	3.44E-08
lincRNA:chr7:26681650-26696300_R	2.45751	0.00597
lincRNA:chr2:129153697-129402710_F	2.45329	0.00218
CAPN5	2.43104	3.12E-13
ALOX5AP	2.40706	1.00E-04
VIT	2.40681	0.00197
RBFOX2	2.39949	0.00217
lincRNA:chrX:56807400-56832200_F	2.39907	0.00275
ST8SIA6	2.39377	4.72E-06
ATXN1L	2.36931	0.00175
LOC100130894	2.36334	0.0016
GRAMD3	2.34525	1.00E-05
ST8SIA6	2.34074	1.10E-06
CD160	2.33864	4.11E-08
VLDLR	2.33705	4.88E-07
HIC1	2.33603	0.00271
SLC4A10	2.33328	9.00E-05
LBH	2.32753	0.00015
LRRC43	2.31456	1.89E-26
ASPM	2.31341	0.00245
HIST1H2AI	2.31142	7.00E-05
SCARNA10	2.29843	0.00145
SPATA9	2.28822	0.00039
C10orf128	2.28247	0.00092
lincRNA:chr15:34935983-34961608_F	2.27281	0.0083
OR10G2	2.27139	0.00834
C12orf34	2.27043	1.74E-06
COLQ	2.27035	3.00E-05
lincRNA:chr20:58662941-58676395_F	2.26791	0.00021
RAD54B	2.25736	0.00143
ZWINT	2.25653	0.0022
AK000950	2.25607	0.00398
TYMS	2.2491	0.00452
RP1-177G6.2	2.24562	0.00922
SMPDL3B	2.24554	0.00068
PALM	2.2433	3.00E-05
FAM110C	2.24314	0.00539
lincRNA:chr2:121828880-121902705_F	2.23146	0.00328
C6orf132	2.2138	0.00264
lincRNA:chr20:58662941-58676395_F	2.21258	0.00098
lincRNA:chr10:47092419-47149419_F	2.21163	3.60E-08
AATK	2.20804	5.00E-05
LDB2	2.19674	0.00027
FADS2	2.19432	4.60E-06
DTL	2.18285	0.00286
MAF	2.18195	8.00E-05
AKR1C4	2.18155	0.00687
KHDC1	2.17511	0.00192
MKI67	2.16407	0.00057
TPX2	2.16276	3.00E-05
CFHR3	2.15765	0.00508
IKZF3	2.15453	1.26E-08

BRIP1	2.14459	0.00057
RECQL	2.13875	0.00483
AKR1C3	2.13692	0.00525
NQO1	2.12707	0.00757
lincRNA:chr12:4958789-4970589_F	2.12358	0.00459
RMRP	2.11267	0.00159
lincRNA:chr4:6672454-6675524_F	2.10136	0.00154
LBH	2.09956	0.0078
MDGA1	2.09779	4.02E-07
CROT	2.09409	0.00556
LOC100270680	2.06854	0.00127
TUBB4	2.06563	5.00E-04
lincRNA:chr1:86062087-86107987_R	2.06092	0.00042
STMN1	2.058	3.05E-06
IRF6	2.05192	0.00015
TNFRSF25	2.04873	0.00043
XPNPEP2	2.03524	0.00068
HIPK2	2.03296	2.88E-12
ENST00000377803	2.0307	0.00465
PVR	2.0279	0.00958
LBH	2.02518	2.73E-30
KCNE1L	2.0237	0.00901
lincRNA:chr1:11351113-11357788_R	2.02304	0.00012
DEPDC7	-2.00164	0.00629
PLCD4	-2.00323	0.00527
lincRNA:chr3:32516011-32517361_F	-2.00878	3.00E-05
LOC203274	-2.01138	4.56E-07
HDAC11	-2.01232	0.00633
TSPAN33	-2.01743	0.00972
MMP25	-2.01923	0.00638
CSDA	-2.02147	0.00441
ANTXR2	-2.02179	1.22E-07
SLC46A1	-2.02666	0.00122
BEGAIN	-2.03308	0.00102
PRAM1	-2.03387	0.00144
lincRNA:chr2:65103471-65188448_R	-2.04328	0.0011
IER5L	-2.05079	0.00779
ENST00000525262	-2.05209	1.60E-09
FAM134B	-2.0521	0.00027
BI056255	-2.05214	0.00832
ZNF280D	-2.05418	1.00E-05
DLL1	-2.06066	0.00458
TMPRSS13	-2.06552	5.00E-05
LOC400927	-2.08121	0.00036
ANTXR2	-2.0827	0.00182
TOP1MT	-2.08673	6.17E-08
LGALS3	-2.08977	6.30E-14
HMGB3P24	-2.0914	0.00405
DERL3	-2.10877	5.00E-05
ASS1	-2.1101	0.00994
STARD10	-2.11199	0.00795
FAM102A	-2.11323	1.00E-05
AHR	-2.11623	0.00522
P2RX5	-2.11799	0.0076
ADAM28	-2.11995	0.00578
TIGD3	-2.12581	0.00196
C19orf38	-2.1261	0.00041
LILRA1	-2.12787	0.0011
LOC100128252	-2.13203	0.00206
GPR155	-2.13386	2.00E-05
RASSF2	-2.13462	0.00186
JUP	-2.13488	2.50E-06
A_33_P3282988	-2.14837	0.00818
A_33_P3383900	-2.14978	0.00766
GPR155	-2.15201	4.00E-05
WDFY4	-2.16269	1.75E-16
UNC93B1	-2.16714	1.31E-10
KLRC1	-2.16816	0.00109
LMNA	-2.17346	0.00197
PROM2	-2.17758	0.00277
LOC284837	-2.18174	0.00471
FGD4	-2.183	0.00305

TNFRSF10A	-2.18626	2.82E-07
SEMA4A	-2.18678	0.00023
FGD4	-2.18706	0.00032
C3	-2.19203	0.00218
lincRNA:chr12:79972444-79982744_R	-2.19549	0.00459
EMR1	-2.1966	0.00013
C16orf74	-2.20452	5.62E-17
CD33	-2.20495	0.00284
MYBPC3	-2.21453	0.0073
PTP4A3	-2.21651	0.00142
FANCD2	-2.22223	0.00078
KLRC1	-2.2271	0.00094
CDHR1	-2.23931	0.00359
MBOAT1	-2.24104	0.00126
CDH23	-2.2411	0.00129
SLC5A2	-2.24157	0.00022
TP53I11	-2.24275	0.00593
TNFRSF10D	-2.24653	0.003
THC2471881	-2.25044	0.00749
FLNB	-2.256	0.00898
NOD2	-2.25629	2.92E-09
BCAR3	-2.25896	0.00315
MILR1	-2.26138	0.00401
FUT7	-2.26166	0.00231
UNC93B1	-2.26225	2.78E-09
CD79A	-2.27096	1.38E-08
IRAK3	-2.27243	0.00339
RALGPS2	-2.27482	3.00E-05
PIK3R6	-2.2757	0.00184
LOC286367	-2.27867	5.40E-06
CSDA	-2.28038	1.00E-04
C11orf63	-2.28169	0.0021
NCF1	-2.28343	2.94E-08
CYB561	-2.28385	0.0086
ITGB5	-2.28725	0.00522
A_33_P3407691	-2.28914	4.05E-06
IL2RA	-2.29669	0.00098
BEND4	-2.29697	0.00099
A_33_P3224800	-2.29827	0.00235
lincRNA:chr16:54952928-54957538_R	-2.30787	0.00191
lincRNA:chr6:34244122-34253868_F	-2.31233	0.00202
SIRPB1	-2.31297	0.00686
lincRNA:chr1:59049237-59065662_R	-2.32474	0.00367
lincRNA:chr3:97540883-97583240_F	-2.33543	2.33E-10
C1orf228	-2.33558	1.99E-16
AXL	-2.34518	0.00448
PPARGC1B	-2.34748	1.82E-07
CELSR1	-2.353	0.00895
EPB41L2	-2.361	0.00456
LOC100130579	-2.36976	0.00305
ITGAX	-2.3762	1.73E-09
PPARGC1B	-2.37666	2.89E-06
COTL1	-2.37932	0.00142
lincRNA:chr7:26530275-26535725_F	-2.38522	0.0049
PVRL3	-2.38918	6.86E-06
PTK6	-2.38918	0.00389
PNKD	-2.39004	0.00078
GNB4	-2.39197	0.00033
KMO	-2.39429	8.17E-13
RAB34	-2.39624	4.36E-07
HVCN1	-2.4	2.78E-07
FAM69B	-2.40197	1.97E-07
HVCN1	-2.40754	7.25E-06
ARHGAP22	-2.40851	0.00382
lincRNA:chr15:25328629-25332952_F	-2.40961	5.66E-06
SNN	-2.41467	0.00224
IQCJ-SCHIP1	-2.41561	0.00023
OSBPL1A	-2.42166	0.00805
MEF2C	-2.43098	4.82E-08
NCF1	-2.43481	9.00E-05
CCDC50	-2.43504	0.00083
MYC	-2.43663	2.70E-06

CXCR3	-2.44338	0.00023
COL4A4	-2.44885	0.00712
TAGLN	-2.46075	5.00E-05
NIPSNAP3B	-2.4662	9.47E-10
COL19A1	-2.46623	0.00818
LEF1	-2.46685	0.00053
PRR21	-2.46794	0.00108
TCF7	-2.47148	0.00782
SLC15A3	-2.47153	0.0076
IFT57	-2.47444	0.00024
HDAC11	-2.47689	0.00738
LTB	-2.48075	3.00E-05
C3orf57	-2.48109	0.00749
RAB31	-2.48593	0.00175
TMEM154	-2.48944	0.00023
BIRC3	-2.4958	4.50E-13
CDCA7L	-2.49948	5.39E-07
TAGLN	-2.50149	9.00E-05
lincRNA:chr15:25309917-25319198_F	-2.50221	0.00183
RNF207	-2.50442	0.00651
A_24_P256063	-2.50447	0.00729
CDC42BPB	-2.50596	3.17E-08
TCF4	-2.51222	3.00E-05
ZDHHC23	-2.51709	3.00E-05
CD2	-2.52003	0.00757
GFI1B	-2.52085	0.00019
SEMA7A	-2.5238	9.29E-10
IFNGR2	-2.52464	8.00E-05
EAF2	-2.52947	8.64E-09
AK024389	-2.54003	0.00029
PRDM8	-2.54361	2.35E-15
FBXL16	-2.54581	0.00672
ZNF365	-2.55061	1.19E-06
PTK2	-2.55334	0.00204
CAPG	-2.55444	0.00167
NCF1	-2.56333	1.00E-05
TTN	-2.56573	0.00123
lincRNA:chr8:129008365-129008906_F	-2.57288	0.00036
RRAGD	-2.57604	0.00541
MGLL	-2.59445	0.00867
SELL	-2.60234	0.00095
AFF3	-2.60377	1.00E-04
MAST4	-2.61453	8.00E-05
TRIM47	-2.61515	2.00E-05
ANXA5	-2.61547	1.00E-05
NCF1	-2.61654	0.00024
CYP2S1	-2.62605	0.00436
CAPG	-2.63446	0.00654
BAIAP3	-2.64421	0.00497
KLF8	-2.64623	0.00065
ADCY3	-2.65828	0.00053
ZNF365	-2.66812	6.40E-07
TMEM14E	-2.66911	0.00746
ENST00000390626	-2.67279	4.00E-05
IL1RL1	-2.67945	0.00893
SLITRK5	-2.69178	0.00048
MYLK	-2.69661	0.00779
lincRNA:chrX:68147000-68166900_F	-2.70328	0.00031
SCT	-2.71803	0.00028
CLIC4	-2.71896	3.35E-08
PDGFA	-2.73896	5.12E-07
TIMP2	-2.74491	1.00E-05
MGC39372	-2.74735	0.00562
TRIP6	-2.75235	6.33E-12
C17orf28	-2.76922	0.00766
TLR9	-2.77394	4.00E-05
SCARB1	-2.77832	4.48E-06
CD74	-2.78259	5.15E-07
ROR1	-2.80093	0.00282
NCF4	-2.81458	3.40E-09
ZFP42	-2.82406	0.00137
CUEDC1	-2.82556	0.00244

ENST00000390295	-2.82934	0.00191
CDKN1A	-2.83808	0.0045
SPIN3	-2.84708	7.00E-05
CXorf38	-2.85337	1.00E-05
lincRNA:chr5:55753680-55777514_R	-2.85989	5.00E-05
ALCAM	-2.861	0.00056
BATF3	-2.86375	0.00249
P2RY14	-2.86611	0.00138
lincRNA:chr10:49893514-50016263_F	-2.87269	7.00E-05
LOC100130992	-2.87687	0.0067
GHRL	-2.88486	0.00179
ENTPD1	-2.88582	6.45E-10
SRGAP1	-2.89155	0.00029
CBLN3	-2.89211	1.00E-05
SNORD3B-1	-2.89741	0.00748
ENST00000390549	-2.9009	0.00014
GYLTL1B	-2.90899	0.00094
NAPSA	-2.91551	0.00025
PTGS1	-2.91877	0.0054
BEST1	-2.92754	0.00018
AJ252276	-2.934	0.00067
PBX1	-2.93404	0.00022
RPS6KA2	-2.93737	0.00907
VAV2	-2.93775	2.64E-08
LY86	-2.95011	8.00E-05
BMF	-2.95998	4.06E-11
THC2564554	-2.97017	6.00E-05
ABCA1	-2.97771	0.00631
WDR86	-2.99416	0.00316
ATP6V0A1	-2.99776	1.00E-05
ENST00000261651	-2.9985	0.00032
IL7R	-3.00865	0.00216
SLC10A7	-3.01234	7.00E-05
SGCA	-3.01739	3.10E-06
UBXN10	-3.01763	0.00179
OBSL1	-3.01878	0.00509
SUPT3H	-3.02338	0.00431
PROC	-3.03447	0.00796
STK33	-3.03742	1.78E-06
TFEC	-3.04289	0.00136
GABRA3	-3.04661	3.96E-07
RIMKLA	-3.04818	0.00851
COL9A2	-3.05141	0.0038
KCNQ1	-3.05838	0.00089
HSPG2	-3.06031	8.93E-07
CHST15	-3.06147	0.0096
ZNF365	-3.063	8.00E-05
lincRNA:chr15:25310225-25312679_F	-3.06351	3.07E-12
CD70	-3.06526	5.87E-08
CLIC4	-3.06717	0.00027
CLEC17A	-3.08327	0.00735
HLA-DMA	-3.08973	4.95E-10
CCR7	-3.10499	0.00139
TMEM63C	-3.11221	0.00243
NEFL	-3.11492	0.0065
HLA-DMA	-3.12425	3.24E-09
P2RY13	-3.13435	0.00473
SELP	-3.13965	0.00501
PPP1R9A	-3.14092	0.00323
ARHGAP40	-3.14403	0.00014
CKB	-3.16876	0.00486
PRDM8	-3.17712	3.64E-06
lincRNA:chr8:129000922-129004320_F	-3.17985	0.00013
GAB1	-3.181	0.00907
ESPNL	-3.18172	0.00275
C2	-3.20135	0.0057
NCRNA00173	-3.2098	0.00029
NLN	-3.21321	0.00209
GPR183	-3.21326	0.00016
CIITA	-3.21872	0.00367
NT5DC3	-3.21935	0.00074
lincRNA:chr1:101548009-101552817_F	-3.22116	0.00024

SMOX	-3.24111	0.0022
FNBP1L	-3.25377	0.00321
LPCAT2	-3.27222	0.00305
DGAT2	-3.30501	0.00025
SPINT2	-3.31266	3.32E-09
DAPP1	-3.32234	4.12E-15
FGD2	-3.32716	5.66E-08
SUSD3	-3.3341	7.44E-07
DOK3	-3.3502	0.00216
ENTPD1	-3.36527	3.39E-08
HLA-DPB1	-3.42995	1.13E-09
RNF207	-3.45211	0.00558
MACC1	-3.45891	2.43E-08
HLA-DRB5	-3.46178	0.00039
ZC3H12D	-3.484	0.00045
MSRB3	-3.48552	0.00213
HLA-DPB1	-3.48653	2.39E-13
MOXD1	-3.48701	0.00299
C5orf20	-3.48771	0.0027
IL3RA	-3.48806	0.00632
lincRNA:chr9:21506160-21506630_R	-3.4889	0.00096
ST3GAL6	-3.49563	0.0018
GABBR1	-3.49774	7.57E-11
MZB1	-3.52507	4.05E-09
ENST00000390600	-3.52767	0.00161
HLA-DRB4	-3.53466	5.06E-13
ULK2	-3.53936	8.25E-06
LOC400958	-3.54187	8.00E-05
BMF	-3.54865	0.00177
EPS8	-3.61123	0.00541
ENST00000390304	-3.62169	9.00E-05
ITLN1	-3.62894	0.00101
HLA-DPB1	-3.64353	6.73E-16
HLA-DPB1	-3.64403	3.07E-20
BIK	-3.64452	0.00128
COL8A2	-3.6539	0.00371
SIT1	-3.65859	0.00199
HLA-DPB2	-3.66025	1.70E-22
CLMN	-3.66634	0.00073
CRIP2	-3.67078	0.00028
ENST00000427632	-3.69072	0.00381
PFN2	-3.6978	0.0052
LOC100505564	-3.71617	0.00023
LYL1	-3.71837	8.72E-06
CDCA7L	-3.73454	3.01E-06
BACE2	-3.75345	7.00E-04
NT5E	-3.76758	3.58E-06
ENST00000547498	-3.78529	0.00068
MYL2	-3.79733	0.00309
HLA-DQB1	-3.81131	0.00428
HLA-DMB	-3.8528	2.32E-11
HLA-DPA1	-3.85479	4.54E-10
ARHGEF17	-3.89792	2.86E-09
PLXNB2	-3.89841	0.00509
ENST00000491977	-3.91379	0.00071
LOC100131654	-3.9179	0.00178
lincRNA:chr8:128807043-128820943_F	-3.92432	0.00051
CSF2RA	-3.94198	0.00045
TIAM2	-3.96166	0.00017
ITM2C	-3.98249	2.00E-05
RNF207	-4.01208	0.00061
EMR3	-4.02083	0.00143
SLC9A7	-4.02307	1.58E-08
ADRBK2	-4.02974	9.99E-10
SLC9A7P1	-4.03385	1.00E-05
ITM2C	-4.04411	1.32E-06
HLA-DPA1	-4.0458	3.82E-12
LOC100510059	-4.04674	3.00E-05
INSR	-4.04917	5.13E-06
FAM164A	-4.07389	0.0021
PKIG	-4.07595	7.00E-05
LOC285286	-4.12393	0.00588

ZNF717	-4.13024	0.008
C1orf186	-4.13788	5.67E-07
lincRNA:chr13:33888375-33923595_F	-4.1761	1.56E-06
LRRK1	-4.19127	0.00066
ENST00000390629	-4.20869	4.53E-06
lincRNA:chr21:45228747-45238991_R	-4.21745	0.00906
TFCP2L1	-4.22608	0.00653
ENHO	-4.24519	1.00E-05
CLEC10A	-4.2499	0.002
NP109356	-4.29531	0.00013
AFF3	-4.29675	0.00025
ENST00000409515	-4.30052	0.00515
LOC100130269	-4.33067	0.00332
ENST00000549427	-4.35274	0.00183
lincRNA:chr2:64455601-64479960_F	-4.37663	0.00017
MYOF	-4.38481	0.00443
VENTX	-4.39871	0.00665
RCN3	-4.40032	0.00018
ENST00000304890	-4.42636	0.00086
HLA-DRB1	-4.45754	8.37E-12
lincRNA:chr6:44059763-44060019_R	-4.4731	5.00E-04
PKIG	-4.50118	0.003
SPINT1	-4.53221	1.00E-04
ALPK1	-4.54765	7.97E-06
LOC100133661	-4.55402	0.00018
ENST00000390291	-4.56886	0.00027
ENST00000531609	-4.58125	0.00962
CLIC4	-4.60886	5.08E-06
BTNL9	-4.63176	1.13E-06
PTPN13	-4.64961	0.00038
ENST00000390298	-4.65547	8.00E-05
ENST00000390305	-4.67001	2.00E-04
ITPRIPL2	-4.70058	0.00239
FZD1	-4.74505	0.00214
ID4	-4.75293	1.88E-11
CD82	-4.75707	5.33E-09
MS4A3	-4.78184	0.00917
FER1L4	-4.78289	0.00016
LOC644145	-4.80635	2.00E-05
TTC21A	-4.93815	6.02E-09
MS4A14	-4.93878	0.00151
GPR55	-4.95481	5.95E-08
ENHO	-4.96401	0.00058
KIAA0125	-4.96416	7.16E-11
NAPSA	-4.96921	0.00043
ZBED2	-4.97636	0.00027
BCAT1	-4.98653	5.00E-05
DQ272581	-4.99906	0.00937
PTPRK	-4.99993	2.86E-07
HLA-DRB3	-5.00611	1.18E-24
FCRL1	-5.01914	7.67E-13
ENST00000390268	-5.03527	3.32E-06
SIGLEC6	-5.06375	9.03E-07
MGAT3	-5.06613	1.77E-09
ICOSLG	-5.06646	0.00029
RALGPS2	-5.06816	2.27E-08
FRAS1	-5.07766	0.00103
ALOX5	-5.11979	1.66E-06
COL8A2	-5.12669	0.00032
DNASE1L3	-5.16055	0.00119
lincRNA:chr5:81650244-81658219_R	-5.19017	0.00416
GAPT	-5.25246	8.00E-05
PROC	-5.25666	1.34E-07
SIGLEC10	-5.28022	0.00059
UGGT2	-5.34713	2.00E-05
DHRS9	-5.35784	0.00143
VMO1	-5.36339	0.00292
SH2B2	-5.36914	4.49E-11
lincRNA:chr7:22611311-22612083_R	-5.39624	9.25E-07
EMP1	-5.41068	0.00694
ANK1	-5.43901	8.85E-10
ENST00000531730	-5.44727	0.00167

CD5	-5.48222	5.41E-17
FAM20A	-5.48698	0.00097
KYNU	-5.52347	2.00E-05
IGLL1	-5.53726	2.19E-09
lincRNA:chr7:22611226-22701411_R	-5.55827	0.00328
BASP1	-5.61519	7.40E-06
APP	-5.65021	1.00E-05
ENST00000390597	-5.70347	0.00232
TUBB6	-5.7052	0.00014
GABBR1	-5.71591	2.77E-11
DKFZP434L187	-5.76035	0.00195
PLEKHG7	-5.80394	1.32E-09
C10orf105	-5.81022	6.00E-05
IL7	-5.81779	6.47E-13
PTPRO	-5.82658	4.90E-09
MCOLN2	-5.84011	2.03E-09
TNS3	-5.93494	4.00E-05
TNFRSF13B	-5.95107	0.00047
BCL7A	-5.99308	2.42E-18
BTK	-6.00759	2.33E-07
EBI3	-6.02016	2.66E-20
FLJ38379	-6.06573	0.00035
BCL11A	-6.15811	2.92E-07
NTNG1	-6.18088	0.0066
DENND5B	-6.24192	5.85E-07
MOBKL2B	-6.3404	1.05E-08
COL4A3	-6.34545	2.76E-13
lincRNA:chr11:117668490-117680359_R	-6.41469	0.00012
ACPP	-6.42353	6.00E-05
LOC200772	-6.43183	0.00044
GNG7	-6.58509	1.38E-18
DENND5B	-6.66034	1.55E-06
HLA-DRA	-6.70384	9.84E-08
TCL1A	-6.7139	2.00E-05
ENST00000390600	-6.72236	2.83E-06
KIAA0125	-6.82828	0.00044
SFTPD	-6.85372	0.00096
BCL11A	-6.94082	2.00E-05
MZB1	-6.98133	2.94E-11
LOC283710	-7.0479	4.06E-11
CIITA	-7.09505	2.21E-20
MPP3	-7.14894	8.64E-08
ENST00000390282	-7.16399	2.89E-12
KMO	-7.24948	2.16E-09
PDE8B	-7.25396	1.00E-05
CBFA2T3	-7.34848	2.44E-08
VPREB3	-7.38934	3.39E-18
BTK	-7.57526	9.14E-12
MOBKL2B	-7.58078	3.76E-06
HLA-DQA2	-7.68084	3.13E-25
LOC284219	-7.68972	7.00E-05
LGMN	-7.69852	3.84E-08
CLIC2	-7.97207	1.28E-06
MRAS	-7.98707	4.00E-05
lincRNA:chr4:26806777-26850102_R	-8.06612	0.00204
COL9A3	-8.0725	7.18E-18
ITFG3	-8.11109	0.00105
COCH	-8.15368	1.00E-05
ABCC3	-8.32751	0.00016
KREMEN2	-8.34269	3.61E-19
IL28RA	-8.58544	8.71E-11
PAPSS2	-8.61726	6.29E-08
GAS6	-8.64176	9.60E-09
C7orf16	-8.70276	3.00E-05
ICAM4	-8.8486	1.28E-06
PLEKHG1	-8.85582	3.87E-14
ENST00000390256	-8.86294	0.00312
ENST00000390265	-8.93873	3.55E-08
CDK14	-8.9893	4.01E-12
AK128421	-9.11695	1.69E-11
LEPREL1	-9.12092	4.00E-05
ENST00000390284	-9.17286	2.31E-09

ENST00000477036	-9.17335	0
ENST00000390301	-9.3575	2.01E-06
PLD4	-9.37914	0.00017
HLA-DQA1	-9.4106	1.25E-30
HLA-DQA1	-9.57875	0
SCARA5	-9.73178	3.55E-06
PPM1J	-9.7912	6.00E-05
HLA-DOA	-9.8198	2.84E-15
HS3ST1	-9.8319	8.39E-21
A_33_P3418321	-9.85503	6.00E-05
PRICKLE1	-10.09737	3.32E-15
KCNN4	-10.11104	2.79E-33
ABCB4	-10.17133	0
ENST00000390312	-10.21327	3.95E-09
FLT3	-10.22403	6.36E-09
NXPH4	-10.28877	5.94E-12
A_33_P3307192	-10.43924	0.00209
LIMS2	-10.7609	1.57E-19
ADAM19	-10.76942	3.11E-39
IGJ	-10.88229	2.00E-05
SYT17	-10.9227	1.36E-08
CXCR5	-11.22639	7.75E-14
TNFRSF13C	-11.2548	1.11E-09
TBC1D9	-11.3747	2.00E-08
SLC2A5	-11.55617	1.14E-17
ENST00000390283	-11.66012	6.00E-05
DNAJC5B	-11.85418	0.00117
LPL	-11.91101	3.54E-06
lincRNA:chr10:65236069-65272880_F	-11.96109	0.0079
LOC96610	-12.07566	7.96E-11
LYPD2	-12.31674	4.06E-06
LOC149773	-12.51689	2.57E-06
CD1C	-12.60621	1.20E-16
DQ098707	-12.61042	8.67E-11
AIM2	-12.71312	7.42E-09
PMEPA1	-12.94315	3.89E-15
LOC283663	-13.04615	3.43E-13
KCNG1	-13.07014	4.12E-19
lincRNA:chr14:58754750-58755876_F	-13.25046	0.00103
ADD2	-13.26871	1.79E-15
CDH1	-13.32591	1.18E-09
L1TD1	-13.45085	1.22E-07
A_33_P3251412	-13.46671	3.00E-05
ENST00000390323	-13.54216	1.35E-12
S77011	-13.55736	1.20E-08
SYNPO	-13.63397	2.65E-15
COBLL1	-13.64927	1.10E-11
LRRC14B	-13.82479	0.00073
FAM129C	-13.87167	6.94E-28
IL6	-14.11133	0.00041
AF058072	-14.50957	9.89E-20
BCL11A	-14.73464	2.37E-11
AF085654	-14.87823	5.92E-21
WDFY4	-14.99211	8.69E-30
HRK	-15.39669	4.59E-10
FCRL5	-15.91267	1.28E-15
WDFY4	-16.09646	1.56E-32
LOC100132941	-16.3032	3.12E-16
BTLA	-16.35479	3.77E-16
TLR10	-16.64017	5.83E-31
SPIB	-17.69522	2.98E-17
FCRL2	-17.82269	4.21E-09
FAM129C	-17.86552	4.18E-14
BLNK	-17.96654	5.96E-16
VPREB3	-18.22386	1.24E-24
ENST00000483158	-18.87628	1.85E-12
ENST00000453166	-20.55688	6.45E-07
BANK1	-20.94769	8.10E-37
FCRL1	-20.97202	2.86E-11
CD24	-21.07023	4.55E-11
ENST00000498435	-21.23822	1.47E-10
ENST00000390549	-21.30495	1.13E-10

SLC4A3	-22.78108	1.87E-09
ENST00000471857	-23.08864	1.36E-20
LOC152225	-23.38226	5.88E-15
BLNK	-24.16102	4.29E-17
ENST00000468879	-24.9297	2.07E-09
CD22	-25.21356	4.14E-14
FCRL2	-25.5361	5.82E-22
ENST00000390602	-25.68971	1.39E-41
ENST00000390556	-25.99785	5.19E-24
ENST00000492446	-28.10088	3.49E-15
AF194718	-28.31807	1.25E-15
ENST00000390294	-28.98927	1.27E-08
FCRLA	-29.70317	0
LOC401847	-29.83713	1.86E-21
ENST00000390297	-30.11857	1.38E-08
PNOC	-30.8357	1.74E-18
CD19	-31.5894	6.08E-36
ENST00000390604	-31.89311	5.33E-24
BF175071	-31.98391	3.41E-12
ENST00000390617	-32.4836	1.24E-14
FCRLA	-32.86758	0
ENST00000492167	-32.96331	6.48E-13
SNX22	-33.10691	5.57E-17
C13orf18	-33.34941	9.88E-21
ENST00000390636	-33.90577	3.18E-20
ZBTB32	-35.76022	2.17E-26
CPNE5	-36.60059	1.87E-33
ENST00000390323	-36.82059	5.10E-16
ENST00000390629	-37.01991	1.77E-16
ENST00000479981	-37.28387	6.59E-12
CR2	-37.45994	0
ENST00000390551	-38.05157	2.73E-12
MS4A1	-38.44199	1.00E-20
ENST00000474213	-39.05642	1.02E-11
ENST00000390632	-39.27282	9.98E-14
ENST00000390237	-43.35363	5.15E-13
OSBPL10	-43.6717	1.26E-31
ENST00000390539	-44.91785	6.63E-15
BLK	-45.01957	1.07E-24
AB363267	-45.75781	1.24E-15
ENST00000390615	-45.99879	1.31E-15
NP113779	-47.00494	3.04E-15
IGLL5	-48.20793	2.05E-21
FCRL5	-49.47239	3.10E-27
ENST00000426099	-49.55975	9.46E-25
ENST00000390243	-54.00483	7.94E-16
ENST00000390624	-54.16075	4.80E-20
ENST00000390547	-55.85385	1.18E-25
POU2AF1	-57.77307	3.62E-41
ENST00000390247	-57.87497	2.28E-24
ENST00000354689	-59.17162	8.42E-26
ENST00000390603	-59.25721	3.97E-30
ENST00000424969	-62.74327	7.03E-23
ENST00000390632	-63.51356	9.40E-34
LOC100510044	-63.59669	4.16E-38
ENST00000390559	-71.19186	0
ENST00000471857	-77.78079	0

Appendix Table VI-2. CyTOF panel for experiments shown in Appendix VI-1.

Atomic mass	Marker	Clone	Company
112	CD3	S1.4	Invitrogen
114	CD3	S1.4	Invitrogen
115	CD57	HCD57	BioLegend
142	CD69	MCA1442	AbD Serotec
143	CD5	UCHT2	BioLegend
144	CD45RO	UCLHL1	BioLegend
145	CTLA-4	BNI3	BD Biosciences
146	CD8	SK1	BioLegend
147	GM-CSF	BVD2-21C11	BioLegend
148	CD45RA	HI100	eBioscience
149	CD4	SK3	BioLegend
150	MIP-1β	D21-1351	BD Biosciences
151	Granzyme B	2CF/F5	BD Biosciences
152	TNFα	MAb11	eBioscience
153	CD107a+b	H4A3, H4B4	BD Biosciences
154	CD27	LG.7F9	eBioscience
156	CD33	P67.6	Santa Cruz
	CD13	WM15	BioLegend
157	CD19	HIB19	BioLegend
158	CD16	3G8	BioLegend
159	CD56	NCAM16.2	BD Biosciences
160	CD28	CD28.2	BD Biosciences
161	CD38	HIT2	BioLegend
162	γδ TCR	FIT-22	BioLegend
165	CD127	A019D5	BioLegend
166	IL-2	MQ1-17h12	eBioscience
167	CD161-APC	191B8	Miltenyi Biotec
168	CCR7	150503	R&D Systems
170	IFNγ	4S.B4	eBioscience
171	HLA-DR	L23	BioLegend
172	CD40L	24-31	eBiosciences
174	CD62L	PE001	BioLegend
176	Perforin	B-D48	AbCam
123, 139	Live/dead	na	DVS Sciences
191, 193	DNA	na	na

7. Discussion

MAIT cells were first identified in 1993 by virtue of their expression of a unique TCR α rearrangement (Porcelli et al., 1993), which was subsequently ascribed to a novel subset of T cells restricted by MR1 (Tilloy et al., 1999). Major advances in our understanding of the role of MAIT cells in the immune system have occurred in the last few years. MAIT cells have been shown to detect a variety of microbes through the recognition of vitamin B metabolites presented by MR1 (Gold et al., 2010; Kjer-Nielsen et al., 2012; Le Bourhis et al., 2010). Furthermore, these cells were found to largely overlap with a unique subset of CD8+ T cells expressing CD161 at a high level, capable of producing IL-17 (Billerbeck et al., 2010; Dusseaux et al., 2011). The ability of these cells to be activated both through their TCR and by innate cytokines (Ussher et al., 2014a) further broadens their potential role in disease, even in the absence of the riboflavin ligand for MR1. In this thesis, further effector functions of human MAIT cells, and whether they may play a role in psoriatic disease, was explored. Furthermore, as all T cells expressing CD161 share a transcriptional signature and innate responsiveness to cytokines associated with MAIT cells (Fergusson et al., 2014), the question of whether this may be extended to NK cells was addressed in a detailed characterization of CD161+ and CD161− NK cells.

7.1. MAIT cells and their effector functions

7.1.1. License to kill: upregulation of GrB by MAIT cells

In Chapter 3, low grade but specific MAIT cell killing of target cells presenting MR1 ligands, but not control target cells, was demonstrated using a novel flow-cytometric killing assay. The low cytotoxicity of resting MAIT cells was associated with their

expression of GrA and GrK, lack of GrB, and low levels of perforin expression compared to conventional CD8+ T cells. Upon short-term bacterial exposure, however, MAIT cells upregulated GrB and perforin, and upon prolonged activation, further enhanced GrB and perforin expression and downregulated GrK expression, which greatly enhanced killing of target cells compared to paired, *ex vivo* MAIT cells.

Early upregulation of GrB induced by bacterial stimulation of MAIT cells was dependent on MR1, but also required costimulation provided by IL-12. Additionally, long-term stimulation with cytokines could also induce the expression of GrB and perforin in a TCR-independent manner. In support of these results, cytokines such as IL-7 (Leeansyah et al., 2015) and IL-15 (Sattler et al., 2015) have been shown to enhance the TCR-induced cytotoxicity of MAIT cells, as well as inducing TCR-independent upregulation of GrB. Together, these results suggest that expression of GrB by MAIT cells is tightly regulated and either requires the presence of an MR1 ligand for early GrB expression, or persistent exposure to proinflammatory or homeostatic cytokines. Whether MAIT cells downregulate GrB expression following the removal of the pathogen or cytokines has not been investigated. Interestingly, however, GrB has been shown to be upregulated in the peripheral blood and adipose tissue MAIT cells of obese patients, and only returned to levels comparable to healthy controls 6 months after bariatric surgery (Magalhaes et al., 2015). GrB may therefore be a useful activation marker of MAIT cells.

An *in vivo* role for GrB expression by MAIT cells and direct cytotoxicity remains to be demonstrated. Recent studies have shown that MAIT cells can lyse cells infected with BCG (Lepore et al., 2014) and *Shigella* (Martin et al., 2013), which may be important for protection, given the abundance of these cells in the lung and gut. Other innate-like T cells also demonstrate polyfunctional ability, secreting a broad range of cytokines, but also mediating killing. γδ T cells can lyse tumour cells through

the recognition of endogenous phosphoantigens, as well as through NKG2D (Meraviglia et al., 2010). iNKT cells can also upregulate GrB upon TLR stimulation (van Gisbergen et al., 2012). However, their anti-tumour activity induced by αGalCer injection in mice is mediated indirectly by IFNγ secretion, which activates NK cells (Kawano et al., 1998; Wingender et al., 2010). Murine models of MAIT cells have also suggested that control of bacterial growth by MAIT cells requires IFNγ, rather than MR1-dependent cytolysis (Chua et al., 2012; Meierovics et al., 2013). Thus, questions remain about the relative importance of direct killing and cytokine production in the antibacterial role of MAIT cells, and about whether MAIT cells have anti-tumour activity, either directly e.g. following NKG2D ligation, or indirectly through IFNγ-mediated NK cell activation.

7.1.2. Can CD4+ MAIT cells kill?

In contrast to CD8+ and DN MAIT cells, which readily degranulated in response to *E. coli*-treated THP1 cells regardless of the content of their cytotoxic granules, CD4+ MAIT cells showed no mobilization of the degranulation marker CD107a (Chapter 4). Furthermore, resting CD4+ MAIT cells expressed significantly less GrA, GrK, and perforin compared to their CD4− counterparts, and showed reduced GrB expression even after activation. Amongst the transcription factors investigated, the greatest difference between the CD4+ and CD4− subsets was the low expression of Eomes by these cells. As Eomes and T-bet expression together regulate the ability of cells to acquire cytotoxic function (Gordon et al., 2012; Intlekofer et al., 2005; Kallies et al., 2011), lack of Eomes expression may be associated with the reduced cytotoxicity of CD4+ MAIT cells. Whether CD4+ MAIT cells are truly unable to lyse target cells or express GrB has not yet been assayed here. Other mechanisms of target cell killing, such as via FasL, may play a larger role for CD4+ MAIT cells. For instance, although CD4+ iNKT cells are similarly low in their capacity to kill via the cytotoxic granule

exocytosis pathway, they are the main iNKT population to express FasL (Gumperz et al., 2002), which is in fact the dominant mechanism by which iNKT cells kill tumour cells in a CD1d-dependent manner (Wingender et al., 2010).

7.1.3. Th2 cytokine production by CD4+ MAIT cells

The low cytotoxic potential of CD4+ MAIT cells was associated with reduced Th1 cytokine production. While CD8+ MAIT cells, and to a lesser extent, DN MAIT cells had a suppressed ability to secrete IL-4 and IL-13, CD4+ MAIT cells were able to secrete significantly more Th2 cytokines. Interestingly, Eomes is induced by the CD8-lineage promoter Runx3, and enforced expression of Runx3 in Th2 cells inhibits IL-4 production (Yagi et al., 2010). Although we have not looked at Runx3 expression, this may be another transcription factor expressed differentially by MAIT cell subsets. Together with their unique enrichment in tonsils, they may be able to perform immunoregulatory functions such as providing help for B cell activation and antibody production (Zeng et al., 2013), and suppressing autoimmunity (Oh & Chung, 2011), as has been demonstrated for CD4+ iNKT cells. The differences and similarities between the subsets of MAIT cells are summarised in Figure 7-1.

7.1.4. Lineage decisions by MAIT cells

The signals that determine the CD4/CD8 lineage of MAIT cells, and therefore their potential effector functions, are unclear. Although iNKT cells do not require CD4 for their development, strong and persistent signaling through their TCR is thought to induce CD4 lineage commitment, and subsequently, a fraction of CD4+ cells downregulates CD4 to become DN cells (Engel et al., 2010; Savage et al., 2008). In a humanized mouse model, CD8+ cells had a lower TCR avidity compared to other iNKT cell subsets, which led to the induction of Eomes (Wen et al., 2015). Thus, it is

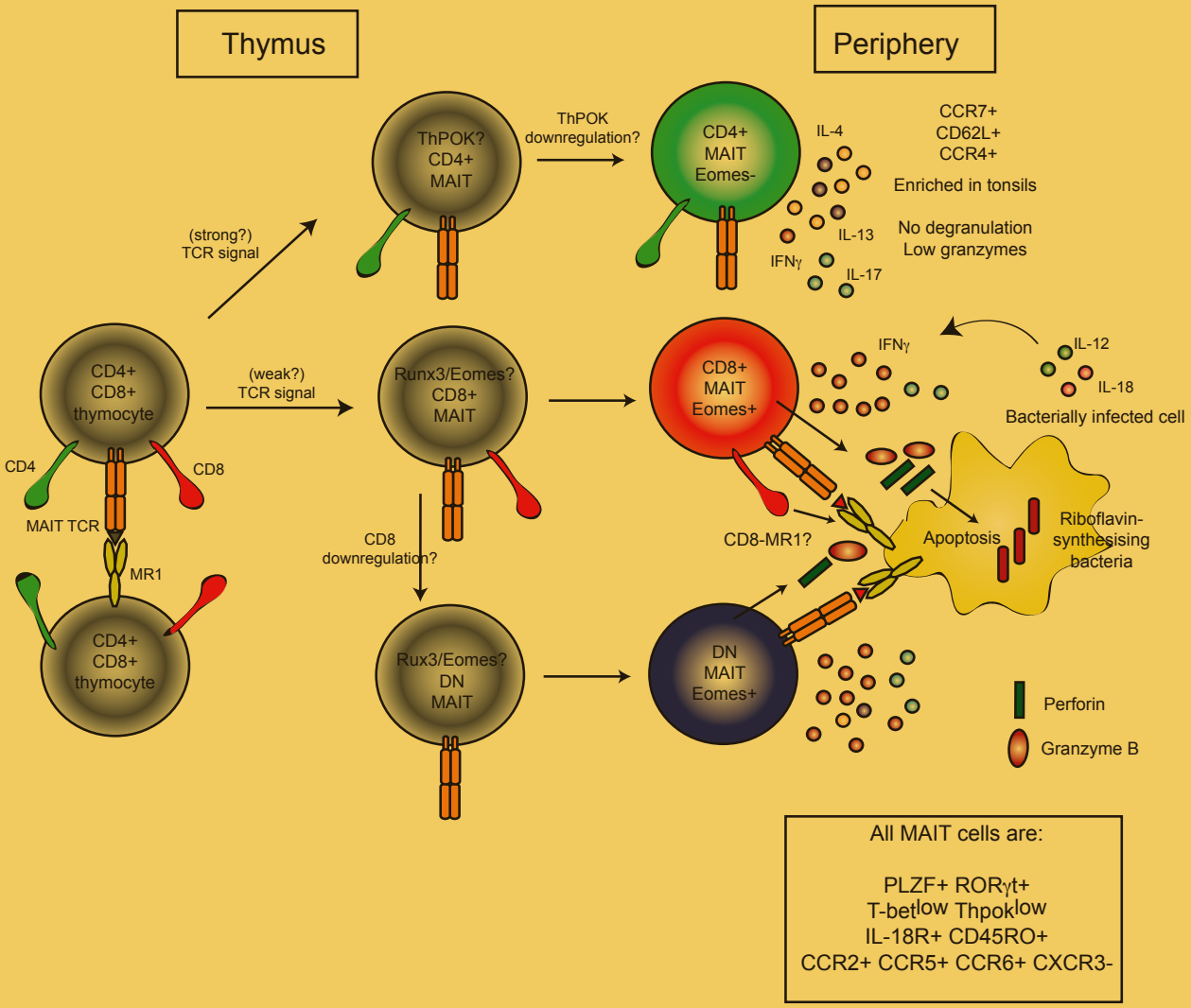


Figure 7-1. Model showing possible developmental and functional differences between MAIT cell subsets. MAIT cells are selected by CD8+CD4+ thymocytes expressing MR1. Coreceptor expression by selected MAIT cells may be determined by the strength of the TCR signal induced, which can induce ThPOK, the master transcription factor of the CD4 lineage, or the repressor of the CD4 lineage, Runx3, which in turn induces Eomes. CD8 may be downregulated on MAIT cells to become double-negative (DN) MAIT cells during development, as the CD4+, CD8+ and DN populations are already present at birth. In the periphery, CD8+ and DN MAIT cells can induce the lysis of cells infected with bacteria possessing the riboflavin synthesis pathway, by upregulating GrB and perforin in response to MR1 stimuli and cytokines. The CD8 coreceptor may also may a role in the activation of CD8+ MAIT cells. CD8+ and DN MAIT cells also secrete abundant IFNγ in response to MR1-induced stimulation as well as IL-12+IL-18, and are the dominant populations in peripheral blood and tissues. CD4+ MAIT cells are enriched in tonsils, in contrast, and express lymphoid tissue homing receptors. They have a greater capacity to secrete IL-4 and IL-13, but cannot mediate cytotoxicity through granule exocytosis. All MAIT cells share RORγt expression, and therefore can secrete IL-17.

tempting to speculate that weaker TCR signaling in the thymus during MAIT cell development leads to the CD8+ phenotype dominant in humans (Figure 7-1). Weaker TCR signaling in γδ T cells also leads to the development of IL-17-secreting γδ T cells (Turchinovich & Hayday, 2011). Given that induction of other transcription factors such as PLZF during innate T cell development is regulated by the strength of TCR signaling (Alonzo et al., 2010; Qiao et al., 2012), it will be important to investigate the signals that induce the transcription factors associated with MAIT cell effector functions.

7.2. MAIT cells and their role in autoimmunity

7.2.1. MAIT cells in psoriatic disease

All subsets of MAIT cells could secrete IL-17 upon stimulation (Chapter 4), which was confirmed to be completely dependent on RORγt using a novel RORγt inhibitor (Chapter 5). Given the importance of IL-17 in driving several autoimmune diseases, including psoriasis and arthritic diseases (Yoo et al., 2012), the function and phenotype of MAIT cells in psoriasis and psoriatic arthritis was investigated. MAIT cells trended towards a lower frequency in the blood of psoriasis patients compared to healthy controls and AD patients, although significance was not reached in this study and needs to be further investigated. MAIT cells were also present in the psoriatic and healthy skin, albeit at low frequencies, which has been demonstrated in a recent study (Teunissen et al., 2014). Much more striking was their presence in the synovial fluid of PsA patients, which correlated with clinical measures of inflammation. As murine MAIT cells have been shown to exacerbate CIA in mice (Chiba et al., 2012), MAIT cells, which made up to 60% of CD8+ T cells in the synovial fluid, have the potential to drive the pathology of PsA.

Interestingly, one PsA patient studied in Chapter 5 had active psoriasis and PsA, and synovial fluid samples were collected before and after treatment with the commonly used anti-rheumatic drug, methotrexate. In this patient, psoriasis was improved by methotrexate treatment but PsA was exacerbated, with a corresponding increase in the frequency of MAIT cells in the synovial fluid. MAIT cells express the multidrug resistance protein 1 (MDR1) (Turtle et al., 2009), which can efflux a variety of drugs from the cytoplasm. Expression of MDR1 confers resistance to immunosuppressive drugs, and thus exposure of CD8+ T cells to cytotoxic chemotherapy drugs selects for the survival of MAIT cells within CD8+ T cells (Turtle et al., 2009). MDR1-conferred resistance is known to affect the outcome of methotrexate treatment in rheumatoid arthritis patients (Kato et al., 2012). Therefore determining the role of MAIT cells in these autoimmune diseases is vital; if found to be actively contributing to pathology, current treatments may be exacerbating the disease by promoting their preferential survival.

MAIT cells showed increased IL-17 production within the synovial fluid of PsA patients, although whether this correlates with disease activity has not been investigated. Furthermore, the effect of the novel RORγt inhibitor on the production of IL-17 from these synovial fluid MAIT cells has not been tested here. However, almost all T cells produced IL-17 in the synovial fluid, and MAIT cells only constituted a small frequency of IL-17+ cells within CD8+ T cells. This is supported by another study looking at IL-17+CD8+ T cells in PsA patients, which showed that IL-17 was mainly produced by non-MAIT CD8+ T cells both in the joint and the periphery (Menon et al., 2014). Furthermore, another study of CD8+ T cells in psoriatic lesions showed that non-MAIT, CD161+ and CD161− CD8+ T cells had the capacity to secrete abundant IL-17 (Teunissen et al., 2014). Thus in inflammatory tissues, and in some cases, the peripheral blood, IL-17 can be produced by non-MAIT CD8+ T cells, and therefore co-expression of CD8 and IL-17 cannot be used as a surrogate for

MAIT cells in clinical studies. What drives this increased capacity of T cells to express IL-17 in psoriasis and PsA is unknown. Preliminary experiments from a small number of PsA synovial samples showed that RORγt expression is not significantly different in T cells from these patients' synovial fluid, compared to T cells from paired blood samples. Ultimately, whether MAIT cells play a unique role in these psoriatic diseases should be further investigated using *in vivo* models, such as the imiquimod-induced model of psoriasis, corroborated with a larger cohort of patients.

7.2.2. Activation of MAIT cells in autoimmune diseases

Although most studies examining IL-17 production in psoriasis and PsA patients use non-specific, PMA/ionomycin stimulation to activate T cells, a factor that may potentiate the specific activation of MAIT cells in autoimmune disease is their ability to be activated by cytokines alone (Jo et al., 2014; Ussher et al., 2014a). Indeed, MAIT cells could be activated in an innate manner by IL-23+IL-18 to produce IFNγ, although innate IL-17 production remains to be demonstrated. Furthermore, culture with Th17-skewing cytokines such as IL-23 enhanced IL-17 production from MAIT cells compared to cells only stimulated with TCR beads, which was not observed in conventional CD4+ T cells. The sensitivity of MAIT cells to IL-23 should therefore be compared directly with other IL-23-responsive populations, such as Th17 cells and γδ T cells. The therapeutic success of IL-23-blocking antibodies in psoriasis (Kauffman et al., 2004; Krueger et al., 2007; Toichi et al., 2006), and recent research highlighting a role for innate, IL-23-responsive populations such as γδ T cells and ILC3 cells in driving psoriatic skin inflammation (Cai et al., 2011; Leijten et al., 2015; Pantelyushin et al., 2012) suggests that IL-23-responsive populations may be the critical drivers of psoriatic diseases. As dermal γδ T cells isolated from psoriatic lesions, but not healthy skin, produced IL-17 in response to IL-23 alone (Cai et al., 2011), MAIT cells isolated from the psoriatic lesions and synovial fluid of PsA

patients should be stimulated with IL-23 to investigate whether they are also able to produce IL-17 in an innate manner.

Another question that remains is whether MAIT cells may be activated in an MR1-dependent manner in autoimmune diseases. Autoimmune conditions are often associated with, or preceded by, bacterial infections. For example, guttate psoriasis is strongly associated with streptococcal infections, as well as *S. aureus* and *C. albicans* (Valdimarsson et al., 2009), although MAIT cells cannot be activated by *S. pyogenes* in an MR1-dependent manner (Le Bourhis et al., 2010). Furthermore, changes in microbiome composition (Gevers et al., 2014), as well as reduced barrier function and increased intestinal permeability, have been shown to affect the development of autoimmune diseases, such as IBD and MS (Fasano & Shea-Donohue, 2005; Miyake et al., 2015; Nouri et al., 2014). Therefore, MAIT cells activated aberrantly following exposure to riboflavin-synthesizing microbes may potentially go on to further drive autoimmune conditions. Furthermore, autoreactive MAIT cells have been described where MR1 is overexpressed, and can be enhanced by modifying a single amino acid residue (López-Sagaseta et al., 2013; Young et al., 2013), providing a potential mechanism by which MAIT cells may be activated in the absence of riboflavin-derived metabolites. Further ligands that may be presented by MR1, including self-ligands, have yet to be identified, and may also explain their involvement in a wide range of autoimmune diseases.

Certain MAIT cell effector functions, such as granule exocytosis, are currently thought to be completely dependent on MR1 (Chapter 3), which may be important in conditions such as graft-versus-host disease (GVHD) where T-cell mediated cytotoxicity is critical for their pathology. Furthermore, as yet, IL-17 production from human MAIT cells has only been demonstrated in the context of TCR stimulation. Thus, the mechanism by which MAIT cells are activated in these diseases will be

important to understand, to give insight into what their role is in the increasing number of autoimmune conditions they have been associated with.

7.3. Innate-ness of cells and CD161

7.3.1. Innate-ness of T cells and CD161

The innate ability of MAIT cells to be activated by cytokines alone and secrete abundant IFNγ is shared with other T cells that express CD161 (Fergusson et al., 2014). This function was strikingly enhanced within non-MAIT, CD4+ CD161++ T cells in the synovial fluid of PsA patients, confirming that innate IFNγ production is restricted to cells expressing CD161 at a high level. Furthermore, the increased frequency of IFNγ-expressing SF CD161++CD4+ T cells in response to IL-12 and IL-18 is most likely not due to increased responsiveness (e.g. expression of IL-18R and PLZF), but due to an increased ability to secrete IFNγ. These results support the notion that innate responsiveness is pre-programmed within T cells expressing CD161 and is not acquired by cells lacking CD161 under chronic inflammatory conditions.

7.3.2. Innate-ness of NK cells and CD161

Chapter 6 explored whether this phenotype may be extended to NK cells. In contrast to T cells, CD161 only partially accounted for the cytokine-responsiveness of NK cells, as $CD56^{bright}$ NK cells were highly responsive to IL-12+IL-18, regardless of CD161 expression. However, within $CD56^{dim}$ NK cells, responsiveness to these cytokines correlated with CD161 expression. Furthermore, CD161+ NK cells had a heightened ability to proliferate in response to cytokines. The cytokine responsiveness of CD161+ NK cells was independent of other markers that have

been previously shown to negatively correlate with cytokine responsiveness, such as CD57, suggesting that this is a novel correlate for NK cell maturation. This was explored further using multidimensional data analysis of CyTOF data, showing that distinct CD161− NK cell populations were absent in cord blood but present in healthy adults, and further expanded and differentiated upon CMV infection. Within these expanded CD161− NK cells, markers of activation in response to IL-12+IL-18 stimulation, including IFNγ, CD69, CD25, and NKp30, were downmodulated compared to other NK cell subsets. Thus, CD161 expression correlates with innate cytokine responsiveness within $CD56^{dim}$ NK cells, and both CD161 expression and responsiveness to IL-12+IL-18 is downregulated upon CMV-induced NK cell terminal differentiation.

7.3.3. PLZF: master transcription factor of innate-ness?

Recently, these CMV-specific terminally differentiated NK cells (CD57++NKG2C+), or “adaptive” NK cells, were demonstrated to have extensively downregulated their expression of PLZF, due to hypermethylation of the *ZBTB16* intronic sequence (Schlums et al., 2015). This was associated with the silencing of signaling molecules such as the SLAM family receptor adaptor molecule EAT-2, as well as CD161, IL-12R, and IL-18R. This is in line with the observation in Chapter 6 that CD161− NK cells are enriched in these adaptive NK cells, and CD161+ NK cells are significantly enriched for PLZF expression, regardless of exposure to CMV.

PLZF is an epigenetic regulator and interacts with proteins such as HDAC1 (Histone Deacetylase 1) and the Cullin-based E3 ubiquitin ligase (CUL3) to induce chromatin modifications (Mathew et al., 2012). The transcriptional programme controlled by PLZF in immune cells is only beginning to be dissected, and the direct and indirect effects of PLZF transcription remains to be delineated. In adaptive NK cells, PLZF

was shown to directly bind the promoters of genes encoding signaling adaptor molecules (Schlums et al., 2015), supporting a direct role for PLZF in regulating signaling molecules. This also explains the increased responsiveness of NK cells from a PLZF-deficient patient to activating receptor ligation (Eidson et al., 2011). Furthermore, PLZF has been consistently associated with the innate-ness and cytokine responsiveness of cells. For example, PLZF-deficient mice are more susceptible to viral infections due to reduced IFNα-induced NK cell cytotoxicity (Xu et al., 2009). Genes encoding subunits of IL-12R and IL-18R are downregulated in PLZF-deficient mice (Gleimer et al., 2012), and, in Chapter 5, gene expression correlation analysis showed that the expression patterns of genes encoding IL-12R and IL-18R are highly correlated with the expression pattern of *ZBTB16* within CD8+ T cells. In addition to γδ T cells, iNKT cells and MAIT cells, newly described murine innate T cells such as the PLZF+ RORγt+ natural Th17 cells (Massot et al., 2014) and PLZF+ T-CD4 T cells (Qiao et al., 2012) also express PLZF, and are highly responsive to cytokines. Thus, PLZF may be a direct regulator of cytokine receptor expression and signaling proteins.

In contrast, despite the repeated association between CD161 and PLZF, the expression of CD161 and PLZF is not always correlated. Although knockdown of *ZBTB16* downregulates CD161 expression in cord blood T cells (Singh et al., 2015), CD161 expression on T and NK cells was not completely lost in a PLZF-deficient patient (Eidson et al., 2011). Chapter 6 also showed that all CD161+ NK cells express PLZF, but not all CD161− NK cell lacked PLZF expression. Additionally, thymic MAIT cells from second trimester fetuses are already CD161++, but do not express PLZF until migration to peripheral tissues (Leeansyah et al., 2014). Furthermore, although CD161++CD8+ T cells have a significantly higher expression of PLZF compared to CD161+ CD8+ T cells, there is no significant difference in their CD161 expression at the mRNA level. PLZF is only expressed by 5% of murine NK

cells (Constantinides et al., 2014), and CD161 lacks a direct homologue in mice, rendering the study of the relationship between CD161 and PLZF in mice difficult. Therefore, techniques such as ChIP-Seq may be required to shed light onto the relationship between CD161, PLZF and innate-ness across T cells and NK cells.

7.4. Parallels between NK cell and CD8+ T cell subsets

As discussed above, in contrast to T cells, the association between CD161 expression on NK cells and the ability to respond to IL-12+IL-18 was weaker, with significant correlation only observed within $CD56^{dim}$ NK cells. $CD56^{bright}$ NK cells, however, were highly responsive to IL-12+IL-18, regardless of CD161 expression. $CD56^{bright}$ cells are uniformly high in IL-18R expression, in a similar manner to CD161++ CD8+ T cells, including both Vα7.2− cells and MAIT cells. In fact, phenotypic analysis of NK cells and CD8+ T cells highlighted more similarities between $CD56^{bright}$ NK cells and CD161++CD8+ T cells, as well as $CD56^{dim}$ and CD161+ CD8+ T cells, than between CD161+ NK cells and CD161++ or CD161+ CD8+ T cells (Figure 7-2). In the following section, functional similarities between subsets of NK cells and subsets of CD8+ T cells will be highlighted.

7.4.1. Cytokine responsiveness

As discussed above, $CD56^{bright}$ NK cells and CD161++CD8+/MAIT cells both have high constitutive expression of several cytokine receptors, including the shared expression of IL-7R (CD127) (Zwirner & Domaica, 2010) and IL-18R (Figure 7-2), the latter enabling abundant secretion of IFNγ in response to IL-12+IL-18 compared to their respective 'dim' counterparts. 'Bright' populations also express unique cytokine receptors such as IL-2Rα (CD25) expressed by $CD56^{bright}$ NK cells (Fehniger et al., 2003), and IL-23R expressed by CD161++CD8+ T cells (Billerbeck et al., 2010),

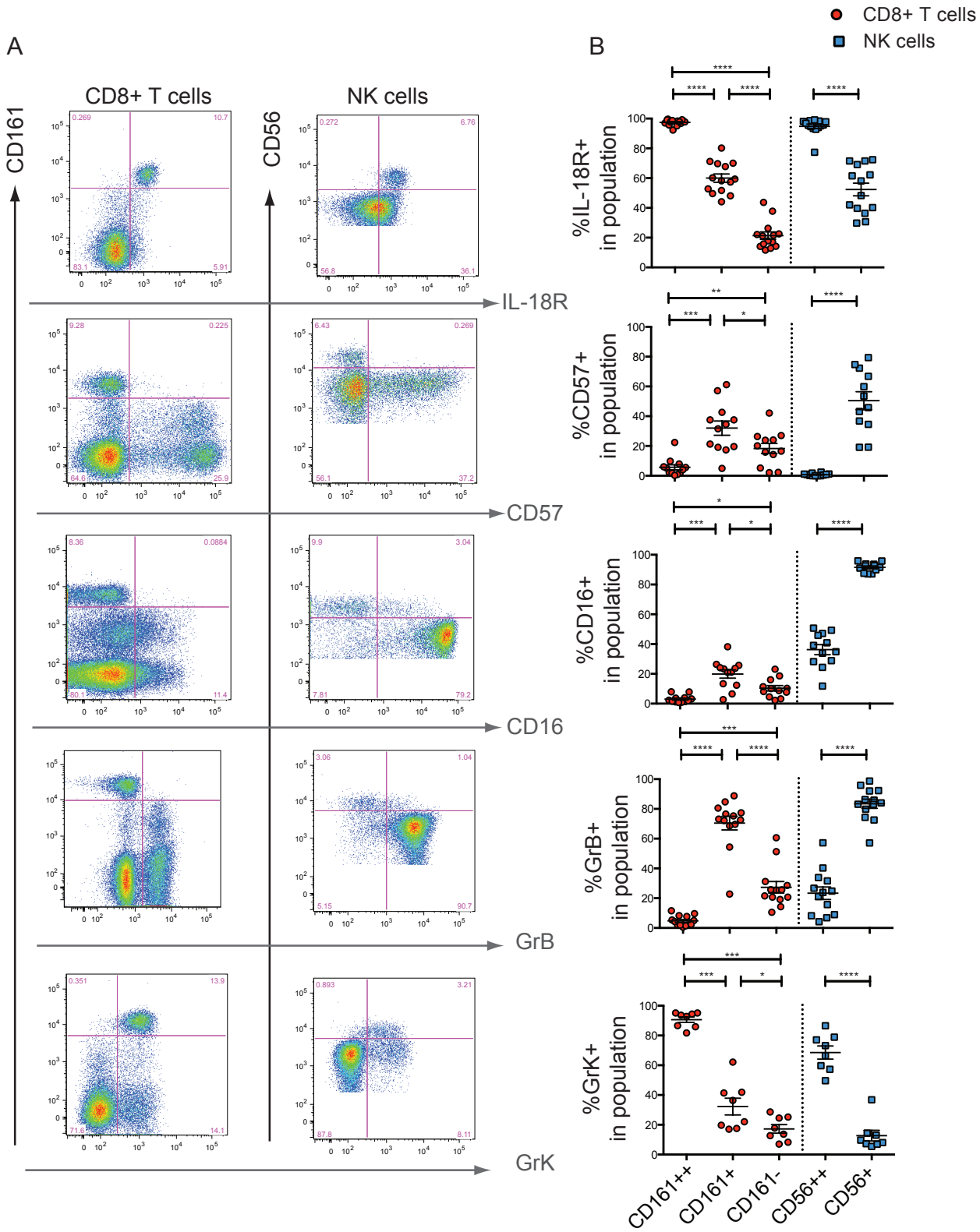


Figure 7-2. Functional and phenotypic similarities between CD8+ T cell and NK cell subsets. A) Representative flow cytometry staining showing expression of various markers against CD161 expression on CD8+ T cells (left), or against CD56 expression on NK cells (right). Each panel shows the expression of the indicated marker within the same healthy donor, gated on CD8+ T cells or NK cells. B) Frequencies of cells expressing the indicated marker within the CD161++, CD161+, and CD161- CD8+ T cells (red), within the $CD56^{bright}$ (CD56++) and $CD56^{dim}$ (CD56+) NK cells (blue), in 8-14 healthy individuals. ****P<0.0001, ***P<0.001, **P<0.01, *P<0.05 by repeated measures one-way ANOVA with Tukey's multiple comparisons test. All other comparisons were non-significant.

which are not expressed by their 'dim' counterparts. Additionally, CD56^{bright} NK cells are known for their proliferative capacity in response to cytokines (Punt et al., 2001), and CD161++ CD8+ T cells are also highly proliferative upon stimulation with IL-12 and IL-15 compared to the CD161+ CD8+ T cell counterparts (Chapter 3).

In turn, CD161++ CD8+ T cells have been described to be hyporesponsive to TCR signaling compared to their CD161+ and CD161− CD8+ T cell counterparts (Turtle et al., 2011). Indeed, MAIT cells did not proliferate in response to PHA, which crosslinks the TCR/CD3 complex, but proliferated extensively when TCR stimulation was supplemented with anti-CD28 and anti-CD2, or with cytokines such as IL-12 and IL-18 during *E. coli*-induced proliferation (Chapter 3). CD56^{dim} NK cells also have a heightened ability to respond to the crosslinking of activating receptors such as NKp30 and CD16 (De Maria et al., 2011; Juelke et al., 2010). In particular, the terminally differentiated CD57++NKG2C+ CD56^{dim} NK cells proliferate extensively in response to ligation of activation receptors such as NKG2C (Rölle et al., 2014). Thus, both CD161++ CD8+ T cells and CD56^{bright} NK cells have high cytokine responsiveness compared to other CD8+ and NK cell subsets, which is associated with a comparatively lower ability to respond to activating receptors alone.

7.4.2. Regulation of cytotoxicity

CD8+ T cells and NK cells constitute the cytotoxic arms of T cells and ILCs, respectively, and thus share the expression of granzymes and perforin. Resting CD161++CD8+ T cells, in particular the MAIT cells, express no GrB and little perforin, and instead are uniquely enriched for GrK expression (Chapter 3). In turn, CD161+CD8+ T cells are enriched for GrB and perforin expression, even compared to their CD161− CD8+ T cell counterparts (Fergusson et al., 2015). The GrK+ GrB− perforin^{low} phenotype of CD161++CD8+ T cells was similar to the phenotype of

CD56^{bright} NK cells (Figure 7-2) (Bratke et al., 2005; Cooper et al., 2001), which are often compared to their highly cytotoxic CD56^{dim} counterparts that express high levels of GrB and perforin. However, both CD56^{bright} NK cells (Nagler et al., 1989) and CD161++ CD8+ T cells (including the MAIT cells, Chapter 3) can be activated to upregulate GrB and perforin, and become efficient killer cells.

Coexpression of the transcription factors T-bet and Eomes is critical for the cytotoxic functions of both CD8+ T cells and NK cells (Gordon et al., 2012; Intlekofer et al., 2005), and the similarities in granzyme and perforin expression in these cells is reflected by their expression of the T-bet and Eomes. Thus both CD56^{dim} NK cells and CD161+ CD8+ T cells are enriched for Eomes+T-bet^{high} cells (Fergusson et al., 2015; Knox et al., 2014), while CD56^{bright} NK cells have an Eomes+T-bet^{low} phenotype (Knox et al., 2014), which was mirrored by CD8+ MAIT cells (Chapter 4). Of note, CD161+CD8+ T cells express higher levels of GrB and perforin even compared to their CD161− CD8+ T cell counterparts, although both populations contain similar frequencies of effector memory T cells and terminally differentiated CD8+ T cells (Fergusson et al., 2015).

7.4.3. Enrichment in inflamed tissues

Perhaps the most interesting similarity between CD56^{bright} NK cells and CD161++ CD8+ T cells is their enrichment in inflammatory sites (Dalbeth et al., 2004). Although CD56^{bright} NK cells express lymphoid homing receptors, which contrasts with CD161++CD8+ T cells, both of these populations express chemokine receptors associated with inflammation such as CCR1, CCR5, as well as CXCR6, which directs cells to rheumatoid joints and livers (Berahovich et al., 2011). Therefore, CD56^{bright} NK cells are highly enriched and activated within synovial fluid from PsA and RA patients (de Matos et al., 2007; Pridgeon et al., 2003), as well as in inflamed

tissues in tuberculosis (Schierloh et al., 2005). MAIT cells are also well-established to be recruited to sites of inflammation (Le Bourhis et al., 2010; Serriari et al., 2014), and indeed within the synovial fluid of PsA patients, MAIT cells composed up to 60% of the CD8+ T cells and their frequency correlated with clinical measures of disease activity (Chapter 5).

7.4.4. Implications of similarities between CD56^{bright} NK cells and MAIT cells

A model summarizing the similarities between NK cell and CD8+ T cell subsets is shown in Figure 7-3. This, of course, disregards the specificity of the TCR that drive CD8+ T cell functions, and many differences are not noted here, including the expression of RORγt within CD8+ T cells but not in NK cells, and the lymphoid tissue homing phenotype of CD56^{bright} NK cells (Berahovich et al., 2011) compared to the peripheral tissue homing phenotype of CD161++CD8+ T cells (Dusseaux et al., 2011). However, the general inverse correlation between cytokine responsiveness and responsiveness to activating receptors may in part, explain the functional similarities between CD8+ T cell and NK cell subsets. These functions are associated with the shared expression of transcription factors that determines their effector functions. Interestingly, although these subsets of NK and T cells can be clearly delineated using markers such as CD56 and CD161, both of these markers are not directly involved in determining the differential functions of these subsets; in fact, CD161 has been suggested to have opposing functions on T and NK cells (Rosen et al., 2008).

The similarities between NK cells and MAIT cells suggest that MAIT cells may share some functions already described in immature NK cells. For instance, the expansion

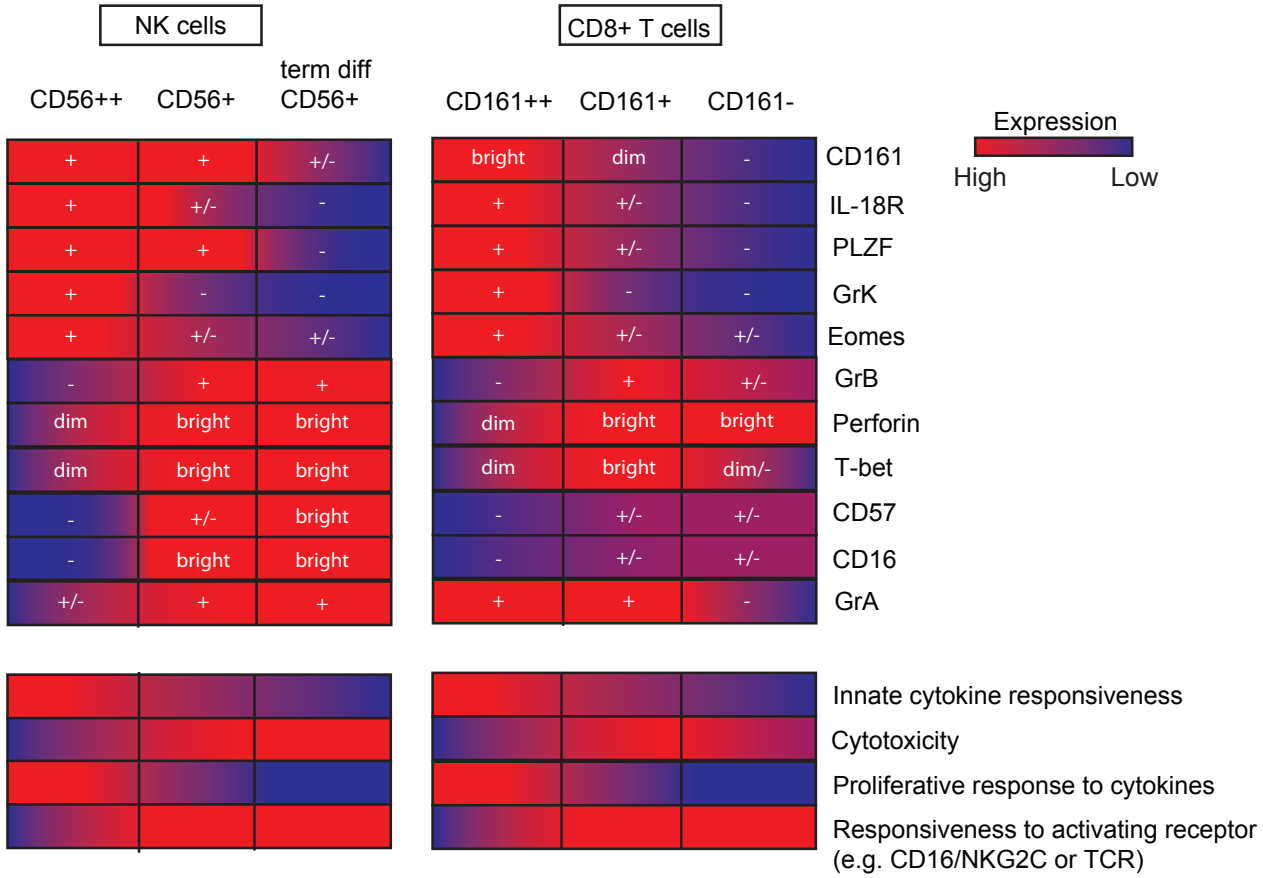


Figure 7-3. Model highlighting functional parallels between CD8+ T cells and NK cells. The ability to respond to cytokines by secreting IFNγ and proliferating inversely correlates with cytoxic potential at rest and responsiveness to activating receptor ligation in both CD8+ T cells and NK cells. The markers and transcription factors correlated with these functional properties are highlighted (top). $CD56^{dim}$ term diff = terminally differentiated $CD56^{dim}$ NK cells. Bright/dim indicate expression levels, + and - signs indicate whether the population is mostly positive or negative for the marker indicated. Both “bright” populations are also enriched in inflammatory sites where they may be activated by cytokines.

of CD56^{bright} NK cells in MS patients during daclizumab treatment is associated with better prognosis, due to their ability to kill pathogenic, highly activated CD4+ T cells (Bielekova et al., 2006). Cytotoxicity is mainly mediated through the expression of GrK (Jiang et al., 2011) and NKG2D (Nielsen et al., 2012). MAIT cells are also enriched in MS lesions and indeed early papers suggested that they play a regulatory role (Croxford et al., 2006; Miyazaki et al., 2011). Whether MAIT cells are protective or pathogenic in MS may depend on their context of activation and the secretion of IL-17, but the regulatory role for MAIT cells could be further examined in the context of NKG2D-induced cytotoxicity. Furthermore, in a similar way that IL-12+IL-18 and TLR stimulation activates MAIT cells (Jo et al., 2014; Ussher et al., 2014a), they may respond to other cytokines that activate NK cells. For example, NK cell sensitivity to IFNα is regulated by PLZF (Xu et al., 2009), and thus PLZF+ MAIT cells may also be able to respond to IFNα.

Innate-like T cells are so called due to the fact that they share several functional features with NK cells. A recent study on iNKT cells indeed demonstrated that iNKT cells share a broader transcriptional programme with NK cells than previously appreciated (Cohen et al., 2013). Many of the effector functions of innate-like T cells may particularly be shared with the more immature NK cells, including CD56^{bright} NK cells and CD161+ CD56^{dim} NK cells. A transcriptional comparison between subsets of NK cells and innate-like T cells, including MAIT cells, will be able to highlight these similarities in an objective manner. Furthermore, terminally differentiated NK cells have been shown to have epigenetic modifications resembling memory CD8+ T cells, particularly those affecting the expression of PLZF, IFNγ, cytokine receptors, and signaling proteins (Luetke-Eversloh et al., 2014; Schlums et al., 2015). Thus, comparison of the epigenetic signature between immature NK cells and innate-like T cells may also reveal important similarities associated with their innate programming, such as the expression of other members of the BTB-ZF protein family.

7.5. Conclusions

MAIT cells are a novel innate-like T cell population, prevalent in humans, and play a critical role in the control of bacterial infections in mice (Le Bourhis et al., 2010; Meierovics et al., 2013). The regulation of the broad effector functions of MAIT cells, however, and markers associated with these functions, have not been fully characterized.

In this thesis, MAIT cells were found to have a unique cytotoxic profile within CD8+ T cells, expressing GrA and GrK, instead of the key effector molecules GrB and perforin which are typically associated with high cytolytic activity. Upon exposure to bacteria, however, MAIT cells rapidly upregulate GrB and perforin in a manner similar to conventional memory CD8+ T cells. The acquisition of this cytotoxic phenotype was associated with the ability to efficiently kill target cells. Whether MAIT cell-mediated killing plays an important role in immunity against bacteria remains to be determined. In contrast to these cytotoxic MAIT cells that express the CD8 coreceptor, MAIT cells expressing the CD4 coreceptor were found to lack the ability to degranulate and upregulate GrB upon bacterial stimulation. Instead, CD4+ MAIT cells showed a higher expression of Th2 cytokines compared to their CD4− counterparts, and were enriched within tonsils. The significance of the heterogeneous effector functions and homing properties between MAIT cell subsets requires further investigation.

All MAIT cell subsets expressed RORγt and could secrete IL-17. As IL-17 has been implicated in the pathology of psoriasis and PsA, the frequency and function of MAIT cells from the blood and tissue of these patients was investigated. This revealed that MAIT cells are present in healthy and psoriatic skin, although their functional capacity within tissues was not investigated here. MAIT cells within the synovial fluid of PsA

patients, however, were highly activated and their frequency correlated with measures of clinical activity. A higher frequency of synovial fluid MAIT cells also expressed IL-17 compared to peripheral blood samples from the same patient, but this increased capacity to make IL-17 was shared with other T cells, in line with a recent study (Menon et al., 2014). Whether MAIT cells play a unique role in these psoriatic diseases is therefore unclear, and requires investigation in murine models of psoriasis and arthritis. If they are found to play a pathological role, the use of RORγt inhibitors, as tested in preliminary experiments here, may be key in inhibiting their IL-17 production.

RORγt inhibition did not affect the expression of CD161 on MAIT cells. Instead, PLZF may be a key regulator of CD161 expression and the associated responsiveness to innate cytokines, as implied by the characterization of CD161+ and CD161− NK cells. Understanding the shared regulators of innate, rapid effector cells such as MAIT cells and NK cells may provide interesting therapeutic options in the future.

References

Achour, A., Baychelier, F., Besson, C., Arnoux, A., Marty, M., Hannoun, L., Samuel, D., Debré, P., & Vieillard, V. (2014). Expansion of CMV-mediated NKG2C+ NK cells associates with the development of specific de novo malignancies in liver-transplanted patients. *Journal of Immunology*, *192*(1), 503–511.

Addison, E. G., North, J., Bakhsh, I., Marden, C., Haq, S., Al-Sarraj, S., Malayeri, R., Wickremasinghe, R. G., Davies, J. K., & Lowdell, M. W. (2005). Ligation of CD8alpha on human natural killer cells prevents activation-induced apoptosis and enhances cytolytic activity. *Immunology*, *116*(3), 354–361.

Ahlenstiel, G., Titerence, R. H., Koh, C., Edlich, B., Feld, J. J., Rotman, Y., Ghany, M. G., Hoofnagle, J. H., Liang, T. J., Heller, T., & Rehermann, B. (2010). Natural Killer Cells Are Polarized Toward Cytotoxicity in Chronic Hepatitis C in an Interferon-Alfa–Dependent Manner. *Gastroenterology*, *138*(1), 325–335.e2.

Ahmad, A., & Menezes, J. (1996). Defective killing activity against gp120/41-expressing human erythroleukaemic K562 cell line by monocytes and natural killer cells from HIV-infected individuals. *AIDS*, *10*(2), 143–149.

Aldemir, H., Prod'homme, V., Dumaurier, M.-J., Retiere, C., Poupon, G., Cazareth, J., Bihl, F., & Braud, V. M. (2005). Cutting edge: lectin-like transcript 1 is a ligand for the CD161 receptor. *Journal of Immunology*, *175*(12), 7791–7795.

Alonzo, E. S., Gottschalk, R. A., Das, J., Egawa, T., Hobbs, R. M., Pandolfi, P. P., Pereira, P., Nichols, K. E., Koretzky, G. A., Jordan, M. S., & Sant'Angelo, D. B. (2010). Development of promyelocytic zinc finger and ThPOK-expressing innate gamma delta T cells is controlled by strength of TCR signaling and Id3. *Journal of Immunology*, *184*(3), 1268–1279.

Alter, G., Jost, S., Rihn, S., Reyor, L. L., Nolan, B. E., Ghebremichael, M., Bosch, R., Altfeld, M., & Lauer, G. M. (2011). Reduced frequencies of NKp30+NKp46+, CD161+, and NKG2D+ NK cells in acute HCV infection may predict viral clearance. *Journal of Hepatology*, *55*(2), 278–288.

Alter, G., Malenfant, J. M., Delabre, R. M., Burgett, N. C., Yu, X. G., Lichterfeld, M., Zaunders, J., & Altfeld, M. (2004). Increased Natural Killer Cell Activity in Viremic HIV-1 Infection. *The Journal of Immunology*, *173*(8), 5305–5311.

Alter, G., Martin, M. P., Teigen, N., Carr, W. H., Suscovich, T. J., Schneidewind, A., Streeck, H., Waring, M., Meier, A., Brander, C., Lifson, J. D., Allen, T. M., Carrington, M., & Altfeld, M. (2007). Differential natural killer cell-mediated inhibition of HIV-1 replication based on distinct KIR/HLA subtypes. *The Journal of Experimental Medicine*, *204*(12), 3027–3036.

Alvaro-Gracia, J. M., Zvaifler, N. J., Brown, C. B., Kaushansky, K., & Firestein, G. S. (1991). Cytokines in chronic inflammatory arthritis. VI. Analysis of the synovial cells involved in granulocyte-macrophage colony-stimulating factor production and gene expression in rheumatoid arthritis and its regulation by IL-1 and tumor necrosis factor-alpha. *Journal of Immunology*, *146*(10), 3365–3371.

Amir, E. D., Davis, K. L., Tadmor, M. D., Simonds, E. F., Levine, J. H., Bendall, S. C., Shenfeld, D. K., Krishnaswamy, S., Nolan, G. P., & Pe'er, D. (2013). viSNE enables visualization of high dimensional single-cell data and reveals phenotypic heterogeneity of leukemia. *Nature Biotechnology*, *31*(6), 545–52.

Anfossi, N., André, P., Guia, S., Falk, C. S., Roetynck, S., Stewart, C. A., Breso, V., Frassati, C., Reviron, D., Middleton, D., Romagné, F., Ugolini, S., & Vivier, E. (2006). Human NK cell education by inhibitory receptors for MHC class I. *Immunity*, *25*(2), 331–342.

Annibali, V., Ristori, G., Angelini, D. F., Serafini, B., Mechelli, R., Cannoni, S., Romano, S., Paolillo, A., Abderrahim, H., Diamantini, A., Borsellino, G., Aloisi, F., Battistini, L., & Salvetti, M. (2011). CD161high CD8+T cells bear pathogenetic potential in multiple sclerosis. *Brain*, *134*(2), 542–554.

Annunziato, F., Cosmi, L., Santarlasci, V., Maggi, L., Liotta, F., Mazzinghi, B., Parente, E., Filì, L., Ferri, S., Frosali, F., Giudici, F., Romagnani, P., Parronchi, P., Tonelli, F., Maggi, E., & Romagnani, S. (2007). Phenotypic and functional features of human Th17 cells. *The Journal of Experimental Medicine*, *204*(8), 1849–1861.

Antoniu, S. A. (2012). Discontinued drugs 2011: pulmonary, allergy, gastrointestinal and arthritis. *Expert Opinion on Investigational Drugs*, *21*(11), 1607–1618.

Arcaro, A., Gregoire, C., Boucheron, N., Stotz, S., Palmer, E., Malissen, B., & Luescher, I. F. (2000). Essential Role of CD8 Palmitoylation in CD8 Coreceptor Function. *The Journal of Immunology*, *165*(4), 2068–2076.

Arican, O., Aral, M., Sasmaz, S., & Ciragil, P. (2005). Serum levels of TNF-alpha, IFN-gamma, IL-6, IL-8, IL-12, IL-17, and IL-18 in patients with active psoriasis and correlation with disease severity. *Mediators of Inflammation*, *2005*(5), 273–279.

Arnon, T. I., Achdout, H., Lieberman, N., Gazit, R., Gonen-Gross, T., Katz, G., Bar-Ilan, A., Bloushtain, N., Lev, M., Joseph, A., Kedar, E., Porgador, A., & Mandelboim, O. (2004). The mechanisms controlling the recognition of tumor- and virus-infected cells by NKp46. *Blood*, *103*(2), 664–672.

Arnon, T. I., Lev, M., Katz, G., Chernobrov, Y., Porgador, A., & Mandelboim, O. (2001). Recognition of viral hemagglutinins by NKp44 but not by NKp30. *European Journal of Immunology*, *31*(9), 2680–9.

Artis, D., & Spits, H. (2015). The biology of innate lymphoid cells. *Nature*, *517*(7534), 293–301.

Asarnow, D. M., Kuziel, W. A., Bonyhadi, M., Tigelaar, R. E., Tucker, P. W., & Allison, J. P. (1988). Limited diversity of gamma delta antigen receptor genes of Thy-1+ dendritic epidermal cells. *Cell*, *55*(5), 837–847.

Aust, J. G., Gays, F., Mickiewicz, K. M., Buchanan, E., & Brooks, C. G. (2009). The expression and function of the NKRP1 receptor family in C57BL/6 mice. *Journal of Immunology*, *183*(1), 106–116.

Austin, L. M., Covens, T. R., Bhardwaj, N., Steinman, R., & Krueger, J. G. (1998). Intraepidermal lymphocytes in psoriatic lesions are activated GMP-17(TIA-1)+CD8+CD3+ CTLs as determined by phenotypic analysis. *Journal of Cutaneous*

Pathology, *25*(2), 79–88.

Austin, L. M., Ozawa, M., Kikuchi, T., Walters, I. B., & Krueger, J. G. (1999). The majority of epidermal T cells in psoriasis vulgaris lesions can produce type 1 cytokines, interferon-gamma, interleukin-2, and tumor necrosis factor-alpha, defining TC1 (cytotoxic T lymphocyte) and TH1 effector populations: a type 1 differentiation bi. *The Journal of Investigative Dermatology*, *113*(5), 752–9.

Azzoni, L., Papasavvas, E., Chehimi, J., Kostman, J. R., Mounzer, K., Ondercin, J., Perussia, B., & Montaner, L. J. (2002). Sustained impairment of IFN-gamma secretion in suppressed HIV-infected patients despite mature NK cell recovery: evidence for a defective reconstitution of innate immunity. *Journal of Immunology*, *168*(11), 5764–5770.

Azzoni, L., Zatsepina, O., Abebe, B., Bennett, I. M., Kanakaraj, P., & Perussia, B. (1998). Differential transcriptional regulation of CD161 and a novel gene, 197/15a, by IL-2, IL-15, and IL-12 in NK and T cells. *Journal of Immunology*, *161*(7), 3493–3500.

Bachmann, M. F., Barner, M., Viola, A., & Kopf, M. (1999). Distinct kinetics of cytokine production and cytolysis in effector and memory T cells after viral infection. *European Journal of Immunology*, *29*(1), 291–9.

Badovinac, V. P., Porter, B. B., & Harty, J. T. (2002). Programmed contraction of CD8+ T cells after infection. *Nature Immunology*, *3*(7), 619–626.

Barakonyi, A., Rabot, M., Marie-Cardine, A., Aguerre-Girr, M., Polgar, B., Schiavon, V., Bensussan, A., & Le Bouteiller, P. (2004). Cutting Edge: Engagement of CD160 by its HLA-C Physiological Ligand Triggers a Unique Cytokine Profile Secretion in the Cytotoxic Peripheral Blood NK Cell Subset. *The Journal of Immunology*, *173*(9), 5349–5354.

Baran, K., Dunstone, M., Chia, J., Ciccone, A., Browne, K. A., Clarke, C. J. P., Lukoyanova, N., Saibil, H., Whisstock, J. C., Voskoboinik, I., & Trapani, J. A. (2009). The molecular basis for perforin oligomerization and transmembrane pore assembly. *Immunity*, *30*(5), 684–695.

Barth, R. J., Mulé, J. J., Spiess, P. J., & Rosenberg, S. A. (1991). Interferon gamma and tumor necrosis factor have a role in tumor regressions mediated by murine CD8+ tumor-infiltrating lymphocytes. *The Journal of Experimental Medicine*, *173*(3), 647–658.

Bas, M., Bier, H., Schirlau, K., Friebe-Hoffmann, U., Scheckenbach, K., Balz, V., Whiteside, T. L., & Hoffmann, T. K. (2006). Gamma-delta T-cells in patients with squamous cell carcinoma of the head and neck. *Oral Oncology*, *42*(7), 691–697.

Bauer, S. (1999). Activation of NK Cells and T Cells by NKG2D, a Receptor for Stress-Inducible MICA. *Science*, *285*(5428), 727–729.

Bauer, S., Groh, V., Wu, J., Steinle, A., Phillips, J. H., Lanier, L. L., & Spies, T. (1999). Activation of NK cells and T cells by NKG2D, a receptor for stress-inducible MICA. *Science*, *285*(5428), 727–729.

Baume, D. M., Robertson, M. J., Levine, H., Manley, T. J., Schow, P. W., & Ritz, J. (1992). Differential responses to interleukin 2 define functionally distinct subsets of human

natural killer cells. *European Journal of Immunology*, *22*(1), 1–6.

Becher, B., Schlitzer, A., Chen, J., Mair, F., Sumatoh, H. R., Teng, K. W. W., Low, D., Ruedl, C., Riccardi-Castagnoli, P., Poidinger, M., Greter, M., Ginhoux, F., & Newell, E. W. (2014). High-dimensional analysis of the murine myeloid cell system. *Nature Immunology*, *15*(12), 1181–1189.

Beckman, E. M., Porcelli, S. A., Morita, C. T., Behar, S. M., Furlong, S. T., & Brenner, M. B. (1994). Recognition of a lipid antigen by CD1-restricted alpha beta+ T cells. *Nature*, *372*(6507), 691–694.

Behrendt, C., Gollnick, H., & Bonnekoh, B. (2000). Up-regulated perforin expression of CD8+ blood lymphocytes in generalized non-anaphylactic drug eruptions and exacerbated psoriasis. *European Journal of Dermatology*, *10*(5), 365–369.

Bendelac, A. (1995). Positive selection of mouse NK1+ T cells by CD1-expressing cortical thymocytes. *The Journal of Experimental Medicine*, *182*(6), 2091–2096.

Bendelac, A., Lantz, O., Quimby, M. E., Yewdell, J. W., Bennink, J. R., & Brutkiewicz, R. R. (1995). CD1 recognition by mouse NK1+ T lymphocytes. *Science*, *268*(5212), 863–865.

Benham, H., Norris, P., Goodall, J., Wechalekar, M. D., FitzGerald, O., Szentpetery, A., Smith, M., Thomas, R., & Gaston, H. (2013). Th17 and Th22 cells in psoriatic arthritis and psoriasis. *Arthritis Research & Therapy*, *15*(5), R136.

Bennett, I. M., Zatsepina, O., Zamai, L., Azzoni, L., Mikheeva, T., & Perussia, B. (1996). Definition of a natural killer NKR-P1A+/CD56-/CD16- functionally immature human NK cell subset that differentiates in vitro in the presence of interleukin 12. *The Journal of Experimental Medicine*, *184*(5), 1845–1856.

Berahovich, R. D., Lai, N. L., Wei, Z., Lewis, L., & Schall, T. J. (2011). Evidence for NK Cell Subsets Based on Chemokine Receptor Expression. *Journal of Immunology*, *177*(11), 7833–7840.

Bernink, J. H., Krabbendam, L., Germar, K., de Jong, E., Gronke, K., Kofoed-Nielsen, M., Munneke, J. M., Hazenberg, M. D., Villaudy, J., Buskens, C. J., Bemelman, W. A., Diefenbach, A., Blom, B., & Spits, H. (2015). Interleukin-12 and -23 Control Plasticity of CD127+ Group 1 and Group 3 Innate Lymphoid Cells in the Intestinal Lamina Propria. *Immunity*, *43*(1), 146–160.

Bernink, J. H., Peters, C. P., Munneke, M., te Velde, A. A., Meijer, S. L., Weijer, K., Hreggvidsdottir, H. S., Heinsbroek, S. E., Legrand, N., Buskens, C. J., Bemelman, W. A., Mjösberg, J. M., & Spits, H. (2013). Human type 1 innate lymphoid cells accumulate in inflamed mucosal tissues. *Nature Immunology*, *14*(3), 221–229.

Bettelli, E., Carrier, Y., Gao, W., Korn, T., Strom, T. B., Oukka, M., Weiner, H. L., & Kuchroo, V. K. (2006). Reciprocal developmental pathways for the generation of pathogenic effector TH17 and regulatory T cells. *Nature*, *441*(7090), 235–238.

Betts, M. R., Brenchley, J. M., Price, D. A., De Rosa, S. C., Douek, D. C., Roederer, M., & Koup, R. A. (2003). Sensitive and viable identification of antigen-specific CD8+ T cells by a flow cytometric assay for degranulation. *Journal of Immunological Methods*, *281*(1-2), 65–78.

Béziat, V., Dalgard, O., Asselah, T., Halfon, P., Bedossa, P., Boudifa, A., Hervier, B., Theodorou, I., Martinot, M., Debré, P., Björkström, N. K., Malmberg, K.-J., Marcellin, P., & Vieillard, V. (2012). CMV drives clonal expansion of NKG2C+ NK cells expressing self-specific KIRs in chronic hepatitis patients. *European Journal of Immunology*, *42*(2), 447–457.

Béziat, V., Descours, B., Parizot, C., Debré, P., & Vieillard, V. (2010). NK cell terminal differentiation: correlated stepwise decrease of NKG2A and acquisition of KIRs. *PloS One*, *5*(8), e11966.

Béziat, V., Liu, L. L., Malmberg, J.-A., Ivarsson, M. A., Sohlberg, E., Björklund, A. T., Retière, C., Sverremark-Ekström, E., Traherne, J., Ljungman, P., Schaffer, M., Price, D. A., Trowsdale, J., Michaëlsson, J., Ljunggren, H.-G., & Malmberg, K.-J. (2013). NK cell responses to cytomegalovirus infection lead to stable imprints in the human KIR repertoire and involve activating KIRs. *Blood*, *121*(14), 2678–2688.

Bielekova, B., Catalfamo, M., Reichert-Scrivner, S., Packer, A., Cerna, M., Waldmann, T. A., McFarland, H., Henkart, P. A., & Martin, R. (2006). Regulatory CD56bright natural killer cells mediate immunomodulatory effects of IL-2Ralpha-targeted therapy (daclizumab) in multiple sclerosis. *Proceedings of the National Academy of Sciences of the United States of America*, *103*(15), 5941–5946.

Bigley, A. B., Lowder, T. W., Spielmann, G., Rector, J. L., Pircher, H., Woods, J. A., & Simpson, R. J. (2012). NK-cells have an impaired response to acute exercise and a lower expression of the inhibitory receptors KLRG1 and CD158a in humans with latent cytomegalovirus infection. *Brain, Behavior, and Immunity*, *26*(1), 177–186.

Billerbeck, E., Kang, Y.-H., Walker, L. J., Lockstone, H., Grafmueller, S., Fleming, V., Flint, J., Willberg, C. B., Bengsch, B., Seigel, B., Ramamurthy, N., Zitzmann, N., Barnes, E. J., Thevanayagam, J., Bhagwanani, A., Leslie, A., Oo, Y. H., Kollnberger, S., Bowness, P., Drognitz, O., Adams, D. H., Blum, H. E., Thimme, R., & Klenerman, P. (2010). Analysis of CD161 expression on human CD8+ T cells defines a distinct functional subset with tissue-homing properties. *Proceedings of the National Academy of Sciences of the United States of America*, *107*(7), 3006–3011.

Biron, C. A., Byron, K. S., & Sullivan, J. L. (1989). Severe herpesvirus infections in an adolescent without natural killer cells. *The New England Journal of Medicine*, *320*(26), 1731–1735.

Bix, M., Liao, N. S., Zijlstra, M., Loring, J., Jaenisch, R., & Raulet, D. (1991). Rejection of class I MHC-deficient haemopoietic cells by irradiated MHC-matched mice. *Nature*, *349*(6307), 329–331.

Björkström, N. K., Lindgren, T., Stoltz, M., Fauriat, C., Braun, M., Evander, M., Michaëlsson, J., Malmberg, K.-J., Klingström, J., Ahlm, C., & Ljunggren, H.-G. (2011). Rapid expansion and long-term persistence of elevated NK cell numbers in humans infected with hantavirus. *The Journal of Experimental Medicine*, *208*(1), 13–21.

Björkström, N. K., Riese, P., Heuts, F., Andersson, S., Fauriat, C., Ivarsson, M. a., Björklund, A. T., Flodström-Tullberg, M., Michaëlsson, J., Rottenberg, M. E., Guzmán, C. a., Ljunggren, H.-G. G., & Malmberg, K.-J. J. (2010). Expression patterns of NKG2A, KIR, and CD57 define a process of CD56dim NK-cell differentiation

uncoupled from NK-cell education. *Blood*, *116*(19), 3853–3864.

Blauvelt, A., Lebwohl, M. G., & Bissonnette, R. (2015). IL-23/IL-17A Dysfunction Phenotypes Inform Possible Clinical Effects from Anti-IL-17A Therapies. *Journal of Investigative Dermatology*, *135*(8), 1946–1953.

Boles, K. S., Barten, R., Kumaresan, P. R., Trowsdale, J., & Mathew, P. a. (1999). Cloning of a new lectin-like receptor expressed on human NK cells. *Immunogenetics*, *50*(1-2), 1–7.

Bonanno, G., Mariotti, A., Procoli, A., Corallo, M., Scambia, G., Pierelli, L., & Rutella, S. (2009). Interleukin-21 induces the differentiation of human umbilical cord blood CD34-lineage- cells into pseudomature lytic NK cells. *BMC Immunology*, *10*, 46.

Boniface, K., Bernard, F.-X., Garcia, M., Gurney, A. L., Lecron, J.-C., & Morel, F. (2005). IL-22 Inhibits Epidermal Differentiation and Induces Proinflammatory Gene Expression and Migration of Human Keratinocytes. *The Journal of Immunology*, *174*(6), 3695–3702.

Boniface, K., Guignouard, E., Pedretti, N., Garcia, M., Delwail, A., Bernard, F.-X., Nau, F., Guillet, G., Dagregorio, G., Yssel, H., Lecron, J.-C., & Morel, F. (2007). A role for T cell-derived interleukin 22 in psoriatic skin inflammation. *Clinical and Experimental Immunology*, *150*(3), 407–415.

Bonneville, M., O'Brien, R. L., & Born, W. K. (2010). Gammadelta T cell effector functions: a blend of innate programming and acquired plasticity. *Nature Reviews Immunology*, *10*(7), 467–478.

Boos, M. D., Yokota, Y., Eberl, G., & Kee, B. L. (2007). Mature natural killer cell and lymphoid tissue-inducing cell development requires Id2-mediated suppression of E protein activity. *The Journal of Experimental Medicine*, *204*(5), 1119–1130.

Bourgeois, E. A., Subramaniam, S., Cheng, T.-Y., De Jong, A., Layre, E., Ly, D., Salimi, M., Legaspi, A., Modlin, R. L., Salio, M., Cerundolo, V., Moody, D. B., & Ogg, G. (2015). Bee venom processes human skin lipids for presentation by CD1a. *The Journal of Experimental Medicine*, *212*(2), 149–163.

Bovenschen, N., Quadir, R., van den Berg, A. L., Brenkman, A. B., Vandenberghe, I., Devreese, B., Joore, J., & Kummer, J. A. (2009). Granzyme K displays highly restricted substrate specificity that only partially overlaps with granzyme A. *The Journal of Biological Chemistry*, *284*(6), 3504–3512.

Bowes, J., Budu-Aggrey, A., Huffmeier, U., Uebe, S., Steel, K., Hebert, H. L., Wallace, C., Massey, J., Bruce, I. N., Bluett, J., Feletar, M., Morgan, A. W., Marzo-Ortega, H., Donohoe, G., Morris, D. W., Helliwell, P., Ryan, A. W., Kane, D., Warren, R. B., Korendowych, E., Alenius, G.-M., Giardina, E., Packham, J., McManus, R., FitzGerald, O., McHugh, N., Brown, M. A., Ho, P., Behrens, F., Burkhardt, H., Reis, A., & Barton, A. (2015). Dense genotyping of immune-related susceptibility loci reveals new insights into the genetics of psoriatic arthritis. *Nature Communications*, *6*, 6046.

Boyman, O., Hefti, H. P., Conrad, C., Nickoloff, B. J., Suter, M., & Nestle, F. O. (2004). Spontaneous development of psoriasis in a new animal model shows an essential role for resident T cells and tumor necrosis factor-alpha. *The Journal of Experimental*

Medicine, *199*(5), 731–736.

Bratke, K., Kuepper, M., Bade, B., Virchow Jr., J. C., & Luttmann, W. (2005). Differential expression of human granzymes A, B, and K in natural killer cells and during CD8+ T cell differentiation in peripheral blood. *European Journal of Immunology*, *35*(9), 2608–2616.

Brenchley, J. M., Karandikar, N. J., Betts, M. R., Ambrozak, D. R., Hill, B. J., Crotty, L. E., Casazza, J. P., Kuruppu, J., Migueles, S. a., Connors, M., Roederer, M., Douek, D. C., & Koup, R. a. (2003). Expression of CD57 defines replicative senescence and antigen-induced apoptotic death of CD8+ T cells. *Blood*, *101*(7), 2711–2720.

Brenner, B. G., Gryllis, C., & Wainberg, M. A. (1991). Role of antibody-dependent cellular cytotoxicity and lymphokine-activated killer cells in AIDS and related diseases. *Journal of Leukocyte Biology*, *50*(6), 628–640.

Brigl, M., Tatituri, R. V. V, Watts, G. F. M., Bhowruth, V., Leadbetter, E. A., Barton, N., Cohen, N. R., Hsu, F.-F., Besra, G. S., & Brenner, M. B. (2011). Innate and cytokine-driven signals, rather than microbial antigens, dominate in natural killer T cell activation during microbial infection. *The Journal of Experimental Medicine*, *208*(6), 1163–1177.

Brown, M. G., Dokun, A. O., Heusel, J. W., Smith, H. R., Beckman, D. L., Blattenberger, E. A., Dubbelde, C. E., Stone, L. R., Scalzo, A. A., & Yokoyama, W. M. (2001). Vital involvement of a natural killer cell activation receptor in resistance to viral infection. *Science*, *292*(5518), 934–937.

Bryceson, Y. T., March, M. E., Ljunggren, H.-G., & Long, E. O. (2006). Synergy among receptors on resting NK cells for the activation of natural cytotoxicity and cytokine secretion. *Blood*, *107*(1), 159–166.

Buchmeier, N. A., & Heffron, F. (1991). Inhibition of macrophage phagosome-lysosome fusion by Salmonella typhimurium. *Infection and Immunity*, *59*(7), 2232–8.

Budd, R. C., Miescher, G. C., Howe, R. C., Lees, R. K., Bron, C., & MacDonald, H. R. (1987). Developmentally regulated expression of T cell receptor beta chain variable domains in immature thymocytes. *The Journal of Experimental Medicine*, *166*(2), 577–582.

Bukowski, J. F. (1985). Adoptive transfer studies demonstrating the antiviral effect of natural killer cells in vivo. *Journal of Experimental Medicine*, *161*(1), 40–52.

Bukowski, J. F., Morita, C. T., & Brenner, M. B. (1994). Recognition and destruction of virus-infected cells by human gamma delta CTL. *Journal of Immunology (Baltimore, Md. : 1950)*, *153*(11), 5133–40.

Buonocore, S., Ahern, P. P., Uhlig, H. H., Ivanov, I. I., Littman, D. R., Maloy, K. J., & Powrie, F. (2010). Innate lymphoid cells drive interleukin-23-dependent innate intestinal pathology. *Nature*, *464*(7293), 1371–1375.

Bush, K. A., Farmer, K. M., Walker, J. S., & Kirkham, B. W. (2002). Reduction of joint inflammation and bone erosion in rat adjuvant arthritis by treatment with interleukin-17 receptor IgG1 Fc fusion protein. *Arthritis and Rheumatism*, *46*(3), 802–805.

Butz, E. A., & Bevan, M. J. (1998). Massive expansion of antigen-specific CD8+ T cells during an acute virus infection. *Immunity*, *8*(2), 167–175.

Cai, Y., Shen, X., Ding, C., Qi, C., Li, K., Li, X., Jala, V. R., Zhang, H., Wang, T., Zheng, J., & Yan, J. (2011). Pivotal role of dermal IL-17-producing γδ T cells in skin inflammation. *Immunity*, *35*(4), 596–610.

Caligiuri, M. A., Zmuidzinas, A., Manley, T. J., Levine, H., Smith, K. A., & Ritz, J. (1990). Functional consequences of interleukin 2 receptor expression on resting human lymphocytes. Identification of a novel natural killer cell subset with high affinity receptors. *The Journal of Experimental Medicine*, *171*(5), 1509–15026.

Campbell, I. K., Bendele, A., Smith, D. A., & Hamilton, J. A. (1997). Granulocyte-macrophage colony stimulating factor exacerbates collagen induced arthritis in mice. *Annals of the Rheumatic Diseases*, *56*(6), 364–368.

Campbell, J. J., Haraldsen, G., Pan, J., Rottman, J., Qin, S., Ponath, P., Andrew, D. P., Warnke, R., Ruffing, N., Kassam, N., Wu, L., & Butcher, E. C. (1999). The chemokine receptor CCR4 in vascular recognition by cutaneous but not intestinal memory T cells. *Nature*, *400*(6746), 776–780.

Capon, F., Di Meglio, P., Szaub, J., Prescott, N. J., Dunster, C., Baumber, L., Timms, K., Gutin, A., Abkevic, V., Burden, A. D., Lanchbury, J., Barker, J. N., Trembath, R. C., & Nestle, F. O. (2007). Sequence variants in the genes for the interleukin-23 receptor (IL23R) and its ligand (IL12B) confer protection against psoriasis. *Human Genetics*, *122*(2), 201–206.

Cargill, M., Schrodi, S. J., Chang, M., Garcia, V. E., Brandon, R., Callis, K. P., Matsunami, N., Ardlie, K. G., Civello, D., Catanese, J. J., Leong, D. U., Panko, J. M., McAllister, L. B., Hansen, C. B., Papenfuss, J., Prescott, S. M., White, T. J., Leppert, M. F., Krueger, G. G., & Begovich, A. B. (2007). A large-scale genetic association study confirms IL12B and leads to the identification of IL23R as psoriasis-risk genes. *American Journal of Human Genetics*, *80*(2), 273–290.

Carlyle, J. R., Jamieson, A. M., Gasser, S., Clingan, C. S., Arase, H., & Raulet, D. H. (2004). Missing self-recognition of Ocil/Clr-b by inhibitory NKR-P1 natural killer cell receptors. *Proceedings of the National Academy of Sciences*, *101*(10), 3527–3532.

Carlyle, J. R., Martin, A., Mehra, A., Attisano, L., Tsui, F. W., & Zúñiga-Pflücker, J. C. (1999). Mouse NKR-P1B, a novel NK1.1 antigen with inhibitory function. *Journal of Immunology*, *162*(10), 5917–5923.

Carolan, E., Tobin, L. M., Mangan, B. A., Corrigan, M., Gaoatswe, G., Byrne, G., Geoghegan, J., Cody, D., O'Connell, J., Winter, D. C., Doherty, D. G., Lynch, L., O'Shea, D., & Hogan, A. E. (2015). Altered Distribution and Increased IL-17 Production by Mucosal-Associated Invariant T Cells in Adult and Childhood Obesity. *The Journal of Immunology*, *194*(12), 5775–5780.

Cascão, R., Vidal, B., Raquel, H., Neves-Costa, A., Figueiredo, N., Gupta, V., Fonseca, J. E., & Moita, L. F. (2012). Effective treatment of rat adjuvant-induced arthritis by celastrol. *Autoimmunity Reviews*, *11*(12), 856–862.

Celis, R., Planell, N., Fernández-Sueiro, J. L., Sanmartí, R., Ramírez, J., González-Álvaro,

I., Pablos, J. L., & Cañete, J. D. (2012). Synovial cytokine expression in psoriatic arthritis and associations with lymphoid neogenesis and clinical features. *Arthritis Research & Therapy*, *14*(2), R93.

Cella, M., Fuchs, A., Vermi, W., Facchetti, F., Otero, K., Lennerz, J. K. M., Doherty, J. M., Mills, J. C., & Colonna, M. (2009). A human natural killer cell subset provides an innate source of IL-22 for mucosal immunity. *Nature*, *457*(7230), 722–725.

Ceredig, R., Lynch, F., & Newman, P. (1987). Phenotypic properties, interleukin 2 production, and developmental origin of a “mature” subpopulation of Lyt-2- L3T4- mouse thymocytes. *Proceedings of the National Academy of Sciences of the United States of America*, *84*(23), 8578–8582.

Chabaud, M., Durand, J. M., Buchs, N., Fossiez, F., Page, G., Frappart, L., & Miossec, P. (1999). Human interleukin-17: A T cell-derived proinflammatory cytokine produced by the rheumatoid synovium. *Arthritis and Rheumatism*, *42*(5), 963–970.

Chabaud, M., Garnero, P., Dayer, J. M., Guerne, P. A., Fossiez, F., & Miossec, P. (2000). Contribution of interleukin 17 to synovium matrix destruction in rheumatoid arthritis. *Cytokine*, *12*(7), 1092–1099.

Chakravarti, S., & Godfrey, D. I. (2010). Directing traffic on the NKT-cell highway: a key role for ThPOK. *European Journal of Immunology*, *40*(9), 2372–2375.

Chan, A., Hong, D.-L., Atzberger, A., Kollnberger, S., Filer, A. D., Buckley, C. D., McMichael, A., Enver, T., & Bowness, P. (2007). CD56bright Human NK Cells Differentiate into CD56dim Cells: Role of Contact with Peripheral Fibroblasts. *The Journal of Immunology*, *179*(1), 89–94.

Chan, J. R., Blumenschein, W., Murphy, E., Diveu, C., Wiekowski, M., Abbondanzo, S., Lucian, L., Geissler, R., Brodie, S., Kimball, A. B., Gorman, D. M., Smith, K., de Waal Malefyt, R., Kastelein, R. A., McClanahan, T. K., & Bowman, E. P. (2006). IL-23 stimulates epidermal hyperplasia via TNF and IL-20R2-dependent mechanisms with implications for psoriasis pathogenesis. *The Journal of Experimental Medicine*, *203*(12), 2577–2587.

Chan, W. L., Pejnovic, N., Hamilton, H., Liew, T. V., Popadic, D., Poggi, A., & Khan, S. M. (2005). Atherosclerotic abdominal aortic aneurysm and the interaction between autologous human plaque-derived vascular smooth muscle cells, type 1 NKT, and helper T cells. *Circulation Research*, *96*(6), 675–683.

Chen, W., Jin, W., Hardegen, N., Lei, K.-J., Li, L., Marinos, N., McGrady, G., & Wahl, S. M. (2003). Conversion of peripheral CD4+CD25- naive T cells to CD4+CD25+ regulatory T cells by TGF-beta induction of transcription factor Foxp3. *The Journal of Experimental Medicine*, *198*(12), 1875–1886.

Cheroutre, H., & Lambolez, F. (2008). Doubting the TCR coreceptor function of CD8alphaalpha. *Immunity*, *28*(2), 149–159.

Cherrier, M., Sawa, S., & Eberl, G. (2012). Notch, Id2, and RORγt sequentially orchestrate the fetal development of lymphoid tissue inducer cells. *The Journal of Experimental Medicine*, *209*(4), 729–740.

Cheung, T. W., & Teich, S. A. (1999). Cytomegalovirus infection in patients with HIV

infection. *The Mount Sinai Journal of Medicine, New York*, *66*(2), 113–24.

Chiba, A., Tajima, R., Tomi, C., Miyazaki, Y., Yamamura, T., & Miyake, S. (2012). Mucosal-associated invariant T cells promote inflammation and exacerbate disease in murine models of arthritis. *Arthritis and Rheumatism*, *64*(1), 153–161.

Chien, Y.-H., Iwashima, M., Kaplan, K. B., Elliott, J. F., & Davis, M. M. (1987). A new T-cell receptor gene located within the alpha locus and expressed early in T-cell differentiation. *Nature*, *327*(6124), 677–682.

Chien, Y.-H., Meyer, C., & Bonneville, M. (2014). γδ T cells: first line of defense and beyond. *Annual Review of Immunology*, *32*, 121–55.

Cho, Y.-N., Kee, S.-J., Kim, T.-J., Jin, H. M., Kim, M.-J., Jung, H.-J., Park, K.-J., Lee, S.-J., Lee, S.-S., Kwon, Y.-S., Kee, H. J., Kim, N., & Park, Y.-W. (2014). Mucosal-associated invariant T cell deficiency in systemic lupus erythematosus. *Journal of Immunology*, *193*(8), 3891–3901.

Chowdhury, D., & Lieberman, J. (2008). Death by a thousand cuts: granzyme pathways of programmed cell death. *Annual Review of Immunology*, *26*, 389–420.

Christophers, E. (2001). Psoriasis - epidemiology and clinical spectrum. *Clinical and Experimental Dermatology*, *26*(4), 314–320.

Chua, W.-J., Kim, S., Myers, N., Huang, S., Yu, L., Fremont, D. H., Diamond, M. S., & Hansen, T. H. (2011). Endogenous MHC-related protein 1 is transiently expressed on the plasma membrane in a conformation that activates mucosal-associated invariant T cells. *Journal of Immunology*, *186*(8), 4744–4750.

Chua, W.-J., Truscott, S. M., Eickhoff, C. S., Blazevic, A., Hoft, D. F., & Hansen, T. H. (2012). Polyclonal mucosa-associated invariant T cells have unique innate functions in bacterial infection. *Infection and Immunity*, *80*(9), 3256–67.

Clark, R. A., Chong, B., Mirchandani, N., Brinster, N. K., Yamanaka, K. -i., Dowgiert, R. K., & Kupper, T. S. (2006). The Vast Majority of CLA+ T Cells Are Resident in Normal Skin. *The Journal of Immunology*, *176*(7), 4431–4439.

Cohen, N. R., Brennan, P. J., Shay, T., Watts, G. F., Brigl, M., Kang, J., & Brenner, M. B. (2013). Shared and distinct transcriptional programs underlie the hybrid nature of iNKT cells. *Nature Immunology*, *14*(1), 90–99.

Colonna, M., Borsellino, G., Falco, M., Ferrara, G. B., & Strominger, J. L. (1993). HLA-C is the inhibitory ligand that determines dominant resistance to lysis by NK1- and NK2-specific natural killer cells. *Proceedings of the National Academy of Sciences*, *90*(24), 12000–12004.

Constantinides, M. G., McDonald, B. D., Verhoef, P. A., & Bendelac, A. (2014). A committed precursor to innate lymphoid cells. *Nature*, *508*(7496), 397–401.

Cookson, S., & Reen, D. (2003). IL-15 drives neonatal T cells to acquire CD56 and become activated effector cells. *Blood*, *102*(6), 2195–2197.

Cooper, D. M., Petchkovsky, D. V., Hackett, T. L., Knight, D. a., & Granville, D. J. (2011). Granzyme K activates protease-activated receptor-1. *PLoS ONE*, *6*(6), e21484.

Cooper, M. A., Bush, J. E., Fehniger, T. A., VanDeusen, J. B., Waite, R. E., Liu, Y., Aguila, H. L., & Caligiuri, M. A. (2002). In vivo evidence for a dependence on interleukin 15 for survival of natural killer cells. *Blood*, *100*(10), 3633–3638.

Cooper, M. A., Fehniger, T. A., Turner, S. C., Chen, K. S., Ghaheri, B. A., Ghayur, T., Carson, W. E., & Caligiuri, M. A. (2001). Human natural killer cells: A unique innate immunoregulatory role for the CD56bright subset. *Blood*, *97*(10), 3146–3151.

Coquet, J. M., Chakravarti, S., Kyparissoudis, K., McNab, F. W., Pitt, L. A., McKenzie, B. S., Berzins, S. P., Smyth, M. J., & Godfrey, D. I. (2008). Diverse cytokine production by NKT cell subsets and identification of an IL-17-producing CD4-NK1.1- NKT cell population. *Proceedings of the National Academy of Sciences of the United States of America*, *105*(32), 11287–11292.

Corbett, A. J., Eckle, S. B. G., Birkinshaw, R. W., Liu, L., Patel, O., Mahony, J., Chen, Z., Reantragoon, R., Meehan, B., Cao, H., Williamson, N. A., Strugnell, R. A., Van Sinderen, D., Mak, J. Y. W., Fairlie, D. P., Kjer-Nielsen, L., Rossjohn, J., & McCluskey, J. (2014). T-cell activation by transitory neo-antigens derived from distinct microbial pathways. *Nature*, *509*(7500), 361–365.

Cosgrove, C., Berger, C. T., Kroy, D. C., Cheney, P. C., Ghebremichael, M., Aneja, J., Tomlinson, M., Kim, A. Y., Lauer, G. M., & Alter, G. (2014). Chronic HCV infection affects the NK cell phenotype in the blood more than in the liver. *PloS One*, *9*(8), e105950.

Cosgrove, C., Ussher, J. E., Rauch, A., Gärtner, K., Kurioka, A., Hühn, M. H., Adelmann, K., Kang, Y. H., Fergusson, J. R., Simmonds, P., Goulder, P., Hansen, T. H., Fox, J., Günthard, H. F., Khanna, N., Powrie, F., Steel, A., Gazzard, B., Phillips, R. E., Frater, J., Uhlig, H., Klenerman, P., Huhn, M. H., Adelmann, K., Kang, Y. H., Fergusson, J. R., Simmonds, P., Goulder, P., Hansen, T. H., Fox, J., Günthard, H. F., Khanna, N., Powrie, F., Steel, A., Gazzard, B., Phillips, R. E., Frater, J., Uhlig, H., Klenerman, P., & Ga, K. (2013). Early and nonreversible decrease of CD161++/MAIT cells in HIV infection. *Blood*, *121*(6), 951–961.

Cosmi, L., De Palma, R., Santarlasci, V., Maggi, L., Capone, M., Frosali, F., Rodolico, G., Querci, V., Abbate, G., Angeli, R., Berrino, L., Fambrini, M., Caproni, M., Tonelli, F., Lazzeri, E., Parronchi, P., Liotta, F., Maggi, E., Romagnani, S., & Annunziato, F. (2008). Human interleukin 17-producing cells originate from a CD161+CD4+ T cell precursor. *The Journal of Experimental Medicine*, *205*(8), 1903–1916.

Costello, P., Bresnihan, B., O'Farrelly, C., & FitzGerald, O. (1999). Predominance of CD8+ T lymphocytes in psoriatic arthritis. *The Journal of Rheumatology*, *26*(5), 1117–1124.

Crowe, N. Y., Coquet, J. M., Berzins, S. P., Kyparissoudis, K., Keating, R., Pellicci, D. G., Hayakawa, Y., Godfrey, D. I., & Smyth, M. J. (2005). Differential antitumor immunity mediated by NKT cell subsets in vivo. *The Journal of Experimental Medicine*, *202*(9), 1279–1288.

Croxford, J. L., Miyake, S., Huang, Y.-Y., Shimamura, M., & Yamamura, T. (2006). Invariant V(alpha)19i T cells regulate autoimmune inflammation. *Nature Immunology*, *7*(9), 987–994.

Cruz-Guilloty, F., Pipkin, M. E., Djuretic, I. M., Levanon, D., Lotem, J., Lichtenheld, M. G.,

Groner, Y., & Rao, A. (2009). Runx3 and T-box proteins cooperate to establish the transcriptional program of effector CTLs. *The Journal of Experimental Medicine*, *206*(1), 51–59.

Cua, D. J., Sherlock, J., Chen, Y., Murphy, C. A., Joyce, B., Seymour, B., Lucian, L., To, W., Kwan, S., Churakova, T., Zurawski, S., Wiekowski, M., Lira, S. A., Gorman, D., Kastelein, R. A., & Sedgwick, J. D. (2003). Interleukin-23 rather than interleukin-12 is the critical cytokine for autoimmune inflammation of the brain. *Nature*, *421*(6924), 744–748.

Dalbeth, N., Gundle, R., Davies, R. J. O., Lee, Y. C. G., McMichael, A. J., & Callan, M. F. C. (2004). CD56bright NK cells are enriched at inflammatory sites and can engage with monocytes in a reciprocal program of activation. *Journal of Immunology*, *173*(10), 6418–6426.

de Jong, A., Cheng, T.-Y., Huang, S., Gras, S., Birkinshaw, R. W., Kasmar, A. G., Van Rhijn, I., Peña-Cruz, V., Ruan, D. T., Altman, J. D., Rossjohn, J., & Moody, D. B. (2014). CD1a-autoreactive T cells recognize natural skin oils that function as headless antigens. *Nature Immunology*, *15*(2), 177–185.

De Maria, A., Bozzano, F., Cantoni, C., & Moretta, L. (2011). Revisiting human natural killer cell subset function revealed cytolytic CD56(dim)CD16+ NK cells as rapid producers of abundant IFN-gamma on activation. *Proceedings of the National Academy of Sciences of the United States of America*, *108*(2), 728–732.

De Maria, A., Fogli, M., Costa, P., Murdaca, G., Puppo, F., Mavilio, D., Moretta, A., & Moretta, L. (2003). The impaired NK cell cytolytic function in viremic HIV-1 infection is associated with a reduced surface expression of natural cytotoxicity receptors (NKp46, NKp30 and NKp44). *European Journal of Immunology*, *33*(9), 2410–2418.

de Matos, C. T., Berg, L., Michaëlsson, J., Felländer-Tsai, L., Kärre, K., & Söderström, K. (2007). Activating and inhibitory receptors on synovial fluid natural killer cells of arthritis patients: role of CD94/NKG2A in control of cytokine secretion. *Immunology*, *122*(2), 291–301.

Della Chiesa, M., Falco, M., Bertaina, A., Muccio, L., Alicata, C., Frassoni, F., Locatelli, F., Moretta, L., & Moretta, A. (2014). Human cytomegalovirus infection promotes rapid maturation of NK cells expressing activating killer Ig-like receptor in patients transplanted with NKG2C-/- umbilical cord blood. *Journal of Immunology*, *192*(4), 1471–1479.

Di Cesare, A., Di Meglio, P., & Nestle, F. O. (2008). A role for Th17 cells in the immunopathogenesis of atopic dermatitis? *The Journal of Investigative Dermatology*, *128*(11), 2569–2571.

Di Cesare, A., Di Meglio, P., & Nestle, F. O. (2009). The IL-23/Th17 axis in the immunopathogenesis of psoriasis. *The Journal of Investigative Dermatology*, *129*(6), 1339–50.

Dieli, F., Troye-Blomberg, M., Ivanyi, J., Fournié, J. J., Krensky, A. M., Bonneville, M., Peyrat, M. A., Caccamo, N., Sireci, G., & Salerno, A. (2001). Granulysin-dependent killing of intracellular and extracellular Mycobacterium tuberculosis by Vgamma9/Vdelta2 T lymphocytes. *The Journal of Infectious Diseases*, *184*(8), 1082–

5.

Dunne, M. R., Elliott, L., Hussey, S., Mahmud, N., Kelly, J., Doherty, D. G., & Feighery, C. F. (2013). Persistent changes in circulating and intestinal γδ T cell subsets, invariant natural killer T cells and mucosal-associated invariant T cells in children and adults with coeliac disease. *PloS One*, *8*(10), e76008.

Dusseaux, M., Martin, E., Serriari, N., Péguillet, I., Premel, V., Louis, D., Milder, M., Le Bourhis, L., Soudais, C., Treiner, E., & Lantz, O. (2011). Human MAIT cells are xenobiotic-resistant, tissue-targeted, CD161hi IL-17-secreting T cells. *Blood*, *117*(4), 1250–1259.

Eckle, S. B. G., Birkinshaw, R. W., Kostenko, L., Corbett, A. J., McWilliam, H. E. G., Reantragoon, R., Chen, Z., Gherardin, N. A., Beddoe, T., Liu, L., Patel, O., Meehan, B., Fairlie, D. P., Villadangos, J. A., Godfrey, D. I., Kjer-Nielsen, L., McCluskey, J., & Rossjohn, J. (2014). A molecular basis underpinning the T cell receptor heterogeneity of mucosal-associated invariant T cells. *The Journal of Experimental Medicine*, *211*(8), 1585–1600.

Eder, L., Chandran, V., Pellet, F., Shanmugarajah, S., Rosen, C. F., Bull, S. B., & Gladman, D. D. (2012). Human leucocyte antigen risk alleles for psoriatic arthritis among patients with psoriasis. *Annals of the Rheumatic Diseases*, *71*(1), 50–55.

Eidson, M., Wahlstrom, J., Beaulieu, A. M., Zaidi, B., Carsons, S. E., Crow, P. K., Yuan, J., Wolchok, J. D., Horsthemke, B., Wieczorek, D., & Sant'Angelo, D. B. (2011). Altered development of NKT cells, γδ T cells, CD8 T cells and NK cells in a PLZF deficient patient. *PloS One*, *6*(9), e24441.

Emoto, M., Emoto, Y., & Kaufmann, S. H. (1995). Interleukin-4-producing CD4+ NK1.1+ TCR alpha/beta intermediate liver lymphocytes are down-regulated by Listeria monocytogenes. *European Journal of Immunology*, *25*(12), 3321–3325.

Emoto, M., Yoshizawa, I., Emoto, Y., Miamoto, M., Hurwitz, R., & Kaufmann, S. H. E. (2006). Rapid development of a gamma interferon-secreting glycolipid/CD1d-specific Valpha14+ NK1.1- T-cell subset after bacterial infection. *Infection and Immunity*, *74*(10), 5903–5913.

Enders, A., Stankovic, S., Teh, C., Uldrich, A. P., Yabas, M., Juelich, T., Altin, J. A., Frankenreiter, S., Bergmann, H., Roots, C. M., Kyparissoudis, K., Goodnow, C. C., & Godfrey, D. I. (2012). ZBTB7B (Th-POK) regulates the development of IL-17-producing CD1d-restricted mouse NKT cells. *Journal of Immunology*, *189*(11), 5240–5249.

Engel, I., Hammond, K., Sullivan, B. A., He, X., Taniuchi, I., Kappes, D., & Kronenberg, M. (2010). Co-receptor choice by V alpha14i NKT cells is driven by Th-POK expression rather than avoidance of CD8-mediated negative selection. *The Journal of Experimental Medicine*, *207*(5), 1015–1029.

Engel, I., Zhao, M., Kappes, D., Taniuchi, I., & Kronenberg, M. (2012). The transcription factor Th-POK negatively regulates Th17 differentiation in Vα14i NKT cells. *Blood*, *120*(23), 4524–32.

Exley, M., Garcia, J., Balk, S. P., & Porcelli, S. (1997). Requirements for CD1d recognition

by human invariant Valpha24+ CD4-CD8- T cells. *The Journal of Experimental Medicine*, *186*(1), 109–120.

Exley, M., Porcelli, S., Furman, M., Garcia, J., & Balk, S. (1998). CD161 (NKR-P1A) costimulation of CD1d-dependent activation of human T cells expressing invariant V alpha 24 J alpha Q T cell receptor alpha chains. *The Journal of Experimental Medicine*, *188*(5), 867–876.

Eysteinsdóttir, J. H., Sigurgeirsson, B., Ólafsson, J. H., Fridriksson, T., Agnarsson, B. A., Davíðsson, S., Valdimarsson, H., & Lúðvíksson, B. R. (2013). The role of Th17/Tc17 peripheral blood T cells in psoriasis and their positive therapeutic response. *Scandinavian Journal of Immunology*, *78*(6), 529–537.

Fallon, P. G., Ballantyne, S. J., Mangan, N. E., Barlow, J. L., Dasvarma, A., Hewett, D. R., McIlgorm, A., Jolin, H. E., & McKenzie, A. N. J. (2006). Identification of an interleukin (IL)-25-dependent cell population that provides IL-4, IL-5, and IL-13 at the onset of helminth expulsion. *The Journal of Experimental Medicine*, *203*(4), 1105–16.

Farr, A. R., Wu, W., Choi, B., Cavalcoli, J. D., & Laouar, Y. (2014). CD1d-unrestricted NKT cells are endowed with a hybrid function far superior than that of iNKT cells. *Proceedings of the National Academy of Sciences of the United States of America*, *111*(35), 12841–12846.

Fasano, A., & Shea-Donohue, T. (2005). Mechanisms of disease: the role of intestinal barrier function in the pathogenesis of gastrointestinal autoimmune diseases. *Nature Clinical Practice. Gastroenterology & Hepatology*, *2*(9), 416–422.

Fauriat, C., Ivarsson, M. A., Ljunggren, H.-G., Malmberg, K.-J., & Michaëlsson, J. (2010a). Education of human natural killer cells by activating killer cell immunoglobulin-like receptors. *Blood*, *115*(6), 1166–74.

Fauriat, C., Long, E. O., Ljunggren, H.-G., & Bryceson, Y. T. (2010b). Regulation of human NK-cell cytokine and chemokine production by target cell recognition. *Blood*, *115*(11), 2167–2176.

Fehniger, T. A., Cooper, M. A., Nuovo, G. J., Cella, M., Facchetti, F., Colonna, M., & Caligiuri, M. A. (2003). CD56bright natural killer cells are present in human lymph nodes and are activated by T cell-derived IL-2: a potential new link between adaptive and innate immunity. *Blood*, *101*(8), 3052–3057.

Fehniger, T. A., Shah, M. H., Turner, M. J., VanDeusen, J. B., Whitman, S. P., Cooper, M. A., Suzuki, K., Wechser, M., Goodsaid, F., & Caligiuri, M. A. (1999). Differential cytokine and chemokine gene expression by human NK cells following activation with IL-18 or IL-15 in combination with IL-12: implications for the innate immune response. *Journal of Immunology*, *162*(8), 4511–4520.

Fergusson, J. R., Fleming, V. M., & Klenerman, P. (2011). CD161-expressing human T cells. *Frontiers in Immunology*, *2*(August), 36.

Fergusson, J. R., Hühn, M. H., Swadling, L., Walker, L. J., Kurioka, A., Llibre, A., Bertoletti, A., Holländer, G., Newell, E. W., Davis, M. M., Sverremark-Ekström, E., Powrie, F., Capone, S., Folgori, A., Barnes, E., Willberg, C. B., Ussher, J. E., & Klenerman, P. (2015). CD161(int)CD8+ T cells: a novel population of highly functional, memory

CD8+ T cells enriched within the gut. *Mucosal Immunology*.

Fergusson, J. R., Smith, K. E., Fleming, V. M., Rajoriya, N., Newell, E. W., Simmons, R., Marchi, E., Björkander, S., Kang, Y.-H., Swadling, L., Kurioka, A., Sahgal, N., Lockstone, H., Baban, D., Freeman, G. J., Sverremark-Ekström, E., Davis, M. M., Davenport, M. P., Venturi, V., Ussher, J. E., Willberg, C. B., & Klenerman, P. (2014). CD161 Defines a Transcriptional and Functional Phenotype across Distinct Human T Cell Lineages. *Cell Reports*, *9*(3), 1075–1088.

Ferlazzo, G., Pack, M., Thomas, D., Paludan, C., Schmid, D., Strowig, T., Bougras, G., Muller, W. A., Moretta, L., & Münz, C. (2004a). Distinct roles of IL-12 and IL-15 in human natural killer cell activation by dendritic cells from secondary lymphoid organs. *Proceedings of the National Academy of Sciences of the United States of America*, *101*(47), 16606–16611.

Ferlazzo, G., Thomas, D., Lin, S.-L., Goodman, K., Morandi, B., Muller, W. A., Moretta, A., & Munz, C. (2004b). The Abundant NK Cells in Human Secondary Lymphoid Tissues Require Activation to Express Killer Cell Ig-Like Receptors and Become Cytolytic. *The Journal of Immunology*, *172*(3), 1455–1462.

Fernandez, C. S., Amarasena, T., Kelleher, A. D., Rossjohn, J., McCluskey, J., Godfrey, D. I., & Kent, S. J. (2015). MAIT cells are depleted early but retain functional cytokine expression in HIV infection. *Immunology and Cell Biology*, *93*(2), 177–188.

Ferrick, D. A., Schrenzel, M. D., Mulvania, T., Hsieh, B., Ferlin, W. G., & Lepper, H. (1995). Differential production of interferon-gamma and interleukin-4 in response to Th1- and Th2-stimulating pathogens by gamma delta T cells in vivo. *Nature*, *373*(6511), 255–257.

Finck, R., Simonds, E. F., Jager, A., Krishnaswamy, S., Sachs, K., Fantl, W., Pe'er, D., Nolan, G. P., & Bendall, S. C. (2013). Normalization of mass cytometry data with bead standards. *Cytometry. Part A : The Journal of the International Society for Analytical Cytology*, *83*(5), 483–494.

Fisch, P., Malkovsky, M., Braakman, E., Sturm, E., Bolhuis, R. L., Prieve, A., Sosman, J. A., Lam, V. A., & Sondel, P. M. (1990). Gamma/delta T cell clones and natural killer cell clones mediate distinct patterns of non-major histocompatibility complex-restricted cytolysis. *The Journal of Experimental Medicine*, *171*(5), 1567–1579.

Foley, B., Cooley, S., Verneris, M. R., Curtsinger, J., Luo, X., Waller, E. K., Anasetti, C., Weisdorf, D., & Miller, J. S. (2012a). Human cytomegalovirus (CMV)-induced memory-like NKG2C(+) NK cells are transplantable and expand in vivo in response to recipient CMV antigen. *Journal of Immunology*, *189*(10), 5082–5088.

Foley, B., Cooley, S., Verneris, M. R., Pitt, M., Curtsinger, J., Luo, X., Lopez-Vergès, S., Lanier, L. L., Weisdorf, D., & Miller, J. S. (2012b). Cytomegalovirus reactivation after allogeneic transplantation promotes a lasting increase in educated NKG2C+ natural killer cells with potent function. *Blood*, *119*(11), 2665–2674.

Fowlkes, B. J., Kruisbeek, A. M., Ton-That, H., Weston, M. A., Coligan, J. E., Schwartz, R. H., & Pardoll, D. M. (1987). A novel population of T-cell receptor alpha beta-bearing thymocytes which predominantly expresses a single V beta gene family. *Nature*, *329*(6136), 251–254.

Freud, A. G., Yokohama, A., Becknell, B., Lee, M. T., Mao, H. C., Ferketich, A. K., & Caligiuri, M. A. (2006). Evidence for discrete stages of human natural killer cell differentiation in vivo. *The Journal of Experimental Medicine*, *203*(4), 1033–1043.

Froelich, C. J., Orth, K., Turbov, J., Seth, P., Gottlieb, R., Babior, B., Shah, G. M., Bleackley, R. C., Dixit, V. M., & Hanna, W. (1996). New paradigm for lymphocyte granule-mediated cytotoxicity. Target cells bind and internalize granzyme B, but an endosomolytic agent is necessary for cytosolic delivery and subsequent apoptosis. *Journal of Biological Chemistry*, *271*(46), 29073–29079.

Fuchs, A., Vermi, W., Lee, J. S., Lonardi, S., Gilfillan, S., Newberry, R. D., Cella, M., & Colonna, M. (2013). Intraepithelial type 1 innate lymphoid cells are a unique subset of IL-12- and IL-15-responsive IFN-γ-producing cells. *Immunity*, *38*(4), 769–781.

Gadola, S. D., Dulphy, N., Salio, M., & Cerundolo, V. (2002). Vα24-JαQ-independent, CD1d-restricted recognition of α-Galactosylceramide by human CD4+ and CD8αβ+ T lymphocytes. *Journal of Immunology*, *168*(11), 5514–5520.

Garcia, K. C., Scott, C. A., Brunmark, A., Carbone, F. R., Peterson, P. A., Wilson, I. A., & Teyton, L. (1996). CD8 enhances formation of stable T-cell receptor/MHC class I molecule complexes. *Nature*, *384*(6609), 577–81.

Gazit, R., Gruda, R., Elboim, M., Arnon, T. I., Katz, G., Achdout, H., Hanna, J., Qimron, U., Landau, G., Greenbaum, E., Zakay-Rones, Z., Porgador, A., & Mandelboim, O. (2006). Lethal influenza infection in the absence of the natural killer cell receptor gene Ncr1. *Nature Immunology*, *7*(5), 517–23.

Georgel, P., Radosavljevic, M., Macquin, C., & Bahram, S. (2011). The non-conventional MHC class I MR1 molecule controls infection by Klebsiella pneumoniae in mice. *Molecular Immunology*, *48*(5), 769–775.

Gérart, S., Sibéril, S., Martin, E., Lenoir, C., Aguilar, C., Lantz, O., Fischer, A., Latour, S., & Dc, W. (2013). Human iNKT and MAIT cells exhibit a PLZF-dependent proapoptotic propensity that is counterbalanced by XIAP. *Blood*, *121*(4), 614–623.

Geremia, A., Arancibia-Cárcamo, C. V, Fleming, M. P. P., Rust, N., Singh, B., Mortensen, N. J., Travis, S. P. L., & Powrie, F. (2011). IL-23-responsive innate lymphoid cells are increased in inflammatory bowel disease. *The Journal of Experimental Medicine*, *208*(6), 1127–1133.

Germain, C., Guillaudeux, T., Galsgaard, E. D., Hervouet, C., Tekaya, N., Gallouet, A.-S., Fassy, J., Bihl, F., Poupon, G., Lazzari, A., Spee, P., Anjuère, F., Pangault, C., Tarte, K., Tas, P., Xerri, L., & Braud, V. M. (2015). Lectin-like transcript 1 is a marker of germinal center-derived B-cell non-Hodgkin's lymphomas dampening natural killer cell functions. *OncoImmunology*, *4*(8), e1026503.

Germain, C., Meier, A., Jensen, T., Knapnougel, P., Poupon, G., Lazzari, A., Neisig, A., Håkansson, K., Dong, T., Wagtmann, N., Galsgaard, E. D., Spee, P., & Braud, V. M. (2011). Induction of lectin-like transcript 1 (LLT1) protein cell surface expression by pathogens and interferon-γ contributes to modulate immune responses. *The Journal of Biological Chemistry*, *286*(44), 37964–37975.

Gevers, D., Kugathasan, S., Denson, L. A., Vázquez-Baeza, Y., Van Treuren, W., Ren, B.,

Schwager, E., Knights, D., Song, S. J., Yassour, M., Morgan, X. C., Kostic, A. D., Luo, C., González, A., McDonald, D., Haberman, Y., Walters, T., Baker, S., Rosh, J., Stephens, M., Heyman, M., Markowitz, J., Baldassano, R., Griffiths, A., Sylvester, F., Mack, D., Kim, S., Crandall, W., Hyams, J., Huttenhower, C., Knight, R., & Xavier, R. J. (2014). The treatment-naive microbiome in new-onset Crohn's disease. *Cell Host & Microbe*, *15*(3), 382–392.

Gibbons, D. L., Haque, S. F. Y., Silberzahn, T., Hamilton, K., Langford, C., Ellis, P., Carr, R., & Hayday, A. C. (2009). Neonates harbour highly active gammadelta T cells with selective impairments in preterm infants. *European Journal of Immunology*, *39*(7), 1794–1806.

Gittler, J. K., Shemer, A., Suárez-Fariñas, M., Fuentes-Duculan, J., Gulewicz, K. J., Wang, C. Q. F., Mitsui, H., Cardinale, I., de Guzman Strong, C., Krueger, J. G., & Guttman-Yassky, E. (2012). Progressive activation of T(H)2/T(H)22 cytokines and selective epidermal proteins characterizes acute and chronic atopic dermatitis. *The Journal of Allergy and Clinical Immunology*, *130*(6), 1344–1354.

Gleimer, M., von Boehmer, H., & Kreslavsky, T. (2012). PLZF Controls the Expression of a Limited Number of Genes Essential for NKT Cell Function. *Frontiers in Immunology*, *3*(374).

Godfrey, D. I., Macdonald, H. R., Kronenberg, M., Smyth, M. J., & Van Kaer, L. (2004). NKT cells : what's in a name ? *Nature Reviews Immunology*, *4*(March), 231–237.

Godfrey, D. I., Stankovic, S., & Baxter, A. G. (2010). Raising the NKT cell family. *Nature Immunology*, *11*(3), 197–206.

Gold, M. C., Cerri, S., Smyk-Pearson, S., Cansler, M. E., Vogt, T. M., Delepine, J., Winata, E., Swarbrick, G. M., Chua, W. J., Yu, Y. Y. L., Lantz, O., Cook, M. S., Null, M. D., Jacoby, D. B., Harriff, M. J., Lewinsohn, D. A., Hansen, T. H., & Lewinsohn, D. M. (2010). Human mucosal associated invariant T cells detect bacterially infected cells. *PLoS Biology*, *8*(6), e1000407.

Gold, M. C., Eid, T., Smyk-Pearson, S., Eberling, Y., Swarbrick, G. M., Langley, S. M., Streeter, P. R., Lewinsohn, D. A., & Lewinsohn, D. M. (2012). Human thymic MR1-restricted MAIT cells are innate pathogen-reactive effectors that adapt following thymic egress. *Mucosal Immunology*, *6*(1), 35–44.

Gold, M. C., McLaren, J. E., Reistetter, J. A., Smyk-Pearson, S., Ladell, K., Swarbrick, G. M., Yu, Y. Y. L., Hansen, T. H., Lund, O., Nielsen, M., Gerritsen, B., Kesmir, C., Miles, J. J., Lewinsohn, D. A., Price, D. A., & Lewinsohn, D. M. (2014). MR1-restricted MAIT cells display ligand discrimination and pathogen selectivity through distinct T cell receptor usage. *The Journal of Experimental Medicine*, *211*(8), 1601–10.

Golden-Mason, L., Kelly, a. M., Doherty, D. G., Traynor, O., McEntee, G., Kelly, J., Hegarty, J. E., & O'Farrelly, C. (2004). Hepatic interleukin 15 (IL-15) expression: Implications for local NK/NKT cell homeostasis and development. *Clinical and Experimental Immunology*, *138*(1), 94–101.

Gordon, S. M., Chaix, J., Rupp, L. J., Wu, J., Madera, S., Sun, J. C., Lindsten, T., & Reiner, S. L. (2012). The transcription factors T-bet and Eomes control key checkpoints of natural killer cell maturation. *Immunity*, *36*(1), 55–67.

Griewank, K., Borowski, C., Rietdijk, S., Wang, N., Julien, A., Wei, D. G., Mamchak, A. A., Terhorst, C., & Bendelac, A. (2007). Homotypic interactions mediated by Slamf1 and Slamf6 receptors control NKT cell lineage development. *Immunity*, *27*(5), 751–762.

Grimaldi, D., Le Bourhis, L., Sauneuf, B., Dechartres, A., Rousseau, C., Ouaaz, F., Milder, M., Louis, D., Chiche, J.-D., Mira, J.-P., Lantz, O., & Pène, F. (2014). Specific MAIT cell behaviour among innate-like T lymphocytes in critically ill patients with severe infections. *Intensive Care Medicine*, *40*(2), 192–201.

Groh, V., Steinle, A., Bauer, S., & Spies, T. (1998). Recognition of stress-induced MHC molecules by intestinal epithelial gammadelta T cells. *Science*, *279*(5357), 1737–1740.

Gu, S., Nawrocka, W., & Adams, E. J. (2015). Sensing of Pyrophosphate Metabolites by Vγ9Vδ2 T Cells. *Frontiers in Immunology*, *5*(688).

Gudjonsson, J. E., Johnston, A., Sigmundsdottir, H., Valdimarsson, H., Gudjonsson, J. E., Johnston, A., Sigmundsdottir, H., & Valdimarsson, H. (2004). Immunopathogenic mechanisms in psoriasis. *Clinical and Experimental Immunology*, *135*(1), 1–8.

Gudjonsson, J. E., Karason, A., Antonsdottir, A., Runarsdottir, E. H., Hauksson, V. B., Upmanyu, R., Gulcher, J., Stefansson, K., & Valdimarsson, H. (2003). Psoriasis patients who are homozygous for the HLA-Cw*0602 allele have a 2.5-fold increased risk of developing psoriasis compared with Cw6 heterozygotes. *British Journal of Dermatology*, *148*(2), 233–235.

Gumá, M., Angulo, A., Vilches, C., Gómez-Lozano, N., Malats, N., & López-Botet, M. (2004). Imprint of human cytomegalovirus infection on the NK cell receptor repertoire. *Blood*, *104*(12), 3664–3671.

Gumá, M., Budt, M., Sáez, A., Brckalo, T., Hengel, H., Angulo, A., & López-Botet, M. (2006). Expansion of CD94/NKG2C+ NK cells in response to human cytomegalovirus-infected fibroblasts. *Blood*, *107*(9), 3624–31.

Gumperz, J. E., Miyake, S., Yamamura, T., & Brenner, M. B. (2002). Functionally distinct subsets of CD1d-restricted natural killer T cells revealed by CD1d tetramer staining. *The Journal of Experimental Medicine*, *195*(5), 625–636.

Guo, J., Hawwari, A., Li, H., Sun, Z., Mahanta, S. K., Littman, D. R., Krangel, M. S., & He, Y.-W. (2002). Regulation of the TCRalpha repertoire by the survival window of CD4+CD8+ thymocytes. *Nature Immunology*, *3*(5), 469–476.

Gutowska-Owsiak, D., Schaupp, A. L., Salimi, M., Selvakumar, T. A., McPherson, T., Taylor, S., & Ogg, G. S. (2012). IL-17 downregulates filaggrin and affects keratinocyte expression of genes associated with cellular adhesion. *Experimental Dermatology*, *21*(2), 104–110.

Halim, T. Y. F., Krauss, R. H., Sun, A. C., & Takei, F. (2012). Lung natural helper cells are a critical source of Th2 cell-type cytokines in protease allergen-induced airway inflammation. *Immunity*, *36*(3), 451–463.

Hamada, S., Umemura, M., Shiono, T., Tanaka, K., Yahagi, A., Begum, M. D., Oshiro, K., Okamoto, Y., Watanabe, H., Kawakami, K., Roark, C., Born, W. K., O'Brien, R., Ikuta, K., Ishikawa, H., Nakae, S., Iwakura, Y., Ohta, T., & Matsuzaki, G. (2008). IL-17A

produced by gammadelta T cells plays a critical role in innate immunity against listeria monocytogenes infection in the liver. *Journal of Immunology*, *181*(5), 3456–3463.

Harari, A., Enders, F. B., Cellerai, C., Bart, P.-A., & Pantaleo, G. (2009). Distinct profiles of cytotoxic granules in memory CD8 T cells correlate with function, differentiation stage, and antigen exposure. *Journal of Virology*, *83*(7), 2862–2871.

Harly, C., Guillaume, Y., Nedellec, S., Peigné, C.-M., Mönkkönen, H., Mönkkönen, J., Li, J., Kuball, J., Adams, E. J., Netzer, S., Déchanet-Merville, J., Léger, A., Herrmann, T., Breathnach, R., Olive, D., Bonneville, M., & Scotet, E. (2012). Key implication of CD277/butyrophilin-3 (BTN3A) in cellular stress sensing by a major human γδ T-cell subset. *Blood*, *120*(11), 2269–2279.

Harms, R. Z., Lorenzo, K. M., Corley, K. P., Cabrera, M. S., & Sarvetnick, N. E. (2015). Altered CD161 bright CD8+ mucosal associated invariant T (MAIT)-like cell dynamics and increased differentiation states among juvenile type 1 diabetics. *PloS One*, *10*(1), e0117335.

Harper, E. G., Guo, C., Rizzo, H., Lillis, J. V, Kurtz, S. E., Skorcheva, I., Purdy, D., Fitch, E., Iordanov, M., & Blauvelt, A. (2009). Th17 cytokines stimulate CCL20 expression in keratinocytes in vitro and in vivo: implications for psoriasis pathogenesis. *The Journal of Investigative Dermatology*, *129*(9), 2175–2183.

Hashimoto, K., Hirai, M., & Kurosawa, Y. (1995). A gene outside the human MHC related to classical HLA class I genes. *Science*, *269*(5224), 693–695.

Havlir, D. V, Ellner, J. J., Chervenak, K. A., & Boom, W. H. (1991). Selective expansion of human gamma delta T cells by monocytes infected with live Mycobacterium tuberculosis. *The Journal of Clinical Investigation*, *87*(2), 729–733.

Havran, W. L., & Allison, J. P. (1988). Developmentally ordered appearance of thymocytes expressing different T-cell antigen receptors. *Nature*, *335*(6189), 443–445.

Hayakawa, Y., Screpanti, V., Yagita, H., Grandien, A., Ljunggren, H.-G., Smyth, M. J., & Chambers, B. J. (2003). NK Cell TRAIL Eliminates Immature Dendritic Cells In Vivo and Limits Dendritic Cell Vaccination Efficacy. *The Journal of Immunology*, *172*(1), 123–129.

Hayhoe, R. P. G., Henson, S. M., Akbar, A. N., & Palmer, D. B. (2010). Variation of human natural killer cell phenotypes with age: identification of a unique KLRG1-negative subset. *Human Immunology*, *71*(7), 676–681.

He, X., He, X., Dave, V. P., Zhang, Y., Hua, X., Nicolas, E., Xu, W., Roe, B. A., & Kappes, D. J. (2005). The zinc finger transcription factor Th-POK regulates CD4 versus CD8 T-cell lineage commitment. *Nature*, *433*(7028), 826–833.

He, X., Park, K., & Kappes, D. J. (2010). The Role of ThPOK in Control of CD4/CD8 Lineage Commitment. *Annual Review of Immunology*, *28*, 295–320.

He, X., Park, K., Wang, H., He, X., Zhang, Y., Hua, X., Li, Y., & Kappes, D. J. (2008). CD4-CD8 lineage commitment is regulated by a silencer element at the ThPOK transcription-factor locus. *Immunity*, *28*(3), 346–58.

Hébert, H. L., Ali, F. R., Bowes, J., Griffiths, C. E. M., Barton, A., & Warren, R. B. (2012). Genetic susceptibility to psoriasis and psoriatic arthritis: implications for therapy. *The British Journal of Dermatology*, *166*(3), 474–482.

Herberman, R. B., Nunn, M. E., Holden, H. T., & Lavrin, D. H. (1975). Natural cytotoxic reactivity of mouse lymphoid cells against syngeneic and allogeneic tumors. II. Characterization of effector cells. *International Journal of Cancer*, *16*(2), 230–239.

Heusel, J. W., Wesselschmidt, R. L., Shresta, S., Russell, J. H., & Ley, T. J. (1994). Cytotoxic lymphocytes require granzyme B for the rapid induction of DNA fragmentation and apoptosis in allogeneic target cells. *Cell*, *76*(6), 977–987.

Hintz, M., Reichenberg, A., Altincicek, B., Bahr, U., Gschwind, R. M., Kollas, A. K., Beck, E., Wiesner, J., Eberl, M., & Jomaa, H. (2001). Identification of (E)-4-hydroxy-3-methyl-but-2-enyl pyrophosphate as a major activator for human gammadelta T cells in Escherichia coli. *FEBS Letters*, *509*(2), 317–322.

Hirota, K., Yoshitomi, H., Hashimoto, M., Maeda, S., Teradaira, S., Sugimoto, N., Yamaguchi, T., Nomura, T., Ito, H., Nakamura, T., Sakaguchi, N., & Sakaguchi, S. (2007). Preferential recruitment of CCR6-expressing Th17 cells to inflamed joints via CCL20 in rheumatoid arthritis and its animal model. *The Journal of Experimental Medicine*, *204*(12), 2803–12.

Holder, K. A., Stapleton, S. N., Gallant, M. E., Russell, R. S., & Grant, M. D. (2013). Hepatitis C virus-infected cells downregulate NKp30 and inhibit ex vivo NK cell functions. *Journal of Immunology*, *191*(6), 3308–3318.

Homey, B., Dieu-Nosjean, M.-C., Wiesenborn, A., Massacrier, C., Pin, J.-J., Oldham, E., Catron, D., Buchanan, M. E., Muller, A., deWaal Malefyt, R., Deng, G., Orozco, R., Ruzicka, T., Lehmann, P., Lebecque, S., Caux, C., & Zlotnik, A. (2000). Up-Regulation of Macrophage Inflammatory Protein-3 /CCL20 and CC Chemokine Receptor 6 in Psoriasis. *The Journal of Immunology*, *164*(12), 6621–6632.

Hoyler, T., Klose, C. S. N., Souabni, A., Turqueti-Neves, A., Pfeifer, D., Rawlins, E. L., Voehringer, D., Busslinger, M., & Diefenbach, A. (2012). The transcription factor GATA-3 controls cell fate and maintenance of type 2 innate lymphoid cells. *Immunity*, *37*(4), 634–648.

Hsieh, C. S., Macatonia, S. E., Tripp, C. S., Wolf, S. F., O'Garra, A., & Murphy, K. M. (1993). Development of TH1 CD4+ T cells through IL-12 produced by Listeria-induced macrophages. *Science*, *260*(5107), 547–549.

Huang, S., Gilfillan, S., Cella, M., Miley, M. J., Lantz, O., Lybarger, L., Fremont, D. H., & Hansen, T. H. (2005). Evidence for MR1 antigen presentation to mucosal-associated invariant T cells. *The Journal of Biological Chemistry*, *280*(22), 21183–21193.

Huang, S., Gilfillan, S., Kim, S., Thompson, B., Wang, X., Sant, A. J., Fremont, D. H., Lantz, O., & Hansen, T. H. (2008). MR1 uses an endocytic pathway to activate mucosal-associated invariant T cells. *The Journal of Experimental Medicine*, *205*(5), 1201–1211.

Huang, Y., Park, Y., Wang-Zhu, Y., Larange, A., Arens, R., Bernardo, I., Olivares-Villagómez, D., Herndler-Brandstetter, D., Abraham, N., Grubeck-Loebenstein, B.,

Schoenberger, S. P., Van Kaer, L., Kronenberg, M., Teitell, M. A., & Cheroutre, H. (2011). Mucosal memory CD8+ T cells are selected in the periphery by an MHC class I molecule. *Nature Immunology*, *12*(11), 1086–1095.

Hueber, W., Patel, D. D., Dryja, T., Wright, A. M., Koroleva, I., Bruin, G., Antoni, C., Draelos, Z., Gold, M. H., Durez, P., Tak, P. P., Gomez-Reino, J. J., Foster, C. S., Kim, R. Y., Samson, C. M., Falk, N. S., Chu, D. S., Callanan, D., Nguyen, Q. D., Rose, K., Haider, A., & Di Padova, F. (2010). Effects of AIN457, a fully human antibody to interleukin-17A, on psoriasis, rheumatoid arthritis, and uveitis. *Science Translational Medicine*, *2*(52), 52ra72.

Hüffmeier, U., Uebe, S., Ekici, A. B., Bowes, J., Giardina, E., Korendowych, E., Juneblad, K., Apel, M., McManus, R., Ho, P., Bruce, I. N., Ryan, A. W., Behrens, F., Lascorz, J., Böhm, B., Traupe, H., Lohmann, J., Gieger, C., Wichmann, H.-E., Herold, C., Steffens, M., Klareskog, L., Wienker, T. F., Fitzgerald, O., Alenius, G.-M., McHugh, N. J., Novelli, G., Burkhardt, H., Barton, A., & Reis, A. (2010). Common variants at TRAF3IP2 are associated with susceptibility to psoriatic arthritis and psoriasis. *Nature Genetics*, *42*(11), 996–9.

Huh, J. R., Leung, M. W. L., Huang, P. X., Ryan, D. A., Krout, M. R., Malapaka, R. R. V, Chow, J., Manel, N., Ciofani, M., Kim, S. V, Cuesta, A., Santori, F. R., Lafaille, J. J., Xu, H. E., Gin, D. Y., Rastinejad, F., & Littman, D. R. (2011). Digoxin and its derivatives suppress T(H)17 cell differentiation by antagonizing ROR gamma t activity. *Nature*, *472*(7344), 486–490.

Huh, J. R., & Littman, D. R. (2012). Small molecule inhibitors of RORγt: targeting Th17 cells and other applications. *European Journal of Immunology*, *42*(9), 2232–2237.

Huntington, N. D., Legrand, N., Alves, N. L., Jaron, B., Weijer, K., Plet, A., Corcuff, E., Mortier, E., Jacques, Y., Spits, H., & Di Santo, J. P. (2009). IL-15 trans-presentation promotes human NK cell development and differentiation in vivo. *The Journal of Experimental Medicine*, *206*(1), 25–34.

Iizuka, K., Naidenko, O. V, Plougastel, B. F. M., Fremont, D. H., & Yokoyama, W. M. (2003). Genetically linked C-type lectin-related ligands for the NKRP1 family of natural killer cell receptors. *Nature Immunology*, *4*(8), 801–807.

Illés, Z., Shimamura, M., Newcombe, J., Oka, N., & Yamamura, T. (2004). Accumulation of Valpha7.2-Jalpha33 invariant T cells in human autoimmune inflammatory lesions in the nervous system. *International Immunology*, *16*(2), 223–30.

Intlekofer, A. M., Takemoto, N., Wherry, E. J., Longworth, S. A., Northrup, J. T., Palanivel, V. R., Mullen, A. C., Gasink, C. R., Kaech, S. M., Miller, J. D., Gapin, L., Ryan, K., Russ, A. P., Lindsten, T., Orange, J. S., Goldrath, A. W., Ahmed, R., & Reiner, S. L. (2005). Effector and memory CD8+ T cell fate coupled by T-bet and eomesodermin. *Nature Immunology*, *6*(12), 1236–1244.

Itohara, S., Farr, A. G., Lafaille, J. J., Bonneville, M., Takagaki, Y., Haas, W., & Tonegawa, S. (1990). Homing of a gamma delta thymocyte subset with homogeneous T-cell receptors to mucosal epithelia. *Nature*, *343*(6260), 754–757.

Ivanov, I. I., McKenzie, B. S., Zhou, L., Tadokoro, C. E., Lepelley, A., Lafaille, J. J., Cua, D. J., & Littman, D. R. (2006). The orphan nuclear receptor RORγt directs the

differentiation program of proinflammatory IL-17+ T helper cells. *Cell*, *126*(6), 1121–1133.

Jacobs, R., Hintzen, G., Kemper, A., Beul, K., Kempf, S., Behrens, G., Sykora, K.-W., & Schmidt, R. E. (2001). CD56bright cells differ in their KIR repertoire and cytotoxic features from CD56dim NK cells. *European Journal of Immunology*, *31*(10), 3121–3127.

Jacobs, R., Stoll, M., Stratmann, G., Leo, R., Link, H., & Schmidt, R. E. (1992). CD16-CD56+ natural killer cells after bone marrow transplantation. *Blood*, *79*(12), 3239–44.

Jacobs, R., Weber, K., Wendt, K., Heiken, H., & Schmidt, R. E. (2004). Altered coexpression of lectin-like receptors CD94 and CD161 on NK and T cells in HIV patients. *Journal of Clinical Immunology*, *24*(3), 281–286.

Jamil, K. M., & Khakoo, S. I. (2011). KIR/HLA Interactions and Pathogen Immunity. *Journal of Biomedicine and Biotechnology*, *2011*, 290348.

Jandus, C., Bioley, G., Rivals, J.-P., Dudler, J., Speiser, D., & Romero, P. (2008). Increased numbers of circulating polyfunctional Th17 memory cells in patients with seronegative spondylarthritides. *Arthritis and Rheumatism*, *58*(8), 2307–2017.

Janeway, C. A. (1992). The T cell receptor as a multicomponent signalling machine: CD4/CD8 coreceptors and CD45 in T cell activation. *Annual Review of Immunology*, *10*, 645–674.

Jawahar, S., Moody, C., Chan, M., Finberg, R., Geha, R., & Chatila, T. (1996). Natural Killer (NK) cell deficiency associated with an epitope-deficient Fc receptor type IIIA (CD16-II). *Clinical and Experimental Immunology*, *103*(3), 408–413.

Jenkins, M. R., Trapani, J. a, Doherty, P. C., & Turner, S. J. (2008). Granzyme K expressing cytotoxic T lymphocytes protects against influenza virus in granzyme AB-/- mice. *Viral Immunology*, *21*(3), 341–346.

Jenkins, M. R., Tsun, A., Stinchcombe, J. C., & Griffiths, G. M. (2009). The strength of T cell receptor signal controls the polarization of cytotoxic machinery to the immunological synapse. *Immunity*, *31*(4), 621–631.

Jensen, K. D. C., Su, X., Shin, S., Li, L., Youssef, S., Yamasaki, S., Steinman, L., Saito, T., Locksley, R. M., Davis, M. M., Baumgarth, N., & Chien, Y. (2008). Thymic selection determines γδ T cell effector fate: antigen-naive cells make Interleukin-17 and antigen-experienced cells make Interferon γ. *Immunity*, *29*(1), 90–100.

Jiang, J., Wang, X., An, H., Yang, B., Cao, Z., Liu, Y., Su, J., Zhai, F., Wang, R., Zhang, G., & Cheng, X. (2014). Mucosal-associated Invariant T-Cell Function Is Modulated by Programmed Death-1 Signaling in Patients with Active Tuberculosis.

Jiang, W., Chai, N. R., Maric, D., & Bielekova, B. (2011). Unexpected role for granzyme K in CD56bright NK cell-mediated immunoregulation of multiple sclerosis. *Journal of Immunology*, *187*(2), 781–790.

Jiang, X., Clark, R. A., Liu, L., Wagers, A. J., Fuhlbrigge, R. C., & Kupper, T. S. (2012). Skin infection generates non-migratory memory CD8+ T(RM) cells providing global skin immunity. *Nature*, *483*(7388), 227–231.

Jo, J., Tan, A. T., Ussher, J. E., Sandalova, E., Tang, X.-Z., Tan-Garcia, A., To, N., Hong, M., Chia, A., Gill, U. S., Kennedy, P. T., Tan, K. C., Lee, K. H., De Libero, G., Gehring, A. J., Willberg, C. B., Klenerman, P., & Bertoletti, A. (2014). Toll-like receptor 8 agonist and bacteria trigger potent activation of innate immune cells in human liver. *PLoS Pathogens*, *10*(6), e1004210.

Joeckel, L. T., Wallich, R., Martin, P., Sanchez-Martinez, D., Weber, F. C., Martin, S. F., Borner, C., Pardo, J., Froelich, C., & Simon, M. M. (2011). Mouse granzyme K has pro-inflammatory potential. *Cell Death and Differentiation*, *18*(7), 1112–1119.

Johnson-Huang, L. M., Suárez-Fariñas, M., Pierson, K. C., Fuentes-Duculan, J., Cueto, I., Lentini, T., Sullivan-Whalen, M., Gilleaudeau, P., Krueger, J. G., Haider, A. S., & Lowes, M. A. (2012). A single intradermal injection of IFN-γ induces an inflammatory state in both non-lesional psoriatic and healthy skin. *The Journal of Investigative Dermatology*, *132*(4), 1177–1187.

Joncas, J., Monczak, Y., Ghibu, F., Alfieri, C., Bonin, A., Ahronheim, G., & Rivard, G. (1989). Brief report: killer cell defect and persistent immunological abnormalities in two patients with chronic active Epstein-Barr virus infection. *Journal of Medical Virology*, *28*(2), 110–117.

Jovanovic, D. V, Di Battista, J. A., Martel-Pelletier, J., Jolicoeur, F. C., He, Y., Zhang, M., Mineau, F., & Pelletier, J. P. (1998). IL-17 stimulates the production and expression of proinflammatory cytokines, IL-beta and TNF-alpha, by human macrophages. *Journal of Immunology*, *160*(7), 3513–3521.

Juelke, K., Killig, M., Luetke-Eversloh, M., Parente, E., Gruen, J., Morandi, B., Ferlazzo, G., Thiel, A., Schmitt-Knosalla, I., & Romagnani, C. (2010). CD62L expression identifies a unique subset of polyfunctional CD56 dim NK cells. *Blood*, *116*(8), 1299–1307.

Juelke, K., Killig, M., Thiel, A., Dong, J., & Romagnani, C. (2009). Education of hyporesponsive NK cells by cytokines. *European Journal of Immunology*, *39*(9), 2548–55.

Kagami, S., Rizzo, H. L., Lee, J. J., Koguchi, Y., & Blauvelt, A. (2010). Circulating Th17, Th22, and Th1 cells are increased in psoriasis. *The Journal of Investigative Dermatology*, *130*(5), 1373–1383.

Kägi, D., Ledermann, B., Bürki, K., Seiler, P., Odermatt, B., Olsen, K. J., Podack, E. R., Zinkernagel, R. M., & Hengartner, H. (1994a). Cytotoxicity mediated by T cells and natural killer cells is greatly impaired in perforin-deficient mice. *Nature*, *369*(6475), 31–7.

Kägi, D., Vignaux, F., Ledermann, B., Bürki, K., Depraetere, V., Nagata, S., Hengartner, H., & Golstein, P. (1994b). Fas and perforin pathways as major mechanisms of T cell-mediated cytotoxicity. *Science*, *265*(5171), 528–530.

Kaiserman, D., Bird, C. H., Sun, J., Matthews, A., Ung, K., Whisstock, J. C., Thompson, P. E., Trapani, J. a, & Bird, P. I. (2006). The major human and mouse granzymes are structurally and functionally divergent. *The Journal of Cell Biology*, *175*(4), 619–630.

Kaiserman, D., Stewart, S. E., Gevaert, K., Damme, P. Van, & Bird, P. I. (2014). Identification of Serpinb6b as a species-specific mouse granzyme A inhibitor

suggests functional divergence between human and mouse granzyme A. *Journal of Biological Chemistry*, *289*(13), 9408–9417.

Kallies, A., Carotta, S., Huntington, N. D., Bernard, N. J., Tarlinton, D. M., Smyth, M. J., & Nutt, S. L. (2011). A role for Blimp1 in the transcriptional network controlling natural killer cell maturation. *Blood*, *117*(6), 1869–79.

Kallies, A., Xin, A., Belz, G. T., & Nutt, S. L. (2009). Blimp-1 Transcription Factor Is Required for the Differentiation of Effector CD8+ T Cells and Memory Responses. *Immunity*, *31*(2), 283–295.

Karlhofer, F. M., Ribaudo, R. K., & Yokoyama, W. M. (1992). MHC class I alloantigen specificity of Ly-49+ IL-2-activated natural killer cells. *Nature*, *358*(6381), 66–70.

Kärre, K., Ljunggren, H. G., Piontek, G., & Kiessling, R. (1986). Selective rejection of H-2-deficient lymphoma variants suggests alternative immune defence strategy. *Nature*, *319*(6055), 675–678.

Kato, T., Hamada, A., Mori, S., & Saito, H. (2012). Genetic Polymorphisms in Metabolic and Cellular Transport Pathway of Methotrexate Impact Clinical Outcome of Methotrexate Monotherapy in Japanese Patients with Rheumatoid Arthritis. *Drug Metabolism and Pharmacokinetics*, *27*(2), 192–199.

Kauffman, C. L., Aria, N., Toichi, E., McCormick, T. S., Cooper, K. D., Gottlieb, A. B., Everitt, D. E., Frederick, B., Zhu, Y., Graham, M. A., Pendley, C. E., & Mascelli, M. A. (2004). A phase I study evaluating the safety, pharmacokinetics, and clinical response of a human IL-12 p40 antibody in subjects with plaque psoriasis. *The Journal of Investigative Dermatology*, *123*(6), 1037–1044.

Kawachi, I., Maldonado, J., Strader, C., & Gilfillan, S. (2006). MR1-restricted V alpha 19i mucosal-associated invariant T cells are innate T cells in the gut lamina propria that provide a rapid and diverse cytokine response. *Journal of Immunology*, *176*(3), 1618–1627.

Kawano, T., Cui, J., Koezuka, Y., Toura, I., Kaneko, Y., Motoki, K., Ueno, H., Nakagawa, R., Sato, H., Kondo, E., Koseki, H., & Taniguchi, M. (1997). CD1d-restricted and TCR-mediated activation of Valpha14 NKT cells by glycosylceramides. *Science*, *278*(5343), 1626–1629.

Kawano, T., Cui, J., Koezuka, Y., Toura, I., Kaneko, Y., Sato, H., Kondo, E., Harada, M., Koseki, H., Nakayama, T., Tanaka, Y., & Taniguchi, M. (1998). Natural killer-like nonspecific tumor cell lysis mediated by specific ligand-activated V 14 NKT cells. *Proceedings of the National Academy of Sciences*, *95*(10), 5690–5693.

Kelly-Rogers, J., Madrigal-Estebas, L., O'Connor, T., & Doherty, D. G. (2006). Activation-induced expression of CD56 by T cells is associated with a reprogramming of cytolytic activity and cytokine secretion profile in vitro. *Human Immunology*, *67*(11), 863–873.

Kennedy, M. K., Glaccum, M., Brown, S. N., Butz, E. A., Viney, J. L., Embers, M., Matsuki, N., Charrier, K., Sedger, L., Willis, C. R., Brasel, K., Morrissey, P. J., Stocking, K., Schuh, J. C., Joyce, S., & Peschon, J. J. (2000). Reversible defects in natural killer and memory CD8 T cell lineages in interleukin 15-deficient mice. *The Journal of*

Experimental Medicine, *191*(5), 771–780.

Khakoo, S. I., Thio, C. L., Martin, M. P., Brooks, C. R., Gao, X., Astemborski, J., Cheng, J., Goedert, J. J., Vlahov, D., Hilgartner, M., Cox, S., Little, A.-M., Alexander, G. J., Cramp, M. E., O'Brien, S. J., Rosenberg, W. M. C., Thomas, D. L., & Carrington, M. (2004). HLA and NK cell inhibitory receptor genes in resolving hepatitis C virus infection. *Science*, *305*(5685), 872–874.

Kiessling, R., Klein, E., & Wigzell, H. (1975). "Natural" killer cells in the mouse. I. Cytotoxic cells with specificity for mouse Moloney leukemia cells. Specificity and distribution according to genotype. *European Journal of Immunology*, *5*(2), 112–117.

Kim, B. S., Siracusa, M. C., Saenz, S. A., Noti, M., Monticelli, L. A., Sonnenberg, G. F., Hepworth, M. R., Van Voorhees, A. S., Comeau, M. R., & Artis, D. (2013). TSLP elicits IL-33-independent innate lymphoid cell responses to promote skin inflammation. *Science Translational Medicine*, *5*(170), 170ra16.

Kim, C. H., Johnston, B., & Butcher, E. C. (2002). Trafficking machinery of NKT cells: Shared and differential chemokine receptor expression among Va24+Vb11+ NKT cell subsets with distinct cytokine-producing capacity. *Blood*, *100*(1), 11–16.

Kim, J.-C., Jin, H.-M., Cho, Y.-N., Kwon, Y.-S., Kee, S.-J., & Park, Y.-W. (2015). Deficiencies of Circulating Mucosal-associated Invariant T Cells and Natural Killer T Cells in Patients with Acute Cholecystitis. *Journal of Korean Medical Science*, *30*(5), 606–611.

Kim, S., Poursine-Laurent, J., Truscott, S. M., Lybarger, L., Song, Y.-J., Yang, L., French, A. R., Sunwoo, J. B., Lemieux, S., Hansen, T. H., & Yokoyama, W. M. (2005). Licensing of natural killer cells by host major histocompatibility complex class I molecules. *Nature*, *436*(7051), 709–713.

Kinjo, Y., Wu, D., Kim, G., Xing, G.-W., Poles, M. A., Ho, D. D., Tsuji, M., Kawahara, K., Wong, C.-H., & Kronenberg, M. (2005). Recognition of bacterial glycosphingolipids by natural killer T cells. *Nature*, *434*(7032), 520–525.

Kjer-Nielsen, L., Patel, O., Corbett, A. J., Le Nours, J., Meehan, B., Liu, L., Bhati, M., Chen, Z., Kostenko, L., Reantragoon, R., Williamson, N. A., Purcell, A. W., Dudek, N. L., Mcconville, M. J., Hair, R. A. J. O., Khairallah, G. N., Godfrey, D. I., Fairlie, D. P., Kjer-Nielsen, L., Patel, O., Corbett, A. J., Le Nours, J., Meehan, B., Liu, L., Bhati, M., Chen, Z., Kostenko, L., Reantragoon, R., Williamson, N. A., Purcell, A. W., Dudek, N. L., Mcconville, M. J., O'Hair, R. A. J., Khairallah, G. N., Godfrey, D. I., Fairlie, D. P., Rossjohn, J., & McCluskey, J. (2012). MR1 presents microbial vitamin B metabolites to MAIT cells. *Nature*, *491*(7426), 717–723.

Klose, C. S. N., Flach, M., Möhle, L., Rogell, L., Hoyler, T., Ebert, K., Fabiunke, C., Pfeifer, D., Sexl, V., Fonseca-Pereira, D., Domingues, R. G., Veiga-Fernandes, H., Arnold, S. J., Busslinger, M., Dunay, I. R., Tanriver, Y., & Diefenbach, A. (2014). Differentiation of type 1 ILCs from a common progenitor to all helper-like innate lymphoid cell lineages. *Cell*, *157*(2), 340–56.

Klose, C. S. N., Kiss, E. A., Schwierzeck, V., Ebert, K., Hoyler, T., D'Hargues, Y., Göppert, N., Croxford, A. L., Waisman, A., Tanriver, Y., & Diefenbach, A. (2013). A T-bet gradient controls the fate and function of CCR6-RORγt+ innate lymphoid cells. *Nature*,

494(7436), 261–265.

Knox, J. J., Cosma, G. L., Betts, M. R., & McLane, L. M. (2014). Characterization of T-bet and eomes in peripheral human immune cells. *Frontiers in Immunology*, *5*, 217.

Koenders, M. I., Lubberts, E., Oppers-Walgreen, B., van den Bersselaar, L., Helsen, M. M., Kolls, J. K., Joosten, L. A. B., & van den Berg, W. B. (2005). Induction of cartilage damage by overexpression of T cell interleukin-17A in experimental arthritis in mice deficient in interleukin-1. *Arthritis and Rheumatism*, *52*(3), 975–983.

Koga, C., Kabashima, K., Shiraishi, N., Kobayashi, M., & Tokura, Y. (2008). Possible pathogenic role of Th17 cells for atopic dermatitis. *The Journal of Investigative Dermatology*, *128*(11), 2625–2630.

Konjević, G., Mirjacić Martinović, K., Vuletić, A., Jurisić, V., & Spuzić, I. (2009). Distribution of several activating and inhibitory receptors on CD3-CD16+ NK cells and their correlation with NK cell function in healthy individuals. *The Journal of Membrane Biology*, *230*(3), 113–123.

Koshy, P. J., Henderson, N., Logan, C., Life, P. F., Cawston, T. E., & Rowan, A. D. (2002). Interleukin 17 induces cartilage collagen breakdown: novel synergistic effects in combination with proinflammatory cytokines. *Annals of the Rheumatic Diseases*, *61*(8), 704–713.

Kotake, S., Nanke, Y., Mogi, M., Kawamoto, M., Furuya, T., Yago, T., Kobashigawa, T., Togari, A., & Kamatani, N. (2005). IFN-gamma-producing human T cells directly induce osteoclastogenesis from human monocytes via the expression of RANKL. *European Journal of Immunology*, *35*(11), 3353–3363.

Kotake, S., Udagawa, N., Takahashi, N., Matsuzaki, K., Itoh, K., Ishiyama, S., Saito, S., Inoue, K., Kamatani, N., Gillespie, M. T., Martin, T. J., & Suda, T. (1999). IL-17 in synovial fluids from patients with rheumatoid arthritis is a potent stimulator of osteoclastogenesis. *The Journal of Clinical Investigation*, *103*(9), 1345–1352.

Kovalovsky, D., Alonzo, E. S., Uche, O. U., Eidson, M., Nichols, K. E., & Sant'Angelo, D. B. (2010). PLZF induces the spontaneous acquisition of memory/effector functions in T cells independently of NKT cell-related signals. *Journal of Immunology*, *184*(12), 6746–6755.

Kovalovsky, D., Uche, O. U., Eladad, S., Hobbs, R. M., Yi, W., Alonzo, E., Chua, K., Eidson, M., Kim, H.-J., Im, J. S., Pandolfi, P. P., & Sant'Angelo, D. B. (2008). The BTB-zinc finger transcriptional regulator PLZF controls the development of invariant natural killer T cell effector functions. *Nature Immunology*, *9*(9), 1055–1064.

Krämer, B., Körner, C., Kebschull, M., Glässner, A., Eisenhardt, M., Nischalke, H.-D., Alexander, M., Sauerbruch, T., Spengler, U., & Nattermann, J. (2012). NKp46High expression defines a natural killer cell subset that is potentially involved in control of hepatitis C virus replication and modulation of liver fibrosis. *Hepatology*, *56*(4), 1201–1213.

Kreslavsky, T., Savage, A. K., Hobbs, R., Gounari, F., Bronson, R., Pereira, P., Pandolfi, P. P., Bendelac, A., & von Boehmer, H. (2009). TCR-inducible PLZF transcription factor required for innate phenotype of a subset of γδ T cells with restricted TCR diversity.

Proceedings of the National Academy of Sciences of the United States of America, *106*(30), 12453–12458.

Krueger, G. G., Langley, R. G., Leonardi, C., Yeilding, N., Guzzo, C., Wang, Y., Dooley, L. T., & Lebwohl, M. (2007). A human interleukin-12/23 monoclonal antibody for the treatment of psoriasis. *The New England Journal of Medicine*, *356*(6), 580–592.

Kryczek, I., Bruce, A. T., Gudjonsson, J. E., Johnston, A., Aphale, A., Vatan, L., Szeliga, W., Wang, Y., Liu, Y., Welling, T. H., Elder, J. T., & Zou, W. (2008). Induction of IL-17+ T cell trafficking and development by IFN-gamma: mechanism and pathological relevance in psoriasis. *The Journal of Immunology*, *181*(7), 4733–4741.

Kubin, M., Cassiano, L., Chalupny, J., Chin, W., Cosman, D., Fanslow, W., Müllberg, J., Rousseau, A. M., Ulrich, D., & Armitage, R. (2001). ULBP1, 2, 3: novel MHC class I-related molecules that bind to human cytomegalovirus glycoprotein UL16, activate NK cells. *European Journal of Immunology*, *31*(5), 1428–37.

Kuijpers, T. W., Baars, P. A., Dantin, C., van den Burg, M., van Lier, R. A. W., & Roosnek, E. (2008). Human NK cells can control CMV infection in the absence of T cells. *Blood*, *112*(3), 914–5.

Kulkarni, A., Paranjape, R., & Thakar, M. (2012). Expansion of Defective NK Cells in Early HIV Type 1C Infection : A Consequence of Reduced CD161 Expression. *AIDS Research and Human Retroviruses*, *28*(1), 100–105.

Kyriakakis, E., Cavallari, M., Andert, J., Philippova, M., Koella, C., Bochkov, V., Erne, P., Wilson, S. B., Mori, L., Biedermann, B. C., Resink, T. J., & De Libero, G. (2010). Invariant natural killer T cells: linking inflammation and neovascularization in human atherosclerosis. *European Journal of Immunology*, *40*(11), 3268–3279.

Lalor, S. J., Dungan, L. S., Sutton, C. E., Basdeo, S. A., Fletcher, J. M., & Mills, K. H. G. (2011). Caspase-1-processed cytokines IL-1beta and IL-18 promote IL-17 production by gammadelta and CD4 T cells that mediate autoimmunity. *Journal of Immunology*, *186*(10), 5738–5748.

Langfelder, P., & Horvath, S. (2008). WGCNA: an R package for weighted correlation network analysis. *BMC Bioinformatics*, *9*, 559.

Langley, R. G. B., Krueger, G. G., & Griffiths, C. E. M. (2005). Psoriasis: epidemiology, clinical features, and quality of life. *Annals of the Rheumatic Diseases*, *64*(Suppl 2), 18–23.

Lanier, L. L., Chang, C., & Phillips, J. H. (1994). Human NKR-P1A. A disulfide-linked homodimer of the C-type lectin superfamily expressed by a subset of NK and T lymphocytes. *Journal of Immunology*, *153*(6), 2417–2428.

Lanier, L. L., Le, A. M., Civin, C. I., Loken, M. R., & Phillips, J. H. (1986). The relationship of CD16 (Leu-11) and Leu-19 (NKH-1) antigen expression on human peripheral blood NK cells and cytotoxic T lymphocytes. *Journal of Immunology*, *136*(12), 4480–4486.

Lantz, O., & Bendelac, A. (1994). An invariant T cell receptor alpha chain is used by a unique subset of major histocompatibility complex class I-specific CD4+ and CD4-8- T cells in mice and humans. *The Journal of Experimental Medicine*, *180*(3), 1097–1106.

Lau, L. L., Jamieson, B. D., Somasundaram, T., & Ahmed, R. (1994). Cytotoxic T-cell memory without antigen. *Nature*, *369*(6482), 648–652.

Laugel, B., van den Berg, H. a, Gostick, E., Cole, D. K., Wooldridge, L., Boulter, J., Milicic, A., Price, D. a, & Sewell, A. K. (2007). Different T cell receptor affinity thresholds and CD8 coreceptor dependence govern cytotoxic T lymphocyte activation and tetramer binding properties. *The Journal of Biological Chemistry*, *282*(33), 23799–23810.

Lazetic, S., Chang, C., Houchins, J. P., Lanier, L. L., & Phillips, J. H. (1996). Human natural killer cell receptors involved in MHC class I recognition are disulfide-linked heterodimers of CD94 and NKG2 subunits. *Journal of Immunology*, *157*(11), 4741–4745.

Le Bourhis, L., Martin, E., Péguillet, I., Guihot, A., Froux, N., Coré, M., Lévy, E., Dusseaux, M., Meyssonnier, V., Premel, V., Ngo, C., Riteau, B., Duban, L., Robert, D., Huang, S., Rottman, M., Soudais, C., & Lantz, O. (2010). Antimicrobial activity of mucosal-associated invariant T cells. *Nature Immunology*, *11*(8), 701–708.

Le Bouteiller, P., Tabiasco, J., Polgar, B., Kozma, N., Giustiniani, J., Siewiera, J., Berrebi, A., Aguerre-Girr, M., Bensussan, A., & Jabrane-Ferrat, N. (2011). CD160: A unique activating NK cell receptor. *Immunology Letters*, *138*(2), 93–96.

Lee, E., Trepicchio, W. L., Oestreicher, J. L., Pittman, D., Wang, F., Chamian, F., Dhodapkar, M., & Krueger, J. G. (2004). Increased expression of interleukin 23 p19 and p40 in lesional skin of patients with psoriasis vulgaris. *The Journal of Experimental Medicine*, *199*(1), 125–130.

Lee, J., Zhang, T., Hwang, I., Kim, A., Nitschke, L., Kim, M., Scott, J. M., Kamimura, Y., Lanier, L. L., & Kim, S. (2015). Epigenetic Modification and Antibody-Dependent Expansion of Memory-like NK Cells in Human Cytomegalovirus-Infected Individuals. *Immunity*, *42*(3), 431–442.

Lee, O.-J., Cho, Y.-N., Kee, S.-J., Kim, M.-J., Jin, H.-M., Lee, S.-J., Park, K.-J., Kim, T.-J., Lee, S.-S., Kwon, Y.-S., Kim, N., Shin, M.-G., Shin, J.-H., Suh, S.-P., Ryang, D.-W., & Park, Y.-W. (2014). Circulating mucosal-associated invariant T cell levels and their cytokine levels in healthy adults. *Experimental Gerontology*, *49*, 47–54.

Lee, P. T., Benlagha, K., Teyton, L., & Bendelac, A. (2002). Distinct functional lineages of human V(alpha)24 natural killer T cells. *The Journal of Experimental Medicine*, *195*(5), 637–641.

Lee, Y., Awasthi, A., Yosef, N., Quintana, F. J., Xiao, S., Peters, A., Wu, C., Kleinewietfeld, M., Kunder, S., Hafler, D. A., Sobel, R. A., Regev, A., & Kuchroo, V. K. (2012). Induction and molecular signature of pathogenic TH17 cells. *Nature Immunology*, *13*(10), 991–999.

Leeansyah, E., Ganesh, A., Quigley, M. F., Sönnerborg, A., Andersson, J., Hunt, P. W., Somsouk, M., Deeks, S. G., Martin, J. N., Moll, M., Shacklett, B. L., & Sandberg, J. K. (2013). Activation, exhaustion, and persistent decline of the antimicrobial MR1-restricted MAIT-cell population in chronic HIV-1 infection. *Blood*, *121*(7), 1124–1135.

Leeansyah, E., Loh, L., Nixon, D. F., & Sandberg, J. K. (2014). Acquisition of innate-like microbial reactivity in mucosal tissues during human fetal MAIT-cell development.

Nature Communications, *5*, 3143.

Leeansyah, E., Svärd, J., Dias, J., Buggert, M., Nyström, J., Quigley, M. F., Moll, M., Sönnerborg, A., Nowak, P., & Sandberg, J. K. (2015). Arming of MAIT Cell Cytolytic Antimicrobial Activity Is Induced by IL-7 and Defective in HIV-1 Infection. *PLoS Pathogens*, *11*(8), e1005072.

LeGrand, A., Fermor, B., Fink, C., Pisetsky, D. S., Weinberg, J. B., Vail, T. P., & Guilak, F. (2001). Interleukin-1, tumor necrosis factor alpha, and interleukin-17 synergistically up-regulate nitric oxide and prostaglandin E2 production in explants of human osteoarthritic knee menisci. *Arthritis and Rheumatism*, *44*(9), 2078–2083.

Leijten, E. F. A., van Kempen, T. S., Boes, M., Michels-van Amelsfort, J. M. R., Hijnen, D., Hartgring, S. A. Y., van Roon, J. A. G., Wenink, M. H., & Radstake, T. R. D. J. (2015). Activated group 3 innate lymphoid cells are selectively enriched in psoriatic arthritis synovial fluid. *Arthritis & Rheumatology*, *67*(10), 2673–2678.

Leipe, J., Grunke, M., Dechant, C., Reindl, C., Kerzendorf, U., Schulze-Koops, H., & Skapenko, A. (2010). Role of Th17 cells in human autoimmune arthritis. *Arthritis and Rheumatism*, *62*(10), 2876–2885.

Leonardi, C., Matheson, R., Zachariae, C., Cameron, G., Li, L., Edson-Heredia, E., Braun, D., & Banerjee, S. (2012). Anti-interleukin-17 monoclonal antibody ixekizumab in chronic plaque psoriasis. *The New England Journal of Medicine*, *366*(13), 1190–1199.

Lepore, M., Kalinichenko, A., Kalinicenko, A., Colone, A., Paleja, B., Singhal, A., Tschumi, A., Lee, B., Poidinger, M., Zolezzi, F., Quagliata, L., Sander, P., Newell, E., Bertoletti, A., Terracciano, L., De Libero, G., & Mori, L. (2014). Parallel T-cell cloning and deep sequencing of human MAIT cells reveal stable oligoclonal TCRβ repertoire. *Nature Communications*, *5*, 3866.

Leung, D. T., Bhuiyan, T. R., Nishat, N. S., Hoq, M. R., Aktar, A., Rahman, M. A., Uddin, T., Khan, A. I., Chowdhury, F., Charles, R. C., Harris, J. B., Calderwood, S. B., Qadri, F., & Ryan, E. T. (2014a). Circulating Mucosal Associated Invariant T Cells Are Activated in Vibrio cholerae O1 Infection and Associated with Lipopolysaccharide Antibody Responses. *PLoS Neglected Tropical Diseases*, *8*(8), e3076.

Leung, J. M., Davenport, M., Wolff, M. J., Wiens, K. E., Abidi, W. M., Poles, M. A., Cho, I., Ullman, T., Mayer, L., & Loke, P. (2014b). IL-22-producing CD4+ cells are depleted in actively inflamed colitis tissue. *Mucosal Immunology*, *7*(1), 124–133.

Li, P., Nijhawan, D., Budihardjo, I., Srinivasula, S. M., Ahmad, M., Alnemri, E. S., & Wang, X. (1997). Cytochrome c and dATP-Dependent Formation of Apaf-1/Caspase-9 Complex Initiates an Apoptotic Protease Cascade. *Cell*, *91*(4), 479–489.

Li, W., Sofi, M. H., Rietdijk, S., Wang, N., Terhorst, C., & Chang, C.-H. (2007a). The SLAM-associated protein signaling pathway is required for development of CD4+ T cells selected by homotypic thymocyte interaction. *Immunity*, *27*(5), 763–774.

Li, W., Sofi, M. H., Yeh, N., Sehra, S., McCarthy, B. P., Patel, D. R., Brutkiewicz, R. R., Kaplan, M. H., & Chang, C.-H. (2007b). Thymic selection pathway regulates the effector function of CD4 T cells. *The Journal of Experimental Medicine*, *204*(9), 2145–2157.

Liang, S. C., Tan, X.-Y., Luxenberg, D. P., Karim, R., Dunussi-Joannopoulos, K., Collins, M., & Fouser, L. A. (2006). Interleukin (IL)-22 and IL-17 are coexpressed by Th17 cells and cooperatively enhance expression of antimicrobial peptides. *The Journal of Experimental Medicine*, *203*(10), 2271–2279.

Lindqvist, U. R. C., Alenius, G.-M., Husmark, T., Theander, E., Holmström, G., & Larsson, P. T. (2008). The Swedish early psoriatic arthritis register- 2-year followup: a comparison with early rheumatoid arthritis. *The Journal of Rheumatology*, *35*(4), 668–673.

Liu, K., Catalfamo, M., Li, Y., Henkart, P. a, & Weng, N. (2002). IL-15 mimics T cell receptor crosslinking in the induction of cellular proliferation, gene expression, and cytotoxicity in CD8+ memory T cells. *Proceedings of the National Academy of Sciences of the United States of America*, *99*(9), 6192–6197.

Liu, T.-Y., Uemura, Y., Suzuki, M., Narita, Y., Hirata, S., Ohyama, H., Ishihara, O., & Matsushita, S. (2008). Distinct subsets of human invariant NKT cells differentially regulate T helper responses via dendritic cells. *European Journal of Immunology*, *38*(4), 1012–1023.

Long, B. R., Ndhlovu, L. C., Oksenberg, J. R., Lanier, L. L., Hecht, F. M., Nixon, D. F., & Barbour, J. D. (2008). Conferral of enhanced natural killer cell function by KIR3DS1 in early human immunodeficiency virus type 1 infection. *Journal of Virology*, *82*(10), 4785–4792.

López-Sagaseta, J., Dulberger, C. L., Crooks, J. E., Parks, C. D., Luoma, A. M., McFedries, A., Van Rhijn, I., Saghatelian, A., & Adams, E. J. (2013). The molecular basis for Mucosal-Associated Invariant T cell recognition of MR1 proteins. *Proceedings of the National Academy of Sciences of the United States of America*, *110*(19), E1771–8.

Lopez-Vergès, S., Milush, J. M., Pandey, S., York, V. a, Arakawa-Hoyt, J., Pircher, H., Norris, P. J. P. J., Nixon, D. F., & Lanier, L. L. (2010). CD57 defines a functionally distinct population of mature NK cells in the human CD56dimCD16+ NK-cell subset. *Blood*, *116*(19), 3865–3874.

Lopez-Vergès, S., Milush, J. M., Schwartz, B. S., Pando, M. J., Jarjoura, J., York, V. A., Houchins, J. P., Miller, S., Kang, S.-M., Norris, P. J., Nixon, D. F., & Lanier, L. L. (2011). Expansion of a unique $CD57^{+}$NKG2Chi natural killer cell subset during acute human cytomegalovirus infection. *Proceedings of the National Academy of Sciences of the United States of America*, *108*(36), 14725–14732.

Lowes, M. A., Kikuchi, T., Fuentes-Duculan, J., Cardinale, I., Zaba, L. C., Haider, A. S., Bowman, E. P., & Krueger, J. G. (2008). Psoriasis vulgaris lesions contain discrete populations of Th1 and Th17 T cells. *The Journal of Investigative Dermatology*, *128*(5), 1207–1211.

Lubberts, E., Joosten, L. A. B., Oppers, B., van den Bersselaar, L., Coenen-de Roo, C. J. J., Kolls, J. K., Schwarzenberger, P., van de Loo, F. A. J., & van den Berg, W. B. (2001). IL-1-Independent Role of IL-17 in Synovial Inflammation and Joint Destruction During Collagen-Induced Arthritis. *The Journal of Immunology*, *167*(2), 1004–1013.

Lubberts, E., Koenders, M. I., Oppers-Walgreen, B., van den Bersselaar, L., Coenen-de

Roo, C. J. J., Joosten, L. A. B., & van den Berg, W. B. (2004). Treatment with a neutralizing anti-murine interleukin-17 antibody after the onset of collagen-induced arthritis reduces joint inflammation, cartilage destruction, and bone erosion. *Arthritis and Rheumatism*, *50*(2), 650–659.

Luetke-Eversloh, M., Hammer, Q., Durek, P., Nordström, K., Gasparoni, G., Pink, M., Hamann, A., Walter, J., Chang, H.-D., Dong, J., & Romagnani, C. (2014). Human cytomegalovirus drives epigenetic imprinting of the IFNG locus in NKG2Chi natural killer cells. *PLoS Pathogens*, *10*(10), e1004441.

Lunemann, S., Malone, D. F. G., Hengst, J., Port, K., Grabowski, J., Deterding, K., Markova, A., Bremer, B., Schlaphoff, V., Cornberg, M., Manns, M. P., Sandberg, J. K., Ljunggren, H.-G., Björkström, N. K., & Wedemeyer, H. (2014). Compromised function of natural killer cells in acute and chronic viral hepatitis. *The Journal of Infectious Diseases*, *209*(9), 1362–1373.

Luteijn, R., Sciaranghella, G., van Lunzen, J., Nolting, A., Dugast, A. S., Ghebremichael, M. S., Altfeld, M., & Alter, G. (2011). Early viral replication in lymph nodes provides HIV with a means by which to escape NK-cell-mediated control. *European Journal of Immunology*, *41*(9), 2729–2740.

Ly, D., Kasmar, A. G., Cheng, T.-Y., de Jong, A., Huang, S., Roy, S., Bhatt, A., van Summeren, R. P., Altman, J. D., Jacobs, W. R., Adams, E. J., Minnaard, A. J., Porcelli, S. A., & Moody, D. B. (2013). CD1c tetramers detect ex vivo T cell responses to processed phosphomycoketide antigens. *The Journal of Experimental Medicine*, *210*(4), 729–741.

Ma, H.-L., Liang, S., Li, J., Napierata, L., Brown, T., Benoit, S., Senices, M., Gill, D., Dunussi-Joannopoulos, K., Collins, M., Nickerson-Nutter, C., Fouser, L. A., & Young, D. A. (2008). IL-22 is required for Th17 cell-mediated pathology in a mouse model of psoriasis-like skin inflammation. *The Journal of Clinical Investigation*, *118*(2), 597–607.

Mackay, L. K., Rahimpour, A., Ma, J. Z., Collins, N., Stock, A. T., Hafon, M.-L., Vega-Ramos, J., Lauzurica, P., Mueller, S. N., Stefanovic, T., Tscharke, D. C., Heath, W. R., Inouye, M., Carbone, F. R., & Gebhardt, T. (2013). The developmental pathway for CD103+CD8+ tissue-resident memory T cells of skin. *Nature Immunology*, *14*(12), 1294–1301.

Madakamutil, L. T., Christen, U., Lena, C. J., Wang-Zhu, Y., Attinger, A., Sundarrajan, M., Ellmeier, W., von Herrath, M. G., Jensen, P., Littman, D. R., & Cheroutre, H. (2004). CD8alphaalpha-mediated survival and differentiation of CD8 memory T cell precursors. *Science*, *304*(5670), 590–593.

Magalhaes, I., Pingris, K., Poitou, C., Bessoles, S., Venteclef, N., Kiaf, B., Beaudoin, L., Da Silva, J., Allatif, O., Rossjohn, J., Kjer-Nielsen, L., McCluskey, J., Ledoux, S., Genser, L., Torcivia, A., Soudais, C., Lantz, O., Boitard, C., Aron-Wisnewsky, J., Larger, E., Clément, K., & Lehuen, A. (2015). Mucosal-associated invariant T cell alterations in obese and type 2 diabetic patients. *The Journal of Clinical Investigation*, *125*(4), 1752–62.

Maggi, L., Santarlasci, V., Capone, M., Peired, A., Frosali, F., Crome, S. Q., Querci, V.,

Fambrini, M., Liotta, F., Levings, M. K., Maggi, E., Cosmi, L., Romagnani, S., & Annunziato, F. (2010). CD161 is a marker of all human IL-17-producing T-cell subsets and is induced by RORC. *European Journal of Immunology*, *40*(8), 2174–2181.

Magram, J., Connaughton, S. E., Warrier, R. R., Carvajal, D. M., Wu, C. Y., Ferrante, J., Stewart, C., Sarmiento, U., Faherty, D. A., & Gately, M. K. (1996). IL-12-deficient mice are defective in IFN-gamma production and type 1 cytokine responses. *Immunity*, *4*(5), 471–481.

Makino, Y., Kanno, R., Ito, T., Higashino, K., & Taniguchi, M. (1995). Predominant expression of invariant V alpha 14+ TCR alpha chain in NK1.1+ T cell populations. *International Immunology*, *7*(7), 1157–1161.

Mallon, E., Bunce, M., Wojnarowska, F., & Welsh, K. (1997). HLA-CW*0602 is a susceptibility factor in type I psoriasis, and evidence Ala-73 is increased in male type I psoriatics. *The Journal of Investigative Dermatology*, *109*(2), 183–186.

Mandelboim, O., Lieberman, N., Lev, M., Paul, L., Arnon, T. I., Bushkin, Y., Davis, D. M., Strominger, J. L., Yewdell, J. W., & Porgador, A. (2001). Recognition of haemagglutinins on virus-infected cells by NKp46 activates lysis by human NK cells. *Nature*, *409*(6823), 1055–60.

Mandelboim, O., Reyburn, H. T., Valés-Gómez, M., Pazmany, L., Colonna, M., Borsellino, G., & Strominger, J. L. (1996). Protection from lysis by natural killer cells of group 1 and 2 specificity is mediated by residue 80 in human histocompatibility leukocyte antigen C alleles and also occurs with empty major histocompatibility complex molecules. *The Journal of Experimental Medicine*, *184*(3), 913–22.

Mangan, P. R., Harrington, L. E., O'Quinn, D. B., Helms, W. S., Bullard, D. C., Elson, C. O., Hatton, R. D., Wahl, S. M., Schoeb, T. R., & Weaver, C. T. (2006). Transforming growth factor-beta induces development of the T(H)17 lineage. *Nature*, *441*(7090), 231–234.

Maricic, I., Girardi, E., Zajonc, D. M., & Kumar, V. (2014). Recognition of lysophosphatidylcholine by type II NKT cells and protection from an inflammatory liver disease. *Journal of Immunology*, *193*(9), 4580–4589.

Martin, E., Bourhis, L. Le, Dusseaux, M., Bohineust, A., Sleurs, D., Serriari, N., Treiner, E., Premel, V., Core, M., Hivroz, C., Sansonetti, P., Gougeon, M., Soudais, C., & Lantz, O. (2013). MAIT Cells Detect and Efficiently Lyse Bacterially- Infected Epithelial Cells. *Plos Pathogens*, *9*(10), e1003681.

Martin, E., Treiner, E., Duban, L., Guerri, L., Laude, H., Toly, C., Premel, V., Devys, A., Moura, I. C., Tilloy, F., Cherif, S., Vera, G., Latour, S., Soudais, C., & Lantz, O. (2009). Stepwise development of mait cells in mouse and human. *PLoS Biology*, *7*(3), e1000054.

Martin, M. P., Gao, X., Lee, J.-H., Nelson, G. W., Detels, R., Goedert, J. J., Buchbinder, S., Hoots, K., Vlahov, D., Trowsdale, J., Wilson, M., O'Brien, S. J., & Carrington, M. (2002). Epistatic interaction between KIR3DS1 and HLA-B delays the progression to AIDS. *Nature Genetics*, *31*(4), 429–434.

Masopust, D., Vezys, V., Marzo, A. L., & Lefrançois, L. (2001). Preferential localization of

effector memory cells in nonlymphoid tissue. *Science*, *291*(5512), 2413–2417.

Massot, B., Michel, M.-L., Diem, S., Ohnmacht, C., Latour, S., Dy, M., Eberl, G., & Leite-de-Moraes, M. C. (2014). TLR-induced cytokines promote effective proinflammatory natural Th17 cell responses. *Journal of Immunology*, *192*(12), 5635–5642.

Mathew, R., Seiler, M. P., Scanlon, S. T., Mao, A., Constantinides, M. G., Bertozzi-Villa, C., Singer, J. D., & Bendelac, A. (2012). BTB-ZF factors recruit the E3 ligase cullin 3 to regulate lymphoid effector programs. *Nature*, *491*(7425), 618–621.

Matsuda, J. L., Zhang, Q., Ndonye, R., Richardson, S. K., Howell, A. R., & Gapin, L. (2006). T-bet concomitantly controls migration, survival, and effector functions during the development of V??14i NKT cells. *Blood*, *107*(7), 2797–2805.

Mattner, J., Debord, K. L., Ismail, N., Goff, R. D., Cantu, C., Zhou, D., Saint-Mezard, P., Wang, V., Gao, Y., Yin, N., Hoebe, K., Schneewind, O., Walker, D., Beutler, B., Teyton, L., Savage, P. B., & Bendelac, A. (2005). Exogenous and endogenous glycolipid antigens activate NKT cells during microbial infections. *Nature*, *434*(7032), 525–529.

Mavilio, D., Lombardo, G., Benjamin, J., Kim, D., Follman, D., Marcenaro, E., O'Shea, M. A., Kinter, A., Kovacs, C., Moretta, A., Fauci, A. S., Shea, M. A. O., Kinter, A., Kovacs, C., Moretta, A., & Fauci, A. S. (2005). Characterization of CD56-/CD16+ natural killer (NK) cells: A highly dysfunctional NK subset expanded in HIV-infected viremic individuals. *Proceedings of the National Academy of Sciences*, *102*(8), 2886–2891.

Mebius, R. E., Rennert, P., & Weissman, I. L. (1997). Developing lymph nodes collect CD4+CD3- LTbeta+ cells that can differentiate to APC, NK cells, and follicular cells but not T or B cells. *Immunity*, *7*(4), 493–504.

Medzhitov, R. (1998). Innate immune recognition and control of adaptive immune responses. *Seminars in Immunology*, *10*(5), 351–353.

Meier, U.-C., Owen, R. E., Taylor, E., Worth, A., Naoumov, N., Willberg, C., Tang, K., Newton, P., Pellegrino, P., Williams, I., Klenerman, P., & Borrow, P. (2005). Shared Alterations in NK Cell Frequency, Phenotype, and Function in Chronic Human Immunodeficiency Virus and Hepatitis C Virus Infections. *Journal of Virology*, *79*(19), 12365–12374.

Meierovics, A., Yankelevich, W. C., & Cowley, S. C. (2013). MAIT cells are critical for optimal mucosal immune responses during in vivo pulmonary bacterial infection. *Proceedings of the National Academy of Sciences of the United States of America*, *110*(33), E3119–E3128.

Mela, C. M., Burton, C. T., Imami, N., Nelson, M., Steel, A., Gazzard, B. G., Gotch, F. M., & Goodier, M. R. (2005). Switch from inhibitory to activating NKG2 receptor expression in HIV-1 infection: lack of reversion with highly active antiretroviral therapy. *AIDS (London, England)*, *19*(16), 1761–9.

Menon, B., Gullick, N. J., Walter, G. J., Rajasekhar, M., Garrood, T., Evans, H. G., Taams, L. S., & Kirkham, B. W. (2014). Interleukin-17+CD8+ T cells are enriched in the joints of patients with psoriatic arthritis and correlate with disease activity and joint damage progression. *Arthritis & Rheumatology*, *66*(5), 1272–1281.

Meraviglia, S., Eberl, M., Vermijlen, D., Todaro, M., Buccheri, S., Cicero, G., La Mendola, C., Guggino, G., D'Asaro, M., Orlando, V., Scarpa, F., Roberts, A., Caccamo, N., Stassi, G., Dieli, F., & Hayday, A. C. (2010). In vivo manipulation of Vgamma9Vdelta2 T cells with zoledronate and low-dose interleukin-2 for immunotherapy of advanced breast cancer patients. *Clinical and Experimental Immunology*, *161*(2), 290–297.

Metkar, S. S., Menaa, C., Pardo, J., Wang, B., Wallich, R., Freudenberg, M., Kim, S., Raja, S. M., Shi, L., Simon, M. M., & Froelich, C. J. (2008). Human and Mouse Granzyme A Induce a Proinfammatory Cytokine Response. *Immunity*, *29*(5), 720–733.

Michie, C. A., McLean, A., Alcock, C., & Beverley, P. C. (1992). Lifespan of human lymphocyte subsets defined by CD45 isoforms. *Nature*, *360*(6401), 264–5.

Migueles, S. A., Osborne, C. M., Royce, C., Compton, A. A., Joshi, R. P., Weeks, K. A., Rood, J. E., Berkley, A. M., Sacha, J. B., Cogliano-Shutta, N. A., Lloyd, M., Roby, G., Kwan, R., McLaughlin, M., Stallings, S., Rehm, C., O'Shea, M. A., Mican, J., Packard, B. Z., Komoriya, A., Palmer, S., Wiegand, A. P., Maldarelli, F., Coffin, J. M., Mellors, J. W., Hallahan, C. W., Follman, D. A., & Connors, M. (2008). Lytic granule loading of CD8+ T cells is required for HIV-infected cell elimination associated with immune control. *Immunity*, *29*(6), 1009–1021.

Miley, M. J., Truscott, S. M., Yu, Y. Y. L., Gilfillan, S., Fremont, D. H., Hansen, T. H., & Lybarger, L. (2003). Biochemical features of the MHC-related protein 1 consistent with an immunological function. *Journal of Immunology*, *170*(12), 6090–6098.

Milush, J. M., López-Vergès, S., York, V. A., Deeks, S. G., Martin, J. N., Hecht, F. M., Lanier, L. L., & Nixon, D. F. (2013). CD56negCD16+ NK cells are activated mature NK cells with impaired effector function during HIV-1 infection. *Retrovirology*, *10*, 158.

Miyake, S., Kim, S., Suda, W., Oshima, K., Nakamura, M., Matsuoka, T., Chihara, N., Tomita, A., Sato, W., Kim, S.-W., Morita, H., Hattori, M., & Yamamura, T. (2015). Dysbiosis in the Gut Microbiota of Patients with Multiple Sclerosis, with a Striking Depletion of Species Belonging to Clostridia XIVa and IV Clusters. *PloS One*, *10*(9), e0137429.

Miyazaki, Y., Miyake, S., Chiba, A., Lantz, O., & Yamamura, T. (2011). Mucosal-associated invariant T cells regulate Th1 response in multiple sclerosis. *International Immunology*, *23*(9), 529–535.

Modlin, R. L., Pirmez, C., Hofman, F. M., Torigian, V., Uyemura, K., Rea, T. H., Bloom, B. R., & Brenner, M. B. (1989). Lymphocytes bearing antigen-specific gamma delta T-cell receptors accumulate in human infectious disease lesions. *Nature*, *339*(6225), 544–548.

Moesta, A. K., & Parham, P. (2012). Diverse functionality among human NK cell receptors for the C1 epitope of HLA-C: KIR2DS2, KIR2DL2, and KIR2DL3. *Frontiers in Immunology*, *3*, 336.

Moffett-King, A. (2002). Natural killer cells and pregnancy. *Nature Reviews. Immunology*, *2*(9), 656–63.

Montaldo, E., Vitale, C., Cottalasso, F., Conte, R., Glatzer, T., Moretta, L., Mingari, M. C., Dc, W., & Ambrosini, P. (2012). Human NK cells at early stages of differentiation

produce CXCL8 and express CD161 molecule that functions as an activating receptor Human NK cells at early stages of differentiation produce CXCL8 and express CD161 molecule that functions as an activating. *Blood*, *119*(17), 3987–3996.

Mootha, V. K., Lindgren, C. M., Eriksson, K.-F., Subramanian, A., Sihag, S., Lehar, J., Puigserver, P., Carlsson, E., Ridderstråle, M., Laurila, E., Houstis, N., Daly, M. J., Patterson, N., Mesirov, J. P., Golub, T. R., Tamayo, P., Spiegelman, B., Lander, E. S., Hirschhorn, J. N., Altshuler, D., & Groop, L. C. (2003). PGC-1alpha-responsive genes involved in oxidative phosphorylation are coordinately downregulated in human diabetes. *Nature Genetics*, *34*(3), 267–273.

Morizane, S., & Gallo, R. L. (2012). Antimicrobial peptides in the pathogenesis of psoriasis. *The Journal of Dermatology*, *39*(3), 225–230.

Moro, K., Yamada, T., Tanabe, M., Takeuchi, T., Ikawa, T., Kawamoto, H., Furusawa, J.-I., Ohtani, M., Fujii, H., & Koyasu, S. (2010). Innate production of T(H)2 cytokines by adipose tissue-associated c-Kit(+)Sca-1(+) lymphoid cells. *Nature*, *463*(7280), 540–544.

Mosmann, T. R., & Coffman, R. L. (1989). TH1 and TH2 cells: different patterns of lymphokine secretion lead to different functional properties. *Annual Review of Immunology*, *7*, 145–173.

Motyka, B., Korbutt, G., Pinkoski, M. J., Heibein, J. A., Caputo, A., Hobman, M., Barry, M., Shostak, I., Sawchuk, T., Holmes, C. F. ., Gauldie, J., & Bleackley, R. C. (2000). Mannose 6-Phosphate/Insulin-like Growth Factor II Receptor Is a Death Receptor for Granzyme B during Cytotoxic T Cell–Induced Apoptosis. *Cell*, *103*(3), 491–500.

Mrózek, E., Anderson, P., & Caligiuri, M. A. (1996). Role of interleukin-15 in the development of human CD56+ natural killer cells from CD34+ hematopoietic progenitor cells. *Blood*, *87*(7), 2632–40.

Mueller, S. N., Zaid, A., & Carbone, F. R. (2014). Tissue-resident T cells: dynamic players in skin immunity. *Frontiers in Immunology*, *5*, 332.

Mulder, W. M. C., Koenen, H., van de Muysenberg, A. J. C., Bloemena, E., Wagsfaff, J., & Scheper, R. J. (1994). Reduced expression of distinct T-cell CD molecules by collagenase/DNase treatment. *Cancer Immunology, Immunotherapy*, *38*(4), 253–258.

Murali-Krishna, K. (1999). Persistence of Memory CD8 T Cells in MHC Class I-Deficient Mice. *Science*, *286*(5443), 1377–1381.

Nagler, A., Lanier, L. L., Cwirla, S., & Phillips, J. H. (1989). Comparative studies of human FcRIII-positive and negative natural killer cells. *Journal of Immunology*, *143*(10), 3183–3191.

Nair, R. P., Duffin, K. C., Helms, C., Ding, J., Stuart, P. E., Goldgar, D., Gudjonsson, J. E., Li, Y., Tejasvi, T., Feng, B.-J., Ruether, A., Schreiber, S., Weichenthal, M., Gladman, D., Rahman, P., Schrodi, S. J., Prahalad, S., Guthery, S. L., Fischer, J., Liao, W., Kwok, P.-Y., Menter, A., Lathrop, G. M., Wise, C. A., Begovich, A. B., Voorhees, J. J., Elder, J. T., Krueger, G. G., Bowcock, A. M., & Abecasis, G. R. (2009). Genome-wide scan reveals association of psoriasis with IL-23 and NF-kappaB pathways. *Nature Genetics*, *41*(2), 199–204.

Nakae, S., Nambu, A., Sudo, K., & Iwakura, Y. (2003). Suppression of Immune Induction of Collagen-Induced Arthritis in IL-17-Deficient Mice. *The Journal of Immunology*, *171*(11), 6173–6177.

Nattermann, J., Feldmann, G., Ahlenstiel, G., Langhans, B., Sauerbruch, T., & Spengler, U. (2006). Surface expression and cytolytic function of natural killer cell receptors is altered in chronic hepatitis C. *Gut*, *55*(6), 869–877.

Navarro, F., Llano, M., Bellón, T., Colonna, M., Geraghty, D. E., & López-Botet, M. (1999). The ILT2(LIR1) and CD94/NKG2A NK cell receptors respectively recognize HLA-G1 and HLA-E molecules co-expressed on target cells. *European Journal of Immunology*, *29*(1), 277–283.

Neill, D. R., Wong, S. H., Bellosi, A., Flynn, R. J., Daly, M., Langford, T. K. A., Bucks, C., Kane, C. M., Fallon, P. G., Pannell, R., Jolin, H. E., & McKenzie, A. N. J. (2010). Nuocytes represent a new innate effector leukocyte that mediates type-2 immunity. *Nature*, *464*(7293), 1367–70.

Newell, E. W., Sigal, N., Bendall, S. C., Nolan, G. P., & Davis, M. M. (2012). Cytometry by time-of-flight shows combinatorial cytokine expression and virus-specific cell niches within a continuum of CD8+ T cell phenotypes. *Immunity*, *36*(1), 142–152.

Nichols, K. E., Hom, J., Gong, S.-Y., Ganguly, A., Ma, C. S., Cannons, J. L., Tangye, S. G., Schwartzberg, P. L., Koretzky, G. A., & Stein, P. L. (2005). Regulation of NKT cell development by SAP, the protein defective in XLP. *Nature Medicine*, *11*(3), 340–345.

Nielsen, N., Ødum, N., Ursø, B., Lanier, L. L., & Spee, P. (2012). Cytotoxicity of CD56(bright) NK cells towards autologous activated CD4+ T cells is mediated through NKG2D, LFA-1 and TRAIL and dampened via CD94/NKG2A. *PloS One*, *7*(2), e31959.

Nograles, K. E., Zaba, L. C., Shemer, A., Fuentes-Duculan, J., Cardinale, I., Kikuchi, T., Ramon, M., Bergman, R., Krueger, J. G., & Guttman-Yassky, E. (2009). IL-22-producing “T22” T cells account for upregulated IL-22 in atopic dermatitis despite reduced IL-17-producing TH17 T cells. *The Journal of Allergy and Clinical Immunology*, *123*(6), 1244–52.e2.

Nouri, M., Bredberg, A., Weström, B., & Lavasani, S. (2014). Intestinal Barrier Dysfunction Develops at the Onset of Experimental Autoimmune Encephalomyelitis, and Can Be Induced by Adoptive Transfer of Auto-Reactive T Cells. *PLoS ONE*, *9*(9), e106335.

Novak, J., Dobrovolny, J., Novakova, L., & Kozak, T. (2014). The decrease in number and change in phenotype of mucosal-associated invariant T cells in the elderly and differences in men and women of reproductive age. *Scandinavian Journal of Immunology*, *80*(4), 271–275.

Nowacki, T. M., Kuerten, S., Zhang, W., Shive, C. L., Kreher, C. R., Boehm, B. O., Lehmann, P. V, & Tary-Lehmann, M. (2007). Granzyme B production distinguishes recently activated CD8(+) memory cells from resting memory cells. *Cellular Immunology*, *247*(1), 36–48.

Noyola, D. E., Fortuny, C., Muntasell, A., Noguera-Julian, A., Muñoz-Almagro, C., Alarcón, A., Juncosa, T., Moraru, M., Vilches, C., López-Botet, M., Mu, C., Juncosa, T., Moraru,

M., Vilches, C., & Miguel, L. (2012). Influence of congenital human cytomegalovirus infection and the NKG2C genotype on NK-cell subset distribution in children. *European Journal of Immunology*, *42*(12), 3256–3266.

O'Reilly, V., Zeng, S. G., Bricard, G., Atzberger, A., Hogan, A. E., Jackson, J., Feighery, C., Porcelli, S. A., & Doherty, D. G. (2011). Distinct and overlapping effector functions of expanded human CD4+, CD8α+ and CD4-CD8α- invariant natural killer T cells. *PloS One*, *6*(12), e28648.

Oh, S. J., & Chung, D. H. (2011). Invariant NKT cells producing IL-4 or IL-10, but not IFN-gamma, inhibit the Th1 response in experimental autoimmune encephalomyelitis, whereas none of these cells inhibits the Th17 response. *Journal of Immunology*, *186*(12), 6815–6821.

Okada, S., Markle, J. G., Deenick, E. K., Mele, F., Averbuch, D., Lagos, M., Alzahrani, M., Al-Muhsen, S., Halwani, R., Ma, C. S., Wong, N., Soudais, C., Henderson, L. A., Marzouqa, H., Shamma, J., Gonzalez, M., Martinez-Barricarte, R., Okada, C., Avery, D. T., Latorre, D., Deswarte, C., Jabot-Hanin, F., Torrado, E., Fountain, J., Belkadi, A., Itan, Y., Boisson, B., Migaud, M., Arlehamn, C. S. L., Sette, A., Breton, S., McCluskey, J., Rossjohn, J., de Villartay, J.-P., Moshous, D., Hambleton, S., Latour, S., Arkwright, P. D., Picard, C., Lantz, O., Engelhard, D., Kobayashi, M., Abel, L., Cooper, A. M., Notarangelo, L. D., Boisson-Dupuis, S., Puel, A., Sallusto, F., Bustamante, J., Tangye, S. G., & Casanova, J.-L. (2015). Impairment of immunity to Candida and Mycobacterium in humans with bi-allelic RORC mutations. *Science*, *349*(6248), 606–613.

Ortega, C., Fernández-A, S., Carrillo, J. M., Romero, P., Molina, I. J., Moreno, J. C., & Santamaría, M. (2009). IL-17-producing CD8+ T lymphocytes from psoriasis skin plaques are cytotoxic effector cells that secrete Th17-related cytokines. *Journal of Leukocyte Biology*, *86*(2), 435–443.

Osada, T., Morse, M. A., Lyerly, H. K., & Clay, T. M. (2005). Ex vivo expanded human CD4+ regulatory NKT cells suppress expansion of tumor antigen-specific CTLs. *International Immunology*, *17*(9), 1143–1155.

Pantelyushin, S., Haak, S., Ingold, B., Kulig, P., Heppner, F. L., Navarini, A. A., & Becher, B. (2012). Rorγt+ innate lymphocytes and γδ T cells initiate psoriasiform plaque formation in mice. *The Journal of Clinical Investigation*, *122*(6), 2252–2256.

Papp, K. A., Langley, R. G., Lebwohl, M., Krueger, G. G., Szapary, P., Yeilding, N., Guzzo, C., Hsu, M.-C., Wang, Y., Li, S., Dooley, L. T., & Reich, K. (2008). Efficacy and safety of ustekinumab, a human interleukin-12/23 monoclonal antibody, in patients with psoriasis: 52-week results from a randomised, double-blind, placebo-controlled trial (PHOENIX 2). *Lancet (London, England)*, *371*(9625), 1675–84.

Papp, K. A., Leonardi, C., Menter, A., Ortonne, J.-P., Krueger, J. G., Kricorian, G., Aras, G., Li, J., Russell, C. B., Thompson, E. H. Z., & Baumgartner, S. (2012). Brodalumab, an anti-interleukin-17-receptor antibody for psoriasis. *The New England Journal of Medicine*, *366*(13), 1181–1189.

Pardo, J., Bosque, A., Brehm, R., Wallich, R., Naval, J., Müllbacher, A., Anel, A., & Simon, M. M. (2004). Apoptotic pathways are selectively activated by granzyme A and/or

granzyme B in CTL-mediated target cell lysis. *The Journal of Cell Biology*, *167*(3), 457–468.

Park, H., Li, Z., Yang, X. O., Chang, S. H., Nurieva, R., Wang, Y.-H., Wang, Y., Hood, L., Zhu, Z., Tian, Q., & Dong, C. (2005). A distinct lineage of CD4 T cells regulates tissue inflammation by producing interleukin 17. *Nature Immunology*, *6*(11), 1133–1141.

Park, S. H., Weiss, A., Benlagha, K., Kyin, T., Teyton, L., & Bendelac, A. (2001). The mouse CD1d-restricted repertoire is dominated by a few autoreactive T cell receptor families. *The Journal of Experimental Medicine*, *193*(8), 893–904.

Pascal, V., Schleinitz, N., Brunet, C., Ravet, S., Bonnet, E., Lafarge, X., Touinssi, M., Reviron, D., Viallard, J. F., Moreau, J. F., Déchanet-Merville, J., Blanco, P., Harlé, J. R., Sampol, J., Vivier, E., Dignat-George, F., & Paul, P. (2004). Comparative analysis of NK cell subset distribution in normal and lymphoproliferative disease of granular lymphocyte conditions. *European Journal of Immunology*, *34*(10), 2930–40.

Pasquier, B., Yin, L., Fondanèche, M.-C., Relouzat, F., Bloch-Queyrat, C., Lambert, N., Fischer, A., de Saint-Basile, G., & Latour, S. (2005). Defective NKT cell development in mice and humans lacking the adapter SAP, the X-linked lymphoproliferative syndrome gene product. *The Journal of Experimental Medicine*, *201*(5), 695–701.

Patel, O., Kjer-Nielsen, L., Le Nours, J., Eckle, S. B. G., Birkinshaw, R., Beddoe, T., Corbett, A. J., Liu, L., Miles, J. J., Meehan, B., Reantragoon, R., Sandoval-Romero, M. L., Sullivan, L. C., Brooks, A. G., Chen, Z., Fairlie, D. P., McCluskey, J., & Rossjohn, J. (2013). Recognition of vitamin B metabolites by mucosal-associated invariant T cells. *Nature Communications*, *4*, 2142.

Patel, O., Pellicci, D. G., Gras, S., Sandoval-Romero, M. L., Uldrich, A. P., Mallevaey, T., Clarke, A. J., Le Nours, J., Theodossis, A., Cardell, S. L., Gapin, L., Godfrey, D. I., & Rossjohn, J. (2012). Recognition of CD1d-sulfatide mediated by a type II natural killer T cell antigen receptor. *Nature Immunology*, *13*(9), 857–863.

Paukkonen, K., Naukkarinen, A., & Horsmanheimo, M. (1992). The development of manifest psoriatic lesions is linked with the invasion of CD8 + T cells and CD11c + macrophages into the epidermis. *Archives of Dermatological Research*, *284*(7), 375–379.

Paust, S., Gill, H. S., Wang, B.-Z., Flynn, M. P., Moseman, E. A., Senman, B., Szczepanik, M., Telenti, A., Askenase, P. W., Compans, R. W., & von Andrian, U. H. (2010). Critical role for the chemokine receptor CXCR6 in NK cell-mediated antigen-specific memory of haptens and viruses. *Nature Immunology*, *11*(12), 1127–1135.

Pavlidis, P., & Noble, W. S. (2001). Analysis of strain and regional variation in gene expression in mouse brain. *Genome Biology*, *2*(10), RESEARCH0042.

Pearce, E. L., Mullen, A. C., Martins, G. A., Krawczyk, C. M., Hutchins, A. S., Zediak, V. P., Banica, M., DiCioccio, C. B., Gross, D. A., Mao, C.-A., Shen, H., Cereb, N., Yang, S. Y., Lindsten, T., Rossant, J., Hunter, C. A., & Reiner, S. L. (2003). Control of effector CD8+ T cell function by the transcription factor Eomesodermin. *Science*, *302*(5647), 1041–3.

Pende, D., Parolini, S., Pessino, A., Sivori, S., Augugliaro, R., Morelli, L., Marcenaro, E.,

Accame, L., Malaspina, A., Biassoni, R., Bottino, C., Moretta, L., & Moretta, A. (1999). Identification and molecular characterization of NKp30, a novel triggering receptor involved in natural cytotoxicity mediated by human natural killer cells. *The Journal of Experimental Medicine*, *190*(10), 1505–1516.

Perera, G. K., Di Meglio, P., & Nestle, F. O. (2012). Psoriasis. *Annual Review of Pathology*, *7*, 385–422.

Petitdemange, C., Becquart, P., Wauquier, N., Béziat, V., Debré, P., Leroy, E. M., & Vieillard, V. (2011). Unconventional repertoire profile is imprinted during acute chikungunya infection for natural killer cells polarization toward cytotoxicity. *PLoS Pathogens*, *7*(9), e1002268.

Piccioli, D. (2002). Contact-dependent Stimulation and Inhibition of Dendritic Cells by Natural Killer Cells. *Journal of Experimental Medicine*, *195*(3), 335–341.

Pieters, J. (2008). Mycobacterium tuberculosis and the macrophage: maintaining a balance. *Cell Host & Microbe*, *3*(6), 399–407.

Pietrzak, A. T., Zalewska, A., Chodorowska, G., Krasowska, D., Michalak-Stoma, A., Nockowski, P., Osemlak, P., Paszkowski, T., & Roliński, J. M. (2008). Cytokines and anticytokines in psoriasis. *International Journal of Clinical Chemistry*, *394*(1-2), 7–21.

Pinkoski, M. J., Hobman, M., Heibein, J. a, Tomaselli, K., Li, F., Seth, P., Froelich, C. J., & Bleackley, R. C. (1998). Entry and trafficking of granzyme B in target cells during granzyme B-perforin-mediated apoptosis. *Blood*, *92*(3), 1044–1054.

Piskin, G., Sylva-Steenland, R. M. R., Bos, J. D., & Teunissen, M. B. M. (2006). In Vitro and In Situ Expression of IL-23 by Keratinocytes in Healthy Skin and Psoriasis Lesions: Enhanced Expression in Psoriatic Skin. *The Journal of Immunology*, *176*(3), 1908–1915.

Pittet, M. J., Speiser, D. E., Valmori, D., Cerottini, J.-C., & Romero, P. (2000). Cutting Edge: Cytolytic Effector Function in Human Circulating CD8+ T Cells Closely Correlates with CD56 Surface Expression. *The Journal of Immunology*, *164*(3), 1148–1152.

Poggi, A., Costa, P., Tomasello, E., & Moretta, L. (1998). IL-12-induced up-regulation of NKRP1A expression in human NK cells and consequent NKRP1A-mediated down-regulation of NK cell activation. *European Journal of Immunology*, *28*(5), 1611–1616.

Poggi, A., Costa, P., Zocchi, M. R., & Moretta, L. (1997). Phenotypic and functional analysis of CD4+ NKRP1A+ human T lymphocytes. Direct evidence that the NKRP1A molecule is involved in transendothelial migration. *European Journal of Immunology*, *27*(9), 2345–50.

Poggi, A., Massaro, A.-M., Negrini, S., Contini, P., & Zocchi, M. R. (2005). Tumor-induced apoptosis of human IL-2-activated NK cells: role of natural cytotoxicity receptors. *Journal of Immunology*, *174*(5), 2653–2660.

Porcelli, S., Yockey, C. E., Brenner, M. B., & Balk, S. P. (1993). Analysis of T cell antigen receptor (TCR) expression by human peripheral blood CD4-8- alpha/beta T cells demonstrates preferential use of several V beta genes and an invariant TCR alpha chain. *The Journal of Experimental Medicine*, *178*(1), 1–16.

Possot, C., Schmutz, S., Chea, S., Boucontet, L., Louise, A., Cumano, A., & Golub, R. (2011). Notch signaling is necessary for adult, but not fetal, development of RORγt(+) innate lymphoid cells. *Nature Immunology*, *12*(10), 949–958.

Poupot, M., Fournié, J.-J., & Poupot, R. (2008). Trogocytosis and killing of IL-4-polarized monocytes by autologous NK cells. *Journal of Leukocyte Biology*, *84*(5), 1298–1305.

Price, A. E., Liang, H.-E., Sullivan, B. M., Reinhardt, R. L., Eisley, C. J., Erle, D. J., & Locksley, R. M. (2010). Systemically dispersed innate IL-13-expressing cells in type 2 immunity. *Proceedings of the National Academy of Sciences of the United States of America*, *107*(25), 11489–11494.

Pridgeon, C., Lennon, G. P., Pazmany, L., Thompson, R. N., Christmas, S. E., & Moots, R. J. (2003). Natural killer cells in the synovial fluid of rheumatoid arthritis patients exhibit a CD56bright,CD94bright,CD158negative phenotype. *Rheumatology*, *42*(7), 870–878.

Prpić Massari, L., Kastelan, M., Laskarin, G., Zamolo, G., Massari, D., & Rukavina, D. (2007). Analysis of perforin expression in peripheral blood and lesions in severe and mild psoriasis. *Journal of Dermatological Science*, *47*(1), 29–36.

Punt, J., Owen, J., & Caligiuri, M. A. (2001). The biology of human natural killer-cell subsets. *Trends in Immunology*, *22*(11), 633–640.

Purbhoo, M. A., Boulter, J. M., Price, D. A., Vuidepot, A. L., Hourigan, C. S., Dunbar, P. R., Olson, K., Dawson, S. J., Phillips, R. E., Jakobsen, B. K., Bell, J. I., & Sewell, A. K. (2001). The human CD8 coreceptor effects cytotoxic T cell activation and antigen sensitivity primarily by mediating complete phosphorylation of the T cell receptor zeta chain. *The Journal of Biological Chemistry*, *276*(35), 32786–32792.

Qiao, Y., Zhu, L., Sofi, H., Lapinski, P. E., Horai, R., Mueller, K., Stritesky, G. L., He, X., Teh, H.-S., Wiest, D. L., Kappes, D. J., King, P. D., Hogquist, K. A., Schwartzberg, P. L., Sant'Angelo, D. B., & Chang, C.-H. (2012). Development of promyelocytic leukemia zinc finger-expressing innate CD4 T cells requires stronger T-cell receptor signals than conventional CD4 T cells. *Proceedings of the National Academy of Sciences of the United States of America*, *109*(40), 16264–16269.

Quinnan, G. V, Kirmani, N., Rook, A. H., Manischewitz, J. F., Jackson, L., Moreschi, G., Santos, G. W., Saral, R., & Burns, W. H. (1982). Cytotoxic t cells in cytomegalovirus infection: HLA-restricted T-lymphocyte and non-T-lymphocyte cytotoxic responses correlate with recovery from cytomegalovirus infection in bone-marrow-transplant recipients. *The New England Journal of Medicine*, *307*(1), 7–13.

Raberger, J., Schebesta, A., Sakaguchi, S., Boucheron, N., Blomberg, K. E. M., Berglof, A., Kolbe, T., Smith, C. I. E., Rulicke, T., & Ellmeier, W. (2008). The transcriptional regulator PLZF induces the development of CD44high memory phenotype T cells. *Proceedings of the National Academy of Sciences*, *105*(46), 17919–17924.

Raffatellu, M., Santos, R. L., Verhoeven, D. E., George, M. D., Wilson, R. P., Winter, S. E., Godinez, I., Sankaran, S., Paixao, T. A., Gordon, M. A., Kolls, J. K., Dandekar, S., & Bäumler, A. J. (2008). Simian immunodeficiency virus-induced mucosal interleukin-17 deficiency promotes Salmonella dissemination from the gut. *Nature Medicine*, *14*(4), 421–428.

Rahimpour, A., Koay, H. F., Enders, A., Clanchy, R., Eckle, S. B. G., Meehan, B., Chen, Z., Whittle, B., Liu, L., Fairlie, D. P., Goodnow, C. C., McCluskey, J., Rossjohn, J., Uldrich, A. P., Pellicci, D. G., & Godfrey, D. I. (2015). Identification of phenotypically and functionally heterogeneous mouse mucosal-associated invariant T cells using MR1 tetramers. *Journal of Experimental Medicine*, *212*(7), 1095–1108.

Ramsburg, E., Tigelaar, R., Craft, J., & Hayday, A. (2003). Age-dependent requirement for gammadelta T cells in the primary but not secondary protective immune response against an intestinal parasite. *The Journal of Experimental Medicine*, *198*(9), 1403–1414.

Rankin, L., Groom, J., Mielke, L. A., Seillet, C., & Belz, G. T. (2013). Diversity, function, and transcriptional regulation of gut innate lymphocytes. *Frontiers in Immunology*, *4*, 22.

Ranson, T., Vosshenrich, C. A. J., Corcuff, E., Richard, O., Laloux, V., Lehuen, A., & Di Santo, J. P. (2003). IL-15 availability conditions homeostasis of peripheral natural killer T cells. *Proceedings of the National Academy of Sciences of the United States of America*, *100*(5), 2663–2668.

Raychaudhuri, S. P., Raychaudhuri, S. K., & Genovese, M. C. (2012). IL-17 receptor and its functional significance in psoriatic arthritis. *Molecular and Cellular Biochemistry*, *359*(1-2), 419–429.

Reantragoon, R., Corbett, A. J., Sakala, I. G., Gherardin, N. A., Furness, J. B., Chen, Z., Eckle, S. B. G., Uldrich, A. P., Birkinshaw, R. W., Patel, O., Kostenko, L., Meehan, B., Kedzierska, K., Liu, L., Fairlie, D. P., Hansen, T. H., Godfrey, D. I., Rossjohn, J., Mccluskey, J., & Kjer-nielsen, L. (2013). Antigen-loaded MR1 tetramers define T cell receptor heterogeneity in mucosal-associated invariant T cells. *Journal of Experimental Medicine*, *210*(11), 2305–2320.

Reantragoon, R., Kjer-Nielsen, L., Patel, O., Chen, Z., Illing, P. T., Bhati, M., Kostenko, L., Bharadwaj, M., Meehan, B., Hansen, T. H., Godfrey, D. I., Rossjohn, J., & Mccluskey, J. (2012). Structural insight into MR1-mediated recognition of the mucosal associated invariant T cell receptor. *The Journal of Experimental Medicine*, *209*(4), 761–774.

Res, P. C. M., Piskin, G., de Boer, O. J., van der Loos, C. M., Teeling, P., Bos, J. D., & Teunissen, M. B. M. (2010). Overrepresentation of IL-17A and IL-22 producing CD8 T cells in lesional skin suggests their involvement in the pathogenesis of psoriasis. *PloS One*, *5*(11), e14108.

Rich, P., Sigurgeirsson, B., Thaci, D., Ortonne, J.-P., Paul, C., Schopf, R. E., Morita, A., Roseau, K., Harfst, E., Guettner, A., Machacek, M., & Papavassilis, C. (2013). Secukinumab induction and maintenance therapy in moderate-to-severe plaque psoriasis: a randomized, double-blind, placebo-controlled, phase II regimen-finding study. *The British Journal of Dermatology*, *168*(2), 402–11.

Riegert, P., Wanner, V., & Bahram, S. (1998). Genomics, isoforms, expression, and phylogeny of the MHC class I-related MR1 gene. *Journal of Immunology*, *161*(8), 4066–4077.

Ritchlin, C., Haas-Smith, S. A., Hicks, D., Cappuccio, J., Osterland, C. K., & Looney, R. J. (1998). Patterns of cytokine production in psoriatic synovium. *The Journal of*

Rheumatology, *25*(8), 1544–1552.

Ritchlin, C. T., Haas-Smith, S. A., Li, P., Hicks, D. G., & Schwarz, E. M. (2003). Mechanisms of TNF-α– and RANKL-mediated osteoclastogenesis and bone resorption in psoriatic arthritis. *Journal of Clinical Investigation*, *111*(6), 821–831.

Rizzo, H. L., Kagami, S., Phillips, K. G., Kurtz, S. E., Jacques, S. L., & Blauvelt, A. (2010). IL-23-Mediated Psoriasis-Like Epidermal Hyperplasia Is Dependent on IL-17A. *The Journal of Immunology*, *186*(3), 1495–1502.

Roark, C. L., French, J. D., Taylor, M. A., Bendele, A. M., Born, W. K., & O'Brien, R. L. (2007). Exacerbation of Collagen-Induced Arthritis by Oligoclonal, IL-17-Producing T Cells. *The Journal of Immunology*, *179*(8), 5576–5583.

Robinette, M. L., Fuchs, A., Cortez, V. S., Lee, J. S., Wang, Y., Durum, S. K., Gilfillan, S., & Colonna, M. (2015). Transcriptional programs define molecular characteristics of innate lymphoid cell classes and subsets. *Nature Immunology*, *16*(3), 306–317.

Roederer, M., Nozzi, J. L., & Nason, M. C. (2011). SPICE: Exploration and analysis of post-cytometric complex multivariate datasets. *Cytometry Part A*, *79 A*(2), 167–174.

Rölle, A., Pollmann, J., Ewen, E.-M., Le, V. T. K., Halenius, A., Hengel, H., & Cerwenka, A. (2014). IL-12-producing monocytes and HLA-E control HCMV-driven NKG2C+ NK cell expansion. *The Journal of Clinical Investigation*, *124*(12), 5305–5316.

Romagnani, C., Juelke, K., Falco, M., Morandi, B., D'Agostino, A., Costa, R., Ratto, G., Forte, G., Carrega, P., Lui, G., Conte, R., Strowig, T., Moretta, A., Munz, C., Thiel, A., Moretta, L., & Ferlazzo, G. (2007). CD56brightCD16- Killer Ig-Like Receptor- NK Cells Display Longer Telomeres and Acquire Features of CD56dim NK Cells upon Activation. *The Journal of Immunology*, *178*(8), 4947–4955.

Romero, P., Zippelius, A., Kurth, I., Pittet, M. J., Touvrey, C., Iancu, E. M., Corthesy, P., Devevre, E., Speiser, D. E., & Rufer, N. (2007). Four Functionally Distinct Populations of Human Effector-Memory CD8+ T Lymphocytes. *The Journal of Immunology*, *178*(7), 4112–4119.

Rooney, T., Murphy, E., Benito, M., Roux-Lombard, P., FitzGerald, O., Dayer, J.-M., & Bresnihan, B. (2004). Synovial tissue interleukin-18 expression and the response to treatment in patients with inflammatory arthritis. *Annals of the Rheumatic Diseases*, *63*(11), 1393–1398.

Rosen, D. B., Bettadapura, J., Alsharifi, M., Mathew, P. a, Warren, H. S., & Lanier, L. L. (2005). Cutting edge: lectin-like transcript-1 is a ligand for the inhibitory human NKR-P1A receptor. *Journal of Immunology*, *175*(12), 7796–7799.

Rosen, D. B., Cao, W., Avery, D. T., Tangye, S. G., Liu, Y.-J., Houchins, J. P., & Lanier, L. L. (2008). Functional consequences of interactions between human NKR-P1A and its ligand LLT1 expressed on activated dendritic cells and B cells. *Journal of Immunology*, *180*(10), 6508–6517.

Ryan, J. C., Turck, J., Niemi, E. C., Yokoyama, W. M., & Seaman, W. E. (1992). Molecular cloning of the NK1.1 antigen, a member of the NKR-P1 family of natural killer cell activation molecules. *Journal of Immunology*, *149*(5), 1631–1635.

Sa, S. M., Valdez, P. A., Wu, J., Jung, K., Zhong, F., Hall, L., Kasman, I., Winer, J., Modrusan, Z., Danilenko, D. M., & Ouyang, W. (2007). The Effects of IL-20 Subfamily Cytokines on Reconstituted Human Epidermis Suggest Potential Roles in Cutaneous Innate Defense and Pathogenic Adaptive Immunity in Psoriasis. *The Journal of Immunology*, *178*(4), 2229–2240.

Sabin, C. A., Phillips, A. N., Lee, C. A., Janossy, G., Emery, V., & Griffiths, P. D. (1995). The effect of CMV infection on progression of human immunodeficiency virus disease is a cohort of haemophilic men followed for up to 13 years from seroconversion. *Epidemiology and Infection*, *114*(2), 361–72.

Saeed, A. I., Sharov, V., White, J., Li, J., Liang, W., Bhagabati, N., Braisted, J., Klapa, M., Currier, T., Thiagarajan, M., Sturn, A., Snuffin, M., Rezantsev, A., Popov, D., Ryltsov, A., Kostukovich, E., Borisovsky, I., Liu, Z., Vinsavich, A., Trush, V., & Quackenbush, J. (2003). TM4: a free, open-source system for microarray data management and analysis. *BioTechniques*, *34*(2), 374–378.

Saeidi, A., Tien Tien, V. L., Al-Batran, R., Al-Darraji, H. A., Tan, H. Y., Yong, Y. K., Ponnampalavanar, S., Barathan, M., Rukumani, D. V, Ansari, A. W., Velu, V., Kamarulzaman, A., Larsson, M., & Shankar, E. M. (2015). Attrition of TCR Vα7.2+ CD161++ MAIT cells in HIV-tuberculosis co-infection is associated with elevated levels of PD-1 expression. *PloS One*, *10*(4), e0124659.

Saghafian-Hedengren, S., Sohlberg, E., Theorell, J., Carvalho-Queiroz, C., Nagy, N., Persson, J.-O., Nilsson, C., Bryceson, Y. T., & Sverremark-Ekström, E. (2013). Epstein-Barr virus coinfection in children boosts cytomegalovirus-induced differentiation of natural killer cells. *Journal of Virology*, *87*(24), 13446–13455.

Saghafian-Hedengren, S., Sverremark-Ekström, E., Linde, A., Lilja, G., & Nilsson, C. (2010). Early-life EBV infection protects against persistent IgE sensitization. *The Journal of Allergy and Clinical Immunology*, *125*(2), 433–438.

Saito, H., Kranz, D. M., Takagaki, Y., Hayday, A. C., Eisen, H. N., & Tonegawa, S. (1984). Complete primary structure of a heterodimeric T-cell receptor deduced from cDNA sequences. *Nature*, *309*(5971), 757–762.

Sakala, I. G., Kjer-Nielsen, L., Eickhoff, C. S., Wang, X., Blazevic, A., Liu, L., Fairlie, D. P., Rossjohn, J., McCluskey, J., Fremont, D. H., Hansen, T. H., & Hoft, D. F. (2015). Functional Heterogeneity and Antimycobacterial Effects of Mouse Mucosal-Associated Invariant T Cells Specific for Riboflavin Metabolites. *Journal of Immunology (Baltimore, Md. : 1950)*, *195*(2), 587–601.

Salimi, M., Barlow, J. L., Saunders, S. P., Xue, L., Gutowska-Owsiak, D., Wang, X., Huang, L.-C., Johnson, D., Scanlon, S. T., McKenzie, A. N. J., Fallon, P. G., & Ogg, G. S. (2013). A role for IL-25 and IL-33-driven type-2 innate lymphoid cells in atopic dermatitis. *The Journal of Experimental Medicine*, *210*(13), 2939–2950.

Sallusto, F., Lenig, D., Förster, R., Lipp, M., & Lanzavecchia, A. (1999). Two subsets of memory T lymphocytes with distinct homing potentials and effector functions. *Nature*, *401*(6754), 708–12.

Sandberg, J. K., Fast, N. M., Palacios, E. H., Fennelly, G., Dobroszycki, J., Palumbo, P., Wiznia, A., Grant, R. M., Bhardwaj, N., Rosenberg, M. G., & Nixon, D. F. (2002).

Selective Loss of Innate CD4+ V 24 Natural Killer T Cells in Human Immunodeficiency Virus Infection. *Journal of Virology*, *76*(15), 7528–7534.

Sandstrom, A., Peigné, C.-M., Léger, A., Crooks, J. E., Konczak, F., Gesnel, M.-C., Breathnach, R., Bonneville, M., Scotet, E., & Adams, E. J. (2014). The intracellular B30.2 domain of butyrophilin 3A1 binds phosphoantigens to mediate activation of human Vγ9Vδ2 T cells. *Immunity*, *40*(4), 490–500.

Sarkar, S., Cooney, L. A., White, P., Dunlop, D. B., Endres, J., Jorns, J. M., Wasco, M. J., & Fox, D. A. (2009). Regulation of pathogenic IL-17 responses in collagen-induced arthritis: roles of endogenous interferon-gamma and IL-4. *Arthritis Research & Therapy*, *11*(5), R158.

Satoh-Takayama, N., Dumoutier, L., Lesjean-Pottier, S., Ribeiro, V. S. G., Mandelboim, O., Renauld, J.-C., Vosshenrich, C. A. J., & Di Santo, J. P. (2009). The natural cytotoxicity receptor NKp46 is dispensable for IL-22-mediated innate intestinal immune defense against Citrobacter rodentium. *Journal of Immunology (Baltimore, Md. : 1950)*, *183*(10), 6579–87.

Sattler, A., Dang-Heine, C., Reinke, P., & Babel, N. (2015). IL-15 dependent induction of IL-18 secretion as a feedback mechanism controlling human MAIT-cell effector functions. *European Journal of Immunology*, *45*(8), 2286–2298.

Savage, A. K., Constantinides, M. G., & Bendelac, A. (2011). Promyelocytic leukemia zinc finger turns on the effector T cell program without requirement for agonist TCR signaling. *Journal of Immunology*, *186*(10), 5801–5806.

Savage, A. K., Constantinides, M. G., Han, J., Picard, D., Martin, E., Li, B., Lantz, O., & Bendelac, A. (2008). The transcription factor PLZF directs the effector program of the NKT cell lineage. *Immunity*, *29*(3), 391–403.

Scandella, E., Bolinger, B., Lattmann, E., Miller, S., Favre, S., Littman, D. R., Finke, D., Luther, S. A., Junt, T., & Ludewig, B. (2008). Restoration of lymphoid organ integrity through the interaction of lymphoid tissue-inducer cells with stroma of the T cell zone. *Nature Immunology*, *9*(6), 667–675.

Scharton, T. M., & Scott, P. (1993). Natural killer cells are a source of interferon gamma that drives differentiation of CD4+ T cell subsets and induces early resistance to Leishmania major in mice. *The Journal of Experimental Medicine*, *178*(2), 567–577.

Schatz, D. G., Oettinger, M. A., & Baltimore, D. (1989). The V(D)J recombination activating gene, RAG-1. *Cell*, *59*(6), 1035–1048.

Schierloh, P., Yokobori, N., Alemán, M., Musella, R. M., Beigier-Bompadre, M., Saab, M. A., Alves, L., Abbate, E., de la Barrera, S. S., & Sasiain, M. C. (2005). Increased susceptibility to apoptosis of CD56dimCD16+ NK cells induces the enrichment of IFN-gamma-producing CD56bright cells in tuberculous pleurisy. *Journal of Immunology*, *175*(10), 6852–6860.

Schlums, H., Cichocki, F., Tesi, B., Theorell, J., Beziat, V., Holmes, T. D., Han, H., Chiang, S. C. C., Foley, B., Mattsson, K., Larsson, S., Schaffer, M., Malmberg, K.-J., Ljunggren, H.-G., Miller, J. S., & Bryceson, Y. T. (2015). Cytomegalovirus infection drives adaptive epigenetic diversification of NK cells with altered signaling and

effector function. *Immunity*, *42*(3), 443–456.

Seach, N., Guerri, L., Le Bourhis, L., Mburu, Y., Cui, Y., Bessoles, S., Soudais, C., & Lantz, O. (2013). Double-positive thymocytes select mucosal-associated invariant T cells. *Journal of Immunology*, *191*(12), 6002–6009.

Seder, R. A., Paul, W. E., Davis, M. M., & Fazekas de St Groth, B. (1992). The presence of interleukin 4 during in vitro priming determines the lymphokine-producing potential of CD4+ T cells from T cell receptor transgenic mice. *The Journal of Experimental Medicine*, *176*(4), 1091–1098.

Serriari, N.-E., Eoche, M., Lamotte, L., Lion, J., Fumery, M., Marcelo, P., Chatelain, D., Barre, A., Nguyen-Khac, E., Lantz, O., Dupas, J.-L., & Treiner, E. (2014). Innate mucosal-associated invariant T (MAIT) cells are activated in inflammatory bowel diseases. *Clinical and Experimental Immunology*, *176*(2), 266–274.

Sheehy, M. E., McDermott, A. B., Furlan, S. N., Klenerman, P., & Nixon, D. F. (2001). A novel technique for the fluorometric assessment of T lymphocyte antigen specific lysis. *Journal of Immunological Methods*, *249*(1-2), 99–110.

Shen, Y., Zhou, D., Qiu, L., Lai, X., Simon, M., Shen, L., Kou, Z., Wang, Q., Jiang, L., Estep, J., Hunt, R., Clagett, M., Sehgal, P. K., Li, Y., Zeng, X., Morita, C. T., Brenner, M. B., Letvin, N. L., & Chen, Z. W. (2002). Adaptive immune response of Vgamma2Vdelta2+ T cells during mycobacterial infections. *Science (New York, N.Y.)*, *295*(5563), 2255–8.

Shi, L., Kam, C. M., Powers, J. C., Aebersold, R., & Greenberg, A. H. (1992). Purification of three cytotoxic lymphocyte granule serine proteases that induce apoptosis through distinct substrate and target cell interactions. *Journal of Experimental Medicine*, *176*(6), 1521–1529.

Shimamura, M., Huang, Y.-Y., Goji, H., Endo, S., Migishima, R., & Yokoyama, M. (2011). Regulation of immunological disorders by invariant Vα19-Jα33 TCR-bearing cells. *Immunobiology*, *216*(3), 374–378.

Shin, H., Günther, O., Hollander, Z., Wilson-McManus, J. E., Ng, R. T., Balshaw, R., Keown, P. A., McMaster, R., McManus, B. M., Isbel, N. M., Knoll, G., & Tebbutt, S. J. (2014). Longitudinal analysis of whole blood transcriptomes to explore molecular signatures associated with acute renal allograft rejection. *Bioinformatics and Biology Insights*, *8*, 17–33.

Shresta, S., MacIvor, D. M., Heusel, J. W., Russell, J. H., & Ley, T. J. (1995). Natural killer and lymphokine-activated killer cells require granzyme B for the rapid induction of apoptosis in susceptible target cells. *Proceedings of the National Academy of Sciences of the United States of America*, *92*(12), 5679–5683.

Simoni, Y., Gautron, A.-S., Beaudoin, L., Bui, L.-C., Michel, M.-L., Coumoul, X., Eberl, G., Leite-de-Moraes, M., & Lehuen, A. (2011). NOD mice contain an elevated frequency of iNKT17 cells that exacerbate diabetes. *European Journal of Immunology*, *41*(12), 3574–3585.

Singer, A., Adoro, S., & Park, J.-H. (2008). Lineage fate and intense debate: myths, models and mechanisms of CD4- versus CD8-lineage choice. *Nature Reviews*

Immunology, *8*(10), 788–801.

Singh, S. P., Zhang, H. H., Tsang, H., Gardina, P. J., Myers, T. G., Nagarajan, V., Lee, C. H., & Farber, J. M. (2015). PLZF regulates CCR6 and is critical for the acquisition and maintenance of the Th17 phenotype in human cells. *Journal of Immunology*, *194*(9), 4350–4361.

Sirianni, M. C., Mezzaroma, I., Aiuti, F., & Moretta, A. (1994). Analysis of the cytolytic activity mediated by natural killer cells from acquired immunodeficiency syndrome patients in response to phytohemagglutinin or anti-CD16 monoclonal antibody. *European Journal of Immunology*, *24*(8), 1874–1878.

Skepner, J., Ramesh, R., Trocha, M., Schmidt, D., Baloglu, E., Lobera, M., Carlson, T., Hill, J., Orband-Miller, L. A., Barnes, A., Boudjelal, M., Sundrud, M., Ghosh, S., & Yang, J. (2014). Pharmacologic inhibition of RORγt regulates Th17 signature gene expression and suppresses cutaneous inflammation in vivo. *Journal of Immunology*, *192*(6), 2564–2575.

Smith, C., Elhassen, D., Gras, S., Wynn, K. K., Dasari, V., Tellam, J., Tey, S.-K., Rehan, S., Liu, Y. C., Rossjohn, J., Burrows, S. R., & Khanna, R. (2012). Endogenous antigen presentation impacts on T-box transcription factor expression and functional maturation of CD8+ T cells. *Blood*, *120*(16), 3237–45.

Smith, D. J., Hill, G. R., Bell, S. C., & Reid, D. W. (2014). Reduced mucosal associated invariant T-cells are associated with increased disease severity and Pseudomonas aeruginosa infection in cystic fibrosis. *PloS One*, *9*(10), e109891.

Sojka, D. K., Plougastel-Douglas, B., Yang, L., Pak-Wittel, M. A., Artyomov, M. N., Ivanova, Y., Zhong, C., Chase, J. M., Rothman, P. B., Yu, J., Riley, J. K., Zhu, J., Tian, Z., & Yokoyama, W. M. (2014). Tissue-resident natural killer (NK) cells are cell lineages distinct from thymic and conventional splenic NK cells. *eLife*, *3*, e01659.

Solt, L. A., Kumar, N., Nuhant, P., Wang, Y., Lauer, J. L., Liu, J., Istrate, M. A., Kamenecka, T. M., Roush, W. R., Vidović, D., Schürer, S. C., Xu, J., Wagoner, G., Drew, P. D., Griffin, P. R., & Burris, T. P. (2011). Suppression of TH17 differentiation and autoimmunity by a synthetic ROR ligand. *Nature*, *472*(7344), 491–494.

Song, R., Lisovsky, I., Lebouché, B., Routy, J.-P., Bruneau, J., & Bernard, N. F. (2014). HIV protective KIR3DL1/S1-HLA-B genotypes influence NK cell-mediated inhibition of HIV replication in autologous CD4 targets. *PLoS Pathogens*, *10*(1), e1003867.

Sonnenberg, G. F., Monticelli, L. A., Alenghat, T., Fung, T. C., Hutnick, N. A., Kunisawa, J., Shibata, N., Grunberg, S., Sinha, R., Zahm, A. M., Tardif, M. R., Sathaliyawala, T., Kubota, M., Farber, D. L., Collman, R. G., Shaked, A., Fouser, L. A., Weiner, D. B., Tessier, P. A., Friedman, J. R., Kiyono, H., Bushman, F. D., Chang, K.-M., & Artis, D. (2012). Innate lymphoid cells promote anatomical containment of lymphoid-resident commensal bacteria. *Science*, *336*(6086), 1321–1325.

Soudais, C., Samassa, F., Sarkis, M., Le Bourhis, L., Bessoles, S., Blanot, D., Hervé, M., Schmidt, F., Mengin-Lecreulx, D., & Lantz, O. (2015). In Vitro and In Vivo Analysis of the Gram-Negative Bacteria-Derived Riboflavin Precursor Derivatives Activating Mouse MAIT Cells. *Journal of Immunology*, *194*(10), 4641–4649.

Souwer, Y., Griekspoor, A., de Wit, J., Martinoli, C., Zagato, E., Janssen, H., Jorritsma, T., Bar-Ephraïm, Y. E., Rescigno, M., Neefjes, J., van Ham, S. M., Wit, J. De, Martinoli, C., Zagato, E., Janssen, H., Rescigno, M., Neefjes, J., Ham, S. M. Van, Jorritsma, T., & Bar-ephraı, Y. E. (2012). Selective Infection of Antigen-Specific B Lymphocytes by Salmonella Mediates Bacterial Survival and Systemic Spreading of Infection. *PLoS ONE*, *7*(11), e50667.

Spada, F. M., Grant, E. P., Peters, P. J., Sugita, M., Melián, A., Leslie, D. S., Lee, H. K., van Donselaar, E., Hanson, D. A., Krensky, A. M., Majdic, O., Porcelli, S. A., Morita, C. T., & Brenner, M. B. (2000). Self-recognition of CD1 by gamma/delta T cells: implications for innate immunity. *The Journal of Experimental Medicine*, *191*(6), 937–948.

Spencer, C. T., Abate, G., Sakala, I. G., Xia, M., Truscott, S. M., Eickhoff, C. S., Linn, R., Blazevic, A., Metkar, S. S., Peng, G., Froelich, C. J., & Hoft, D. F. (2013). Granzyme A Produced by γ9δ2 T Cells Induces Human Macrophages to Inhibit Growth of an Intracellular Pathogen, *9*(1).

Spits, H., Artis, D., Colonna, M., Diefenbach, A., Di Santo, J. P., Eberl, G., Koyasu, S., Locksley, R. M., McKenzie, A. N. J., Mebius, R. E., Powrie, F., & Vivier, E. (2013). Innate lymphoid cells - a proposal for uniform nomenclature. *Nature Reviews Immunology*, *13*(2), 145–149.

Spits, H., & Cupedo, T. (2012). Innate Lymphoid Cells : Emerging Insights in Development , Lineage Relationships, and Function. *Annual Review of Immunology*, *30*(April), 647–675.

Stein-Streilein, J., & Guffee, J. (1986). In vivo treatment of mice and hamsters with antibodies to asialo GM1 increases morbidity and mortality to pulmonary influenza infection. *Journal of Immunology*, *136*(4), 1435–1441.

Stetson, D. B., Mohrs, M., Reinhardt, R. L., Baron, J. L., Wang, Z.-E., Gapin, L., Kronenberg, M., & Locksley, R. M. (2003). Constitutive cytokine mRNAs mark natural killer (NK) and NK T cells poised for rapid effector function. *The Journal of Experimental Medicine*, *198*(7), 1069–1076.

Stinchcombe, J. C., Majorovits, E., Bossi, G., Fuller, S., & Griffiths, G. M. (2006). Centrosome polarization delivers secretory granules to the immunological synapse. *Nature*, *443*(7110), 462–465.

Strid, J., Roberts, S. J., Filler, R. B., Lewis, J. M., Kwong, B. Y., Schpero, W., Kaplan, D. H., Hayday, A. C., & Girardi, M. (2008). Acute upregulation of an NKG2D ligand promotes rapid reorganization of a local immune compartment with pleiotropic effects on carcinogenesis. *Nature Immunology*, *9*(2), 146–154.

Subramanian, A., Tamayo, P., Mootha, V. K., Mukherjee, S., Ebert, B. L., Gillette, M. A., Paulovich, A., Pomeroy, S. L., Golub, T. R., Lander, E. S., & Mesirov, J. P. (2005). Gene set enrichment analysis: a knowledge-based approach for interpreting genome-wide expression profiles. *Proceedings of the National Academy of Sciences of the United States of America*, *102*(43), 15545–15550.

Sun, J. C., Beilke, J. N., & Lanier, L. L. (2009). Adaptive immune features of natural killer cells. *Nature*, *457*(7229), 557–561.

Sun, J. C., Madera, S., Bezman, N. A., Beilke, J. N., Kaplan, M. H., & Lanier, L. L. (2012). Proinflammatory cytokine signaling required for the generation of natural killer cell memory. *The Journal of Experimental Medicine*, *209*(5), 947–954.

Sun, Z., Unutmaz, D., Zou, Y. R., Sunshine, M. J., Pierani, A., Brenner-Morton, S., Mebius, R. E., & Littman, D. R. (2000). Requirement for RORγ in thymocyte survival and lymphoid organ development. *Science (New York, N.Y.)*, *288*(5475), 2369–73.

Susanto, O., Stewart, S. E., Voskoboinik, I., Brasacchio, D., Hagn, M., Ellis, S., Asquith, S., Sedelies, K. A., & Bird, P. I. (2013). Mouse granzyme A induces a novel death with writhing morphology that is mechanistically distinct from granzyme B-induced apoptosis. *Cell Death and Differentiation*, *20*(9), 1183–1193.

Sutton, C. E., Lalor, S. J., Sweeney, C. M., Brereton, C. F., Lavelle, E. C., & Mills, K. H. G. (2009). Interleukin-1 and IL-23 induce innate IL-17 production from gammadelta T cells, amplifying Th17 responses and autoimmunity. *Immunity*, *31*(2), 331–341.

Sutton, V. R., Davis, J. E., Cancilla, M., Johnstone, R. W., Ruefli, A. A., Sedelies, K., Browne, K. A., & Trapani, J. A. (2000). Initiation of Apoptosis by Granzyme B Requires Direct Cleavage of Bid, but Not Direct Granzyme B-Mediated Caspase Activation. *Journal of Experimental Medicine*, *192*(10), 1403–1414.

Sykes, M. (1990). Unusual T cell populations in adult murine bone marrow. Prevalence of CD3+CD4-CD8- and alpha beta TCR+NK1.1+ cells. *Journal of Immunology*, *145*(10), 3209–3215.

Szabo, S. J., Kim, S. T., Costa, G. L., Zhang, X., Fathman, C. G., & Glimcher, L. H. (2000). A novel transcription factor, T-bet, directs Th1 lineage commitment. *Cell*, *100*(6), 655–669.

Szabo, S. K., Hammerberg, C., Yoshida, Y., Bata-Csorgo, Z., & Cooper, K. D. (1998). Identification and quantitation of interferon-gamma producing T cells in psoriatic lesions: localization to both CD4+ and CD8+ subsets. *The Journal of Investigative Dermatology*, *111*(6), 1072–1078.

Szelc, C. M., Mitcheltree, C., Roberts, R. L., & Stiehm, E. R. (1992). Deficient polymorphonuclear cell and mononuclear cell antibody-dependent cellular cytotoxicity in pediatric and adult human immunodeficiency virus infection. *The Journal of Infectious Diseases*, *166*(3), 486–493.

Takahashi, T., Chiba, S., Nieda, M., Azuma, T., Ishihara, S., Shibata, Y., Juji, T., & Hirai, H. (2002). Cutting Edge: Analysis of Human Vα24+CD8+ NK T Cells Activated by α-Galactosylceramide-Pulsed Monocyte-Derived Dendritic Cells. *The Journal of Immunology*, *168*(7), 3140–3144.

Takahashi, T., Dejbakhsh-Jones, S., & Strober, S. (2005). Expression of CD161 (NKR-P1A) Defines Subsets of Human CD4 and CD8 T Cells with Different Functional Activities. *The Journal of Immunology*, *176*(1), 211–216.

Takatori, H., Kanno, Y., Watford, W. T., Tato, C. M., Weiss, G., Ivanov, I. I., Littman, D. R., & O'Shea, J. J. (2009). Lymphoid tissue inducer-like cells are an innate source of IL-17 and IL-22. *The Journal of Experimental Medicine*, *206*(1), 35–41.

Tanaka, Y., Morita, C. T., Nieves, E., Brenner, M. B., & Bloom, B. R. (1995). Natural and

synthetic non-peptide antigens recognized by human γδ T cells. *Nature*, *375*(6527), 155–158.

Tang, X., Jo, J., Tan, A. T., Sandalova, E., Chia, A., Tan, K. C., Lee, K. H., Adam, J., Libero, G. De, Bertoletti, A., & Gehring, A. J. (2013). IL-7 Licenses Activation of Human Liver Intrasinusoidal Mucosal-Associated Invariant T Cells. *Journal of Immunology*, *190*(7), 3142–3152.

Tarazona, R., Casado, J. G., Delarosa, O., Torre-cisneros, J., Villanueva, J. L., Sanchez, B., Galiani, M. D., Gonzalez, R., Solana, R., & Pena, J. (2002). Selective Depletion of CD56 dim NK Cell Subsets and Maintenance of CD56 bright NK Cells in Treatment-Naive HIV-1-Seropositive Individuals, *22*(3), 176–183.

Terabe, M., Tagaya, Y., Zhu, Q., Granger, L., Roederer, M., Waldmann, T. A., & Berzofsky, J. A. (2008). IL-15 Expands Unconventional CD8αα NK1.1+ T Cells but Not Vα14Jα18+ NKT Cells. *The Journal of Immunology*, *180*(11), 7276–7286.

Teunissen, M. B. M., Koomen, C. W., de Waal Malefyt, R., Wierenga, E. A., & Bos, J. D. (1998). Interleukin-17 and interferon-gamma synergize in the enhancement of proinflammatory cytokine production by human keratinocytes. *The Journal of Investigative Dermatology*, *111*(4), 645–649.

Teunissen, M. B. M., Yeremenko, N. G., Baeten, D. L. P., Chielie, S., Spuls, P. I., Rie, M. A. De, Lantz, O., Res, P. C. M., de Rie, M. A., Lantz, O., & Res, P. C. M. (2014). The IL-17A-Producing CD8+T-Cell Population in Psoriatic Lesional Skin Comprises Mucosa-Associated Invariant T Cells and Conventional T Cells. *The Journal of Investigative Dermatology*, *134*(12), 2898–2907.

Tilloy, F., Treiner, E., Park, S. H., Garcia, C., Lemonnier, F., de la Salle, H., Bendelac, A., Bonneville, M., & Lantz, O. (1999). An invariant T cell receptor alpha chain defines a novel TAP-independent major histocompatibility complex class Ib-restricted alpha/beta T cell subpopulation in mammals. *The Journal of Experimental Medicine*, *189*(12), 1907–1921.

To, K., Agrotis, A., Besra, G., Bobik, A., & Toh, B.-H. (2009). NKT cell subsets mediate differential proatherogenic effects in ApoE-/- mice. *Arteriosclerosis, Thrombosis, and Vascular Biology*, *29*(5), 671–677.

Toda, M., Leung, D. Y. M., Molet, S., Boguniewicz, M., Taha, R., Christodoulopoulos, P., Fukuda, T., Elias, J. A., & Hamid, Q. A. (2003). Polarized in vivo expression of IL-11 and IL-17 between acute and chronic skin lesions. *Journal of Allergy and Clinical Immunology*, *111*(4), 875–881.

Toichi, E., Torres, G., McCormick, T. S., Chang, T., Mascelli, M. A., Kauffman, C. L., Aria, N., Gottlieb, A. B., Everitt, D. E., Frederick, B., Pendley, C. E., & Cooper, K. D. (2006). An Anti-IL-12p40 Antibody Down-Regulates Type 1 Cytokines, Chemokines, and IL-12/IL-23 in Psoriasis. *The Journal of Immunology*, *177*(7), 4917–4926.

Tomura, M., Maruo, S., Mu, J., Zhou, X. Y., Ahn, H. J., Hamaoka, T., Okamura, H., Nakanishi, K., Clark, S., Kurimoto, M., & Fujiwara, H. (1998). Differential capacities of CD4+, CD8+, and CD4-CD8- T cell subsets to express IL-18 receptor and produce IFN-gamma in response to IL-18. *Journal of Immunology*, *160*(8), 3759–3765.

Toossi, Z., Wu, M., Rojas, R., Kalsdorf, B., Aung, H., Hirsch, C. S., Walrath, J., Wolbink, A., van Ham, M., Silver, R. F., Ham, M. Van, & Silver, R. F. (2011). Induction of Serine Protease Inhibitor 9 by Mycobacterium tuberculosis Inhibits Apoptosis and Promotes Survival of Infected Macrophages. *Journal of Infectious Diseases*, *205*(1), 144–151.

Townsend, M. J., Weinmann, A. S., Matsuda, J. L., Salomon, R., Farnham, P. J., Biron, C. A., Gapin, L., & Glimcher, L. H. (2004). T-bet regulates the terminal maturation and homeostasis of NK and Valpha14i NKT cells. *Immunity*, *20*(4), 477–94.

Treiner, E., Duban, L., Bahram, S., Radosavljevic, M., Wanner, V., Tilloy, F., Affaticati, P., Gilfillan, S., & Lantz, O. (2003). Selection of evolutionarily conserved mucosal-associated invariant T cells by MR1. *Nature*, *422*(6928), 164–169.

Trichet, V., Benezech, C., Dousset, C., Gesnel, M.-C., Bonneville, M., & Breathnach, R. (2006). Complex Interplay of Activating and Inhibitory Signals Received by Vγ9Vδ2 T Cells Revealed by Target Cell β2-Microglobulin Knockdown. *The Journal of Immunology*, *177*(9), 6129–6136.

Triebel, F., & Hercend, T. (1989). Subpopulations of human peripheral T gamma delta lymphocytes. *Immunology Today*, *10*(6), 186–188.

Trotta, R., Parihar, R., Yu, J., Becknell, B., Allard, J., Wen, J., Ding, W., Mao, H., Tridandapani, S., Carson, W. E., & Caligiuri, M. A. (2005). Differential expression of SHIP1 in CD56bright and CD56dim NK cells provides a molecular basis for distinct functional responses to monokine costimulation. *Blood*, *105*(8), 3011–8.

Tsukamoto, K., Deakin, J. E., Graves, J. A. M., & Hashimoto, K. (2013). Exceptionally high conservation of the MHC class I-related gene, MR1, among mammals. *Immunogenetics*, *65*(2), 115–124.

Turchinovich, G., & Hayday, A. C. (2011). Skint-1 identifies a common molecular mechanism for the development of interferon-γ-secreting versus interleukin-17-secreting γδ T cells. *Immunity*, *35*(1), 59–68.

Turtle, C. J., Delrow, J., Joslyn, R. C., Swanson, H. M., Basom, R., Tabellini, L., Delaney, C., Heimfeld, S., Hansen, J. a., & Riddell, S. R. (2011). Innate signals overcome acquired TCR signaling pathway regulation and govern the fate of human CD161(hi) CD8α^{+} semi-invariant T cells. *Blood*, *118*(10), 2752–2762.

Turtle, C. J., Swanson, H. M., Fujii, N., Estey, E. H., & Riddell, S. R. (2009). A Distinct Subset of Self-Renewing Human Memory CD8+ T Cells Survives Cytotoxic Chemotherapy. *Immunity*, *31*(5), 834–844.

Uldrich, A. P., Le Nours, J., Pellicci, D. G., Gherardin, N. A., McPherson, K. G., Lim, R. T., Patel, O., Beddoe, T., Gras, S., Rossjohn, J., & Godfrey, D. I. (2013). CD1d-lipid antigen recognition by the γδ TCR. *Nature Immunology*, *14*(11), 1137–1145.

Ussher, J. E., Bilton, M., Attwod, E., Shadwell, J., Richardson, R., Lara, C. De, & Willberg, C. B. (2013). CD161 ++ CD8 + T cells , including the MAIT cell subset , are specifically activated by IL-12 + IL-18 in a TCR-independent manner, 1–9.

Ussher, J. E., Bilton, M., Attwod, E., Shadwell, J., Richardson, R., Lara, C. De, Willberg, C. B., de Lara, C., Mettke, E., Kurioka, A., Hansen, T. H., Klenerman, P., & Willberg, C. B. (2014a). CD161++CD8+ T cells, including the MAIT cell subset, are specifically

activated by IL-12+IL-18 in a TCR-independent manner. *European Journal of Immunology*, *44*(1), 195–203.

Ussher, J. E., Klenerman, P., & Willberg, C. B. (2014b). Mucosal-associated invariant T-cells: new players in anti-bacterial immunity. *Frontiers in Immunology*, *5*, 450.

Vahl, J. C., Heger, K., Knies, N., Hein, M. Y., Boon, L., Yagita, H., Polic, B., & Schmidt-Supprian, M. (2013). NKT cell-TCR expression activates conventional T cells in vivo, but is largely dispensable for mature NKT cell biology. *PLoS Biology*, *11*(6), e1001589.

Valdimarsson, H., Thorleifsdottir, R. H., Sigurdardottir, S. L., Gudjonsson, J. E., & Johnston, A. (2009). Psoriasis-as an autoimmune disease caused by molecular mimicry. *Trends in Immunology*, *30*(10), 494–501.

Valitutti, S., Müller, S., Dessing, M., & Lanzavecchia, A. (1996). Different responses are elicited in cytotoxic T lymphocytes by different levels of T cell receptor occupancy. *The Journal of Experimental Medicine*, *183*(4), 1917–1921.

van Beelen, A. J., Teunissen, M. B. M., Kapsenberg, M. L., & de Jong, E. C. (2007). Interleukin-17 in inflammatory skin disorders. *Current Opinion in Allergy and Clinical Immunology*, *7*(5), 374–381.

Van Belle, A. B., de Heusch, M., Lemaire, M. M., Hendrickx, E., Warnier, G., Dunussi-Joannopoulos, K., Fouser, L. A., Renauld, J.-C., & Dumoutier, L. (2012). IL-22 is required for imiquimod-induced psoriasiform skin inflammation in mice. *Journal of Immunology*, *188*(1), 462–469.

van de Wetering, D., de Paus, R. a., van Dissel, J. T., & van de Vosse, E. (2009). IL-23 modulates CD56+/CD3- NK Cell and CD56+/CD3+ NK-like T Cell function differentially from IL-12. *International Immunology*, *21*(2), 145–153.

van den Berg, H. A., Ladell, K., Miners, K., Laugel, B., Llewellyn-Lacey, S., Clement, M., Cole, D. K., Gostick, E., Wooldridge, L., Sewell, A. K., Bridgeman, J. S., & Price, D. A. (2013). Cellular-level versus receptor-level response threshold hierarchies in T-cell activation. *Frontiers in Immunology*, *4*, 250.

van den Broek, M. E. (1996). Decreased tumor surveillance in perforin-deficient mice. *Journal of Experimental Medicine*, *184*(5), 1781–1790.

van der Fits, L., Mourits, S., Voerman, J. S. A., Kant, M., Boon, L., Laman, J. D., Cornelissen, F., Mus, A.-M., Florencia, E., Prens, E. P., & Lubberts, E. (2009). Imiquimod-induced psoriasis-like skin inflammation in mice is mediated via the IL-23/IL-17 axis. *Journal of Immunology*, *182*(9), 5836–5845.

van Gisbergen, K. P. J. M., Kragten, N. A. M., Hertoghs, K. M. L., Wensveen, F. M., Jonjic, S., Hamann, J., Nolte, M. A., van Lier, R. A. W., Gisbergen, K. P. J. M. Van, Kragten, N. A. M., Hertoghs, K. M. L., Wensveen, F. M., Jonjic, S., Hamann, J., Nolte, M. A., & Lier, R. A. W. Van. (2012). Mouse Hobit is a homolog of the transcriptional repressor Blimp-1 that regulates NKT cell effector differentiation. *Nature Immunology*, *13*(9), 864–871.

Van Rhijn, I., Kasmar, A., de Jong, A., Gras, S., Bhati, M., Doorenspleet, M. E., de Vries, N., Godfrey, D. I., Altman, J. D., de Jager, W., Rossjohn, J., & Moody, D. B. (2013). A

conserved human T cell population targets mycobacterial antigens presented by CD1b. *Nature Immunology*, *14*(7), 706–713.

Veldhoen, M., Hirota, K., Westendorf, A. M., Buer, J., Dumoutier, L., Renauld, J.-C., & Stockinger, B. (2008). The aryl hydrocarbon receptor links TH17-cell-mediated autoimmunity to environmental toxins. *Nature*, *453*(7191), 106–109.

Vitale, M., Della Chiesa, M., Carlomagno, S., Romagnani, C., Thiel, A., Moretta, L., & Moretta, A. (2004). The small subset of CD56brightCD16- natural killer cells is selectively responsible for both cell proliferation and interferon-gamma production upon interaction with dendritic cells. *European Journal of Immunology*, *34*(6), 1715–1722.

Vitale, M., Falco, M., Castriconi, R., Parolini, S., Semenzato, G., Biassoni, R., Bottino, C., & Moretta, A. (2001). Identification of NKp80, a novel triggering molecule expressed by human NK cells. *European Journal of Immunology*, *31*(1), 233–242.

Vonarbourg, C., Mortha, A., Bui, V. L., Hernandez, P. P., Kiss, E. A., Hoyler, T., Flach, M., Bengsch, B., Thimme, R., Hölscher, C., Hönig, M., Pannicke, U., Schwarz, K., Ware, C. F., Finke, D., & Diefenbach, A. (2010). Regulated expression of nuclear receptor RORγt confers distinct functional fates to NK cell receptor-expressing RORγt+ innate lymphocytes. *Immunity*, *33*(5), 736–751.

Vossen, M. T. M., Matmati, M., Hertoghs, K. M. L., Baars, P. A., Gent, M.-R., Leclercq, G., Hamann, J., Kuijpers, T. W., & van Lier, R. A. W. (2008). CD27 defines phenotypically and functionally different human NK cell subsets. *Journal of Immunology*, *180*(6), 3739–3745.

Walker, L. J., Kang, Y. H., Smith, M. O., Tharmalingham, H., Ramamurthy, N., Fleming, V. M., Sahgal, N., Leslie, A., Oo, Y., Geremia, A., Scriba, T. J., Hanekom, W. A., Lauer, G. M., Lantz, O., Adams, D. H., Powrie, F., Barnes, E., & Klenerman, P. (2012). Human MAIT and CD8αα cells develop from a pool of type-17 precommitted CD8 + T cells. *Blood*, *119*(2), 422–433.

Walker, L. J., Tharmalingam, H., & Klenerman, P. (2014). The Rise and Fall of MAIT Cells with Age. *Scandinavian Journal of Immunology*, *80*(6), 462–463.

Walsh, C. M., Matloubian, M., Liu, C. C., Ueda, R., Kurahara, C. G., Christensen, J. L., Huang, M. T., Young, J. D., Ahmed, R., & Clark, W. R. (1994). Immune function in mice lacking the perforin gene. *Proceedings of the National Academy of Sciences of the United States of America*, *91*(23), 10854–10858.

Wang, H., Henry, O., Distefano, M. D., Wang, Y.-C., Räikkönen, J., Mönkkönen, J., Tanaka, Y., & Morita, C. T. (2013). Butyrophilin 3A1 plays an essential role in prenyl pyrophosphate stimulation of human Vγ2Vδ2 T cells. *Journal of Immunology*, *191*(3), 1029–1042.

Wang, L., Carr, T., Xiong, Y., Wildt, K. F., Zhu, J., Feigenbaum, L., Bendelac, A., & Bosselut, R. (2010). The sequential activity of Gata3 and Thpok is required for the differentiation of CD1d-restricted CD4+ NKT cells. *European Journal of Immunology*, *40*(9), 2385–2390.

Wang, Y., Xu, H., Zheng, X., Wei, H., Sun, R., & Tian, Z. (2007). High expression of

NKG2A/CD94 and low expression of granzyme B are associated with reduced cord blood NK cell activity. *Cellular & Molecular Immunology*, *4*(5), 377–382.

Warfield, K. L., Perkins, J. G., Swenson, D. L., Deal, E. M., Bosio, C. M., Aman, M. J., Yokoyama, W. M., Young, H. A., & Bavari, S. (2004). Role of natural killer cells in innate protection against lethal ebola virus infection. *The Journal of Experimental Medicine*, *200*(2), 169–179.

Wen, X., Kim, S., Xiong, R., Li, M., Lawrenczyk, A., Huang, X., Chen, S.-Y., Rao, P., Besra, G. S., Delabona, P., Casorati, G., Porcelli, S. A., Akbari, O., Exley, M. A., & Yuan, W. (2015). A Subset of CD8αβ+ Invariant NKT Cells in a Humanized Mouse Model. *Journal of Immunology*, *195*(4), 1459–1469.

Wende, H., Colonna, M., Ziegler, A., & Volz, A. (1999). Organization of the leukocyte receptor cluster (LRC) on human Chromosome 19q13.4. *Mammalian Genome*, *10*(2), 154–160.

Wendt, K., Wilk, E., Buyny, S., Buer, J., Schmidt, R. E., & Jacobs, R. (2006). Gene and protein characteristics reflect functional diversity of CD56dim and CD56bright NK cells. *Journal of Leukocyte Biology*, *80*(6), 1529–1541.

Wensink, A. C., Kemp, V., Fermie, J., García, M. I., Poll, T. Van Der, & Hack, C. E. (2014). Granzyme K synergistically potentiates LPS-induced cytokine responses in human monocytes, *4*, 1–6.

Wherry, E. J., Teichgräber, V., Becker, T. C., Masopust, D., Kaech, S. M., Antia, R., von Andrian, U. H., & Ahmed, R. (2003). Lineage relationship and protective immunity of memory CD8 T cell subsets. *Nature Immunology*, *4*(3), 225–34.

Wiekowski, M. T., Leach, M. W., Evans, E. W., Sullivan, L., Chen, S.-C., Vassileva, G., Bazan, J. F., Gorman, D. M., Kastelein, R. A., Narula, S., & Lira, S. A. (2001). Ubiquitous Transgenic Expression of the IL-23 Subunit p19 Induces Multiorgan Inflammation, Runting, Infertility, and Premature Death. *The Journal of Immunology*, *166*(12), 7563–7570.

Wierenga, E. A., Snoek, M., Jansen, H. M., Bos, J. D., van Lier, R. A., & Kapsenberg, M. L. (1991). Human atopen-specific types 1 and 2 T helper cell clones. *Journal of Immunology*, *147*(9), 2942–2949.

Willberg, C. B., Ward, S. M., Clayton, R. F., Naoumov, N. V, McCormick, C., Proto, S., Harris, M., Patel, A. H., & Klenerman, P. (2007). Protection of hepatocytes from cytotoxic T cell mediated killing by interferon-alpha. *PloS One*, *2*(8), e791.

Williams, M. A., & Bevan, M. J. (2007). Effector and memory CTL differentiation. *Annual Review of Immunology*, *25*, 171–192.

Willing, A., Leach, O. A., Ufer, F., Attfield, K. E., Steinbach, K., Kursawe, N., Piedavent, M., & Friese, M. A. (2014). CD8(+) MAIT cells infiltrate into the CNS and alterations in their blood frequencies correlate with IL-18 serum levels in multiple sclerosis. *European Journal of Immunology*, *44*(10), 3119–3128.

Wilson, N. J., Boniface, K., Chan, J. R., McKenzie, B. S., Blumenschein, W. M., Mattson, J. D., Basham, B., Smith, K., Chen, T., Morel, F., Lecron, J.-C., Kastelein, R. A., Cua, D. J., McClanahan, T. K., Bowman, E. P., & de Waal Malefyt, R. (2007). Development,

cytokine profile and function of human interleukin 17-producing helper T cells. *Nature Immunology*, *8*(9), 950–957.

Wilson, R. P., Ives, M. L., Rao, G., Lau, A., Payne, K., Kobayashi, M., Arkwright, P. D., Peake, J., Wong, M., Adelstein, S., Smart, J. M., French, M. A., Fulcher, D. A., Picard, C., Bustamante, J., Boisson-Dupuis, S., Gray, P., Stepensky, P., Warnatz, K., Freeman, A. F., Rossjohn, J., McCluskey, J., Holland, S. M., Casanova, J.-L., Uzel, G., Ma, C. S., Tangye, S. G., & Deenick, E. K. (2015). STAT3 is a critical cell-intrinsic regulator of human unconventional T cell numbers and function. *Journal of Experimental Medicine*, *212*(6), 855–864.

Winchester, R., Minevich, G., Steshenko, V., Kirby, B., Kane, D., Greenberg, D. A., & FitzGerald, O. (2012). HLA associations reveal genetic heterogeneity in psoriatic arthritis and in the psoriasis phenotype. *Arthritis and Rheumatism*, *64*(4), 1134–1144.

Wingender, G., Krebs, P., Beutler, B., & Kronenberg, M. (2010). Antigen-specific cytotoxicity by invariant NKT cells in vivo is CD95/CD178-dependent and is correlated with antigenic potency. *Journal of Immunology (Baltimore, Md. : 1950)*, *185*(5), 2721–2729.

Wolk, K., Witte, E., Wallace, E., Döcke, W.-D., Kunz, S., Asadullah, K., Volk, H.-D., Sterry, W., & Sabat, R. (2006). IL-22 regulates the expression of genes responsible for antimicrobial defense, cellular differentiation, and mobility in keratinocytes: a potential role in psoriasis. *European Journal of Immunology*, *36*(5), 1309–1323.

Wong, E. B., Akilimali, N. A., Govender, P., Sullivan, Z. A., Cosgrove, C., Pillay, M., Lewinsohn, D. M., Bishai, W. R., Walker, B. D., Ndung'u, T., Klenerman, P., & Kasprowicz, V. O. (2013). Low levels of peripheral CD161++CD8+ mucosal associated invariant T (MAIT) cells are found in HIV and HIV/TB co-infection. *PloS One*, *8*(12), e83474.

Wong, M. T., Chen, J., Narayanan, S., Lin, W., Anicete, R., Kiaang, H. T. K., De Lafaille, M. A. C., Poidinger, M., & Newell, E. W. (2015). Mapping the Diversity of Follicular Helper T Cells in Human Blood and Tonsils Using High-Dimensional Mass Cytometry Analysis. *Cell Reports*, *11*(11), 1822–1833.

Wu, J., Groh, V., & Spies, T. (2002). T cell antigen receptor engagement and specificity in the recognition of stress-inducible MHC class I-related chains by human epithelial gamma delta T cells. *Journal of Immunology*, *169*(3), 1236–1240.

Xiong, N., Kang, C., & Raulet, D. H. (2004). Positive selection of dendritic epidermal gammadelta T cell precursors in the fetal thymus determines expression of skin-homing receptors. *Immunity*, *21*(1), 121–131.

Xu, D., Holko, M., Sadler, A. J., Scott, B., Higashiyama, S., Berkofsky-Fessler, W., McConnell, M. J., Pandolfi, P. P., Licht, J. D., & Williams, B. R. G. (2009). Promyelocytic leukemia zinc finger protein regulates interferon-mediated innate immunity. *Immunity*, *30*(6), 802–816.

Xue, L., Fergusson, J. R., Salimi, M., Panse, I., Ussher, J. E., Hegazy, A. N., Vinall, S. L., Jackson, D. G., Hunter, M. G., Pettipher, R., Ogg, G., & Klenerman, P. (2015). Prostaglandin D2 and leukotriene E4 synergize to stimulate diverse TH2 functions and TH2 cell/neutrophil crosstalk. *The Journal of Allergy and Clinical Immunology*,

135(5), 1358–1366.e11.

Yagi, R., Junttila, I. S., Wei, G., Urban, J. F., Zhao, K., Paul, W. E., & Zhu, J. (2010). The transcription factor GATA3 actively represses RUNX3 protein-regulated production of interferon-gamma. *Immunity*, *32*(4), 507–517.

Yajima, T., Nishimura, H., Sad, S., Shen, H., Kuwano, H., & Yoshikai, Y. (2005). A Novel Role of IL-15 in Early Activation of Memory CD8+ CTL after Reinfection. *The Journal of Immunology*, *174*(6), 3590–3597.

Yamaguchi, H., Kurosawa, Y., & Hashimoto, K. (1998). Expanded genomic organization of conserved mammalian MHC class I-related genes, human MR1 and its murine ortholog. *Biochemical and Biophysical Research Communications*, *250*(3), 558–564.

Yang, C.-S., Yuk, J.-M., & Jo, E.-K. (2009). The role of nitric oxide in mycobacterial infections. *Immune Network*, *9*(2), 46–52.

Yang, X. O., Pappu, B. P., Nurieva, R., Akimzhanov, A., Kang, H. S., Chung, Y., Ma, L., Shah, B., Panopoulos, A. D., Schluns, K. S., Watowich, S. S., Tian, Q., Jetten, A. M., & Dong, C. (2008). T helper 17 lineage differentiation is programmed by orphan nuclear receptors ROR alpha and ROR gamma. *Immunity*, *28*(1), 29–39.

Yao, Z., Painter, S. L., Fanslow, W. C., Ulrich, D., Macduff, B. M., Spriggs, M. K., & Armitage, R. J. (1995). Human IL-17: a novel cytokine derived from T cells. *Journal of Immunology*, *155*(12), 5483–5486.

Yawalkar, N., Schmid, S., Braathen, L. R., & Pichler, W. J. (2001). Perforin and granzyme B may contribute to skin inflammation in atopic dermatitis and psoriasis. *British Journal of Dermatology*, *144*(6), 1133–1139.

Yokota, K., Miyazaki, T., Hirano, M., Akiyama, Y., & Mimura, T. (2006). Simvastatin inhibits production of interleukin 6 (IL-6) and IL-8 and cell proliferation induced by tumor necrosis factor-alpha in fibroblast-like synoviocytes from patients with rheumatoid arthritis. *The Journal of Rheumatology*, *33*(3), 463–471.

Yokota, Y., Mansouri, A., Mori, S., Sugawara, S., Adachi, S., Nishikawa, S., & Gruss, P. (1999). Development of peripheral lymphoid organs and natural killer cells depends on the helix-loop-helix inhibitor Id2. *Nature*, *397*(6721), 702–706.

Yoo, I. S., Lee, J. H., Song, S. T., Kim, J. H., Lee, H. J., & Kang, S. W. (2012). T-helper 17 cells: the driving force of psoriasis and psoriatic arthritis. *International Journal of Rheumatic Diseases*, *15*(6), 531–537.

Yoon, J. C., Lim, J.-B., Park, J. H., & Lee, J. M. (2011). Cell-to-cell contact with hepatitis C virus-infected cells reduces functional capacity of natural killer cells. *Journal of Virology*, *85*(23), 12557–12569.

Young, M. H., U'Ren, L., Huang, S., Mallevaey, T., Scott-Browne, J., Crawford, F., Lantz, O., Hansen, T. H., Kappler, J., Marrack, P., & Gapin, L. (2013). MAIT cell recognition of MR1 on bacterially infected and uninfected cells. *PloS One*, *8*(1), e53789.

Yu, J., Freud, A. G., & Caligiuri, M. A. (2013). Location and cellular stages of natural killer cell development. *Trends in Immunology*, *34*(12), 573–82.

Yu, J., Mao, H. C., Wei, M., Hughes, T., Zhang, J., Park, I., Liu, S., McClory, S., Marcucci,

G., Trotta, R., & Caligiuri, M. A. (2010). CD94 surface density identifies a functional intermediary between the CD56bright and CD56dim human NK-cell subsets. *Blood*, *115*(2), 274–281.

Zaba, L. C., Cardinale, I., Gilleaudeau, P., Sullivan-Whalen, M., Suárez-Fariñas, M., Suárez Fariñas, M., Fuentes-Duculan, J., Novitskaya, I., Khatcherian, A., Bluth, M. J., Lowes, M. A., & Krueger, J. G. (2007). Amelioration of epidermal hyperplasia by TNF inhibition is associated with reduced Th17 responses. *The Journal of Experimental Medicine*, *204*(13), 3183–3194.

Zeng, S. G., Ghnewa, Y. G., O'Reilly, V. P., Lyons, V. G., Atzberger, A., Hogan, A. E., Exley, M. A., & Doherty, D. G. (2013). Human invariant NKT cell subsets differentially promote differentiation, antibody production, and T cell stimulation by B cells in vitro. *Journal of Immunology*, *191*(4), 1666–1676.

Zhang, T., Scott, J. M., Hwang, I., & Kim, S. (2013). Cutting edge: antibody-dependent memory-like NK cells distinguished by FcRγ deficiency. *Journal of Immunology (Baltimore, Md. : 1950)*, *190*(4), 1402–6.

Zhao, T., Zhang, H., Guo, Y., & Fan, Z. (2007). Granzyme K directly processes bid to release cytochrome c and endonuclease G leading to mitochondria-dependent cell death. *The Journal of Biological Chemistry*, *282*(16), 12104–12111.

Zheng, W., & Flavell, R. A. (1997). The Transcription Factor GATA-3 Is Necessary and Sufficient for Th2 Cytokine Gene Expression in CD4 T Cells. *Cell*, *89*(4), 587–596.

Zheng, Y., Danilenko, D. M., Valdez, P., Kasman, I., Eastham-Anderson, J., Wu, J., & Ouyang, W. (2007). Interleukin-22, a T(H)17 cytokine, mediates IL-23-induced dermal inflammation and acanthosis. *Nature*, *445*(7128), 648–651.

Zhong, W., & Reinherz, E. L. (2005). CD8 alpha alpha homodimer expression and role in CD8 T cell memory generation during influenza virus A infection in mice. *European Journal of Immunology*, *35*(11), 3103–3110.

Zhou, D., Mattner, J., Cantu, C., Schrantz, N., Yin, N., Gao, Y., Sagiv, Y., Hudspeth, K., Wu, Y.-P., Yamashita, T., Teneberg, S., Wang, D., Proia, R. L., Levery, S. B., Savage, P. B., Teyton, L., & Bendelac, A. (2004). Lysosomal glycosphingolipid recognition by NKT cells. *Science*, *306*(5702), 1786–1789.

Zhu, J., Peng, T., Johnston, C., Phasouk, K., Kask, A. S., Klock, A., Jin, L., Diem, K., Koelle, D. M., Wald, A., Robins, H., & Corey, L. (2013). Immune surveillance by CD8αα+ skin-resident T cells in human herpes virus infection. *Nature*, *497*(7450), 494–497.

Zwirner, N. W., & Domaica, C. I. (2010). Cytokine regulation of natural killer cell effector functions. *BioFactors*, *36*(4), 274–288.

List of publications

Kurioka, A., Ussher, J. E., Cosgrove, C., Clough, C., Fergusson, J. R., Smith, K., Kang, Y.-H., Walker, L. J., Hansen, T. H., Willberg, C. B., & Klenerman, P. (2015). MAIT cells are licensed through granzyme exchange to kill bacterially sensitized targets. *Mucosal Immunology*, *8*(2), 429–40.

Cosgrove, C., Ussher, J. E., Rauch, A., Gärtner, K., Kurioka, A., Hühn, M. H., Adelmann, K., Kang, Y.-H., Fergusson, J. R., Simmonds, P., Goulder, P., Hansen, T. H., Fox, J., Günthard, H. F., Khanna, N., Powrie, F., Steel, A., Gazzard, B., Phillips, R. E., Frater, J., Uhlig, H., & Klenerman, P. (2013). Early and nonreversible decrease of CD161++/MAIT cells in HIV infection. *Blood*, *121*(6), 951–61.

Ussher, J. E., Bilton, M., Attwod, E., Shadwell, J., Richardson, R., de Lara, C., Mettke, E., Kurioka, A., Hansen, T. H., Klenerman, P., & Willberg, C. B. (2014). CD161++ CD8+ T cells, including the MAIT cell subset, are specifically activated by IL-12+IL-18 in a TCR-independent manner. *European Journal of Immunology*, *44*(1), 195–203.

Fergusson, J. R., Hühn, M. H., Swadling, L., Walker, L. J., Kurioka, A., Llibre, A., Bertoletti, A., Holländer, G., Newell, E. W., Davis, M. M., Sverremark-Ekström, E., Powrie, F., Capone, S., Folgori, A., Barnes, E., Willberg, C. B., Ussher, J. E., & Klenerman, P. (2015). CD161(int)CD8+ T cells: a novel population of highly functional, memory CD8+ T cells enriched within the gut. *Mucosal Immunology*. doi: 10.1038/mi.2015.69.

Fergusson, J. R., Smith, K. E., Fleming, V. M., Rajoriya, N., Newell, E. W., Simmons, R., Marchi, E., Björkander, S., Kang, Y.-H., Swadling, L., Kurioka, A., Sahgal, N., Lockstone, H., Baban, D., Freeman, G. J., Sverremark-Ekström, E., Davis, M. M., Davenport, M. P., Venturi, V., Ussher, J. E., Willberg, C. B., & Klenerman, P. (2014). CD161 Defines a Transcriptional and Functional Phenotype across Distinct Human T Cell Lineages. *Cell Reports*, *9*(3), 1075–1088.

Barnes, E., Folgori, A., Capone, S., Swadling, L., Aston, S., Kurioka, A., Meyer, J., Huddart, R., Smith, K., Townsend, R., Brown, A., Antrobus, R., Ammendola, V., Naddeo, M., O'Hara, G., Willberg, C., Harrison, A., Grazioli, F., Esposito, M. L., Siani, L., Traboni, C., Oo, Y., Adams, D., Hill, A., Colloca, S., Nicosia, A., Cortese, R., & Klenerman, P. (2012). Novel Adenovirus-Based Vaccines Induce Broad and Sustained T Cell Responses to HCV in Man. *Science Translational Medicine*, *4*(115), 115ra1.

Colloca, S., Barnes, E., Folgori, A., Ammendola, V., Capone, S., Cirillo, A., Siani, L., Naddeo, M., Grazioli, F., Esposito, M. L., Ambrosio, M., Sparacino, A., Bartiromo, M., Meola, A., Smith, K., Kurioka, A., O'Hara, G. A., Ewer, K. J., Anagnostou, N., Bliss, C., Hill, A. V. S., Traboni, C., Klenerman, P., Cortese, R., & Nicosia, A. (2012). Vaccine Vectors Derived from a Large Collection of Simian Adenoviruses Induce Potent Cellular Immunity Across Multiple Species. *Science Translational Medicine*. *4*(115), 115ra2.

Swadling, L., Capone, S., Antrobus, R. D., Brown, A., Richardson, R., Newell, E. W., Halliday, J., Kelly, C., Bowen, D., Fergusson, J. R., Kurioka, A., Ammendola, V., Del Sorbo, M., Grazioli, F., Esposito, M. L., Siani, L., Traboni, C., Hill, A., Colloca, S., Davis, M., Nicosia, A., Cortese, R., Folgori, A., Klenerman, P., & Barnes, E. (2014). A human vaccine strategy based on chimpanzee adenoviral and MVA vectors that primes, boosts, and sustains functional HCV-specific T cell memory. *Science Translational Medicine*, *6*(261), 261ra153.

OPEN

MAIT cells are licensed through granzyme exchange to kill bacterially sensitized targets

A Kurioka[1], JE Ussher[1], C Cosgrove[1], C Clough[1], JR Fergusson[1], K Smith[1], Y-H Kang[1], LJ Walker[1], TH Hansen[2], CB Willberg[1,3] and P Klenerman[1,3]

Mucosal-associated invariant T (MAIT) cells are an innate-like T-cell population restricted by the non-polymorphic, major histocompatibility complex class I-related protein 1, MR1. MAIT cells are activated by a broad range of bacteria through detection of riboflavin metabolites bound by MR1, but their direct cytolytic capacity upon recognition of cognate target cells remains unclear. We show that resting human MAIT cells are uniquely characterized by a lack of granzyme (Gr) B and low perforin expression, key granule proteins required for efficient cytotoxic activity, but high levels of expression of GrA and GrK. Bacterial activation of MAIT cells rapidly induced GrB and perforin, licensing these cells to kill their cognate target cells. Using a novel flow cytometry-based killing assay, we show that licensed MAIT cells, but not *ex vivo* MAIT cells from the same donors, can efficiently kill *Escherichia coli*-exposed B-cell lines in an MR1- and degranulation-dependent manner. Finally, we show that MAIT cells are highly proliferative in response to antigenic and cytokine stimulation, maintaining high expression of GrB, perforin, and GrA, but reduced expression of GrK following antigenic proliferation. The tightly regulated cytolytic capacity of MAIT cells may have an important role in the control of intracellular bacterial infections, such as *Mycobacterium tuberculosis*.

INTRODUCTION

Mucosal-associated invariant T (MAIT) cells are an evolutionarily conserved sub-population of T cells in mammals, characterized by the expression of the semi-invariant Vα7.2-Jα33 chain of the T-cell receptor (TCR), which restricts them to the non-polymorphic, major histocompatibility complex class I-related protein 1, MR1.[1–3] In murine models, MAIT cells are critical for the control of Bacillus Calmette-Guérin (BCG),[4] *Klebsiella pneumonia*[5] and *Francisella tularensis*[6] infections. Their broad reactivity to microbes has recently been attributed to their ability to recognize ligands bound to MR1 originating from metabolic intermediates of riboflavin.[7] MAIT cells are enriched in the intestine and liver, and represent 1–20% of $CD8^+$ T cells in the periphery in man.[1,8–10] In adult blood, MAIT cells are the dominant population among $CD8^+$ T cells that express the C-type lectin-like receptor CD161 at high levels.[8,10,11] These $CD161^{++}CD8^+$ T cells are functionally and transcriptionally distinct from other $CD8^+$ T-cell populations,[11,12] with the ability to respond to cytokines interleukin-12 (IL-12) and IL-18 in a TCR-independent manner.[13]

Previous studies into $CD161^{++}$/MAIT cell effector functions have focused principally on their production of Tc1 and Tc17 cytokines.[8,9,12–13] Recently, MAIT cells were shown to kill epithelial cells infected by *Shigella dysenteriae*.[14] However, the factors regulating the cytotoxicity of MAIT cells and whether they can kill antigen-presenting cells (APCs), which in many infections provide a survival niche for intracellular bacteria, still remains to be addressed. This is a critical point, given their high frequencies in tissues, "effector-memory" phenotype[11] and cytotoxic potential; such activity must be tightly regulated in order to limit immunopathology.

The primary mechanism by which cytotoxic cells induce apoptosis in tumor or virus-infected cells is granule exocytosis. This is dependent upon granzymes gaining entry to the cytoplasm of the target cell through the action of perforin;[15] without perforin, internalized granzymes are retained in

[1]Peter Medawar Building for Pathogen Research, Nuffield Department of Medicine, University of Oxford, Oxford, UK. [2]Department of Pathology and Immunology, Washington University School of Medicine, St Louis, Missouri, USA and [3]National Institute for Health Research Oxford Biomedical Research Centre, University of Oxford, Oxford, UK. Correspondence: A Kurioka (ayako.kurioka@ndm.ox.ac.uk)

Received 28 April 2014; accepted 26 July 2014; published online 1 October 2014. doi:10.1038/mi.2014.81

endosome-like vesicles, and do not induce apoptosis.[16] In humans, there are five granzymes with diverse substrate specificities: granzyme (Gr) A, GrB, GrH, GrK, and GrM. A hierarchy among these molecules determines cytotoxic efficiency, with perforin and GrB, but not GrA or GrK, correlating with lytic ability.[17–20] Instead, recent studies have suggested that GrA and GrK are primarily non-cytotoxic molecules promoting proinflammatory responses.[21–23] Perforin and GrB can be upregulated upon activation and proliferation,[17,24] and are regulated by transcription factors such as T-bet and Blimp1.[25,26]

In this study, we have performed a comprehensive characterization of the cytotoxicity of $CD161^{++}CD8^{+}$ T cells, including the MAIT cells, and probe the relative contribution of TCR and innate cytokine signals regulating their granule content. Furthermore, we show that MAIT cells are highly proliferative *in vitro* and rapidly acquire high expression of GrB, GrA, and perforin. This cytotoxic phenotype "licenses" them to specifically kill target cells in an MR1-dependent manner.

RESULTS

Resting blood-derived human MAIT cells have a unique cytotoxic profile

First, we confirmed our previous finding[12] that *ex vivo*, peripheral blood $CD161^{++}CD8^{+}$ T cells expressed almost no GrB ($3.1 \pm 0.9\%$) compared with either $CD161^{+}$ (47.6%, $P<0.0001$) or $CD161^{-}$ sub-populations (18.5%, $P<0.01$; **Figure 1a**). The amount of perforin expressed by these cells, as measured by geometric mean fluorescence intensity, was also significantly lower than other $CD8^{+}$ T-cell sub-populations (both $P<0.0001$). In contrast, $CD161^{++}CD8^{+}$ T cells expressed high levels of GrA ($96.6 \pm 1.2\%$) compared with $CD161^{+}$ (87.2%, $P<0.05$) and $CD161^{-}CD8^{+}$ T cells (31.3%, $P<0.0001$). $CD161^{++}CD8^{+}$ T cells also uniquely expressed high levels of GrK ($91.1 \pm 1.2\%$) compared with $CD161^{+}CD8^{+}$ T cells (32.9%, $P<0.0001$) and $CD161^{-}CD8^{+}$ T cells (16.3%, $P<0.0001$). Consistent with transcriptional profiling,[11] cord blood $CD161^{++}CD8^{+}$ T cells were also $GrA^{+}GrK^{+}$ (**Supplementary Figure S1A** online), suggesting this is an inherent feature of this subset.

Next, we asked whether this cytotoxic profile was characteristic of MAIT cells, or of the $CD161^{++}CD8^{+}$ T-cell population as a whole. T cells possessing the Vα7.2 TCR within the $CD161^{++}CD8^{+}$ T-cell population are defined as MAIT cells throughout this study (**Figure 1b**). Within $CD161^{++}CD8^{+}$ T cells, there was no difference in expression of GrA and perforin between $V\alpha7.2^{+}$ cells and $V\alpha7.2^{-}$. However, GrB expression was significantly lower ($P<0.05$) and GrK expression was significantly higher ($P<0.001$) in the $V\alpha7.2^{+}$ MAIT cells (**Figure 1c**). Analysis of the simultaneous expression of perforin and granzymes in MAIT cells confirmed that the majority of the population coexpressed GrA and GrK, whereas a mean of 30% of MAIT cells coexpressed GrA, GrK, and perforin (**Supplementary Figure S1B** and **C**).

Using ImageStream technology, GrA was seen to colocalize with CD107α, a marker of cytotoxic granules, as well as with GrK in $CD161^{++}CD8^{+}$ T cells (**Figure 1d**), suggesting that GrA and GrK are preformed within lytic granules. Thus, $CD161^{++}CD8^{+}$ T cells, including the MAIT cells, have the potential to release GrA, GrK, and perforin immediately upon target cell interaction.

Physiologic stimulation via MR1 leads to degranulation and changes in cytotoxic profile of MAIT cells

We next investigated the regulation of cytotoxic potential in an *in vitro* model of MAIT cell activation. We have recently shown that MAIT cells can be activated both through the cognate interaction between MR1 and the TCR, as well as through IL-12 and IL-18 stimulation in a TCR-independent manner.[13] Therefore, we tested if either pathway, or a combination of these signals, could induce a cytotoxic phenotype within MAIT cells.

Using our previously described model,[13] THP1 cell lines were pre-exposed to paraformaldehyde (PFA)-fixed *Escherichia coli*, and then cultured with enriched $CD8^{+}$ T cells overnight, after which the cytotoxic profile of MAIT cells was evaluated (**Figure 2**). MAIT cells degranulated extensively in response to *E. coli* as measured by CD107α expression (**Figure 2a**; 66.3%, $P<0.0001$). This was almost completely blocked by an anti-MR1-blocking antibody (20.9%; $P<0.0001$), whereas blocking IL-12 or IL-18 had minimal effect on the degranulation of the cells.

We then examined whether the expression of the key cytotoxic effector molecules, GrB and perforin, is modified by activation in this model. The frequency of MAIT cells expressing GrB increased to ~35% in response to *E. coli* ($P<0.0001$; **Figure 2b**). Importantly, the addition of either anti-MR1-blocking antibody, or anti-IL-12-blocking antibody, significantly reduced the induction of GrB (6.5%, $P<0.001$; 12.2%, $P<0.001$, respectively), and the combination of anti-MR1, anti-IL-12, and anti-IL-18-blocking antibodies inhibited GrB upregulation completely (2.28%, $P<0.001$). Confirming the need for a TCR signal, direct stimulation of MAIT cells with anti-CD3/CD28/CD2 beads, but not with anti-CD3 beads or cytokines alone, also led to significant upregulation of GrB (**Supplementary Figure S2A**). This suggests that TCR signals are necessary for GrB upregulation in response to *E. coli*, and that costimulation either with IL-12 or CD2/CD28 is also required. Of note, there was a dose-dependent increase of GrB expression with increasing concentrations of *E. coli* (**Supplementary Figure S3A** and **B**). At the highest BpC, however, there was no further increase in GrB expression, although these cells were maximally activated as measured by CD69 expression (**Supplementary Figure S3A**). This may be due to the downregulation of the TCR upon exposure to high doses of bacteria, as shown by Vα7.2 downregulation, in turn limiting further TCR-mediated upregulation of GrB. There was a loss of the $CD161^{++}$ population with increasing doses of *E. coli* as previously described,[27] but there was no visible loss of CD161 expression from the maximally activated MAIT cells (**Supplementary Figure S3A**). There was no difference in the frequency of MAIT cells or other $CD8^{+}$ T-cell populations when the cells were stained extracellularly or intracellularly for CD161 after activation (data not shown). Therefore, in this

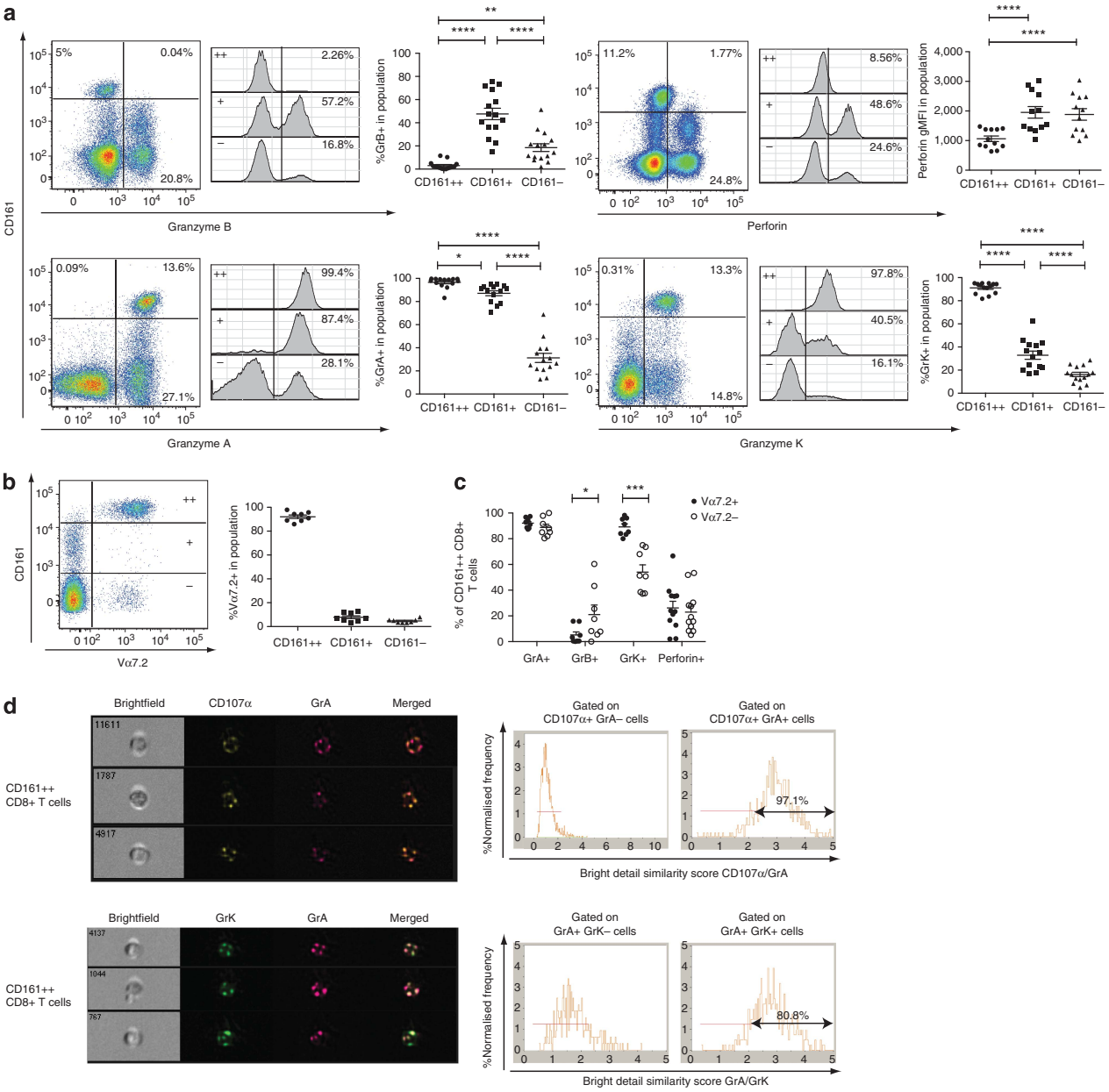


Figure 1 Resting blood-derived human mucosal-associated invariant T (MAIT) cells have a unique cytotoxic profile. (**a**) Expression of granzyme (Gr) B, perforin, GrA, and GrK in peripheral blood CD8$^+$ T cells from healthy donors according to CD161 expression levels. For each marker, representative staining gated on CD8$^+$ T cells (left), representative staining gated on CD161^{++}, CD161$^+$, and CD161$^-$ CD8$^+$ T cells (middle), and cumulative data for 12–15 healthy individuals (right) are shown. Results shown as mean ± s.e.m., analyzed by repeated-measures one-way analysis of variance (ANOVA), with Bonferroni's multiple comparisons test. *$P<0.05$, **$P<0.01$, ***$P<0.001$, ****$P<0.0001$. (**b**) CD161^{++}CD8$^+$ T cells are predominantly Vα7.2$^+$, compared with CD161$^+$ and CD161$^-$ CD8$^+$ T cells. Representative staining of Vα7.2 T-cell receptor (TCR) on CD8$^+$ T cells according to CD161 expression levels and cumulative data are shown ($n=8$). (**c**) Expression of GrB, perforin, GrA, and GrK in Vα7.2$^+$ and Vα7.2$^-$ cells, gated within the CD161^{++}CD8$^+$ T-cell population. Cumulative data are shown, analyzed by paired *t*-test ($n=8$–12). (**d**) Representative images showing Imagestream analysis of colocalization of GrA, GrK, and CD107α expression within CD161^{++}CD8$^+$ T cells. Histograms of normalized cell frequency against colocalization as measured by Bright Detail Similarity scores; >2.0 is defined as colocalized (see **Supplementary Methods**).

activation model, we do not observe CD161 downregulation in MAIT cells.

We also observed perforin to be upregulated in this coculture model (20.8% vs. 66.7%, $P<0.0001$; **Figure 2c**). However, unlike GrB, perforin upregulation could not be blocked by the addition of the MR1-blocking antibody. IL-12-blocking antibody also had only a small effect on the upregulation of perforin (66.7% vs. 54.3%, $P<0.01$). Therefore, multiple factors may be contributing to perforin upregulation; indeed, direct stimulation of MAIT cells with IL-7, IL-15, or IL-2 upregulated perforin (**Supplementary Figure S2B**). This contrasts with the TCR- and costimulation-dependent GrB upregulation

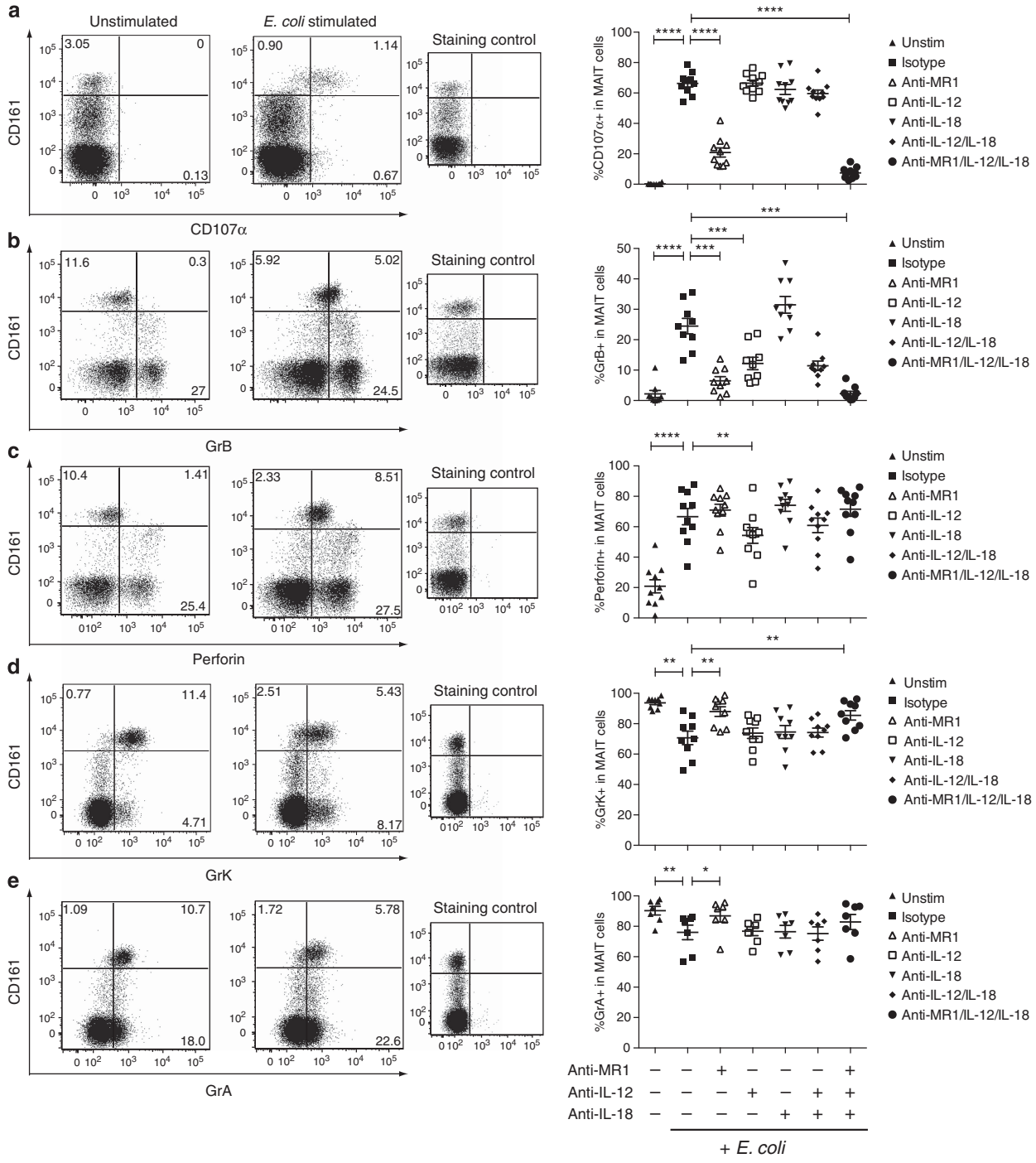


Figure 2 Bacterial stimulation leads to degranulation and changes in cytotoxic profile of mucosal-associated invariant T (MAIT) cells. Enriched CD8$^+$ T cells were cocultured with THP1 cells exposed to *E. coli*, in the presence or absence of blocking antibodies against MR1, interleukin (IL)-12, IL-18 or isotype controls, and assayed for the expression of (**a**) CD107α, (**b**) granzyme (Gr) B, (**c**) perforin, (**d**) GrK, and (**e**) GrA. Representative plots gated on CD8$^+$ T cells are shown on the left panel and cumulative data on the right panel for each marker, with bars indicating mean ± s.e.m. ($n = 7$–10). Staining control shows isotype control (conjugated with matched fluorochromes) used for gating for each marker. Note that GrA and GrK staining control is the same for each donor as both conjugated to the same flurochrome, and CD107α staining uses the unstimulated control for gating. Results are analyzed by repeated-measures one-way analysis of variance (ANOVA), with Bonferroni's multiple comparisons test. *$P<0.05$, **$P<0.01$, ***$P<0.001$, ****$P<0.0001$.

described above, and suggests that GrB expression in MAIT cells may be more tightly regulated than perforin.

In contrast to GrB and perforin, the frequency of GrK- and GrA-expressing MAIT cells were both significantly reduced in response to *E. coli* (**Figure 2d** and **e**), and this loss was blocked by the anti-MR1 antibody. Stimulation of MAIT cells directly with anti-CD3/CD28/CD2 beads or phorbol 12-myristate 13 acetate/ionomycin, but not cytokines, also reduced the percentage of

MAIT cells expressing GrK, and to a limited extent, GrA, although this did not reach significance (**Supplementary Figure S2C** and **D**). There was also no significant increase in GrA or GrK expression as measured by geometric mean fluorescence intensity when cells were directly stimulated with cytokines, such as IL-12 + IL-18. Furthermore, there was no significant upregulation of granulysin or FasL when MAIT cells were stimulated with anti-CD3/CD28/CD2 beads or *E. coli* (**Supplementary Figure S2E** and **F**). Thus, MAIT cells modify their granule contents upon physiological activation.

Licensed MAIT cells can kill target cells in an MR1-dependent manner

MAIT cells are activated by a broad range of bacteria through recognition of their ligand, a metabolic precursor of riboflavin, presented by MR1.[7] Whether this recognition leads to cytotoxicity, and what mechanisms are involved, have not been probed in detail. Furthermore, when administered to target cells, GrA and GrK, expressed by resting MAIT cells, have been suggested not to induce apoptosis, while GrB, not expressed by resting MAIT cells, induces apoptosis at equivalent concentrations.[21,34]

To test the capacity of *ex vivo* MAIT cells to kill target cells, a flow cytometry-based killing assay was developed, based on the published FATAL assay.[28] Briefly, Epstein–Barr virus-transformed B-cell lines (BCLs) were either incubated with PFA-fixed *E. coli* or sterility control overnight and stained with carboxyfluorescein succinimidyl ester (CFSE) and CellTrace Violet (CTV) dyes, respectively. These were mixed at a 1:1 ratio and cocultured with enriched $CD8^+$ T cells at various E:T ratios. Specific killing of $CFSE^+$ target cells, but not CTV^+ control cells, was then calculated based on the ratio of $CFSE^+$ and CTV^+ cells in wells without effector cells. In addition, taking advantage of the capacity of modern flow cytometers to measure a greater number of parameters, CD107α externalization by the $CD161^{++}CD8^+$ T cells was measured. Therefore, by combining the FATAL assay with the LAMP-1 assay[29] and phenotyping the effector cells, our assay allows the identification of the cell population responsible for cytolysis; thus, removing the necessity to sort enrich specific or rare effector populations. The gating strategy is shown in **Supplementary Figure S4A**. Using this modified FATAL assay, we found that resting MAIT cells only killed 30% of *E. coli*-exposed BCLs even the highest E:T ratios, in an MR1-dependent manner (**Figure 3a** and **b**).

Next, we asked whether pre-activation of MAIT cells, eliciting a more cytotoxic phenotype, would enhance their cytotoxic capacity. Peripheral blood mononuclear cells (PBMCs) isolated from the same donors were either pre-stimulated with PFA-fixed *E. coli* for 6 days (licensed) or freshly thawed (*ex vivo*); both were enriched for $CD8^+$ T cells in parallel. Licensed MAIT cells were significantly more cytotoxic compared with *ex vivo* MAIT cells, killing up to 70% of *E. coli*-exposed BCLs ($P<0.0001$; **Figure 3c** and **d**). The frequency of $CD161^{++}CD8^+$ T cells did not significantly differ between *ex vivo* and licensed cells (**Supplementary Figure S4B**), and indeed *post hoc* adjustment of the E:T to the actual ratio of $CD161^{++}CD8^+$ T cells to target cells showed licensed MAIT cells were more cytotoxic on a per cell basis (**Supplementary Figure S4C**). Target cell killing by the *E. coli*-stimulated $CD8^+$ T cells was abolished with the addition of the anti-MR1-blocking antibody, confirming MAIT cells were mediating the killing (**Figure 3e**). Inhibition of degranulation and perforin polymerization with ethylene glycol tetra-acetic acid also prevented killing, suggesting this process was degranulation mediated. Blocking FasL did not affect this killing, consistent with the low FasL expression on activated MAIT cells (**Supplementary Figure S2F**).

In addition, we confirmed that the $CD161^{++}CD8^+$ T-cell population was responsible for target cell killing as only this $CD8^+$ T-cell population degranulated in response to *E. coli*-exposed BCLs (**Figure 3f** and **g**). Furthermore, this novel cytotoxicity assay uses two amine-reactive dyes that bind to both cytosolic and membrane proteins, which are less prone to dye transfer than the lipophilic dye used in the original FATAL assay; thus, we were able to measure trogocytosis of the target cell membrane by the T cells, indicating prior synapse formation.[30] This showed that $CD161^{++}CD8^+$ T cells made immunological synapses with the $CFSE^+$ target cells, and not with the CTV^+ control cells (**Figure 3g** and **Supplementary Figure S3D**). *Ex vivo* $CD161^{++}CD8^+$ T cells degranulated more readily than *E. coli*-stimulated $CD161^{++}CD8^+$ T cells in response to the same target cells (**Figure 3f**), yet were less cytotoxic than the latter, consistent with the hypothesis that MAIT cells needed licensing by granzyme exchange to become highly cytotoxic. When $CD107\alpha^+$ cells within $CD161^{++}CD8^+$ T cells were compared, the frequency of cells that had acquired CFSE was significantly higher in the *E. coli*-stimulated cells than in *ex vivo* cells (**Figure 3h**), suggesting there is also increased synapse formation between the target cells and *E. coli*-stimulated $CD161^{++}CD8^+$ T cells compared with *ex vivo* $CD161^{++}CD8^+$ T cells.

Overall, these data suggest that *E. coli*-stimulated, licensed MAIT cells maintain the capacity to degranulate and possess enhanced killing capacity compared with *ex vivo* MAIT cells.

Rapid GrB upregulation in MAIT cells is associated with Blimp1 and T-bet expression

Next, we probed the kinetics of this MAIT cell licensing by examining GrB and perforin upregulation in response to *E. coli*. MAIT cells showed no change in the expression of GrB and perforin within the first 6 h of stimulation (**Figure 4a** and **b**), but markedly upregulated these effector molecules by 18 h, with most cells expressing GrB and perforin by 30 h. This upregulation was specific to the MAIT cell population, the kinetics of which was similar to anti-CD3/CD28/CD2 stimulation (**Figure 4c** and **d**).

The transcription factors T-bet and Blimp1 are both important for GrB expression in $CD8^+$ T cells.[25,26] To investigate whether these transcription factors are associated with GrB upregulation in MAIT cells, PBMCs were stimulated with *E. coli* for 24 h, with or without the addition of MR1- and IL-12-

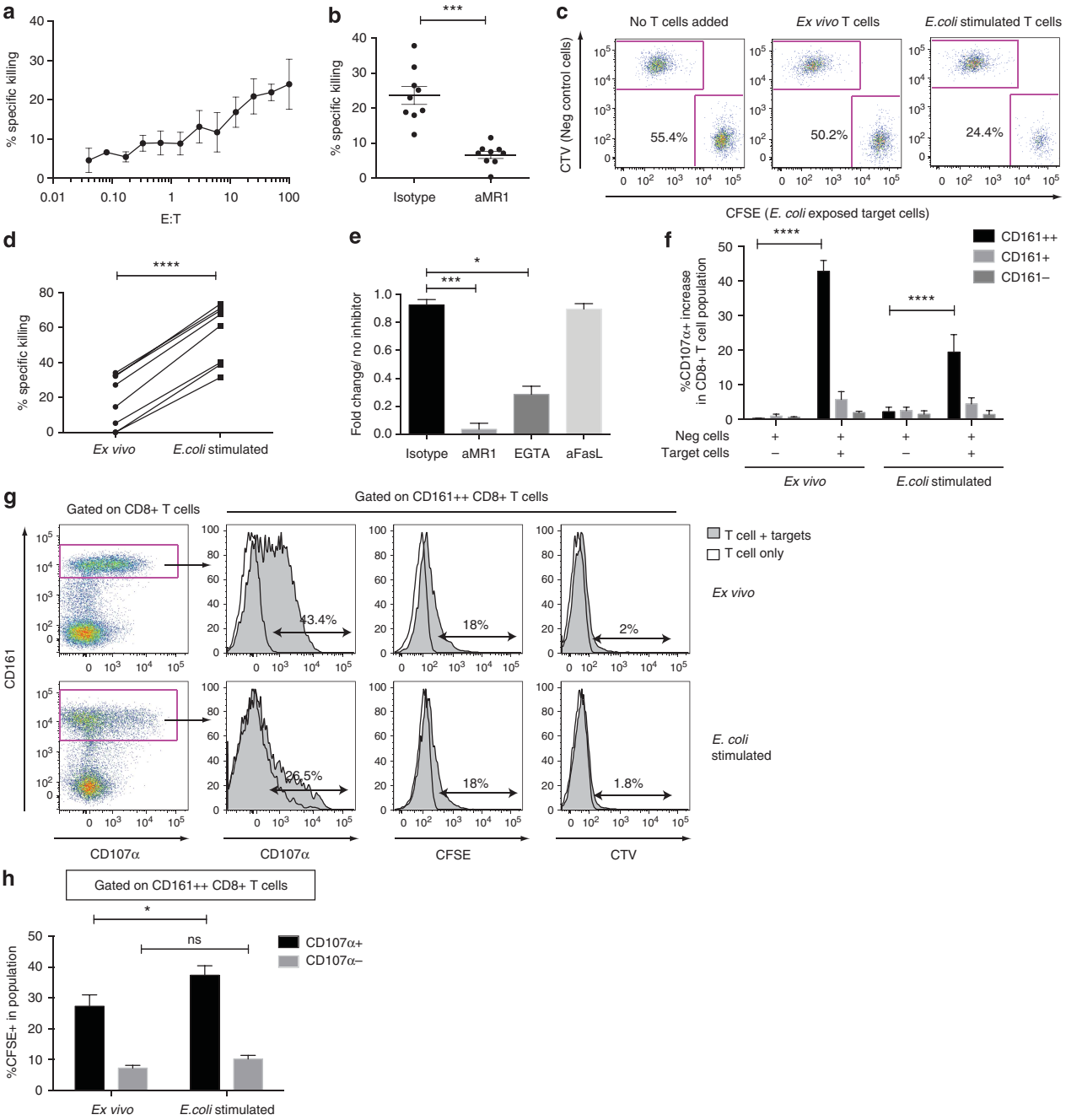


Figure 3 *E.coli*-stimulated mucosal-associated invariant T (MAIT) cells can efficiently kill target cells in an MR1- and degranulation-dependent manner. B-cell lines (BCLs) were either incubated with paraformaldehyde (PFA)-fixed *E. coli* or sterility control and stained with carboxyfluorescein succinimidyl ester (CFSE) and CellTrace Violet (CTV) dyes, respectively, and cocultured with enriched $CD8^+$ T cells. (**a**) Percentage of specific killing of target BCLs by *ex vivo* MAIT cells at various E:T ratios. Mean ± s.e.m. of duplicate results of three independent experiments shown ($n = 10$). (**b**) Percentage of specific killing of target cells by *ex vivo* MAIT cells with and without an anti-MR1-blocking antibody at E:T = 50:1. ($n = 9$). (**c**) Example plots showing the frequency of live *E. coli*-exposed BCLs and negative control BCLs without effector cells (left), with *ex vivo* MAIT cells (middle), or with MAIT cells stimulated with *E. coli* for 6 days (right), added at E:T = 10:1. (**d**) Percentage of specific killing of target cells by *ex vivo* and *E. coli*-stimulated MAIT cells from the same donors at E:T = 10:1. Mean ± s.e.m. of duplicate results of three independent experiments are shown. ($n = 8$). (**e**) Inhibition of killing at E:T = 10:1 by *E. coli*-stimulated MAIT cells in presence of anti-MR1 antibody, ethylene glycol tetra-acetic acid (EGTA), or anti-FasL antibody, compared with killing with no inhibitor. Repeated-measures one-way analysis of variance (ANOVA), with Bonferroni's multiple comparisons test. ($n = 5$) (**f**) Cumulative data showing increase in $\%CD107\alpha^+$ cells in indicated $CD8^+$ T-cell populations compared with wells with T cells only. Analyzed by two-way ANOVA, comparing increase in $CD107\alpha^+$ expressing cells when target cells are added, within each $CD8^+$ T-cell population, with Bonferroni's multiple comparisons test. $CFSE^+$ *E. coli*-exposed BCL = Target cells, CTV^+ negative control BCL = Neg cells. ($n = 8$). (**g**) Representative plots of *ex vivo* and *E. coli*-stimulated CD8 T cells from the killing assays. Histograms showing expression of CD107α, and CFSE and CTV acquired through trogocytosis in $CD161^{++}CD8^+$ T cells. (**h**) Trogocytosis of CFSE from *E. coli*-exposed BCL membranes onto degranulating $CD161^{++}CD8^+$ T cells ($n = 8$). Analyzed by two-way ANOVA, comparing wells with *ex vivo* and *E. coli*-stimulated cells, with Bonferroni's multiple comparisons test. NS, nonsignificant. $^*P < 0.05$, $^{***}P < 0.001$, $^{****}P < 0.0001$.

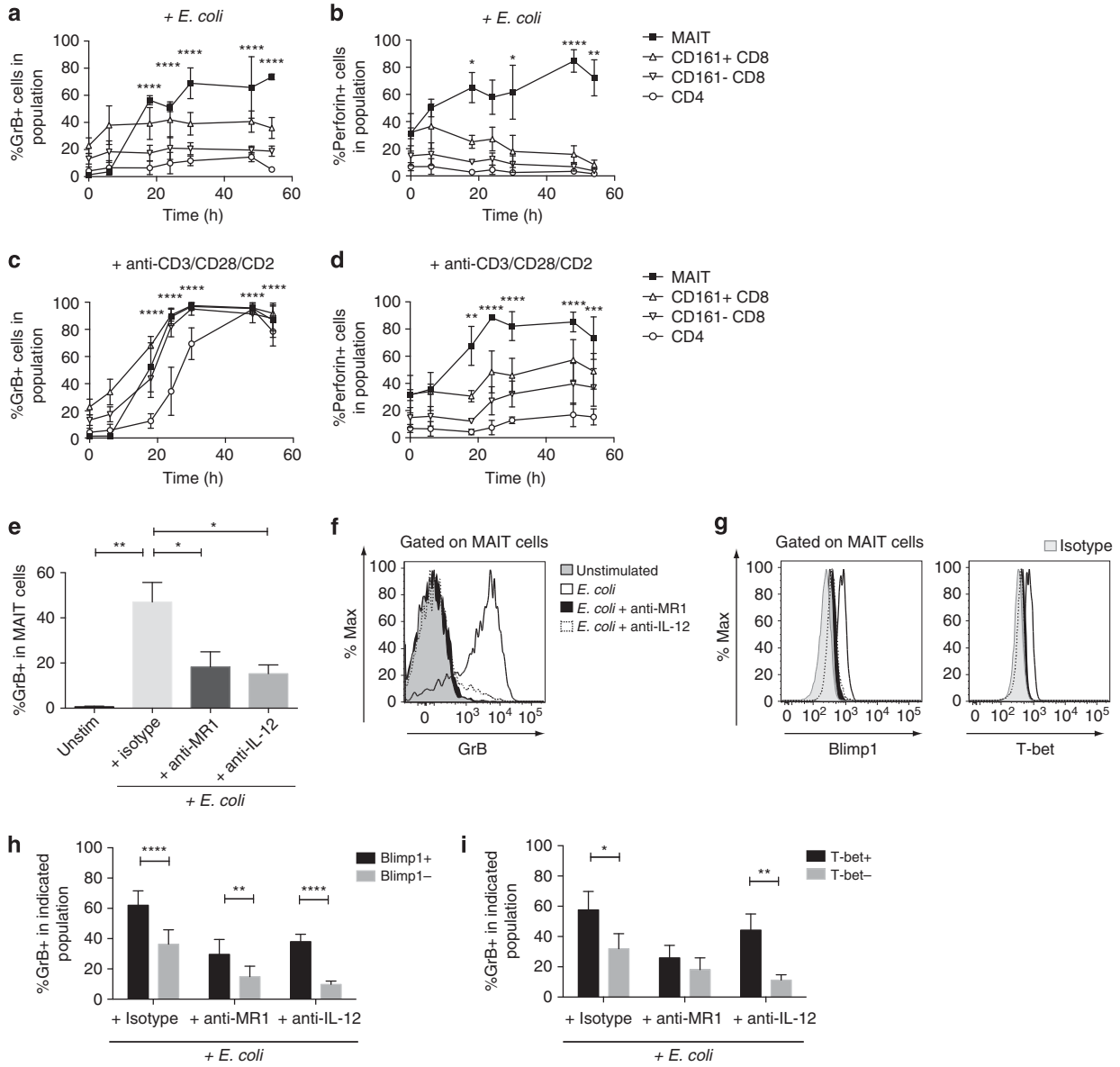


Figure 4 Granzyme (Gr) B and perforin upregulation in *E. coli*-stimulated mucosal-associated invariant T (MAIT) cells is rapid and associated with Blimp1 and T-bet expression. (**a**–**d**) Peripheral blood mononuclear cells (PBMCs) were stimulated with (**a**, **b**) paraformaldehyde (PFA)-fixed *E. coli*, or (**c**, **d**) anti-CD3/CD28/CD2 coated beads, and stained for GrB and perforin at the indicated time points ($n=3$). Asterisks (*) indicate significant increases in effector molecules in MAIT cells compared with the unstimulated controls, by a two-way analysis of variance (ANOVA), with Bonferroni's multiple comparisons test. (**e**–**i**) PBMCs were stimulated with PFA-fixed *E. coli* for 24 h with and without blocking antibodies to MR1 and interleukin (IL)-12, and stained for GrB, T-bet, and Blimp1 ($n=7$). (**e**) Cumulative data for frequency of GrB expressing MAIT cells and (**f**) representative example of GrB expression in MAIT cells after *E. coli* stimulation, ± blocking antibodies to MR1 or IL-12. One-way ANOVA, Bonferroni's multiple comparisons test. (**g**) Representative T-bet and Blimp1 expression in MAIT cells unstimulated or stimulated with PFA-fixed *E. coli* ± blocking antibodies to MR1 or IL-12. For figure legend, see panel **f**. (**h**) Frequency of GrB-expressing cells in T-bet$^+$ or T-bet$^-$ MAIT cells. (**i**) Frequency of GrB-expressing cells in Blimp1$^+$ or Blimp1$^-$ MAIT cells. Results analyzed by two-way ANOVA with Bonferroni's multiple comparisons test. Bars indicate mean ± s.e.m. *$P<0.05$, **$P<0.01$, ***$P<0.001$, ****$P<0.0001$.

blocking antibodies. As expected from the THP1 coculture model (**Figure 2**), MAIT cells stimulated with *E. coli* upregulated GrB (**Figure 4e** and **f**), but also coexpressed T-bet and Blimp1 in an MR1- and IL-12-dependent manner (**Figure 4g**). Cells expressing T-bet or Blimp1 were more likely to express GrB (**Figure 4h** and **i**), supporting a role for these transcription factors in the upregulation of GrB in MAIT cells.

MAIT cells readily proliferate in response to *E. coli* and maintain a highly cytotoxic profile

Finally, we asked whether the granule content of MAIT cells were sustained during proliferation. When CTV-labeled PBMCs were cultured with PFA-fixed *E. coli* for 6 days, MAIT cells proliferated in a dose-dependent manner to *E. coli* (**Figure 5a** and **b**). The proliferation of MAIT cells was

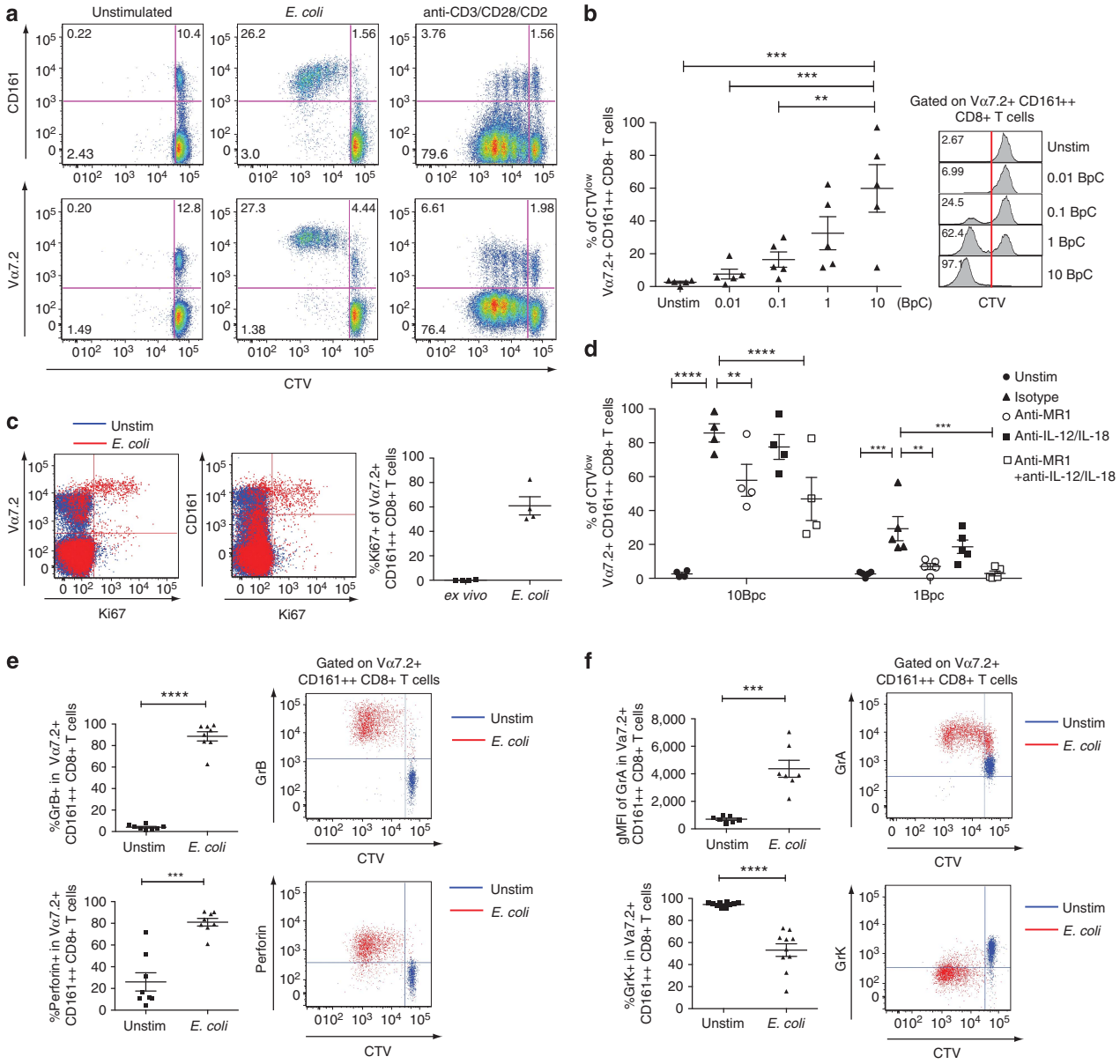


Figure 5 Mucosal-associated invariant T (MAIT) cells are readily proliferative in response to *E. coli* and maintain a highly cytotoxic profile. Peripheral blood mononuclear cells (PBMCs) from healthy donors were CellTrace Violet (CTV)-labeled and cultured with paraformaldehyde (PFA)-fixed *E. coli* for 6 days. BpC = bacteria per cell ratio. (**a**) Representative plot showing dilution of CTV against CD161 expression (upper panel) and Vα7.2 expression (lower panel) at 10 BpC or with anti-CD3/CD28/CD2 beads, gated on $CD8^+$ T cells. (**b**) Cumulative data (left) and representative flow cytometry histograms are shown for each BpC. One-way analysis of variance (ANOVA), with Bonferroni's multiple comparisons test. (**c**) Representative plot (left) and cumulative data (right) showing Ki67 staining in $CD8^+$ T cells after *E. coli*-stimulation at 10 BpC ($n = 4$). (**d**) Proliferation of $V\alpha7.2^+CD161^{++}CD8^+$ T cells in response to *E. coli* with anti-MR1, interleukin (IL)-12, and IL-18-blocking antibodies at the indicated BpCs. Results pooled from two independent experiments and analyzed by two-way ANOVA, with Bonferroni's multiple comparisons test. (**e**) GrB and perforin, and (**f**) GrA and GrK expression in CTV-labeled $V\alpha7.2^+CD161^{++}CD8^+$ T cells following *E. coli* stimulation for 6 days. Cumulative data (left) and representative staining is shown (right). Gating for granzymes and perforin based on isotype controls. Results analyzed by paired *t*-test ($n = 8$). Bars indicate mean ± s.e.m. $^*P < 0.05$, $^{**}P < 0.01$, $^{***}P < 0.001$, $^{****}P < 0.0001$.

confirmed by Ki67 staining (**Figure 5c**), and was inducible when enriched $CD8^+$ T cells were directly stimulated with *E. coli*-exposed THP1 cells (**Supplementary Figure S5A**), confirming this is a specific effect and not bystander proliferation. Interestingly, although most cells remained $CD161^{++}$ (**Figure 5a**, **Supplementary Figure S5A**), CD161 was downregulated on MAIT cells with increasing rounds of cell divisions (**Supplementary Figure S5B**). In addition, although both CD8αα and CD8αβ subsets of MAIT cells proliferated, there was greater proliferation of the CD8αβ subset (**Supplementary Figure S5C**). To investigate the relative contributions of the TCR signal and innate cytokines for MAIT

cell proliferation, blocking antibodies to MR1 or IL-12 and IL-18 were added. Addition of the MR1-blocking antibody, but not IL-12- or IL-18-blocking antibodies, significantly inhibited MAIT cell proliferation (**Figure 5d**), demonstrating that *E. coli*-induced MAIT cell expansion is largely TCR dependent; this was further confirmed with enriched $CD8^+$ T cells (**Supplementary Figure S5A**). Of note, proliferation of MAIT cells at 10BpC could not be completely inhibited by the anti-MR1-blocking antibody, suggesting that other cytokines may be contributing to their proliferation. Indeed, $CD161^{++}$ $CD8^+$ T cells readily proliferated in response to IL-2, IL-15, or IL-12 in the absence of exogenous TCR stimulation (**Supplementary Figure S4D–G**).

We next probed how the cytotoxic prolife of MAIT cells changed as they proliferated. PFA-fixed *E. coli* were added to CTV-stained PBMCs, and after 6 days GrB, perforin, GrK, and GrA expression was assessed. MAIT cells cultured with *E. coli* acquired a highly cytotoxic profile; ~100% of cells expressed GrB and ~90% of cells expressed perforin. GrB and perforin expression did not require proliferation, as CTV^{high}, non-proliferating cells also expressed high levels of both cytotoxic mediators (**Figure 5e**). Although resting MAIT cells all express GrA, stimulated MAIT cells upregulated GrA as measured by geometric mean fluorescence intensity (**Figure 5f**). In turn, there was a significant loss of GrK expression by activated MAIT cells (**Figure 5f**).

Therefore, MAIT cells are highly proliferative to antigenic and cytokine stimuli *in vitro*, and antigenic stimulation, irrespective of proliferation, is associated with increased expression of perforin, GrB, and GrA, and decreased expression of GrK.

DISCUSSION

In this article, we demonstrate that the unique cytotoxic granule content of resting MAIT cells changes markedly upon activation, licensing these cells to kill target cells with greater efficiency. Importantly, to our knowledge this is the first study to investigate the regulation of MAIT cell cytotoxicity and their ability to kill APCs. Our findings support a role for MAIT cells in the control of intracellular bacterial infection.

At rest, almost all $CD161^{++}CD8^+$ T cells, including MAIT cells, express GrA and GrK within cytotoxic granules and, therefore, are poised to release these immediately upon degranulation. In contrast, they express low levels of perforin, no GrB, and little granulysin or FasL (**Supplementary Figure S2E** and **F**). GrA and GrK are closely related trypsin-like serine proteases[15] originally believed to function as pro-apoptotic proteases,[31–33] however, recent studies have suggested that they are inefficient inducers of cell death.[21,22,34] Human GrA is significantly less cytotoxic than mouse GrA,[35,36] and in virus-specific $CD8^+$ T cells, cytotoxicity inversely correlated with GrK expression, whereas GrA expression did not correlate with lytic ability.[17] Instead, GrA and GrK have been shown to activate monocytes to produce proinflammatory cytokines such as IL-1β and tumor necrosis factor-α.[21–23,34] Intriguingly, a recent paper by Wensink *et al.*[37] has demonstrated *in vivo* and *in vitro* that GrK binds to Gram-negative bacteria and lipopolysaccharide, synergistically increasing lipopolysaccharide-induced release of proinflammatory cytokines. GrA release by γδ T cells is also critical in the control of BCG growth by inducing tumor necrosis factor-α production in infected macrophages,[38] and similarly, degranulation of resting MAIT cells may assist in the control of bacterial infection through phagocyte activation. Once GrA and GrK are released from the cell, the signals that may increase the production of these granzymes and aid the replenishment of the granules are unknown. Of note, direct stimulation of MAIT cells with various cytokines such as IL-12 + IL-18 did not significantly increase the amount of GrA or GrK expressed by *ex vivo* MAIT cells as measured by geometric mean fluorescence intensity, although IL-15 induced a slight increase in GrA in 6/10 donors (**Supplementary Figure S2C** and **D**).

Following antigen exposure, MAIT cells rapidly transition to a more classical cytotoxic cell type, displaying high levels of GrB and perforin. This is consistent with previous work showing that activated MAIT cells can secrete GrB,[8] and that GrB expression in $CD8^+$ T cells positively correlates with antigenic stimulation.[17,39] When we probed the mechanisms controlling the early upregulation of GrB by activated MAIT cells, we found this to be dependent upon engagement of the TCR with MR1 and IL-12 or costimulation through CD2/CD28. This is in contrast to degranulation, which is dependent solely on the interaction of the TCR with MR1, and perforin upregulation, which could be induced by multiple cytokines. Among the granzymes, GrB is the most potent, especially in humans where it induces apoptosis in a caspase-independent manner.[15,40] Thus, the requirement for a second signal for maximal expression of GrB in TCR-stimulated MAIT cells may be important to prevent unwanted tissue damage. The relative importance of MR1- and cytokine-mediated regulation of MAIT cell cytotoxicity *in vivo* will be crucial in harnessing the cytotoxic potential of these cells. Our data also suggest that the transcription factors Blimp1 and T-bet may be involved in this regulation of GrB expression in MAIT cells. In conventional $CD8^+$ T cells, T-bet and Blimp1 are independently regulated, with Blimp1 deficiency resulting in a failure to produce GrB.[25,26] Whether Blimp1 and T-bet has a similarly critical role in GrB expression in MAIT cells remains to be determined.

Highly cytotoxic, licensed MAIT cells were able to kill up to 70% of *E. coli*-exposed BCLs. Although both *ex vivo* and licensed MAIT cells degranulated upon exposure to target cells, *ex vivo* MAIT cells showed significantly less cytotoxicity compared with licensed MAIT cells, consistent with changes in granule content with activation. Blocking experiments showed killing by these licensed MAIT cells was dependent on TCR-mediated degranulation, and not Fas-mediated killing, which is important in invariant natural killer T-cell cytotoxicity.[41]

Interestingly, $CD161^{++}$ cells within the few $CD8^-$ T cells in the killing assays degranulated in response to *E. coli*, and indeed $CD8^-CD4^-$ MAIT cells could be activated by *E. coli* as readily as $CD8^+$ MAIT cells (**Supplementary Figure S6**). Although we cannot rule out CD8 downregulation, conventional $CD8^+$

T-cell responses also do not necessarily require, but can be augmented by, the CD8 coreceptor. In conventional $CD8^+$ T cells, CD8 coreceptor enhances the binding of the TCR to the peptide-major histocompatibility complex, and cytolytic responses may be abrogated when coreceptor binding is inhibited.[42] However, in the context of high-affinity agonist ligands, APCs expressing wild-type or CD8-null human leukocyte antigen molecules induces CD107α externalization by $CD8^+$ T cells to a similar extent across a range of peptide concentrations, whereas abrogation of coreceptor binding inhibits degranulation in response to low-affinity peptide variants, even at high peptide concentrations.[43] Molecular analyses have shown that MR1 can accommodate a range of riboflavin-derived ligands with different binding affinities,[10,44] and given that murine MAIT cells are mostly $CD8^-$,[10] the role of the CD8 coreceptor in MAIT cell cytotoxicity and biology is a question that warrants further investigation.

The ability of activated MAIT cells to kill target cells may have an important role in bacterial control *in vivo*. A recent paper showed that MAIT cells can kill epithelial cells infected with *S. flexneri*,[14] suggesting that this function may be important for preventing cytosolic bacteria from crossing the mucosal barrier. Other intracellular bacteria such as *Mycobacterium tuberculosis* can replicate in macrophages[45] and B cells,[46] surviving inside a segregated endosomal compartment. Efficient killing of infected APCs by MAIT cells may lead to enhanced clearance of such bacteria. Intriguingly, an *in vivo* model using BCG found that IL-12 rather than recognition of MR1 by murine MAIT cells was required for their control of BCG growth,[4] suggesting that degranulation was not critical in this model. Similarly, murine MAIT cell control of *F. tularensis* growth *in vitro* was mediated by cytokine production, not infected cell lysis.[6] Successful killing of infected cells will ultimately depend upon various factors including ligand availability for MR1 loading, inhibitors of cytolysis expressed by the infected cell,[47,48] and inhibitory/costimulatory signals. Indeed, we found that CD161 is a costimulatory molecule on MAIT cells, and its ligation induces a substantial increase in target cell killing (Fergusson *et al*., in press,[49] and Smith *et al*., unpublished data). Thus, whether cytotoxicity has a significant role in protection mediated by MAIT cells *in vivo* will most likely depend on both the pathogen and the infected host cell in question.

In this study, we also demonstrate that adult MAIT cells proliferate in response to cytokines as well as TCR stimulation. MAIT cell expansion could be induced through *E. coli* stimulation in an MR1-dependent manner, a property recently shown to be acquired during fetal development.[50] Interestingly, MAIT cells downregulated CD161 with increasing rounds of cell division (**Supplementary Figure S5B**), in agreement with previous observations that MAIT cell clones can be $CD161^-$.[3] In our hands, we do not observe CD161 downregulation during short-term activation of MAIT cells (**Supplementary Figure S3**), as has been shown previously,[51] but as CD161 costimulates T-cell proliferation,[52] downregulation of CD161 with proliferation may be beneficial for the continued survival of the cells by limiting activation-induced cell death. In contrast to previous studies,[8,53] a greater proportion of $CD161^{++}$ $CD8^+$ T cells, including the $V\alpha7.2^+$ MAIT cells, proliferated when stimulated with IL-2 or IL-15 compared with $CD161^+$ $CD8^+$ T cells, whereas phytohaemagglutinin induced limited proliferation despite high activation (**Supplementary Figure S5C** and **D**). Given the sensitivity of MAIT cells to activation-induced cell death,[27,54] MAIT cell proliferation most likely depends on a balance between expansion and activation-induced cell death, and may explain the variation between MAIT cell proliferation studies. *In vivo*, once MAIT cells are attracted to sites of infection/inflammation, their functional impact, including cytotoxic activity, may be further perpetuated by their proliferation.

Overall, our results show that MAIT cell cytotoxicity is suppressed in the resting state, but upon continued exposure to bacteria, they rapidly acquire a cytotoxic phenotype, licensing them to kill target cells. Maximum expression of GrB requires both TCR stimulation and a second signal, provided by IL-12 or costimulation, whereas perforin can be induced by multiple factors. Release of these cytotoxic mediators, however, is ultimately dependent on MR1. This tight regulation of MAIT cell cytotoxicity may have an important role in the control of intracellular bacterial infections, such as *M. tuberculosis*, while limiting immune-mediated pathology. Further elucidation of the relative role of MR1-dependent and cytokine-mediated regulation of MAIT cell function *in vivo* will be important in addressing this issue.

METHODS

Donors. Healthy donors were laboratory volunteers and leukocyte cones (NHS Blood Services, Oxford, UK). Umbilical cord blood samples were provided by the NHS Blood Services. All subjects were recruited in agreement with the local ethics committees of all participating institutions. PBMCs were isolated using Lymphoprep (AxisShield, Oslo, Norway). Cells were thawed and washed in RPMI 1640 with 10% fetal calf serum, L-glutamine, and penicillin/streptomycin (all Sigma-Aldrich, Dorset, UK).

Flow cytometry. For immunofluorescence staining, dead cells were excluded with the Near-IR Dead-Cell stain (Invitrogen, Paisley, UK). Antibodies used were: anti-CD3 PE-Cy7 or APC, anti-CD8 PerCP-Cy5.5 or eFluor 450, anti-CD69 FITC (eBioscience, Hatfield, UK); anti-CD161 PE or APC, anti-CD4 VioGreen (Miltenyi Biotec, Surrey, UK); anti-Vα7.2 PE or FITC or PE-Cy7, anti-CD107α PE-Cy7, anti-GrA PerCP-Cy5.5, anti-Perforin Pacific Blue, anti-granulysin PE, anti-FasL PE (Biolegend, London, UK); anti-GrB AlexaFluor700, anti-Perforin FITC, anti-Ki67 FITC (BD Biosciences, Oxford, UK), anti-GrB APC (Invitrogen); anti-GrK FITC (Immunotools, Friesoythe, Germany); anti-T-bet PE (Santa Cruz Biotechnology, Heidelberg, Germany); anti-GrA FITC, anti-Blimp1 AlexaFluor488 (R&D Systems, Abingdon, UK); and anti-CD8β PE (Beckman Coulter, High Wycombe, UK).

Data were collected on the flow cytometers LSRII (BD Biosciences) or MACSQuant (Miltenyi Biotec), and was analyzed using FlowJo v9.6 (TreeStar, Ashland, OR). For ImageStream analysis, see **Supplementary Methods**.

***In vitro* stimulation**. *E. coli* (DH5α, Invitrogen) was fixed in 2% PFA for 20 min, and washed extensively. A sterility control was prepared in identical manner and used as a negative control. In coculture experiments, *E. coli*, or the negative control, was added to THP1 cells (ECACC, Wiltshire, UK) at 25 Bacteria-per-Cell (BpC) overnight. Subsequently, THP1 cells were washed and $CD8^+$ T cells isolated

using CD8 Microbeads (Miltenyi Biotec; purities were $\geq$90%) and anti-CD107α antibody were added to the wells overnight. For further details, see **Supplementary Methods**.

Killing assays. The assay was based on the FATAL assay.[28] BCLs were either coincubated with PFA-fixed *E. coli* at 25BpC or the negative control overnight. Cells were harvested and the *E. coli*-exposed BCLs were stained with CellTrace CFSE (CFSE; Invitrogen), whereas the negative control BCLs were stained with CTV (Invitrogen) according to the manufacturer's protocol. After extensive washing, the CFSE- and CTV-labeled cells were mixed at a 1:1 ratio before plating.

$CD8^+$ T cells were isolated from PBMCs using CD8 Microbeads (Miltenyi Biotec), and added to the wells at the indicated E:T ratios overnight, with an anti-CD107α antibody. E:T indicates ratio of $CD8^+$ T cells to $CFSE^+$ target cells, unless otherwise indicated. $CD8^+$ T-cell purities were $\geq$90%. Experiments were done in duplicate. An MR1-blocking antibody (clone 26.5), a FasL-blocking antibody (clone NOK-1, BioLegend) or an appropriate isotype control was added at 5 μg ml^{-1} for blocking experiments. To block degranulation, 5 mM ethylene glycol tetra-acetic acid (Sigma-Aldrich) with 1 mM $MgCl_2$ (Affymetrix, High Wycombe, UK) was used.

Following incubation, cells were stained with a live–dead maker (Invitrogen) before fixation/permeabilization for the staining of relevant markers. Gating is shown in **Supplementary Figure S4A**. Based on the %survival of $CFSE^+$ cells in wells containing no effectors (E:T = 0:1), the expected frequency of target cells can be found:

$$\text{Expected ratio (ER)} = \%\,CFSE^+\,\text{cells} / \%\,CTV^+\,\text{cells}$$

Using this ratio, the % specific killing can be calculated:

$$\%\,\text{specific killing} = 100 \times [(ER \times \%\,CTV^+\,\text{cells}) - \%\,CFSE^+\,\text{cells}] / (ER \times \%\,CTV^+\,\text{cells})$$

For the *post hoc* estimation of the actual E:T ratio in each well, the frequency of $CD161^{++}CD8^+$ T cells within live cells was divided by the expected frequency of $CFSE^+$ cells in each well (ER × %CTV^+ cells).

Proliferation assays. PBMCs were labeled with CTV (Invitrogen) according to the manufacturer's protocol, and cultured for 6 days with either PFA-fixed *E. coli* at the indicated BpC, or the sterility control. An MR1-blocking antibody (clone 26.5), IL-12p40/70-blocking antibody (eBioscience), IL-18-blocking antibody (clone 126-2H, MBL International, Woburn, MA) or an appropriate isotype control was used at 5 μg ml^{-1} for blocking experiments. Alternatively, THP1 cells were cultured with *E. coli* at 25BpC overnight before irradiation and were cocultured with CTV-labeled $CD8^+$ T cells enriched with CD8 Microbeads for 6 days, with autologous irradiated feeder cells. For cytokine-induced proliferation, CTV-labeled PBMCs were cultured for 6 days with the following stimuli: recombinant human IL-2 (100 IU ml^{-1}), IL-15 (25 ng ml^{-1}), IL-18 (50 ng ml^{-1}), IL-12 (50 ng ml^{-1}), phytohaemagglutinin (2 μg ml^{-1}), anti-CD3-coated or anti-CD3/CD28/CD2-coated beads (Miltenyi Biotec) at a 1:1 ratio, or the indicated combinations.

Statistical analysis. All graphs and statistical analyses were completed using GraphPad Prism software Version 6.0b (La Jolla, CA). Coexpression analysis was performed with SPICE software Version 5.3.[55] Statistical significance was assessed using paired Student's *t*-test, repeated-measures one-way analysis of variances or two-way analysis of variances, with Bonferroni's correction for multiple comparison assays. All data presented as means with s.e.m., unless otherwise indicated.

SUPPLEMENTARY MATERIAL is linked to the online version of the paper at http://www.nature.com/mi

ACKNOWLEDGMENTS

This work was supported by the Wellcome Trust (WT091663MA); the Medical Research Council; the NIHR Biomedical Research Centre (Oxford); the Nuffield Department of Clinical Medicine (Oxford); the James Martin School for the 21st Century (Oxford); the National Institutes of Health (NIAD 5U19A082630 and AI046553), and the Oxford Dominions Trust.

DISCLOSURE

The authors declared no conflict of interest.

© 2015 Society for Mucosal Immunology

REFERENCES

1. Treiner, E. *et al.* Selection of evolutionarily conserved mucosal-associated invariant T cells by MR1. *Nature* **422**, 164–169 (2003).
2. Le Bourhis, L. *et al.* Antimicrobial activity of mucosal-associated invariant T cells. *Nat. Immunol.* **11**, 701–708 (2010).
3. Gold, M.C. *et al.* Human mucosal associated invariant T cells detect bacterially infected cells. *PLoS Biol.* **8**, e1000407 (2010).
4. Chua, W.J. *et al.* Polyclonal mucosal-associated invariant T cells have unique innate functions in bacterial infection. *Infect. Immun.* **80**, 3256–3267 (2012).
5. Georgel, P., Radosavljevic, M., Macquin, C. & Bahram, S. The non-conventional MHC class I MR1 molecule controls infection by *Klebsiella pneumoniae* in mice. *Mol. Immunol.* **48**, 769–775 (2011).
6. Meierovics, A., Yankelevich, W.-J.C. & Cowley, S.C. MAIT cells are critical for optimal mucosal immune responses during *in vivo* pulmonary bacterial infection. *Pro. Natl. Acad. Sci. USA* **110**, E3119–E3128 (2013).
7. Kjer-Nielsen, L. *et al.* MR1 presents microbial vitamin B metabolites to MAIT cells. *Nature* **491**, 717–723 (2012).
8. Dusseaux, M. *et al.* Human MAIT cells are xenobiotic-resistant, tissue-targeted, CD161hi IL-17-secreting T cells. *Blood* **117**, 1250–1259 (2011).
9. Tang, X.-Z. *et al.* IL-7 licenses activation of human liver intrasinusoidal mucosal-associated invariant T cells. *J. Immunol.* **190**, 3142–3152 (2013).
10. Reantragoon, R. *et al.* Antigen-loaded MR1 tetramers define T cell receptor heterogeneity in mucosal-associated invariant T cells. *J. Ex. Med* **210**, 2305–2320 (2013).
11. Walker, L.J. *et al.* Human MAIT and CD8αα cells develop from a pool of type-17 precommitted CD8+ T cells. *Blood* **119**, 422–433 (2012).
12. Billerbeck, E. *et al.* Analysis of CD161 expression on human CD8+ T cells defines a distinct functional subset with tissue-homing properties. *Proc. Natl. Acad. Sci. USA* **107**, 3006–3011 (2010).
13. Ussher, J.E. *et al.* $CD161^{++}CD8^+$ T cells, including the MAIT cell subset, are specifically activated by IL-12+IL-18 in a TCR-independent manner. *Eur. J. Immunol.* **44**, 195–203 (2014).
14. Le Bourhis, L. *et al.* MAIT cells detect and efficiently lyse bacterially-infected epithelial cells. *PLoS Pathog.* **9**, e1003681 (2013).
15. Chowdhury, D. & Lieberman, J. Death by a thousand cuts: granzyme pathways of programmed cell death. *Annu. Rev. Immunol.* **26**, 389–420 (2008).
16. Pinkoski, M.J. *et al.* Entry and trafficking of granzyme B in target cells during granzyme B-perforin-mediated apoptosis. *Blood* **92**, 1044–1054 (1998).
17. Harari, A., Enders, F.B., Cellerai, C., Bart, P.A. & Pantaleo, G. Distinct profiles of cytotoxic granules in memory CD8 T Cells correlate with function, differentiation stage, and antigen exposure. *J. Virol.* **83**, 2862–2871 (2009).
18. Wolint, P., Betts, M.R., Koup, R.A. & Oxenius, A. Immediate cytotoxicity but not degranulation distinguishes effector and memory subsets of CD8+ T cells. *J. Exp. Med.* **199**, 925–936 (2004).
19. Bratke, K., Kuepper, M., Bade, B., Virchow, J.C. & Luttmann, W. Differential expression of human granzymes A, B, and K in natural killer cells and during CD8+ T cell differentiation in peripheral blood. *Eur. J. Immunol.* **35**, 2608–2616 (2005).
20. Curtsinger, J.M., Lins, D.C., Johnson, C.M. & Mescher, M.F. Signal 3 tolerant CD8 T cells degranulate in response to antigen but lack granzyme B to mediate cytolysis. *J. Immunol.* **175**, 4392–4399 (2005).
21. Metkar, S.S. *et al.* Human and mouse granzyme A induce a proinflammatory cytokine response. *Immunity* **29**, 720–733 (2008).
22. Cooper, D.M., Pechkovsky, D.V., Hackett, T.L., Knight, D.A. & Granville, D.J. Granzyme K activates protease-activated receptor-1. *PLoS One* **6**, e21484 (2011).

23. Sower, L.E. *et al.* Extracellular activities of human granzyme A. Monocyte activation by granzyme A versus alpha-thrombin. *J. Immunol.* **156**, 2585–2590 (1996).
24. Makedonas, G. *et al.* Rapid up-regulation and granule-independent transport of perforin to the immunological synapse define a novel mechanism of antigen-specific CD8 + T cell cytotoxic activity. *J. Immunol.* **182**, 5560–5569 (2009).
25. Kallies, A., Xin, A., Belz, G.T. & Nutt, S.L. Blimp-1 transcription factor is required for the differentiation of effector CD8 + T Cells and memory responses. *Immunity* **31**, 283–295 (2009).
26. Cruz-Guilloty, F. *et al.* Runx3 and T-box proteins cooperate to establish the transcriptional program of effector CTLs. *J. Exp. Med.* **206**, 51–59 (2009).
27. Cosgrove, C. *et al.* Early and nonreversible decrease of CD161 $^{++}$ /MAIT cells in HIV infection. *Blood* **121**, 951–961 (2013).
28. Sheehy, M.E., McDermott, A.B., Furlan, S.N., Klenerman, P. & Nixon, D.F. A novel technique for the fluorometric assessment of T lymphocyte antigen specific lysis. *J. Immunol. Methods* **249**, 99–110 (2001).
29. Betts, M.R. *et al.* Sensitive and viable identification of antigen-specific CD8 + T cells by a flow cytometric assay for degranulation. *J. Immunol. Methods* **281**, 65–78 (2003).
30. Poupot, M., Fournié, J.-J. & Poupot, R. Trogocytosis and killing of IL-4-polarized monocytes by autologous NK cells. *J. Leukoc. Biol.* **84**, 1298–1305 (2008).
31. Jiang, W., Chai, N.R., Maric, D. & Bielekova, B. Unexpected role for granzyme K in CD56^{bright} NK cell-mediated immunoregulation of multiple sclerosis. *J. Immunol.* **187**, 781–790 (2011).
32. Jenkins, M.R., Trapani, J.A., Doherty, P.C. & Turner, S.J. Granzyme K expressing cytotoxic T lymphocytes protects against influenza virus in granzyme AB $^{-/-}$ Mice. *Viral Immunol.* **21**, 341–346 (2008).
33. Zhao, T. *et al.* Granzyme K cleaves the nucleosome assembly protein SET to induce single-stranded DNA nicks of target cells. *Cell Death Differ.* **14**, 489–499 (2007).
34. Joeckel, L.T. *et al.* Mouse granzyme K has pro-inflammatory potential. *Cell Death Differ.* **18**, 1112–1119 (2011).
35. Kaiserman, D. *et al.* Identification of Serpinb6b as a species-specific mouse granzyme A inhibitor suggests functional divergence between human and mouse granzyme A. *J. Biol. Chem.* **289**, 9408–9417 (2014).
36. Susanto, O. *et al.* Mouse granzyme A induces a novel death with writhing morphology that is mechanistically distinct from granzyme B-induced apoptosis. *Cell Death Differ.* **20**, 1183–1193 (2013).
37. Wensink, A.C. *et al.* Granzyme K synergistically potentiates LPS-induced cytokine responses in human monocytes. *Proc. Natl. Acad. Sci. USA* **111**, 5974–5979 (2014).
38. Spencer, C.T. *et al.* Granzyme A produced by $\gamma_9\delta_2$ T cells induces human macrophages to inhibit growth of an intracellular pathogen. *PLoS Pathog.* **9**, e1003119 (2013).
39. Migueles, S.A. *et al.* Lytic granule loading of CD8 + T cells is required for HIV-infected cell elimination associated with immune control. *Immunity* **29**, 1009–1021 (2008).
40. Kaiserman, D. *et al.* The major human and mouse granzymes are structurally and functionally divergent. *J. Cell Biol.* **175**, 619–630 (2006).
41. Wingender, G., Krebs, P., Beutler, B. & Kronenberg, M. Antigen-specific cytotoxicity by invariant NKT cells in vivo is CD95/CD178-dependent and is correlated with antigenic potency. *J. Immunol.* **185**, 2721–2729 (2010).
42. Purbhoo, M.A. *et al.* The human CD8 coreceptor effects cytotoxic T cell activation and antigen sensitivity primarily by mediating complete phosphorylation of the T cell receptor chain ζ. *J. Biol. Chem.* **276**, 32786–32792 (2001).
43. Laugel, B. *et al.* Different T cell receptor affinity thresholds and CD8 coreceptor dependence govern cytotoxic T lymphocyte activation and tetramer binding properties. *J. Biol. Chem.* **282**, 23799–23810 (2007).
44. López-Sagaseta, J. *et al.* MAIT recognition of a stimulatory bacterial antigen bound to MR1. *J. Immunol.* **191**, 5268–5277 (2013).
45. Buckner, M.M.C. & Finlay, B.B. Host-microbe interaction: innate immunity cues virulence. *Nature* **472**, 179–180 (2011).
46. Souwer, Y. *et al.* Selective infection of antigen-specific B lymphocytes by *Salmonella* mediates bacterial survival and systemic spreading of infection. *PLoS One* **7**, e50667 (2012).
47. Toossi, Z. *et al.* Induction of serine protease inhibitor 9 by *Mycobacterium tuberculosis* inhibits apoptosis and promotes survival of infected macrophages. *J. Infect. Dis.* **205**, 144–151 (2012).
48. Willberg, C.B. *et al.* Protection of hepatocytes from cytotoxic T cell mediated killing by interferon-alpha. *PLoS One* **2**, e791 (2007).
49. Fergusson, R.J. *et al.* CD161 defines a transcriptional and functional phenotype shared across distinct human T cell lineages. *Cell. Rep.* (in press).
50. Leeansyah, E., Loh, L., Nixon, D.F. & Sandberg, J.K. Acquisition of innate-like microbial reactivity in mucosal tissues during human fetal MAIT-cell development. *Nat. Commun* **5**, 3143 (2014).
51. Leeansyah, E. *et al.* Activation, exhaustion, and persistent decline of the antimicrobial MR1-restricted MAIT-cell population in chronic HIV-1 infection. *Blood* **121**, 1124–1135 (2013).
52. Germain, C. *et al.* Induction of lectin-like transcript 1 (LLT1) protein cell surface expression by pathogens and interferon-γ contributes to modulate immune responses. *J. Biol. Chem.* **286**, 37964–37975 (2011).
53. Turtle, C.J. *et al.* Innate signals overcome acquired TCR signaling pathway regulation and govern the fate of human CD161^{hi} CD8α^{+} semi-invariant T cells. *Blood* **118**, 2752–2762 (2011).
54. Gérart, S. *et al.* Human iNKT and MAIT cells exhibit a PLZF-dependent proapoptotic propensity that is counterbalanced by XIAP. *Blood* **121**, 614–623 (2013).
55. Roederer, M., Nozzi, J.L. & Nason, M.C. SPICE: exploration and analysis of post-cytometric complex multivariate datasets. *Cytometry A* **79**, 167–174 (2011).

This work is licensed under the Creative Commons Attribution-NonCommercial-No Derivative Works 3.0 Unported License. To view a copy of this license, visit http://creativecommons.org/licenses/by-nc-nd/3.0/